CONCRETE NZ

CONFERENCE 2022

TECHNICAL PAPERS

Energy Events Centre, Rotorua | 13 – 15 October 2022

THE ORGANISERS GRATEFULLY ACKNOWLEDGE THE FOLLOWING COMPANIES FOR MAKING THIS CONFERENCE POSSIBLE

CONFERENCE PATRONS

Golden Bay

www.goldenbay.co.nz

Holcim

www.holcim.co.nz

PACIFIC STEEL
CERTAIN STRENGTH

www.pacificsteel.co.nz

Sika®

www.sika.co.nz

CONFERENCE SPONSORS

BuildingPoint™

www.buildingpoint.com.au

CONEQUIP
CONCRETE PLANTS AND EQUIPMENT

www.conequip.co.nz

Firth

www.firth.co.nz

Fletcher Reinforcing
STRUCTURED FOR STRENGTH

www.fletcherreinforcing.co.nz

GPIL
GEOSYNTHETIC PARTNERS INTERNATIONAL

www.gpil.co.nz

Leviat
A CRH COMPANY

www.leviat.com

reid™
Construction Systems

www.reids.co.nz

tws

www.techweld.nz

MASTER® BUILDERS SOLUTIONS
bluey

www.master-builders-solutions.com

concretenz BUILDING RESILIENCE
CONFERENCE 2022
13-15 October 2022
Energy Events Centre | Rotorua

Concrete NZ Conference 2022 Technical Programme

THURSDAY 13 OCTOBER			
10.00 – 17.00	**Registration desk open**		
11.00 – 12.00	**Concrete NZ – Precast Meeting**	**11.30 – 12.00**	**Concrete NZ – Readymix Annual Meeting**
11.30 – 12.45	**Lunch**		
12.45 – 13.00	**Conference Opening**		
13.00 – 14.45	**Session 1** **Chair: Alessandro Palermo** **KEYNOTE:** The Future of Concrete ***Santiago Pujol*** *(University of Canterbury)* A Vision for Fast Decarbonisation of the NZ Concrete Industry ***Kevin Larcombe*** *(Holcim NZ)* Americas Cup 36 – Hobson Wharf Extension Design and Construction ***Joshua Paterson, Ted Polley*** *(Beca Ltd) and* ***Murray Ford*** *(Downer)*		
14.45 – 15.30	**Afternoon Tea**		
15.30 – 17.00	**Session 2A** **Chair: Alistair Russell**	**Session 2B** **Chair: John Marshall**	
	A Dissipative Controlled Rocking Column Solution for Bridge Piers on Monopiles ***Sabina Piras, Alessandro Palermo, Gabriele Chiaro*** *(University of Canterbury)*	Mix Design and Fresh Properties of 3D Printed Concrete ***Giuseppe Loporcaro, Don Clucas*** *(University of Canterbury)*	
	Effect of Accelerated Curing and Admixtures on Concrete Shrinkage ***Hossein Askarinejad, Jonathan Chantarawitoon, Kiran Joshipandey*** *(Ara Institute of Canterbury);* ***Trevor Sawyer*** *(Firth Concrete)*	Evaluation of the Durability of AutoCast Concrete Pipe Against Machine-Made Concrete Pipe ***Americo Dos Santos, Tim MacIntosh*** *(Hynds Pipe Systems Ltd);* ***Daksh Baweja, Hayden Duffy*** *(BG&E)*	
	Pioneering a New Way of Building Bridge Piers ***Hugo Jackson, Alison Craigie*** *(Fulton Hogan Civil)*	Fibre-Reinforced Concrete: A Technical Consideration on Application and Design ***Kyle Hundloe*** *(Master Builders Solutions Pty Ltd)*	
	Low Damage Rocking Concrete Wall Structures with Resilient Hold-downs and No Post-Tensioning: Applications, Stiffness and Case Study ***Ashkan Hashemi, Nicholas Chan, Rick Henry, Pierre Quenneville*** *(University of Auckland);* ***Chris Wallington, Samir Govind*** *(Beca);* ***Pouyan Zarnani*** *(Auckland University of Technology)*	Carbonation Resistance Factor for Concrete ***Vineet Shah, Allan Scott*** *(University of Canterbury);* ***James Mackechnie*** *(Concrete NZ/Allied Concrete Ltd)*	
17.00 – 18.00	**Concrete NZ Learned Society / Concrete NZ AGMs**		
18.30	**President's Reception – Exhibition Hall**		
19.00	**Casual Conference Dinner & Entertainment**		

FRIDAY 14 OCTOBER		
8.00 – 13.30	**Registration desk open**	
8.30 – 10.15	**Session 3** **Chair: Dave McGuigan** Strength Classification and Durability of Concrete Made from Industrial or Natural Supplementary Cementitious Materials ***James Mackechnie*** *(Concrete NZ/Allied Concrete Ltd);* ***Vineet Shah, Allan Scott*** *(University of Canterbury)* Waikato Expressway – Hamilton Section ***Ted Polley*** *(City Edge Alliance)* It's Okay Not to Be Okay – Your Daily Mental Health Journey ***Mike Botherway*** *(Higgins Concrete Ltd)* Northland Rail Upgrade – Fast-tracked Replacement of Five Bridges Using Post-Tensioned Segmental Construction ***Matthew Ireland, Aidan Summers*** *(Holmes Consulting);* ***Rafael Ballen*** *(KiwiRail)*	
10.15 – 11.00	**Morning Tea**	
11.00 – 12.45	**Session 4A** **Chair: Moustafa Al-Ani**	**Session 4B** **Chair: Kerry Newton**
	Design and Construction of Te Wananga – A New Waterfront Space for Auckland ***Alex Vink*** *(Tonkin & Taylor);* ***Alex Foxon*** *(Isthmus Group Ltd);* ***Kiel Heeks-Purell*** *(HEB Construction)*	Rubberised Concrete: Material Characterization and Mechanical Behaviour ***Ernesto Hernandez, Royce Liu, Alessandro Palermo, Gabriele Chiaro, Allan Scott*** *(University of Canterbury)*
	Overview of the Cyclic Shear Behaviour of Corrosion Damaged RC Circular Columns ***Benjamin Matthews, Alessandro Palermo and Allan Scott*** *(University of Canterbury)*	Chemical and Mineral Admixture Concrete Mix Design for Sustainability Using Simplex Centroid Model ***Jarod Wilson, Ezra Jones*** *(Sika)*
	Glass Fibre-Reinforced Polymer (GFRP) Bars – A Durable Reinforcement Alternative for Concrete Bridge Piers ***Cain Stratford, Alessandro Palermo, Allan Scott*** *(University of Canterbury)*	Effect of Curing Condition and Weather on Concrete Cylinder Compressive Strength ***Opinder Saggi, Nasser Almesfer, Craig Bezett*** *(Allied Concrete Ltd)*
	Tokomaru Bay - Historic Wharf Restoration Using Modern Materials ***Ray Hudd, Mark Dyer, James Brott*** *(University of Waikato)*	The Revised NZS 3104 Specification for Concrete Production and the Concrete NZ Plant Audit Scheme ***James Mackechnie*** *(Concrete NZ/Allied Concrete Ltd);* ***Rob Gaimster, Adam Leach, Dave McGuigan*** *(Concrete NZ)*
	Half Moon Bay Marina Precast Concrete Breakwater: Production Lessons Learnt ***Jamal Almulla*** *(Wilco Precast Ltd)*	Golden Bay Cement's Waste End-of-Life Tyre Project ***Gian Raffainer*** *(Golden Bay Cement);* ***David Welsh*** *(Fletcher Building)*
12.45 – 13.30	**Lunch**	
13.30 - onwards	**Range of Social Activities**	
18.30	**Pre-dinner Drinks**	
19.00	**Formal Conference Dinner & Awards Evening**	

SATURDAY 15 OCTOBER		
8.00 – 13.00	**Registration desk open**	
8.30 – 10.15	**Session 5A** **Chair: Ralf Kessel**	**Session 5B** **Chair: Paul Dillon**
	Case Study of Solar Panel Installation at Concretec New Zealand Ltd ***Justin Bragg*** *(Concretec New Zealand Ltd)*	The Sound of Music: University of Otago – Music and Theatre Redevelopment Project ***Alex Kelly, John Heenan, Neill Lewis*** *(Beca)*
	Getting Ahead of the Curve on Decarbonisation and Sustainability ***Bernie Napp*** *(Concrete NZ)*	Effect of Multifaceted Technologies on Concrete in the 2020s ***Sue Freitag, Mary Ann Halliday*** *(WSP)*
	Hawkes Bay Airport Terminal Redevelopment ***James Behan, Brendon Cornell, Jessica Jacks*** *(WSP Wellington)*	A Review of Concrete Specifications in the New Zealand Industry and the Complications Associated with Them in Practice ***Paul Donoghue, Trevor Sawyer*** *(Firth Industries)*
	Proposed Test Programme for Concrete-Filled Metal Deck Applications: Bridging the Gap for ETA Approved Mechanical Anchors ***Emanuele Naccini*** *(Ramset);* ***Enrique Del Rey Castillo*** *(University of Auckland)*	High and Ultra-High Performance Concrete for New Zealand Bridges: A Natural Pathway to Sustainable Design ***Rosie Pagel, Alessandro Palermo, Ernesto Hernandez*** *(University of Canterbury);* ***Hannah Weise*** *(WSP)*
	Carbon Mitigation Options in the Cement Industry ***Allan Scott*** *(University of Canterbury);* ***Chris Oze*** *(Occidental College);* ***Vineet Shah*** *(Callaghan Innovation)*	Projects and People – What Does the Right Workforce Look Like ***Mark Williams*** *(Waihanga Ara Rau),* ***Greg Durkin*** *(BCITO)*
10.15 – 10.45	**Morning Tea**	
10.45 – 12.45	**Session 6** **Chair: Rick Henry** A Sustainability Check of Some Recently Constructed Concrete Bridges – A Case Study ***Jamil Khan*** *(Beca Ltd)* Construction of Tekapo a New Intake Gate and Shaft ***Mark Hedley*** *(Downer NZ);* ***Alex Parfitt*** *(Parfitt Construction Ltd)* Testing of Flange Hung Double Tee Units with Loop Bars ***Rick Henry, Matthew Jenkins, Ken Elwood*** *(University of Auckland)* Underpinning of Auckland's Chief Post Office Building ***Niraj Ranjit, Dale Burtenshaw, Michael Chung*** *(Aurecon);* ***Nick Craig*** *(Downer Soletanche Bachy JV)* Building the Largest Floor Slab in New Zealand and the Future of High-Performance Floors – A Case Study on Foodstuffs North Island Distribution Centre (NIDC) ***Tim Walker*** *(Face Consultants / RDT Pacific),* ***Sam Datlen-Carter*** *(Conslab)*	
12.45 – 13.00	**Sandy Cormack Award and Conference Closure**	

SESSION 1

Chair:
Alessandro Palermo

concretenz
BUILDING RESILIENCE
CONFERENCE 2022
13-15 October 2022
Energy Events Centre | Rotorua

THE CONCRETE OF THE FUTURE

S. PUJOL[1]

[1] Civil Engineering, University of Canterbury, NZ

SUMMARY

There are accounts that link the beginning of civilization -as we know it- with the origin of (lime) concrete approximately 12,000 years ago, preceding the start of agriculture. Whether that is accurate or not, there is no denying that concrete has been an integral part of the human experience for thousands of years. Today's concrete, owed to the likes of Vitruvius, Smeaton, Lambot, Talbot, Abrams, Richart, Cross, and many others, has served society well. But we must recognize it has two critical Achilles' heels: its durability, as affected mostly by reinforcement corrosion, and its carbon footprint. These challenges must prompt us to rethink what we do. At least three steps seem imperative:

1. Find better ways to revamp and reuse the existing inventory of concrete structures.
2. Build more durable and more robust structures.
3. Explore ways to combine the undeniable advantages of concrete with the attributes of other more sustainable materials.

In relation to Step 1: there are scores of structures with either limited remaining life spans, or well-known vulnerabilities, especially to dynamic demands such as earthquake. Given what we are seeing in our climate, we cannot afford to demolish and rebuild all these structures from scratch. We must find efficient ways to strengthen them so that we can keep using them.

Step 2 was made abundantly clear by the Canterbury Earthquakes of 2010 and 2011. It is true that the details of insurance policies and socioeconomic factors played a crucial role. But damage to RC buildings played a part too, leading to the demolition and reconstruction 2 out of every 3 buildings in its central business district. The rebuild is not favouring concrete, and even if it was: can we afford a similar experiment in Wellington or, for that matter, in San Francisco? In contrast, cities in Japan and Chile go through larger earthquakes with more frequency and more success. What prevents us from imitating what they do?

If Step 2 requires more abundant use of more robust structural systems, given the current challenge with carbon emissions, we may need to admit that other materials are more sustainable and can be suitable for use together with RC. In Step 3, can we combine RC and timber or recycled plastics, for instance, to achieve a more sustainable practice?

Not exploring these steps is likely to result in more damaged concrete buildings on the news in the next disaster, more reluctance to use RC in future construction, and more justified challenges from environmental organizations. The concrete of the future has to be a different concrete: reused and reusable, robust, and combined with other materials. The time to go back to the drawing board is now. Given what happened in Christchurch and what is expected for Wellington, Aotearoa -New Zealand- has the opportunity to lead the way.

concretenz BUILDING RESILIENCE
CONFERENCE 2022
13-15 October 2022
Energy Events Centre | Rotorua

A VISION FOR FAST DECARBONISATION OF THE NZ CONCRETE INDUSTRY

KEVIN LARCOMBE

Executive General Manager (New Zealand), Holcim New Zealand

There are numerous examples of cement and concrete organisations globally developing a science-based target (SBTi) roadmap to reduce carbon dioxide[1] yet the concrete sector in New Zealand is yet to follow that road. Up to 80% of embodied CO2 in concrete is from cement and the population of New Zealand (NZ) consumes about 1.6 million tonnes of cement annually, equating to around 1.3 million tonnes CO2. Cement manufacture for the local construction industry generates the equivalent of 2% of this country's entire carbon budget[2], so our sector is uniquely positioned to do its part to limit global warming.

Our industry can be at the leading edge of decarbonisation by changing to low carbon cement solutions. Yet we've been held back by a few factors, including a reluctance to use low clinker cement, low availability of cement substitutes (with no domestic granulated blast furnace slag available), and the technical risk inherent in natural pozzolans.

Minimising clinker in the cementitious component of concrete is the key to decarbonisation and Holcim New Zealand (Holcim) is responding. We are breaking the link between clinker and concrete in the short term with four initiatives:

- Deliver the country's first dedicated low carbon cement replacement grinding station at Ports of Auckland in early 2023, providing Ground Granulated Blast Furnace Slag (GGBFS) at a comparable cost to cement;
- Introduce a new range of low carbon blended cements to the NZ market, branded EcoPlanet;
- Increasing the Mineral Component (MIC) in GP cement progressively to 10%; and
- Use Holcim's global sourcing and innovation capability to ensure fly ash continues to be available in NZ as Genisys reduces coal burn.

Holcim is best placed to help make a real difference by offering low carbon cement solutions. As the world's global leader in building solutions, it has the largest footprint, and a real commitment to sustainability including a net zero pledge, SBTi validated 2030 targets, sector-leading R&D and the world's broadest range of low carbon materials.

The low carbon products available from 2023, represent a prime opportunity to improve environmental outcomes.

The construction industry should be at the leading edge of decarbonisation due to the relative ease of making a quick impact. We have a clear vision for the concrete industry's response to climate change: accelerate decarbonisation by breaking the link between clinker and concrete.

---

[1] https://sciencebasedtargets.org/sectors/cement

[2] https://environment.govt.nz/what-government-is-doing/areas-of-work/climate-change/emissions-reduction-targets/greenhouse-gas-emissions-targets-and-reporting/

If the New Zealand concrete industry achieves more than a 25% replacement of Type GP Cement with low carbon alternatives, as Australia and the UK are currently doing, we achieve the equivalent of taking 128,000 petrol cars off the road every year.[3] Holcim is challenging the concrete industry - from engineers and specifiers to cement and ready mix manufacturers - let's deliver 25 by 25. Substitute 25% of traditional cement with low carbon alternatives by 2025.

We can make a difference, without economic sacrifice. Holcim will deliver solutions. Will you join us?

[3] https://environment.govt.nz/publications/measuring-emissions-a-guide-for-organisations-2022-summary-of-emission-factors/

concretenz BUILDING RESILIENCE
CONFERENCE 2022
13-15 October 2022
Energy Events Centre | Rotorua

AMERICAS CUP 36 – HOBSON WHARF EXTENSION DESIGN AND CONSTRUCTION

JOSHUA PATERSON[1], TED POLLEY[2], MURRAY FORD[3]

[1]Structural Engineer – Civil Structures, Beca Ltd, Auckland, New Zealand
[2]Technical Director – Civil Structures, Beca Ltd, Auckland, New Zealand
[3]Project Manager – Infrastructure Projects, Downer, Auckland, New Zealand

SUMMARY

The Wynyard Edge Alliance was formed to deliver the infrastructure required to support the 36th Americas Cup event held within Auckland in 2020 / 2021.

The structural aspects of the project involved repairs, modifications and upgrades to aging existing infrastructure as well as construction of many new structures including: two wharves, six bridges, multiple piled breakwater structures and an outfall structure.

This paper focuses on the larger of the two wharves, the Hobson Wharf Extension, required to house the challenger of record, Luna Rossa, base.

INTRODUCTION

To meet the challenge of hosting the 36th America's Cup event in Auckland's Wynyard Quarter, in April 2018, the New Zealand Government (MBIE) and Auckland Council formed their first commercial alliance committing close to $250M to prepare Auckland's waterfront for the AC36 event. The Wynyard Edge Alliance (WEA) brought together a high-performing team of designers, constructors and owner representatives, working in a highly charged, dynamic environment to: "create the stage for the America's Cup and a waterfront destination that Kiwis love".

At the time, nobody knew how many teams were coming, where they would be located, or how the bases would be configured. The uncertainty and risk associated with AC36 preparations required a leap of faith by all partners. The non-owner participant team of McConnell Dowell, Downer, Beca and Tonkin+Taylor adjusted quickly to changes in scope and delivered the bases to each team's requirements, with the last milestone met on 30th November 2020.

The AC36 project was delivered safely, in a constrained and highly visible urban and marine environment, with strict consent conditions, complex technical elements, a fixed budget and timeframe, and for good measure - with clients that were new to Alliance construction. What could possibly go wrong? Success was paramount – failure was definitely not an option.

The project's marine location and complicated construction sequencing, dictated by a tight programme, required rapid construction activities across a sprawling worksite compounded by

up to 13 work fronts being accessed via open water or through public spaces. The different types of construction contributed to the projects complexity of delivery and included contaminated soil, marine dredging, pile casing driving and drilling, marine works, site wide utility works with many installed under wharfs, paving, wharf assembly, 100-year-old wharf repair works, architectural finishes and many more.

One of the main challenges of this important project was the diversity and complexity of the design and construction. The structural aspects of the project involved repairs, modifications and upgrades to aging existing infrastructure as well as construction of many new structures including: two wharves, six bridges, multiple piled breakwater structures and an outfall structure. Refer Figure 1 for project extent.

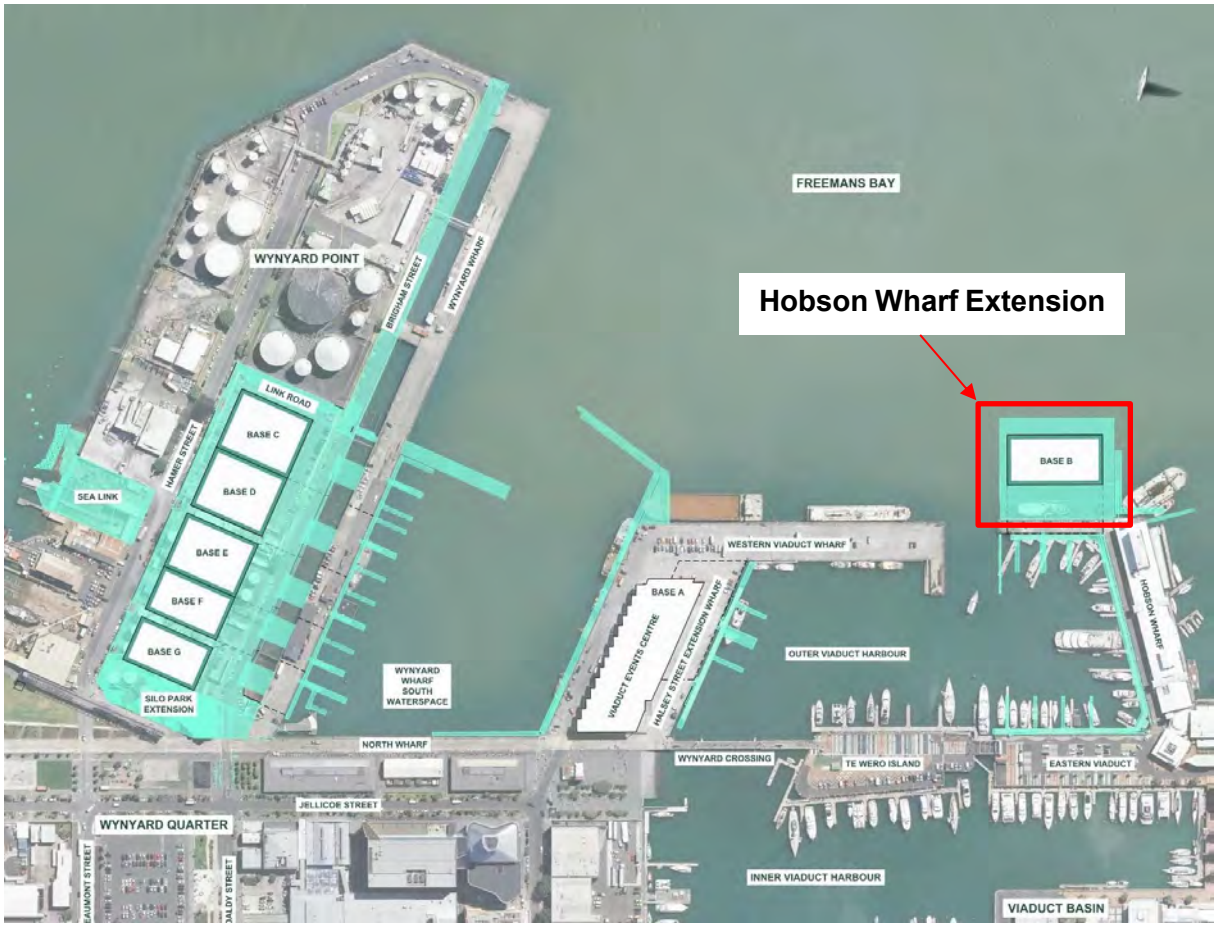

Figure 1. Project extent and location of Hobson Wharf Extension.

Specific to the Hobson Wharf Extension (HWE), the larger of the two wharves, this paper focuses on all aspects of design and construction from the concept phase through to the finished product, and everything in between.

The delivery of the wharf needed to meet extremely tight time constraints while achieving value for money. To achieve this goal, the Alliance developed a modular precast concrete solution which utilised barge transport of elements from Whangarei. Six barge loads transported a total of 8,800 tonnes of precast, pile casings and pile reinforcing cages direct to the worksite. This eliminated hundreds of truck deliveries on the already congested downtown Auckland city streets. After extensive analysis of land-based (from the existing wharf) versus water-based construction techniques, a large floating barge, the AMS Gladstone, was fitted out with a 400-tonne crane and piling equipment to construct the 84 reinforced concrete bored piles and install precast elements directly from the supply barge – akin to an ‘island location’ methodology.

Early designs of the base building for Luna Rossa included statement schemes developed by internationally renowned architects. However, uncertainty around the design of the building and its associated structural form and services significantly increased the complexity of the wharf design in order to accommodate a large degree of flexibility. This was further compounded by the resource consent directing that the building be temporary in nature, leaving uncertainty around the future uses of the wharf through its 100-year design life.

This meant that in addition to supporting the AC36 event infrastructure the wharf also needed to be able to accommodate potential future uses for events, the provision of public open space or commercial wharf operations. The provision of services and drainage also posed a significant challenge due to the wharf's location, being over 200m from the nearest public landside service connections in Quay Street.

STRUCTURE DESCRIPTION

The HWE is situated at the northern end of the existing Harbour Entrance Protection Wharf (HEPW) and sits adjacent to the existing Maritime Museum (refer Figure 1). The extension was sized to accommodate the required footprint of the base building as well as achieving the necessary clearances required between the building and the edge of the wharf deck for public access.

The HWE measures approximately 72m N-S and 81m E-W covering an area of approximately 5832m^2. The wharf is located in the Outer Viaduct harbour to cater for the base of operations for the AC36 challenger of record, Luna Rossa syndicate.

The wharf structure consists of 84 reinforced concrete bored piles supporting 576 precast elements (corbel rings, headstocks, tie planks and deck planks) with an overlaid in-situ concrete deck.

A total of 84 piles of varying length are arranged on a grid pattern of approximately 12m (North-South direction) by 7.5m (East-West direction). Each pile is typically socketed 6-12m into the underlying ECBF rock through a process of driving 813mm diameter steel casings 2-3m into the rock to achieve a seal, followed by socket drilling, reinforcing cage installation and tremie poured concrete.

The piles support a configuration of precast headstock beams (1550mm wide x 775mm deep) that run in the East-West direction which form a series of moment resisting frames when the headstocks are made integral with the piles. Precast slab units (typically 550mm deep planks) span between the headstocks to form the deck area. These planks are then structurally integrated by means of a 150mm deep cast in-situ reinforced concrete topping. Once installed the topping brings the total depth of the deck (precast and in-situ) to 700mm with a total headstock depth of 1500mm.

The planks are detailed as being integral with the headstocks, thereby also achieving moment continuity in the North-South direction and minimising the need for expansion joints. Expansion joints are instead only provided at the interface with the existing Hobson Wharf.

Over the width of the wharf, the deck is pitched in the North-South direction from a central crest situated along Gridline H-D at a 1% slope. Stormwater is directed towards the wharf's northern and southern edges, where it is collected by slot drains that feed into precast treatment chambers suspended underneath the wharf deck. During boat wash-down operations, automated valves located in the stormwater network divert the wash-water to the wastewater system.

The precast wastewater holding chamber, also suspended underneath the wharf, discharges effluent by pump to a rising main suspended under the original Hobson Wharf which discharges into the land-side public sewage network in Quay Street.

SEISMIC DESIGN PHILOSOPHY

It was not considered economical to design the structure to behave elastically under seismic inertia loads. Instead the wharf extension is designed to be a “limited ductility” structure (μ=3), allowing for a mechanism of potential plastic hinges to form at the top of the piles (immediately underneath the superstructure) and at depth. For the lower hinges, the presence of the steel casing means that a complete mechanism may not necessarily form until after the design displacement has been reached. Over-strength shears are instead limited to those generated at the Major Event displacement (defined by the New Zealand Transport Agency Bridge Manual (NZTABM) as 1.5 times the ULS return period factor). From a detailing perspective the structure is detailed for a ductility level of μ = 6, thereby adopting more robust detailing provisions.

The wharf extension is isolated from the existing Harbour Entrance Protection Wharf by way of a seismic gap and expansion joint. The gaps are sized to avoid contact between structures for most earthquakes however some inter-structure pounding has been allowed for during ULS events.

The wharf extension is not situated in an area which is susceptible to earthquake induced liquefaction.

Seismic design actions were assessed following the provisions of NZTABM. Inertia loads are resisted by the frame action created by the headstocks and piles in the East-West direction, and by the wharf deck and piles in the North-South direction.

ANALYSIS METHODOLOGY

Substructure

Structural modelling of the substructure was carried out using the software package SPACEGASS for which a three-dimensional linear elastic frame model was used in the analysis. All key elements of the wharf were modelled, including headstocks, deck and piles. Vertical geometry of the wharf and foundations were considered in the analysis. The deck slab was modelled as a series of rigid in-plane beam elements spanning between piles to represent the deck’s diaphragm action.

Piles were modelled as frame elements and were connected to the deck by rigid link members. Winkler springs were used to model the soil-structure interaction between the piles and founding soil material. Soil properties were adopted as per the Hobson Wharf Extension Geotechnical Design Report (WEA, 2018b). Spring stiffness values were based on the modulus of subgrade reaction and the anticipated soil profile at each pile location. The soil was modelled using bilinear springs and was checked for yielding under all load cases. In instances where yielding occurs, the affected springs are limited to the materials passive pressure limit. Pile group interaction effects were also considered.

Seismic analysis was undertaken using the Equivalent Static Force Analysis approach outlined in the NZTABM. The seismic weight was applied at the superstructures centre of mass. To account for the simultaneous occurrence of earthquake shaking in two perpendicular horizontal directions, the effects resulting from each direction are combined as per the Bridge Manual (i.e 100% x-x & 30% y-y, & 100%y-y + 30% x-x).

Superstructure

The wharf superstructure was also modelled using the software package SPACEGASS for which a grillage model was used to determine the transverse spread of concentrated loads between adjacent precast units. Within the model, traffic loads were applied as moving loads to obtain the worst-case loading configuration.

A single line beam element was used to determine environmental effects arising from differential temperature, differential creep and shrinkage. Design actions arising from seismic load cases were evaluated separately using the substructure model and were then super-imposed to obtain resultant demands.

Within the model, each composite precast plank was modelled as a spine beam along the beam's centreline. The deck slab was modelled as discretely spaced continuous transverse members passing over the precast plank spine beams. These transverse members consisted of two distinct regions: the region that passes over the precast planks (A) and the region that spans between the units (B). However, in order to minimise the number of members contained within the grillage model, each run of transverse members, representing both regions A & B, were instead modelled as a singular member of equivalent stiffness, following the recommendations of E.C Hambly Bridge Deck Behaviour 1991.

3D MODELLING

The wharf structural form consists of multiple interconnecting precast concrete elements. The ability to correctly place and orientate the precast elements was dependent upon achieving the tolerances agreed with the construction team throughout the design phase. Further to this, the design also relied upon the pile cage being oriented correctly to ensure the precast headstock could be placed. Any rotation of the pile cage from the design position resulted in loss of tolerance for subsequently placed elements. Extensive 3D modelling, shown in Figure 2, was undertaken to confirm the structure was buildable with construction safety, budget and achievable tolerance conditions being paramount.

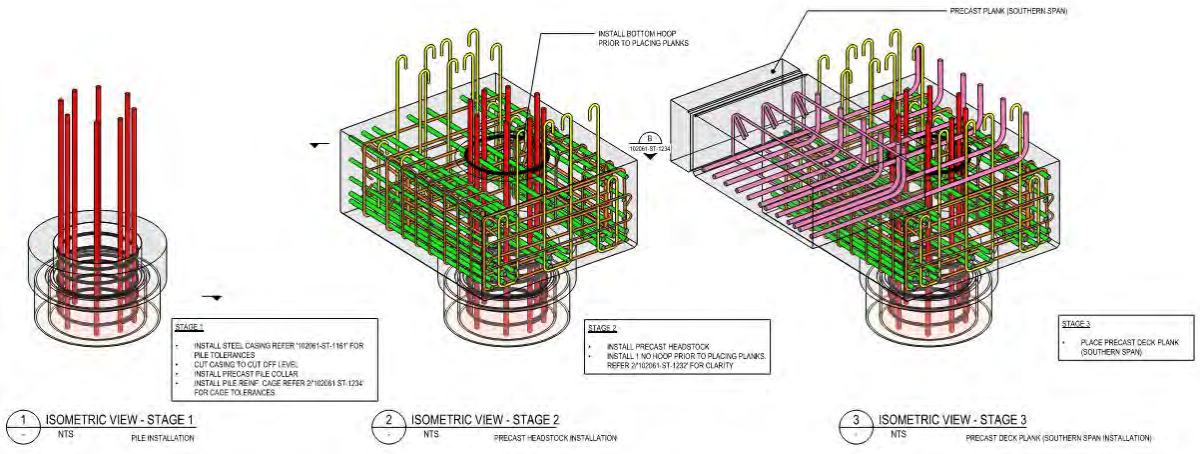

Figure 2a. 3D modelling of deck-pile joint region.

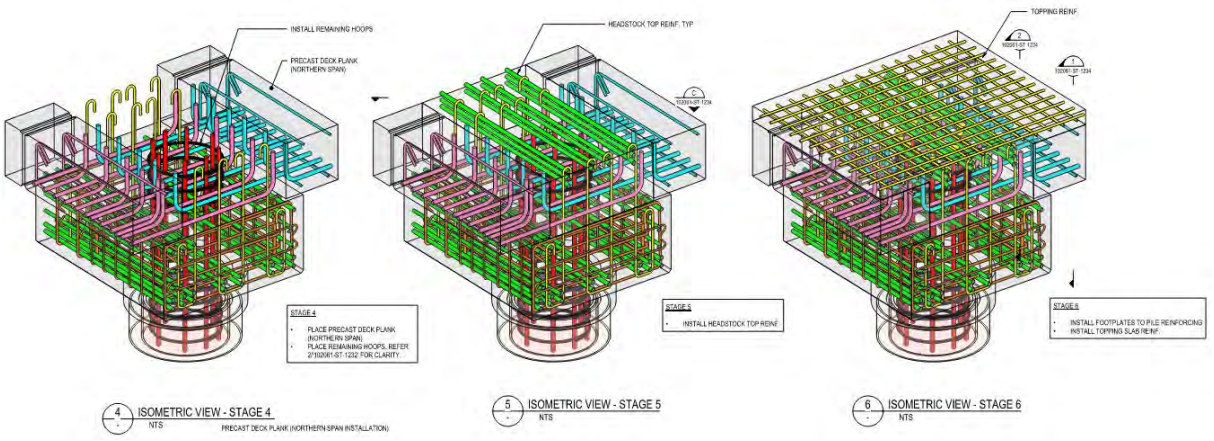

Figure 2b. 3D modelling of deck-pile joint region.

SUSTAINABILITY AND ENVIRONMENTAL CONSIDERATIONS

The sensitive coastal location and significant marine construction works posed significant environmental risks. WEA managed a comprehensive framework of adverse environmental effects including noise and vibration, traffic impacts, social impacts, business disruption, and unplanned discharges to air, land, and water. Key mitigations are included below.

Design for Sea Level Rise

To accommodate the effects of sea level rise, the design allows for a new deck structure to be constructed on top of the original wharf extension. In order to do so, it is intended that portions of the original deck will firstly be removed, such that there is no net increase in loading to the piles. To facilitate future removal prior to installing the new deck, the slabs are spaced with 30mm width gaps. The gaps are spanned with fibrous board ahead of topping concrete, similar to rib and infill floor construction. The seismic design of the piles allows for the mass of the deck to be relocated +1m higher than the original deck.

Pile Top ‘bathtubs’

To mitigate the risk of concrete discharge and facilitate safe work platforms during piling concrete pours over water, WEA developed pile top containers (shaped like bathtubs) to capture over-pour and concrete contaminated water. The containers also included plastic inserts for ease of disposal of concrete waste. These were one of the many innovations that saved time, money and enhanced environmental outcomes.

Marine Mammal Observation

Given WEA’s strong environmental commitment, a Marine Mammal Observer (MMO) programme was established. The risk of impact to marine mammals by underwater noise from piling installation works was identified during the consenting process as common dolphins and Orca are known to frequent Waitematā Harbour as well as the presence of a resident leopard seal at nearby Westhaven Marina.

To mitigate risks to marine life, a MMO protocol was developed based on the principles used in seismic survey works; scaled down to suit piling works using underwater monitoring data. After 100 hours of piling work, WEA produced a technical document outlining practical construction protocols which have been shared within the industry. This MMO practice has since been adopted on other marine projects including Calliope Wharf Extension at Devonport

Naval Base, Downtown Infrastructure Development Programme, and Port of Nelson Wharf Replacement, with training provided to construction teams by the WEA MMOs.

Noise and Vibration Management

In compliance with construction noise and vibration standards for the project, WEA identified sensitive locations, including the Maritime Museum where 130 piles were installed for the breakwater structure within 10m of the museum's western wall and sensitive exhibits.

The construction team engaged early with museum staff to identify high risk areas and installed long-term vibration monitors in sensitive locations within the museum. Real-time vibration monitoring was undertaken during piling works, and WEA adapted their approach where necessary to comply with limits. One initiative was the adoption of a variable frequency vibratory hammer with controlled ramp up-and-down features to eliminate shudders when stopping and starting the hammer.

Driven Piles

Following consultation with neighbours on Princes Wharf during the consenting phase, WEA switched from full-depth driven piles to bored piles. Adopting bored piles in favour of driven piles significantly reduced construction noise and vibration and led to improved relationships with key stakeholders, including local residents, that lasted for the duration of the project.

Use of HDPE Sleeves on Perimeter Piles

HDPE sleeves were installed on the perimeter piles. Traditionally, piles in and around the Freeman's Bay area have not been covered with HDPE sleeves, but rather have been installed using steel casings that are either cut down after installation or alternatively left to corrode. The use of HDPE sleeves is a practice which is more common overseas and is considered to improve the aesthetics of the structure and provides a legacy beyond the project of a low maintenance and environmentally friendly solution. This initiative was also adopted for the multiple piled breakwater structures.

SITE FACTORS

Working across both marine and landside spaces with as many as 13 active work fronts at any one time, was a significant logistical challenge. Works included; installing casings in the seabed using a barge mounted crane and separate drill, dredging of silt, demolition, building a wharf over tidal conditions, capping and stabilisation of contaminated soil, structural strengthening of a 100 year old wharf, paving, large diameter pipeline installation, a major programme of utilities relocation and upgrades, the creation of a new park and other architectural and cultural elements - all happening in different physical environments in a highly sensitive stakeholder community and within tightly constrained milestones and budgets.

The site was severely exposed to the elements from all directions being located right on the waterfront. All marine operations were weather and tidal dependant. Additionally, there was a significant risk of works interruption due to high winds that could shut down crane operations when limits were exceeded. Of note, the site was hit by a small tornado.

PRECAST CONCRETE MODULARISATION

WEA had to be efficient with design and construction to meet the fixed timeframes. The programme to design and construct the extension the conventional way (i.e. closely spaced

piles with staging and insitu poured deck) would not meet the ambitious programme. WEA created a solution using precast concrete elements, which met the project delivery timeline, was less expensive, maximised controlled off-site work for improved quality, and significantly reduced working over water. This culminated in constructing this 84 pile, 5832m² wharf extension in an impressive seven-month timeframe from first pile install to last concrete pour.

The early decision to precast concrete elements off-site and barge them to site was a major health and safety win for Auckland, significantly reducing transportation safety risks to the public and freight transporters. Barging also avoided risk from freight breakdowns while transporting from truck to storage at each site, which in turn contributed to the Zero Harm goal.

The intentional modularisation of precast elements facilitating adaption of shared moulds across subsequent breakwater structures on the AC36 project, provided opportunities for both time and cost savings. Additionally, on Breakwater 2, precast beams were lifted in place pre-fitted with temporary walkways and handrails to eliminate “fall from height to water” risk for workers fitting reinforcement and forming the insitu concrete topping.

PROCUREMENT

Early procurement activities involved investigating pre-cast locations and access to berthing with suitable crane capability for barge loading. Northport was identified as the preferred point of delivery for precast supply for loading onto a barge operated by WEA. Busck Prestressed Concrete was selected as the precast supplier with a 2.5hectare greenfield site at Marsden Point, 4 km from Northport.

Early subcontractor engagement identified several critical path procurement items, including site establishment, reinforcing steel, production crane, mould design and mould fabrication. To mitigate programme risk, a number of items were procured during the Interim Project Alliance Agreement (iPAA) phase, ahead of formal supplier agreements.

Busck had procured land near Marsden Point to develop long-line prestressing production capability so AC36 provided the opportunity to upscale their amenities, construct new casting platforms, develop storage areas and invest in a heavy-lift crane.

TECHNICAL SPECIFICATIONS AND QUALITY ASSURANCE

Three 50 MPa concrete mix designs were used to satisfy the 100-year material durability in a Class C marine environment. The concrete specification included the following mix designs:

- 50MPa mix, 8% micro silica for Zone C application – precast (7-day water curing);
- 50MPa mix, 30% flyash for Zone C application – insitu (7-day water curing); and
- 50MPa mix, 40% flyash for Zone C application – insitu (7-day form curing).

These mixes were found to have average 28-day compressive strengths of 70-90MPa due to a combined high GP cement and supplementary cementitious material (SCM) content.

With concerns surrounding precast strength gain during colder months, and heat curing not permitted, early testing of both GP and HE cement mixes was undertaken to verify HE mixes for Zone C applications. Permeability testing verified both mixes met requirements however, through a combination of element concrete mass plus thermal blankets, the GP mix was used throughout.

To ensure an effective water curing regime, slabs were constructed complete with sumps and edge bunds thus facilitating precast soffit submersion plus recycling of curing water. Recirculation pumps, installed in the sumps and connected to sprinklers, ensured all units remained fully wet within hessian enclosures.

The CONQA system was used by Busck and WEA to capture and maintain all Quality Assurance (QA) documents for the precast including; rebar tracking, pre- and post-pour inspections, concrete testing, water curing and pre-dispatch inspections.

WEA maintained a full-time site engineer at Busck undertaking QA inspections and testing with concrete being tested on site for stripping strength followed by IANZ laboratory testing for 7 and 28 day strengths.

For the Hobson Wharf structure, a total of 576 elements (84 corbel rings, 42 headstocks, 72 tie planks and 378 deck planks) were cast over a twenty four week period consuming 3,345m^3 concrete plus 860t of reinforcing steel. Included in the rebar tonnage is the supply of insitu stitch lap bars projecting from the precast and stirrups pre-assembled onto the precast headstock projection bars. This facilitated safe erection followed by construction of the 4.5m long insitu joints.

TRANSPORTATION

Shipping this quantum of product involved six barge loads transporting a total of 8,800 tonnes of precast concrete, pile casings and pile rebar cages direct to the worksite. The barge ‘Cronus’ was secured for the project duration providing on-site storage when not collecting product.

The numerous delivery trips needed to be coordinated with piling operations and berth availability. Once the barge berthed, it became a detailed process of loading the stored planks between deliveries of 39.5 tonne headstocks and 27 tonne tie planks that required direct truck to barge transfer. Each barge loading plan was pre-approved by a maritime surveyor. Northport’s large cargo crane was ideally suited for loading the materials into designated locations on the barge.

The transfer of units from Busck’s yard to wharf achieved load cycle times of 25 minutes per load, with one unit delivered every six minutes using four trucks.

Concurrent with loading precast, each barge load also included pile casings, pile cage sets and corbel rings for each bent, hence 129 lifts per load at a respectable 4 minutes per lift.

Commencing with a 900 tonne load in February, four subsequent loads at 1,450 tonnes each, and a final load of 2,200 tonnes in early July 2020 completed the supply of precast to Hobson Wharf.

Concrete for the HWE was pumped 185m along existing Hobson Wharf to a boom pump which subsequently pumped a further 40m to piles, insitu headstock moulds and topping slab locations. This was required due to adjacent AC36 breakwater construction activities.

CONSTRUCTION SEQUENCE

The construction sequence adopted for each wharf bent is outlined in Table 1 and illustrated in Figure 3.

Table 1. Hobson Wharf Extension construction sequence.

Stage 1	• Steel casings driven into ECBF rock from floating barge + 400T crane • Steel casing cut to level • Pile drilled to depth and reinforcing cage installed ensuring correct orientation • HDPE sleeve installed (perimeter piles only) • Precast pile collar + working platform installed • Pile tremie poured and 'type b' construction joint formed at pile top
Stage 2	• Precast headstocks placed to required tolerances
Stage 3	• Pile plugs poured (to lock the precast headstocks in place) • Precast tie planks installed to required tolerances
Stage 4	• Headstock insitu stiches formed and poured
Stage 5	• Deck planks installed to required tolerances
Stage 6	• Insitu topping poured • Under wharf utilities and precast utility chambers installed • Bollards, fendering and other wharf furniture installed

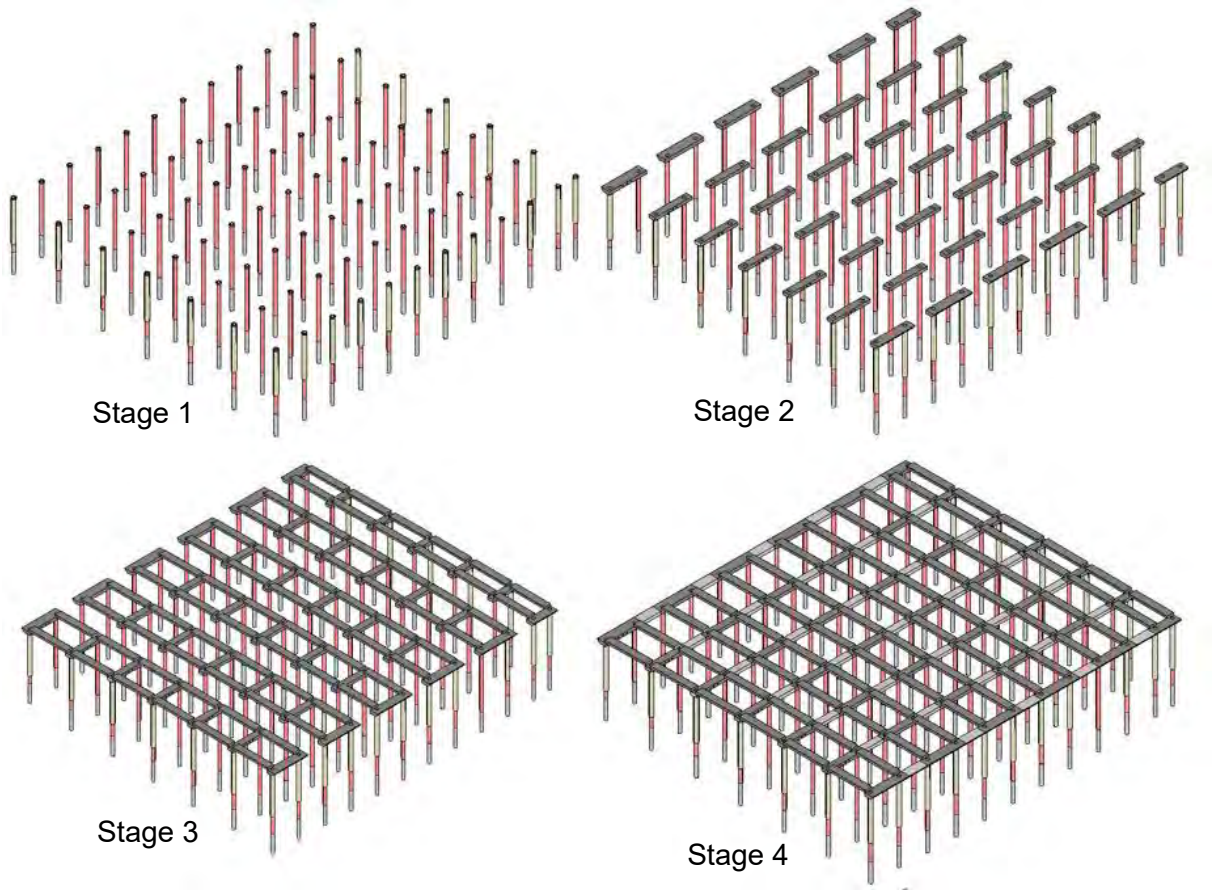

Figure 3a. Construction sequence.

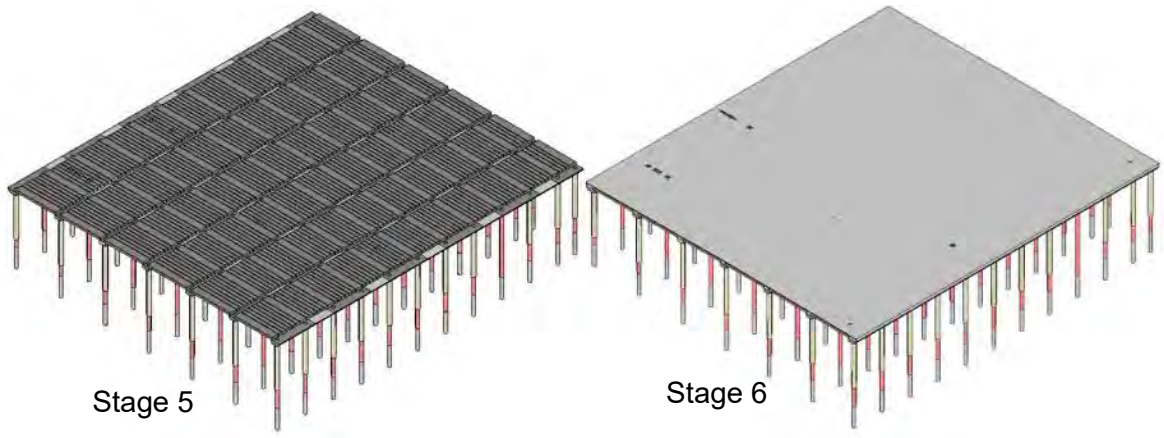

Figure 3b. Construction sequence.

FEEDBACK AND CLIENT SATISFACTION

> **The fast-track construction of Hobson Wharf Extension for AC36 is a credit to the WEA team of designers and constructors who have worked tirelessly in the face of budget constraints, very tight deadlines and methodology challenges. The success is testament to collaborative behaviours involving smart thinking, challenging the status quo and development of great ideas within an over-riding team ethos (adopted from ETNZ) 'Will it make the boat go faster'. We achieved our targets and celebrate our success as a Team.**

Barry Potter, Director, Infrastructure and Environmental Services, Auckland Council.

REFERENCES

Wynyard Edge Alliance (2021), D&C of Hobson Wharf Extension, AC36, SESOC Award Submission.

Wynyard Edge Alliance (2021), Creating the Stage for the 36th Americas Cup, ACE Awards 2021.

Wynyard Edge Alliance and Busck Prestressed Concrete (2019), Design & Construction of Hobson Wharf Extension for AC36, Concrete NZ, Concrete Awards 2019.

Wynyard Edge Alliance (2018a), ST01: Hobson Wharf Extension Design Report, Rev 1, Issued for Construction 19 December 2018.

Wynyard Edge Alliance (2018b), Hobson Wharf Extension Geotechnical Design Report, Rev 1, Issued for Construction 20 December 2018.

New Zealand Transport Agency (2016), Bridge Manual (SP/M/022), Third Addition, Including Amendment 2 Effective from May 2016.

E. C. Hambly (1991), Bridge Deck Behaviour, Second Edition 1991.

PHOTOS

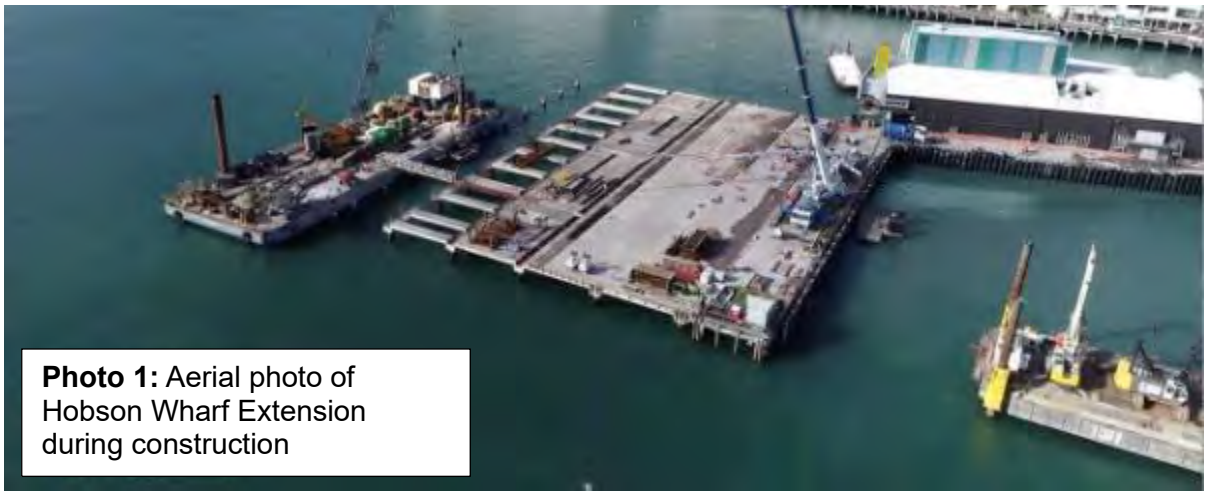

Photo 1: Aerial photo of Hobson Wharf Extension during construction

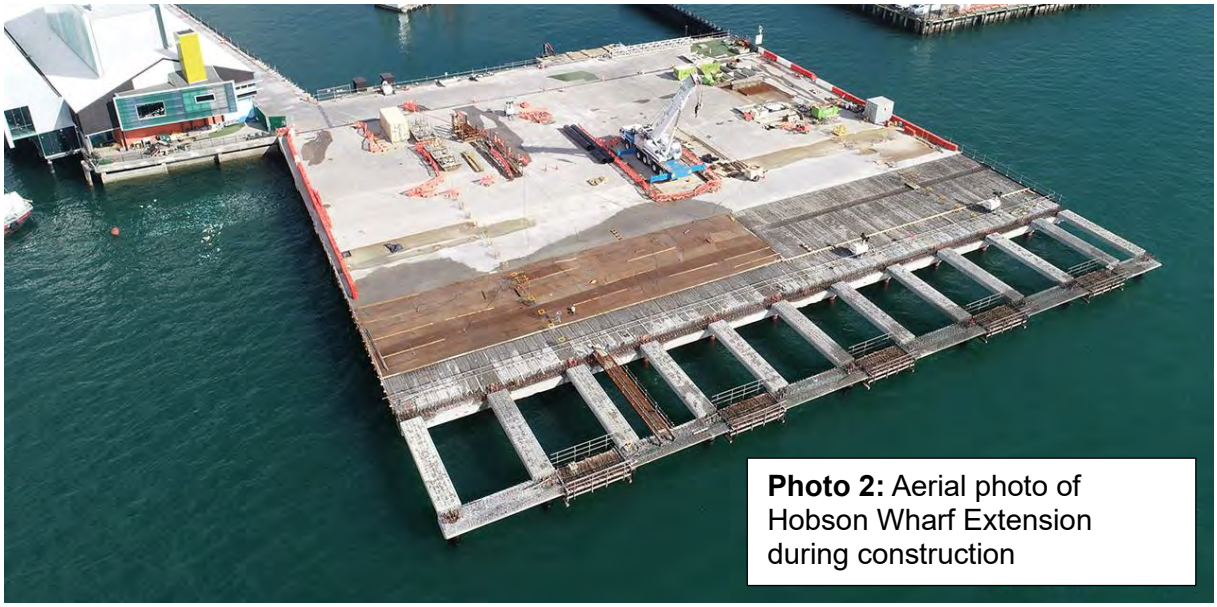

Photo 2: Aerial photo of Hobson Wharf Extension during construction

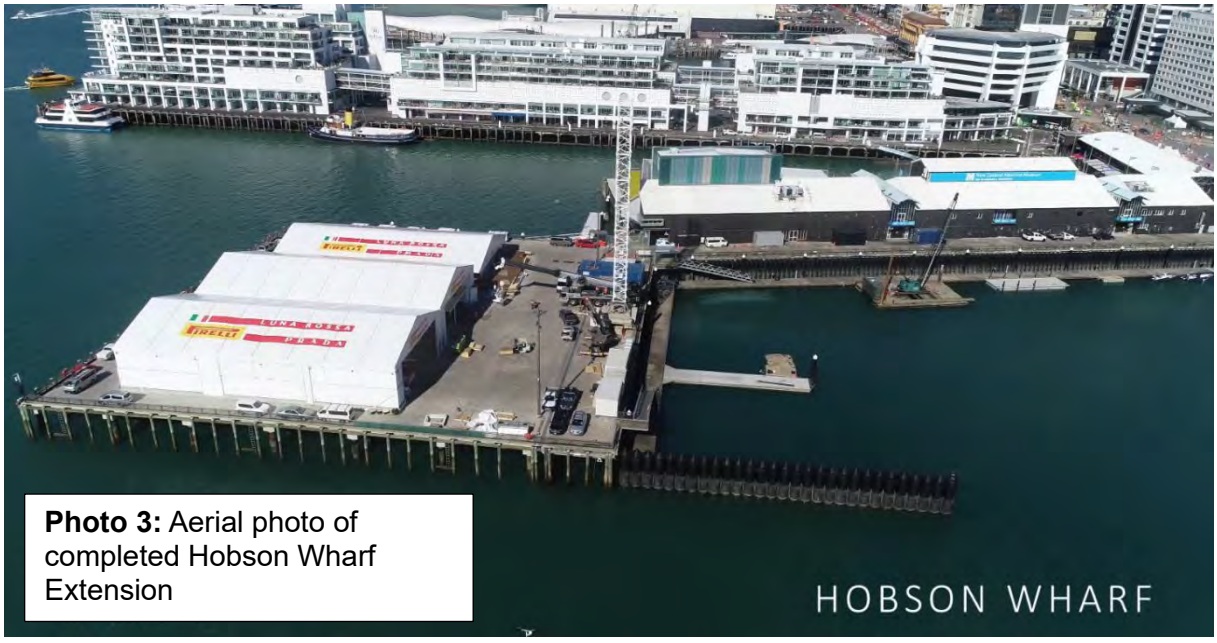

Photo 3: Aerial photo of completed Hobson Wharf Extension

Photo 4: Precast concrete deck planks at Busck Prestressed Concrete Ltd. yard

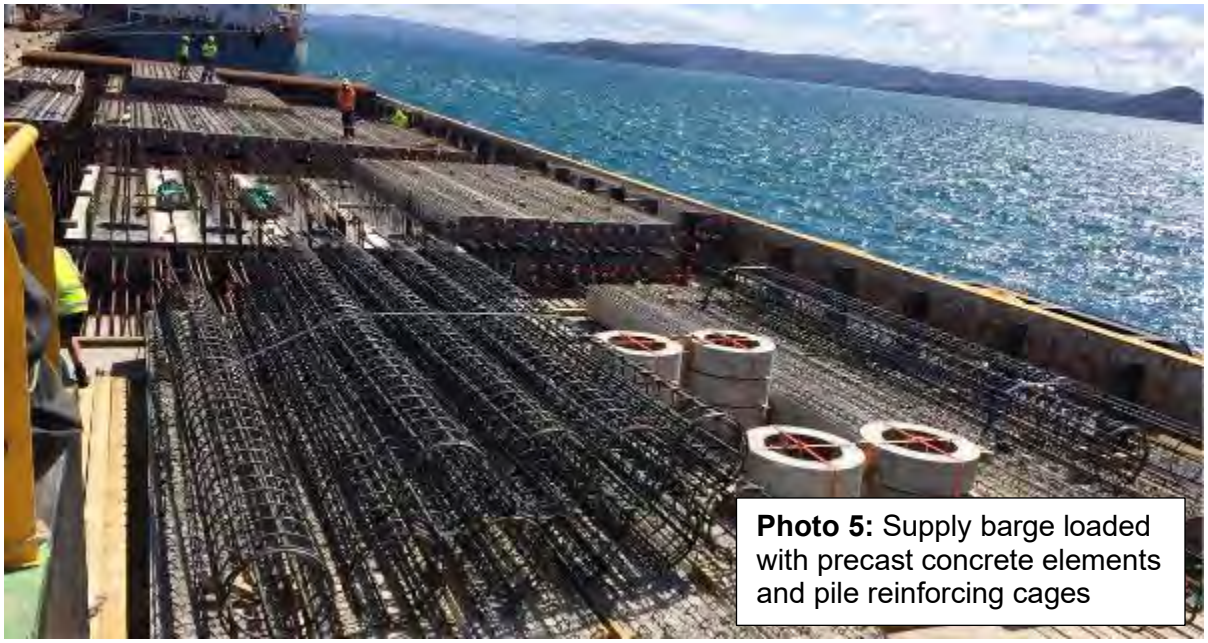

Photo 5: Supply barge loaded with precast concrete elements and pile reinforcing cages

Photo 6: Precast concrete corbels and headstocks installed on piles

SESSION 2A

Chair:
Alistair Russell

concretenz
BUILDING RESILIENCE
CONFERENCE 2022
13-15 October 2022
Energy Events Centre | Rotorua

A DISSIPATIVE CONTROLLED ROCKING COLUMN SOLUTION FOR BRIDGE PIERS ON MONOPILES

SABINA PIRAS, PROF. ALESSANDRO PALERMO, DR. GABRIELE CHIARO

Department of Civil and Natural Resources Engineering, University of Canterbury, New Zealand

SUMMARY

A dissipative controlled rocking (DCR) connection is a low-damage system that replaces the plastic hinge in a column and aims to minimise and potentially eliminate the repair time and costs to a bridge after an earthquake. A DCR system combines unbonded post-tensioning and replaceable dissipaters to provide self-centring and energy absorption capabilities for the bridge pier, respectively. Current research on DCR column systems has focused on the performance of bridge piers founded on a fixed foundation, which ignores any soil-foundation-structure interaction. This paper describes the research undertaken at the University of Canterbury that has developed a DCR solution for bridge columns founded on monopile foundations with passive soil resistance. An emphasis is made on utilising conventional construction materials and forms for the low-damage pier that yields a similar construction cost as a monolithic cast-in-place joint. Lastly, this paper will present an overview of the experimental work conducted as part of this research.

INTRODUCTION

Capacity design in the current bridge seismic design philosophy ensures that the most desirable energy dissipating mechanism forms in the substructure as a result of a significant earthquake (NZ Transport Agency 2018; Caltrans 2019; Eurocode 8 2004). Substructure elements, such as piles and columns, are detailed to have a large ductility to protect the structure from collapse and dissipate energy through localised plastic deformations in the plastic hinges. However, this design approach can result in damage to critical structural members, like in the Mason River bridge in Figure 1a as a result of the 2016 Kaikōura Earthquake. Additionally, the formation of plastic hinges can produce large residual lateral displacements that are not recoverable after severe earthquakes. An example is the Wandle River Bridge which displaced as a result of the 2016 Kaikōura earthquake and required demolition (Figure 1b).

DCR systems are an established engineering technology that has been successfully adopted into building design (Canterbury Earthquake Royal Commission 2012) and experimentally validated for application of bridge columns (Mashal and Palermo 2019; Han et al. 2019). DCR systems, when applied to column joints, combine a self-centring mechanism with dissipation devices to reduce structural damage at plastic hinge zones and residual displacements in columns. The combination of recentring and dissipating components typically results in a “flag-shaped” hysteresis response that passes through the origin, indicating zero residual column displacement.

(a) **(b)**

Figure 1. (a) Localised plastic hinge formation in Mason River Bridge as a result of the 2016 Kaikōura Earthquake. (b) Permanent residual displacements in Wandle River Bridge. Images reprinted from Palermo et al. 2017.

Past experimental research on the application of DCR systems to concrete bridge columns have shown such technologies to significantly improve seismic performance in comparison to their monolithically constructed or emulative counterparts in terms of restricting damage to internal or external devices and eliminating the majority of residual drift (Mander and Cheng 1997; Palermo et al. 2004, 2005, 2007; Wacker et al. 2005; Palermo and Pampanin 2008; Marriott 2009; White and Palermo 2016; Guerrini et al. 2015; Mashal and Palermo 2019). However, all research to-date has assumed a rigid foundation at the base of the column. There is a current lack of knowledge regarding system response due to soil-foundation-structure interaction, similar to that demonstrated in Figure 2.

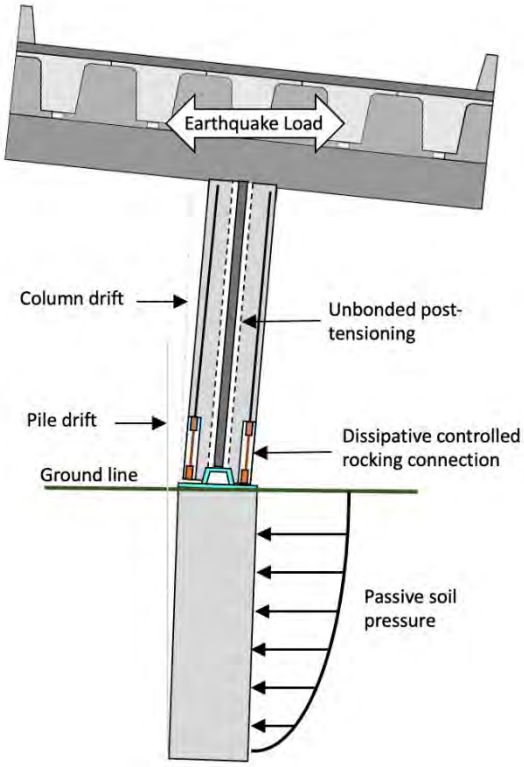

Figure 2. Seismic response of a DCR bridge column founded on a monopile foundation with soil-pile-structure interaction.

Research has been undertaken at the University of Canterbury, which develops a low-damage and replaceable DCR solution for bridge piers founded on monopile foundations. The prototype

developed in this research utilises internal dissipative devices and central post-tensioning to minimise bridge damage during earthquakes and minimise life-cycle costs of the structure, including construction, maintenance and repair costs, and time delays associated with these activities.

This paper aims to provide an introduction and overview of the DCR system developed as part of this research. An outline of the research undertaken will be given, which includes a description of the specimen, an overview of the experimental campaign and a discussion of the results.

TEST SPECIMEN

The prototype structure chosen for this research is representative of a typical New Zealand highway bridge. The bridge is assumed to be of importance level 3, have a 100-year design life, located in Christchurch on non-liquefiable soil, and is not susceptible to near-fault effects. The specimen investigated as part of this experimental research is scaled one-third in size. The specimen is a post-tensioned single cantilever bridge pier with a replaceable DCR connection type at the base of the column where a plastic hinge is likely to form, as shown in Figure 2. The detail adopted for the DCR connection utilizes conventional construction materials and forms.

The pier consists of a 500 mm diameter precast column with a design height of 2.1 m and is supported on a single 600 mm diameter precast pile. Only the length of the pile measured to its theoretical point of zero moment was constructed as part of this study, which equated to 1.9 m in length. Additionally, the pile was pinned at the base, which allows the pile head to experience rotations. The effects of translation do not need to be considered since only relative displacements are of relevance. Refer to Figure 3 for an illustration of the test specimen.

NZS 3101:2006 (Standards New Zealand 2006) was used to design and detail the reinforcement cage in the column and pile. The PRESSS design handbook (Pampanin et al. 2010) was used to size the required fuse area and fuse length of the dissipaters and determine the size and initial post-tensioning force required for the central post-tensioning bar.

The specimen is post-tensioned for self-centring using a single 50 mm diameter fully threaded post-tensioning bar. The post-tensioning bar is debonded inside a 75 mm diameter drossbach duct the full length of the column and pile. The post-tensioning bar is mechanically fixed at the bottom of the pile and tensioned at the top of the column. In actual application, the post-tensioning bar will be cast into the pile and post-tensioned in the pier capping beam.

Replaceable internal dissipaters are used at the rocking joint for dissipation, consisting of grade 300 fully threaded steel rods (Figure 4). The dissipaters are 16 mm in diameter, 380 mm in length, and debonded from the concrete using debonding grease tape (Denso Tape). Debonding reduces the strain concentrations in the dissipaters and prevents premature yielding of the bars under seismic loading. The dissipaters are joined to the permanent longitudinal column and pile reinforcement through Ancon threaded couplers. The use of fully threaded bars facilitates the installation and replacement of the dissipative bars because the couplers and locknuts can be fully screwed back onto the threaded rods before being screwed to the connecting column and pile longitudinal reinforcement. Additionally, the threaded dissipater bars have the advantage of being cut to any length, which reduces fabrication costs and allows for additional adjustments at the installation time.

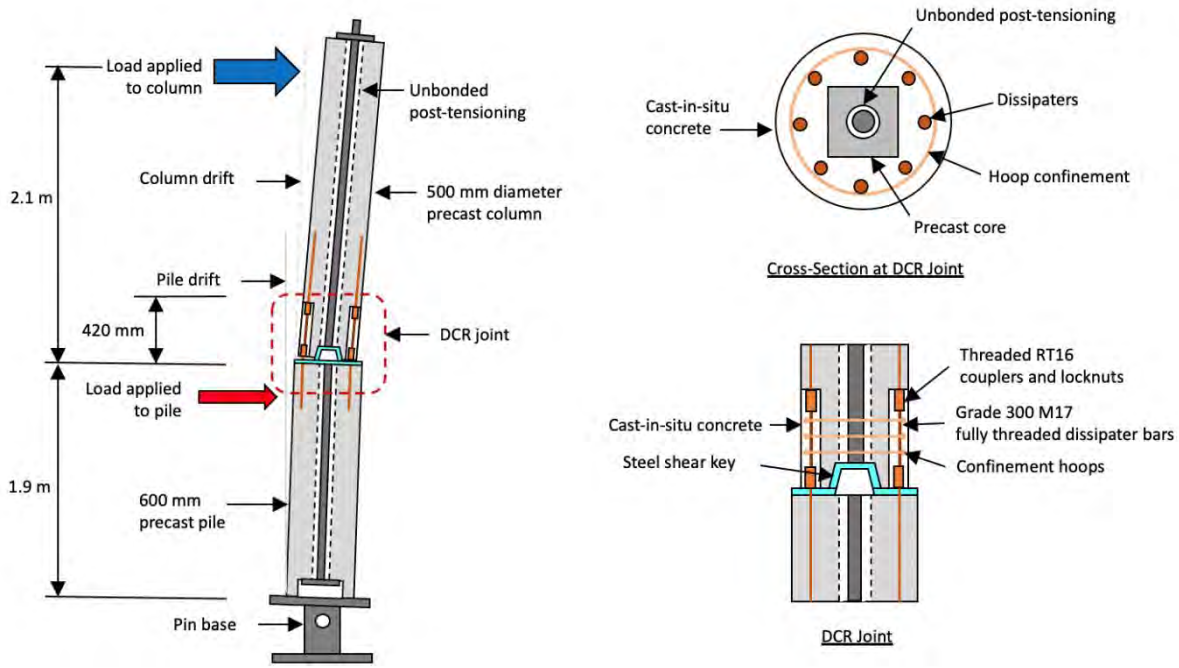

Figure 3. Test specimen.

A steel shear key is provided at the rocking joint for shear and torsion restraint, as well as protection at the rocking surface (Figure 5). The shear key is fabricated from welded plates to form a rectangle with inclined edges at the centre of the column. An opening is provided at the centre of the shear key to allow post-tensioning to pass through. The shear key assembly is welded on a 600 mm diameter base plate, which sits on the pile. Bolts that restrain the shear key assembly are cast into the pile, which allows the shear key to be easily installed or removed. Additional holes were tapped into the shear key's base plate for the longitudinal reinforcement to pass through.

Figure 4. Fully threaded dissipators in the DCR joint. Dissipaters are coupled to permanent column and pile reinforcement by means of threaded couplers.

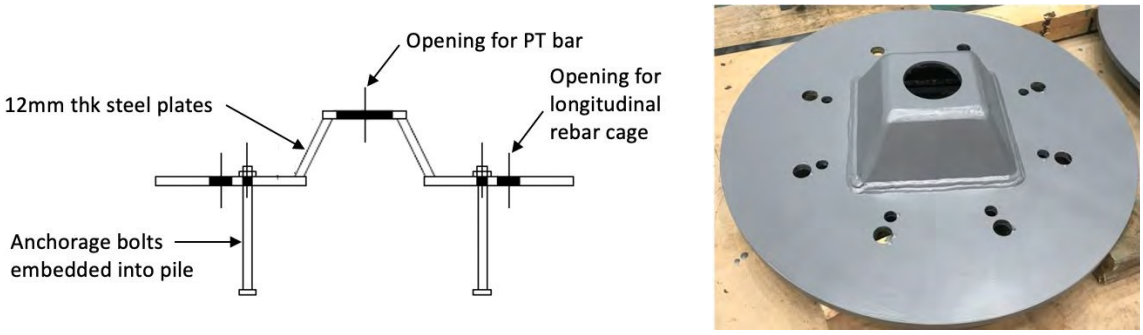

Figure 5. Steel shear key.

CONSTRUCTION

The precast pile and column were fabricated at a commercial prefabrication yard. The concrete mix specified for the precast segments was 40 MPa with 13 mm aggregate chips. The column and pile were reinforced with 16 mm diameter deformed longitudinal bars that were terminated by threaded ends and coupled to the internal dissipaters. The column was constructed with a reduced diameter at the DCR joint that measured 280 mm by 280 mm and was formed to the shape of the shear key.

The precast elements were transported to the University of Canterbury Structural Engineering Lab for assembly and testing. The pile was first erected on the pin support with the post-tensioning bar and shear key. The column, dissipaters and joint hoops were lifted onto the pile. The internal dissipater bars were coupled to the permanent column and pile longitudinal reinforcement, then wrapped in debonding tape. Next, the hoop reinforcement was distributed along the height of the DCR joint. Refer to Figure 6 for a detailed depiction of the joint installation. Finally, a fibre-reinforced (poly monofilament fibre) grout (Sika MonoTop®-438 R) was used to cast the joint. The joint was given seven days to cure until applying vertical post-tensioning to the pier.

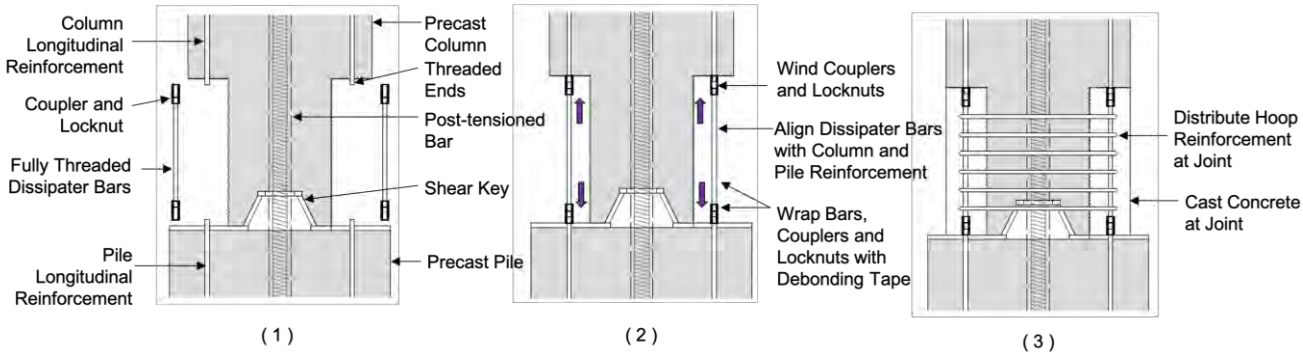

Figure 6. Installation methodology of internal dissipaters.

TESTING ARRANGEMENT AND VARIABLES

Simulation of the seismic loading was achieved through uniaxial, cyclic, quasi-static loading of the bridge in the transverse direction. The experimental setup is depicted in Figure 7. The pier was loaded by two 1000 kN hydraulic rams: one at the top of the column to simulative transverse inertial loading of the specimen from the superstructure, and one at the pile to simulative the soil-pile interaction. A third ram was attached at mid-height of the column to prevent out-of-plane movement but remained unloaded. Gravity loads on the column were applied through the unbonded post-tensioning in addition to the post-tensioning load required for self-centring.

The variable control between each test is the passive soil resistance from the hydraulic ram at the pile. Three soil properties – loose sand, medium-dense sand, and dense sand – were used to represent the variability in soil stiffness. A summary of the test programme is presented in Table 1. Since only one specimen was used, the DCR joint was required to be repaired or replaced between each test, which also enabled the evaluation of the residual capacity of the pier after subsequent large-magnitude earthquakes. Refer to Figure 8 for the joint replacement methodology adopted.

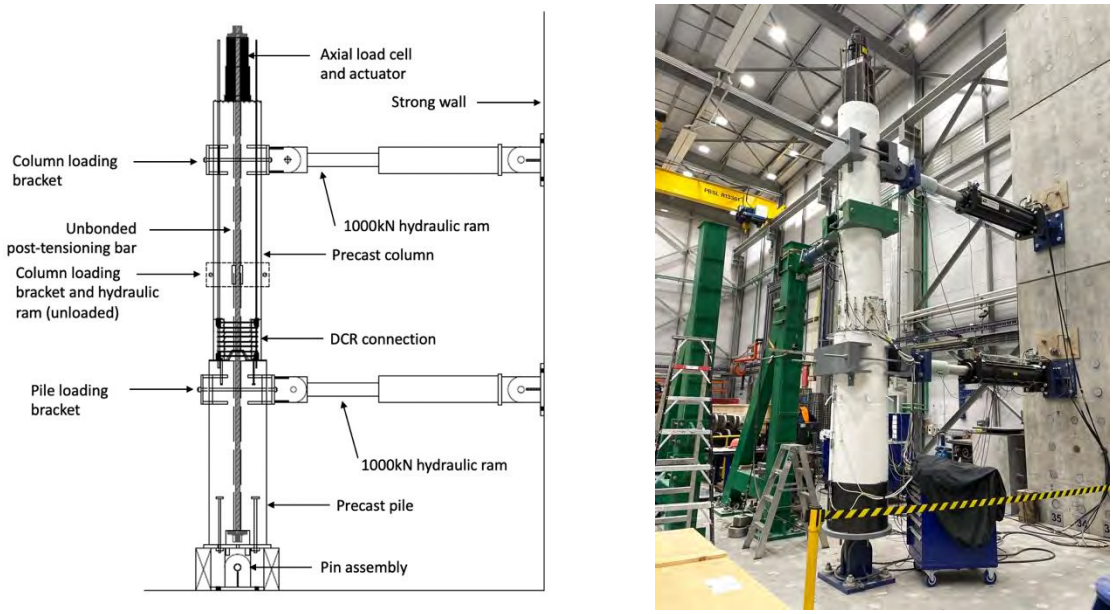

Figure 7. Experimental test setup.

Table 1. Experimental programme.

Test	Description	Soil type
1	DCR connection	Loose sand
2A	DCR connection - replaced	Medium-dense sand
2B	DCR connection with repaired concrete cover	Medium-dense sand
3A	DCR connection - replaced	Dense Sand
3B	DCR connection with repaired concrete cover	Dense Sand
4	Benchmark test: high damage bent	Dense sand

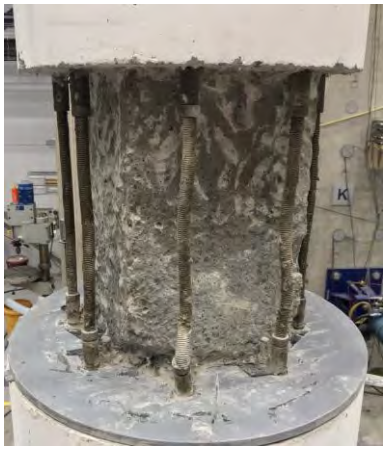

Step 1: Break out concrete in DCR joint.

Step 2: Cut and remove dissipaters and hoops.

Step 3: Install new dissipaters.

Step 4: Wrap dissipaters with debonding tape.

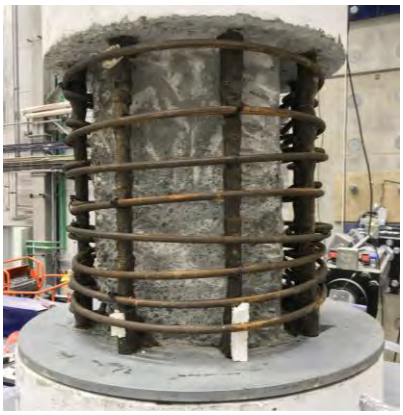

Step 5: Install confinement hoops (2 halves with 180-degree hooks).

Step 6: Pour grout at joint.

Figure 8: Joint replacement methodology adopted in this study.

EXPERIMENTAL RESULTS

This experiment was conducted as a means of obtaining experimental evidence to validate the theoretical predictions used to design the DCR system proposed. Each column was loaded to the assumed maximum considered earthquake (MCE), which corresponded to a factor of 1.5 beyond the design level drift ratio or ultimate limit state (ULS).

There was no fracture to any dissipaters during the tests. However, there was minor buckling in the dissipaters, shown in Figure 8 (Step 1). The precast columns and pile had minor flexural cracking. Concrete damage was contained to the rocking joint where cracks only penetrated through the cover concrete. Concrete crushing was initiated at ULS; however, crushing did not propagate into the core concrete. Thus, there was no loss in structural capacity after the DCR joint was repaired or replaced. Additionally, no damage was observed to the shear key, which successfully prevented column movement due to twisting or stepping. Further, the shear key protected the pile from damage at the rocking interface.

The flexibility of the foundation had a direct effect on the seismic response of the DCR column, which was primarily due to the energy dissipation in the soil. An increase in foundation flexibility reduced the column stiffness, which delayed the onset of column rocking. As shown in Figure

9, larger drifts were required in the pier to reach the design base shear. For smaller lateral drifts, the column remained elastic and undamaged.

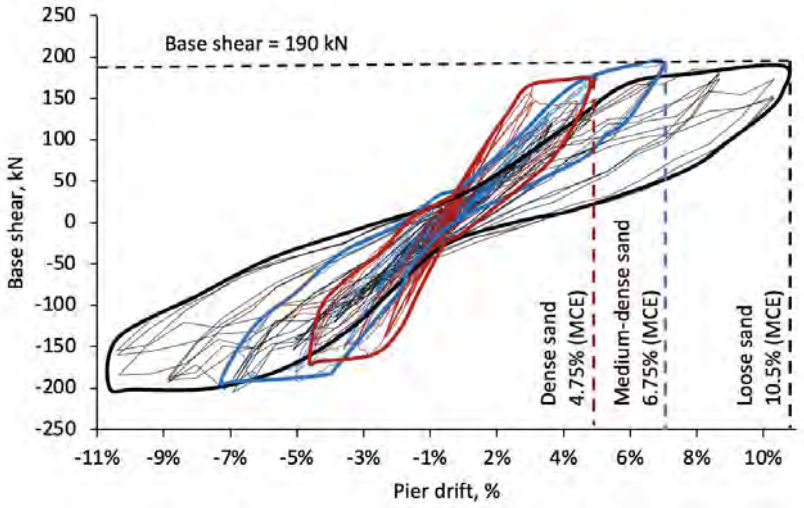

Figure 9. Hysteresis response of DCR column from soil-pile-structure interaction.

The performance of the DCR bent was compared with an equivalent benchmark bent that incorporated a grouted duct connection between the column and the pile, which emulated the behavior of a monolithic or cast-in-place joint. The column longitudinal reinforcement, which consisted of eight 16 mm diameter deformed bars, were grouted into drossbach bars cast into the pile. Given the emulative behavior, the bent relied on the formation of a plastic hinge in the column; therefore, it is referred to as a high damage bent (HDB). The HDB was tested under the same loading protocol as Test 3. Observations from the testing showed the formation of a plastic hinge in the column, which is expected of a system emulating cast-in-place construction.

Crushing and spalling of the concrete occurred at the plastic hinge, followed by buckling of the longitudinal bars. Additionally, there was extensive flexural cracking up the height of the column. The extent of the damage in the HDB's plastic hinge was not repairable, unlike the DCR connection.

The pile, which is a capacity protected member, had significant damage due to pull-out forces in the grouted bars of the HDB. Figure 10 compares the observed damage in the HDB and DCR bent at the end of testing.

CONCLUSION

Low-damage seismic design offers better seismic performance compared to emulative cast-in-place construction. In this paper, a low-damage dissipative controlled rocking bridge column supported on a monopile foundation is investigated, in which the potential plastic hinge zone is replaced by a repairable joint. The dissipative controlled rocking connection adopted in this research utilised a combination of unbonded post-tensioning and internal dissipaters to provide self-centring and energy dissipation for the bridge substructure during an earthquake, respectively. The construction of the proposed low-damage pier utilises conventional construction materials and forms.

The research presented in this paper was validated through experimental testing of a pier scaled one-third of the prototype, in which the system response from the soil-pile-structure interaction was validated. Results showed self-centring and good seismic performance of the specimen. The residual capacity of the column after it was repaired and or replaced was not

affected. Foundation flexibility delayed the onset of column rocking; however, the bent remained elastic and undamaged until rocking was initiated. Damage in the DCR column was limited to crushing of the cover concrete and minor buckling of the dissipating bars. However, the concrete and dissipating bars in the DCR joint proved to be easily repairable.

The performance of the specimen was compared with that of an equivalent bent with emulative, cast-in-place construction, referred to as a high damage bent (HDB). The HDB suffered damage in the plastic hinge in terms of concrete spalling and bar buckling under seismic loading. Damage from pull-out forces in the grouted bars also caused significant damage to the pile. Overall, the results prove the effectiveness of the DCR system to provide an earthquake-resilient solution that can be easily repaired after a large-seismic event.

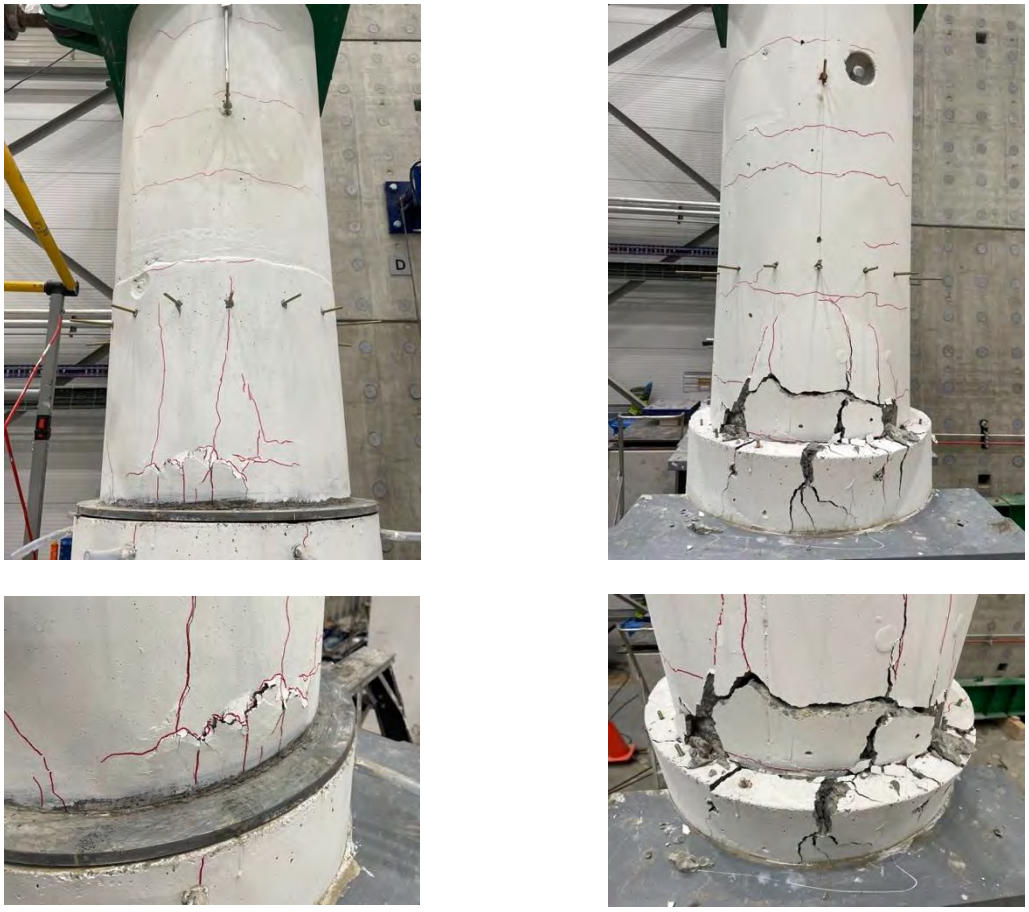

(a) (b)

Figure 10. (a) Column damage in the DCR column at peak drift that resulted in concrete crushing at the rocking joint. No damage in the pile. (b) Column damage in the benchmark structure (high damage bent) at peak drift that resulted in significant flexural cracks in the column and damage to the pile head due to bar buckling at the joint.

ACKNOWLEDGEMENTS

The authors would like to express their gratitude to QuakeCoRE, Ancon, Freyssinet, Sika, Contech, Everitt Site Supplies, and iNFORCE for their financial support and material donations. Additionally, the authors would like to acknowledge Busck Prestressed Concrete Ltd., and Etech and RMI Steel Services for manufacturing the specimens.

REFERENCES

Caltrans, S. D. C. (2019). Seismic Design Criteria Version 2.0.

Canterbury Earthquake Royal Commission (2012). “Final Report Volume 3: Low-Damage Building Technologies.

Eurocode 8 (2004). Design of Structures for Earthquake Resistance.

Guerrini, G., Restrepo, J. I., Massari, M., and Vervelidis, A. (2015). Seismic behavior of posttensioned self-centering precast concrete dual-shell steel columns. Journal of Structural Engineering, Vol 141(4).

Han, Q., Jia, Z., Xu, K., Zhou, Y., and Du, X. (2019). “Hysteretic behavior investigation of self-centering double-column rocking piers for seismic resilience.” Engineering Structures, 188, 218–232.

Mander, J. B. and Cheng, C. (1997). Seismic resistance of bridge piers based on damage avoidance design. Technical Report NCEER-97-0014.

Marriott, D. (2009). “The Development of High-Performance Post-Tensioned Rocking Systems for the Seismic Design of Structures.” PhD thesis, University of Canterbury.

Mashal, M. and Palermo, A. (2019). Low-damage seismic design for accelerated bridge construction. *Journal of Bridge Engineering*, Vol 24(7), 1–13.

NZ Transport Agency (2018). Bridge Manual.

Pampanin, S., Marriott, D., Palermo, A., and Bolognini, D. (2010). PRESSS Design Handbook. New Zealand Concrete Society.

Palermo, A. and Pampanin, S. (2008). Enhanced seismic performance of hybrid bridge systems: Comparison with traditional monolithic solutions. *Journal of Earthquake Engineering*, Vol 12(8), 1267–1295.

Palermo, A., Pampanin, S., and Calvi, G. (2004). Use of “Controlled Rocking” in the seismic design of Bridges. *13th World Conference on Earthquake Engineering*, Vancouver, B.C., Canada.

Palermo, A., Pampanin, S., and Calvi, G. (2005). Concept and development of hybrid solutions for seismic resistant bridge systems. *Journal of Earthquake Engineering*, Vol 9(6), 899–921.

Palermo, A., Pampanin, S., and Marr. (2007). Design, modelling, and experimental response of seismic resistant bridge piers with posttensioned dissipating connections. *Journal of Structural Engineering*, Vol 133(11), 1648–1661.

Palermo, A., Liu, R., Rais, A., McHaffie, B., Pampanin, S., Gentile, R., Nuzzo I., Granerio M., Loporcaro, G., McGann, C., and Wotherspoon, L. (2017). Performance of road bridges during the 14 November 2016 Kaikoura earthquake.

Standards New Zealand. (2006). NZS3101 Concrete Structures Standard: Part 1 - the Design of Concrete Structures.

Wacker, J.M., Hieber, D.G., Stanton, J.F. and Eberhard, M.O. (2005). Design of precast concrete piers for rapid bridge construction in seismic regions (No. WA-RD 629.1). University of Washington.

White, S. and Palermo, A. (2016). Quasi-Static Testing of Posttensioned Nonemulative Column-Footing Connections for Bridge Piers. *Journal of Bridge Engineering*, Vol 21(6), 04016025.

concretenz BUILDING RESILIENCE
CONFERENCE 2022
13-15 October 2022
Energy Events Centre | Rotorua

EFFECT OF ACCELERATED CURING AND ADMIXTURES ON CONCRETE SHRINKAGE

J CHANTARAWITOON[1]; H ASKARINEJAD[1]; K JOSHIPANDEY[1]; T SAWYER[2]

[1] Department of Engineering and Architectural Studies, Ara Institute of Canterbury Ltd, Christchurch
[2] Firth Concrete, Christchurch, New Zealand

SUMMARY

The magnitude and rate of concrete shrinkage depends on various factors including the mix design, admixtures, curing process, and environmental conditions. In this research an experimental investigation is undertaken where the effect of admixtures and the accelerated curing condition on the concrete shrinkage behaviour and compressive strength were examined. Three high-strength concrete mix designs (containing shrinkage reducer or accelerator) and two curing conditions including the normal standard curing and steam curing were replicated to compare the shrinkage and strength results.

INTRODUCTION

Concrete shrinkage is a time-dependent strain in a specimen, and it is usually considered to be the sum of drying shrinkage and autogenous shrinkage. Drying shrinkage is caused mainly by the loss of water during the drying process while autogenous shrinkage is mainly due to various chemical reactions within the cement paste and occurs in the early stages after casting (Ian Gilbert et al. 2017). Shrinkage (in particular, drying shrinkage) is considered to be one of the main causes of cracking in concrete structures. For example, when the concrete is restrained for instance by the reinforcements, the shrinkage will result in tensile stresses which can cause cracking if it surpasses the tensile strength leading to reduction of the tensile load-bearing capacity. Additionally, shrinkage can lead to curling in concrete slabs when the upper slab surface shrinks at a different rate to the bottom surface (Shelton 2015).

The mechanism of shrinkage has been discussed in various publications such as (Ian Gilbert, et al. 2017; Nguyen et al. 2019; Bouziadio et al. 2016; Long et al. 2014: Lura et al. 2001; Ramezanianpour et al. 2014). However, there are limited studies reported in the literature on the shrinkage behaviour of high strength concrete subject to accelerated curing. Accelerated curing is particularly popular in precast concrete industry considering its advantages to gain early strength and to reduce costs and curing time in the production of precast members. However, concerns with accelerated curing are the potential for increased moisture loss during the curing process plus possible problems in strength gain over time (ACI 517.2R 1992; Yazdani et al. 2010; Han et al. 2021; Ekolu 2016).

In this study, three high-strength concrete mix designs and two curing conditions were considered for the shrinkage investigation. The three mix designs included (1) standard concrete mix (control mix), (2) concrete mix containing a shrinkage reducing admixture and (3)

concrete mix containing a non-chloride accelerator. All mix designs were produced with the consistent w/c ratio in a concrete lab using commercially available materials. The specimens produced using the standard concrete mix and the shrinkage reducer mix were split into two groups to cure in two different conditions including normal standard curing according to NZS 3112 (1982) and steam curing. In total 15 concrete beams were produced, and the shrinkage was measured in 14, 21, 28 and 56 days as per AS 1012:13: 2015. Additionally, concrete cylinders were prepared and cured in the same conditions as the beam specimens for compressive testing. The shrinkage and compressive test results obtained from different groups of specimens are analysed and compared.

LAB EXPERIMENT

Table 1 presents the specimen groups used in this study. All mix designs were produced with the consistent w/c ratio. The concrete mix without the shrinkage reducer and accelerator admixtures is shown as the 'Normal Mix' in this table. The Normal Mix here refers to the mix containing cement, water, sand and aggerates, plus water reducing and superplasticizer admixtures. As shown in Table1, shrinkage reducing admixture was added in two of the specimen groups. These admixtures are commercially available and can be used in ready-mix or precast concrete structures requiring shrinkage reduction. Group 5 specimens contain non chloride accelerator. This admixture is used to accelerate the setting time of the concrete. Table 2 shows a summary of the admixtures used in each mix.

Table 1. Specimens produced in the lab

Group	Concrete Mix	Curing method
1	Normal Mix	Normally cured
2	Normal Mix	Steam cured
3	Containing shrinkage reducing admixture	Normally cured
4	Containing shrinkage reducing admixture	Steam cured
5	Containing non-chloride accelerator	Normally cured

Table 2. Admixtures used in each mix for this study

Group	Mid-range water reducer	Super Plasticiser	Viscosity Modifier	Shrinkage reducing	Non-Chloride Accelerator
1	√	√	√	-	-
2	√	√	√	-	-
3	√	√	√	√	-
4	√	√	√	√	-
5	√	√	√	-	√

The mixes used in this study are common to be used by precast specialist in large precast elements where high early strengths are required to facilitate early stripping and lifting of the elements. For large precast elements the moulds are incredibly expensive as these are engineered elements fabricated from heavy steel, so productivity is a key value driver. For this reason, the admixtures used are selected to maximise water reduction but also reduce setting

times. Modern third generation Polycarboxylate based admixtures not only reduce water but have one and in some cases two additional functions.

The admixtures used here reduce significant volumes of water but does not retain slump for much longer that 45 minutes and reduces setting times. This facilitates early finishing and the shorter setting times reduces the risk of plastic shrinkage cracking. This also allows for accelerated curing to proceed in a predictable and manageable time which suits the precast production environment. The use of accelerators in large precast elements is not a common practice, but as part of the work there was interest to assess the impact an accelerator would have on the shrinkage test when performed according to the AS 1012:13: 2015.

Sample preparation and curing process

In total 15 concrete beams (three beams per group) were produced. The beam moulds were prepared by applying oil and placing studs in referenced to the gauge length bar. The specimens were levelled on the top and were compacted as per AS 1012.13:2015. Figure 1 shows different preparation stages of the specimens. As shown in Table 1, the specimens were either normally cured or steam cured. Additionally, concrete cylinders were prepared and cured in the same conditions as the beam specimens for compressive testing. The curing processes are discussed below:

A. Normal curing process:
The specimens were left in a controlled environment at 20°C for 24 hours before demoulding. After demoulding the samples were then placed into a controlled water bath for five days at 20°C. On day 5 the beam samples were plastic wrapped to prevent moisture loss and sent to a testing facility.

B. Steam curing process:
The specimens remained in a controlled environment at 20°C for 2 hours. They were then placed inside the steam chamber with the temperature rising at the rate of 20°C per hour. When the chamber reached 60°C, the temperature remained constant for a period of 6 hours. After that the specimens cooled at the rate of 20°C per hour to and temperature of 20°C where they were kept for 12 hours. The samples were then demoulded and stored in a water curing tank for 5 days at 20°C. On day 5 the beam samples were plastic wrapped same as the normally cured specimens and sent to a testing facility.

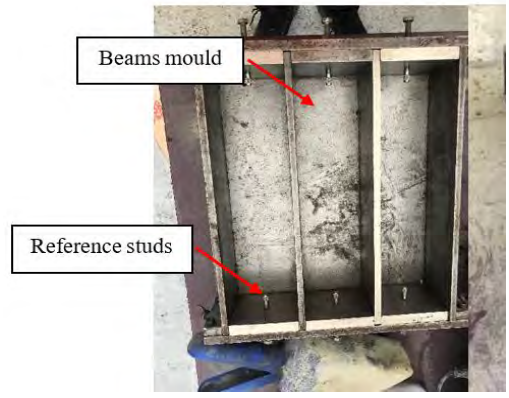

a) Casting the test beams

b) Curing in controlled water bath

c) Steam curing

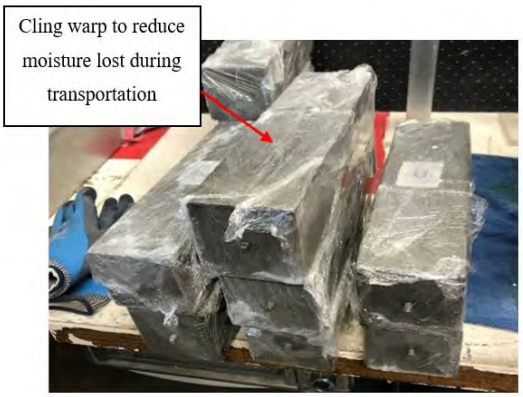

d) plastic wrapped prior to transportation

Figure 1. Preparation of concrete test specimens

Test Setup

The shrinkage test was conducted according to AS 1012.13: 2015 and the shrinkage was measured in 14, 21, 28 and 56 days. Before any measurement, the shrinkage measuring apparatus was required to recalibrated with the reference bar. The beam specimens were marked to identify the top end and were cleaned on both ends to remove the dust particles. The beam samples were then placed in the measuring apparatus with the top end against the dial gauge (Figure 2) to record the sample length measurement.

a) compressive test

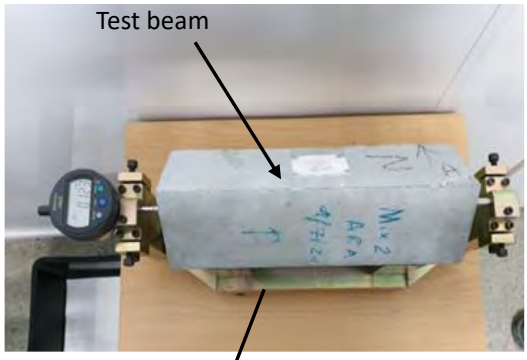

b) shrinkage test

Figure 2. Test setup

TEST RESULTS AND DISCUSSIONS

Shrinkage Test Results

The average shrinkage values between three test results for each group were calculated. The shrinkage measurements were undertaken on days 14, 21, 28 and 56. Figure 3 demonstrates the shrinkage results obtained from the tests. To better clarify the findings, the results are shown in three graphs (Figures 3 (a) to 3 (c)). Figure 3 (a) compares the shrinkage rate and values between normally cured and steam cured concrete samples. It can be observed that there are about 40% difference between shrinkage of normally cured and steam cured samples at 28 days. However, the difference is reduced to about 8% at 56 days.

Figure 3 (b) compares the shrinkage between the two steam cured samples (Group 2 vs Group 4). It can be observed that there are about 47% difference between shrinkage of steam cured samples with and without shrinkage reducing admixture at 28 days. The rate of shrinkage for both groups stay almost the same over time showing 46% difference between two groups at 56 days. Figure 3 (c) compares the shrinkage results between three normally cured groups with different admixtures. The mix with the accelerator (Group 5) does not show any significant difference compared to the normal mix (Group 1) in terms of shrinkage rate and final magnitude. The mix with the shrinkage reducer shows about 23% lower shrinkage at 28 days which eventually increased to 58% difference at 56 days.

Compressive Test Results

The compressive test results after 7 days and 28 days are presented in Figure 4. As shown in this figure there is no significant increase in compressive strength between day 7 and day 28 for the steam cured samples. This can be explained by rapid initial hydration and high temperature during steam curing. However, for the normally cured samples the strength development is a normal strength development for a HE-type cement where the 7-day strengths are in the region of 85% of the 28-day strengths.

In average, the 28-day strength of the steam cured, and normally cured samples are 61.5 MPa and 67.5 MPa respectively which means the 28-day strength of the steam cured samples is about 10% lower than normally cured samples. This is consistent with the relevant literature such as Yazdani et al. 2010.

Comparing the obtained compressive test results with the shrinkage behaviour, for the mix designs and curing conditions studied here, it is evident that the shrinkage of the elements is not necessarily correlated with the strength development as there was a significant amount of shrinkage that occurred in the accelerated samples after they had achieved their 24-hour strength which would indicate that the shrinkage is predominantly due to drying of the element.

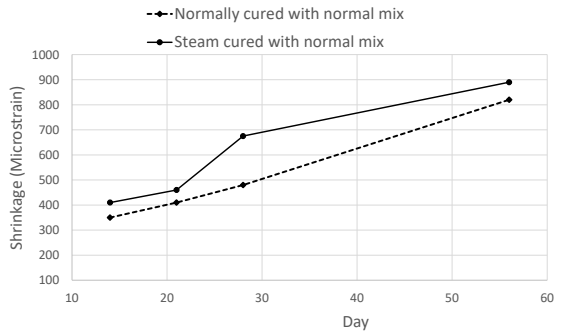

a) Effect of steam curing on shrinkage

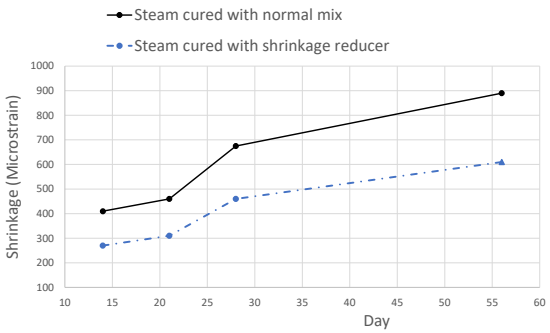

b) Effect of shrinkage reducing admixture on shrinkage of samples that were steam cured

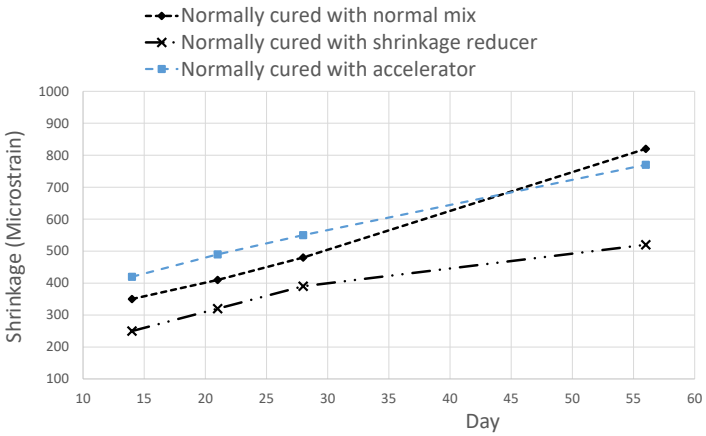

c) Effect of shrinkage reducer and accelerator admixtures on shrinkage

Figure 3. Shrinkage test results

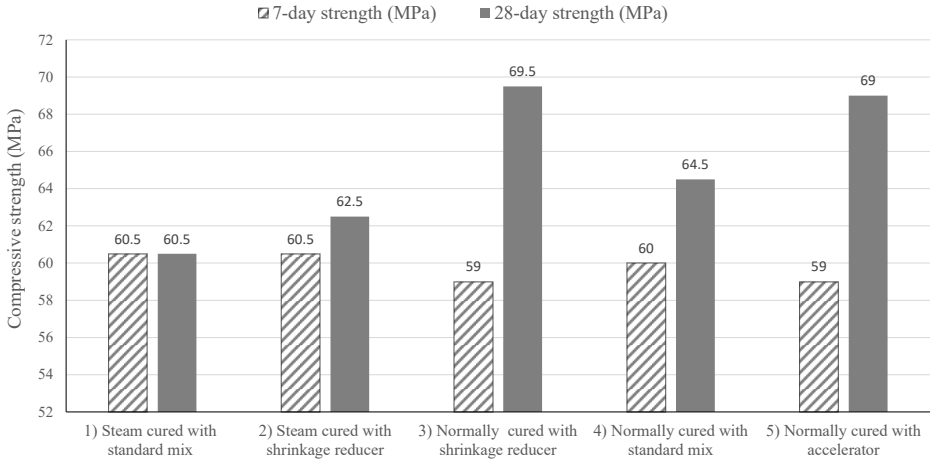

Figure 4. Compressive test results

CONCLUSIONS

The magnitude and rate of concrete drying shrinkage and compressive strength in five groups of high-strength concrete samples were compared. Below is summary of the main findings:

- Steam curing showed a significant effect on the shrinkage at 28 days (40% increase in shrinkage) compared to normal curing; however, the difference reduced over time. The shrinkage magnitude at 56 days is close to the samples that were normally cured (only 8% higher).

- The shrinkage reducer admixture showed a significant effect on the shrinkage values as expected (about 50% reduction in shrinkage magnitude at 56 days). The accelerator admixture did not show any considerable effect on the shrinkage behaviour

- The steam cured samples showed lower strength gain over time compared to normally cured samples. In average, the 28-day strength of the steam cured samples were 10% lower than normally cured samples.

It should be noted that the experiments in this study were conducted on specific mix designs and curing conditions and thus are not necessarily applicable to other concrete types and applications.

ACKNOWLEDGEMENTS
The authors would like to acknowledge the lab technicians who helped with the samples preparations and test setup.

REFERENCES

ACI Committee 517.2 Report (1992). “Accelerated Curing of Concrete at Atmospheric Pressure – State of the Art”. *ACI Manual of Concrete Practice*. American Concrete Institute, Farmington Hills, MI.

AS 1012.13 (2015). “Methods of testing concrete - Method 13: Determination of the drying shrinkage of concrete for samples prepared in the field or in the laboratory”. Standards Australia.

Bouziadi, F., Boulekbache, B., & Hamrat, M. (2016). ” The effects of fibres on the shrinkage of high-strength concrete under various curing temperatures”. *Construction and Building Materials*, Vol.114, July, pp.40-48.

Combrinck, R., & Boshoff, W. P. (2009). ”Plastic Shrinkage Cracking of Fresh Concrete”. Stellenbosch University.

Ekolu S.O (2006). “Heat curing practice in concrete precasting technology - problems and future directions”. 939 Concrete Beton, *Journal of the Concrete Society of Southern Africa*, 114, 5-10.

Han, X.; Fu, H.; Li, G.; Tian, L.; Pan, C.; Chen, C. ;Wang, P (2021). “Volume Deformation of Steam-Cured Concrete with Slag during and after Steam Curing”. *Materials*, 14, 1647.

Ian Gilbert R., Castel A., Khan I., South W., Mohammadi J. (2018). “An Experimental Study of Autogenous and Drying Shrinkage”. In: Hordijk D., Luković M. (eds) High Tech Concrete: Where Technology and Engineering Meet. Springer, Cham. https://doi.org/10.1007/978-3-319-59471-2_5

Long, G., Wang, M., Xie, Y., & Ma, K., (2014). ”Experimental Investigation on Dynamic Mechanical Characteristics and Microstructure of Steam-Cured Concrete”. *Science China Technological Sciences*, Vol. 57(10), October, pp.1902-1908.

Lura, P., van Breugel, K., & Maruyama, I., (2001). ”Effect of Curing Temperature and Type of Cement on Early-Age Shrinkage of High-Performance Concrete”. *Cement and Concrete Research*, Vol.31(12), June, pp.1867-1872.

Nguyen, D., Zhang, Y., Chilwesa, M., Castel, A., South, W., (2019). “Concrete Drying Shrinkage–Test Methods and Specifications in Australia”. Concrete 2019, Concrete Institute of Australia's Biennial National Conference, Sydney, Australia.

NZS 3112 (1982). " Methods of test for concrete”. Standards New Zealand, Wellington, NZ

Ramezanianpour, A. M., Esmaeili, K., Ghahari, S. A., & Ramezanianpour, A. A., (2014). ”Influence of Initial Steam Curing and Different Types of Mineral Additives on Mechanical and Durability Properties of Self-Compacting Concrete”. Construction and Building Materials, Vol.73, September, pp.187-194.

Shelton, R.H, 2015. Revisiting concrete ground floor slabs, Study Report SR340SR340. Building Research Association of New Zealand, Judgeford, New Zealand.

Yazdani N, Filsaime, M., and Manzur, T., (2010). “Effect of Steam Curing on Shrinkage of Concrete Piles with Silica Fume”. Second International Conference on Sustainable Construction Materials and Technologies, Italy.

concretenz BUILDING RESILIENCE
CONFERENCE 2022
13-15 October 2022
Energy Events Centre | Rotorua

PIONEERING A NEW WAY OF BUILDING BRIDGE PIERS

HUGO JACKSON[1] / ALISON CRAIGIE[2]

[1] Project Manager Fulton Hogan Civil, Auckland, New Zealand
[2] Project Engineer Fulton Hogan Civil, Auckland, New Zealand

SUMMARY

This paper outlines a new way of constructing bridge piers in the marine environment. This method was developed and successfully used to construct the piers of the new Panmure Busway Bridge as part of Auckland's AMETI Busway Project.

INTRODUCTION

The Panmure Busway Bridge is a new busway, cycling and walking bridge across the Tamaki Estuary, alongside the existing Panmure Bridge. The new bridge consists of a composite superstructure supported on two reinforced concrete, piled piers in the water and a piled abutment on either bank. The bridge is a Beca design for Auckland Transport.

The Fulton Hogan tender team faced two main issues in developing a construction methodology for pricing. These were the best method to construct the two piers in the Tamaki Estuary and how the superstructure could safely be erected.

The length and weight of the steel beams of the superstructure were near the maximum capacity of cranes available in NZ and positioning these in the river would have required extremely heavy duty staging or the importation of very large barges. Historic structures and Archaeological issues limited the locations where temporary staging could be installed. For these reasons the superstructure was assembled on the Eastern bank and pushed to the West using an incremental launch procedure.

The construction of the two marine piers was complicated by their large size, their position in the tidal range and Resource Consent conditions that prevented the construction of sheet piled, dewatered cofferdams. A floating cofferdam (boat) that could be piled through and which would act as the formwork of the pile cap was developed as the solution.

The size and weight of the pile cap boat was such that it couldn't be lifted with cranes and so an innovative construction and launch procedure was developed.

Each pier consists of 8 number 1.2 m diameter piles terminating at a 17 m x 7.5 m x 2.7 m deep concrete pile cap. Twin flared concrete piers are constructed from each pile cap to support the superstructure.

TEMPORARY ACCESS STAGING

Piling, pile cap and pier construction required heavy machinery in close proximity to each pier. The temporary access staging was installed along the bridge centreline, to support pier construction and then removed prior to superstructure launch.

The Eastern staging was installed at low level. The Western staging had to be accessed from the Mokoia pa headland, approx. 18 metres above the estuary level. This meant that this staging is thought to be the highest installed in NZ.

The temporary staging allowed safe access for an RT3, crane mounted drill rig and a 100 tonne crane which were required for the piling and to support pile cap and pier construction.

The crane mounted RT3 drill rig was preferred over “Soilmec” type rigs as it had greater reach that allowed all piles to be drilled from the end of the access staging.

TEMPORARY SUPPORT OF THE BOAT

The system required that the boat is flooded during piling and this necessitated the construction of a temporary support frame to support it until the loads could be transferred to the permanent piles.

The temporary support system consisted of 4 circular steel casings supporting a square grillage of steel beams and the boat was hung from this temporary support structure by 12 Macalloy bars.

This frame was constructed, prior to the boat launch with equipment working from the temporary access staging. As the piers were constructed sequentially, only one temporary support system was required and this was removed after construction of the first pier and reused at the second.

The temporary support system had provision for adjustment of the boats height and position. However, this capacity was not utilised as the boat was accurately located into the support frame and no settlement occurred after load transfer or during the piling operations.

BOAT CONSTRUCTION

The tender concept of a concrete bottomed and concrete sided boat was discarded and replaced by a steel sided and concrete bottomed boat. This was largely driven by delays in producing and signing off the Construction Management plans required for work to commence at site. By adopting the steel sides their construction could commence off site and this avoided project delays.

The steel sides and hatch components were constructed at Hornell Industries site in Waiuku.

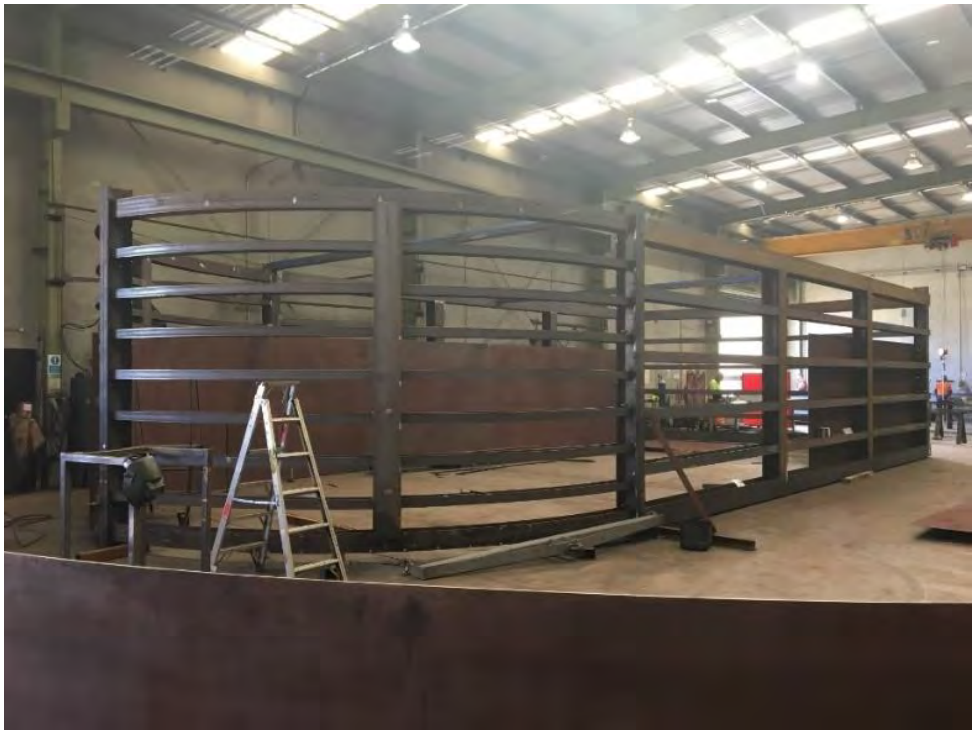

Figure 1: Boat being constructed at Hornell Industries

The steel sides were designed with 5 vertical bolted joints for ease of handling. As the steel sides would be removed and reused for the second pier the construction team chose to paint the steel sides, for longevity and to ensure a high quality finish to the sides of the concrete pile caps.

The top of the pile cap coincided with a normal full tide. To prevent engulfment during construction the sides were made over height to include allowance for waves and exceptional tides. The steel sides were heavily stiffened to avoid external water and internal concrete pressure. In addition an arrangement of ties and props was installed at the top of the boat to limit deflections.

The boats were constructed on a disused boat ramp within the site.

The steel sides were erected, bolted together at the 5 vertical joints around the perimeter and sealed, watertight. The 8 prefabricated steel hatches were lifted in and placed at the pile locations. The steel reinforcing was then tied and the base poured.

The connection between the sides and base consisted of a double row or bolts through the steel sides and terminating in the concrete base. This system in conjunction with a gunned sealant applied to the steel sides, prior to the concrete pour, provided a fully watertight and durable seal.

The completed boats weighed in excess of 120 tonnes and it was not possible to position cranes of adequate size in a position where the completed boats could be lifted into the water. A single double acting hydraulic ram was used to push the completed boat down the inclined ramp and into the water. This ram reacted between the boat and a temporary pile, installed at the top of the ramp, via a Megashor prop. As the ram stroke was only 300 mm the launching process was in small increments with a series of plates or sections of Megashor.

prop being added with each stroke of the ram. Despite the small stroke the launch team developed a rhythm and the process was completed in two days.

Figure 2: Boat being slid down ramp using hydraulic ram

Ram forces varied but were generally around 50 tonne which corresponds to a friction factor of 0.4.

Figure 3: Boat Launched and secured prior to tug arrival.

Once the boat had been pushed down the ramp, a tug was used to direct the boat into the temporary support frame.

Launch and hanging operations had to be aligned with the tidal cycle so that the boat could be launched at high tide, positioned into the lifting frame at mid tide and fully hung and flooded by low tide. A concern was that failure to flood the boat would allow it to rise with the incoming tide and lift the support frame from the temporary piles.

Flooding, after hanging of the boat, could have been undertaken by opening the two valves cast into the floor. However, this was not required as the team were able to remove all 8 bolted hatch covers, after hanging and before the tide rose above the hatch covers.

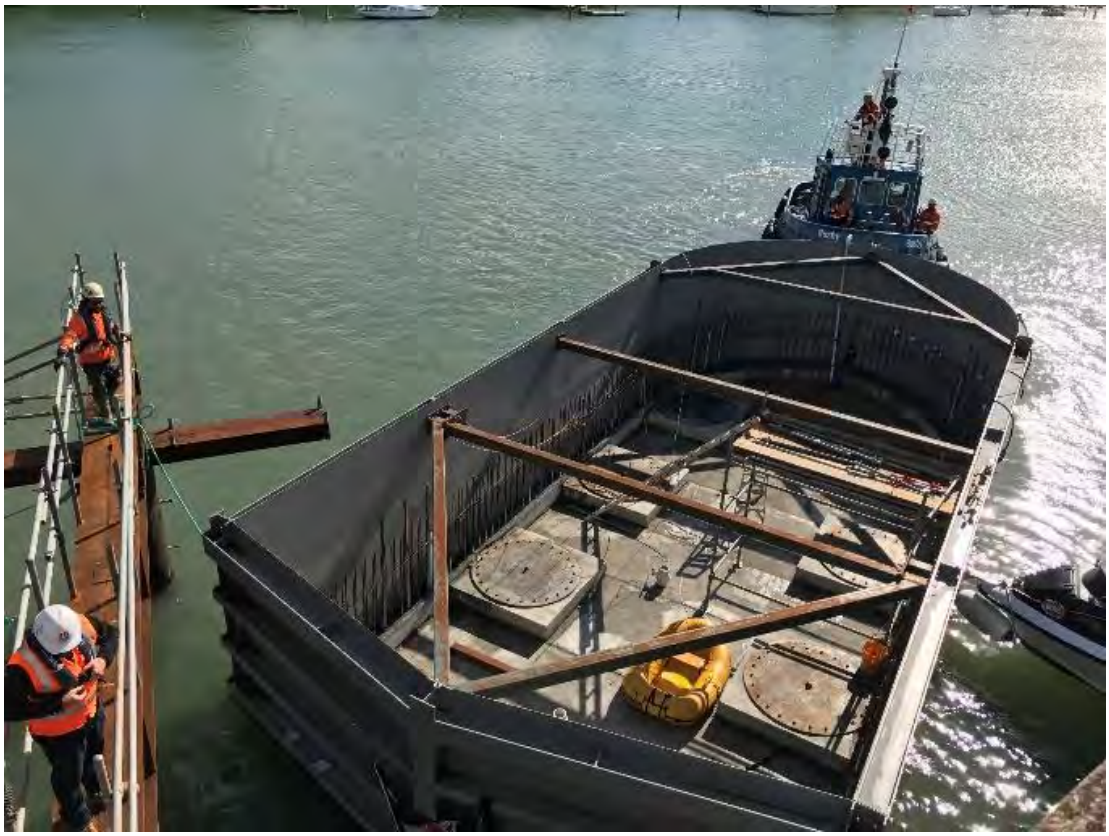

Figure 4: Boat being pushed into support frame

At this stage the boat was secure, hung from the temporary support frame and would flood and empty with each tide, through the open hatches.

PILING

The pier piles consisted of permanent steel casings driven to East Coast Bays formation rock and then bored out and concrete filled.

Casings were vibrated to depth with a crane slung vibro hammer and then the rotary drilling table was used to excavate the spoil and drill the 13 m rock socket.

The reinforcing cages were assembled in pre-tied segments, due to the depth of the piles and the length of boom rigged the reinforcing cages were not installed in a full length and were spliced in position. The piles were poured using a boom pump and tremie.

Figure 5: Piling through the Boat, from staging

SECURING AND DEWATERING THE BOAT

A primary objective of this system is to create an all tide dry area where the pile caps can be constructed and this requires that the boat is structurally connected to the piles and for this connection to be watertight.

This connection consisted of circular steel plates bolted to the hatch inserts and welded to the pile casings. These were constructed from the original hatch covers and each had the central hole cut out, to match the final pile position within the slightly oversize hatch. In order to ensure correct fit, the relationship between each pile to its hatch were measured at low tide, and the holes cut to these measurements. The covers were also split into two halves to make fitting easier.

A weld preparation bevel was also cut into the connection plates at the same time as the circular hole was cut.

A particularly low tide was chosen to fit and seal the connection between the piles and the hatches. On a falling tide near the low tide the boat had drained to a point where the connection plates could be bolted to the hatches.

For the first boat a team of 4 welders made the weld connection between the plates and the casings and they were able to install the sealing pass during the low tide. They continued to weld as the tide rose and had sealed and structurally welded all connections by the time the water rose to a point where the boat would have floated. These initial welds proved capable of resisting the full buoyancy forces that occurred at full tide. The following day additional weld material was added to strengthen the joint, to resist the design condition, of the boat full of wet concrete at low tide, which occurs during the pile cap pour. Tides were less favourable for the second boat and three tidal cycles were required to complete the seal welds.

Figure 6: Welding of pile to hatch connections

The stage, during construction, where the connection between the pile casing and the boat hatches is made has some flexibility. The connection could be made after driving of the casing but before drilling and concreting of the piles. If this choice is made then there is a risk that the floatation forces may dislodge the casing. There is also a risk that a casing may have to be further advanced if weak strata are encountered during rotary drilling. This is much more difficult after the connection has been made.

To avoid these risks and to provide continuity to the piling team a choice was made to delay making this connection until after all the piling had been completed. This required that the over-poured concrete which had set in the casings had to be manually broken back after the connection had been made and the excess casing cut away.

After the boat had been sealed and the piles broken back we had a completely dry environment where we could tie the reinforcing for the pile cap, at all stages of the tide.

As the welded connection was of sufficient capacity to resist the loads from the pile cap pour, the exterior temporary support frame was removed at this stage.

Reinforcing was lifted into the boat and tied into cages insitu.

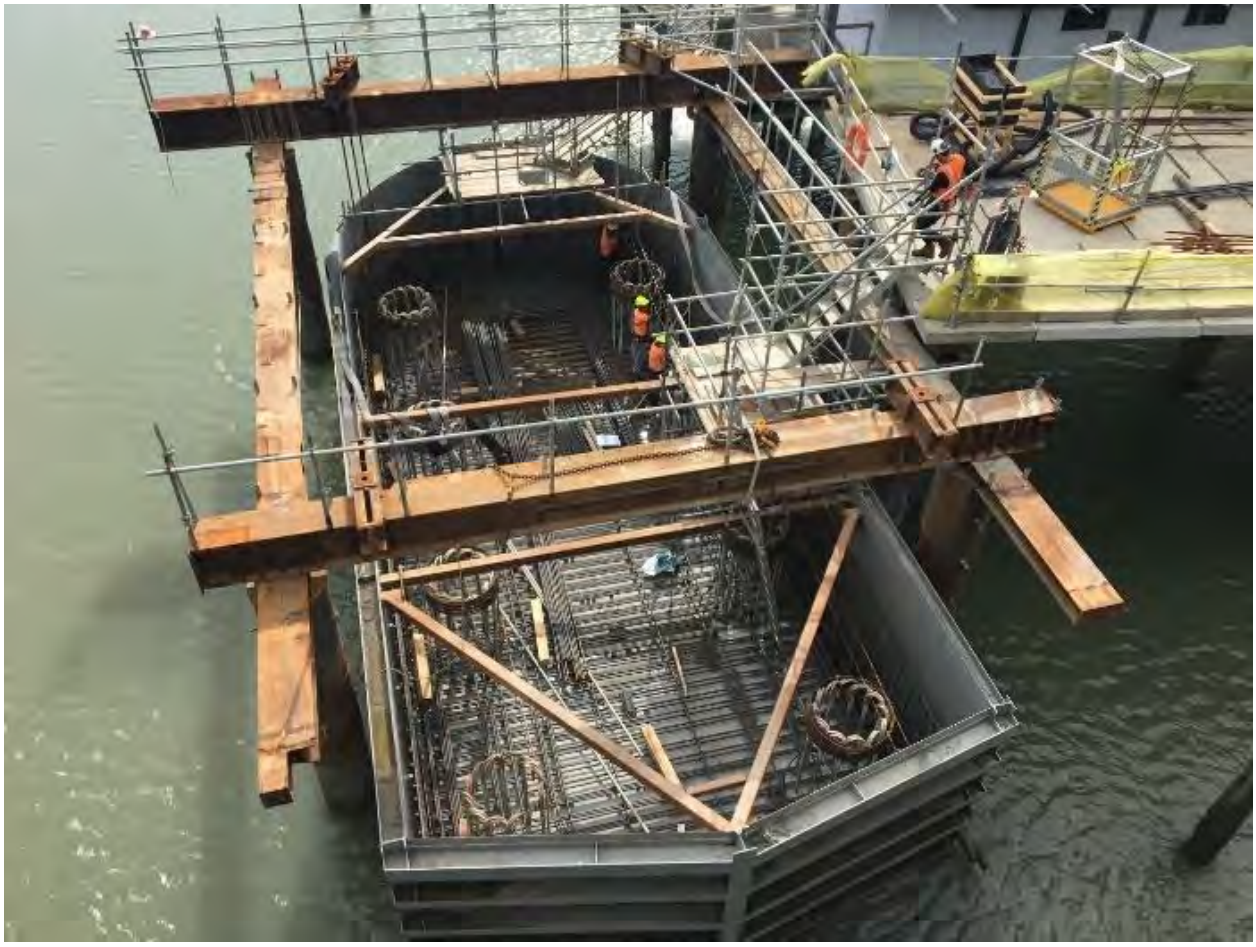

Figure 7 Boat hung and sealed with pile cap reinforcing being installed.

The pile caps were poured utilising a boom pump located at the end of the temporary staging. Agitator trucks drove on and off the staging to feed the pump. Rate of pour had to be controlled to prevent excessive pressures developing on the boat sides.

Heat of hydration was a concern and we worked with our supplier to design and trial a mix to limit development of heat.

PIER CONSTRUCTION

The twin piers were constructed, cast insitu utilising reusable steel forms.

As the top of the pile cap and the base of the piers was below high tide level we delayed removing the steel sides of the boats until after the piers had been poured.

Figure 8 Pier columns cast and the boat stripped.

STRIPPING THE BOAT

Divers were used to remove the bolts that connected the steel sides of the boat to the concrete base and also to remove the bolts between the 5 segments of the sides.

The sides were then individually removed and craned back to the boat ramp for reuse at the second pier.

These were then bolted back together and the process repeated.

After construction of the second pier the flat sides of the boat were repurposed and utilised as flat panel precast beds. The bow and stern sections, being of unusual shape had to be scrapped.

CONCLUSIONS

The methodology developed for this project proved successful in practice.

The benefits to the project were economic as work could be undertaken at all stages of the tide, reducing down time and shortening the programme. The dry environment also allowed the pile caps to be constructed with increased safety. The quality of work performed in this environment was enhanced and was easy for the supervising engineers to inspect.

Performing the piling within the boat sides lead to better containment of drill spoil and improved containment of cement products.

Another benefit was that the boat could be constructed offline and in conjunction with construction of the access staging.

An enhanced method is the preferred methodology for marine pier construction for the Waitemata Harbour Crossing section of the Northern Pathway Project.

REFERENCES

ACKNOWLEDGEMENTS

Nick Bamford, Bamford Consultants.

Hamish Stanaway, Stanaway Marine Services.

Clint Hornell,Hornell Industries.

concretenz BUILDING RESILIENCE
CONFERENCE 2022
13-15 October 2022
Energy Events Centre | Rotorua

LOW DAMAGE ROCKING CONCRETE WALL STRUCTURES WITH RESILIENT HOLD-DOWNS AND NO POST-TENSIONING: APPLICATIONS, STIFFNESS AND CASE STUDY

ASHKAN HASHEMI[1], CHRIS WALLINGTON[2], NICHOLAS CHAN[3], SAMIR GOVIND[4], RICK HENRY[5], POUYAN ZARNANI[6], PIERRE QUENNEVILLE[7]

[1] Lecturer, The University of Auckland, Auckland, New Zealand
[2] Associate, Beca, Christchurch, New Zealand
[3] PhD Student, The University of Auckland, Auckland, New Zealand
[4] Technical Director, Beca, Christchurch, New Zealand
[5] Senior Lecturer, The University of Auckland, Auckland, New Zealand
[6] Lecturer, Auckland University of Technology, Auckland, New Zealand
[7] Professor, The University of Auckland, Auckland, New Zealand

SUMMARY

Rocking concrete walls are strong, stiff and reliable lateral-load resisting elements that can minimise damage and reduce response drifts during seismic events. Conventional low damage rocking concrete walls typically use unbonded Post-tensioned (PT) elements to control the inelastic demand and increase the walls' moment capacity. This paper presents a new generation of rocking concrete walls that can provide a low damage performance by using resilient seismic devices at the base of the walls as hold-down connectors. These connections provide a flag-shaped hysteresis and a self-centring behaviour. The PT elements are removed from the system to add to the simplicity while providing similar performance. The key performance advantages of this system are described and discussed in the paper. While there have been numerous researches on the stiffness of rocking concrete walls with PT elements, there is a knowledge gap for the wall systems without PT elements. This paper provides insights on the stiffness of these walls based on the numerical studies carried out. Lastly, a case study project in Christchurch, New Zealand, is presented where the introduced system is adopted. This structure is a three-storey IL3 building designed by Beca and is one of the first projects where rocking concrete walls with resilient hold-downs are used.

INTRODUCTION

A controlled level of ductile damage to concrete structures was perceived as an improvement over brittle collapse, thereby meeting the life safety objective. However, the associated economic losses remained substantial in various earthquakes around the world (Rodgers et al. 2016). This has resulted in greater societal demand for the next generation of structures to be built/rebuilt to withstand minimal damage and disruption (Bruneau and MacRae 2017).

There is an increasing number of low-damage concepts for both structural and non-structural systems (Pampanin 2015). The rocking concrete wall is one such system, as shown in Figure 1 (Darani et al. 2018; Shannon et al. 2019). Various types of supplemental damping devices can be incorporated to dissipate seismic energy. They are often compact mechanical devices adjoining the structural members. As 'fuses', they activate at extreme loads to limit the forces sustained in the structural members. This paper provides some insights on the stiffness of such

systems, introduces a resilient connection system and presents a case study where the technology is implemented.

Figure 1. Supplemental damping devices in rocking wall systems, such as (a) hold-downs at rocking toes, and (b) shear links at boundary columns.

Rocking wall systems using RC panels can take advantage of the high stiffness to resist overturning moments and provide an even distribution of storey drifts, thereby avoiding soft-storey mechanisms (Grigorian and Grigorian 2016). In contrast to cast-in-place walls, the panel is usually designed for smaller deformation and is not intended to sustain significant damage. There are two reasons why it is inappropriate to use the first yield stiffness derived for cast-in-place walls for rocking walls:

1. In rocking systems with supplemental damping devices, the links have become the source of ductility. So, the RC walls are usually capacity-designed not to yield even at the ultimate limit state.
2. Unlike cast-in-place walls, wall panels in rocking systems are unbonded to the foundation, and this difference in boundary conditions leads to different behaviour.

Twigden et al. (Twigden et al. 2017) obtained effective stiffness values I_{eff}/I_g from 0.61 to 0.79 from testing post-tensioned rocking concrete walls with aspect ratios of 3 and 3.5. However, it is not clear whether this is the stiffness of the panel only or the stiffness of the whole system, which is influenced by the post-tensioning.

In this paper, an energy-based method is used to extract the shear and flexural deformations from the numerical simulations. It is based on the principle of virtual work, applied separately to the shear and flexural strain energies (Iyer 2005). The sample wall model is a 1.2 m by 2.4 m panel with corner cut-outs measuring 0.2 m by 0.4 m to accommodate the hold-down (Figure 2). The thickness is 200 mm throughout the panel. In these pushover analyses, only the hold-down working in tension is modelled because it accounts for almost all the moment resistance. In this preliminary analysis, only the linear behaviour is simulated as this is sufficient to obtain the effective stiffnesses up to the first yield. Table 1 shows the range of parameters used in these preliminary analyses.

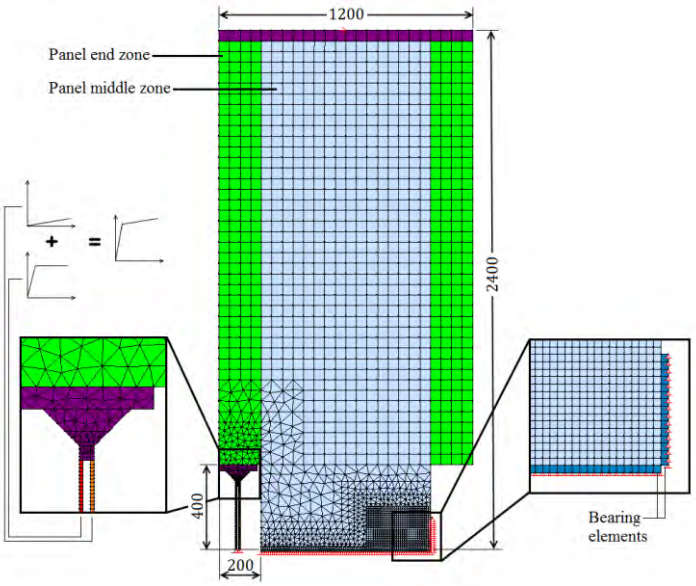

Figure 2. Numerical model of the rocking wall in VecTor2 (Wong et al. 2013).

Table 1. Parameters used in the rocking wall models.

Parameter	Symbol	Values
Longitudinal reinforcement in end zones	$\rho_{end,\ longitudinal}$	1%, 3%
Longitudinal reinforcement in middle zone	$\rho_{middle,\ longitudinal}$	1%, 3%
Transverse reinforcement in end zones	$\rho_{end,\ transverse}$	1%, 3%
Transverse reinforcement in middle zone	$\rho_{middle,\ transverse}$	= $\rho_{end,\ transverse}$
Stiffness of hold-down	$k_{hold\ down}$	200 kN/mm, 500 kN/mm
Concrete elastic modulus	E_c	26.4 GPa
Concrete shear modulus	G_c	11.5 GPa
Concrete compressive strength	f'_c	34.5 MPa
Reinforcement yield strength	f_y	345 MPa
Reinforcement ultimate strength	f_u	415 MPa
Wall width	b	1200 mm
Wall height	h	2400 mm
Wall thickness	t	200 mm

Figure 3 shows a typical pattern of cracking in the RC panel at first yield. Initial cracks appeared almost simultaneously at two locations: (a) horizontal/inclined cracks at the hold-down where large tensile forces occur, and (b) vertical cracks near the rocking toe where the panel uplifts and loses contact with the foundation. Figure 4 shows pushover curves for all the walls modelled. It appears that the flexibility of the hold-down contributes to a substantial portion of the overall displacement at the top. In real applications, the hold-down will become the main source of top displacement (ductility) once nonlinear behaviour commences, while the panel reinforcement remains within the elastic range.

The effective section properties are shown in Figure 5 up to the load at first yield. For the Ie/Ig plot, the lowest value is 0.40, and the highest value is 0.85. There are two visibly distinct bands of curves according to the longitudinal reinforcement ratios (1% and 3%) that determine the strength of the panel. In each band, one can observe a large effect from the stiffness of the hold-down, a moderate effect from the longitudinal reinforcement in the middle zone, and a minor effect from the transverse reinforcement ratio. As can be seen, Ie/Ig does not fall below 0.4 for all cases. This is because some of the deformations have been attributed to the shear component (Ae/Ag variable). By reducing the shear stiffness (by means of Ae/Ag) it allows larger values of the flexural stiffness (via larger Ie/Ig). If the shear and flexural deformations were not distinguished, then the lower bound of Ie/Ig would fall below 0.4.

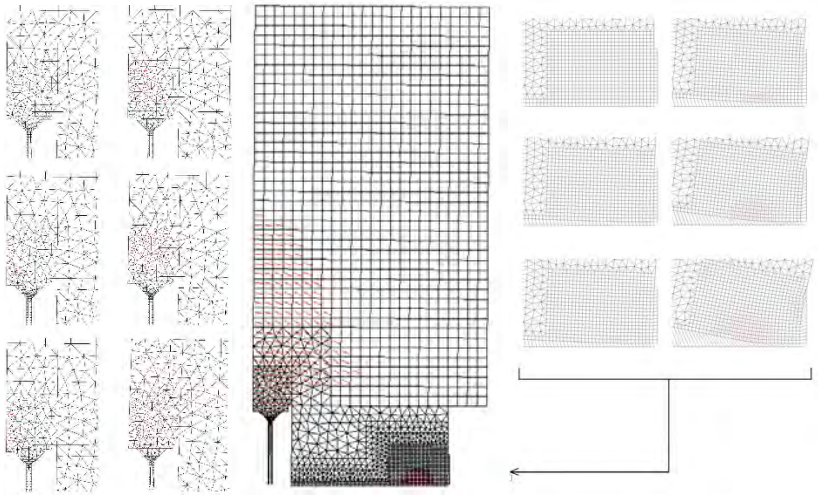

Figure 3. Typical cracking pattern in the reinforced concrete panel.

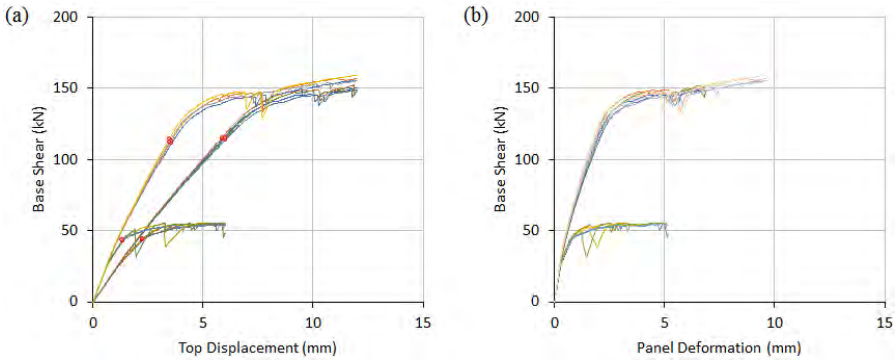

Figure 4. Pushover curves of the rocking walls where the x-axis shows the (a) total top displacement, (b) panel deformation. The red circles indicate the instances of first yield.

From the results, it appears that the stiffness of the hold-down plays an important role on both effective stiffnesses (Ie/Ig and Ae/Ag). This was explained by the increased rotation at the pivot that can lead to additional vertical cracks along the base. A possible remedy is to increase the amount of transverse reinforcement along the base only. If the extent of cracking/damage is reduced here, it may be possible to obtain a stiffer response from the panel. In addition, it may be necessary to investigate the effect of the foundation stiffness also. The degree of rotation and associated cracking at the pivot could very well depend on the relative stiffnesses of the vertical load-bearing elements (hold-down and bearing foundation).

Normalising the base shear by the load at first yield reveals that, for a given load ratio, higher stiffness modifiers are possible in walls with smaller reinforcement ratios. This is simply because these walls have smaller yield loads (but same cracking load) such that a larger proportion of the strength occurs in the uncracked state. For a given design load, this suggests that designing thicker walls with lower reinforcement ratios will produce the stiffest members, albeit with greater risk and reliance on the tensile strength of concrete. Effectively, this means that the RC panel would be designed as an elastic (uncracked) member as the role of the wall reverts from a weak link to a strong link. The potential to double the effective stiffness however (Ie/Ig and Ae/Ag) makes this worthy of further investigation.

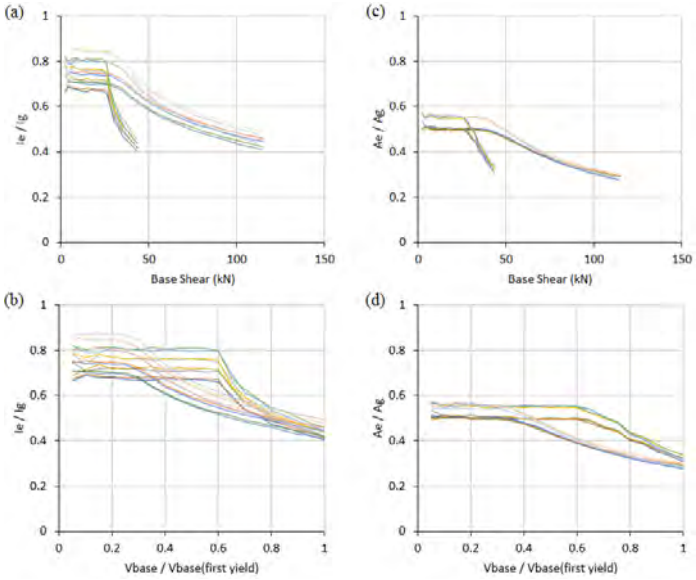

Figure 5. Effective section properties for (a, b) flexure, and (c, d) shear. Each curve ranges from 5% to 100% of the load at first yield.

The Resilient Slip Friction Joint for rocking RC walls

The Resilient Slip Friction Joint (RSFJ) technology was introduced in 2015 (Zarnani and Quenneville 2015). This device is a friction device that can dissipate the seismic energy and provide a re-centering behaviour with a flag-shaped hysteresis. Figure 6 depicts the configuration and the load-deformation relationship of the RSFJ. Similar to conventional friction joints, the RSFJ dissipates energy via the sliding movement of the clamped plates.

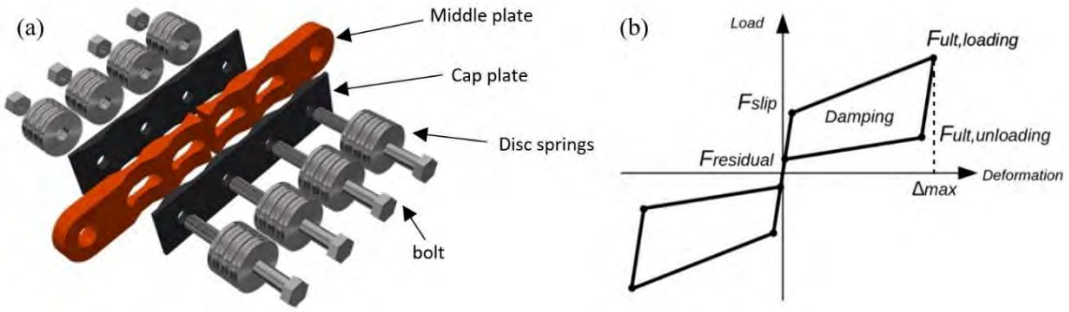

Figure 6: Resilient Slip Friction Joint (RSFJ): (a) configuration (b) hysteretic behavior

Figure 6(a) shows the assembly and different components of an RSFJ specimen. The hysteretic parameters (F_{slip}, $F_{ult,loading}$, $F_{ult,unloading}$, $F_{residual}$ and Δ_{max}) shown in the figure can be determined in accordance with the design requirements. The behaviour and performance of the RSFJ have previously been verified via joint component tests and large-scale experiments. Hashemi et al. experimentally tested full-scale rocking Cross Laminated Timber (CLT) (Hashemi et al. 2017) and Laminated Veneer Lumber (LVL) (Hashemi et al. 2020) walls with RSFJ hold-own connections. Bagheri et al. (Bagheri et al. 2020) tested steel tension-only braces with RSFJs and Yousef-Beik et al. (Yousef-Beik et al. 2019) investigated the performance of tension-compression braces with RSFJs.

The RSFJ Over-strength Mechanism

The RSFJ is designed in a way that all components remain elastic up to the design load (F_{ult} of the device). However, with the aim of collapse prevention in cases that the applied loads are higher than the design earthquake loads, an over-strength mechanism in the body of the RSFJ is considered. When the load on the RSFJ increases beyond its maximum capacity (F_{ult}), the clamping bolts (or rods) start to yield. Inelastic elongation of the bolts provides additional travel distance for the joint allowing it to maintain a ductile behaviour whilst bolts travel across the slotted holes in the RSFJ middle plate. With this mechanism activated, the maximum force will be 1.25 times higher than the design F_{ult}. So, the over-strength factor applicable for the RSFJ is a minimum 1.25 to maintain the hierarchy of strengths following the capacity design principles. An over-strength factor of 1.35 is usually recommended for the attachments and the main structural members.

Figure 7 shows an example of a secondary fuse test performed on an RSFJ configuration related to the case study described in this paper. The specified characteristics of this configuration (ULS) were $F_{ult,loading}$=375 kN at Δ_{ult}=60 mm displacement. As can be seen, the red dashed rectangle shows the hysteretic performance at the specified design values, and the green dashed rectangle demonstrates the over-strength performance. It can be seen that the capacity of the device increased to about 450 kN, corresponding to 1.2 times of the F_{ult}. Also, the device continued displacing to 100 mm, which is about 1.7 times the design level displacement. Therefore, The avaliable extra force and displacement provides additional capacity for events in excess of ULS. Nevertheless, this can be analysed and investigated for different case scenarios and for different structures.

Case- study: Lincoln University Sciences North project

The Sciences North project is a new flagship science building for Lincoln University. The project comprises a Teaching Building and Research Building, located adjacent to one another but separated by a seismic gap, as well as a standalone Ancillary Building. Refer to Figure 8 for an overview of the buildings. The Teaching Building includes teaching spaces and laboratories, whilst the Research Building houses research laboratories, offices, and collaboration spaces.

The lateral system for the Research Building initially included concrete shear walls and steel concentrically braced frames (CBFs) in the transverse and longitudinal directions, respectively (refer Figure 9). The primary driver for introducing shear walls and CBFs was to provide a stiff lateral structure that limited interstorey drifts. CBFs were positioned on three bracing lines, the northern and southern elevations, and a central gridline in the middle of the building. CBFs are an efficient structural lateral system and were considered well integrated to the architecture on the perimeter of the building and at the interface between the laboratories and offices. Six shear walls were positioned on four bracing lines. Four of these walls were integrated into the laboratories, located on either side of a central corridor and one bay in from each end of the laboratory. The advantage of bringing the shear walls in one bay from the ends of the building allows for additional gravity loading to counteract uplift forces at the ends of the walls. Although the research laboratories were heavily serviced, the chosen shear wall arrangement kept the central corridor free of vertical structure.

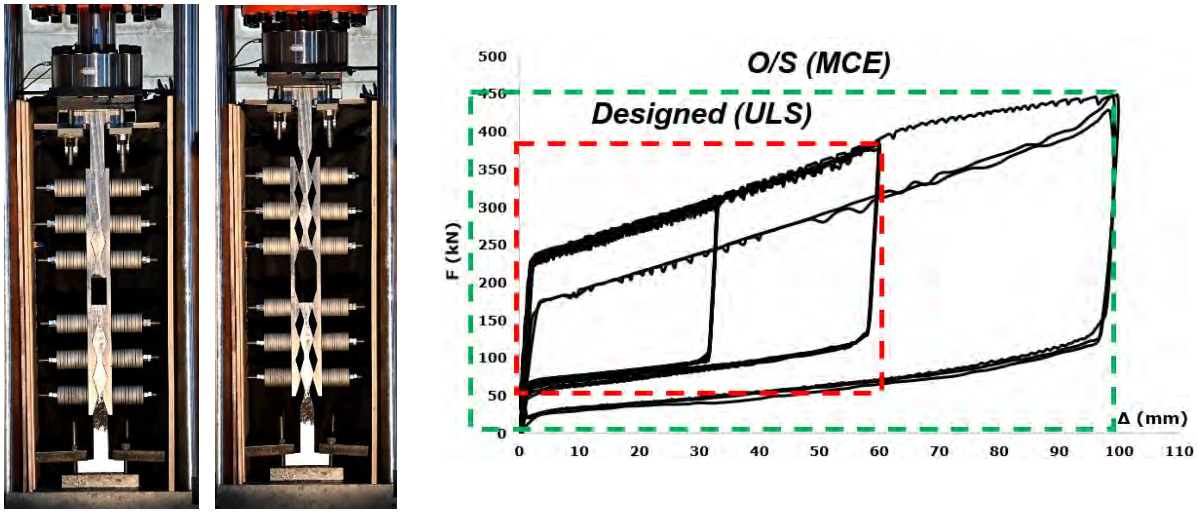

(a) (b) (c)

Figure 7. RSFJ over-strength testing: (a) the damper at rest (b) the damper at maximum displacement (c) test results

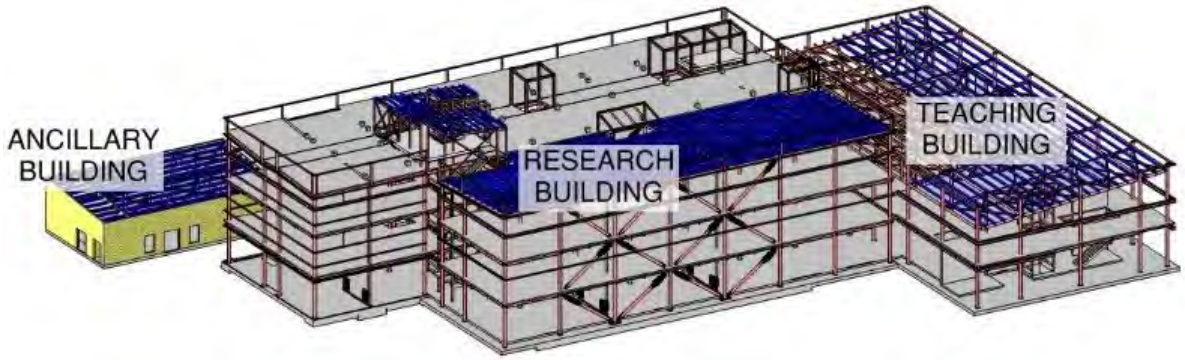

Figure 8. Sciences North building layout

The two remaining walls were placed in the offices with even distribution to those in the laboratory. The walls are between 5.15 m to 5.85 m long, 300 mm thick, and three storeys high with no construction joints along their height. Refer to Figure 10 for an elevation of the shear walls. During concept design, Resilient Slip Friction Joints (RSFJs) were suggested to be implemented at the ends of shear walls and at one end of braces in the CBF direction.

The intention was to concentrate energy dissipation at the RSFJs and design the remaining building elements and connections for the corresponding building movements to avoid structural damage up to an Ultimate Limit State (ULS) event. The RSFJ devices could also be designed to limit device movements so that interstorey drifts could remain limited. An added advantage of shear walls with RSFJs is that large in-plane stiffness of the shear walls means they act as a stiff backbone and promote movement in the RSFJ devices. RSFJ devices were not considered appropriate for the Teaching and Ancillary buildings, given various attributes of these buildings.

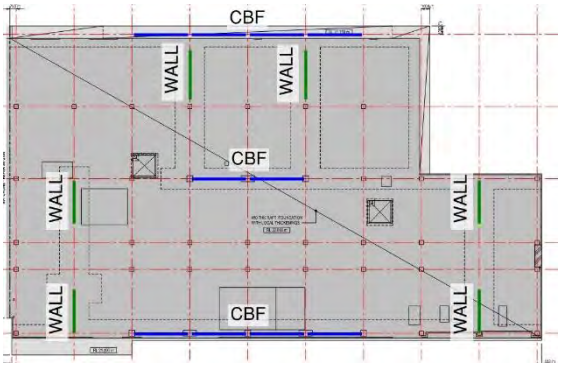

Figure 9 – Research Building lateral load resisting system

Figure 10 –Section across building showing shear walls

Rocking Walls Design and Detailing

The shear walls were modelled in the structural analysis software as shell elements. Each shear wall was modelled with notches at the base to allow for the RSFJ devices. The design required 4-1250kN devices at each end of each shear wall. The devices were modelled as a single link element, with compression-only springs at the base of the wall adjacent to the devices, and lateral restraints provided at the middle of the wall as the shear key.

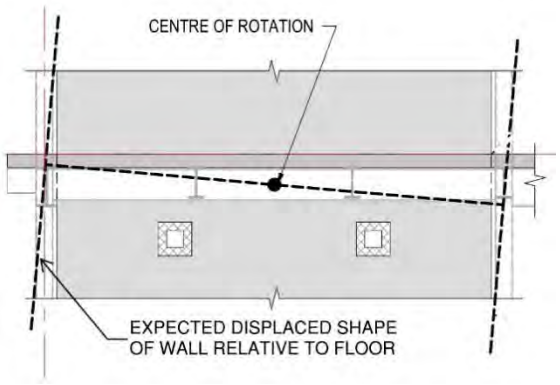

Figure 11 – Expected wall movement

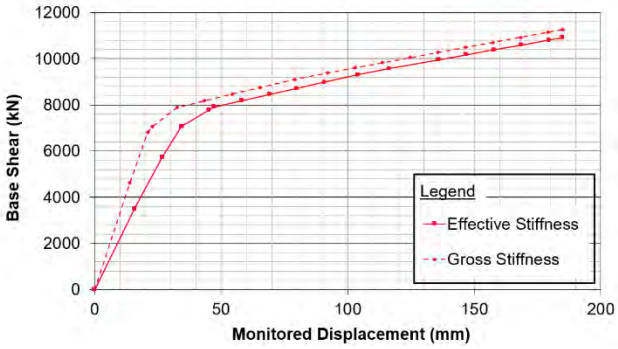

Figure 12 – Shear wall pushover curves using gross (dashed line) and effective (solid line) stiffness

Differential movement can cause damage at the interface of suspended slabs and rocking walls, as indicated in Figure 11. To avoid damage at this location, it was decided to detach the slabs from the walls. This approach required providing gravity columns at either end of the shear walls to support the floor at the walls. Vertical loading on the wall in the seismic load combinations provides additional moment capacity to the shear walls. As the slabs were detached from the walls, only the weight of the wall was considered in the lateral analysis.

At ULS loading it was calculated that the flexural demand in the shear walls exceeded the cracking moment capacity. Thus, indicating that the flexural stiffness of the walls should be reduced to allow for the effect of cracking. NZS 3103 Table C6.5 suggests an effective section property of 0.25 x Ig for a wall at ULS with low axial load and Grade 500 reinforcement. Applying an effective stiffness of 0.25 x Ig up the height of the wall was considered overly conservative as this underestimated the flexural stiffness of the walls at higher levels. NZS 3101 gives a calculation method for determining the effective stiffness for a beam based on moment demand and section properties. Applying this method for the shear walls allowed for the effective stiffness to be calculated up the height of the walls. The adopted values were

between 0.3 and 1.0 as a proportion of gross stiffness. The pushover analysis using gross and effective section properties predicted displacements of 33mm and 47mm at slipping of the RSFJ devices, refer to Figure 12. The difference of 14 mm was maintained beyond the slipping of the devices. This behaviour infers that the SLS performance was somewhat affected by the wall stiffness, but ULS performance was largely influenced by the performance of the RSFJs and not by the stiffness of the shear walls.

Foundations

The Research Building foundations comprise of typically a 450mm thick raft with 800-1200mm deep thickenings under the shear walls and CBFs. The thickenings typically join at intersections between bracing lines. A separate analysis model was created for the foundations. Point reactions were imported from the superstructure analysis model. The structural foundation model was aligned with the geotechnical model by determining the appropriate soil springs so that foundation deformations were comparable between the structural and geotechnical models. A sensitivity study was done on the upper and lower bound soil springs to determine the foundation design actions.

The overall building drift is a function of the superstructure and substructure (foundation and soil) movements. In the shear wall direction, rotation of the foundations at the base of the shear walls was found to contribute approximately 20% to the overall building drift. The additional drift from the foundations arises from soil settlement at the compression wall end and hogging of the foundation at the tension wall end. The rotation at the base of the wall was estimated from predicted displacements at the nodes at base of the walls over the corresponding length. The foundation rotations were reduced by detailing a common thickening between the shear walls (effectively adding a coupling element between the walls), enlarging the thickening at the toe of some walls to better distribute localised loading, and adding extensions around the perimeter foundation to increase resistance to overturning (which also reduced local bearing pressures). Refer to Figure 13 & 14 for plans showing these foundation details.

Connection Design

As described previously, the suspended slabs were detailed so that they weren't directly connected to the walls. This avoided the slab needing to accommodate differential movement at the ends of the walls which were expected to lift upwards by up to 60mm. To transfer lateral loads to the shear walls a pair of custom welded parallel flange channels are provided either side of the shear walls. Shear studs connect the suspended slab to the wall and the CWPFC is connected to the wall with six M36 threaded rods in vertically slotted holes, refer to Figure 15. The bolt spacing was minimised to reduce the distance to each bolt from the centroid of the bolt group. From the expected rotation at the bolt group, it was possible to predict the expected bolt positions. The movements were determined to be <3mm, which was considered not to impose any excessive demands on the bolts given the slotted hole geometry.

A shear key (refer to Figure 16) was required at the base of each shear wall to transfer lateral loading at the base of the wall to the foundations, whilst also allowing for movement of the wall. It was not considered practical to have a reinforced concrete extension of the shear wall into a pocket, given tolerance and strength requirements.

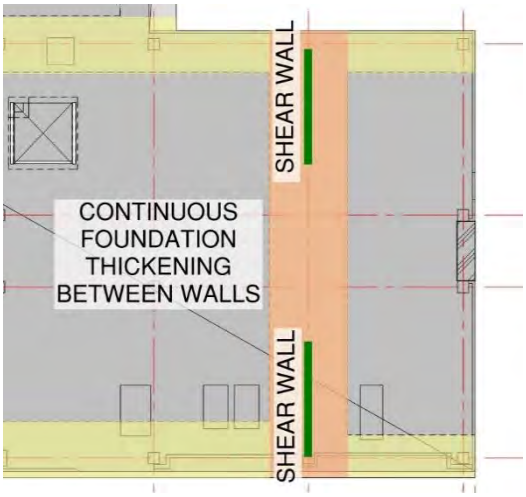

Figure 13 – Foundation coupling element

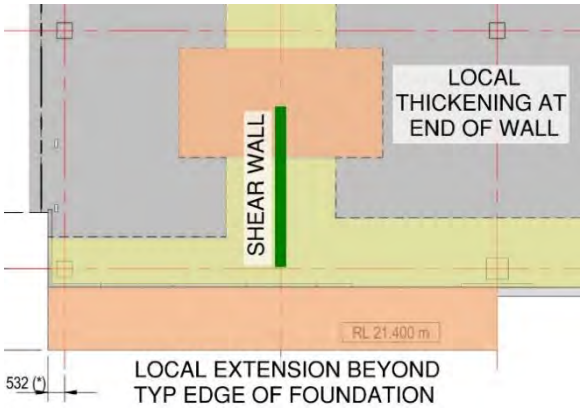

Figure 14 – Foundation localised thickening and extension

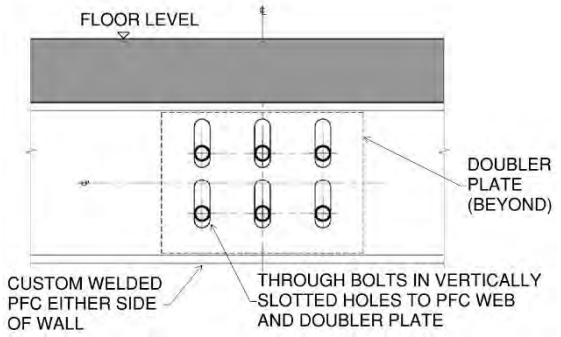

Figure 15 - Suspended floor to wall connection detail

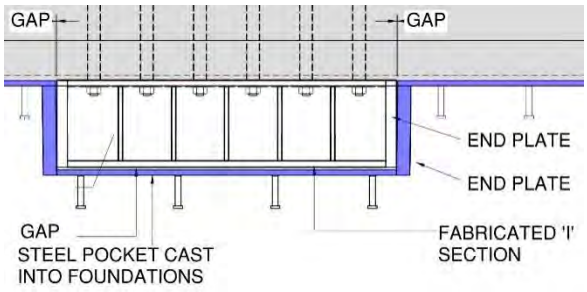

Figure 16 – Shear wall shear key detail

The design solution was for a steel shear key to be bolted to the base of the shear wall and located within a steel pocket cast into the foundations. Twelve M48 threaded rods were detailed to be cast into the wall. These rods were located with a fabricated steel channel also cast into the base of the wall, which provided the correct set out of the rods and armoured the base of the wall. A fabricated steel section with thick end plates and stiffeners connect to the threaded rods. This assembly is in a pocket with thick end plates. A significant benefit of the adopted detailing is that the steel shear key can be constructed to relatively stringent tolerances and test fitted prior to installation to ensure that the shear wall can be installed without risk of shear key not fitting.

The endplates of the pocket were detailed a slight taper to allow for the expected rotation of the wall. A geometrical check was done to validate that the shear key would not be expected to bind up at the design wall rotation. The intended performance was for the endplates to bear uniformly against each other on the side transferring load, and not coming into contact with each other on the opposite side. Another aspect of the connection provides additional shear reinforcement at both ends of the shear key to strengthen the potential concrete breakout wedge. The shear reinforcement was detailed with Reidbar and steel Flange Nuts to develop the reinforcement either side of the potential failure plane.

Beca worked closely with Leighs Construction, the design and build contractor for the project, to determine the appropriate construction methodology and preferred structural detailing. It was confirmed that the shear walls could be constructed as single precast panels without

splices and remain transportable from a local precast yard to the project site. In situ and tilt-up construction were discounted due to programme and site space requirements.

When the panels are brought to the site, they will be erected on the foundation and temporarily propped. The panels will be lifted with RSFJ devices and shear key attached to the panel. Strong backs are to support the RSFJ devices whilst the panels are lifted from horizontal to vertical. The temporary propping arrangement is such that the internal faces of the panels remain free of props. This allows for concrete pours to connect the bracing lines and avoid re-entrant corner pours. Once the walls are connected to the slab, the propping is intended to be removed and final slab pours can be made. This construction sequence avoided penetrations to suspended slabs arising from temporary propping, and any subsequent making good of the floor.

CONCLUSIONS

This paper provided initial findings of a numerical study on the stiffness of rocking concrete walls without post-tensioning. From the preliminary results, it is demonstrated that these walls will have relatively high stiffness compared to fixed based walls, so higher stiffness modifier values are expected for the design. Also, this paper presented a case study project in Christchurch where these walls with Resilient Slip Friction Joint (RSFJ) hold-downs are used. Performance objectives, design approach, and different details of the project are discussed. This paper provides an insight for the engineering community for the potential of self-centring rocking concrete walls for low damage design of structures.

REFERENCES

Bagheri, Hamed et al. 2020. “New Self-Centering Tension-Only Brace Using Resilient Slip-Friction Joint: Experimental Tests and Numerical Analysis.” *Journal of Structural Engineering* 146(10): 04020219–18.

Bruneau, Michel, and Gregory A. MacRae. 2017. The Quake Centre, University of Canterbury *Reconstructing Christchurch: A Seismic Shift in Building Structural Systems*.

Darani, Farhad Mohammadi et al. 2018. “Application of New Resilient Slip Friction Joint for Seismic Damage Avoidance Design of Rocking Concrete Shear Walls.” In *Proceedings of the New Zealand Society for Earthquake Engineering (NZSEE) Conference*, Auckland, New Zealand.

Grigorian, Carl E., and Mark Grigorian. 2016. “Performance Control and Efficient Design of Rocking-Wall Moment Frames.” *Journal of Structural Engineering* 142(2): 04015139.

Hashemi, A., P. Zarnani, R. Masoudnia, and P. Quenneville. 2017. “Seismic Resistant Rocking Coupled Walls with Innovative Resilient Slip Friction (RSF) Joints.” *Journal of Constructional Steel Research* 129.

Hashemi, Ashkan et al. 2020. “Enhanced Seismic Performance of Timber Structures Using Resilient Connections: Full-Scale Testing and Design Procedure.” *Journal of Structural Engineering* 146(9): 04020180.

Hashemi, Ashkan, Pouyan Zarnani, Reza Masoudnia, and Pierre Quenneville. 2017. “Experimental Testing of Rocking Cross Laminated Timber (CLT) Walls with Resilient Slip Friction (RSF) Joints.” *Journal of Structural Engineering* 144(1): 04017180–81 to 04017180–16.

Iyer, Hariharan. 2005. M.Sc. Thesis “The Effects of Shear Deformation in Rectangular and Wide Flange Sections.” Virginia Polytechnic Institute and State University.

Pampanin, Stefano. 2015. 2 Perspectives on European Earthquake Engineering and Seismology *Towards the “Ultimate Earthquake-Proof” Building: Development of an Integrated Low-Damage System*.

Rodgers, Geoffrey W., John B. Mander, J. Geoffrey Chase, and Rajesh P. Dhakal. 2016. “Beyond Ductility: Parametric Testing of a Jointed Rocking Beam-Column Connection Designed for Damage Avoidance.” *Journal of Structural Engineering* 142(8): 1–10.

Shannon, Tim, Jamaledin Borzouie, and Helen Trappitt. 2019. “TŪRANGA LIBRARY CHRISTCHURCH – HYBRID ROCKING PRECAST CONCRETE WALL PANELS.” In *Concrete NZ Conference*, Dunedin, New Zealand.

Twigden, K. M., S. Sritharan, and R. S. Henry. 2017. “Cyclic Testing of Unbonded Post-Tensioned Concrete Wall Systems with and without Supplemental Damping.” *Engineering Structures* 140: 406–20.

Twigden, K M, and R S Henry. 2019. “Shake Table Testing of Unbonded Post-Tensioned Concrete Walls with and without Additional Energy Dissipation.” *Soil Dynamics and Earthquake Engineering* 119: 375–89.

Wong, P. S., F. J. Vecchio, and H. Trommels. 2013. University of Toronto: Toronto, ON, Canada *VecTor2 & FormWorks User’s Manual (2nd Edn)*.

Yousef-Beik, Seyed Mohammad Mehdi et al. 2019. “Damage-Avoidance Timber Brace Using a Self-Centring Friction Damper.” *Pacific Conference on Earthquke Engineering (PCEE2019), Auckland, New Zealand*.

Zarnani, Pouyan, and Pierre Quenneville. 2015. “A Resilient Slip Friction Joint.” : 2015.; NZ IP Office; Patent No. WO2016185432A1.

SESSION 2B

Chair:
John Marshall

concretenz BUILDING RESILIENCE
CONFERENCE 2022
13-15 October 2022
Energy Events Centre | Rotorua

MIX DESIGN AND FRESH PROPERTIES OF 3D PRINTED CONCRETE

GIUSEPPE LOPORCARO & DON CLUCAS

University of Canterbury

SUMMARY

Digital fabrication and additive manufacturing may revolutionize the construction industry due to their potential advantages such as faster construction, waste minimisation, less human labour, improved accuracy and on-site safety improvements. Moreover, concrete additive manufacturing has a unique advantage over typical concrete construction because of its ability to construct architectural and structural components without the use of formwork. Although additive manufacturing in construction has been researched for over a decade, little research is available in the New Zealand context.

3D printing consists of the deposition of successive layers of concrete which is generally pumped to a nozzle which size may vary from 9 to 30 mm, approximately. The nozzle may be attached to either a robotic arm, a frame or a gantry system and it is computer controlled. This type of construction method requires that the material meets requirements that are not usually required for ordinary in-situ casted concrete.

At the University of Canterbury, a medium-scale custom-made 3D printer for concrete has been designed and built. After an introduction to the design and construction of the 3D concrete printer, this paper discusses the development of three mix designs of 3D printable concrete and compare the experimental results concerning the fresh material properties of these mixes.

The mixes were evaluated based on extrudability (through a 10-mm nozzle), workability, open time and buildability. The mix designs that varied in ratios of locally sourced New Zealand materials (river sand, Portland cement, fly ash and silica fume) were compared based on the latter properties. The mixes also contained various quantities of super plasticiser and fibre reinforcements (no fibre, polyvinyl alcohol or polypropylene). The mixes containing fibres had the most desirable workability characteristics as the fibres improved the binding properties of the mix. The mix containing polypropylene fibres showed the lowest workability in the ASTM drop table test, which was consistent in further testing as it extruded a narrower and less consistent filament. The optimum mix was the mix containing PVA fibres with a 3:2 sand-binder and 0.27 water-cement ratio. This mix had optimal workability and extrudability characteristics and showed little deformation under the load of the subsequent layers.

INTRODUCTION

The use of concrete in construction dates back to the Roman Empire in the third century BC. Concrete (*opus caementicium*) for construction was made by mixing sandy volcanic ash and lime mortar such as that used in the Pantheon. Modern concrete, made of Portland cement

and coarse aggregate, was produced from the beginning of the 1800s. The invention of reinforced concrete is often attributed to Joseph Monier, who patented the idea of combining concrete and round steel bars in flexural members in 1877. However, it is the French constructor François Hennebique who gave the biggest impulse to the spread of reinforced concrete in construction (Soderstrom, 2020). Statistics from Stats NZ show that the use of ready-mixed concrete was approximately 4 million cubic metres over the last five years (http://infoshare.stats.govt.nz/).

The success of reinforced concrete is due to multiple reasons such as its strength which allow obtaining slender structures able to span long distances, the resistance to fire and the ability to be moulded and shaped in different forms, providing flexibility in terms of material placement, handling and creative geometry. However, it typically involves formwork and steel reinforcement which requires considerable time and labour to set up and constrains building geometries.

New age construction has seen digital fabrication and additive manufacturing as promising avenues of construction due to its potential advantages such as faster construction, increased geometric complexity, waste minimisation, less human labour, improved accuracy and on-site safety improvements (Zhao & Loporcaro, 2019). Introducing this freeform method of construction into the concrete industry has the potential to create new innovative concrete shapes without formwork, and thus having a unique advantage over typical concrete construction.

Concrete additive manufacturing consists of the deposition of successive layers of concrete that is generally pumped to a nozzle whose size may vary in shape and dimensions (Bos et al., 2016). The nozzle can be attached to either a robotic arm, a frame or a gantry system and it is computer controlled. Cementitious materials used in additive manufacturing must possess characteristics different from those possessed by ordinary concrete. 3D printed concrete mix needs to have acceptable extrudability so it could be extruded through a small-size (e.g. 10 to 40 mm) nozzle. It must also have adequate open time to ensure adhesion between filament layers occurs and no cold joints are formed. The material must have sufficient buildability characteristics for the structure to be laid down correctly, remain self-supported and hold its shape under the increasing load generated by subsequent layers. The performance of the concrete is reliant on these characteristics, which are highly influenced by the workability of the material.

Although research on additive manufacturing of concrete is being conducted in many universities, research institutes and private companies, the technology is still in its infancy (Buswell et al., 2018). New Zealand is lagging behind. More research is required to develop solutions that account for the local requirements. In this paper, preliminary results are presented on the development of concrete mixes that will form the basis for further research currently being conducted at the University of Canterbury.

LITERATURE REVIEW

Printing technologies

Additive manufacturing has been employed in different industries (e.g. biomedical, aerospace, manufacturing, construction) over the last few decades. Almost any type of material can be 3D printed, from plastic to ceramics and from metals to concrete (Ngo et al., 2018). The origins of additive manufacturing are dated to the early 1980s when Charles Hull patented the stereolithography (SLA) process that used liquid photosensitive resins as printing materials (Hull, 2015). This process was soon followed by other 3D printing technologies such as material extrusion (MEX) binder jetting (BJT) , and Powder Bed Fusion (PBF). These technologies are well suited for polymers and metals. Also, they have provided the basis

technologies for large scale 3D printing. For cementitious materials, other 3D printing processes have been developed. The most common are Contour Crafting (Khoshnevis, 2004), Concrete Printing (S. Lim, 2009), and D-shape (Dini). Due to the large scale of the 3D printing machines, the nozzle (the depositing head) is either mounted on a frame, a robot or a gantry. Contour crafting, patented by Prof. Behrokh Khoshnevis at the University of Southern California in 2004 was developed for in-situ applications. It comprises a gantry system, a pump and a nozzle. The concrete material is pumped to the nozzle from which the material is extruded, then the surface of the material printed is smoothed with a trowel (Khoshnevis, 2004). Concrete printing, developed by a research team from the University of Loughborough, employs a similar process based on concrete extrusion. This technology was conceived for off-site applications, however, in-situ applications are also possible. The concrete is pumped to a nozzle and then extruded. No trowelling system is employed. Concrete printing allows for greater control of the 3D printed geometries (Le et al., 2012). Similarly to Concrete Printing, the D-shape process was developed for off-site applications. It uses a powder deposition process where a binder is used to hardened selective layers of materials. Each layer of material is placed to the required thickness on the printing platform, then the nozzle deposits the binder only where the building material needs to be solidified. When the 3D object is completed, the loose material that has not hardened is removed. Examples of full-scale objects printed using the contour crafting, concrete printing and D-shape processes are shown in Figure 1.

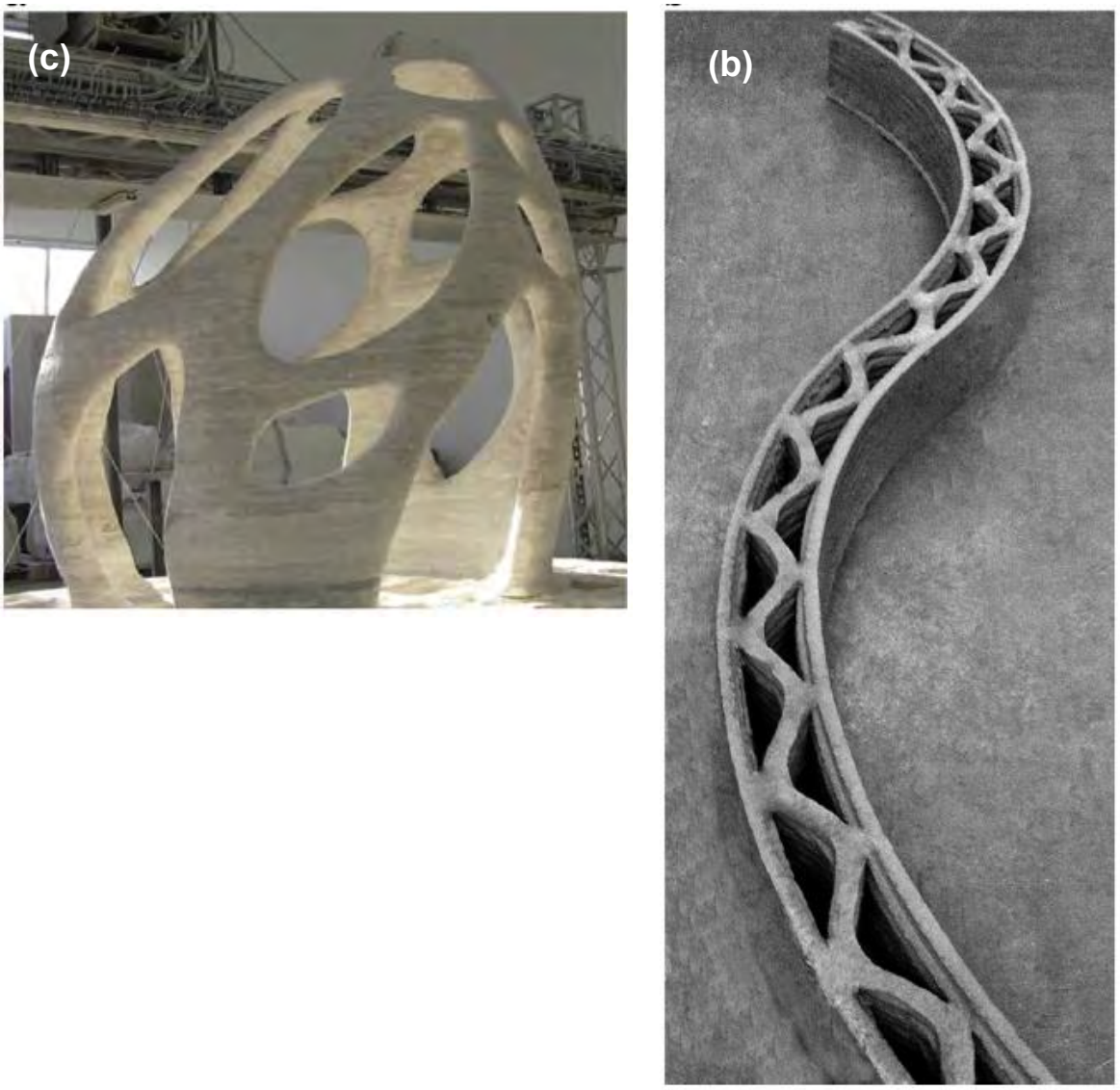

Figure 1 Examples of full-scale samples from Concrete Printing (a), Contour Crafting (b) and D-shape (c). Images are taken from Lim et al. (2012).

Concrete fresh properties and material mixes

Several concrete mixes have been developed by researchers involved in concrete additive manufacturing. The mixes are designed to suit the requirements of the 3D printer process adopted. Nevertheless, the fresh properties of concrete are the key to the success of 3D printing. The fresh properties that 3D concrete mixes must possess to be extruded by a nozzle are pumpability or workability, printability (or extrudability), open time, and buildability (Le et al., 2012; Lim et al., 2012).

Pumpability refers to the ease and reliability of pumping the concrete through the delivery system (from the pump to the nozzle). Printability or extrudability refers to the capacity of the material to be extruded through a nozzle as a continuous filament. The filament should have no or minimal deformation of cross-section as well as an acceptable level of splitting or tearing (Buswell et al., 2018). Buildability is the ability of the extruded layers of concrete to withstand the load applied by layers placed above without notable slumping. The printed concrete filaments must possess sufficient strength and stiffness to avoid significant deformation once further filaments are laid upon them. The open time is the time during which a concrete mix

can be used in a 3D concrete printer. If the concrete is extruded beyond the open time, the mix may be too hard to be extruded. Also, the open time is associated with the hydration rate of the concrete mix. There must be sufficient adhesion between subsequent layers with no cold joints formed between them. The open time influences pumpability and extrusion. On the other hand, the open time is highly influenced by the mix viscosity, the yield strength (the minimum stress to initiate flow) and for how long the ideal value is maintained constant. The open time needs to be calibrated as a function of the volume of the printed object and its area (since this determines the total length of the deposited material per layer).

Concrete mix design developments have been carried out at Loughborough University by Le et al. (Le et al., 2012) using the concrete printing process. The 3D printer utilised was a prototype concrete machine supported by a 5.4 m (length) x 4.4 m (width) x 5.4 m (height) steel frame. The concrete material was fed from a container mounted on top of the printing head. A concrete pump was used to transport the mix from the container to the 9-mm printing nozzle. The printing head was digitally controlled in the X, Y and Z directions by a CNC machine. The optimum printable mix consisted of a 3:2 sand-binder ratio. The maximum size of the sand was 2 mm. This limit was governed by the size of the printing nozzle. The binder was made of cement CEM type I 52.5 (70%), fly ash (20%) and silica fume. A superplasticiser, a retarder and an accelerator were added to improve workability, to maintain a sufficient open time, and to control setting, respectively. Polypropylene fibres were used to reduce shrinkage and deformation in the plastic state (1.2 kg/m^2). The mix proportion of the optimum mix is summarised in Table 1. Paul et al. (Paul, 2018) investigated the fresh and the hardened properties of three types of mixes. The first mix was an alkali-activated geopolymer mortar with no cement. The second and third mixes were printable mortars made of sand (max size 1 mm), cement, fly ash, silica fume, plasticiser and water. The mix proportions of the cement-based mixes were the same. However, in mix 3, glass fibre was used to improve the flexural strength. In Table 1, only the proportion of mix 3 is presented (Paul, 2018). All three mixes were successfully printed with a robotic printer. The geopolymer mix was printed using a 10 mm x 20 mm rectangular nozzle, while the cement-based mortars were printed with an 8-mm diameter circular nozzle. It was found that to ensure better pumpability, the thixotropy of the 3D printed materials should be greater than 10000 [Nmm rpm], Also, the flexural and compressive strength of the printed samples were influenced by the shape of the nozzle orifice and the complexity of the printed objects. Kazemian et al. (Kazemian et al., 2017) investigated the fresh properties of 3D printing mixes studying the effects of nano-clay, silica fume, and fibres inclusions. ASTM C150 Type II Portland cement was used. Sand of 2.36 mm maximum size was used as aggregate. A polycarboxylate-based high-range water-reducing admixture (HRWRA) was used to reduce the amount of water and achieving the required flowability. Also, a viscosity modifying admixture (VMA) was added to increase plastic viscosity and cohesion. Polypropylene (PP) fibres 6-mm long were used to control shrinkage cracking. Silica fume was used as supplementary cementitious material to improve the cohesion of fresh concrete, the mechanical strength and the impermeability of the hardened concrete. In Table 1, two of the four mixes developed by Kazemian et al. are presented. The printer employed was a linear concrete printing machine capable to print up to ten layers of 1.2-m long filaments. The concrete was extruded through a 38.1 mm x 25.4 mm nozzle. It was found that small additions of nano-clay produced a noticeable increase in viscosity and cohesion. Trial-and-error experiments were carried out to determine the ideal mix proportions. A mix design was deemed successful when when the printed layers did not not have any surface defect; the layers edges were visible and squared (because a rectangular shape nozzle was used) and dimension conformity and consistency were satisfied. Dimension conformity guaranteed that the width of each layer was within 10% error from the target width (38.1 mm); meanwhile, dimension consistency required that any change in width of the single filament was less than 10% of the target width. The experimental results showed that additions of nano-clay and silica fume improved shape stability (buildability).

The mix designs discussed in this section and presented in Table 1 formed the basis of the mix developed in this research.

Table 1 Mix proportion of 3D printed concrete materials from selected literature

Material	**Mix proportion (kg/m^3)**			
	Le et al. (Le et al., 2012)	**Paul et al. (Paul, 2018)**	**Kazemian et al. (Kazemian et al., 2017)**	**Kazemian et al. (Kazemian et al., 2017)**
Sand	1241	1211	1357	1379
Cement	579	290	540	600
Fly ash	165	278		
Silica fume	83	145	60	
Fibres	1.2 (PP)	13.5 (glass)		1.18 (PP)
Water	232	284	259	259
Superplasticiser	1%[a]	7	0.16%[b]	0.06[b]
Retarder	0.5%[a]			
VMA				0.10[b]

[a] The percentages are reported by binder weight.
[b] The percentages are reported by cementitious materials mass.

Research aim and objectives

This research aims to develop and test the fresh properties of 3D concrete printing mixes from locally sourced materials and printed through a custom-design and built 3D concrete printer.

The following objectives have been identified:

- Develop three concrete mixes that can be extruded from the 10-mm nozzle available;
- Investigate and compare the fresh properties of the three mixes;
- Provide recommendations for future mix and machine development.

MATERIALS, METHODOLOGY AND TESTING

Mix design

A review of 3D printed concrete mixes available in the literature informed the design of three initial mixes (Table 1). Trial-and-error tests were performed to identify the proportion of the materials. The three selected mixes, named hereafter mix 1, 2 and 2, contained a different proportion of Portland Cement, aggregate (river sand, size smaller than 2.36 mm), fly ash, silica fume, water, a modified polycarboxylate-based superplasticiser, and polymer fibres.
The dry components (cement, sand, river sand, fly ash, silica fume) were added to a 5 L mortar mixer with water and a small amount of superplasticiser to reduce the water demand while increasing workability. Mix 1 was designed with no addition of fibres, mix 2 included polyvinyl alcohol (PVA) fibres and mix 3 polypropylene fibres. The three mixes required fine-tuning before being fully investigated. They had to be extruded through the nozzle with little or no deformation of the filament. Also, a 4-layer tall element could be built noticeable deformation of the bottom layer.

Custom-designed and built 3D concrete printer

In the additive manufacturing industry, there are many architectures of machine design for planar Material Extrusion (MEX) systems. Some use robotic arms with up to six degrees of freedom but for planar extrusion, only three are required, *x,y,* and *z*. Robotic arms are very effective, however, they are also very expensive, especially if a long reach and/or a heavy print head is required. A more cost-effective option is to use a Cartesian system controlling the x and y planar motion and z motion for the layer height. A scaled-down prototype machine has

been manufactured and has been used in this research. The build volume is 1.5m x 2m x1.5m (*xyz*).

Where possible, industry-standard componentry was used. Low backlash ball screws on each axis provide an adequate reduction ratio to allow direct coupling of stepper motors. Similarly, a stepper motor is directly coupled to the screw extruder. The motor control system uses an Arduino microprocessor and standard electronic motor drives. Linear bearings are used for each slide. To avoid corrosion and the requirement to paint the structure, aluminium, stainless steel, and 3D printed polymer parts are used.

For ease of use and creating the G-Code for controlling the axes stepper motors, industry-standard Marlin firmware is used. The G-Code can be manually written using a text editor or, preferably, an industry-standard graphical user interface such as PrusaSlicer is used. This slicer is used on *xyz* polymer printers such as the low-cost Prusa MEX machines used by students at schools and universities. After customising the machine default settings, it is as simple as loading the component file and exporting the G-Code file for the printer. Specialist robotics know-how is not required to run the machine.

Figure 2 The UC custom-built 3D concrete printing machine.

Experimental testing: fresh properties

The fresh properties under investigation were: workability, extrudability, buildability and open time. Experimental tests were selected from a review of previous research and available standards. For each mix design, three samples were tested.

The custom-made printer was not provided with a pump, workability was tested instead of printability. For standard concrete, workability is evaluated using several conventional tests such as slump, compacting factor and flow tests (Kazemian et al., 2017; Le et al., 2012). In this research, the workability of the mixes was quickly assessed using the ASTM drop table test following the ASTM C1437-20 standard (International, 2020). The test requires placing the freshly mixed concrete into a mould, tamping it 20 times with a tamper to ensure uniform filling of the mould, then dropping the table 25 times in 15 seconds. The spread in four directions is then measured using a Vernier calliper and averaged for three different mix designs.

Extrudability was tested using a filament test proposed by Le et al. (Le et al., 2012). This involved printing a U-shape filament with the longest sides being 300 mm long, while the shortest side was 40 mm. This configuration allowed to test the concrete extrudability and the corner section properties. The lines were extruded with a 9 mm clearance from the printer build platform board at a linear speed of 2,000 mm/min. Filaments were scored on a scale between 1 and 5, with 5 being the lines perfectly extruded and consistent without any significant deformation, tearing or splitting and 1 if the concrete did not extrude at all. This test ensured the mix came out consistently without any significant deformation.

Buildability was measured by extruding four layers of concrete one on top of the other. A two-minute setting time in between each layer was allowed for the concrete to partially set. The width of the top and bottom layers was measured using a Vernier calliper approximately 24 hours after the extrusion. Measurements were taken at three different locations for each layer. The three results were averaged. A percentage difference was taken between the top and bottom layer widths.
Two separate methods were adopted to determine the open time. The first method consisted in measuring the change in shear strength with time using a shear vane apparatus (Le et al., 2012). Austin et al. (Austin et al., 2005) adopted the shear vane test typically used to measure the shear strength of soil to determine concrete workability. The concrete mixes under investigation were placed into a rectangular base 100 mm x 100 mm x 50 mm deep container, the shear strength was recorded at set intervals of 0 (for workability), 5, 15, 30, 60, 90 and 120 minutes using a 19-mm diameter shear vane apparatus. The shear vane had a height of 29mm, which was inserted into the concrete samples, as shown in Figure 3.

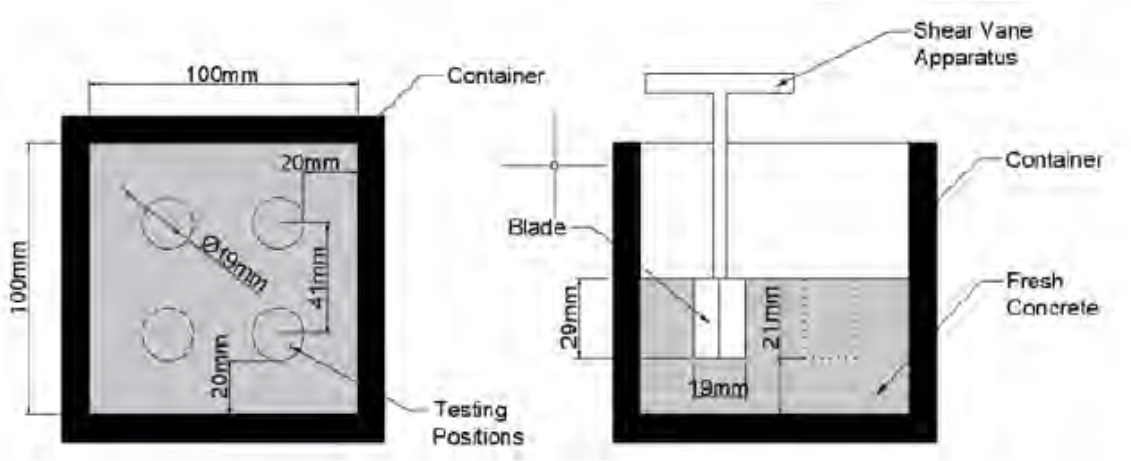

Figure 3 Diagram of the shear vane used for the open time testing

The second test method to evaluate the open time consisted in visually inspecting 3D printed samples for imperfections such as cold joints (Buswell et al., 2018; Jo et al., 2020). Cross-section tests were taken on all the samples printed using the three mix designs. The four-filament tall samples used for buildability were let to set for approximately 24 hours, then cut through. This enabled the inspection of air bubbles, cold joints and other imperfections. The condition of the cross-section of the sample was scored on a scale from 1 to 5, with 1 being a section with major imperfections (e.g. air bubbles and cold joints), and 5 being a section with no imperfections.

RESULTS AND DISCUSSION

Mix design

The tested mix designs are presented in Table 2. These mix designs were all printable using the UC custom-made 3D printer and could be replicated when the volume of the mix was increased. The total density of the three mixes varied between 2260 kg/m^3 and 2311 kg/m^3.

Table 2. Proportions of the tested mix designs.

Materials	**Mix proportion [kg/m^3]**		
	Mix 1	**Mix 2**	**Mix 3**
Sand	1140	1229	1334
Cement	644	571	503
Fly ash	188	163	144
Silica fume	94	82	72
Water	241	217	202
Fibres	0	1.2 (PVA)	1.2 (Polypropelene)
Superplasticiser	4	4.3	4.6
Total	2311	2267	2260
W/C ratio	0.26	0.27	0.28
Binder to sand ratio	0.81	0.66	0.54

As aggregate river sand was used,sieve analysis was performed on the sand to determine the particle size distribution (Figure 4). The aggregate is relatively well-graded. Using a better-graded aggregate would increase the density of the mix design and in turn, increase the ultimate strength of the concrete. If required, the density can also be increased through proper vibration of the sample to reduce entrapped air and using a suitable curing system to prevent water evaporation and decrease porosity.

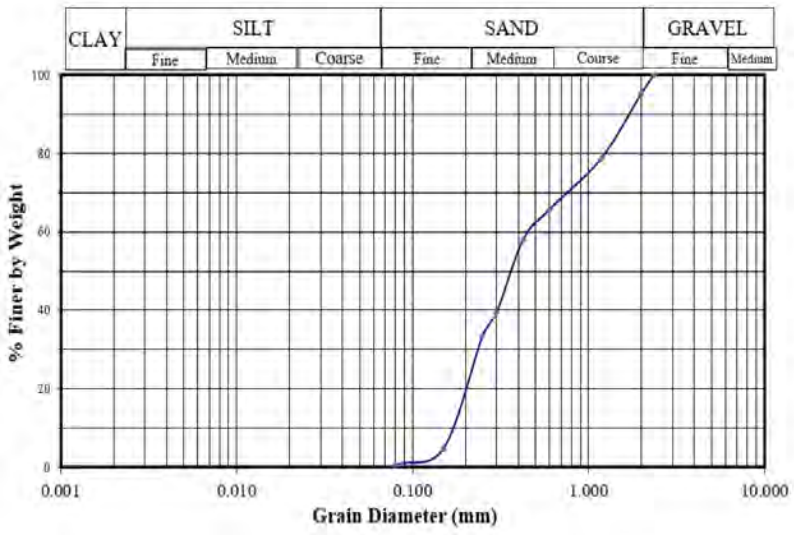

Figure 4. Particle distribution curve for river sand.

Workability

The drop table test was performed three times for each mix design. The results were then averaged. They are summarised in Table 3. The variability of the results from the drop table test among the mixes is largely due to the presence and the type of reinforcement fibres used.

The role of the fibres is to reduce plastic shrinkage and deformation at the fresh state. Mix design 1, with the largest spread, has no reinforcement. The workability is lower in mix three with the polypropylene fibres than that of the mix with PVA fibres due to the nature of the polypropylene fibres. PVA fibres ($E \approx$ 30-40 GPa) are stiffer than polypropylene fibres ($E \approx$ 3.5 GPa). This means they are less inclined to mould and bond with the surrounding particles. The polypropylene fibres are very flexible and will combine throughout the mix to provide tensile resistance and hold the shape most effectively.

Table 3. ASTM drop table test average spread results

	Mix 1	**Mix 2**	**Mix 3**
Average lateral spread [mm]	193.42	180.63	171.33

Extrudability

The extrudability test was performed on each of the mixes twice. The maximum and minimum width and depth of each of the extruded filaments were measured. The results are presented in Table 4. The results show that the mix with the polypropylene fibres (mix 3) extruded a narrower and less consistent filament, with the width varying by over 7 mm in trial two. The widths of the filament extruded with Mix 1 and 2 were similar (~23mm). Moreover, they were more consistent in both width and depth in the two tests. Figure 5 shows the extruded single and double filament from the first test of the mix with the PVA fibres (mix 2).

Table 4 Extrudability test results: max and min-width and depth of a single layer filament

	Mix 1	**Mix 2**	**Mix 3**
Max width [mm]	24.180	24.080	18.745
Min width [mm]	22.480	22.095	11.635
Max depth [mm]	10.005	10.415	9.000
Min depth [mm]	9.230	10.065	7.145

Figure 5 Mix 2 with PVA extrudability test trial one.

It must be noted that after 24 hours, shrinkage cracks were noticed on the filaments of mix 1, most likely caused by the lack of fibre reinforcement. A subjective “extrudability score” was assigned on both trials of the three mixes. The scores are summarised in Table 5

Table 5 Extrudability scores for mix 1, 2 and 3 and trial 1 and 2

	Score	Total
Mix 1, Trial 1	5	9.5
Mix 1, Trial 2	4.5	
Mix 2, Trial 1	4	9
Mix 2, Trial 2	5	
Mix 3, Trial 1	2.5	5.5
Mix 3, Trial 2	3	

Open time

The open time was determined by measuring the increase in shear strength (τ) with time (t) using the shear vane apparatus. Shear strength was measured at 0, 5, 15, 30, 60, 90 and 120 minutes. Each data point in Figure 6 represents the average of three measurements. A linear regression analysis was performed to fit the testing results.

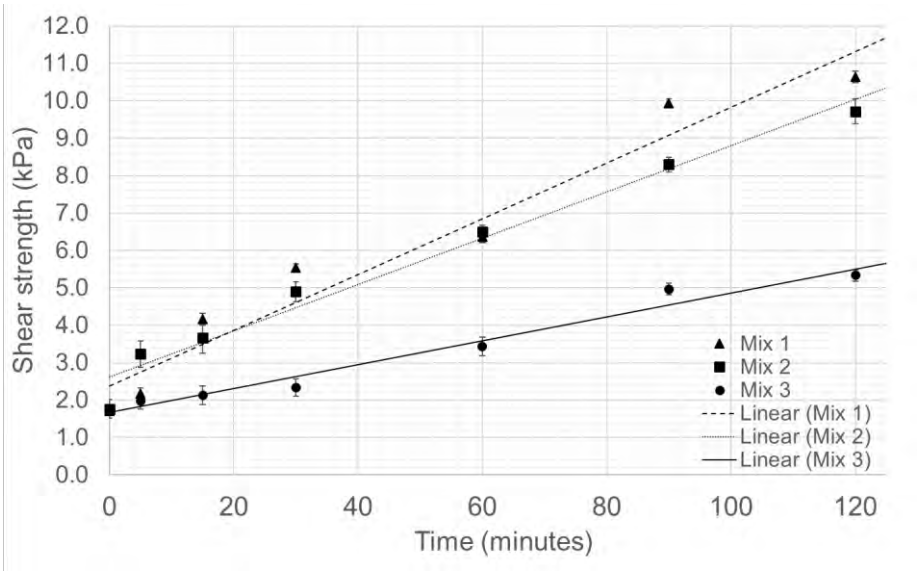

Figure 6 Shear vane test results for workability: shear strength versus time

The linear regressions derived from the shear strength versus time data are represented by the following equations:

Mix 1	$\tau = 0.0745\ t + 2.3814$	$R^2 = 0.952$
Mix 2	$\tau = 0.0618\ t + 2.6145$	$R^2 = 0.976$
Mix 3	$\tau = 0.032\ t + 1.6664$	$R^2 = 0.974$

The initial shear strength (at $t = 0$) of the concrete mixes was approximately similar ranging between 1.5 and 2 kPa. However, the rate of shear strength increase varied. The increase in shear strength of mix 3 was significantly slower compared to mix 1 and 2. Therefore, mix 3 was much slower to gain shear strength. Accelerated hydration of concrete may result in a shorter open time and possibly cold joints at the interface between layers. It was observed that once the shear strength of the concrete increased by 1 kPa, the mixture became difficult to be extruded. Therefore, it was established that the open time was the time required for the mix to gain 1 kPa shear strength. Based on this criterion and using the linear regression equations derived from the shear strength versus time data, the calculated open times are: 13’ 42” for mix 1, 16’ 18” for mix 2 and 31’ 25” for mix 3.

A visual inspection of the cross-section of the concrete filament was performed to observed any cold joint. Inspections were performed 24 hours after printing 500-mm long and 4-layer tall

filaments. It must be noted that a 2-minute pause was allowed between the printing of each layer. The visual inspection (see Figure 7) showed that no cold joints had formed between layers for any of the samples. There was also no notable air bubbles or other imperfections.

Figure 7 Visual inspection of the filament cross-section (Mix 1 on the left, Mix 2 on the centre and Mix 3 on the right image)

Buildability

Buildability was assessed as the ability of the concrete filament to hold its structure without significant deformation (lateral spread) once layers were added on the top. The 4-layer tall filament samples used for the open time test were used (see Figure 7). For each mix, the width of the top and bottom layers were measured. Then, the percentage change of the bottom layer width compared to the top filament width are presented in Figure 7.

Table 6 Buildability test results

	Mix 1	**Mix 2**	**Mix 3**
Botton layer width [mm]	34.18	27.375	22.80
Top layer width [mm]	17.32	26.51	17.87
Percentage change in width	97.3 %	3.3%	27.6%

Mix 1 which did not contain fibres underwent the largest deformation under the load produced by the top layers. The increase in width was 97.3%. Mix 1 had difficulties with withstanding the load from the top layers due to the lack of fibre reinforcement. Mix 2 and 3, which contained fibres performed better with a 3.3% and 27.6% increase in the bottom layer width, respectively. Mix 2, containing the PVA fibres, performed the best by maintaining a constant width. This may be attributed to the lowest water-cement ratio and superplasticiser content.

CONCLUSIONS

Concrete additive manufacturing is a promising technology. It has the potential to revolutionise the concrete construction industry due to its ability to manufacture architectural and structural components without the constraints of formwork, the opportunity to automate the design and construction phases, increase concrete placement accuracy, improve workers' health and safety, etc.

High performance 3D printable concrete mixes were developed. Fresh properties such as extrudability, buildability, open time and workability were investigated. The results showed that mix 2 was best suited for 3D printing and further research is required for further improvements. The mix had a 3:2 sand-binder and 0.27 water-cement ratio. The binder was approximately 70% cement, 20% fly ash and 10% silica fume. PVA fibres in the quantity of 1.2 kg/m^3 were added to the mix to avoid plastic shrinkage. The mix showed the best workability and

extrudability through a 10 mm printer nozzle. It also showed little deformation under loading caused the subsequent top layers. 3D concrete.

ACKNOWLEDGEMENTS

The authors would like to acknowledge the Civil Engineering students Jake Potton, Richard, for performing the testing; Mechanical Engineering students Mink Witowski and Talyah Mayron who assisted with the design of the 3D concrete printing machine; Tim Perigo, Julian Phillips, Mechanical Engineering staff, for building the machine and Associate Professor Allan Scott for sharing his knowledge.

REFERENCES

Austin, S. A., Goodier, C. I., & Robins, P. J. (2005, 2005/03/01). Low-volume wet-process sprayed concrete: pumping and spraying. *Materials and Structures, 38*(2), 229. https://doi.org/10.1007/BF02479348

Bos, F., Wolfs, R., Ahmed, Z., & Salet, T. (2016, 2016/07/02). Additive manufacturing of concrete in construction: potentials and challenges of 3D concrete printing. *Virtual and Physical Prototyping, 11*(3), 209-225. https://doi.org/10.1080/17452759.2016.1209867

Buswell, R. A., Leal de Silva, W. R., Jones, S. Z., & Dirrenberger, J. (2018, 2018/10/01/). 3D printing using concrete extrusion: A roadmap for research. *Cement and Concrete Research, 112*, 37-49. https://doi.org/https://doi.org/10.1016/j.cemconres.2018.05.006

Dini, E. *D-shape*. https://d-shape.com/

Hull, C. W. (2015). The birth of 3D printing. *Research-Technology Management, 58*(6), 25-30.

International, A. (2020). *C1437-20*. West Conshohocken, PA 19428-2959. United States.

Jo, J. H., Jo, B. W., Cho, W., & Kim, J.-H. (2020, 2020/03/03). Development of a 3D Printer for Concrete Structures: Laboratory Testing of Cementitious Materials. *International Journal of Concrete Structures and Materials, 14*(1), 13. https://doi.org/10.1186/s40069-019-0388-2

Kazemian, A., Yuan, X., Cochran, E., & Khoshnevis, B. (2017, 2017/08/01/). Cementitious materials for construction-scale 3D printing: Laboratory testing of fresh printing mixture. *Construction and Building Materials, 145*, 639-647. https://doi.org/https://doi.org/10.1016/j.conbuildmat.2017.04.015

Khoshnevis, B. (2004, 2004/01/01/). Automated construction by contour crafting—related robotics and information technologies. *Automation in Construction, 13*(1), 5-19. https://doi.org/https://doi.org/10.1016/j.autcon.2003.08.012

Le, T. T., Austin, S. A., Lim, S., Buswell, R. A., Gibb, A. G. F., & Thorpe, T. (2012, 2012/08/01). Mix design and fresh properties for high-performance printing concrete. *Materials and Structures, 45*(8), 1221-1232. https://doi.org/10.1617/s11527-012-9828-z

Lim, S., Buswell, R. A., Le, T. T., Austin, S. A., Gibb, A. G. F., & Thorpe, T. (2012, 2012/01/01/). Developments in construction-scale additive manufacturing processes. *Automation in Construction, 21*, 262-268. https://doi.org/https://doi.org/10.1016/j.autcon.2011.06.010

Ngo, T. D., Kashani, A., Imbalzano, G., Nguyen, K. T. Q., & Hui, D. (2018, 2018/06/15/). Additive manufacturing (3D printing): A review of materials, methods, applications and challenges. *Composites Part B: Engineering, 143*, 172-196. https://doi.org/https://doi.org/10.1016/j.compositesb.2018.02.012

Paul, S. C., Tay, Y. W. D., Panda, B., & Tan, M. J. (2018). Fresh and hardened properties of 3D printable cementitious materials for building and construction. *Archives of civil and mechanical engineering, 18*, 1-8.

S. Lim, T. L., J. Webster, R. Buswell, S. Austin, A. Gibb, T. Thorpe. (2009). *Fabricating construction components using layer manufacturing technology* Global Innovation in Construction Conference, Loughborough University, Leicestershire, UK.

Soderstrom, M. (2020). *Concrete : From Ancient Origins to a Problematic Future*. University of Regina. http://ebookcentral.proquest.com/lib/canterbury/detail.action?docID=6362824

Zhao, A., & Loporcaro, G. (2019, October 2019). *Exploring opportunities and limitations of 3D concrete printing technology in New Zealand* Concrete NZ conference, Dunedin.

concretenz BUILDING RESILIENCE
CONFERENCE 2022
13-15 October 2022
Energy Events Centre | Rotorua

EVALUATION OF THE DURABILITY OF AUTOCAST CONCRETE PIPE AGAINST MACHINE-MADE CONCRETE PIPE

AMERICO DOS SANTOS[1], DAKSH BAWEJA[2], HAYDEN DUFFY[3] AND TIM MACINTOSH[4]

[1] Technical Services Manager, Hynds Pipe Systems Ltd
[2] Director-Materials, BG&E
[3] Principal/NZ Manager, BG&E
[4] National Engineering Manager, Hynds Pipe Systems

SUMMARY

Steel reinforced concrete pipe is recognised as the most durable and economical solution for drainage pipelines and has been manufactured in Australasia for more than 100 years.

Spun, Bi-Di Packerhead and Vertical Dry Cast are considered Machine-made processes in AS/NZS 4058:2007. The most recent manufacturing process also considered Machine-made is AutoCast, which is a highly automated vertical casting manufacturing process using high performance SCC.

This paper reviews concrete pipe manufacturing methods and evaluates durability testing of machine-made pipe against AutoCast manufactured concrete pipes.

Durability tests undertaken covering chloride ingress, carbonation, water absorption and acid attack show comparable results for pipe concrete across all manufacturing processes investigated, meeting the durability requirements of AS/NZS 4058: 2007, and all processes exceed those of standard cast in-situ concrete.

INTRODUCTION AND BACKGROUND

Steel reinforced concrete pipe is recognised as the most durable and economical solution for drainage pipelines and these products have been manufactured in Australia and New Zealand for more than 100 years (CPAA 2007). Materials and pipe manufacturing techniques have developed over time. Two horizontal spinning processes (centrifugal wet spinning and roller suspension) were developed in the early 1900s and these became the driving force of the concrete pipe manufacturing industry in Australasia and world wide (Ruffles et al. 2017). These technologies produce thin walled concrete pipe and were a major driver of production efficiency and durability of concrete pipe in this region.

The consistent quality and in-service performance of these pipes has been recognised over time and this superior performance over other precast concrete elements is reflected in the current manufacturing Standard AS/NZS 4058: Precast Concrete Pipes (Pressure and Non-Pressure) (Standards Australia/Standards New Zealand 2007).

In the 1960's and 1970's, development particulalry in the United States led to new manufacturing processes and systems with increased efficiency and reduced waste, such as

the vertical dry cast Radial Press technology, now known as Bi-Di Packerhead or Rollerhead (pfeiffer aktuell 1971). Similarly new technnology was emerging in Europe such as vertical drycast vibrating core technology.

By the early 2000's there were a number of the numbers of processes for manufacturing pipes which included:-

- Horizontal centrifugal spinning;
- Horizontal roller suspension spinning;
- Vertical Bi-Di Packerhead;
- Vertical Vibrating Core;
- Wet cast – 50 MPa (predominantly for some larger diameter pipes)

Prior to AS/NZS 4058: 2007, the earlier Standard AS 4198, made no mention of the manufacturing process. With the publication of AS/NZS 4058:2007 all that changed with the introduction of the terms "machine-made" and "wet cast". No definitions of these terms were included other than wet cast had to be "50 MPa Concrete" (CPAA 2007, Ruffles et al. 2017).

Around 2007, machine-made pipe was generally accepted as processes using very low or zero slump concrete with low water:binder ratio, placed in steel moulds and compacted by centrifugal forces, low frequency high amplitude vibration or by direct mechanical compaction (Ruffles et al. 2017). Wet casting was used for the manufacture of larger diameter pipe (typically >2 m diameter). In this case, conventional slump concrete is placed in rigid steel moulds and compacted using either a combination of internal and external form vibrators, or external form vibrators alone.

AS/NZS 4058:2007 has larger cover requirements for wet cast pipe (25 mm) compared to machine-made pipe (10 mm) for Normal environments, as defined in that Standard. The higher covers for the larger wet cast pipes suited their manufacture as larger aggregates were typically used in the concrete mix and wall thicknesses were relatively large, in part, due to load requirements on the pipe. This resulted in the cover as a percentage of the wall thickness being much less for wet cast pipe.

In the late 1990's, self-compacting or super workable concrete started appearing first in cast in-situ construction and by the early 2000's was being used for precast concrete products in Japan and Europe. This included a modern highly automated pipe manufacturing process using very controlled concrete batching, placing and curing techniques. The self-compacting or super workable concrete used in this process had much higher performance requirements than nominated in AS/NZS 4058:2007 for 50 MPa wet cast concrete. These requirements translated into a more durable concrete with hardened properties that are more closely aligned to concrete produced in the machine-made pipe manufacturing process.

A study was undertaken to compare of the quality and durability properties of concrete pipe manufactured using the high performance self-compacting concrete with pipe manufactured by a number of machine-made processes. The machine made pipes included spun and Vertical Dry Cast Bi-Di Packerhead maufacturing processes.

<u>The mechanical and durability parameters considered were:</u>

1. Concrete strength;
2. Water absorption;
3. Apparent Volume of Permanent Voids (AVPV);
4. Chloride Diffusion and Migration;
5. Accelerated Carbonation, and
6. Resistance to Acid Exposure at 1% and 10% concentration.

TESTING PROGRAM

The testing programme involved sourcing 600 or 675mm diameter concrete pipe from the standard production processes and coring test samples from the finished product. The cored test samples were cylindrical and cut radially through the entire thickness of the concrete pipe wall with faces corresponding to the internal and external surfaces of the pipe.

The protocol followed was that developed by the CPAA for a testing programme carried out some years ago. Each set of cored test samples were extracted from 2 pipes, with cores uniquely identified such that individual test samples across all test sets always came from the same locations on the pipes. Test sets were cored from pipe samples manufactured using the the following processes:

1. Horizontal centrifugal spinning;
2. Vertical Bi-Di Packerhead VCT, and
3. Automated SCC

All the cores were extracted from the pipe samples between 14 and 21 days from date of manufacture. After extraction the cores wrapped in a damp cloth or paper and placed in plastic bags for delivery to the testing laboratory.

Mix design details for concrete used in pipe manufacture are summarised in Table 1. The testing program was undertaken over a number of phases over a period of time from December 2018 to April 2021.

Table 1: Mix Designs Details of Pipe Test Specimens

Component	Unit	Spun	VCT	Automated SCC
Binder Content	kg/m3	>350	>400	>500
w/b Ratio	-	<0.4	<0.4	≤0.35

Note: Superplasticisers and slump retention admixtures were used in all concretes.

LABORATORY TESTING

The testing was carried out by an independent testing laboratory, with all the testing commencing at an age of 28 days after manufacture.

Water Absorption

The water absorption was carried out in accordance with AS/NZS 4058: 2007 – Appendix F-Absorption test for concrete pipe (Standards Australia/Standards New Zealand 2007). The test is an Industry standard classification and quality control test for precast concrete pipe. It is the only durability parameter test required by AS/NZS 4058: 2007. The test measures the increase in weight of oven dried samples after boiling in water for 5 hours.

Apparent Volume of Permeable Voids (AVPV)

This test was carried out in accordance with AS 1012.21 (Standards Australia 2004). It measures the volume of permeable voids within the concrete by weight increase due to absorption from dried to boiling conditions. Details of the test and how it can be used to assess concrete performance are described in the literature (CIA 2015, CCAA 2009).

Chloride Diffusion and Migration

Chloride diffusion and migration testing were carried out in accordance with Nordtest Build 443 (NordTest 1995) and Nordtest Build 492 (NordTest 1999) test methods respectively. The

former test provides the diffusion rate of chlorides whilst the latter test provides the migration rate of chlorides into the concrete specimen.

Accelerated Carbonation

Accelerated carbonation testing was undertaken to a test was carried out in accordance the independent testing laboratory in-house procedure which is equivalent to the EFNARC method. This test provides a comparative indication of the carbonation rate of the different concrete sample.

Acid resistance

This test was carried out in accordance with the independent testing laboratory in-house method for both 1% and 10% H_2SO_4 acid solutions. Loss measurements were carried out at regular intervals up to 10 and 26 weeks for 10% and 1% H_2SO_4 acid solutions respectively. The test provides a comparative indication of the resistance of the concrete to an aggressive acidic environment.

TEST RESULTS

This testing programme compared the same durability parameters across a range of machine-made manufacturing processes which included:

- Horizontal centrifugal spinning;
- Horizontal roller suspension spinning and
- Vertical Vibrating Core

The upper and lower values of data collected by the Concrete Pipe of Australasia (CPAA) from a testing programme carried out in 2015 and 2016 are included in the detailed results. The test results from the various durability parameters are detailed below.

Water Absorption

Data for concrete samples taken from the different pipes is detailed in Figure 1. As expected, all concretes conform to the requirements of limits set in AS4058 (<6%) and are generally within the range of values derived by the CPAA study that are reflective of concrete currently used in machine-made pipe manufacture.

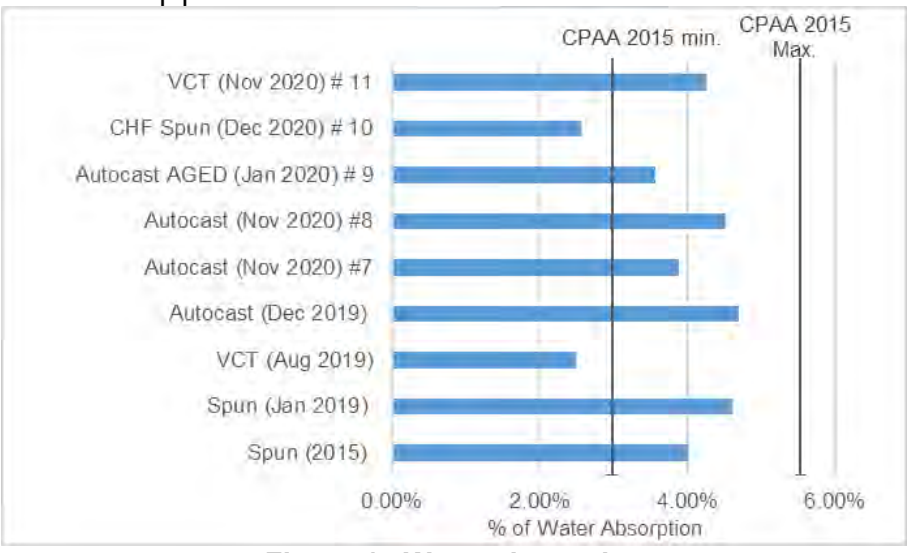

Figure 1. Water absorption.

Apparent Volume of Permeable Voids (AVPV)

Data for AVPV on samples taken from concrete pipes investigated in this study are presented in Figure 2. The most used guidelines for this test are provided in VicRoads Specification 610, which is discussed in Concrete Institute of Australia Recommended Practice Z7-07 (CIA 2015). AVPV performance assessment criteria for structural applications in this specification nominate a maximum value of 14% for cores for concrete having a characteristic compressive strength of 55 MPa.

Data in Figure 2 show that for all pipe concretes investigated results were within a range of 8% to 14%. This is significantly lower than the limit noted. In addition, AVPV data for concrete from the pipes investigated was within the range found in the CPAA study of commercial pipe concrete in 2015.

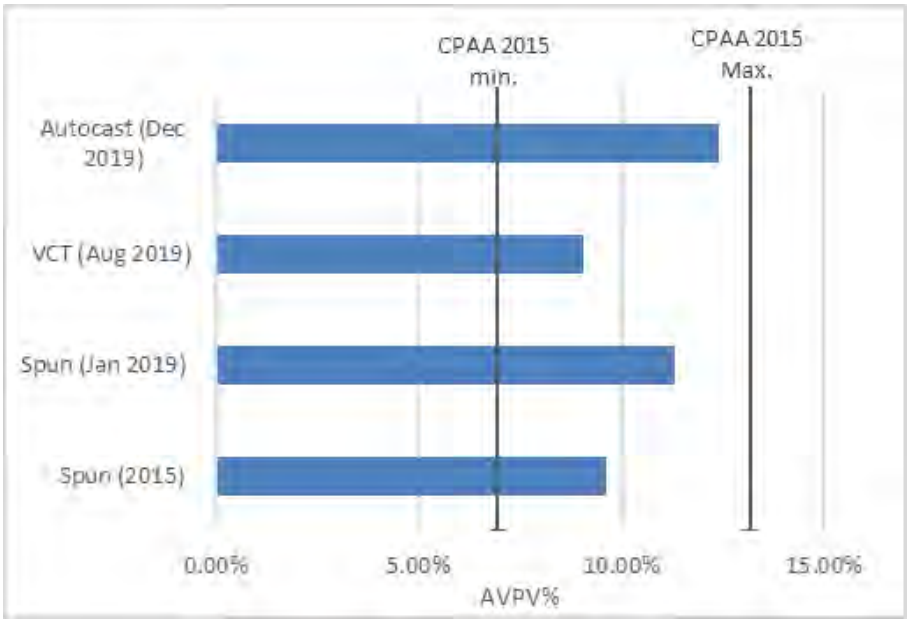

Figure 2. Average volume of permeable voids.

Chloride Diffusion and Migration

The results for both NT Build 443 and 492 are presented in Figures 3(a) and 3(b) respectively. Chloride ingress is not considered critical in a normal environment as defined in Appendix E of AS/NZS 4058: 2007 when the chloride ion concentrations in the soil are < 20 000 ppm (Standards Australia/Standards New Zealand 2007). Chloride diffusion was assessed using the NT Build 443 test method having 35 days of exposure to chloride. This is a very short timeframe for significant levels of chloride to ingress into concrete.

Therefore, given this early age, some variations can be expected in the data (CIA 2015, CCAA 2009). It was found that the difference in the derived chloride diffusion coefficient between spun concrete and the vertical cast concretes is marginal and within the testing error of NT Build 443. Further, the range of chloride diffusion values found in the CPAA study of 2015 were similar to values derived in this study with the exception of two samples. Chloride migration data for the set of pipe concrete investigated in this study were generally lower than those determined for pipes in the CPAA study of 2015.

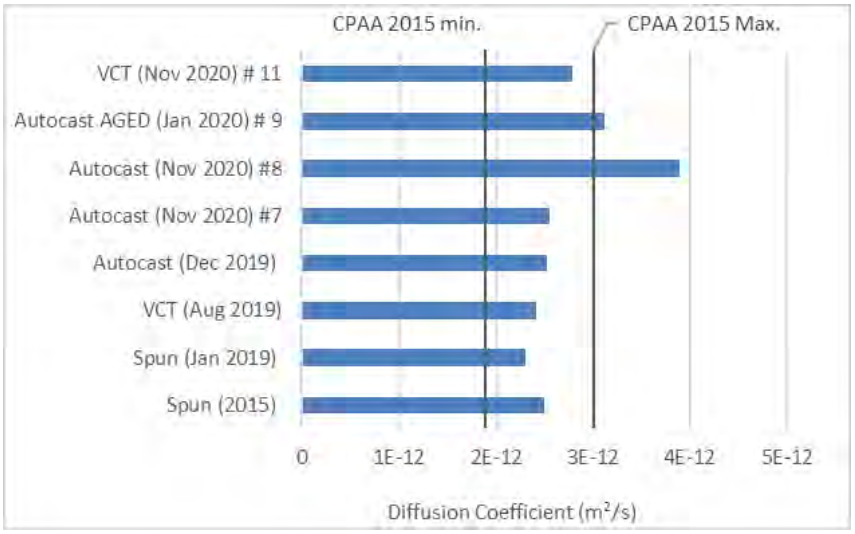

(a) Chloride diffusion (NT Build 443)

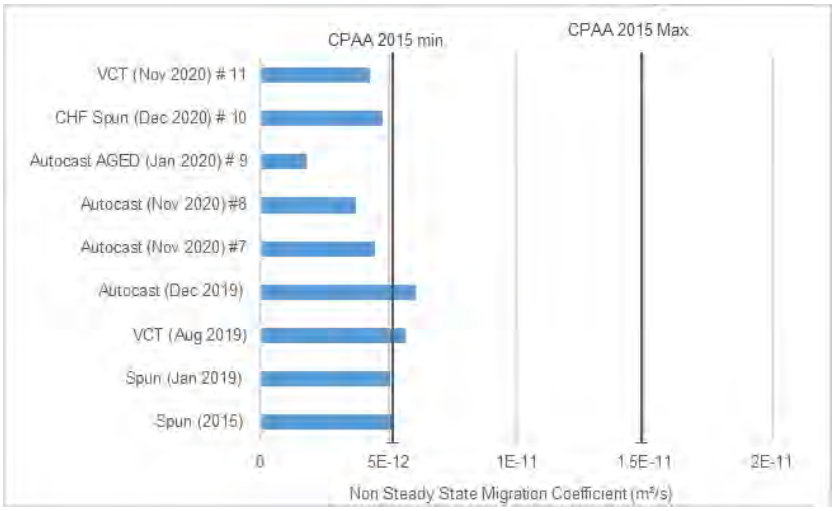

(b) Chloride migration (NT Build 492)

Figure 3. Chloride diffusion and migration.

Accelerated Carbonation

Carbonation testing is undertaken under accelerated conditions and therefore the results are indicative of the relative carbonation rates. Accelerated carbonation testing is highly variable particularly over the short time frame over which the measurements are taken. The accelerated test method is not representative of the actual service conditions of the pipe and cannot be used to directly infer the performance of the pipe in-situ.

Carbonation is generally considered low risk for pipes as carbonation is limited in regions of high humidity typical of the internal and external environments of the pipe. Carbonation is only of concern in arid areas where the internal pipe has long dry periods where carbonation can occur. In Figure 5, data for carbonation for all concretes investigated in this study were relatively low and significantly lower than that derived for concrete in pipes investigated in the 2015 CPAA study, and lower than for 50 MPa cast in-situ concrete.

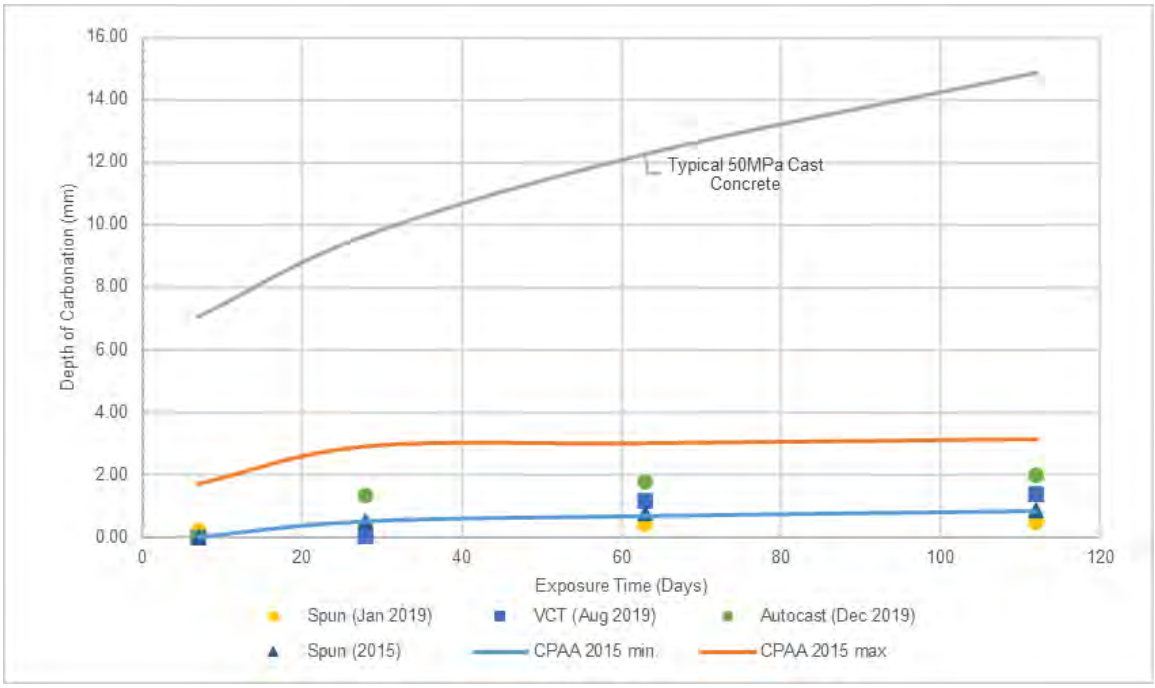

Figure 4. Accelerated carbonation.

Acid Resistance

The resistance of the concrete to acid attack, shown in Figures 5 and 6, provides a comparative assessment of the various concrete compositions associated with the different manufacturing processes. The testing is not related to the resistance of the concrete to acid sulphate soil exposure. The resistance of the concrete to acid sulphate soils is largely based on prescriptive mix requirements. Data in Figures 5 and 6 show that for 1% H_2SO_4 exposure and 10% H_2SO_4 exposure, the difference between spun pipe concrete and AutoCast pipe concrete was similar, and below the values derived from the 2015 CPAA study.

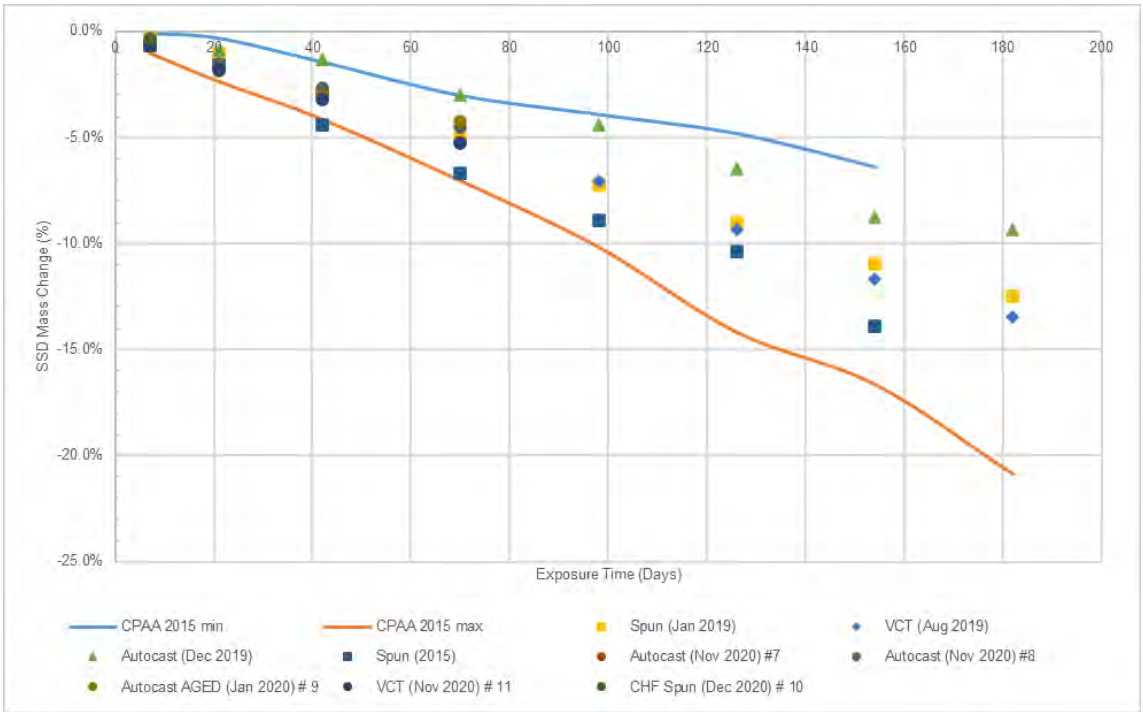

Figure 5. Resistance to 1% H_2SO_4 Exposure.

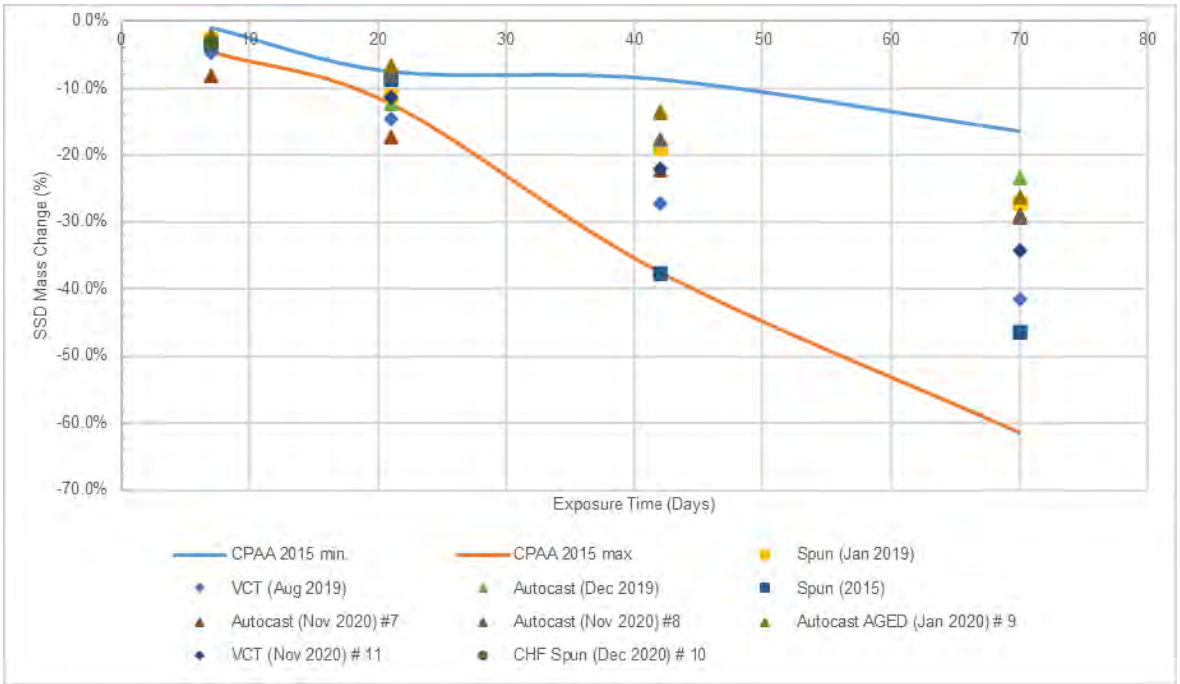

Figure 6. Resistance to 10% H_2SO_4 Exposure.

CONCLUSIONS

This study compared the durability of concrete pipe cores from two machine made manufacturing processes (Spun and Vertical Bi-Di Packerhead) with cores from concrete pipe manufactured using SCC in an automated production process. These results were also benchmarked against similar durability tests results from a CPAA test program which covered a wider range of machine-made concrete pipe. The following test results were compared:

- Water absorption.
- Apparent volume of permeable voids (AVPV);

- Chloride diffusion using Nordtest Build 443;
- Chloride migration using Nordtest Build 492;
- Carbonation, and
- Resistance to Acid Exposure at 1% and 10% concentration.

It is important to note that the tests were performed on cores extracted from actual pipes manufactured, whilst testing samples for standard concretes are generally extracted from laboratory cast cylinders. Therefore, comparisons between data for standard concretes do not necessarily directly compare with that of pipe concrete. However, the results show there is a significant difference between the quality of concrete used to manufacture concrete pipe and that supplied for general structural concrete conforming to NZS 3101 and AS 3600.

The results show that all pipe manufacturing methods reported meet the durability requirements of AS/NZS 4058: 2007. The other durability tests undertaken show comparable results for pipe concrete across all manufacturing processes considered.

ACKNOWLEDGEMENT

The authors thank the Concrete Pipe Association of Australasia (CPAA) for making the data from the 2015 study of machine-made pipe durability available for inclusion in this paper.

REFERENCES

1. Cement Concrete and Aggregates Australia (CCAA), “Chloride Resistance of Concrete”, Report, Available from www.ccaa.com.au, June 2009.

2. Concrete Institute of Australia, “Performance Tests to Assess Concrete Durability”, Concrete Durability Series, Recommended Practice Z7/07, ISBN 978 0 9941738 2 9, Available from www.concreteinstitute.com.au, 2015.

3. Concrete Pipe Association of Australia, “Designing Durable Concrete Pipelines”, Engineering Guideline” Available from www.cpaa.asn.au, Circa, 2007.

4. NordTest, “Concrete, Hardened: Accelerated Chloride Penetration”, NT BUILD 443, Espoo, Finland, 1995.

5. NordTest, “Concrete, Mortar and Cement-Based Repair Materials: Chloride Migration Coefficient from Non-Steady-State Migration Experiments”, NT BUILD 492, Espoo, Finland, 1999.

6. pfeiffer aktuell, Information and Company News, March 1971.

7. Ruffles, A., Matthews, D., Underwood, G. and Degenhardt, G., “New Developments in Concrete Pipe Specification”, Proceedings, Concrete 2017, Concrete Institute of Australia, 28th Biennial Conference, Adelaide, Australia, October 2017.

8. Standards Australia, Australian Standard AS1012 Part 21, "Methods of Testing Concrete – Determination of Water Absorption and Apparent Volume of Permeable Voids in Hardened Concrete", SAI Global, 1999 (R2014).

9. Standards Australia/Standards New Zealand, "Precast Concrete Pipes (Pressure and Non- Pressure)", AS/NZS 4058, ISBN 0 7337 8161 6, SAI Global, 2007.

FIBRE-REINFORCED CONCRETE: A TECHNICAL REFRESHER ON THE APPLICATION AND DESIGN

KYLE HUNDLOE[1]

[1] Master Builders Solutions Pty Ltd Australia. kyle.hundloe@mbcc-group.com

SUMMARY

Reinforcing brittle materials with fibrous material is a practice dating back to ancient times. In recent decades, randomly orientated and discrete fibres - typically of steel or polypropylene – have been used to enhance the plastic and hardened properties of plain or reinforced concrete. Fibres can be used to minimise plastic shrinkage, control bleed, prevent freeze-thaw damage, eliminate explosive spalling, and provide impact and abrasion resistance. Fibre-reinforced concrete also demonstrates ductile failure due to a macrofibres ability to provide post-residual, post-crack flexural strength allowing for the reduction or replacement of conventional temperature and shrinkage reinforcement. This technical paper aids to be an informative refresher on the application, mechanical properties, specification, and design of fibre-reinforced concrete.

INTRODUCTION

Fibre as a reinforcement for brittle materials such as concrete is not a new technology. The first true modern fibre-reinforced concrete composite was asbestos-cement; however, it became evident in the 1960s to 1970s the severe health effects of asbestos (Bentur & Mindess 2007, p. 343). The most common fibres for concrete on the market today are steel and synthetic; The primary synthetic fibres commercially available globally are polypropylene, polyethylene, and polyvinyl alcohol (Pakravan & Ozbakkaloglu 2019, p. 491-518). Of the three, polypropylene (PP) is the most used material due to being hydrophobic (nil water absorption) and alkali resistant (Laning 1992).

Fibres provide an array of benefits to the concrete, ready-mix plants, mines, procurement team, concreters, engineers, and asset owners. Fibres have been promoted as concrete additives to improve the plastic and hardened properties of concrete by minimising shrinkage, controlling bleed water, freeze-thaw damage mitigation, fire safety, impact/abrasion resistance, providing energy absorption, and post-cracking strength (MB Solutions 2022). There is an increasing interest into the benefits provided by steel and synthetic fibres, but they're often met with confusion as to how fibres aid in concrete properties, how to design with structural fibres, and how to specify for concrete mix design or structural usage. This paper aids to clarify how and why the plastic and hardened properties of concrete can improve with the use of fibres, how to specify for inclusion of fibre, and provide an overview of the design method for the ultimate moment capacity of fibre-reinforced concrete in slabs-on-ground.

FIBRE CLASSIFICATION

Macro & micro-synthetic fibres

The European Standard DIN EN 14889-2 divides micro-synthetic fibres into two distinct classes:

- Class Ia: Mono-filamented microfibre with a diameter less than 0.30mm
- Class Ib: Fibrillated microfibre with a diameter less than 0.30mm

Macro-synthetic fibres are defined as Class II fibres in DIN EN 14889-2 and have a diameter greater than 0.30mm.

Class Ia: Forta Econo-Mono (Forta 2022)

Class Ib: MasterFiber F 018 (Hundloe 2022)

Class II: MasterFiber 141 (Hundloe 2022)

Steel fibres

Steel fibres are to conform with DIN EN 14889-1 and can be separated into the following groups:

- Group I: cold-drawn wire
- Group II: cut sheet
- Group III: melt extracted
- Group IV: shaved cold drawn wire
- Group V: milled from blocks

Steel fibres, like macro-synthetic fibres, are commonly used where an increase in residual flexural strength is required.

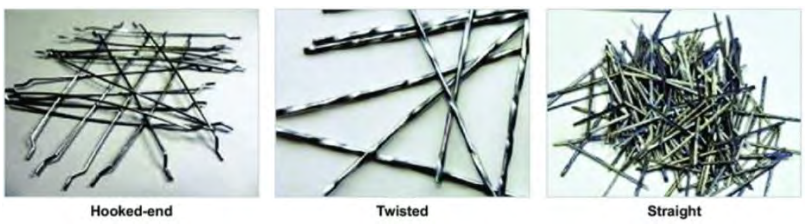

Various steel fibres (Buttignol, Sousa, & Bittencourt 2017)

PLASTIC SHRINKAGE

Plastic shrinkage is caused by the contraction of the concrete during the curing process where the rate of evaporation exceeds the rate of bleeding (Plastic shrinkage cracking 2005, p. 2). Microfibres have been marketed globally as one of the solutions to reducing plastic shrinkage. Mixing class Ia or Ib synthetic fibres at low volume fractions (approximately 0.1 to 0.2%) in concrete disperses the fibre throughout the concrete matrix which has a considerable influence on the plastic shrinkage properties. Naaman, Wongtanakitcharoen, & Hauser (2005) found that the addition of fibre with a diameter less than 40 μm and an aspect ratio greater than 200 will eliminate plastic shrinkage cracking in concrete when dosed at greater than or equal to 0.2% volume fraction. A 2001 plastic shrinkage study (Wang, Shah, & Phuaksuk 2001, p. 458-464) determined that a reduction of 30 to 40% of the total plastic shrinkage crack area was observed when a 0.1% volume fraction of synthetic microfibre was used. Zollo & Hays (1991) theorised that the fibres contribution was by stabilising the matrix and preventing consolidation. Whereas Hamedanimojarrad et al. (2012) proposed that the mechanism for shrinkage reduction was due to the hydrophobic nature of conventional microfibres interrupting moisture transfer from the capillary structure of the matrix minimising moisture loss. Ultimately, the use of fibres for plastic shrinkage prevention is proven and beneficial in compensating for poor finishing and curing practices; when cured and finished properly they play a minimal part as minimal plastic shrinkage should be observed when proper techniques are used (Soroushian, Mirza, & Alhozaimy 1995, p. 553-560).

BLEED CONTROL

‘Bleeding’ in concrete refers to the transfer of free water towards the surface; bleed water can be beneficial, but also problematic when in excess (Goguen 2014). Most fibre technical data sheets, fibre companies, and organisational bodies agree that fibre (particularly microfibre) display better bleed characteristics in the field. However, there is a lack of accessible research data on the topic that concludes the fibre geometry, length, material, and volume fractions effect on concrete bleed.

Goguen discusses that microfibres have been shown to decrease bleed rates due to the control of water migration to the surface while also playing a role in the settlement of fine and coarse particles. Richardson, Coventry, & Wilkinson (2012, p. 49-56) found concrete containing micro fibre exhibited low bleed characteristics. The Concrete Society (2022) states that the addition of 0.9 kg/m^3 of microfibres stabilise the movement of solid particles which blocks bleed water channels, slowing down the rate of bleed and helping to minimise plastic settlement. Zeyad (2020, pp. 4147-4158) found that in a self-compacting concrete containing PP microfibres there was a 75% reduction in bleed water versus plain self-compacting concrete (SCC).

Zeyad found that the addition of hook-end steel fibre, mild steel fibre, and curved steel fibre reduced bleed water by 72%, 56%, and 61% respectively. However, Uygunoglu (2011, p. 766-772) found the opposite in that with an increase in steel fibre dosage there was a proportional increase in bleed water content. From the limited scientific data on the topic, it appears that there is an agreeance on microfibres playing a role in decreasing bleed water rates whereas the role of steel and macro-synthetic fibres is still up for debate.

FREEZE-THAW DURABILITY

Another such way microfibres have been marketed is their ability to increase durability to freeze-thaw cycles. When concrete goes through cycles of freezing and thawing, the moisture within the concrete pores expands by up to 9%, this pressure change over multiple iterations can eventually lead to expansion and cracking (Portland Cement Association 2019). Richardson, Coventry, & Wilkinson (2012, p. 49-56) studied the freeze-thaw effects of a polypropylene fibre reinforced concrete in detail and found that the improvement to freeze-thaw durability was likely due to the microfibres ability to entrain air. The analysis showed that a conventionally air entrained concrete was 76 times more effective versus plain concrete whereas a 0.9 kg/m^3 addition of PP microfibres was 88 times more effective. Within the study it was theorised that the air entrainment came from the microfibres ability to impart low bleed characteristics, producing higher cement paste volumes that eventually dry out leaving behind small voids simulating an air entrained system. The study concluded that a 0.9kg/m^3 addition of microfibre provided a 16% improvement to the durability factor versus air entrained concrete without microfibre.

EXPLOSIVE SPALLING MITIGATION

Impermeable and highly brittle concrete is prone to a phenomenon known as explosive spalling caused by a combination of mechanisms during a fire: pore pressure rising due to increased water evaporating, a thermal gradient in the cross-section, and a difference in material rates of expansion (Gravit & Golub 2018, p. 1-7). Analysis of tests performed by Gravity and Golub (2018) determined that the addition of 6 to 12 mm PP microfibre completely prevented explosive spalling before the onset of the ultimate limit state (extending the limit state by 17 minutes). The study concluded that 1kg/m^3 of PP microfibre increased the fire resistance of the structure by completely preventing explosive spalling during fire exposure. Al-Najjar et al. (2020) outlines that there are two hypothesised mechanisms behind PP microfibres ability to prevent spalling: pressure induced tangential space (PITS) & microcracking mechanism.

Khoury's PITS concept describes the water vapour superseding the PP's contraction as it is melted, pushing between the liquid PP and concrete matrix along the fibre's length. This mechanism relies on an overlapping of the fibres path and thus is likely why performance is seen in PP microfibres with a thickness of 18μm or less. The alternative hypothesized mechanism is the 'microcracking mechanism' proposed by Sullivan (2001) which argues that due to PP's higher frictional heating coefficient versus concrete, microcracks are formed when the PP fibre melts causing a chain reaction creating a fine microcrack network that allows steam to flow to the concrete surface. Khoury also considers Sullivan's hypothesis in that the large difference in thermal expansion causes incredible tensile stresses on the matrix. Saka (2009, p. 510-518) confirmed this tensile stress through finite element analysis that found a considerable amount of stress was caused to a mortar matrix when a single PP fibre was heated to 140ºc. Al-Najjar et al. (2020) concludes that to guarantee an increase in concrete fire performance using fibre, the fibre must be proven to provide such benefits, conform with DIN EN 14889-2 specifications, and that the maximum fibre size shall be 12mm long and 32μm thick (with emphasis on higher performance using 18μm diameter fibre).

IMPACT AND ABRASION RESISTANCE

Yoo and Banthia (2019) hypothesize that the increase in impact resistance of concrete containing fibre is due to the fibre bridging effect at crack surfaces, more effectively absorbing

energy under impact. Yoo and Banthia highlight that this increase in impact resistance is dependant on fibre type and geometry. Mindess and Vondran (1988, p. 109-115) used an instrumented drop-weight impact machine and found that 19mm class Ib microfibres added at a rate of 0.1% to 0.5% increased both the fracture energy and the impact strength of concrete. In a separate study undertaken by Mindess, Yang, and Vondran (1989, p. 545-549) it was found that the inclusion of class Ib fibres in addition to conventional reinforcement increased the impact resistance greater than the sum of the PP fibres and reinforcement considered separately. Manolis et al. (1997, p. 341-349) also found that fibrillated PP fibres in different volume fractions improved the impact resistance proportional to the fibre volume.

The abrasion resistance of concrete is influenced primarily by its compressive strength, with an increase typically requiring a modification to the concrete's water:cement ratio (Concrete NZ, 2022). Shurpali et al. (2017, p. 521-534) found that a 41% and 61% improvement in abrasion resistance was seen by using steel fibres at a volume fraction of 0.5% and 1% respectively. In this study, they concluded that polyfibres were less effective in abrasion resistance however still contributed, maintaining a 10% improvement at a 0.3% addition. The ACI 544.4R committee (1988) reports that in both laboratory and field trials that steel fibre reinforced concrete has enhanced resistance to cavitation forces due to high flowing water and any impact of waterborne debris.

REPLACEMENT OF SECONDARY REINFORCEMENT IN SLABS, PRECAST, AND SHOTCRETE

From a structural perspective, fibres do not typically provide any improvements to modulus of rupture. However, they do provide residual flexural strength and energy absorption which the flexural values can be used in the design of concrete structures such as slabs-on-ground (FRCA 2020). ACI 360R-10 Chapter 11 (2010, p. 40-44) highlights the usage of steel and macro-synthetic fibre as a replacement to conventional shrinkage and temperature steel mesh; macro-synthetic fibre is used in the range of 2 to 9 kg/m^3 whereas steel fibre is used between 20 to 40kg/m^3.

The use of steel and macro-synthetic fibres in precast are used to increase production speed; reduce labour, materials, transport, storage, and remedial costs; reduce element thickness; and provide added durability. A typical precast element suitable for fibres is small precast drainage pits (MRTS273 2020) and cattle troughs. Structural fibres have also been used in larger precast elements such as the precast segment linings used in The Clem Jones Tunnel (Clem 7) in Brisbane, Australia. Microfibres are also commonly used in precast tunnel linings to aid in fire resistance of the lining (Fuente et al. 2013).

Fibres are added to shotcrete as a replacement to the use of steel mesh; they provide a more even distribution of reinforcement through the shotcrete, improve overall economy, simplified logistics, reduce rebound, and aid in compaction. Fibre-reinforced shotcrete also allows the reinforcement to follow uneven substrate profiles more efficiently than conventional mesh. Steel and macro-synthetic fibre's role in shotcrete is primarily the increase in energy absorption they provide allowing for the reduction or replacement of steel mesh. Microfibres can be used in shotcrete, but only aid in plastic shrinkage and rebound reduction (Australian Shotcrete Society 2010).

A recommended method for specifying fibres for post-crack performance in fibre-reinforced concrete:

Steel & macro-synthetic fibres

1. Shall conform with ASTM C1116/C1116M, EN 14889-1, or EN 14889-2
2. Shall provide a minimum average equivalent flexural strength, f_{e3}, of ____ MPa when tested in accordance with ASTM C1609/C1609M or BS EN 14651
3. Dosage shall be recommended by the manufacturer

Several sources provide guidance on the design of steel or macro-synthetic fibre replacing traditional steel for various structures (slabs-on-ground, slabs-on-piles, residential walls, precast, shotcrete). Some example sources are listed below:

- ACI 544.4R-2018: Guide to Design with Fiber-Reinforced Concrete
- ACI 360R-10: Guide to Design of Slabs-on-Ground
- AS 3600-2018, Section 16: Steel Fibre Reinforced Concrete
- Technical Report 34: Concrete Industrial Ground Floors: A guide to design and construction

DESIGN METHOD FOR CONCRETE SLABS REINFORCED WITH STEEL OR MACRO-SYNTHETIC FIBRE

Using yield line theory is one such way to design for concrete slabs-on-ground reinforced with steel or macro-synthetic fibre. The yield line method is based off the work by Meyerhof (1962, p. 89-117) and considers three separate load cases.

Case 1: Central load

$$M_0 = \left(1 + \frac{R_{e3}}{100}\right)\left(\frac{f_r b h^2}{6}\right) \quad \text{(Equation 1)}$$

$$P_o = 6\left(1 + \frac{2a}{L}\right) M_o \quad \text{(Equation 2)}$$

Case 2: Edge load

$$M_0 = \left(1 + \frac{R_{e3}}{100}\right)\left(\frac{f_r b h^2}{6}\right) \quad \text{(Equation 3)}$$

$$P_o = 3.5\left(1 + \frac{3a}{L}\right) M_o \quad \text{(Equation 4)}$$

Case 3: Corner load

$$M_0 = \left(\frac{f_r b h^2}{6}\right) \quad \text{(Equation 5)}$$

$$P_0 = 2\left(1 + \frac{4a}{L}\right) M_0 \quad \text{(Equation 6)}$$

Where:

a = radius of circle with area equal to that of the post base plate (mm)

b = unit width (1 mm)

f_r = concrete modulus of rupture (MPa)

h = slab thickness (mm)

L = radius of relative stiffness (mm) – ACI 360R Section 7.2

$M_o = M_n + M_p$ = negative slab moment + positive slab moment (Nmm)

P_o = ultimate load strength of the slab (N)

R_{e3} = residual strength factor (%)

*ACI 360R-10 recommends that the minimum residual flexural strength (R_{e3}) value be greater than 30%.

Technical Report 34 by The Concrete Society also provides an alternative method to the design of slabs-on-ground, that can be applied to fibre-reinforced concrete that demonstrates strain softening. Assuming the concrete reaches its limiting compressive strain simultaneously with its tensile strain, and assuming that the neutral axis is a constant function of the section depth the following conservative, simplified design method can be followed:

$$\sigma_{r1} = 0.45 f_{R1} \quad \text{(Equation 7)}$$

$$\sigma_{r2} = 0.37 f_{R4} \quad \text{(Equation 8)}$$

$$N \geq T_{2.1} + T_{2.2} \quad \text{(Equation 9)}$$

$$N = 0.078 h f_{ck} \quad \text{(Equation 10)}$$

$$T_{2.1} = 0.88 h \sigma_{r4} \quad \text{(Equation 11)}$$

$$T_{2.1} = 0.44 h (\sigma_{r1} - \sigma_{r4}) \quad \text{(Equation 12)}$$

$$M_u = \frac{h^2}{\gamma_m}(0.29\sigma_{r4} + 0.16\sigma_{r1}) \quad \text{(Equation 13)}$$

Where:

f_{R1} = the residual flexural strength at CMOD 0.5 (MPa) from EN 14651

f_{R4} = the residual flexural strength at CMOD 3.5 (MPa) from EN 14651

h = depth of slab (mm)

f_{ck} = Characteristic compressive cylinder strength (MPa)

γ_m = partial safety factor for materials, concrete with fibre (1.5)

M_u = ultimate moment capacity per m width

Technical Report 34 also provides guidance on fibre-reinforced concrete containing steel reinforcement, a simplified approach can be taken when the area of steel is less than 0.15% of the gross cross-sectional area.

$$N \geq T_1 + T_{2.1} + T_{2.2} \quad \text{(Equation 14)}$$

$$T_1 = A_s E_s \varepsilon_s \leq A_s f_{yk} \quad \text{(Equation 15)}$$

$$M_u = \frac{T_{2.1}}{\gamma_m}\left(\frac{0.877h}{2} + 0.075h\right) + \frac{T_{2.2}}{\gamma_m}\left(\frac{0.877h}{3} + 0.075h\right) + \frac{T_1}{\gamma_s}(d - 0.048h) \qquad \text{(Equation 16)}$$

Where:

A_s = cross-sectional area of reinforcement (mm)

E_s = modulus of elasticity for reinforcing steel (GPa)

E_s = strain in steel

f_{yk} = yield strength of reinforcement (MPa)

γ_m = partial safety factor for reinforcing = 1.15

d = effective depth of reinforcement cross-section

ACI 360R-10 and Technical Report 34 also provide guidance on fibre-reinforced concrete punching shear and other design considerations.

CONCLUSION

Fibre-reinforced concrete is a composite material that has potential benefits over plain or conventionally reinforced concrete. Microfibres help aid in plastic shrinkage reduction, freeze-thaw damage mitigation, and explosive spalling prevention. It is commonly understood that microfibres aid in more finite bleed control, but further research needs to be undertaken to determine if the same can be said for macrofibres. Macrofibre's primary role in concrete is providing residual flexural strength and energy absorption which allows for the partial or complete removal of secondary reinforcement. There are currently multiple reliable sources that provide guidance on the design of fibre-reinforced concrete, with a strong focus on slabs-on-ground.

REFERENCES

ACI Committee 2010, *Guide to design of slabs-on-ground*, *ACI 360R-10*, American Concrete Institute, Indiana USA.

ACI Committee 1988, *Design consideration for steel fibre reinforced concrete, ACI 544.4R-1988*, American Concrete Institute, Indiana USA.

Al-Najjar, A, Sultan, H, Musa, S 2020, 'Polypropylene fibers to resist concrete spalling caused by fire', *TEST engineering and management*, vol. 83, pp. 8914-8924.

Australian Shotcrete Society 2022, *Recommended practice: Shotcreting in Australia*, 2nd edn, Concrete Institute of Australia, Rhodes Australia.

Bentur, A, Mindess, S 2007, *Fibre reinforced cementitious composites*, 2nd edn, Taylor & Francis Group, New York USA.

Buttignol, T, Sousa, J, Bittencourt, T 2017, 'Ultra high-performance fiber-reinforced concrete (UHPFRC): a review of material properties and design procedures, *IBRACON Structures and Materials Journal*, vol. 10, no. 4, pp. 957-971.

Concrete NZ 2022, Concrete NZ Wellington, viewed 22 August 2022, < https://concretenz.org.nz/page/abrasion>.

Department of Transport and Main Roads 2020, *Transport and Main Roads Specifications MRTS273 Fibre-reinforced Concrete*, Queensland Government, Brisbane Australia.

Deutsches Institut fur Normung E.V. (DIN) 2006, *Fibres for concrete – Part 1: Steel fibres – Definitions, specifications and conformity*, DIN EN 14889-1, Deutsches Institut fur Normung E.V. (DIN), Berlin Germany.

Deutsches Institut fur Normung E.V. (DIN) 2006, *Fibres for concrete – Part 2: Polymer fibres – Definitions, specifications and conformity*, DIN EN 14889-2, Deutsches Institut fur Normung E.V. (DIN), Berlin.

Fiber-Reinforced Concrete Association (FRCA) 2020, *Fibers-in-Practice: FAQs*, Fiber-Reinforced Concrete Association, Tennessee USA.

Forta 2022, *Class Ia: Forta Econo-Mono*, image of Forta Econo-Mono, Forta Concrete Fiber, Pennsylvania USA.

Fuente, A, Blanco, A, Pujadas, P, Aguado, A 2013, 'Advances on the use of fibres in precast concrete segmental linnings', *Engineering a concrete future: Technology, modelling & construction*, April 2013, Aviv Israel.

Goguen, C 2014, 'Concrete Bleeding', *Precast Inc. Magazine*, 17 September, viewed 9 September 2022, <https://precast.org/2014/09/concrete-bleeding/>.

Gravit, M, Golub, E 2018, 'Increase of fire resistance of reinforced concrete structures with polypropylene microfibre', *International Scientific Conference on Energy, Environmental and Construction Engineering*, St. Petersburg Polytechnic University, Russia, pp. 1-7.

Hamedanimojarrad, P, Adam, G, Ray, A, Thomas, P, Vessalas, K 2012, 'Development of shrinkage resistant microfibre-reinforced cement-based composites', *Central European Journal of Engineering*, vol. 2, no. 2, pp. 289-295.

Hundloe, K 2022, *Class Ib: MasterFiber F 018*, image of MasterFiber F 018, MB Solutions Pty Ltd, Brisbane Australia.

MB Solutions 2022, *Class II: MasterFiber 141*, image of MasterFiber 141, MB Solutions Pty Ltd, Brisbane Australia.

Khoury, G 2000, 'Effect of fire on concrete and concrete structures', *Progress in structural engineering and materials*, vol. 2, no. 4, pp. 429-447.

Laning, A 1992, *Synthetic fibers*, C920525, Benefits of using synthetic fibres in concrete, The Aberdeen Group, viewed 22 August 2022, < https://www.concreteconstruction.net/how-to/repair/synthetic-fibers_o>.

Manolis, G, Gareis, P, Tsonos, A, Neal, J 1997, 'Dynamic properties of polypropylene fiber-reinforced concrete slabs', *Cement and Concrete Composites*, vol. 19, no. 4, pp. 341-349.

MB Solutions 2022, *MasterFiber*, MB Solutions Pty Ltd, viewed 6 August 2022, < https://www.master-builders-solutions.com/en-au/products/masterfiber>.

Meyerhof, G 1962, 'Load-carrying capacity of concrete pavements', *Journal of the soil mechanics and foundations division*, ASCE, June, pp. 89-117

Mindess, S, Vondran, G 1988, 'Properties of concrete with fibrillated polypropylene fibres under impact loading', *Cement and Concrete Research*, vol. 18, no. 1, pp. 109-115.

Mindess, S, Yang, C, Vondran, G 1989, 'Impact resistance of concrete containing both conventional steel reinforcement and fibrillated polypropylene fibres', *ACI Materials Journal*, vol. 86, pp. 545-549.

Naaman, A E, Wongtanakitcharoen, T, Hauser, G 2005, 'Influence of different fibers on plastic shrinkage cracking of concrete', *ACI Materials Journal*, vol. 102, no. 1, pp. 49-58.

Pakravan, H, Ozbakkaloglu, T 2019, 'Synthetic fibers for cementitious composites: A critical and in-depth review of recent advances', *Construction and Building Materials*, vol. 207, pp. 491-518.

Plastic shrinkage cracking 2005, Compact look into plastic shrinkage cracking by the CCAA, Cement Concrete & Aggregates Australia, St Leonards NSW, viewed 22 August 2022, <https://www.ccaa.com.au/documents/Library%20Documents/CCAA%20Datasheets/DS2005PlasticShrinkageTBR.pdf>.

Portland Cement Association 2019, *Freeze-thaw resistance*, Portland Cement Association, Skokie Illinois, viewed 24 August 2022, <https://www.cement.org/Learn/concrete-technology/durability/freeze-thaw-resistance>.

Richardson, A, Coventry, K, Wilkinson, S 2012, 'Freeze/thaw durability of concrete with synthetic fibre additions', *Cold Regions Science and Technology*, vol. 83-84, pp. 49-56.

Saka, T 2009, 'Spalling potential of fire exposed structural concrete', *Proceedings of 1st International Workshop on Concrete Spalling due to Fire Exposure*, Leipzig Germany, pp. 510-518

Shurpali, A, Edwards, J, Kernes, R, Lange, D, Barkan, C 2017, 'Improving the abrasion resistance of concrete to mitigate concrete crosstie rail seat deterioration (RSD)', *Materials Performance and Characterization,* vol. 6, no. 1, pp. 521-534.

Soroushina, P, Mirza, F, Alhozaimy, A 1995, 'Plastic shrinkage cracking of PP fiber reinforced concrete', *ACI Materials Journal*, vol. 92, pp. 553-560.

Sullivan, P 2001, 'Deterioration and spalling of high strength concrete under fire', *Report for UK Health and Safety Executive*, City University London.

The Concrete Society 2016, *Concrete Industrial Ground Floors: A guide to design and construction Technical Report 34*, The Concrete Society, Surrey UK.

The Concrete Society 2022, Concrete at your fingertips: *Polypropylene micro-fibres*, The Concrete Society, Surrey UK, viewed 27 August 2022, < https://www.concrete.org.uk/fingertips-nuggets.asp?cmd=display&id=550>.

Uygunoglu, T 2011, 'Effect of fiber type and content on bleeding of steel fiber reinforced concrete', *Construction and Building Materials*, vol. 25, no. 2, pp. 766-772.

Wang, K, Shah, S, Phuaksuk, P 2001, 'Plastic Shrinkage Cracking in Concrete Materials – Influence of Fly Ash and fibers', *ACI Materials Journal*, vol. 98, no. 6, pp. 458-464.

Yoo, D, Banthia, N 2019, 'Impact resistance of fiber-reinforced concrete – A review', *Cement and concrete composites*, vol. 104.

Zollo, R, Hays, C 1991, ‘Fibers vs. WWF as non-structural slab reinforcement’, *Concrete International*, vol. 13, no. 11, pp. 50-55.

concretenz BUILDING RESILIENCE
CONFERENCE 2022
13-15 October 2022
Energy Events Centre | Rotorua

CARBONATION RESISTANCE FACTOR FOR CONCRETE

VINEET SHAH[1], ALLAN SCOTT[1], JAMES MACKECHNIE[2]

[1] Department of Civil and Natural Resources Engineering, University of Canterbury, NZ
[2] Concrete NZ

SUMMARY

Clinker factor, binder type, temperature, CO_2 concentration, relative humidity and water to binder ratio are the key parameters that influence the rate of diffusion of CO_2 and carbonation of concrete. Although individually the effect of these parameters has been clearly established, it is difficult to represent the rate of carbonation of different concrete mixes through one single parameter. In this study, concrete mixes were prepared using 4 different SCMs at the same replacement level (30%). Concrete samples were placed in accelerated carbonation conditions for 56 days. The extent of carbonation was compared against concrete properties (porosity, oxygen permeability, resistivity and compressive strength) measured after 28 days of curing. None of the conventional concrete properties showed a compelling relationship with carbonation depth. However, a carbonation resistance factor was postulated using concrete resistivity, porosity and cement content, which exhibits a reasonable correlation with the extent of carbonation.

INTRODUCTION

Carbonation induced corrosion is one of the major cause for deterioration of reinforced concrete structures (Richardson 2002). The continual efforts to improve the sustainability quotient of the cement industry has led to increased usage of supplementary cementitious materials (SCMs) (Lothenbach et al. 2011; UN Environment et al. 2018). The carbonation resistance of SCM incorporated concrete is generally lower as compared to conventional Portland cement (PC) concrete because of dilution effect (overall lower amount of PC) and pozzolanic reaction (consumption of calcium hydroxide (CH) by SCM) (Panesar and Zhang 2020; Šavija and Luković 2016; Shah and Bishnoi 2019; Sisomphon and Franke 2007). The clinker factor, SCM type, environmental condition (temperature, relative humidity and CO_2 concentration) and concrete mix design primarily govern the rate of progress of carbonation in concrete (Leemann et al. 2015; Otieno et al. 2020; Shah and Bishnoi 2018).

Different SCMs exhibits different carbonation performance even at a same clinker factor. The calcium-rich SCMs like slag and Class C fly ash show better carbonation resistance as compared to other SCMs like Class f fly ash, pumice, clay, etc. due to the additional CO_2 buffering capacity provided by calcium present in the SCM (Ribeiro et al. 2018; Shah et al. 2020; Shi et al. 2009). The carbonation resistance of non/low-calcium SCM concrete differs from one another even at the same cement content/clinker factor. The reason for the deviation in the carbonation performance is not well understood. A higher reactive SCM tend to consume more CH due to the pozzolanic reaction, however, which does not necessarily imply the carbonation performance of the system would be inferior due to lower buffering capacity. (Tavares et al. 2020) showed better carbonation resistance for silica fume mix as compared to

quartz powder mix that had a higher amount of CH available at the cement replacement level. Similarly, (Shi et al. 2016) reported an overall lower extent of carbonation in metakaolin substituted cement as compared to limestone substituted cement despite with higher CO_2 binding capacity i.e. higher calcium hydroxide content in the hydrated sample. This indicates that the amount of CH available in the hydrated system is not the only governing factor that affects the rate of carbonation in concrete. The higher carbonation resistance of silica fume (Tavares et al. 2020) and metakaolin (Shi et al. 2016) mixes could be attributed to the denser and refined microstructure, which restricts the diffusion/ingress of CO_2. The extent of modification occurring in the microstructure depends on the magnitude of pozzolanic reaction of SCM and type of hydration products formed thus affecting the movement of CO_2 (Dhandapani and Santhanam 2020). Few studies have tried establishing a relation between physical and transport parameters of concrete with the rate of carbonation (Leemann et al. 2015; Salvoldi et al. 2015; Shah and Bishnoi 2018). However, the correlation is not general and limited to a particular binder type.

The aim of this study is to understand the relationship between the rate of carbonation and different transport properties of concrete. In this investigation four different SCMs were selected to prepare concrete samples at a same cement replacement level of 30%.

MATERIALS AND EXPERIMENTS

Fly ash, pumice, perlite and kaolinite clay were the four SCMs used in the study, all sourced from within New Zealand. The general purpose cement used in the study was obtained from Golden Bay Cement, New Zealand. The kaolinite clay was calcined at a temperature of 800 °C for two hours in a static furnace. Subsequently, the perlite and clay were ground to fine powder using a rod mill. River sand and river gravel with a nominal sizes of 4.75 mm and 12 mm respectively were used to prepare concrete. Superplasticizer was used to obtain a consistent slump of 140±20 mm across different concrete mixes. Table 1 summarizes the concrete mix design.

Table 1: Details of concrete mix design

Notations	PC-1	Fly Ash	Pumice	Perlite	Clay-1
Cement (kg/m^3)	350	245	245	245	245
SCM (kg/m^3)	0	105	105	105	105
Fine Aggregate (kg/m^3)	835	805	805	805	805
Coarse Aggregate (kg/m^3)	1100	1100	1100	1100	1100
Water (kg/m^3)	160	160	160	160	160
Admixture (L/m^3)	1.8	1.4	2.0	2.0	2.2
Slump (mm)	140	150	150	130	120

Cylinders of 100 mm × 200 mm were cast for the measurement of compressive strength, carbonation and transport properties. The cylinders were demoulded 24 hours after casting and were subsequently placed in a curing tank maintained at 20 °C for 28 days. After the end of the curing regime, the two cylinders were preconditioned at 65% relative humidity and 20 °C for 7 days. The preconditioned cylinders were placed in an environmental chamber for accelerated carbonation study (2.5% CO_2, 20 °C temperature and 60% relative humidity). The carbonation depth was measured after 14, 28 and 60 days of exposure using the phenolphthalein indicator test (Rilem CPC-18 1988). The compressive strength was measured after the end of the 28 days curing period using an automatic compression testing machine with a load capacity of 3000 KN. The porosity, oxygen permeability and resistivity of the concrete mixes were determined using disc specimens (30 mm thick) obtained from slicing the 28 days cured concrete cylinders. The porosity and oxygen permeability tests were carried out in accordance with South African Durability Index tests (Beushausen and Alexander 2008). For resistivity measurements, the disc specimens were saturated with 3% salt solution in order to ensure similar ion concentrations in the pore solution of different concrete mixes. The saturated disc specimens were placed between electrodes and a voltage of 250 mV was applied to measure the current, which was used to compute the resistivity values.

RESULTS

The extent of carbonation was higher in SCM incorporated concrete as compared to control PC concrete. Although the cement content in all the SCM incorporated concrete mixes was the same, the rate of carbonation was significantly different. Table 2 summarizes the carbonation coefficient of different concrete mixes.

Table 2: Summary of the carbonation coefficient of the concrete mixes

Concrete Mixes/Concrete Properties	Carbonation Coefficient ($mm/year^{1/2}$)
PC	8.4
Fly ash	25.4
Pumice	22.9
Perlite	38.2
Clay	20.1

In general, the higher the porosity of the concrete faster is the rate of carbonation due to the availability of overall higher pore volume for the diffusion of CO2. Figure 1 compares the relation between porosity and carbonation coefficient of concrete mixes investigated in this study. The rate of carbonation was higher for more porous concrete, however, the trend was not consistent with all the mixes.

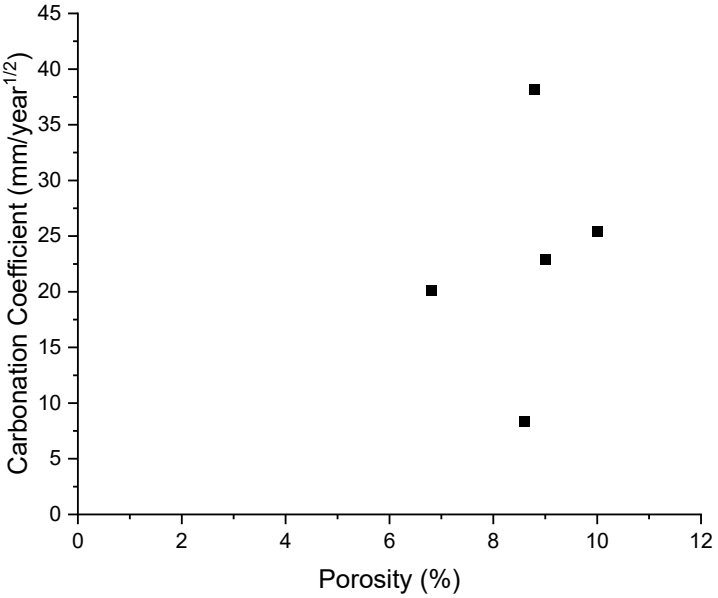

Figure 1: Relation between porosity and carbonation coefficient

A high resistivity or a low permeability value of concrete indicates a presence of denser/refined pore structure that could hinder the diffusion of CO2 (Garboczi 1990; Sengul 2014). Figures 2 and 3 compare the relation between permeability and resistivity respectively with the rate of carbonation. No obvious trend was observed between the two transport parameters and the rate of carbonation. The results imply that a low permeability or high resistivity of concrete does not necessarily result in a reduction in the rate of carbonation.

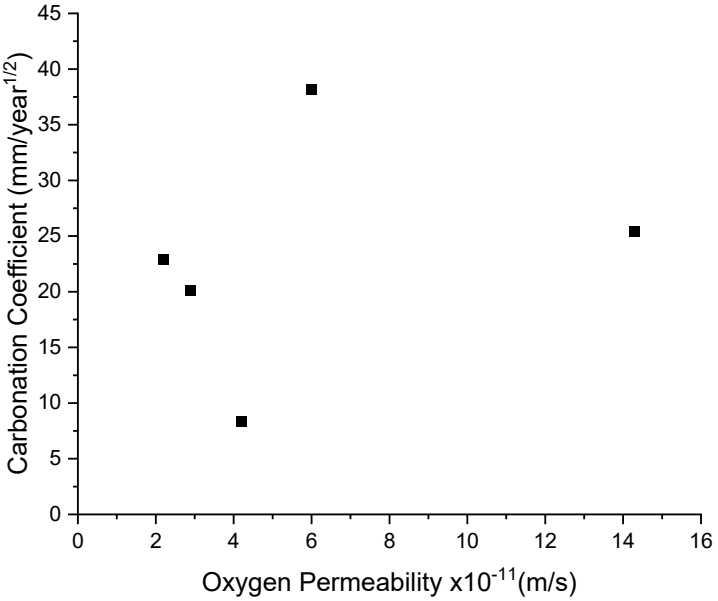

Figure 2: Relation between oxygen permeability and carbonation coefficient

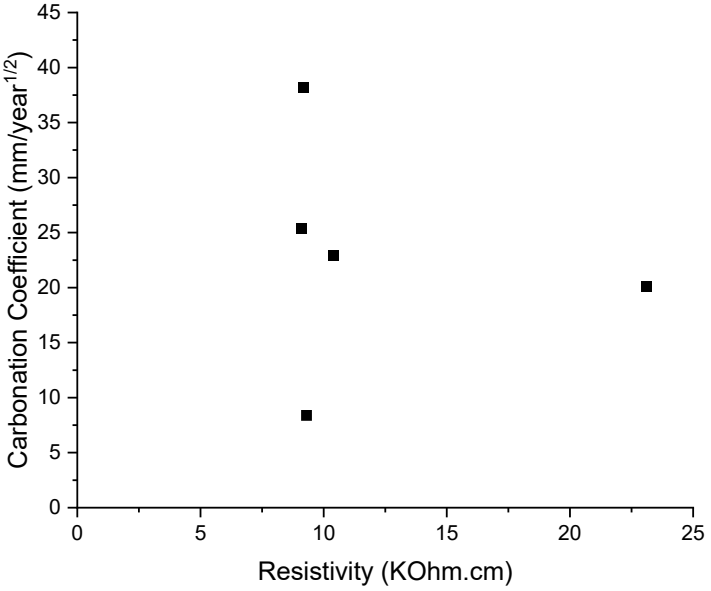

Figure 3: Relation between resistivity and carbonation coefficient

The rate of diffusion of CO2 in concrete is influenced by both the total porosity and size/interconnectedness of pores. Individually porosity and resistivity fails to provide a parameter that could be used to describe the deviation in the rate of carbonation between different concrete mixes. In addition, the carbonation coefficient of PC concrete is significantly lower as compared to SCM mixes due to its higher cement content providing higher CO2 buffering capacity. The above inferences indicate that it is necessary to consider both the cement content and pore structure (porosity and connectivity) simultaneously to develop an effective relation to describe the rate of carbonation for different concrete mixes.

The tortuosity in a concrete system could be described using electrical measurements which indicates the diffusive pathway of an ion (Dhandapani and Santhanam 2020). The electrical tortuosity can be estimated using Equation 1.

$$\tau = \left(\frac{\emptyset \times \sigma_o}{\sigma}\right)^{\frac{1}{2}} \quad (1)$$

where τ is the tortuosity, $\emptyset$ is the porosity, σ is the bulk conductivity of the concrete and σ_o is the conductivity of the pore solution. The reciprocal of electrical resistivity of concrete corresponds to the bulk conductivity value of concrete. The conductivity of the pore solution is the same as the salt solution conductivity as it was used to saturate the concrete specimens for resistivity measurement (44 S/m). The tortuosity factor takes into account both the porosity and connectivity characteristics of pore structure, however, it does not include a parameter that could account for CO2 buffering capacity.

Hence, in this study, the authors propose a “carbonation resistance factor” that captures all the aspects needed to describe the rate of carbonation. The proposed carbonation resistance factor is defined below (Equation 2):

$$Carbonation\ resitance\ factor: Cement\ content\ (kg/m^3) \times \tau \quad (2)$$

Figure 4 compares the relation between the proposed carbonation resistance factor and carbonation coefficient for all the mixes. The higher the carbonation resistance factor lower is the rate of the carbonation. The observed relation is best among all the other relations investigated in this study. Moreover, the carbonation resistance factor helps in clearly discerning the carbonation performance of different SCMs along with the PC control mix.

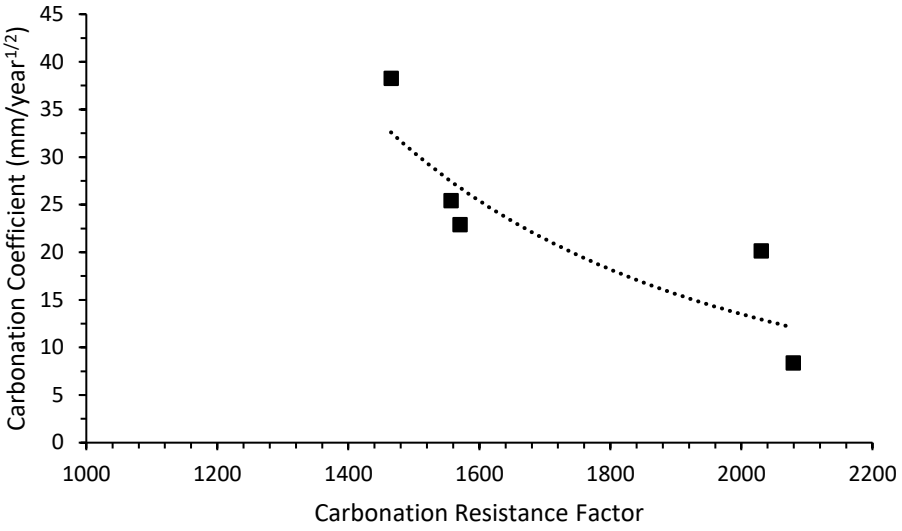

Figure 4: Relation between carbonation resistance factor and carbonation coefficient

CONCLUSIONS

The objective of this study was to understand which transport parameter of concrete could be used to describe the rate of carbonation in concrete. None of the usual transport parameters (porosity, permeability and resistivity) of concrete was able to elucidate the carbonation performance of concrete containing different SCMs. A carbonation resistance factor is proposed in the study, which takes into consideration both the chemical and physical parameters of concrete to effectively describe the rate of carbonation. The proposed factor provides an easy way to compare carbonation resistance of different SCMs using relatively simple laboratory tests. It is important to validate the study with larger data set (more number of SCMs, different concrete mixes, etc.) to demonstrate its applicability on a wider scale.

ACKNOWLEDGEMENTS

The authors would like to acknowledge BRANZ and Concrete NZ for providing the financial support.

REFERENCES

Beushausen, H., and Alexander, M. G. (2008). “The South African durability index tests in an international comparison.” *Journal of the South African Institution of Civil Engineering*, 50(1), 25–31.

Dhandapani, Y., and Santhanam, M. (2020). “Investigation on the microstructure-related characteristics to elucidate performance of composite cement with limestone-calcined clay combination.” *Cement and Concrete Research*, Elsevier, 129(December 2019), 105959.

Garboczi, E. J. (1990). “Peremeability, diffusivity, and microstructural parameters: A critical review.” *Cement and Concrete Research*, 20, 591–601.

Leemann, A., Nygaard, P., Kaufmann, J., and Loser, R. (2015). “Relation between carbonation resistance, mix design and exposure of mortar and concrete.” *Cement and Concrete Composites*, 62, 33–43.

Lothenbach, B., Scrivener, K., and Hooton, R. D. (2011). “Supplementary cementitious materials.” *Cement and Concrete Research*, 41(12), 1244–1256.

Otieno, M., Ikotun, J., and Ballim, Y. (2020). “Experimental investigations on the effect of concrete quality, exposure conditions and duration of initial moist curing on carbonation rate in concretes exposed to urban, inland environment.” *Construction and Building Materials*, Elsevier Ltd, 246, 118443.

Panesar, D. K., and Zhang, R. (2020). “Performance comparison of cement replacing materials in concrete: Limestone fillers and supplementary cementing materials – A review.” *Construction and Building Materials*, Elsevier Ltd, 251, 118866.

Ribeiro, A. B., Santos, T., and Gonçalves, A. (2018). “Performance of concrete exposed to natural carbonation: Use of the k-value concept.” *Construction and Building Materials*, Elsevier Ltd, 175, 360–370.

Richardson, M. G. (2002). *Fundamentals of durable reinforced concrete*. Taylor & Francis, London and New York.

Rilem CPC-18. (1988). “Measurement of hardened concrete carbonation depth.” *Materials and Structures*, 21(6), 453–455.

Salvoldi, B. G., Beushausen, H., and Alexander, M. G. (2015). “Oxygen permeability of concrete and its relation to carbonation.” *Construction and Building Materials*, 85, 30–37.

Šavija, B., and Luković, M. (2016). “Carbonation of cement paste: Understanding, challenges, and opportunities.” *Construction and Building Materials*, 117, 285–301.

Sengul, O. (2014). “Use of electrical resistivity as an indicator for durability.” *Construction and Building Materials*, Elsevier Ltd, 73, 434–441.

Shah, V., and Bishnoi, S. (2018). “Carbonation resistance of cements containing SCMs and its realtion to various parameters of concrete.” *Construction and Building Materials*, 178, 219–232.

Shah, V., and Bishnoi, S. (2019). “Carbonation performance of OPC-SLAG-fly ash binder system.” *Indian Concrete Journal*, 93(4).

Shah, V., Parashar, A., Medepalli, S., and Bishnoi, S. (2020). “Prediction of carbonation with reactivity test methods for pozzolanic materials.” *Advances in Cement Research*, 32(7).

Shi, H. sheng, Xu, B. wan, and Zhou, X. chen. (2009). “Influence of mineral admixtures on compressive strength, gas permeability and carbonation of high performance concrete.” *Construction and Building Materials*, Elsevier Ltd, 23(5), 1980–1985.

Shi, Z., Lothenbach, B., Geiker, M. R., Kaufmann, J., Leemann, A., Ferreiro, S., and Skibsted, J. (2016). “Experimental studies and thermodynamic modeling of the carbonation of Portland cement, metakaolin and limestone mortars.” *Cement and Concrete Research*, 88, 60–72.

Sisomphon, K., and Franke, L. (2007). “Carbonation rates of concretes containing high volume of pozzolanic materials.” *Cement and Concrete Research*, 37(12), 1647–1653.

Tavares, L. R. C., Junior, J. F. T., Costa, L. M., da Silva Bezerra, A. C., Cetlin, P. R., and Aguilar, M. T. P. (2020). “Influence of quartz powder and silica fume on the performance of Portland cement.” *Scientific Reports*, Nature Publishing Group UK, 10(1), 1–15.

UN Environment, Scrivener, K. L., and John, V.M. and Gartner, E. M. (2018). “Eco-efficient cements: Potential, economically viable solutions for a low-CO2 cement based industry.” *Cement and Concrete Research*, 114, 64.

SESSION 3

Chair:
Dave McGuigan

concretenz BUILDING RESILIENCE
CONFERENCE 2022
13-15 October 2022
Energy Events Centre | Rotorua

STRENGTH CLASSIFICATION AND DURABILITY OF CONCRETE MADE FROM INDUSTRIAL OR NATURAL SUPPLEMENTARY CEMENTITIOUS MATERIALS

JAMES MACKECHNIE [1,2], VINEET SHAH [2] AND ALLAN SCOTT [2]

[1] Concrete NZ, [2] University of Canterbury

SUMMARY

Predicting the performance of concrete made with supplementary cementitious materials (SCMs) is required to improve confidence using these materials by designers and suppliers. This research investigated classification and performance of concrete containing natural and industrial pozzolans. SCMs investigated in this research included Class C and F fly ash, silica fume, perlite, natural pozzolan and calcined clay. The current classification method AS 3583.6 measures the relative strength of mortar mixes and is primarily a screening test for identifying materials of high-water demand and/or low reactivity. Findings from this research showed that predictions of strength performance of SCM concrete could be significantly improved using either modified strength activity testing, isothermal calorimetry or bound water from thermo-gravimetric analysis. Durability performance of concrete made with these SCMs is also presented including chloride resistance, carbonation, alkali silica reaction, permeability, resistivity and porosity. Concrete made with natural pozzolans or calcined clay showed reasonable strength performance and good durability that is comparable with established SCMs such as fly ash and slag.

INTRODUCTION

In New Zealand there has been a 15% reduction in carbon emissions associated with Portland cement production since 2005 despite concrete production increasing by 13% during the same period [1]. This has been achieved by better process efficiencies at existing cement factories and by replacing less efficient production facilities. Kiln efficiency at local cement factories has been achieved by utilising waste materials such as biomass and tyres that reduce coal consumption and by adopting advanced process control measures.

Combining the good practices in cement kiln efficiency and process control with better use of SCMs could reduce NZ carbon emission by a further 15% by 2030. Achieving this target will require a better understanding of how industrial and natural SCMs can be best used in concrete construction. SCMs are either sourced from industrial wastes such as fly ash, ground granulated blast-furnace slag (GGBS) and silica fume or from natural materials that are beneficiated into pozzolans such as pumicite, micro-silica, diatomite and calcined clays such as metakaolin. SCMs have diverse chemical and physical properties that affects their reactivity and interaction with PC [2]. The range of chemical compositions of cementitious materials is shown in Figure 1 below.

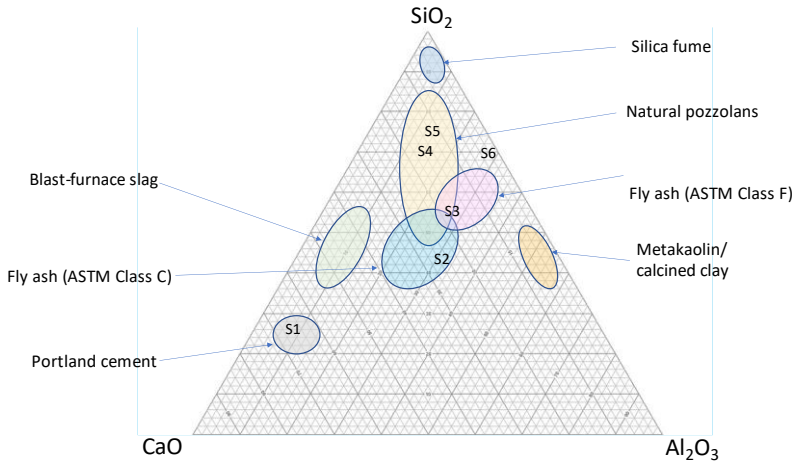

Figure 1: Ternary diagram showing chemical composition of Portland cement and SCMs

SCMs made from industrial waste such as fly ash, GGBS or silica fume are widely used in countries with a strong industrial base where these waste materials are generated. These materials have been used in concrete for more than 50 years and performance of blended cements in concrete is well understood although characterisation techniques are improving with better understanding.

Natural pozzolans are primarily alumino-silicates or amorphous silica that react with hydroxyl ions in concrete to produce secondary pozzolanic reactions. Four main types of natural pozzolan may be defined and found in New Zealand [3]:

- Volcanic glass deposits of pyroclastic origin that includes non-consolidated volcanic ash and pumice with variable pozzolanic activity depending on their siliceous content and fineness (e.g. pumice and volcanic ash)
- Amorphous silica from either biogenic or hydrothermal activity that form relatively soft clastic rock types such as diatomite or amorphous silica deposits (e.g. diatomaceous earth and amorphous silica)
- Zeolites produced by lithification of volcanic glass deposits that are partially transformed from amorphous to crystalline but still retains pozzolanic activity due to their microporous nature (e.g. tuffs and ignimbrite)
- Clay minerals such as bentonite or kaolinite that are very mildly reactive but can be made significantly more reactive when calcined at 700-800 ^{0}C (e.g. metakaolin or calcined clays)

The geology of New Zealand has significant resources of natural pozzolans and clay minerals, including [4]:

- Pumice deposits that can be ground to form pumicite that has been shown to have similar reactivity to that of fly ash
- Amorphous silica in the Rotorua region that have in the past been able to provide very high reactivity similar with silica fume
- Tuff and ignimbrite resources that are widespread and have reasonable reactivity as SCMs by being partially amorphous and microporous
- Kaolin deposits that when contaminated with iron and/or magnesium cannot be used as pigments and fillers but could theoretically be activated at moderate temperatures (e.g. 700 ^{0}C) to form metakaolin

- Other reactive silica sources such as diatomaceous earth that have shown promise when tested in the 1980's and 1990's but may be difficult to extract due to concerns about silica dust

New Zealand geological resources are well documented 60 years ago by DSIR [5]. Kennerley and Clelland from NZ DSIR investigated a wide range of natural pozzolans including rhyolite, pumicite, ignimbrite, andesite tuff and basaltic tuff. This early testing included petrographic examination, chemical analysis, mortar and concrete tests of blends of cement and pozzolan. Reactivity of natural pozzolans in New Zealand was found to increase with fineness and glass content as shown in Figure 2 below.

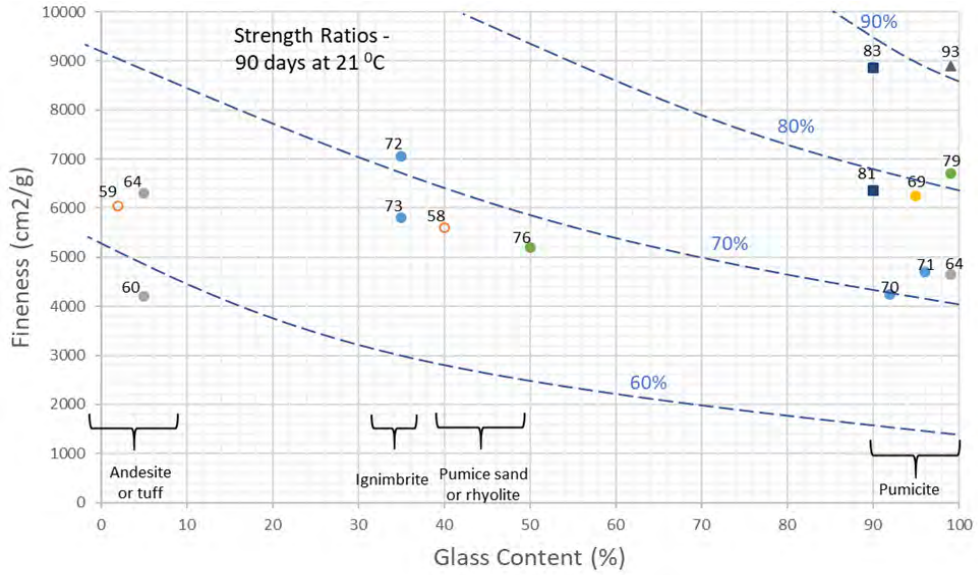

Figure 2: Strength ratios of mortar made with 35% replacement of natural pozzolans [5]

CHARACTERISATION OF SCMs

The quality of Portland cement is characterised primarily by the strength performance of mortar or concrete samples made from the material. The chemical and physical properties of Portland cement have a significant bearing on this hardened performance and modern cements tend to fall within a narrow range and the cement hydration reaction is predictable giving reliable and repeatable results. When SCMs are considered using a similar classification system, performance of concrete becomes more difficult to predict. The poorer correlation between strength activity index testing and concrete strength for SCM concrete is due to the following [6]:

- Portland cement has consistent density values whereas SCMs may be considerably lighter than cement such that replacement levels should not be based on weight but volume
- Classification tests are generally done on mortar mixes where no chemical admixtures are used to compensate for the higher absorption of some pozzolanic materials, which leads to variable water/binder ratios
- Testing age is typically at 28 days, which tends to favour more reactive SCMs and often means that more slowly reactive natural pozzolans are excluded
- Mortar cubes are cast at relatively lower consistence levels that means that some binder combinations are difficult to compact and result in excess void contents in hardened mortar

MATERIALS AND EXPERIMENTAL

An experimental program was developed in 2020 to investigate how best to utilise SCMs in concrete construction, with the following research objectives [7]:

- Better classification systems for potential SCMs to complement existing methods
- Assessing fresh properties of SCM concrete including bleed, setting and workability
- Strength development and durability performance of SCM concrete
- Benchmarking of typical performance using industrial SCMs such as fly ash or slag

To undertake this experimental work the following materials were investigated and provided a wide range of reactivity and performance (see also Figure 3):

- Two sources of GP cement for standard concrete mixes
- Two sources of HE cement for higher strength mixes
- Two types of fly ash (ASTM Class F and Class C)
- Blast-furnace slag from Australia
- Perlite and natural pozzolana from New Zealand
- Calcined clay using moderate grade kaolinite (55%) from New Zealand

HYDRATION STUDIES

Characterization of PC and SCMs used in this research are shown in Table 1 and 2 where physical characteristics and chemical composition are summarised. Details of other properties such as XRF, TGA and binder calorimetry are given in the SCM final report published by Concrete NZ [8].

Table 1: Characterisation of Portland cements and SCMs (GBC & Holcim cement)

Symbol/ Name	**S1 GP**	**S2 FAG**	**S3 FAH**	**S4 PM**	**S5 PL**	**S6 CC**	**S7 SF**	**S8 HE**
Description	Portland cement	Huntly fly ash	Adani fly ash	Natural pozzolan	Perlite	Calcined clay	Silica fume	Portland cement
Processing of material	As received	As received	As received	As received	Milled to powder	Milled & calcined	As received	As received
Blaine fineness (m^2/kg)	350 325	426	279	595	133*	1445	19.4 m^2/g BET	500 445
S.G.	3.17 3.15	2.72	2.65	2.56	2.39	2.83	2.20	3.15 3.15

Note: Slag denoted SD (GGBS) was added to this research but was used as a General Blended (GB) cement

Table 2: XRF oxide analysis of Portland cements and SCMs

Compound	**S1**	**S2**	**S3**	**S4**	**S5**	**S6**	**S7**	**S8**
CaO	64.10	21.98	14.65	4.46	0.91	0.21	0.43	0.27
SiO_2	21.04	36.64	42.15	70.43	74.56	66.20	91.55	94.85
Al_2O_3	3.80	15.73	18.71	13.02	12.17	26.70	0.71	0.57
Fe_2O_3	2.63	13.02	11.39	2.52	2.18	2.13	2.45	0.33
SO_3	2.46	0.91	0.99	0.03	0.01	0.01	2.20	0.05
Na_2O	0.20	1.06	1.52	3.54	3.62	0.03	0.07	0.33

K_2O	0.49	0.75	1.57	2.44	3.79	2.28	0.25	0.76
LOI	3.34	0.45	0.24	2.35	2.51	0.62	2.14	1.94

CLASSIFICATION OF SCMs

Before new supplementary cementitious materials (SCMs) can be used in concrete these materials need to be assessed in an objective and reliable manner. Classification of SCMs in New Zealand is currently based on the relative strength approach outlined in AS3583.6 where prescribed mortar mixes made with SCM combinations are compared with control mortar mixes made using Portland cement [10,11].

Four classification methods were used to assess the SCMs (see also Table 3):

- Relative water and strength assessment in accordance with AS 3583.6 where PC/SCM blends were used in standard mortar mixes without chemical admixture (i.e. varying w/b ratios) [11]
- Modified strength activity testing where PC/SCM blends where used in mortar mixes but adjustment was made chemical admixtures to maintain a constant w/b ratio [12]
- Isothermal calorimetry that measures heat flow at constant temperature for PC/SCM blends in a cementitious paste with a fixed w/b ratio [8]
- Thermogravimetric analysis of cementitious pastes where the weight loss between 110-400 ^{0}C is used to quantify the bound water released from calcium silicate hydrate [13]

Table 3: Comparison between classification systems for SCMs in concrete

Classification method	Standard or reference	Advantages of the technique	Limitations of methodology	Correlation with strength
Relative strength	AS 3583.6	Simple equipment well established	Water demand allowed to vary	Poor (R^2 = 0.003)
Modified strength activity index	EN 196.1 (constant w/b)	Simple equipment easy adjustment	Require careful dosing & testing	Good (R^2 = 0.87)
Isothermal calorimetry	EN 196-8 2010	Quick and very accurate	Specialist test equipment - expensive	Good (R^2 = 0.89)
Bound water analysis	Avet et al [18]	Accurate and easy with correct gear	Specialist test equipment - moderate	Very good (R^2 = 0.93)

The biggest hurdle to a broader adoption of SCMs into concrete construction is the reliance on a test method (AS 3583.6) that is unable to accurately predict the reactivity of SCMs, especially when assessing natural pozzolans. This is best illustrated by comparing the poor relative water requirement and relative strength of concrete containing calcined clay assessed using AS 3583.6 with the excellent concrete strengths achieved. It is recommended that the New Zealand standard NZS 3123 be revised and alternate classification systems be adopted (e.g. modified EN 197.1, isothermal calorimetry and/or bound water from thermogravimetric analysis).

STRENGTH DEVELOPMENT OF CONCRETE

Strength development of SCM concrete is expected to differ compared with control concrete made with Portland cement. This was found to be the case to be the case when

compressive strength results were analysed (see Figure 3 below) [14]. The rate of strength development was found to dependent on the type of SCM as well as the type of GP cement (GBC GP has higher C_2S content than Holcim GP).

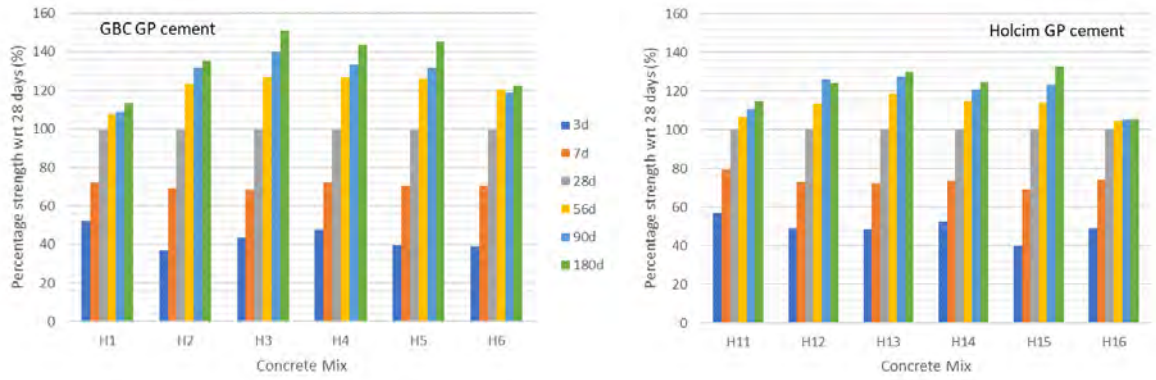

Figure 3: Strength development as a percentage of 28-day strength

Subtle differences were found in the strength development of concrete made with either GBC or Holcim cement. This was not surprising for the two GP cements given the different cement chemistry of these two materials, namely that GBC GP cement has lower C_3S and higher C_2S contents that those found in Holcim GP cement. This resulted in consistently higher long-term strength development of concrete containing GBC GP cement (shown in the left chart in Figure 3).

TRANSPORT PROPERTIES OF CONCRETE

Movement of aggressive agents causing deterioration of concrete is dependent on the transport properties of the material that allow ingress. Table 4 provides a summary of porosity, permeability and resistivity results measured after 28 and 90 days for control and SCM concrete mixes. Comparison of these results is provides the following indications:

- Porosity values below 10.0% indicates and dense microstructure while values below 8.0% are very low [15]
- Oxygen permeability index is a log scale with values above 10.0 indicating low permeability while values above 10.5 indicate very low permeability [15]
- Resistivity of concrete reduces with microstructural refinement and while PC concretes are rarely more than 15 kOhm.cm in the saturated condition, SCM concrete may exceed 20 kOhm.cm over time, which would limit corrosion rates of embedded reinforcement [16]

Table 4: Summary of transport properties of concrete after 28 or 90 days

Property (units)	Age (days)	H1 100%GP	H2 30%FAG	H3 30%FAH	H4 30%PM	H5 30%PL	H6 30%CC	H7 30%SF	H8 30%HE
Porosity (%)	28	8.61	10.05	8.22	8.98	8.81	6.75	6.00	7.00
	90	6.78	8.39	7.56	7.76	7.76	5.85	5.27	6.97
OPI (log scale)	28	10.41	9.99	10.54	10.56	10.22	10.72	10.79	10.52
	90	10.38	10.26	10.44	10.32	10.54	10.60	10.68	10.29
Resist-ivity (kOhm.cm)	28	9.32	9.13	12.42	10.40	9.23	23.11	19.26	10.71
	90	11.18	10.05	13.51	17.09	12.66	30.27	28.81	12.32

Results from permeability and resistivity testing show the improved microstructure of most SCM concretes after 90 days compared with PC concrete. Porosity measurements were variable across the range of concrete mixes and as this is a bulk property provides only a rough indication of durability potential similar with strength.

CONCRETE DURABILITY

Three durability tests were conducted on these concrete mixes; accelerated carbonation, migrating chloride testing and expansion due to alkali silica reaction. Details of these tests is given below while a summary of the results is shown in Table 5.

- Accelerated carbonation done in accordance with ISO 1920 (21 ^{0}C, 65% R.H and 2.5% carbon dioxide exposure for 56 days) – concrete moist cured for 3, 7 or 28 days with 3 day cured concrete shown in the table below [17]
- Migrating chloride coefficient measured in accordance with NTB 492 where concrete is exposed to 30V for periods of 24-48 hours and the depth of chloride ingress measured using a silver nitrate indicator [18]
- Concrete prism testing to measure potential expansion of concrete subject to alkali silica reaction (CPT38 run at 38 ^{0}C, CPT50 run at 50 ^{0}C) with a concrete alkali content of 5.25 kg/m^3 and containing reactive andesite coarse aggregate (PAP7) [19,20]

Table 5: Summary of durability properties of control and SCM concrete at 28 or 90 days

Property (units)	Age (days)	H1 100%GP	H2 30%FAG	H3 30%FAH	H4 30%PM	H5 30%PL	H6 30%CC	H7 30%SF	H8 30%HE
Acc. Carb.	28	5.82	9.76	11.30	11.39	15.94	10.66	5.93	4.58
(mm)	90	6.34	11.52	12.46	13.66	21.82	12.85	10.78	4.95
MCR	28	18.33	22.63	17.76	22.88	32.76	10.43	8.40	11.45
(x10 $^{-12}$)	90	9.99	8.26	5.65	5.49	13.18	5.35	2.81	8.35
CPT38	180	0.2152	0.1016	0.0012	0.0076	0.0056	-0.0036	NT	NT
(% Exp.)	300	0.2296	0.1396	0.0060	0.0176	0.0160	-0.0032		
CPT50	120	0.3258	0.0988	0.0008	0.0084	0.0148	-0.0108	NT	NT
(% Exp.)	180	0.3378	0.1384	0.0092	0.0324	0.0364	-0.0112		

Durability performance was variable depending on the SCM used in concrete and properties need to be considered individually. It should be noted that comparisons are made on the basis of equal binder content rather than equal strength, which is the basis for comparison in practice.

Accelerated carbonation

Control concrete containing either GP or HE cement had lower carbonation depths than SCM concretes regardless of curing regime. This can be seen in Figure 4 where all concrete mixes and curing regimes are compared. The poorer carbonation resistance of SCM concrete was due to the slower maturity of these materials and the lower level of calcium hydroxide as a result of pozzolanic reaction. Generally carbonation depths were relatively low with only concrete containing low reactive perlite having levels of more than 15 mm of carbonation.

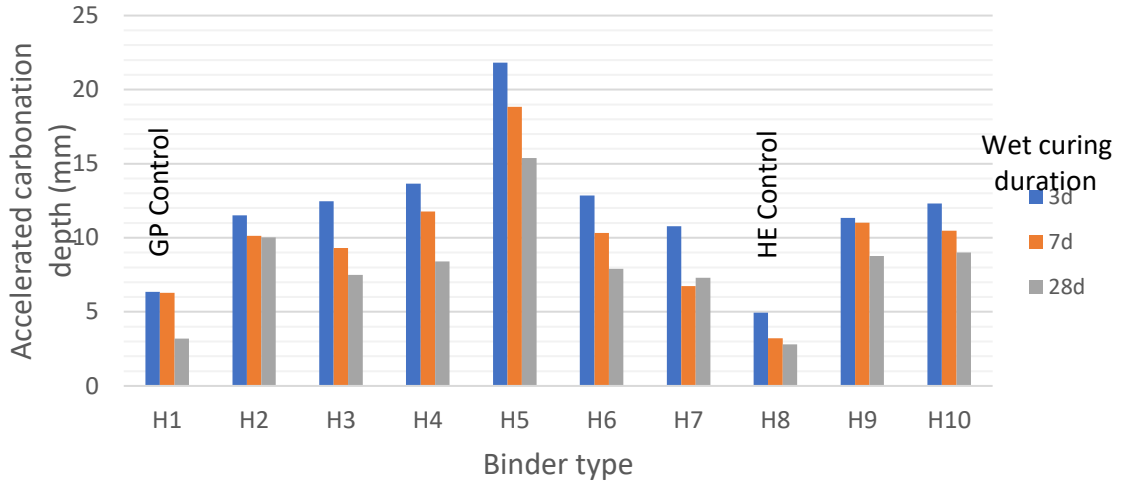

Figure 4: Accelerated carbonation after 56 days exposure (21 ^{0}C, 65% R.H. & 2.5% CO_2)

Migrating chloride resistance

Rapid testing of the chloride resistance of concrete was undertaken using the Nordic chloride migration test (NTB 492). Results measured after 28 and 90 days are shown in Figure 5 below for both GBC and Holcim cement. SCM concrete was found to have significantly higher chloride resistance than control concrete (e.g. mixes H1, H11, H8 & H18) when compared after 90 days. Only concrete containing perlite did not follow the trend for SCM concretes with relatively poor chloride resistance due to the lower reactivity of this SCM.

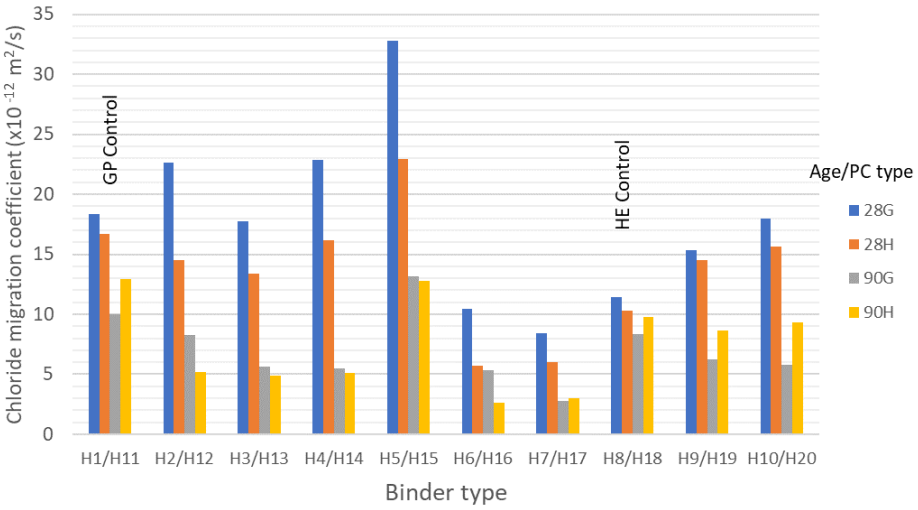

Figure 5: Chloride resistance of control and SCM concrete

Expansion from alkali silica reaction (ASR)

Expansion was measured weekly and later monthly for a period of 6 & 12 months for CPT38 and CPT50 respectively (summary shown in Figure 6 below). Control concrete containing GP cement was found to exceed the reactivity limit of 0.04% within the first few weeks or months of the monitoring and final expansion was sufficient to cause cracking damage. Concrete containing 30% Huntly fly ash allowed longer-term expansion to occur with final expansion exceeding the reactive limit in all cases. Testing at 35% replacement of Huntly fly ash was found to prevent significant expansion (e.g. values below 0.02%).

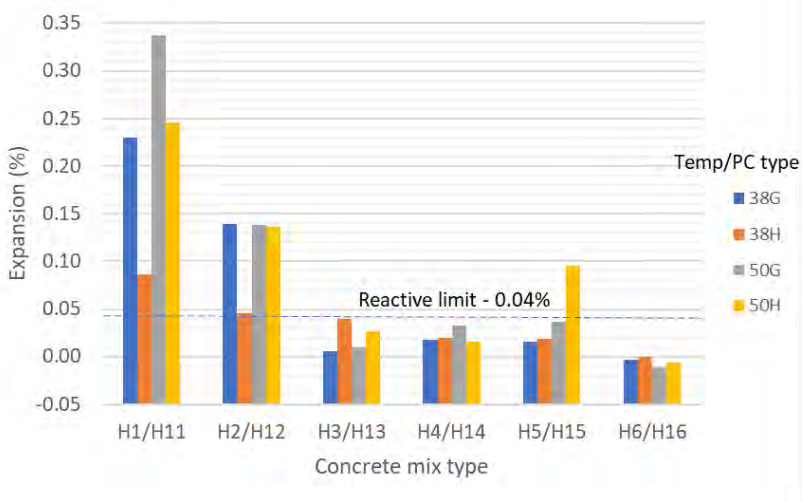

Figure 6: Expansion of concrete subject to ASR (CPT38 @300 days, CPT50 @ 180 days)

Summary of SCM performance with regards to preventing ASR-induced expansion were as follows:

- Class C fly ash (Huntly) can prevent expansion induced by ASR but replacement levels above 30% should be considered
- Class F fly ash (Adani) can prevent ASR-induced expansion at 30% while other SCMs such as natural pozzolans and calcined clay could be effective at 25% replacement of Portland cement

EMBODIED CARBON DIOXIDE OF BINDER COMBINATIONS

Comparisons of embodied carbon for different concrete mixes was made by normalising strength at 50 MPa. The average 28-day strength of concrete mixes made with either GBC or Holcim cement was used to provide a simpler comparison. A linear approximation was made to determine the water/binder ratio of each concrete mix to produce a 28-day strength of 50 MPa. From this calculation, the total binder content was determined assuming a water demand of 170 L/m^3, being the national average value for structural concrete mixes. Figure 7 shows the embodied carbon dioxide using a range of binder combinations.

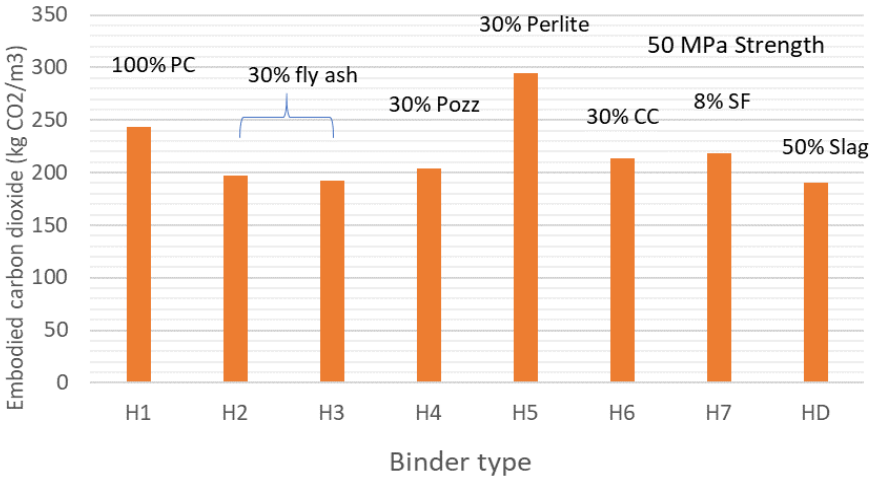

Figure 7: Embodied carbon dioxide in 50 MPa PC and SCM concrete

These indicative values are based on international reported eCO_2 values (e.g. PC – 850 kg/T, calcined clay – 330 kg/T, slag – 100 kg/T, natural pozzolans – 50 kg/T, fly ash or silica

fume – 25 kg/T) [2]. Comparison with the PC concrete shows a reduction of 20% carbon dioxide is possible, which could be improved with further material optimisation.

CONCLUSIONS

The largest barrier to adoption of new SCMs into concrete construction is the reliance on a test method (AS 3583.6) that is unable to accurately predict the reactivity of SCMs, especially when assessing natural pozzolans. The New Zealand standard NZS 3123 should be revised to allow alternate classification systems to be adopted (e.g. modified EN 197.1, isothermal calorimetry and/or bound water from thermogravimetric analysis).

This research showed promising durability performance such that concrete made with more reactive SCMs (e.g. fly ash, ignimbrite, calcined clay and silica fume) had consistently lower porosity and permeability and improved resistivity and chloride resistance. All SCMs showed a beneficial effect in reducing expansion associated with alkali silica reaction although some materials were more effective in the longer-term. SCM concretes did however have poorer carbonation resistance compared with control concrete regardless of the curing regime.

Findings from this research showed that replacement of 30% Portland cement with SCMs was able to achieve reasonable strengths and superior durability properties in some cases. Finer SCMs such as calcined clay and silica fume were most effective in concrete with lower water/binder ratios that achieve higher compressive strength. Fly ash was more effective in lower strength grades since workability was not negatively affected by water demand issues. Slag concrete was not the primary study of this research but results indicated good performance across all properties measured.

ACKNOWLEDGEMENTS

BRANZ and Concrete NZ who provided funding of this research that was undertaken at the University of Canterbury in 2020 and 2021.

REFERENCES

1. Thinkstep, (2019), Under construction – hidden emissions and untapped potential of buildings for New Zealand's 2050 zero carbon goal, Unpublished report for NZGBC, Wellington.

2. Scrivener, K.L., John, V.M. and Gartner, E.M., (2016), Eco-efficient cement: potential economically viable solutions for a low CO_2 cement-based materials industry, UNEP, Paris.

3. South, Warren, (2009), A study of the compressive strength and drying shrinkage of cementitious binders prepared using natural pozzolans, PhD thesis, University of Wollongong, Australia.

4. Christie, A.B., Thompson, B., Brathwaite, R., (2007), Mineral commodity report 20 – Clays, Institute of Geological and Nuclear Sciences, Wellington.

5. Kennerley, R.A., and Clelland, J., (1959), An investigation of New Zealand pozzolans – Part 1 & 2, Bulletin 133, NZ DSIR, Wellington.

6. American Society for Testing and Materials, (2002), ASTM C311 – Standard test methods for sampling and testing fly ash or natural pozzolans for use in Portland cement concrete, ASTM International.

7. Mackechnie, J.R., (2021), Removing the barriers to the use of significant levels of SCMs in concrete production in New Zealand as a major step towards decarbonising concrete construction, Concrete NZ.

8. American Society for Testing and Materials, (2017), ASTM C1679-17, Standard practice for measuring hydration kinetics of hydraulic cementitious mixtures using isothermal calorimetry, ASTM.

9. American Society for Testing and Materials, (2018), ASTM C114-18, Standard test methods for chemical analysis of hydraulic cements.

10. Standards New Zealand, (2009), NZS 3123 – Specification for Portland pozzolan cement (type PP cement), Wellington.

11. Australian Standards, (2018), AS 3583.6 - Methods of test for supplementary cementitious materials, Method 6: Determination of relative water requirement and strength index, Australia.

12. European Standard, (2005), EN 196-5 – Methods of testing cements Part 5 – Pozzolanicity tests for pozzolanic cements, European Committee for Standardization, Brussels.

13. Avet, F., Snellings, R., Diaz, A.A., Haha, M.H. and Scrivener, K., (2016), New rapid, relevant and reliable test method to evaluate the pozzolanic reactivity of calcined kaolinitic clays. Cement and Concrete Research, 85, pp 1-11.

14. Standards New Zealand, NZS 3112 – method of test for fresh and hardened concrete, 1988, Wellington.

15. Alexander, M.G., Mackechnie, J.R. and Ballim, Y., (2009), Durability index testing procedure manual, COMSIRU, University of Cape Town.

16. American Society for Testing and Materials, (2019), ASTM C1876 – Standard test method for bulk electrical resistivity or bulk conductivity of concrete, ASTM International

17. International Standards Organization, (2015), ISO 1920-12: Determination of the carbonation resistance of concrete – accelerated carbonation method, Geneva.

18. Nordtest Method, (1999), NT Build 492 – Chloride migration coefficients from non-steady-state migration experiments, Finland.

19. RILEM. (2016), RILEM Recommendations for the Prevention of Damage by Alkali Aggregate Reactions in New Concrete Structures. State-of-the-Art Report of RILEM Technical Committee 219-ACS. Eds Nixon, P.J. and Sims, I. RILEM State-of-the Art reports v.17.

20. American Society for Testing and Materials, (2020), ASTM C1293-20a, Standard test method for determination of length change of concrete due to alkali-silica reaction, ASTM.

concretenz BUILDING RESILIENCE CONFERENCE 2022
13-15 October 2022
Energy Events Centre | Rotorua

WAIKATO EXPRESSWAY – HAMILTON SECTION

TED POLLEY

City Edge Alliance, Hamilton

SUMMARY

The Hamilton section of the Waikato Expressway is a key piece of infrastructure supporting this growth and will be the primary strategic transport corridor for the Waikato region. It is the largest roading project ever undertaken in the Waikato, a region considered to be highly susceptible to liquefaction during a seismic event.
The Hamilton section is being delivered by the City Edge Alliance comprised of Waka Kotahi (client); Fletcher Construction and Higgins (constructors); and Beca and Coffey (designers). The 22km expressway involves 4 million m3 of earthworks, 17 bridges, and five major intersections.
This paper discusses innovative detailing allows rapid and reliable reinstatement for traffic, thereby providing structural resilience for a key lifeline route.

INTRODUCTION

The Waikato Expressway forms the key transport corridor between Auckland and Hamilton. It has been constructed in stages over the last several decades. The expressway will improve economic growth and productivity through efficient movement of people and freight. A key outcome is to significantly reduce the number of fatal and serious injury crashes in this area. The Hamilton section is the final stage to complete the Waikato Expressway.
The Hamilton section forms 22km of expressway, commencing at the Lake road junction (end of the Ngaruawahia section of the Waikato Expressway). It then runs south to the east of Hamilton, connecting to the existing Tamahere Interchange which was constructed as part of the Cambridge Bypass section of expressway. The Hamilton section has 17 bridge structures and 5 major intersections (see Figure 1 below). There is approximately 4 million m3 of earthworks for approximately 22km of expressway. The construction programme is four years, with completion expected late 2021.

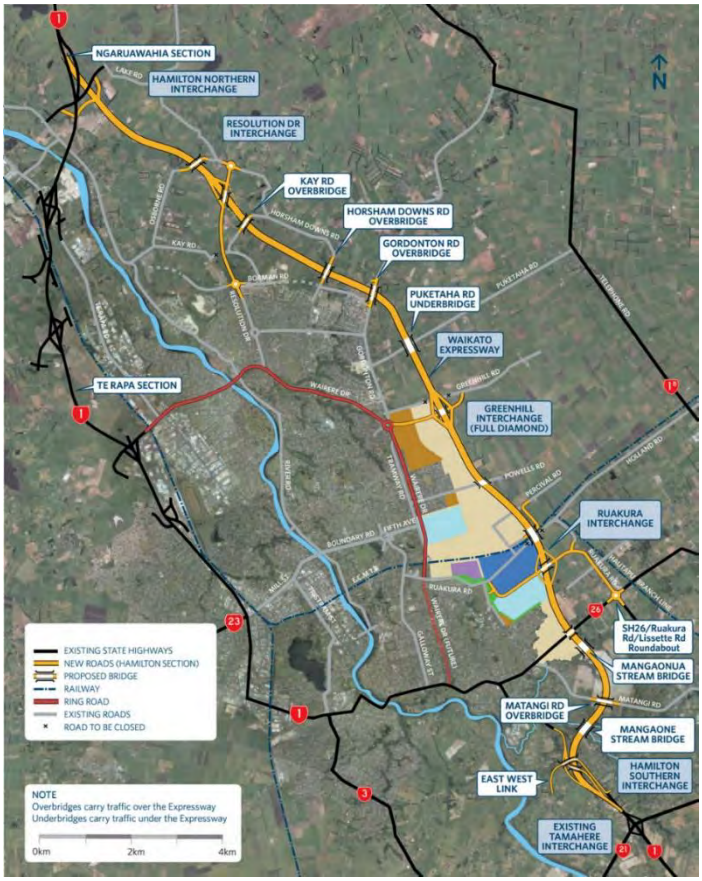

Figure 1: Plan of Hamilton Section of Waikato Expressway showing major structures

This section of the expressway is delivered as an Alliance. The Alliance partners are: Waka Kotahi as the Client, Fletcher Construction and Higgins (now part of FCL) as the Constructors, and finally Beca and Coffey as the Designers. A sub-Alliance with Hic Bros was formed to generate efficiencies with the earthworks.

SEISMICITY

A site-specific spectrum was prepared by GNS Science for the Waikato Expressway in 2010. Seismic accelerations were slightly lower than NZS 1170.5 spectra values for the Waikato region. In addition to the seismic Design Event (DE), the updated Waka Kotahi Bridge Manual (3rd edition, Amendment 1) required the design to consider the effects from the Major Earthquake (ME = 1.5xDE) and to detail the structure to avoid collapse under this load case.
The nearest active faults are more than 20km away, so near fault factors were not required.
The site subsoil classification for most of the Hamilton Expressway was Class D for deep and soft soil sites. However, in some locations of particularly poor soils such as the gully bases, subsoil Class E category was considered more appropriate.
Bridges carrying the expressway were designed for Importance Level 3 loading (2500-year return period). Bridges crossing above the expressway were designed for Importance Level 2 (1000-year return) as specified in accordance with the project Minimum Requirements.

LIQUEFACTION ASSESSMENT

The Hamilton section of the Waikato Expressway is located in the middle of the Hamilton Basin shown in Figure 2 below. The light pale areas shown in the geological map are extensive low-

lying areas with thick sequences of relatively young soils. Many of them are volcanic pumiceous sediments deposited by the Waikato river. These low-lying deposits of mostly young pumiceous sands typically have a high-water table, particularly in the northern end of the Hamilton Basin.

Figure 2: Geology of Region

Based on previous experience, it was anticipated that there would be a significant liquefaction risk in the young pumiceous soils of the lowlands of the Hamilton Basin. Historically, liquefaction potential has been assessed using what is referred to as the Simplified Method. The Simplified Method involves undertaking some penetrometer-based testing which involves pushing or hammering a device into the ground measuring the resistance. This resistance is then compared to a plot of conditions where liquefaction has and has not been observed in the past.

Over time penetrometer-based methods have become more sophisticated and the Simplified Method has become more complex. The penetrometer methods all have the potential to crush the pumice in the soils and conservatively underestimate the liquefaction resistance. The Waikato pumice matrix is different from the Canterbury pumice (which is where the Simplified Method was developed) and so it was decided to use shear wave velocity-based assessment for determining the onset of liquefaction. This method uses low amplitude seismic waves to measure the stiffness of the soil. Shear wave velocity-based method was considered less conservative than the Simplified Method, resulting in significantly less ground improvement as discussed further in this paper.

In order to demonstrate to the client that shear wave velocity was a more realistic assessment, a paleo liquefaction study was carried out (meaning study of ancient liquefaction) to investigate if historically liquefaction has happened at the site. The results were used as a check on whether the penetrometer-based method or the shear wave velocity-based method predicted liquefaction most reliably. Practically, the paleo liquefaction study involved digging trenches across selected parts of the site to look for features indicating historic liquefaction.

As seen from the Christchurch earthquake, liquefaction often causes ejecta to travel up from the liquefied layer, through cracks in the ground to escape on the surface. The locations where these features were found along the Hamilton Expressway Section tied nicely with the locations identified as being liquefiable from the shear wave velocity-based assessment. On the basis of this study, it was concluded that the project team could adopt the liquefaction potential indicated by the shear wave velocity-based assessment.

GROUND IMPROVEMENT AT STRUCTURES

The Specimen Design incorporated extensive ground improvement at the bridge structures. The process for the liquefaction triggering assessment described above, together with the adopted bridge structural forms allowed a significant reduction in quantity of ground improvements at the structures (as compared to the Specimen Design). Refinements to the vertical alignment and groundwater control measures further contributed to the reduction of ground improvement for the project.

In general, ground improvement was deemed not necessary at any of the structures located in cuts or the stream gully bridges. The exception was the Mangaharakeke Stream southern bridge where a row of driven piles below the northern abutment was required to stabilise the abutment slope.

Limited ground improvement was still required at all of the structures located in fill zones, although the extent and depth were significantly reduced from the specimen design. The ground improvement comprised of lattices using low strength overlapping concrete columns constructed with a continuous flight auger (CFA). Depth of the ground improvement was typically 5 to 6m.

The ground improvement blocks at the fill bridges extend two to three metres beyond the MSE wall block to support the higher stresses near the face of the MSE walls and promoted uniform load transfer / settlements over the full footprint of the block.

STRUCTURES DESCRIPTION

The aim of the design was to achieve simple, robust, reliable, and seismically resilient structures.

Concrete structures have typically been used for all local road overbridges and short span expressway bridges. These comprise single / twin span standard precast pre-stressed Super-T girders. A long span steel structure was used for the Mangaonua Stream Bridge. The long span was used because of the expensive substructure caused from a very deep soft peat layer.

Construction details were standardised to achieve construction efficiency and economy and to provide a consistent and unified project design. Consistency in bridge barrier shape and urban design features has been used throughout the project.

All bridge superstructures are semi-integral with the abutments except the Mangaonua Stream Bridge (steel structure) and the Southern Interchange Cambridge Road on ramp, both which use expansion joints due to length or skew. This therefore eliminates the need for movement joints and the associated future maintenance on all but two bridges.

Foundations for the bridges in cut, the stream gully bridges, and the Southern Interchange bridges all used traditional bottom driven steel tube piles. The exception was Mangaonua

(long steel bridge) which is located in deep liquefiable soils and required larger diameter bored piles for lateral resistance.

All single span bridges with abutments located on fill comprise spread footings supported by MSE (Mechanically Stabilised Earth) walls built with in-extendable steel reinforcement. These walls are detailed to allow movement under the seismic Design Event.

All bridges on the project were detailed to accommodate large post-earthquake permanent movements. It is expected that many will not require any intervention / require repairs following the Design Event earthquake. Post-earthquake reinstatement works for the fill bridges was eliminated or reduced, compared to more conventional piled solutions. This was due to the innovative bridge form which allows the abutments and structure above to accommodate more movement. The fill bridge form is considerably more resilient than a conventional piled solution and so will be able to accommodate displacements even larger than the expected movements. This resilience is a major advantage over the more conventional piled abutment solution and is discussed in detail below.

Bridges in Fill – Resilient Floating Abutments

The review of ground conditions at the bridge sites in fill indicated deep soil zones that exhibited risk of liquefaction. Analysis indicated that the triggering of liquefaction typically occurred between the 1/250 and 1/500 AEP events for these bridges.

A soil-structure interaction analysis was carried out at each bridge location assuming no deep ground improvement. The results indicated that a reliable and robust solution appropriately detailed could developed at each site that achieved the performance requirements of both, the Project Minimum Requirements, and the Waka Kotahi Bridge Manual, with targeted and limited ground improvement.

These bridges use simply supported Super-T beams and are considered to be “locked-in” longitudinally with semi-integral abutments supported on spread footing abutment beams. All bridges located in fill have the bridge superstructure seated on free float pot bearings which are connected to abutment spread footings, in turn are seated on MSE walls. The girders are detailed as simply supported for better performance during the post seismic vertical and horizontal movements.

Longitudinal resistance is provided by passive resistance of the abutment via a back wall cast at the end of the girders. Free float pot bearings have been detailed to accommodate the anticipated post seismic movement of the MSE walls. Elastomeric bearings did not have sufficient lateral displacement capacity to be used.

Transverse concrete shear keys are provided at the abutments. The transverse seismic load is transferred from abutment beam to MSE wall via friction. (See Figures 3 and 4 below).

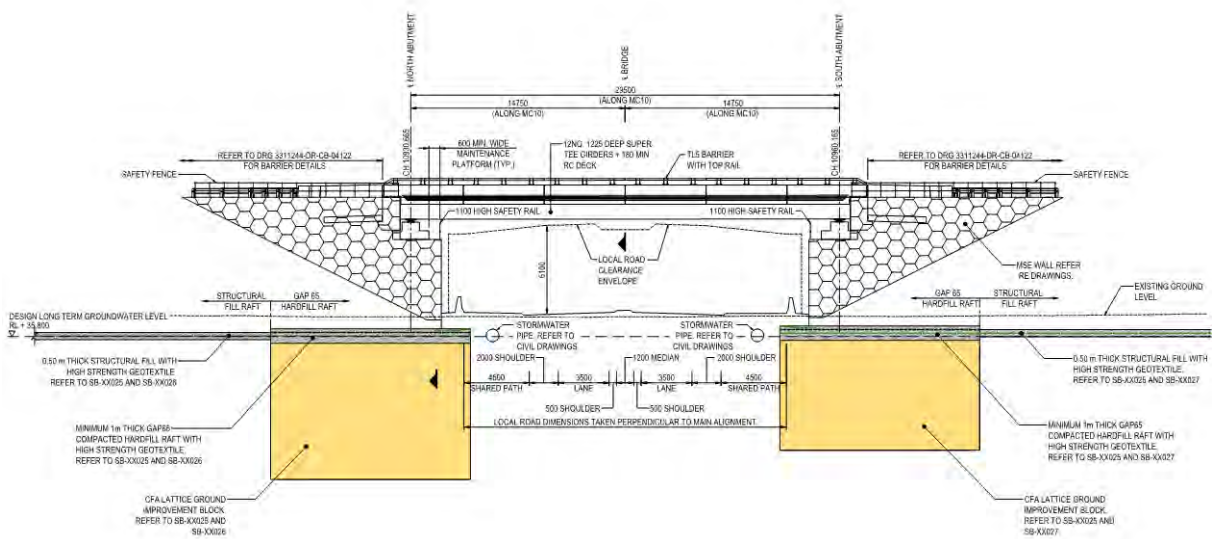

Figure 3: Typical Bridge in Fill

The MSE walls are considerably more resilient and more able to cope with the anticipated post seismic movements compared to a bridge supported on piles. Both the structure and the supporting MSE walls were detailed not only to accommodate the design seismic events, but to enable rapid and reliable reinstatement for traffic in the event of an earthquake. Hence, achieving the performance requirements of the bridge manual as summarised below:

- Emergency traffic able to use the bridge immediately after the seismic Design Event.
- After remediation / repairs, bridge is open to all traffic.
- Usable by emergency traffic after repair if subjected to a seismic Major Event.

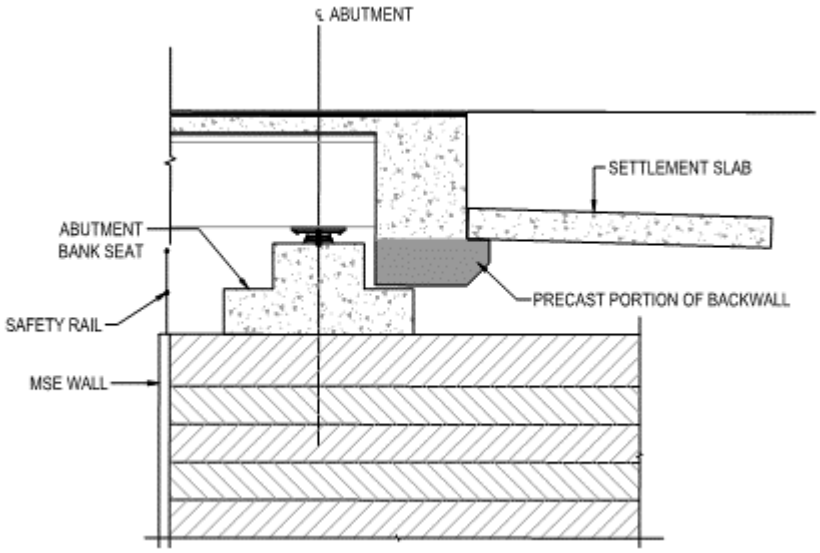

Figure 4: Floating Abutment Detail

The fill bridges meet the performance requirements of Table 5.1 of the Waka Kotahi Bridge Manual by specific details described below:

- The bridge backwalls were designed for full seismic passive pressures using upper bound soil properties.
- Using free float pot bearings to allow for large post seismic horizontal embankment movements whilst still being able to support full dead load with emergency traffic.
- The bridge detailing allowed for vertical jacking of the bridge back to original levels in the event of the MSE walls settling under liquefaction.

The global stability analyses indicated that the fill bridges will experience horizontal displacements of up to 300mm in a seismic Design Event and would require little or no intervention prior to reopening of the bridge to traffic. The bridge MSE walls are located far enough back that there is no reduction in the required horizontal clearance at each bridge site.

It is important to note that with this design approach, both the bridge and approaches will move together in a more sympathetic fashion. Analysis indicated that settlements for both structure and the adjacent embankment will be of a similar order of magnitude, substantially reducing the extent and impact of differential settlement. This will significantly improve the post-earthquake performance and reduce the quantum and extent of reinstatement works. It is expected that only minor works will be required to reopen these bridges to traffic after a seismic event.

Vertical settlement of between 100 to 300mm may occur at either one or both abutments, requiring inspection and possible jacking and re-levelling of bridge bearings. The extent of re-levelling required will depend on the level of differential movement between the bridges and the adjacent approach embankments. The bridge superstructure has been assessed for 50% differential settlement across one abutment. Emergency traffic can access the bridge immediately, although it will be at limited speed.

In contrast, the more rigid approach using piled bridge foundations at these locations would have likely resulted in substantial differential settlements between approach embankments and bridge structures, requiring additional reinstatement work and potentially more detailed structural inspections to confirm structural adequacy of the piles. Hence, piled structures were typically avoided for bridges in fill.

The anticipated response of the floating abutment bridge and approach embankments with respect to the Major Seismic Event was also assessed and confirmed that the structural solution meets the “no collapse” criteria of the Bridge Manual. A key feature of this type of bridge form is its ability to withstand displacements that are even larger than those anticipated with little increase in the extent of repair.

Damage to these structures at the Major Earthquake event would be expected. Damage would likely include significant cracking of MSE wall panels, potentially beyond the point of repair. The bridge may still be suitable for traffic, depending on the nature and magnitude of settlement, although this would be subject to a significant amount of reinstatement work on the approach embankments.

As noted earlier all bridges will be designed and detailed to accommodate jacking for bearing replacement (as a maintenance function). This functionality also provides for re-levelling after abutment settlement (for both design and major events).

If piled bridges were adopted for all bridges, we would expect greater differential settlements between the bridge and adjacent embankment, potentially leading to a different damage profile. In the Major Event, damage to bridge piles is likely to be substantial, most likely leading to demolition of the structure, whereas the more resilient reinforced earth abutment solution is likely to be more usable, perhaps with a new precast concrete facing system applied.

Another principal benefit of the proposed MSE block abutments over other foundation options is that they substantially reduce the extent and depth of ground improvement at each abutment because larger post seismic movements can be accommodated by the structure when detailed appropriately. This significantly reduced cost and critical path programme during construction.

Bridges in Cut - Piled Bridges

The bridges located in cut areas are constructed using the “top down” method i.e., construct the bridge first at existing ground level, then excavate the soil material underneath after. Therefore, these bridges are piled. As noted earlier, post seismic movements are expected to be much lower for these structures since the cut slopes were designed to limit global stability movements.

The cut geometry comprises one vertical to two horizontal cut slopes at the bridge locations. Longitudinal subsoil drains are provided at the base of the cuts to maintain a permanent lowered groundwater level.

These bridges use Super-T structures and are considered to be “locked-in” longitudinally with semi-integral abutments supported on bottom driven steel tube piles. Longitudinal resistance is provided by passive resistance of the abutment via a back wall cast at the end of the girders. Tall elastomeric bearings have been detailed to accommodate the anticipated movements required to develop passive resistance so negligible longitudinal load is carried by the abutment piles. Pier piles have been designed for the maximum longitudinal displacement which occurs as the abutment backwall develops passive resistance i.e., a displacement-based design approach.

Transversely the bridges were designed as limited ductile structures. Transverse concrete shear keys are provided at the abutments and the piers. The relatively short length of bridge means most of the transverse bridge loads are transferred directly to the bridge abutment piles. The piled piers are flexible relative to the abutments and the number of piles at each pier were determined from Ultimate Limit State (ULS) dead and live loads.

The typical multi span local road bridge piers consists of a reinforced concrete pier headstock beam with bottom driven steel tube piles extending up into the headstock. The exposed section of steel casing was considered non-structural, but corrosion protection was still applied to the exposed section of the steel tube piles for aesthetic reasons.

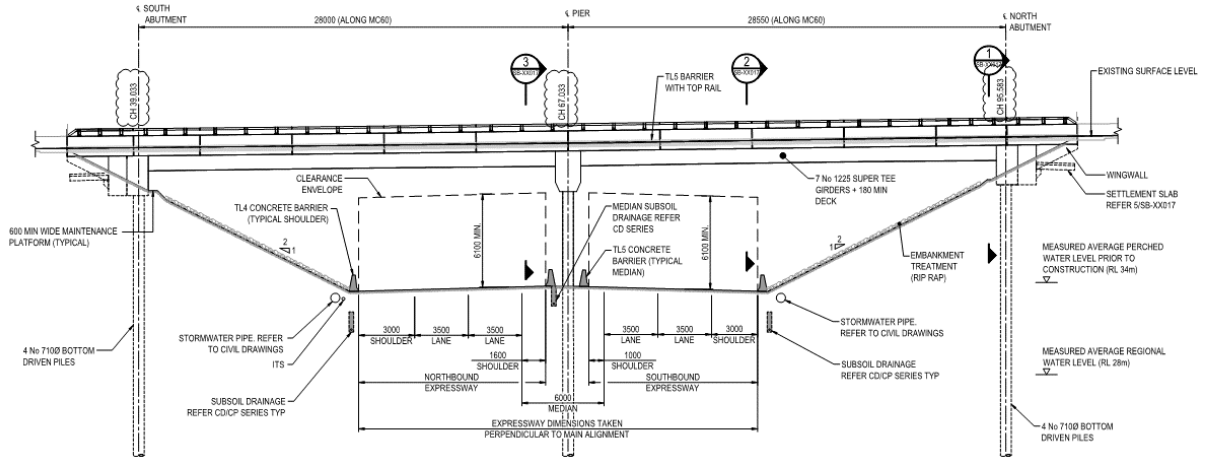

Figure 5: Typical Bridge in Cut

The abutment piles were required to accommodate relatively small (compared to the fill bridges) post seismic movements. These piles were assessed using Waka Kotahi R553 method which models a soil block pushing on the piles by imposing displacements on soil members as shown in the Figure 6 below.

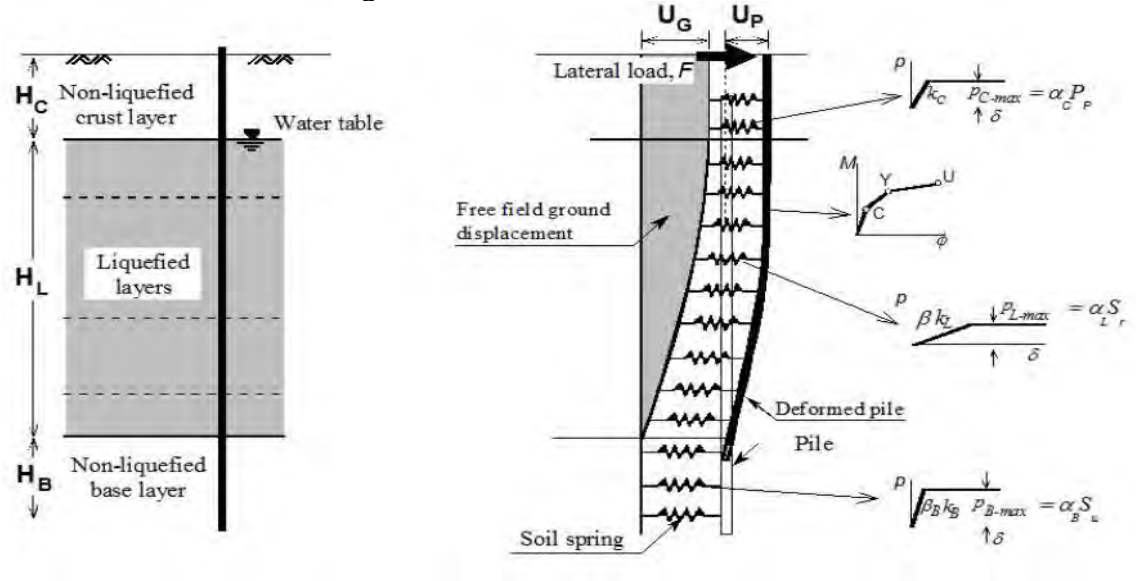

Figure 6: Pile Design for post seismic embankment movement using R553 Method

It should be noted that the seismic Design Event was not considered additive to the post seismic liquefied movements for ULS design since liquefaction induced embankment movements typically commences near the end of a seismic event.

All piles were detailed as fully ductile (mu=6) although allowable rotation curvatures in flexural plastic hinges were restricted to limited ductile limits for the two Design Event cases noted above.

In addition, the piles had to carry significant negative skin friction loads due to post seismic event settlements.

Steel Bridge

The Mangoanua Stream Bridge (see Figure 7 below) was designed as a three span 150m long steel ladder bridge due to the ground conditions in the gully. Maximum bridge span was 55m. Deep piles compounded by construction complexity of piling through, and aquifer meant that the substructure foundations were particularly expensive.

Four girders were used with crossbeams between the two pairs of girders at nominal 3.5m centres. Each girder was supported on a column linked together by a single long pile cap. Ten 1200 diameter piles per pier supported the bridge.

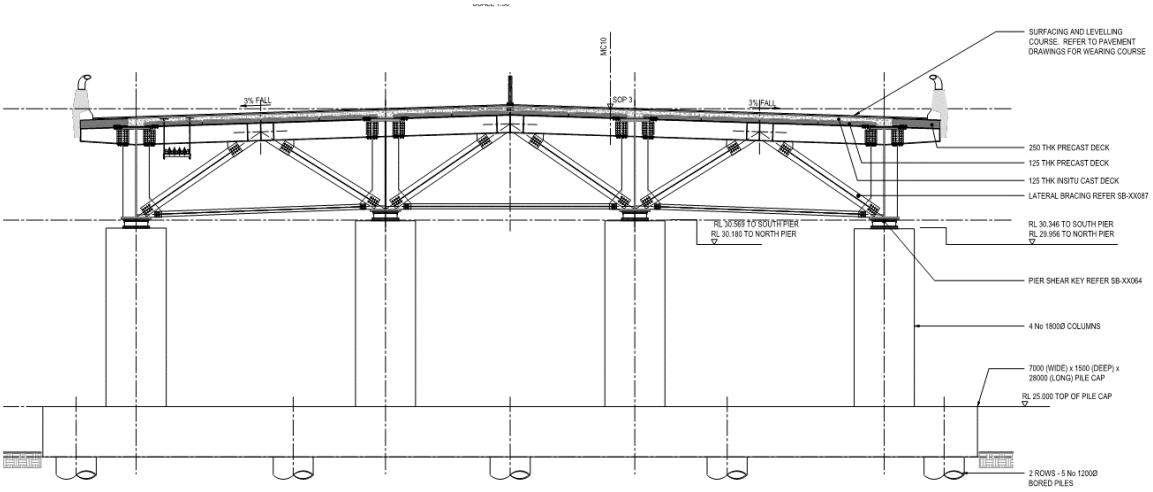

Figure 7: Mangaonua Stream Bridge

The soft ground conditions meant that girder erection was a critical load condition for the pile design. The large 600T crane placed lateral loads onto the piles which were considered to be locked in. The existing site was preloaded to remove a large proportion of the settlement and lateral loading which were expected during girder erection.

Liquefaction of the bridge site was expected over the top. However, due to the geography, the effects of liquefaction were expected to only reduce the soil stiffness to near zero, but not place significant lateral loading onto the piles. The large diameter piles combined with the pile cap provided the required stiffness by portal action since the top layers of ground provided very little lateral resistance.

CONCLUSION

The “floating abutment” solution for all bridges constructed in fill was to support the bridge on free float pot bearings seated on abutment spread footings located on Mechanically Stabilised Earth (MSE) foundations. The reinforced earth foundations are considerably more flexible and more able to cope with the anticipated post seismic ground movements compared to a bridge supported on piles. Both the structure and the supporting reinforced earth foundations were detailed not only to accommodate the design seismic events, but also enable rapid and reliable reinstatement for traffic after an earthquake event, achieving the performance requirements of the Waka Kotahi Bridge Manual.

The solution which allows the bridge abutments to move with the ground meant that costly ground improvement was significantly reduced, providing Waka Kotahi with a value for money solution while also improving the whole of life performance. The floating abutment solution is considerably more resilient than a conventional piled solution and so will be able to accommodate much larger than anticipated movements if required. This was a major advantage over the more conventional piled solution for this project.

concretenz BUILDING RESILIENCE
CONFERENCE 2022
13-15 October 2022
Energy Events Centre | Rotorua

IT'S OKAY NOT TO BE OKAY – YOUR DAILY MENTAL HEALTH JOURNEY.

MIKE BOTHERWAY

Higgins Concrete Limited

THE STORY. A real-life account of the battle with Mental Health from a survivor in their own words. (Source Brendon Cooley 1)

Chapter 1 – I am Better!

September 2017. Everything in my life is going well. I have a job, a wife, three children and my own house. Life is good. I take medication for depression – but that started 12 years ago, so I decide I don't need to be medicated anymore. I am not depressed. I have been better for 12 years. I am better.

When the idea of weaning myself off medication was brought up, Meaghan – my wife – was not so confident. She encouraged me to first discuss this with the GP and to do it slowly under guidance. If I had my way, I would have weaned myself in a few weeks - something that should never be attempted by anyone. The doctor agreed to help me. I can be very persuasive when I want to do something. Meaghan was not comfortable with the idea; however, we are all responsible for our own choices. At about the same time, unbeknownst to me, my dad was about to hit us with the biggest bombshell of our lives.

While stopping my medication in 2017 was the catalyst for my downturn, I am proud for giving it a go. At the same time, if I had been given a chance to avoid the pain it caused, I would have taken my decision back in an instant.

Chapter 2 - When worlds collide

If there is one thing that I have learnt through this ordeal is that we are only responsible for our own decisions and not those of others. We cannot carry another person, we cannot cure them, we cannot put ourselves in their place.

10 months later, in July 2018, I wake and know this is the day it will end. I have failed as a father, son, husband, and teacher. My thoughts are telling me this world will be better off without me. I believe them, I write a note and prepare everything, then suddenly I think, no I don't want to do it. I sit up to try and turn the car off but all I remember afterwards is falling back.

I had a close family that gave me normal upbringing, full of good morals, which turned me into a well-behaved person, who always tried his best. Good at most sports, successful sprinter and rugby player, head boy, later a PE teacher. Beautiful wife, three amazing children, great friends, a house and all else that is required to have a great life. Loved, valued, and respected. If you are willing to give up on all this, depression is real.

What caused this "chemical imbalance in my brain", as I like to call it? Was it running 400m when growing up (i.e., stress and pain); the concussions suffered in rugby (i.e., damage); working two years with some of the most difficult kids in England (i.e., more stress); the high expectations I put on myself (i.e., even more stress and pressure)? Or perhaps my dad questioning after 45 years whether I'm his son (i.e., hurt). Or is it just my thoughts and thinking patterns – anxiety and pressure? I will never know and the more you try and figure it out the harder it is to get on the other side.

Chapter 3 - Journey and recovery

I wake and I'm in Waikato Hospital. I don't remember much but my cousin is there and helping to take me to the toilet. The staff advise me to be taken home – this must change, in my opinion; do not send home someone who has tried to take their life. Sending survivors home is too dangerous and hard on families, especially if they try again and are successful. A few-day compulsory hospital stay should be put in place, so the patient can be reviewed, medication sorted and hopefully a change in their mindset started.

I choose to go to the Henry Bennett Centre; I am unwell and causing so much stress to my family. It's a challenge. Mental illness affects young and old, all ethnicities. It affects people in so many ways and it's hard to watch others around you. I feel safe, though, and extremely well looked after, they have some good initiatives to help your recovery.

"No medications seem to be working so we think you would benefit from ECT (Electroconvulsive Therapy)". I thought it had been outlawed years ago – clearly not. I didn't want to give up and so was scheduled for 20 sessions of shocks that cause tiny seizures, under anaesthetics. You have it done in a unilateral way (one side) or bilateral (two sides) – I had both ways. The major side effect for me was short term memory loss but the change in my behaviour, thoughts and feelings was so good that I didn't care. The treatment allowed my old antidepressant to start working again, which was a big relief.

While at Henry Bennett, I realised I wasn't alone. Mental illness is so frustrating because to look at me there seemed to be nothing wrong with me, but if only people could see the games your brain plays with you. Reading "Out of the Woods" by Brent Williams really helped me as I had felt the same as he had, and it gave me hope that I could get better. I also grew up idolising John Kirwan, believing he made it a lot easier to talk about mental wellbeing. I love what he has done for mental illness in NZ and that's why my third son's middle name is Kirwan. I love Mike King and Gumboot Friday. I think providing counselling for young people is critical today, as technology has exposed them to everything and I'm unsure of the effects that it is going to have.

Eight months of hell that nearly ended in tragedy has made me the person I am today, and I hope that sharing this may help another person with their own struggles, help them to get through. I will be forever grateful to my family, friends, colleagues, doctors, psychiatrists, psychologists, counsellors, ECT staff, and the Henry Rongomau Bennett staff for never giving up on me.

THE STATISTICS

Nationally Last Year:
Covid 19 claimed 26 NZ lives (2)
320 road deaths last year (3), but
654 New Zealanders took their own life (4).
In the next 48-hour period 2 males and 1 female will end their own life (5), and
New Zealand has the highest rate of youth suicide in the OECD (6)

1 in 5 New Zealanders will experience mental illness in their lifetime, over half before the age of 25 (7).
New Zealand is grappling with a pandemic of our own – Mental Health!

STRESS

Stress is inevitable in our daily lives and we cannot change this, but it is important to deal with it. Stress triggers a fight-or-flight response, it manifests itself in anxiety or anger. We don't realise that it is going on in our bodies. Stress releases cortisol and adrenalin into our body's system, and these hormones tense your body. Without understanding stress, we are not going to make the changes we need to make - positive wellbeing.

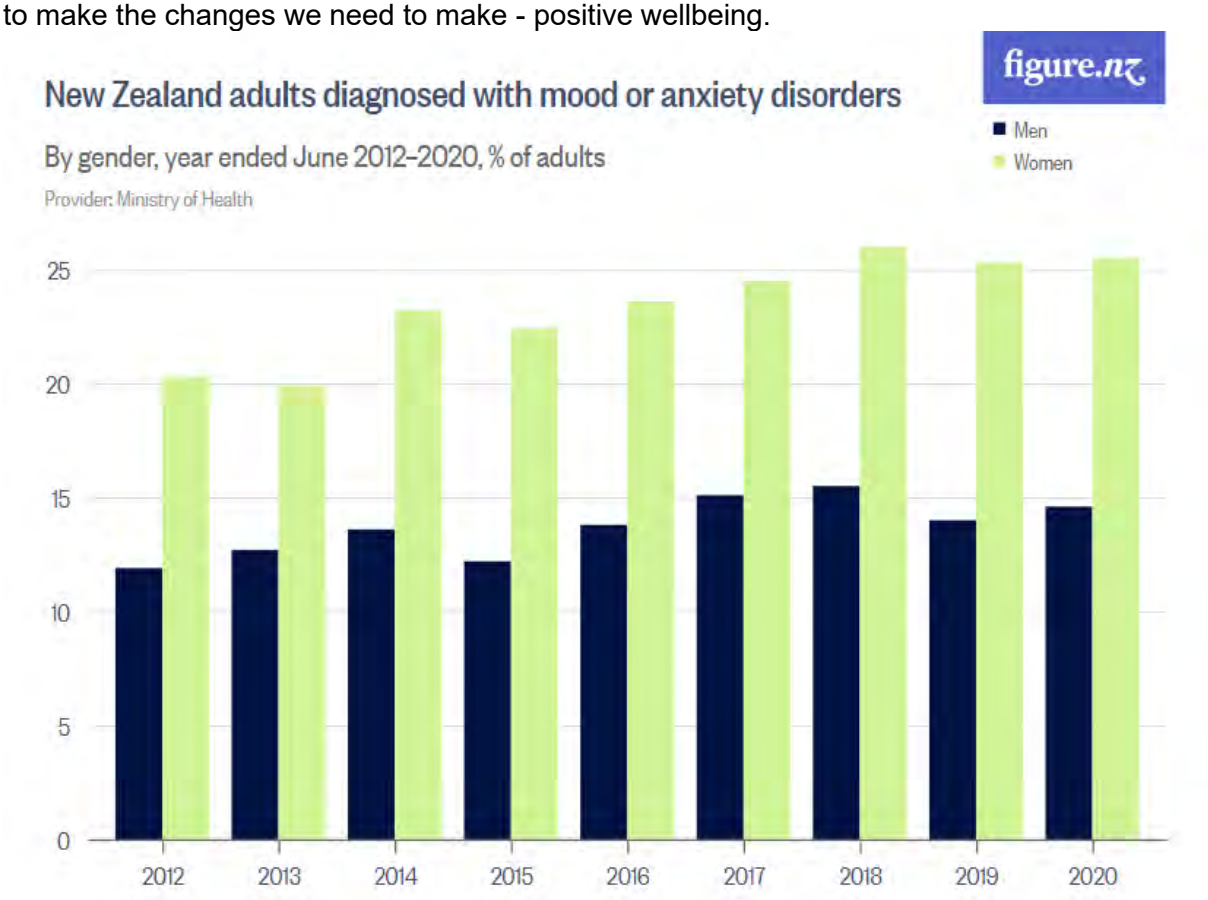

UNDERSTANDING THE SCIENCE

Serotonin (9)

Serotonin is a neurotransmitter, meaning it's used to transmit messages between nerve cells (neurons). Inside your body, there are a number of naturally occurring chemicals that carry messages around – kind of like an internal text messaging system. Serotonin influences your mood, your sleep, your appetite levels, and your digestion.
Some of the most important roles of serotonin include:
Mood regulation
If your serotonin levels are right, you'll feel happier, better able to focus, and more emotionally stable. On the flipside, an imbalance in serotonin levels has been linked to depression.
Appetite and digestion
Serotonin influences how your bowel works. If you eat something dodgy, your intestines will make more serotonin to help get it out of your body (from both ends) more quickly. It also helps reduce your appetite as you eat.

Sleep regulation
Serotonin helps regulate your sleep/wake cycle. Low serotonin levels can interfere with your sleep, which in turn can affect your health and wellbeing.
Self esteem
Serotonin has been labelled the confidence neurochemical. Higher serotonin activity is related to greater feelings of confidence, which in turn gives you the drive to do the things that build self-esteem.
Memory
Serotonin also influences memory and learning. In particular, serotonin seems to improve the speed of learning.
Blood clotting
When you cut yourself, serotonin gets to work helping your blood clot to stop the bleeding.

Dopamine (10)

The body uses dopamine to create chemicals called norepinephrine and epinephrine. Dopamine plays an integral role in the reward system, a group of brain processes that control motivation, desire, and cravings. Dopamine levels also influence your mood, your sleep, blood flow as well as movement and alertness.
Dopamine relays signals between neurons that control body movements and coordination. This neurotransmitter also plays a role in the brain's pleasure and reward centre, and it drives many behaviours. Eating certain foods, taking illicit drugs, and engaging in behaviours such as gambling can all cause dopamine levels in the brain to spike.
Higher levels of dopamine can lead to feelings of euphoria, bliss, and enhanced motivation and concentration. Therefore, exposure to substances and activities that increase dopamine can become addictive to some people.

Endorphins (10)

The word endorphin comes from putting together the words "endogenous," meaning from within the body, and "morphine," which is an opiate pain reliever. In other words, endorphins got their name because they are natural pain relievers. They are tiny neurochemicals released by your body.
Endorphins consist of a large group of peptides. They are produced by the central nervous system and the pituitary gland. Since endorphins act on the opiate receptors in our brains, they reduce pain and boost pleasure, resulting in a feeling of well-being. Endorphins are released in response to pain or stress, but they're also released during other activities, like eating, exercise, or sex.
What is the purpose of endorphins?
Not all of the role's endorphins play in the body are completely understood. What is known is that endorphins are important to reduce pain and enhance pleasure.
Endorphins are involved in our natural reward circuits and are related to important activities like eating, drinking, physical fitness, and sexual intercourse. Endorphins also surge during pregnancy. They minimize discomfort and pain and maximize pleasure. This helps us to continue functioning despite injury or stress.
Since humans naturally seek to feel pleasure and avoid pain, we're more likely to do an activity if it makes us feel good. From an evolutionary standpoint, this helps ensure survival. Humans are social creatures, and we thrive in communities. Endorphins have been shown to also help reinforce social attachments.

MAKING THE SCIENCE WORK FOR YOU

Get a move on
Exercise increases serotonin and endorphin production and release. Whether it's walking, running, yoga or playing sport, regular exercise makes you feel good and is great for your overall health.
Eat your way to health and happiness
Eating certain foods can help boost serotonin and dopamine levels. These include salmon, spinach, poultry, eggs, soy products, milk, nuts and seeds, chocolate.
Remember the time when …
When you think about something good that's happened in the past, your brain will increase serotonin production. Chatting with someone, looking at old photos or visualising a happy moment can all improve your mood.
Let there be light
Getting a good dose of natural sunlight every day helps increase your serotonin and levels. Being exposed to sunlight in the morning also helps your brain and body wake up. At night, avoid blue light from computer screens as this interferes with the conversion of serotonin into melatonin (the hormone that makes you feel sleepy).
Massage to happiness
Several studies have shown massage increases serotonin levels, which is why you always feel so damn good after one.
Listen to Music
Listening to music can be a fun way to stimulate dopamine release in the brain by up to 9%.
Getting Enough Sleep
Lack of Sleep can reduce dopamine sensitivity in the brain, resulting in excessive feelings of sleepiness. Getting a good night's rest may help regulate your body's natural dopamine.
Goal Achievement
When we achieve one of our goals, our brain releases dopamine. The brain finds this dopamine rush very rewarding. It seeks out more dopamine by working toward another goal. However, it's best to start with small goals to improve your chances of success. Short-term goals can add up to achieve a long-term goal (and a bigger reward). This pattern keeps a steady release of dopamine in your brain.

MENTAL WELLBEING

We need to be our authentic selves. We all have good days and bad days, and we need to all understand that bad days are okay, and they do not define us, either as individuals or as part of a team.
Sir John Kirwan, Mental Health ambassador and Mentemia co-founder recalls: "I wanted to jump out the window in Buenos Aires". "The guy sitting next to me said, 'JK, you have got a good heart'. That person saved my life." He likens a proactive approach to mental health to putting your knee out at a game of touch. You see the GP, get a referral to a specialist, and some weeks later, an operation and recovery. The brain is the same. If it is ill, you need to treat it. Stress accumulates in the body and mind day after day if nothing is done about it, Kirwan says. "I learned to get rid of it on a daily basis. We are not going to change the stress in our day." Mental Health is an illness and needs to be treated as such and being vulnerable and seeking help is a sign of strength, not weakness (11).

Finding your sweet spot
Mental Health and Wellbeing is all about active and positive practices, or daily rituals that ensure that our own mental health is being looked after. These rituals are personal, but when practised everyday will provide us with the right balance of neurotransmitters to ensure our good days are great and our bad days are few and you are able to deal with and manage daily stress.
Set your own plan for wellbeing, be true to yourself, be vulnerable, be authentic.

Here is a guide:

LEAD (12)

L ook After you It all starts with small daily habits. When we are following our own wellbeing plan, we are better able to bounce back from stress, build resilience and feel happier in our everyday lives.

E xperiment Create a daily plan involving using Mentemia's six pillars of wellbeing.

- *CHILL* Find proven ways to help your body and mind to fully unwind.
- *MOVE* Tune in to your physical self and help release your brain's feel-good chemicals, endorphins.
- *DO* Get busy with activities that engage your brain.
- *ENJOY* Allow fun and laughter in your day.
- *CONNECT* Practise gratitude, acknowledge your strengths and weaknesses. Celebrate your wins.

A dapt Practise to find your right formula, and don't be afraid to change.

D evelop Habits Make time, make a plan, and get doing.

By focusing on yourself and your own wellbeing means that you are then able to demonstrate to those around you the benefits of having a personal wellbeing plan and practising it. To do this:

SHOW (12)

S et an Example Talk openly about what you've found and what has helped. Don't be afraid to show vulnerability, and let them know that you take it seriously, and you are human too. Most importantly, let it be seen that you are incorporating your well-being habits into your day.

H elp It is up to everyone to make their own plan. Encourage them to experiment until they have found their formula.

O bserve Look for ways that you can encourage daily habits.

W ork As a Team Teamwork makes the dream work, so find ways people can practise your habits together.

The benefits of a collective approach where individuals and teams are prioritising, and practising wellbeing will ensure vulnerability and being authentic will be commonplace.

Because we all have a bad day, there will be times when those around us may be struggling or need some extra help. Here is how we can help:

CARE (12)

C heck in Checking in regularly with people will help to build a sense of trust, and if you do recognise that someone is in distress then checking in about how they are and what they need is critical. A check in does not need to be searching questions, just a simple "How are you?"

A ctively Listen Your most important job is just to listen, give your undivided attention. No need to rush in with solutions or attempt to solve all their problems.

R eassure Reassure that this is not a burden and it is ok to talk. It's not about having the answers, it's about making sure help that is needed is sourced.

E ncourage This is about encouragement to seek the right help to support wellbeing.

SUMMARY

“**Daily habits that will change your life**” **(1)**

One hour of exercise

Two litres of water

Three cups of tea

Four colours on the plate

Five minutes of meditation

Six songs that motivate you

Seven minutes of laughter

Eight hours of sleep

Nine pages of a book

Ten reasons to be thankful

It’s important to be your authentic self and it is Okay not to be Okay!

References.

1. Brendon Cooley, Voices of Hope, www.thevoicesofhope.org 2021
2. www.covid19.govt.nz
3. New Zealand Police 2020
4. Mental Health Foundation August 2020
5. Coronial Services of New Zealand 2020
6. Mental Health Foundation 2020
7. MidCentral District Health Board 2020
8. Ministry of Health 2020
9. Mentemia – New Zealand Mental health and Wellbeing Organisation
10. Healthline 2017
11. Sir John Kirwan, Mental Health ambassador and Mentemia co-founder
12. Doctor Fiona Crichton Health Psychology Specialist and Mentemia Clinical Lead

concretenz BUILDING RESILIENCE
CONFERENCE 2022
13-15 October 2022
Energy Events Centre | Rotorua

NORTHLAND RAIL UPGRADE – FAST-TRACKED REPLACEMENT OF FIVE BRIDGES USING POST-TENSIONED SEGMENTAL CONSTRUCTION

M IRELAND[1]; R BALLEN[2]; A SUMMERS[1]

[1] Holmes Consulting
[2] KiwiRail

SUMMARY

Following a successful application for funding from the Provincial Growth Fund, the Northland Rail Upgrade (NRU) project team began the arduous task of upgrading the railway line between West Auckland and Whangarei. Starting in late 2019, the projects vision was to rejuvenate rail operations on the North Auckland Line (NAL) and improve the economy of Northland. In doing so, it has improved asset health and resilience on the line, reduced rail freight journey time by easing current speed restrictions and enabled Hi-cube container freight capability. This paper focuses on the successes and challenges related to the replacement of five existing timber piled bridges that formed part of the programme of works for the Northland Rail Upgrade project. These are Bridges 88, 89, 100, 126 and 168 on the NAL.

INTRODUCTION

New Zealand's railway has a long history, operating since the mid-nineteenth century. The railways were built to connect people and places and enable efficient movement of freight around the country. Inevitably, certain periods in the past were not all conducive for railway transportation due to various political pressures. This meant substantial rail infrastructure was either not adequately maintained for a long period or discontinued due to limited patronage. Resurgence of rail is nothing new and recently KiwiRail with support from New Zealand Government has made a concerted effort to rejuvenate some of these long-neglected railways.

Following successfully receiving funds from the government, KiwiRail began upgrading the North Auckland Line (NAL) in late 2019. There are thirteen tunnels and 88 bridges between Swanson and Whangarei on the NAL. All the tunnels required maintenance and repairs including lowering all of the tunnel floors to provide sufficient clearance for Hi-cube container freight. Of the 88 bridges, five of the timber piled bridges were identified for replacement, along with one bridge that required lowering to align with the adjacent lowered tunnel floor. Additionally, track renewal works involving the replacement of 50,000 sleepers, the placement of 50,000m^3 of ballast, improvements to drainage, and vegetation clearance were performed.

Figure 1. Northland Rail Upgrade Overview

KIWIRAIL'S OBJECTIVES FOR THE PROJECT

With the vision of improving the economy of Northland and rejuvenating the North Auckland Line, KiwiRail had the following primary objectives for the NRU project:

- Enable existing speed restrictions to be lifted in areas being attended, reducing the rail freight journey time between Northland and Auckland.
- Make the network more resilient and reliable, reducing the number of outages.
- Provide conditions that will enable rail freight growth in Northland.
- As much as possible, utilise Northland based contractors and locally sourced materials for construction.

Another key criteria for the project was that most of the construction was to be completed within a five month of Block-of-Line (BoL) period to limit disruption to rail services to a confined block of time. This single criterion was critical to many design decisions.

THE EXISTING BRIDGES

KiwiRail identified five bridges on the NAL with low bridge health index scores that required replacement (Bridges 88, 89, 100, 126 & 168 NAL). These five bridges ranged in age from 80 to 100+yrs old and were a mix of steel and timber spans, predominately supported on timber piled piers. Bridge 89 NAL and Bridge 100 NAL prior to replacement are shown in Figure 2.

Primary reasons for these bridges requiring replacement included:

- Deteriorated condition of timber elements.
- Piles founded at shallow depths and at risk of scour.
- Timber piles in marine environment vulnerable to attack from Teredo worm (a form of marine borer).
- Low strength rating of timber and steel spans. Limiting train axle loading and line speed.

- Some steel spans having exceeded theoretical fatigue life.
- Improving safety for railway maintenance staff by providing across structure walkways.

Figure 2. Bridge 89 and Bridge 100 NAL before replacement

THE REPLACEMENT BRIDGES

From the onset of the project the design team faced the challenge of a very compressed design programme for the replacement bridges, to enable construction during the planned BoL. The concept development for replacement bridges took just over two weeks to investigate the plausible configuration (number of spans), superstructure types, and substructure details for all five bridges. With only preliminary investigations of geotechnical and hydraulics for each site available at this stage. From beginning concept design to practical completion of construction, 9 months had been allowed.

A series of key design drivers were considered when developing concepts for the replacement bridges. These included:

- Span configuration - single, two and three span bridges were considered suitable. Bridges with a greater number of spans were not considered as they would require more in-stream work (minimising in-stream work helped reduce complications with consenting) and shorter spans were not considered economical.
- Requirement to minimise or eliminate the need for any track raising to avoid disturbing existing embankments.
- Adopt tried and tested construction techniques used in New Zealand, to minimise potential for cost and programme over run.
- Standardisation and simplification. To reduce design and construction time.
- KiwiRail's preference for ballast deck structure to minimise on-going maintenance costs.

Following a series of concept development workshops including all the project team, a standardised design was selected for the five bridges. This consisted of three-span bridge structures for Bridge 88 & 89 NAL and two-span structures for Bridges 100, 126 & 168 NAL. For the bridge superstructures a post-tensioned concrete ballast tray form was adopted, which was designed using a segmental precast concrete approach. This form of construction had previously been implemented successfully on KiwiRail bridges during the NCTIR (North Canterbury Transport Infrastructure Recovery) project and lessons from that project were taken forward on the NRU project. A more conventional substructure form was adopted, typically consisting of twin bored piles and an insitu concrete capping beam.

Figure 3. 3D image of Bridge 88 NAL .

Superstructure Form

The standardised superstructure form adopted for all five bridges was a segmental post-tensioned concrete ballast tray. The superstructure spans are simply supported on plain rubber elastomeric bearing pads, with a span length of 16m between bearing centrelines. The ballast trays have an overall depth of 1.35m, with the inside width of the tray being 4.1m and an overall width of 6.1m. On either side of the ballast tray, 1m wide outstands act as a structural elements, whilst also allowing maintenance walkways to be incorporated on each side of the bridge. A typical cross section of the superstructure is shown in Figure 4.

The post-tensioned ballast trays were designed and constructed using a match-cast segmental precast concrete approach. Each span consisted of six precast segments, with each segment being 2.75m in length and weighing approximately 22 tonnes. The units were transported individually and joined together on-site. Some of the key advantages of this approach included:

- Precast segments were fabricated and cured off-site in the controlled environment of a precast yard.
- Reduced on-site construction time to enable completion during BoL period.
- Match casting of one segment against the face of the previous segment ensured perfect fitment of segments.
- Segments could be made of a manageable size and weight for transportation and handling.

On-site the six segments that formed a span were placed on temporary works. Locator keys were incorporated into the match cast faces of the precast segments to help align adjacent segments. Epoxy was then applied to the joint faces before a temporary stressing force was applied whilst the epoxy cured. A specialised segmental bridge adhesive (epoxy) was specified, as they have been formulated to both lubricate the segments during fitment and provide the required shear transfer and durability across the joints once cured.

After the epoxy had cured the permanent post-tensioning strands were installed and stressed to complete the span. The BoL period allowed the spans to be constructed on the existing rail alignment, therefore once completed they only needed to be lowered down from the temporary works onto the new piers and bearings. Once lowered, the spans were secured in-place using a combination of reinforced concrete headwalls and stainless steel dowel bars. Refer Figure 5 and Figure 6 for examples of temporary works implemented.

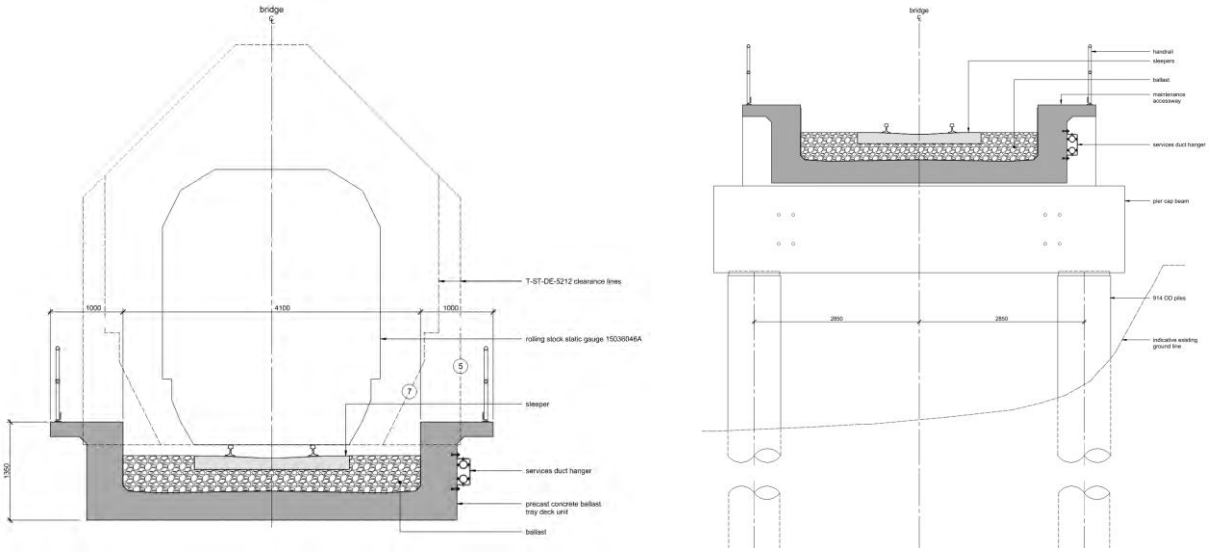

Figure 4. Typical superstructure cross-section and pier elevation

Figure 5. Precast segments supported on temporary works at Bridge 100 NAL

Figure 6. Trial fitment of segments at Bridge 126 NAL

Substructure Form

The piers and abutments consisted of two piles and a reinforced concrete cap beam. The piles were spaced at 5.7m centres to enable installation of the piles before the planned BoL if required. At Bridges 88, 89, 100 and 168 permanently cased bored piles that socketed into the founding rock layer were adopted. These were typically 900mm diameter, except at Bridge 168 where 1050mm diameter piles were required due to the increased depth of the founding rock layer. At Bridge 126 the Northland Allochthon founding rock layer was not considered suitable for bored pile construction, therefore driven steel tubes were specified. A typical pier elevation is shown in Figure 4.

The abutment and pier capping beams were typically 1.3m-1.4m wide x 1.5m deep and were designed to be constructed in-situ. As part of this project, localised improvements were performed on the embankments directly behind the abutments. These improvements were performed to reduce the likelihood and magnitude of static soil creep and seismic soil displacements, which cause large demands on the piles. At the abutments of each bridge, 4m long settlement slabs were provided, along with wingwalls to retain the embankment and ballast.

DESIGN CHALLENGES AND SUCCESSES

As with all projects of this size there were several challenges during the design and construction phase of these bridges which required solving. These challenges however lead too many successes that should be celebrated and shared by the parties involved. Further detail on how some of these more significant challenges were successfully navigated by the project team is provided in the following sections.

One Team Collaborative Approach:

The compressed design and construction programme required a cohesive project team to avoid the inherent time losses that come with a disjointed team.

The structural design was led by Holmes Consulting with three design offices being used to resource the bridge design and internal verification. An ECI (Early Contractor Involvement) process early in the design phase ensured that the bridge design suited Contractor's experience, plant and the availability of materials to avoid delays associated with design/construction mismatch. Together with Geotechnical, Hydraulic and Geometric sub-consultants, work was often completed in parallel with each other to develop, design and detail solutions to meet programme milestones. While originally intending to work out of a project office, Covid-19 restrictions forced the project to go online early in the detailed design process.

The five bridges were constructed by three main contractors, with precast work being completed by a further two sub-contractors. During construction, a full-time design representative was required to monitor construction QA and attend site, with the five bridges progressing in parallel. Microsoft Teams was implemented across the project for both communications and document control.

Standardisation and Segmental Construction:

From concept design, it was identified that standardisation was a key driver to ensure the design and construction teams could successfully deliver the work in the required programme. This led to all five bridges having the same length span, with either two or three spans for each structure. Coupled with segmental bridge construction, each bridge span was broken into six equal length match-cast precast units. In total, the bridge superstructures incorporated 72 precast units.

Whilst a standardised approach was adopted where possible, unique constraints relating to the location of the site or ground conditions meant that each bridge had some unique challenges that required consideration during design and construction. A summary of the most significant unique features working against the standardisation philosophy are provided below:

- Bridges 88 & 89 – Located in a marine environment with limited freeboard.
- Bridge 100 – High approach embankments requiring mechanically stabilized retaining walls. Farm access track passing beneath bridge.
- Bridge 126 – Piles founded in sensitive Northland allochthon rock which is not suitable for bored pile construction, therefore driven piles were adopted instead. No-exit local road passing beneath bridge.
- Bridge 168 – Located in a marine environment with a curved track alignment. Spans skewed to accommodate curved track within the ballast tray with sufficient clearance. Increased depth to founding rock layer meant larger diameter piles required.

Limited freeboard

The existing bridges over the tidal waterways (Bridges 88 and 89 NAL) did not have adequate freeboard for the design flood event of 100-year ARI (Average Recurrence Interval), when considering the future sea level rise and climate change effects. Even without the consideration of future sea level rise, these two bridges had nil or substandard freeboard.

To satisfy future freeboard requirements, including possible future sea level rise and accounting for the effective depth of the new superstructure, the track would need to be raised 700 – 1,250mm. As this is only a possible future requirement it was agreed not to raise the soffit levels of these two bridges at this time but to design-in a method for the bridge superstructures to be lifted. By doing so, this work could be completed at a later date, and in parallel with adjacent line raising.

To allow for the potential future lifting of Bridges 88 and 89, recesses have been provided in the top of the abutment caps, which allow jacks to be installed to enable the superstructure to be raised. At the piers, horizontal ducts have been provided through the piers which will allow temporary jacking corbels to be attached using post-tensioning bars. The depth of the abutment and pier caps will then need to be increased to permanently support the superstructure at its new height through insitu concrete pours. The substructure was then designed considering increased seismic mass and an increase in the effective seismic inertia height.

Soil loads at the bridge abutments

A risk was identified that the existing embankments could impose creep and/or seismic soil displacements on the structure, as the approaches often sat anywhere from 3-6m proud of the surrounding ground. An optimisation exercise was carried out to balance approach embankment improvements with the structural capacity of the structure to sustain soil displacements.

Soil improvements were limited to localised replacement of material behind the abutments with geogrid improved gravel rafts. Additional oversized pile sleeves and approach setbacks were too provided to limit the improved material imposing large passive earth pressures on the structure should movement occur. Where only shallow sleeves were required, inexpensive and readily available precast concrete risers were used. Approach setback details typically used across the replacement bridges can be seen in Figure 7 (left). In the instance of Bridge 100

NAL which required a mechanically stabilized earth wall embankment, the entire approach was set back behind the piles as shown in Figure 7 (right). The settlement slabs then acted as land spans to bridge the gap between the approach embankment and the abutments.

Given the improvements noted, the bridge structures were then designed to accommodate any residual creep and seismic soil displacements. Estimated soil creep displacements ranged between 80 and 300mm whilst the seismic displacements ranged between 40 and 300mm. These displacements are predominantly expected to take place in the longitudinal direction of the bridge.

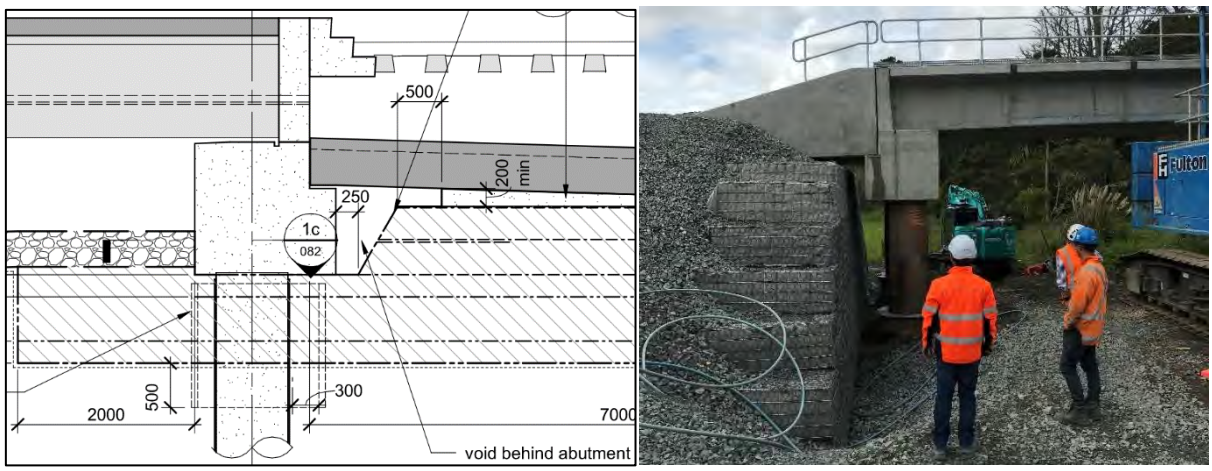

Figure 7. Approach setbacks, left – typical across bridges, right - Brigde 100 NAL

Early Procurement of Materials

Early procurement of pile casing was crucial to starting construction on time. For the case of the NRU programme, this meant confirming the pile size very early in the design process. Having sized the piles for vertical loads, seismic inertia checks were found to not be not critical given the bridges low seismic hazard zone. The piles were however very sensitive to both creep and seismic soil ground displacements. With limited geotechnical investigations and detailed embankment modeling still underway this was a challenge. An exercise was therefore undertaken to identify the outstanding risk at each bridge site and what mitigation measures could be implemented through design. The following were all considered:

- Form plastic hinges in the piles when subject to seismic soil movements.
- Pile casings considered as permanent structural elements to increase moment capacity in highly loaded areas.
- Increase extent of ground improvement behind the abutments to reduce expected movements.
- Increase the length of oversized sleeves provided.
- Construction of the embankments before the piles, to enable short term construction sequence related movements to take place prior to pile installation.
- Apply seismic philosophy to the design of creep soil movements, allowing plastic hinges to form in selected locations while insuring stability when subject to dead and live loads.
- Install monitoring equipment to track slope movements and implement a traffic light system to identify movements that may trigger slope stabilisation works being required.

SUMMARY
The completion of the Northland Rail Upgrade project has improved the conditions for rail freight growth between Northland and Auckland by providing a more resilient and reliable network, reducing journey times, and enabling High-cube container freight. This will help reduce road congestion by reducing road freight movements, which will also reduce overall transport emissions.

The replacement of five bridges has provided a more resilient and reliable network as they have been designed to current design standards which has enabled speed restrictions to be eased and axle load limitations that were in place for the existing bridges to be removed. The ballast tray form of the new bridges also requires less maintenance than the directly fastened track bridge structures that they replace. Safety for railway maintenance staff has also been improved by the provision of walkways with handrails, across either side of each new bridge.

The standardisation of the bridge forms, in particular that of the superstructure and the adoption of match-cast segmental construction proved to be key to the success of this project. As it significantly reduced the on-site construction time enabling the compressed programme to be met.

Another key objective of the project was to bring economic benefits to the Northland communities. This was achieved through the design team engaging local consultancies to participate in the design delivery and utilising locally sourced material and labour for construction, such as precast concrete. One of the three contractors engaged to build the bridges was also locally based in Northland, and they constructed both Bridges 126 and 168, located near Wellsford and Whangarei respectively. This enabled the upskilling of the local staff, in addition to bringing economic returns to the region. The ultimate prize for the Northland communities is the rejuvenated NAL, which enables improved and effective freight movement, additionally allowing for the connection to the future proposed Marsden Point Link.

The objectives the project setout to achieve were successfully completed on-time and on-budget and the Hi-Cube capable NAL re-opened for rail traffic on the 11th of January 2021.

Figure 8. New Bridge 88 NAL

Figure 9. Bridge 126 NAL near completion and Bridge 168 NAL

ACKNOWLEDGEMENTS

KiwiRail – Client;
Tonkin + Taylor – Geotechnical & Hydraulics;
Vitruvius – Alignment;
Cook Costello/MacroVentures – Design/Construction Sub-consultants
HEB, Fulton Hogan and United Civil – Contractors
Novare Design – Structural Peer Review

SESSION 4A

Chair:
Moustafa Al-Ani

concretenz
BUILDING RESILIENCE
CONFERENCE 2022
13-15 October 2022
Energy Events Centre | Rotorua

DESIGN AND CONSTRUCTION OF TE WĀNANGA A NEW WATERFRONT SPACE FOR AUCKLAND

ALEX VINK[1], ALEX FOXON[2], KIEL HEEKS-PURELL[3]

[1] Tonkin + Taylor, Auckland, New Zealand
[2] Isthmus Group ltd, Auckland, New Zealand
[3] HEB Construction, Auckland, New Zealand

SUMMARY

This paper presents an overview of the design and construction of Te Wānanga, located on Quay Street, Auckland. Te Wānanga provides unprecedented connectivity between Auckland's central city and the Waitematā Harbour, with a coastal Pōhutukawa grove floating above the sea. The public space comprises an approximately 1,600 m^2 suspended reinforced concrete wharf with both an organic seaward edge form and numerous irregularly shaped apertures for architectural features, including deck-mounted sunken steel planters which hold large Pōhutukawa and native flora, woven suspended nets, and open apertures with sculpted steel balustrades.

INTRODUCTION

As part of the Downtown Infrastructure Development Programme in Auckland, a new wharf structure, called Te Wānanga was proposed to provide a new public space. Te Wānanga, which was designed to blend the boundary between the city and the harbour, is located in Quay Street, Auckland Central. Te Wānanga consists of reinforced concrete-filled steel tube piles supporting a reinforced concrete deck, which has both an organic seaward edge form and numerous irregularly shaped apertures within the extent of the deck (refer to Figure 1). These apertures create space for a number of architectural features; including deck-mounted suspended steel planters which hold large Pōhutukawa trees, woven suspended Kupenga (nets) and open apertures with sculptural steel balustrades. The steel planters consist of flat plate elements welded together with both base and wall stiffeners and are cast into the deck using headed steel studs. The concrete slab is nominally a flat slab, but in fact consists of a constant soffit level with a varying topping level which resulted in a deck thickness varying from a nominal 500 mm to 1000 mm with a 330 mm terraced step down towards the western end.

Figure 1 Te Wānanga Architectural Render

DESIGN METHODOLOGY

The design of Te Wānanga was delivered using the Early Contractor Involvement (ECI) process to improve constructability whilst retaining key architectural features and meeting project programme constraints. This resulted in a more collaborative design approach than a traditional construction project.

Architectural Design

The design of Te Wānanga aimed to create an elevated tidal shelf for human and coastal ecology. Making space for and creating a closer connection between people and marine life at the edge of Downtown Auckland. Conceptualised as an eroded sandstone shelf, the high shell content concrete mix, varied surface finishes and organic forms took inspiration from the historical coastline that has since disappeared as the city has evolved. The organic line of the deck creates a non-linear edge to the city, more in-keeping with that of the marine environment that Te Wānanga interacts with, rather than the usual linear encroachment of harbour edge developments.

The apertures create a porosity to the deck, which provides the opportunity for interaction with the water below. Woven kupenga (nets) and sculptural balustrades fixed to the internal edges of open apertures create visual and auditory connection to the water below, reveal heritage elements that have been hidden for many years and bring to focus the constructed ecology ropes system fixed between deck and seabed.

As the form of the deck took inspiration from the sandstone shelves of the Waitemata, it was important to create a concrete mix to suit. Through thorough design team and contractor coordination, a sampling process was undertaken to create a mix that had the warmth of local

sandstone and included a high shell content, exposed to varying degrees, to provide connection to the marine environment. All while achieving the strength requirements for the assigned design life of the structure.

Structural Design Philosophy

Te Wānanga was designed as an importance level 3 structure with a 50 year design life in accordance with AS/NZS 1170. All concrete elements were detailed to achieve a 100 year durability design life. Load combinations from AS/NZS 1170 and AS 4997 were adopted for design. All reinforced concrete elements were designed and detailed in accordance with NZS 3101 and all steel elements were designed in accordance with NZS 3404 with appropriate allowances for corrosion losses in accordance with SNZ TS 3404.

The structural analysis was carried out using the software package SAP2000 for which a 3D non-linear static model was created. The key structural elements were modelled (refer to Figure 3) with the piles and steel planters modelled as frame elements, and the reinforced concrete flat slab modelled as shell elements (each section property is shown in a different colour). Rigid frame elements were used to connect the planters to the deck slab at stiffener locations.

A series of non-linear springs were required for the structural model in SAP2000 to model the soil. The p-y curves of the soil were generated using the software LPile and were subsequently converted into non-linear lateral springs for input. These non-linear springs representing the soil were applied as compression only springs at the quarter points around the circumference of each pile and at 1 m intervals along the pile length.

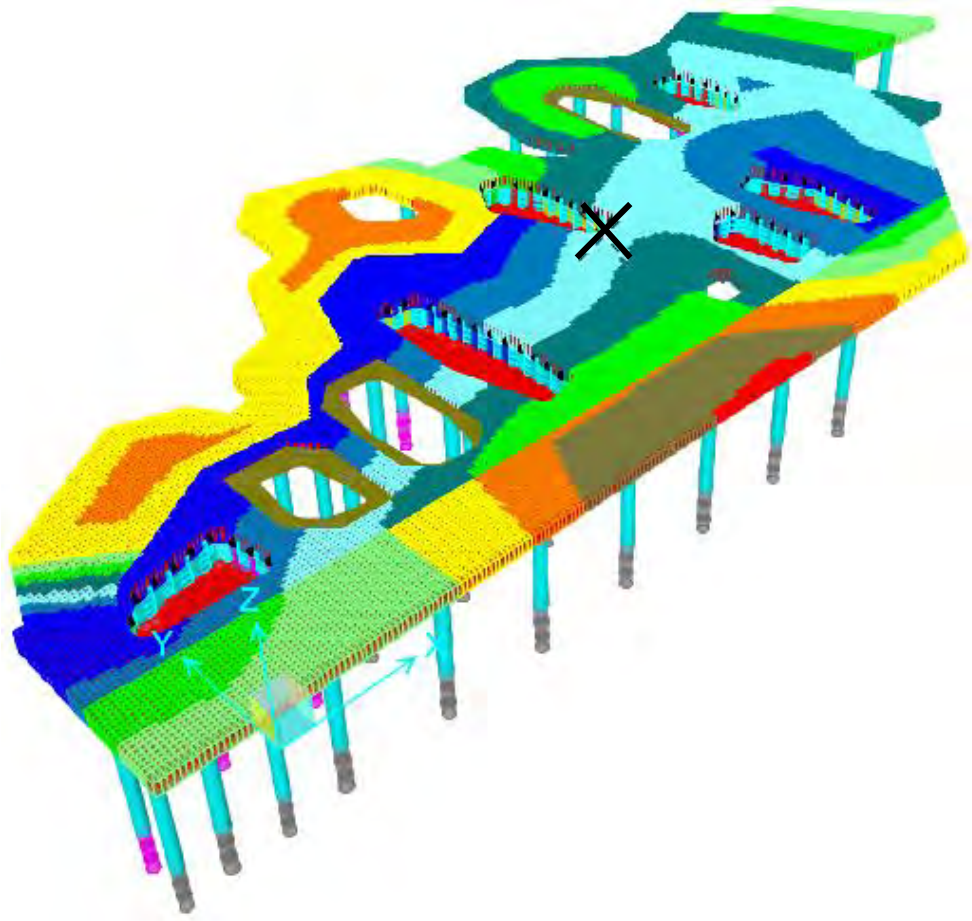

Figure 2: Te Wānanga SAP2000 model isometric view

Pushover Analysis

Seismic analysis was carried out using the non-linear static procedure (more commonly referred to as pushover analysis) in accordance with the guidance set out on ASCE 41-17 and ASCE 61-14, but adopting the material properties and load regimes in the relevant New Zealand standards. Pushover analysis broadly involves the creation of an analysis model which is representative of the structure. The relevant non-linear elements (in this case plastic hinges and soil stiffness) are also modelled. Horizontal forces of increasing magnitude (in this case proportional to the mass lumped at each node) are applied to the model until the plastic hinges reach a predetermined rotation limit. The displacement of a target node (in this case the centroid of the deck which is marked by a cross in Figure 3) at a rotation limit is then compared to the displacement demand of the structure for a design level earthquake. The boundary conditions in the horizontal direction were modelled by non-linear p-y curves which represent the supporting ground, and the vertical support was modelled by a vertical restraint at the pile toe. The structure was displaced in both positive and negative directions, parallel and perpendicular to the shoreline.

Column hinge properties were modelled in accordance with the relevant sections of ASCE 41-17 and ASCE 61-14. ASCE guidelines for the seismic design of wharves suggest allowing for a “weak column – strong deck” hierarchy. Accordingly, plastic hinges were allowed to form at both the head of the column and in the ground within the prescribed hinge rotation limits. ASCE 61-14 guidance gives allowable material strains and hence plastic hinge rotations for a given earthquake event. These rotations relate to a level of damage rather than an Ultimate Limit State (ULS) or a Maximum Credible Earthquake (MCE). The hinge rotations for “Controlled and Repairable Damage” were treated as the maximum rotations for the ULS earthquake. Similarly, the hinge rotations for “Life Safety Protection” were treated as the maximum rotations for the MCE earthquake.

The displacement demand for the ULS earthquake at the target node, ranged from approximately 125mm to 225mm. The displacement ductility demand on the structure at ULS ranged between 1.75 and 2.0. The reasons for the range in displacement and ductility demands result from the sensitivity cases that were carried out to assess how certain assumptions affected overall seismic performance.

For most analysis scenarios, the steel tube pile casings were treated as being composite with the reinforced concrete piles for the purposes of calculating stiffness, but ignored for strength considerations. Under this assumption, the structure was found to be relatively stiff with fundamental elastic periods in the order of 0.8s, and therefore displacements were towards the lower end of the displacement range in the preceding paragraph.

As part of the sensitivity analyses, the casing was ignored for the calculation of stiffness. This scenario represented long term corrosion loss of the casing or a total debond of the casing from the reinforced concrete piles and gave a longer period of approximately 1.2s and displacements towards the upper end of the range above.

CONSTRUCTION METHODOLOGY

The construction of Te Wānanga proved challenging due to a very densely reinforced deck slab and a high level of architectural finish required. These factors, combined with the irregular geometry, multiple apertures and congested worksite in Downtown Auckland provided for a very challenging construction phase.

As the project was run under an ECI agreement this gave the Constructor the opportunity to add value to the construction phase during the design stage of the project. One of these

changes was the standardisation of pile spacing; this allowed the use of a standardised falsework system which could also be re-used throughout the construction duration as opposed to using bespoke panels for each deck pour. As this was identified during the ECI phase, changes were able to be made to the design of the slab in a timely manner and the overall user experience/aesthetics of the space was not negatively impacted.

The construction of the piles was undertaken from a jack up barge in the basin. 31 out of the 49 structural piles had an oversize casing to protect the piles from displacement of the rock armour during a seismic event. The addition of these oversize casings meant that the installation of the piles required additional processes to normal pile construction. First the oversize casings were installed, vibro-hammered to the correct embedment and drilled out to depth. Then the internal, structural casings were installed inside the oversize casings with consideration given to maintain a clear annulus around the pile; before vibro-hammering to depth, drilling and placement of concrete. HDPE sleeves were also required surrounding the oversize casings and the annulus between the HDPE sleeve and oversize casings filled with grout to complete the piles.

The density of the reinforcement (approximately 500 kg/m3) in the deck slab, combined with the complex geometry, meant that careful planning and sequencing were required to ensure efficiency was maintained throughout the construction phase and the strict project programme was adhered to. As construction advanced, learnings were used from the process and alternative construction sequences were introduced to further ease the construction process.

TECHNICAL CHALLENGES

The irregular plan arrangement of Te Wānanga presented a number of challenges for both analysis and construction. Due to these complexities, and the additional challenging programme requirements, Te Wānanga project used the Early Contractor Involvement (ECI) as the delivery model.

Deck Slab

Valuable feedback from the constructors included that a structure with a flat soffit would offer significant programme savings and end up being cheaper than a conventional “beam and slab” structure. A flat soffit also provides better pile-slab connections by eliminating the need for an additional beam pour; this also improves the corrosion resistivity of the slabs structure by removing a potential cold joint. The design requirements of having a step in top surface of the slab, and an architectural preference to eliminate deck joints resulted in a thicker continuous slab than what would be conventionally needed for strength purposes.

The conventional seismic design approach of a “weak column – strong deck” hierarchy associated with wharves makes minimising pile strength a desirable design outcome as this allows the deck to be reduced in size. The minimum thickness of Te Wānanga deck slab was dictated by both anchorage of the pile bars into the deck slab and overstrength considerations at the thinnest section of the deck. Due to the stormwater drainage requirements, the outer edge of the deck was raised to provide falls back to landside raingardens. This provided the opportunity to include a 330mm high terraced step which increased the deck thickness up to 1000mm in parts. This increased deck thickness presented a number of technical challenges due to an increase in seismic mass, concrete deck shrinkage and temperature effects. Temperature effects and concrete deck shrinkage ended up being the dominant factors in the design, particularly when considering crack width.

Pushover analysis was adopted to minimise the size of the piles, which would minimise the deck thickness and reduce the effects of shrinkage and temperature as far as practical. Pushover analysis also allowed more accurate consideration of the increased seismic mass,

as well as both the irregular mass distribution resulting from the plan layout, and the irregular stiffness distribution due to variable soil levels and profiles, compared to conventional force based design.

Serviceability design for durability, specifically the crack width maximum recommended limits in NZS 3101 for a coastal environment, was the governing consideration for the design of the deck slab reinforcing arrangement. The positive differential temperature case (where the top of the concrete deck is hotter than the bottom due to solar radiation) led to large tension and bending forces in the concrete deck.

Shrinkage was also a governing design consideration for durability as this induced very large tension forces in the concrete deck. The risk of cracking was exacerbated by the constructor's preferred construction sequence, whereby the deck is poured sequentially in five pours from east to west, with the first four pours being two spans wide and the final pour being four spans wide. The differential shrinkage effects due to restraint between the pours results in large tension forces on the newer pour, which are effectively "locked-in" at the start of the structure's design life.

Due to the significance of shrinkage on the overall design of Te Wānanga's deck slab, both shrinkage limits for the deck were specified, and shrinkage beam tests were carried out. The effects of the construction sequencing and shrinkage on the stresses induced in the deck were considered during the detailed design of Te Wānanga. This analysis also considered the uncertainty associated with the construction programme by assessing the likely shrinkage to have occurred at both the maximum and minimum times between pours and specifying these timeframes in coordination with the constructors.

Figure 3: Reinforcing in concrete slab prior to pour (Rebate for planter in foreground)

The installation of the planters was carried out in a two-stage pour sequence: A first stage concrete pour was carried out at the time of the main deck pours with a subsequent second concrete topping pour occurring when the steel planters were suspended in place to finish the deck surface. This two-stage pour resulted in additional “locked-in” bending stresses due to the differential shrinkage between the main concrete pours and the second infill pour.

The combination of large net shrinkage forces and differential shrinkage forces associated with the construction staging combined with the significant thermal effects resulted in a large reinforcing content (refer **Error! Reference source not found.**) requirement to ensure that the crack width was below the maximum recommended limits in NZS 3101 for a coastal environment.

Kupenga Openings

The design of the concrete cantilevers, which overhang the woven, suspended Kupenga nets, to conceal the Kupenga fixings, required a novel solution to comply with the relevant code provisions. The cantilever needed to be as slender as possible to minimise the step down from the deck surface level to the Kupenga nets.

Figure 4: Kupenga slab reinforcing. Note that insulating tape has not been applied to the stainless reinforcing bars at the time of photography.

Analysis indicated that there were very large tension forces in these slender slabs as a result of deck shrinkage in particular. Effectively, the thicker surrounding deck imparted large tension forces into the cantilever slab. Design analysis indicated that using large reinforcing bars was not a viable option as the cantilever slab would be over reinforced, which could result in brittle compression failure in the concrete rather than a ductile failure of yielding of the reinforcing bar. To overcome this challenge, small stainless steel reinforcing bars, which would yield under flexural loading, were provided with minimal cover to resist bending stresses, while large hooked tension bars in orthogonal directions closer to the mid depth of the slab were used to resist the large tension forces (refer Figure 4).

CONCLUSION

This paper presents a case study of the construction of a public space, which seeks to make space for and create a closer connection between people and marine life at the edge of Downtown Auckland. Achieving the project vision presented a number of unique architectural, engineering and construction challenges which, when overcome by the entire project team, has delivered outstanding results and an enduring legacy for both Aucklanders and those who visit the city to enjoy for generations to come.

ACKNOWLEDGEMENTS

The authors are grateful to the clients, Auckland Transport and Auckland Council, for their permission to use their project as a case study to prepare this paper and for their vision. The authors would also like to thank our collaborators Mana Whenua Working Group: Ngāti Whātua Ōrākei, Ngaati Whanaunga, Ngai Tai ki Tāmaki, Ngāti Maru, Ngāti Te Ata, Te Akitai Waiohua, Te Patukirikiri, Ngāti Tamaoho, Ngāti Paoa, Ngāti Whātua Runanga, Ngāti Whātua ki Kaipara and Te Ahiwaru.

REFERENCES

American Society of Civil Engineers (2017). Seismic Design of Piers and Wharves (ASCE 41-17).

American Society of Civil Engineers (2014). Seismic Evaluation and Retrofit of Existing Buildings (ASCE 61-14).

Computers & Structures Inc (2020). SAP2000 (Version 21.0.2) [Computer Software]. https://www.csiamerica.com/products/sap2000

Ensoft Inc (2018). LPile (Version 2018.10.09) [Computer Software]. https://www.ensoftinc.com/products/lpile/

Standards Australia. (2002-2011). Structural Design Actions (AS/NZS 1170).

Standards Australia. (2005). Guidelines for the Design of Maritime Structures (AS 4997:2005).

Standards New Zealand. (1997-2009). Steel Structures Standard (NZS 3404).

Standards New Zealand. (2006). Concrete Structures Standard (NZS 3101).

Standards New Zealand. (2018). Durability Requirements for Steel Structures and Components (SNZ TS 3404).

concretenz
BUILDING RESILIENCE
CONFERENCE 2022
13-15 October 2022
Energy Events Centre | Rotorua

OVERVIEW OF THE CYCLIC SHEAR DETERIORATION OF CORROSION DAMAGED REINFORCED CONCRETE CIRCULAR COLUMNS

BENJAMIN MATTHEWS[1], ALESSANDRO PALERMO[1], ALLAN SCOTT[1]

Department of Civil and Natural Resources Engineering, University of Canterbury, Christchurch, New Zealand

Abstract

Reinforced concrete (RC) elements suffer continuous deterioration across their lifetime from in-situ aggressive environmental factors. Spiral reinforcing corrodes preferentially to longitudinal reinforcing, due to the smaller nominal diameter and thickness of protective cover concrete. Therefore, identifying the current shear resistance of an RC member in its deteriorated state is critical when assessing the seismic reliability of a structure. This research addresses the issue of chloride-induced corrosion damage in RC circular bridge piers, specifically focusing on the degradation rate of the seismic shear capacity. The paper covers five RC concrete columns, four of which are artificially corroded to two design damage levels, at two imposed current densities - 200 μA/cm^2 and 300 μA/cm^2. The results indicate the peak shear capacity is adversely affected by corrosion at severe deterioration levels. However, ultimate displacement suffers much heavier degradation, with a maximum reduction of 66 % recorded. The transverse steel is more susceptible to chloride-induced corrosion, deteriorating at a much faster rate than the respective longitudinal steel.

Introduction

Reinforced concrete offers prodigious economic and structural benefits, making it one of the most widely sought-after materials across the globe. However, the non-homogeneous nature of concrete allows aggressive corrosive agents to continually depreciate the material throughout its service life. Water infiltration and chemical ingress activate premature deterioration of critical structural elements and reduce the serviceability and ultimate service life of structures. Within New Zealand, RC is a principal structural material, used across construction disciplines because of its economic efficiency and robustness. Since many current in-service bridges across New Zealand were constructed between the 1950s and 1970s, they do not conform to modern seismic design and durability requirements practiced today [1, 2].

The residual shear capacity of aged RC members exposed to corrosive environments is a crucial consideration that must be recognized when performing any seismic assessment. Since the transverse reinforcement is typically detailed as the outer-facing reinforcement with the least amount of concrete cover, in conjunction with being detailed with a smaller diameter than the larger longitudinal bars – it has a much higher susceptibility to severe corrosive effects than the longitudinal reinforcement. To this day, a paucity of experimental data has been collected on the seismic shear behavior of circular bridge piers with increasing levels of chloride-induced deterioration [3, 4]. This provides an opportunity for further research, with a

particular interest in quantifying the rate of seismic shear strength degradation of in-service coastal New Zealand bridge piers. The experimental campaign presented herein focuses on the design, artificial corrosion, and structural testing of four RC circular columns. The effects of corrosion on the cyclic response are evaluated and discussed in relation to an uncorroded benchmark of identical design.

Experimental Program

Specimen design

Five reinforced concrete circular columns were designed to fail primarily in shear, under cyclic lateral loading. Each column was designed with a 500 mm diameter and 25 mm of concrete cover to the transverse steel. All columns had a total height of 1850 mm and a clear height of 1075 mm, corresponding to a low aspect ratio of 2.15 to ensure shear failure was achieved. All specimens were detailed with 18 H25 Grade500E deformed longitudinal bars, corresponding to a longitudinal steel ratio of 4.5 %, which falls within the acceptable range as defined by NZS3101 [5]. Alternating bars were detailed with hooked ends at 150 mm radii to improve anchorage and enable sufficient stress development. Because of the high steel volume, there was not enough space to hook every bar. To that end, a high strength 70 MPa design mix was used for the base 600 mm of each column, further promoting sufficient development in the longitudinal steel. The structural height of each column was cast using standard 30 MPa design mixes. Table 1 summarises the key design properties of each column. All transverse reinforcement was 10 mm Grade300E round spiral bars at 65 mm spacing within the structural zone – corresponding to a transverse volumetric ratio of 1.1 %. Figure 1 illustrates the standard reinforcement and geometric design of each column specimen.

Test Setup

Each test was performed under displacement-controlled quasi-static fully reversed cyclic loading, following ACI T1.1 [6] standard loading protocol guidelines (Figure 2c). Cyclic lateral loading was induced via a 1000 kN hydraulic actuator operating at 3000 psi, attached to a steel loading collar pretensioned to the concrete column (Figure 2b). A constant axial compression ratio of 2 % was applied to every test specimen, based on the concrete cylinder

Table 1. Specimen design properties

Column ID	f'_c (28 days) (MPa)	f'_c (test day) (MPa)	d_b (mm)	d_{sp} (mm)	s (mm)
BM	34.2	35.9	25	10	65
L1	49.2	56.7	25	10	65
L2	34.2	38.6	25	10	65
S1	49.2	56.7	25	10	65
S2	41.9	46.7	25	10	65

Note: BM = Benchmark uncorroded specimen; L = low target corrosion level; and S = severe corrosion target level.

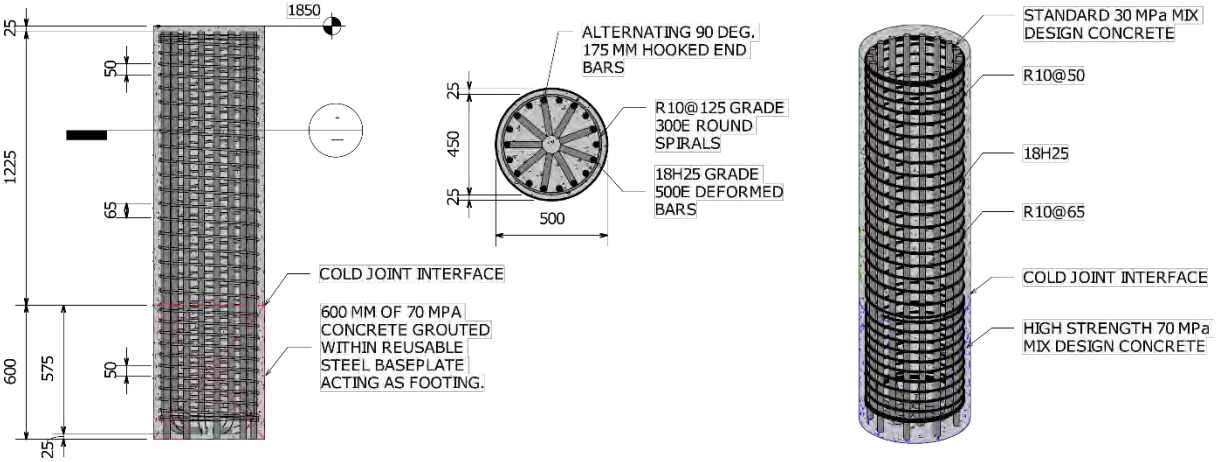

Figure 1. Specimen design

compressive strength of the specimen on the day of testing (Table 1). Axial load was applied through a concentrically placed spreader beam loaded via two vertical 440 kN hydraulic actuators as shown in Figure 2b. The vertical actuators operated on an adaptive self-centering program to ensure that the axial remained concentric through the column section at positive and negative drifts.

Columns were cast monolithically and confined inside of a 600 mm tall reusable steel baseplate acting as the footing detail. A high-performance 65 MPa grout was cast inside the baseplate central tube to effectively confine each specimen. The baseplate collar and floor connections were pretensioned to ensure confinement and realistic conditions were maintained throughout each test. Additional stiffening work was carried out on the baseplate and loading collar prior to testing to minimize deflection in critical areas. Shear keys were installed in the load direction to minimize baseplate slip at high shear stresses.

Artificial Corrosion

Artificially accelerated chloride-induced corrosion was induced through an application of the impressed-current technique, incorporating wet and dry phasing to create more realistic corrosion distributions [7 - 8]. Two target damage levels were designed for – low and severe corrosion, corresponding to approximately 2 % and 12.5 % mass loss of the longitudinal steel, respectively. Two corrosion current densities were applied – 200 μA/cm^2 and 300 μA/cm^2 to investigate whether there were any observable differences in the corrosion distribution or structural behavior. Because artificial corrosion methodologies often pose a risk of over-accelerating the process, creating unrealistic distributions of corrosion morphologies and bond conditions, low imposed current densities are often preferred. El-Maaddawy and Soudki [9] determined that a current density of 300 μA/cm^2 is the maximum desired limit of electrical input before unrealistic corrosion morphologies become prevalent in specimens and the steel-concrete bond interaction is adversely affected. The duration of each corrosion incubation period was estimated using Faraday's Law of Electrolysis (Equation 1) [10]. Table 2 summarises the key corrosion design parameters used in this study.

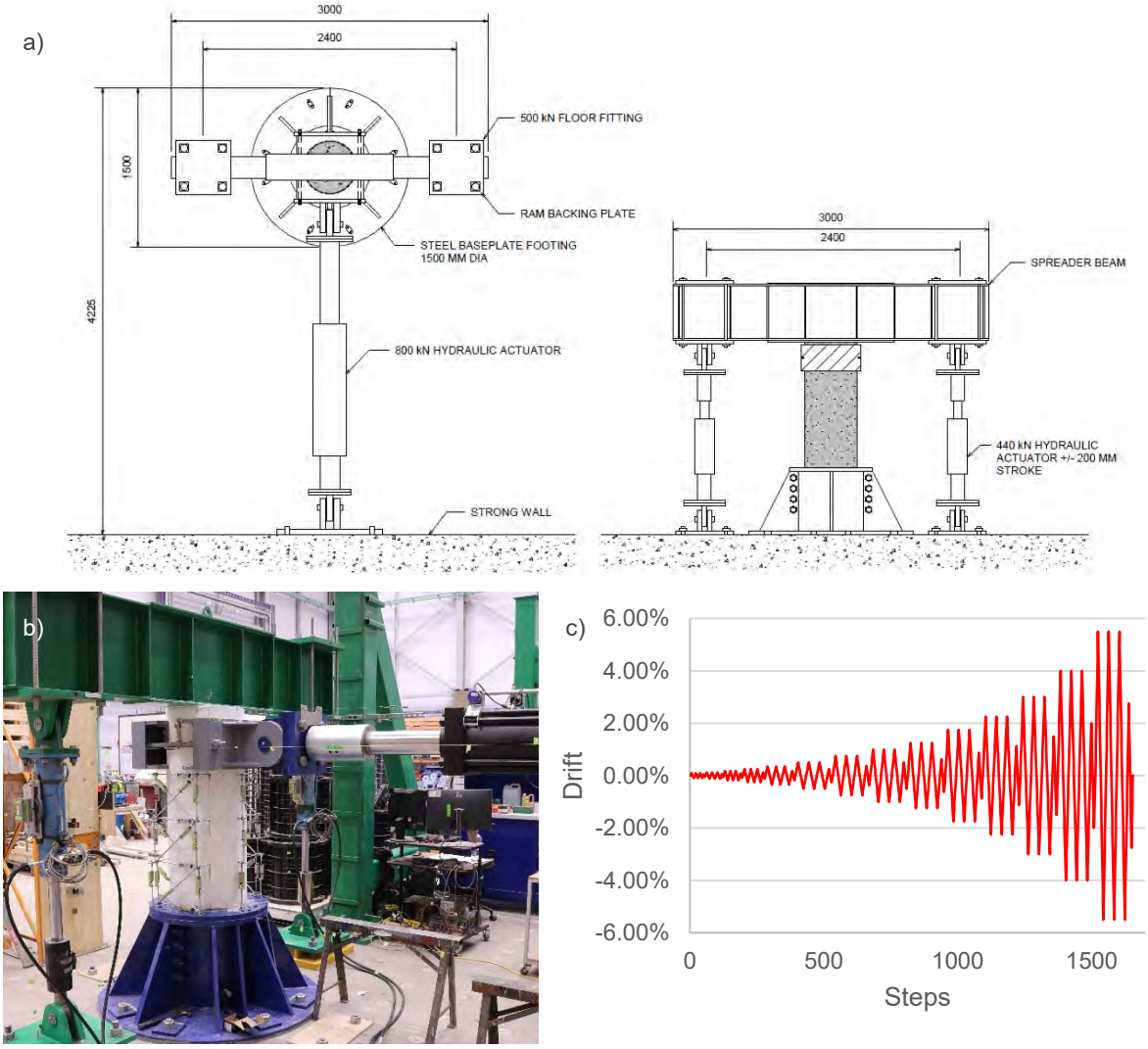

Figure 2. Test setup plan and front views (a); photograph of test setup (b); reveresed cyclic loading protocol based on ACI T1.1 (2001) guidelines (c).

$$t = \frac{ZF\Delta m}{IA} \quad (1)$$

Where t is the corrosion duration in days, Z is the ionic valency of the reacting electrode (iron = 2), F is Faraday's constant (96487 A.s), Δm is the design mass loss target in grams (also presented in terms of percentage as η), and A the molar mass of iron (55.847 g). The imposed current I (amps) is the product of the design current density, i in μA/cm^2, and the surface area of the reacting anodic steel, a, in cm^2.

A ratio of 4 days saturated to 3 days drying was implemented across the full duration of corrosion incubation. A separate holding tank is used to store the saltwater solution while the specimens are drying (Figure 3). During each drying period, the electrical current is stopped to reduce the diffusion of chloride ions and promote a semi-natural reaction rate. At the end of each drying period, the water was returned to the corrosion tank and the impressed-current regime resumed. A 3.5 % NaCl solution was used across the program, with regular quality monitoring through specific conductance, pH, and temperature measurements. Non-iodized salt was used to achieve the desired solution concentration. When the solution exceeded a

Table 2. Corrosion design parameters

Specimen ID	η_L (%)	η_{sp} (%)	i (μA/cm^2)	Current, I (Amps)	Duration (days)
L1	2	5	200	4.47	20
L2	2	5	300	6.70	13
S1	12.5	31.25	200	4.47	123
S2	12.5	31.25	300	6.70	82

predefined conductance and total dissolved solid threshold, the tank was emptied, cleaned, and replaced.

Each column was flipped before being placed inside the solution to ensure full submergence of the structural height. Areas outside of the structural zone were protected by 3 mm thick neoprene rubber sheeting, attached to the concrete surface through a high bonding strength contact adhesive. The rubber sheeting provides an impervious insulating barrier to stop moisture ingress through the concrete surface, while also disrupting the electrical field. Six 25 mm x 3 mm stainless steel flat bars were arranged evenly around the circumference of each column to act cathodically in the corrosion circuit, causing the embedded reinforcement within the reactive zone to become anodic. Figure 3 demonstrates the standard corrosion setup for each column specimen.

Corrosion Damage Assessment

After loading until failure, each column was demolished to extract the corroded steel and evaluate the samples to determine the true mass loss percentage. Every second longitudinal bar was removed to develop an understanding of the corrosion distribution around the column circumference. Each sample was then cut into equal 460 mm segments and compared back to uncorroded counterparts of identical lengths. Spirals were cut and measured on a per-leg basis. Sandblasting was undertaken as a mechanical cleaning methodology to remove rust by-products from the steel samples and prepare them for gravimetric assessment. Once cleaned, the corrosion damage of each sample was measured using a simple gravimetric evaluation, shown by Equation 2 below. Table 3 summarizes the average mass loss percentages calculated for each test specimen.

$$\eta = \frac{m_0 - m_c}{m_0} \times 100 \quad (2)$$

Where η is the mass loss percentage of the corroded reinforcement, m_0 is the initial mass in grams and m_c is the corroded mass of the reinforcement sample after cleaning.

Structural Test Results

Minor flexural cracks began forming consistently around 0.5 % drift in the extreme tension fibers, during each respective push and pull cycle. Diagonal struts formed at 1.25 % drift for the lowly corroded columns, L1 and L2, and benchmark column BM. S1 and S2 demonstrated earlier damage states with struts forming closer to 1.00 % drift. Throughout the early drift magnitudes, across all corroded tests, structural damage appeared to proliferate from the pre-existing corrosion cracks, until the load exceeded the tensile splitting capacity of the concrete. This effect was verified by the higher degree of structural damage sustained by the uncorroded

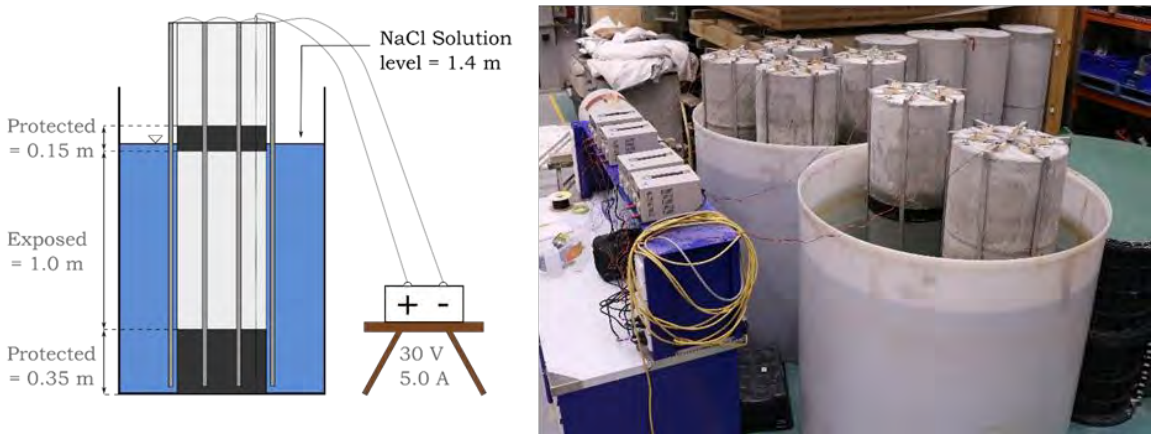

Figure 3. Artificial corrosion setup schematic (left); photograph of impressed-current setup (right).

benchmark column during the early drift magnitudes. Figure 4 displays the damage photos of each column, taken at the point of concrete cover spalling.

Final failure mechanisms showed a clear transition as corrosion increased through the specimens. Columns BM, L1, and L2 all displayed shear failure mechanisms with a limited amount of ductility. Table 3 summarises the key structural parameters measured throughout each test. Yield load and displacements were estimated based on the equivalent reduced stiffness at $0.75P_{peak}$, adapted from recommendations by Park [11]. Ultimate deflection is measured as $0.85P_{peak}$. Specimen L1 outperformed the uncorroded benchmark specimen by a margin of 10.9 %. This was likely caused by the significant difference in final concrete compressive strength on the day of testing. Due to supplier variation and continual Covid-19-related delays, final recorded compressive strengths varied significantly between columns. Despite this, as corrosion increases, clear structural deterioration is still observable in the recorded responses. Specimen L2 demonstrated only minor reductions to peak load-bearing capacity (R_p) and ultimate displacement (R_Δ). At severe deterioration levels, however, specimens S1 and S2 showed considerable reductions of 37.5 % and 28.5 % in peak load-bearing capacity, respectively. Alarmingly, the rate of degradation in ultimate displacement capacity was almost double that of the load-bearing capacity, measuring at 66.1 % and 53.8 % for specimens S1 and S2 respectively. Both severely corroded columns demonstrated

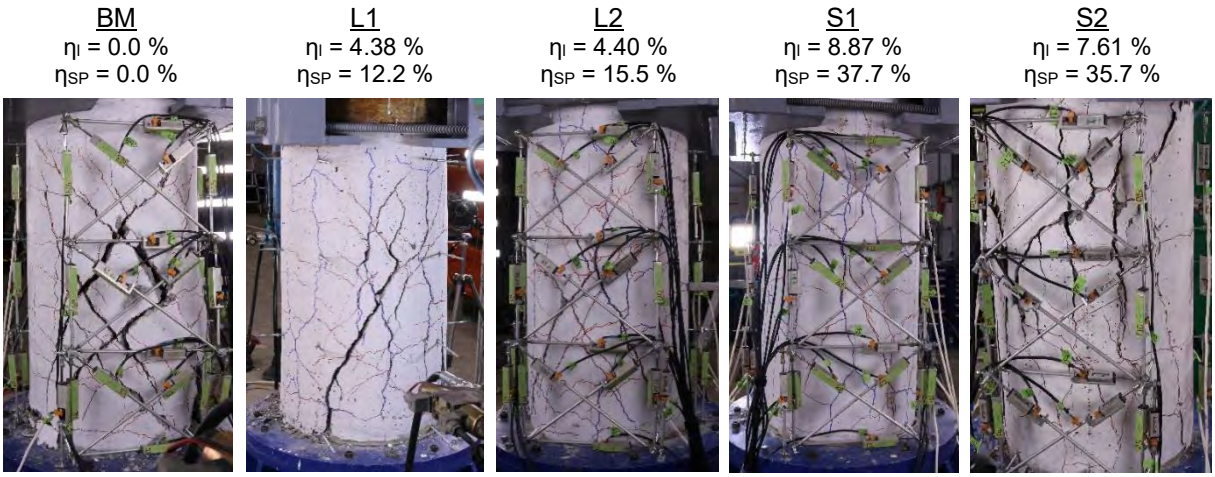

Figure 4. Damage photos at point of spalling.

extremely brittle shear-bond-dominated failure modes. Figure 5 displays the hysteresis behavior of each tested column. The degree of deterioration can be visualized by the comparative skeleton plot shown in Figure 5. After removing the concrete cover following the test, it was observed that both S1 and S2 had several discrete locations of 100 % spiral mass loss. Because of the nature of the spiral reinforcement, once the continuous loop is disrupted, the effective confinement provided to the core is lost, as whole cage sections are

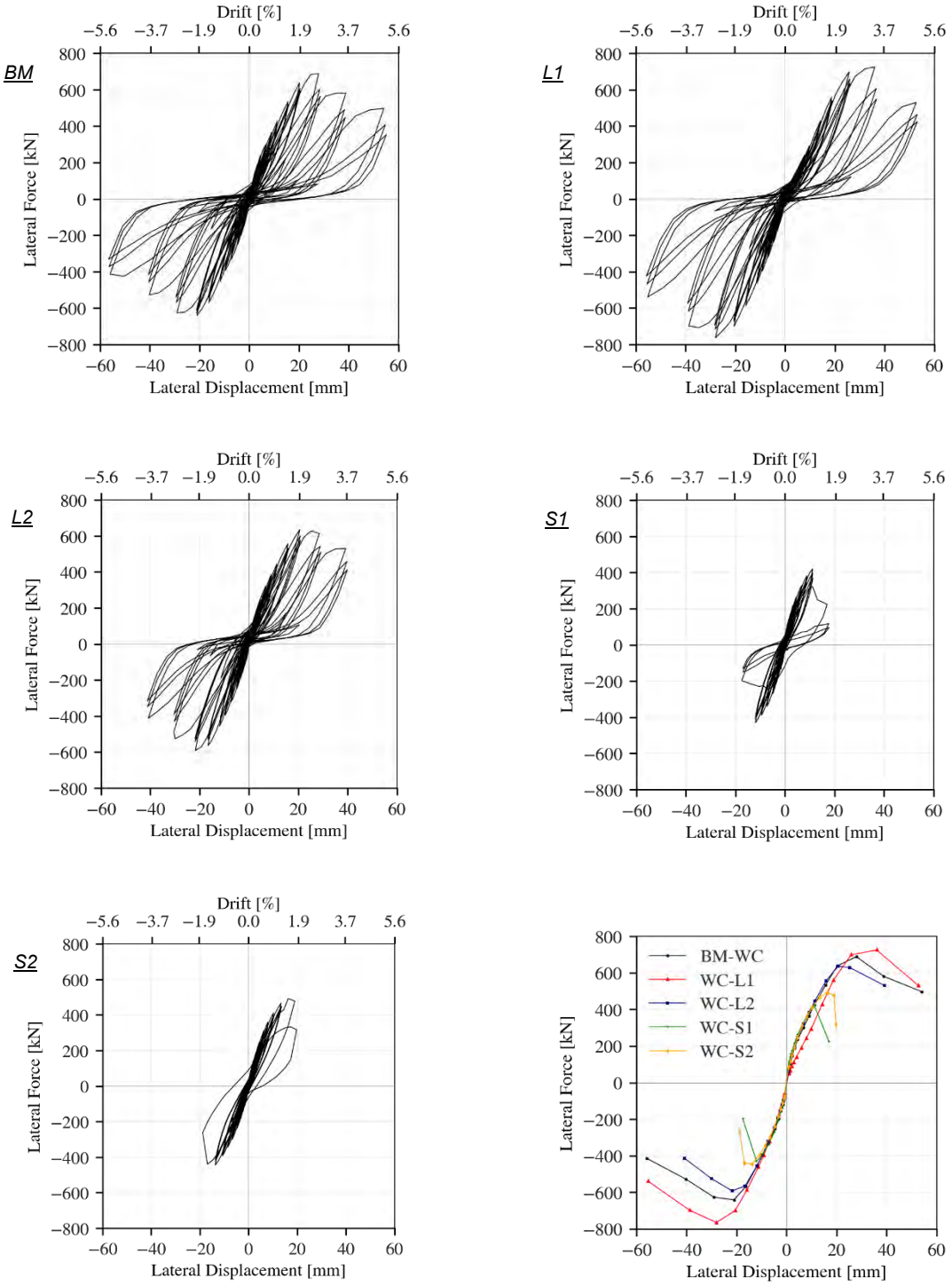

Figure 5. Cyclic hysteresis loop of each test specimen and combined skeleton curves (bottom right).

Table 3. Key corrosion and structural test parameters.

Spec ID	$\eta_{L,ave}$ (%)	$\eta_{sp,ave}$ (%)	Δ_y (mm)	$P_{peak,\ push}$ (kN)	$P_{peak,\ pull}$ (kN)	Δ_u (mm)	ΔV_n (kN)	R_P (%)	$R_{\Delta u}$ (%)
BM	0	0	20.9	689	640	38.4	-	-	-
L1	4.38	12.2	24.2	725	764	40.3	-75	-10.9	-4.95
L2	4.40	15.5	17.1	637	592	37.4	52	7.58	2.68
S1	8.87	37.7	8.3	420	430	13.0	259	37.5	66.1
S2	7.61	35.7	11.7	493	444	17.8	196	28.5	53.8

no longer anchored outside of the loaded zone.

Conclusions

The cyclic response of four artificially corroded RC circular columns and one uncorroded benchmark column was investigated in this study. The following conclusions can be drawn from the reported results of this study.

- Structural damage to the concrete initiates at earlier stages as corrosion increases. At early drift magnitudes, damage concentrates at the locations of pre-existing corrosion cracking – typically longitudinal in nature – but proliferates at higher deflections.
- At low corrosion damage, only minor reductions to peak shear capacity and ultimate displacement are observed. Because of the difference in concrete compressive strength on the day of testing, specimen L1 outperformed the benchmark specimen making direct comparison difficult. No changes in the failure mechanism occurred at low-induced corrosion damage, with all columns displaying shear failure with limited ductility.
- At severe corrosion damage, significant reductions in peak shear capacity are observed, however, the ultimate deflection degrades by almost a factor of two, with a maximum reduction factor of 66 %. Several locations experienced 100 % deterioration of the spiral reinforcement, essentially losing all ability to confine the concrete core effectively. At this stage of deterioration, the final failure mode transitioned to an extremely brittle shear-bond dominated mode.

Acknowledgments

The authors wish to acknowledge the QuakeCore Centre for Earthquake Resilience for their financial support throughout the experimental campaign. Special thanks are given to the University of Canterbury Structural Engineering Laboratory technical staff for their continued practical and technical support. Lastly, the authors would like to acknowledge the Civil and Natural Resources Engineering Department for their contributions and financial support, without whom, this experimental work would not be possible.

References

[1] New Zealand Transport Agency. 1998. “Transfund New Zealand Research Report 129: Durability of Concrete Road Bridges in New Zealand.” Wellington, New Zealand. Retrieved from: https://www.nzta.govt.nz/assets/resources/research/reports/129/129-Durability-of-concrete-road-bridges-in-New-Zealand.pdf

[2] Rogers, Rhys. 2016. “Assessing pre-tensioned reinforcement corrosion within the New Zealand concrete bridge stock.” Ph.D. diss., Auckland University, Auckland, New Zealand.

[3] Gergely, Ioan, and Chris P. Pantelides, Ralph J. Nuismer, Lawrence D. Reaveley. 1998. “Bridge pier retrofit using fiber-reinforced plastic composites.” *Journal of composites for construction, 2*(4), 165-174.

[4] Cardone, Donatello, and Perrone, G., Sofia, S. 2013. “Experimental and numerical studies on the cyclic behavior of R/C hollow bridge piers with corroded rebars.” *Earthquakes and Structures, 4*(1), 41-62. Accessed September 19, 2020. doi: 10.12989/eas.2013.4.1.041

[5] Standards New Zealand, NZS3101, Concrete Structures Standard. 2006: Wellington, New Zealand.

[6] Committee, A.C.I., T1.1-01/T1.1R-01: Acceptance Criteria for Moment Frames Based on Structural Testing. Technical Documents.

[7] Yuan, Yingshu, and Yongsheng Ji and Surendra P. Shah 2007. “Comparison of two accelerated corrosion techniques for concrete structures.” *ACI Structural Journal, 104*(3), 344.

[8] Nguyen, Chinh Van, and Paul Lambert, 2018. “Effect of current density on accelerated corrosion of reinforcing steel bars in concrete.” *Structure and Infrastructure Engineering, 14*(11), 1535-1546. Accessed February 8, 2021. doi: 10.1080/15732479.2018.1459745

[9] El Maaddawy, Tamer A., and Khaled A. Soudki. 2003. “Effectiveness of impressed current technique to simulate corrosion of steel reinforcement in concrete.” *Journal of Materials in Civil Engineering, 15*(1), 41-47. Accessed November 11, 2020. doi: 10.1061/(ASCE)0899-1561(2003)15:1(41)

[10] Mangat, P. and M. Elgarf, Strength and serviceability of repaired reinforced concrete beams undergoing reinforcement corrosion. Magazine of concrete research, 1999. 51(2): p. 97-112.

[11] Park, R., Evaluation of ductility of structures and structural assemblages from laboratory testing. Bulletin of the new Zealand society for earthquake engineering, 1989. 22(3): p. 155-166.

concretenz
BUILDING RESILIENCE
CONFERENCE 2022
13-15 October 2022
Energy Events Centre | Rotorua

GLASS FIBRE-REINFORCED POLYMER (GFRP) BARS - A DURABLE REINFORCEMENT ALTERNATIVE FOR CONCRETE BRIDGE PIERS

C. STRATFORD[1], A. PALERMO[1] & A. SCOTT[1]

[1]Department of Civil and Natural Resources Engineering, University of Canterbury, Christchurch, NZ

SUMMARY

The corrosion of steel reinforcement can have a significant impact on the structural performance and service life of reinforced concrete (RC) bridges. Non-metallic reinforcement alternatives, such as Glass Fibre-Reinforced Polymer (GFRP) bars, are a promising new-build solution to enhance durability and increase life cycles. Despite recent advancements, applications of the bars are currently limited to non-seismic zones and members under bending and shear, such as bridge decks and slabs. This paper briefly reviews the issue of corrosion in RC bridges and introduces GFRP as an alternative reinforcement material. Secondly, an experimental program investigating their application in RC bridge piers is summarised.

INTRODUCTION

As a small island nation surrounded by sea, much of New Zealand's local road and state highway network lie in close proximity to the coastline, making the bridge infrastructure particularly susceptible to the effects of chloride-induced corrosion. In 1999, the New Zealand Transport Agency estimated approximately 80% of the bridges within this network incorporate reinforced concrete (RC) elements – a total of more than 10,500 structures – with this number expected to be even larger today. In addition to this, 40% of all bridges were affected by maintenance and durability problems, with reinforcement corrosion deemed the most threatening for concrete durability (Bruce et al. 1999). These harsh environmental conditions, combined with an ever-increasing population of ageing structures, has highlighted the potential vulnerability of New Zealand bridges to the long-term effects of corrosion-related degradation.

CORROSION IN REINFORCED CONCRETE

The corrosion of steel reinforcement is a gradual process that degrades the member from the inside out, making it difficult to detect until the damage is already advanced (Figure 1). Chlorides, generally from sea spray or splashing, penetrate the concrete through small pores or cracks, eventually reaching the internal bars. The subsequent build-up of corrosion products causes the bar to expand in volume, exerting outward pressure and radial tensile stresses into the surrounding concrete. Over time, cracks propagate to the surface of the member and the concrete cover spalls, further exposing the reinforcement to the environment. This degradation generally initiates in the transverse reinforcement due to its proximity the concrete surface and has proven to have a detrimental impact on both the material and section properties of RC members (Soltani, Safiey, & Brennan, 2019). Steel bars experience significant reductions in strength and ductility, which can trigger unanticipated brittle failure mechanisms. Concrete

spalling reduces the cross-sectional area, compromising the member's ability to safely support vertical gravity loads or bending.

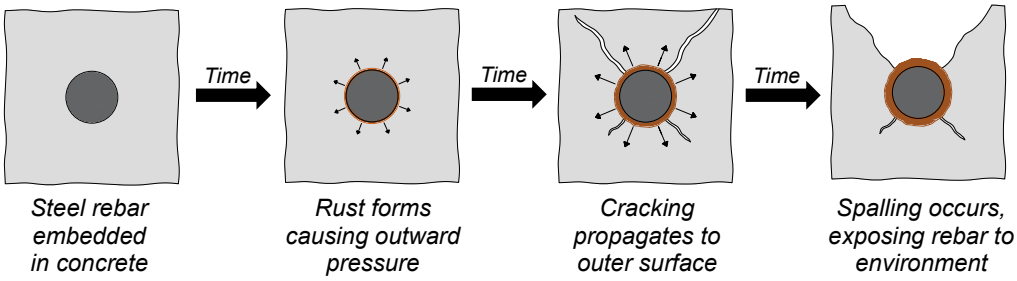

Figure 1. The corrosion process and its effect on reinforced concrete sections.

(Andisheh, 2017) investigated the cyclic response of RC bridge piers, which were artificially corroded to two distinct levels (Figure 2). The non-corroded (NC) benchmark exhibited a stable and ductile cyclic response, reaching a maximum drift of 6%. The corroded piers (CL1 & CL2) experienced accelerated degradation in both strength and stiffness leading to failure at 4% and 2.5% drift - a reduction in displacement ductility of 28% and 42%, respectively. The level of corrosion reduced the amount of hysteretic energy dissipated by the piers before failure, denoted by the area enclosed within the force-displacement loops. This was as much as 50% for CL1 and 73% for CL2. The potential risk this degradation imposes on the seismic performance of RC members, along with the substantial resources required to maintain their integrity and longevity, makes the corrosion of steel-reinforced concrete an important issue among the civil engineering industry.

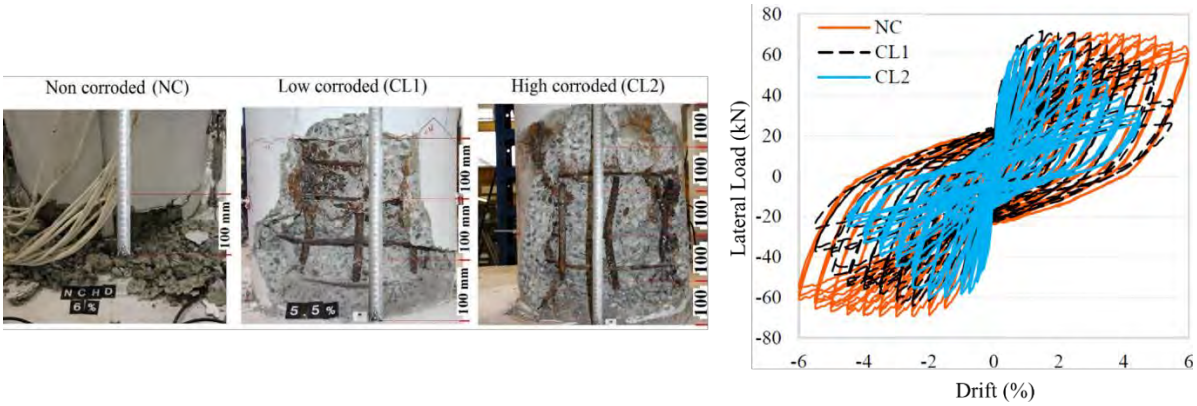

Figure 2. Cyclic response of artificially-corroded RC bridge piers (Andisheh, 2017).

Glass Fibre-Reinforced Polymer (GFRP) Bars: A Non-Metallic Alternative

The substitution of steel with non-metallic reinforcement materials is a promising solution to eliminate the effects of corrosion and increase the life cycle of RC structures. Of the materials readily available, GFRP bars have proved a viable alternative due to their non-corrosive nature, competitive cost, and high tensile strength - all whilst being one-quarter of the weight. Despite these advantages, significant care must be taken to account for the materials unique mechanical properties compared to conventional steel. The linear-elastic stress-strain behaviour up until a brittle failure (Figure 3) means a change in design philosophy is required, in which the section is generally over-reinforced to adopt concrete crushing as the preferred failure mechanism. Furthermore, the lower modulus of elasticity often results in serviceability criteria governing design, with higher reinforcement ratios required to meet deflection limits.

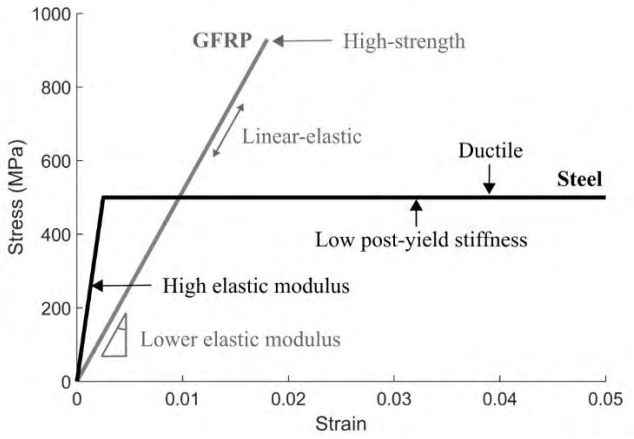

(a) (b)

Figure 3. (a) GFRP Mateenbar used in this study, and (b) comparison of idealised stress-strain behaviour with Grade 500E steel.

Significant research efforts on GFRP-RC members have led to the development of a range of international codes and guidelines (ACI, 2015; CSA, 2012; fib, 2007; JSCE, 1997) and the successful implementation of the bars in various structures around the world, including bridge decks, foundation slabs, seawalls, retaining walls, tunnel structures and buildings (Arduini & Balconi, 2020; FDOT, 2019; Rossini, Cadenazzi, Nolan, & Nanni, 2019). Although recent advancements have been considerable, uncertainty around the reduced compressive strength of the bars and the implications of their brittle failure mechanism has current applications limited to members under flexure or shear and structures within non-seismic regions. In addition to this, limited experimental and analytical data compared to steel and a lack of local design guidelines means New Zealand has yet to realise the full potential of GFRP as a primary reinforcement material. The research summarised in this paper builds on previous studies by investigating the applicability of GFRP bars to bridge piers located in seismically active regions.

GFRP-REINFORCED BRIDGE PIERS

In the seismic design of bridges, RC pier members resist lateral forces induced by seismic accelerations, whilst also supporting the vertical gravity loads of the structure. Capacity design principles are used to concentrate inelastic deformations in carefully detailed ‘plastic hinges’ in the pier, where seismic energy can be dissipated through ductile failure mechanisms. As a result, the seismic performance of the bridge relies heavily on the strength, stiffness, deformability and energy dissipation capabilities of the pier member. With modern bridges designed for a service life of 100 years, long-term durability is crucial to ensure the structure can maintain its resilience and functionality within the transport network.

To achieve this desired combination of durability and seismic performance, two novel reinforcement configurations incorporating GFRP bars were proposed in this study. A hybrid option combining steel longitudinal bars with GFRP spirals (Figure 4b) aims to increase the cover concrete to corrodible reinforcement, whilst maintaining the well-documented ductile response associated with steel longitudinal bars. (Pantelides, Gibbons, & Reaveley, 2013) showed the corrosion rate for steel longitudinal reinforcement could be reduced by two-thirds when steel spirals were replaced with GFRP, allowing hybrid columns to maintain a ductile failure mechanism after significant exposure to harsh environments. An all-GFRP option (Figure 4c) substitutes both the longitudinal and transverse reinforcement with GFRP, eliminating the risk of corrosion-induced deterioration completely. Limited experimental work in this area has shown that all-GFRP RC columns exhibit a softer cyclic response with little strength degradation or residual drift, however, a lower initial stiffness and reduced energy dissipation has also been observed (Ali & El-Salakawy, 2016; Elshamandy, Farghaly, & Benmokrane, 2018; Shamim & Zahra, 2018).

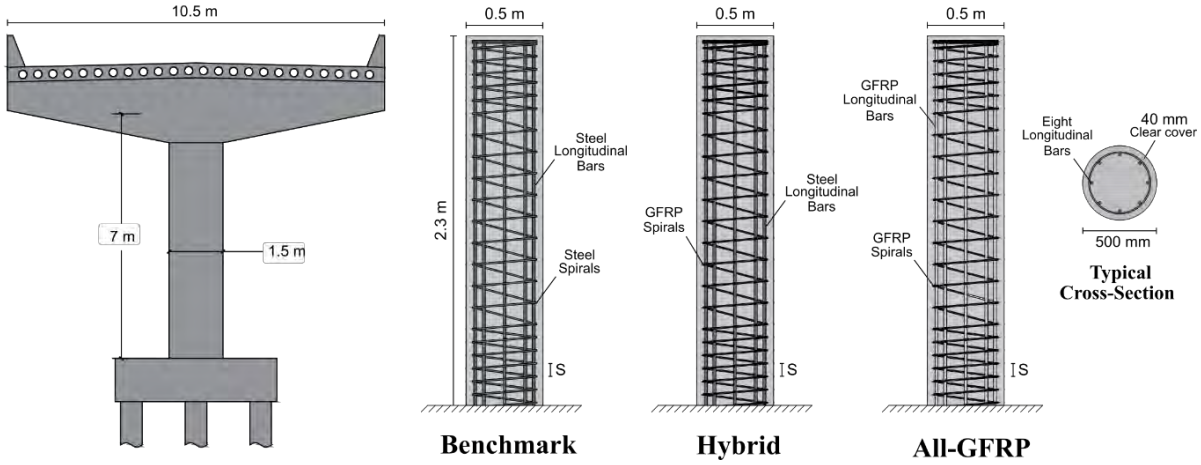

(a) (b)

Figure 4. (a) Prototype bridge used for design of piers, and (b) three unique reinforcement configurations investigated in one-third scale specimens.

EXPERIMENTAL PROGRAM

An experimental program at the University of Canterbury investigated the cyclic response of concrete bridge piers reinforced with conventional steel, hybrid or all-GFRP bars. This paper provides an overview of this experiment and a comparison between three specimens - one from each reinforcement category. A prototype bridge structure was chosen for the design of the test specimens which represents a typical two-span, two-lane RC bridge in New Zealand (Figure 4a). The gravity load was determined from the weight of the superstructure, whilst the design lateral load was computed using the New Zealand Earthquake Design Actions standard (NZS, 2004). To simulate seismic testing of the central pier in the laboratory, the structure was scaled to one-third and replicated in the laboratory using the test setup in Figure 5b.

Specimen Design

The cantilever pier specimens (Table 1) were designed to fail via flexural hinging at the base, with a clear height of 2300 mm and a diameter of 500 mm. All specimens had eight equally-spaced longitudinal bars and a clear cover of 40 mm to the spirals to maintain a comparable cross-section. The benchmark steel-RC specimen was designed in accordance with the 'New Zealand Concrete Structures Standard' (NZS, 2006), whilst the Canadian 'Design and Construction of Building Structures with FRP' (CSA, 2012) was used for design of the hybrid and all-GFRP specimens, where necessary. The all-GFRP pier was over-reinforced to minimise the loss of post-cracking stiffness associated with the low-modulus bars and adopt crushing of the concrete core as the preferred failure mechanism, protecting the GFRP reinforcement from damage.

Table 1. Details of test specimen.

Category	f'_c (MPa)	d_b (mm)	p_l (%)	d_v (%)	S (mm)	p_v (%)
Benchmark	51	20	1.28	10	85	0.90
Hybrid	44	20	1.28	14	85	1.78
All-GFRP	46	27.5	2.33	14	85	1.78

Steel longitudinal reinforcement consisted of Grade 500 deformed bars with 180-degree hooks for development in the footing, whilst Grade 500 round spirals were used transversely. GFRP longitudinal reinforcement had a guaranteed tensile strength of 860 MPa, elastic modulus of 59 GPa and ultimate strain of 1.46%. Although bend products are available, straight bars were utilised in this study with high-strength concrete used in the footing region as a temporary solution for development of the bars. GFRP spirals had a guaranteed tensile strength of 750 MPa and elastic modulus of 54 GPa. These spirals were lap spliced outside of the plastic hinge detailing length when required due to manufacturing limitations on the continuous spiral length. A splice length equal to a full circumference of the spiral was provided.

Specimen Construction

All aspects of specimen construction were carried out in the Structural Engineering Laboratory at the University of Canterbury (Figure 4). The piers were cast using conventional ready mixed concrete with a target 28-day compressive strength of 40 MPa, slump of 120 mm and maximum aggregate size of 19 mm. Layers of 500 mm were poured at a time with vibration carried out between each layer. The specimens were cured in the formwork for seven days, before being removed and stored in the laboratory until the target strength was reached. On the day of testing, three 100x200 mm cylinders were crushed to give the in-situ compressive strength of the concrete, as specified in Table 1.

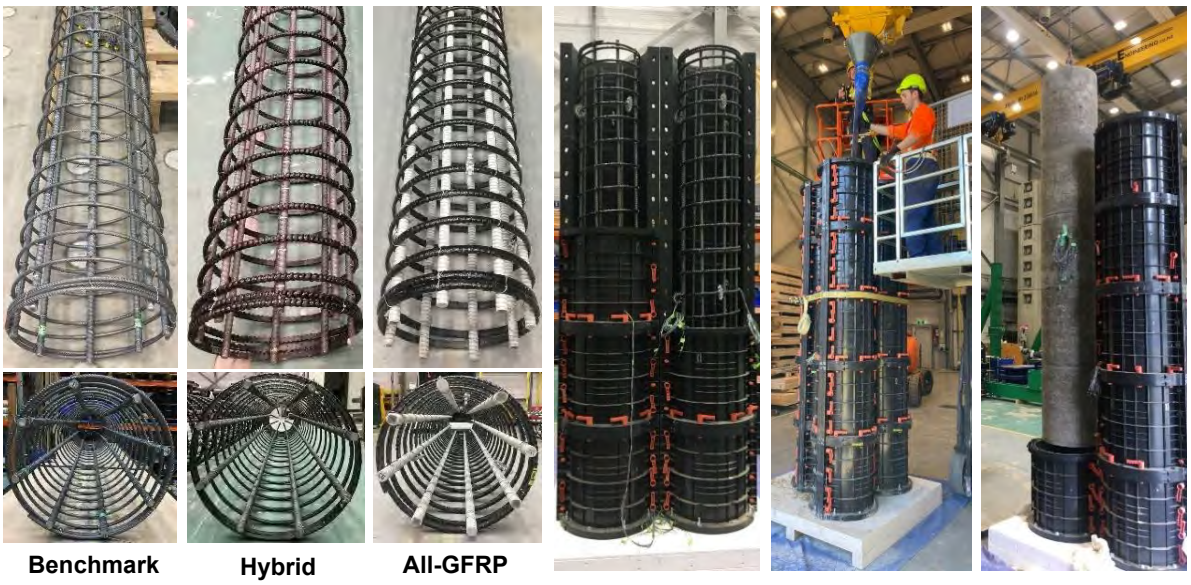

(a) (b)

Figure 4. (a) Reinforcement cages, and (b) construction process of bridge pier specimens.

Test Setup and Procedure

The piers were fixed to the strong floor using a reusable steel socket footing (Figure 5a). A 10 mm gap between the pier base and footing interface was pumped with Sika 212 grout to secure the pier and eliminate the occurrence of stress concentrations. Two vertical actuators connected to a steel spreader beam applied a 360 kN axial load to the pier to simulate the gravity loads of the bridge deck and pier cap. These actuators were automatically checked and adjusted at each loading step to maintain a constant axial load throughout the test. A horizontal actuator connecting the top of the pier to a reaction frame applied quasi-static, cyclic lateral load following the protocol in Figure 5b. Testing was terminated when a significant failure mechanism was observed, or the actuator reached its stroke limit. A series of linear and rotary potentiometers were used to capture the deformations of the pier throughout the test.

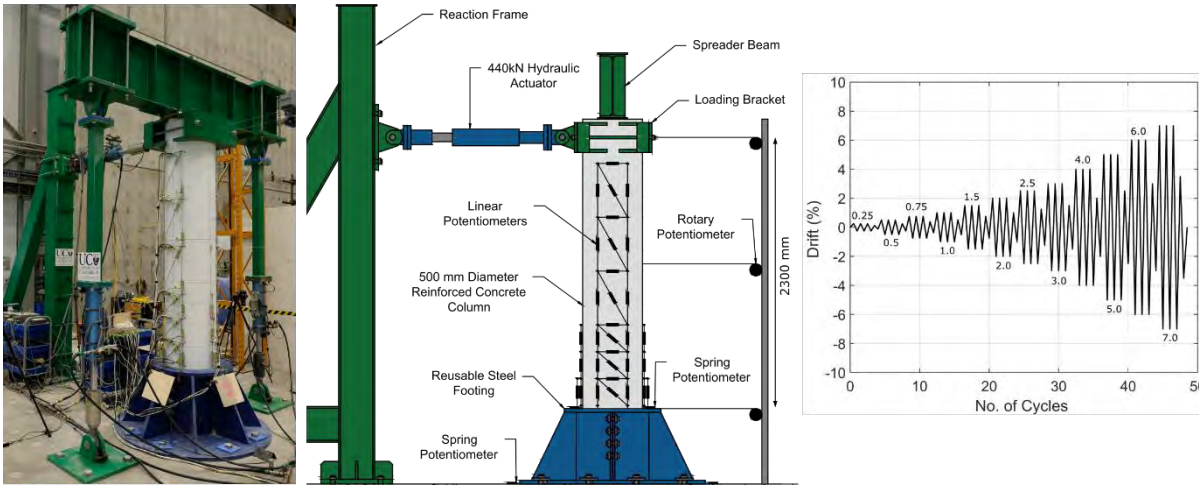

(a) (b)

Figure 5. (a) Details of the test setup, and (b) cyclic loading protocol.

RESULTS

The force versus lateral drift response for the three different reinforcement configurations are shown in Figure 6, where locations of important failure mechanisms are highlighted. Key performance parameters are tabulated, including the maximum moment resisted (M_{max}), max shear force resisted (V_{max}), ultimate drift when the capacity reduced to 80% of its peak value (θ_{80}), accumulative energy dissipation denoted by the area enclosed within the force-displacement loops ($E_{acc,80}$) and displacement ductility taken as the ultimate drift divided by the effective yield drift (μ_{Δ}). The effective yield drift was defined as the intersect of a secant line through origin and 65% of the peak capacity and a horizontal line at the peak capacity.

DISCUSSION

Conventional Steel-Reinforced Benchmark

The benchmark steel-reinforced pier exhibited a ductile cyclic response with good energy dissipation capabilities and residual capacity at large drift levels. The gradual reduction in post-peak strength can be attributed to the progression of concrete crushing and inelastic buckling of the longitudinal bars. The specimen showed typical damage mechanisms observed in several New Zealand RC bridges after significant earthquake events (Palermo et al., 2017). Most notable was the onset of longitudinal bar buckling between a single spiral spacing, which led to low-cycle fatigue damage in the form of cracks on the concave face of the buckled bar. It is anticipated that these bars would have fractured with further cyclic loading. This indicated that, although the spiral diameter provided sufficient stiffness to concentrate the buckling mechanism between one spacing, providing more stringent spacing requirements could limit the impact this failure mode has on the strength and ductility of the member.

The benchmark pier resisted a peak lateral force and bending moment of 142 kN and 323 kNm, respectively. Assuming failure had occurred when the capacity of the pier had decreased to 80% of the peak value, an ultimate drift of 5.6% and displacement ductility of 6.0 was achieved. Significant yielding of the steel longitudinal reinforcement allowed the specimen to dissipate large amounts of hysteretic energy, denoted by the thickness of the force versus drift loops. A consequence of this phenomenon was extensive reinforcement damage and a residual drift of around 4.2% at the conclusion of testing.

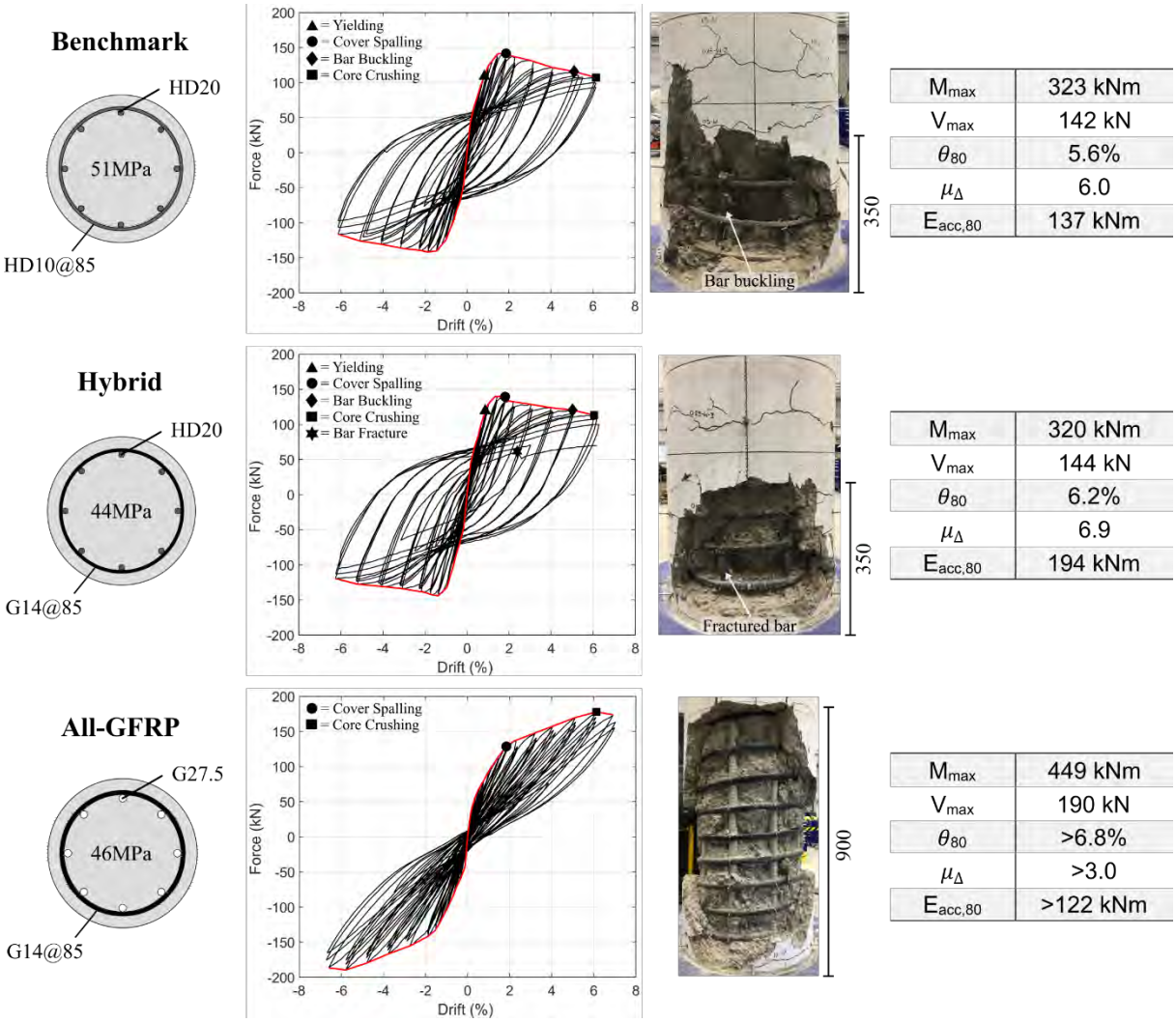

Figure 6. Cyclic response, damage and key seismic performance parameters of the three key reinforcement configurations.

Hybrid-Reinforced

The hybrid-reinforced pier displayed a very similar cyclic response to the benchmark. The main variation observed was the slope of the post-peak descending branch due to the difference in transverse reinforcement material. The elastic nature of the GFRP spirals meant they maintained their stiffness at large strains, providing increased levels of confinement as the concrete core dilated. This phenomenon delayed the buckling of the steel longitudinal bars, reduced concrete core damage, and limited the severity of the buckling at the conclusion of the test (Figure 6). In contrast, yielding of the steel spirals in the benchmark caused the material's stiffness to plateau, limiting the confining stress and anti-buckling resistance at large drift levels. The final failure mode of the pier was fracture of the steel longitudinal bars because of low-cycle fatigue damage in the buckled region.

As anticipated, the specimen achieved a peak moment and shear capacity consistent with the benchmark. The superior confinement properties of the GFRP spirals reduced the progression of damage in the concrete core and longitudinal bars, allowing the pier to reach an ultimate drift and displacement ductility of 6.2% and 6.9, respectively. As a result, a 41% increase in hysteretic energy dissipation was observed relative to the benchmark. These results indicate that when detailed correctly, hybrid-reinforced bridge piers can achieve similar or enhanced cyclic performance compared to conventional steel-reinforced piers.

All-GFRP-Reinforced

The all-GFRP-RC pier had a softer cyclic response due to the lower modulus of elasticity of the GFRP longitudinal bars. In contrast to the benchmark and hybrid specimens, the linear-elastic nature of the bars caused the pier's capacity to increase after concrete spalling, with a second peak in strength observed. This ascending branch plateaued, and the capacity decreased as the concrete core crushed at around 6.0% drift. The lack of concentration of plastic deformations in the hinge, in addition to the bond stresses induced by the high-strength GFRP bars, resulted in more extensive concrete spalling throughout the height of the pier (Figure 6). Despite this, no damage was observed in the GFRP longitudinal bars or spirals. The maximum stroke of the actuator was reached at 7.0% before the pier could be failed.

The higher strength of the GFRP longitudinal bars and the increase in reinforcement ratio caused the all-GFRP-RC pier to reach a shear capacity of 190 kN - 34% larger than the benchmark. This overstrength would need to be optimised in the design phase to minimise the size of foundations required for the bridge structure. The lack of yielding in the longitudinal bars meant energy dissipated by the member could be attributed to bond-slip and concrete crushing. At an equivalent level of drift, the pier dissipated approximately half the energy of the benchmark, however, the increase in deformability before failure allowed it to reach comparable levels of energy dissipation by the conclusion of the test. A benefit of the linear-elastic nature of the bars was the development of a self-centering mechanism, where the GFRP pulled the member back to zero displacement like elastic bands. This limited the residual drift to 0.7%, compared to 4.2% for the benchmark. The reduction in residual displacement, in addition to the lack of damage in the longitudinal or transverse reinforcement, makes the repair of the member a simple process involving conventional concrete patching techniques.

CONCLUSIONS

This paper introduced GFRP bars as a durable reinforcement alternative for RC bridge piers. The experimental results presented within this paper led to the following conclusions:

1. Hybrid-reinforced piers exhibit a comparable cyclic response to conventional steel-reinforced piers and when detailed correctly, can maintain similar or even enhanced post-peak cyclic performance.
2. The linear-elastic nature of GFRP spirals meant a constant confining stiffness was maintained throughout the tests, compared to the post-yield plateau of stiffness for steel. As a result, GFRP was more effective at confining the concrete core and providing anti-buckling resistance at larger drift levels.
3. The piers with GFRP longitudinal bars exhibited a softer cyclic response, with a larger over-strength and reduced stiffness and energy dissipation capabilities. Despite this, the linear-elastic nature of the bars reduced damage in the pier and resulted in a self-centring mechanisms that limited residual displacements.

ACKNOWLEDGEMENTS

The authors would like to acknowledge Callaghan Innovation for funding this research and Pultron Composites for generously supplying materials. The experimental assistance of the technical staff in the Structural Engineering Laboratory (SEL) of the University of Canterbury is also gratefully acknowledged.

REFERENCES

ACI. (2015). *ACI440.1R: Guide for the Design and Construction of Structural Concrete Reinforced with FRP bars*. Farmington Hills, MI: American Concrete Institute.

Ali, M. A., & El-Salakawy, E. (2016). Seismic Performance of GFRP-Reinforced Concrete Rectangular Columns. *Journal of Composites for Construction, 20*(3), 04015074. https://doi.org/doi:10.1061/(ASCE)CC.1943-5614.0000637

Andisheh, K. (2017). *Seismic performance of corroded reinforced concrete bridge piers*, University of Canterbury, Christchurch, New Zealand).

Arduini, M., & Balconi, G. (2020). Applications of Non-metallic Concrete Reinforcements.

CSA. (2012). *CAN/CSA S806-12: Design and construction of building components with fibre reinforced polymers*. Rexdale, Canada: Canadian Standards Association.

Elshamandy, M. G., Farghaly, A., & Benmokrane, B. (2018, 03/01). Experimental Behavior of Glass Fiber-Reinforced Polymer-Reinforced Concrete Columns under Lateral Cyclic Load. *Aci Structural Journal, 115*. https://doi.org/10.14359/51700985

FDOT. (2019). *Project Case Studies on GFRP Reinforcing Bars.* Paper presented at the 2nd International Workshop on GFRP Bars for Concrete Structures, Orlando, Florida, USA.

fib. (2007). *fib Bulletin 40: FRP Reinforcement in Concrete Structures*. Luasanne: fib - International Federation for Structural Concrete.

JSCE. (1997). *Recommendations for design and construction of concrete structures using continuous fibre reinforcing materials*. Tokyo, Japan: Research Committee on Continuous Fiber Reinforcing Materials, Japan Society of Civil Engineers.

NZS. (2004). *NZS1170.5: Structural design actions - Part 5: Earthquake actions*. Standards New Zealand.

NZS. (2006). *NZS3101: Concrete structures standard*. Standards New Zealand.

Palermo, A., Liu, R., Rais, A., McHaffie, B., Andisheh, K., Pampanin, S., . . . Wotherspoon, L. (2017, 06/01). Performance of road bridges during the 14 November 2016 Kaikōura Earthquake. *Bulletin of the New Zealand Society for Earthquake Engineering, 50*, 253-270. https://doi.org/10.5459/bnzsee.50.2.253-270

Pantelides, C. P., Gibbons, M. E., & Reaveley, L. D. (2013). Axial Load Behavior of Concrete Columns Confined with GFRP Spirals. *Journal of Composites for Construction, 17*(3), 305-313. https://doi.org/doi:10.1061/(ASCE)CC.1943-5614.0000357

Rossini, M., Cadenazzi, T., Nolan, S., & Nanni, A. (2019). SEACON and Resilient FRP-RC/PC Solutions: The Halls River Bridge. In (pp. 165-180).

Shamim, S., & Zahra, K. (2018, 8/10/2018). GFRP-Reinforced Concrete Columns Subjected to Seismic Loads. *ACI Symposium Publication, 326*.

Soltani, M., Safiey, A., & Brennan, A. (2019, 05/13). A State-of-the-Art Review of Bending and Shear Behaviors of Corrosion-Damaged Reinforced Concrete Beams. *Aci Structural Journal, 116*, 53-64. https://doi.org/10.14359/51714481

concretenz BUILDING RESILIENCE
CONFERENCE 2022
13-15 October 2022
Energy Events Centre | Rotorua

TOKOMARU BAY - HISTORIC WHARF RESTORATION USING MODERN MATERIALS

R HUDD[1], M DYER[1], J BROTT[1]

[1, 2, 3] School of Engineering, University of Waikato, NZ

SUMMARY

The Tokomaru Bay concrete wharf was constructed in the late 1930's to service the local meat freezing works. In recent years, the wharf structure has exhibited increasing levels of deterioration with extensive concrete spalling from the supporting piles resulting in its closure to the public in 2017 due to safety concerns. A community desire to preserve this piece of local history led to the development of a proposal to restore the structure. This paper gives details of a repair system developed using self-compacting concrete (SCC) and fibre reinforced plastic (FRP) rebar which was trialled successfully on two of the wharf piles in early 2021.

BACKGROUND

Tokomaru Bay is a small coastal settlement on the East Coast of New Zealand approximately 90 km north of Gisborne. The economy of the area developed from wool and meat exports. In the early 20th century a freezing works and timber wharf was constructed at Waima at the northern end of the bay. The original timber wharf was extended to cater for larger vessels and a large section 'optimistically' replaced with a concrete structure between 1937 and 1940 (Gundry 2014). Coastal freight declined following the Second World War and with the closure of the freezing works in 1952 the regular coastal service to the bay ended in 1963. The wharf continued to be used by the local community for recreational activities and was given a Category 2 heritage listing in 1984 (Pattison 2013). Over time, the wharf structure has exhibited increasing levels of deterioration with cracking and concrete spalling from the beams and supporting piles (Figure 1). It was closed to the public in 2017 due to safety concerns (Gisborne District Council 2017).

Figure 1. Cracking and Spalling of Concrete on the Wharf Structure

Local Heritage

The wharf is one of a number of structures associated with the industrial heritage of the area. A desire to preserve this and other pieces of local history prompted the establishment of the Tokomaru Bay Heritage Trust in 2015. In addition, the heritage, and its significance to the local community, were the subject of University of Waikato research projects in 2019 and 2020.

The Wharf Structure

The general structure and approximate metric dimensions of the wharf are described below based on values taken from copies of the original 1936 drawings.

The concrete section is approximately 240 m long running roughly North West - South East out to the remains of the original timber wharf head which extends a further 80 m. The structure consists of a series of trestles or bents made of pairs of inclined piles connected by a headstock. These are connected by pairs of longitudinal beams with a cast in-situ concrete deck forming a double ‘T’ section. The majority of the bents are spaced at 6.1 m along the wharf at the landward end out to a low tide water level of approximately 1 m a further ten bents are spaced at 5.2 m out to the junction with the timber wharf with a low tide water level of approximately 2 m.

The ‘Government Standard Pattern’ piles are of the ‘Considère’ type (Marsh 1905 cited by Reed P et al. 2008) with a 405 mm octagonal section, inclined at 1 in 6 to the vertical. The drawings show the piles as 355 mm but a note has been added that they be ‘increased to 16” dia. instead of 14” dia.’ Longitudinal reinforcement for the piles consisted of eight evenly distributed 22 mm plain steel bars. Circumferential steel consisted of 5 mm (No.6 gauge) wire spiral reinforcement throughout the pile length but concentrated at the top and bottom. Concrete cover to the reinforcement is shown as 40 mm. It is understood the piles were manufactured in Auckland and shipped to site.

Figure 2. Photograph Showing Profile of the Headstocks and Longitudinal Beams

The drawings show that, after installation, the concrete at the pile ends was removed and the longitudinal steel bent out to be integrated into the cast in situ headstocks. The headstocks are of rectangular cross section, 405 mm wide, varying in depth from 600 mm over the centre 900 mm, then tapering to a depth of 915 mm over the piles. (Figure 2). The tops of the piles are 2.1 m apart.

Each bent is connected by two 405 mm wide by 470 mm deep beams with a 3.7 m wide by 250mm thick cast in situ deck. The beam depths increase from 470 mm to 520 mm over a

660mm taper where the beams join the headstocks. Based on the detailing and physical inspection, the headstocks, longitudinal beams and deck were cast together. Reinforcement in the headstocks and beams ranges from 13 to 25 mm diameter with 10 mm stirrups at 200 to 300 mm centres and an indicated minimum cover of 60 mm.

The deck was reinforced with 10 mm longitudinal bars at 305 mm centres top and bottom and straight 13 mm transverse bars at 380 mm centres top and bottom alternating with cranked bars at 380 centres in the top. The deck had a 13 mm cross camber with indicated cover of 40 mm in the bottom and 75 mm in the top. A '3' Gauge' (915 mm) rail line using 28lb Darlington rail was cast into the top.

Details of the concrete mix designs were not available at the time of writing. It is worth noting that the local creek would have provided a source of fresh water. The marine aggregates in this location are not ideal for concrete although it is reported that beach sand was used in the construction of the Tologa Bay Wharf to the South (Williams 2009).

CONCRETE DETERIORATION

Concrete in its simplest form of cement, aggregate and water is a very versatile and cost effective construction material. Locally produced it can be used for a wide range of applications by relatively unskilled labour. In normal applications, when well-proportioned and constructed, concrete structures exhibit excellent durability. Even in more challenging environments it has often proven to be very resilient. Despite this, in some situations, concrete is affected by mechanical or chemical agents resulting in physical damage to the elements or breakdown of the cementing matrix.

Reinforcement Corrosion

Although it can be used in its own right for mass concrete elements, concrete's poor tensile strength limits its use unless it is combined with materials with good tensile performance such as steel. Although steel corrodes in air, the highly alkaline environment in concrete forms a stable 'passive' layer on the metal's surface. This, combined with the physical barrier provided by the surface layer of concrete, usually prevents corrosion from being a concern.

However, if the passive layer on the steel breaks down due to chemical action, corrosion can take place. Neutralisation of the passive layer can occur in the presence of acidic agents, such as atmospheric carbon dioxide (a process known as carbonation), or chlorides. Chlorides can come from a wide range of sources including: the raw materials used to make the concrete, such as sea dredged aggregates or sea water; chloride containing admixtures; or, external environmental sources such as the marine environment.

The corrosion process results in the parent steel being replaced by higher volume iron oxides. This volume increase creates bursting forces which over time crack the concrete surface layers. Aside from the visual impact, the cracking removes the physical barrier provided by the concrete allowing the corrosion reactions to continue unhindered. If untreated, this results in increased cracking and spalling as pieces of cracked concrete become detached.

Where corrosion results from carbonation, cracking and spalling is often apparent over large areas of the structure well before a significant loss of steel has occurred. In the case of chloride induced corrosion however, electrochemical currents can be generated which can create highly localised corrosion. In marine structures especially, this can be manifested as cracking, rust staining and spalling damage to structural elements in the intertidal 'splash' zone (Standards Australia 2005). Within this zone, periodic immersion keeps the concrete wet enough to maintain electrical conductivity while still allowing ingress of oxygen necessary for the corrosion process. Other parts of the structure can be affected to varying degrees

depending on a range of factors including exposure, and the depth and quality of the cover concrete.

In modern concrete structures, these risks are recognised and precautions are taken to avoid or reduce the effects through appropriate design, construction and maintenance. However, in older structures, built prior to these effects being recognised or understood, this type of deterioration is quite commonplace. Because of this, repair of affected elements is frequently necessary to maintain the serviceability of the structures.

CONCRETE REPAIR

There are a range of potential approaches to treat concrete deterioration including:

- No action;
- Stabilisation - treating the structure to slow down or stop the deterioration processes;
- Cosmetic repair to restore the original appearance;
- Structural strengthening or stabilisation to reduce the risk of major structural failure;
- Restoration to an original form and function;
- Enhancement to improve the form or function to allow for a change of use, increase in structural capacity, extension of the design life or other performance requirements.

The chosen option or combination of options will be influenced by a range of factors including the underlying causes of the deterioration, the importance of the structure, the ease and potential success of any repairs, and the cost.

Repair Materials and methods

A wide range of materials are used for concrete repair, the choice usually influenced by the size of the repairs and the desired outcomes. Common materials include conventional mortars or concrete, and proprietary polymer modified cementitious systems. For special applications such as crack repair or where very good chemical resistance is required epoxy or other resin based systems can be used.

Application of repair materials can be carried out using the same methods employed for normal cement based materials. These include: hand placing, wet or dry spraying, or in situ casting using grouts, mortars or concretes depending on volume and accessibility.

Repair to damage caused by reinforcement corrosion

Where corrosion of steel is identified as a cause of the deterioration, in addition to repairing damaged concrete, the causes of the corrosion also need to be addressed. If this is not done, the corrosion mechanism will continue resulting in further deterioration.

In addition, loss of steel to corrosion may require replacement reinforcement to restore the strength of the structure. Conventional steel can be used in these cases, however if corrosion prevention measures are not applied, corrosion of the new steel or accelerated corrosion of existing steel may occur due to galvanic effect. Some protection can be provided by applying impermeable resins or anti-corrosion priming systems to the steel. In addition, many repair materials give improved protection to the reinforcement.

Where chlorides are present additional protection options may be required. These may include more corrosion resistant reinforcement such as galvanised, epoxy coated and stainless steels or FRP composites. Additionally, corrosion prevention or inhibition measures may be applied to the repair or the structure. These include: water repellent surface treatments to help the concrete to dry out and reduce its electrical conductivity; corrosion inhibiting admixtures,

corrosion inhibiting surface treatments; electrochemical chloride removal and cathodic protection systems to control corrosion currents (Standards Australia 2005).

Repair of Historic Structures

Repair of historic structures can adopt similar treatment processes to those outlined above. However, there are some specific considerations which should be taken into account (New Zealand Historic Places Trust 2007):

- Work should generally match the original in terms of quality, materials and detailing;
- Repairs should generally be with original or similar materials;
- Repairs to a higher standard may be justified where life expectancy is being increased;
- Alteration should be avoided whenever possible.

It is also important to note that applying 'new building' design requirements can be excessive or in some cases impossible to meet with historic structures. In such cases alternative methods of analysis or 'an observational method' may be more appropriate to establish a suitable approach (International Council on Monuments and Sites 2003).

In essence, repairs to historic structures, in addition to providing restoration of performance and/ or functionality, should be sympathetic to the nature and significance of the structure. The interpretation and application of these recommendations to this project is discussed in more detail elsewhere (Hudd et al 2021).

PROPOSED REPAIR METHODOLOGY FOR TOKOMARU BAY

Inspection of the wharf between 2007 and 2013 attributed the observed spalling and loss of reinforcement to chloride induced corrosion due to the age of the structure in the marine environment (Tokomaru Bay Heritage Trust 2014). The effects were apparent to varying degrees throughout the structure but most obviously in the wharf piles. Based on the overall condition of the structure, repair was considered to be feasible with restoration of the piles as the highest priority. It was judged that no action would lead to increasing loss of structural integrity with failure of individual elements with either a progressive or a catastrophic collapse of the entire structure. Restoration options suggested at the time were either: complete replacement of the damaged piles; or, repair with a concrete jacket similar to the methodology employed for the Tologa Wharf Restoration (Williams 2009).

The former option had the advantage of being able to use piles of the same size and shape as the original ones thus retaining the structure's appearance. This methodology does however present significant challenges, with total replacement requiring removal of other parts of the structure to allow the new piles to be driven. Jacketing the piles, while much more feasible, was a less visually acceptable option.

At the time these recommendations were made no action was taken. However, the closure of the wharf in 2017 increased the local community's desire for action resulting in a formal proposal for trial repairs of four of the deteriorated piles in 2019.

Trial Repair Proposal 2019

The proposed method followed conventional practice, removing the damaged concrete and steel, and strengthening the remaining core concrete with a concrete jacket reinforced with FRP rebars. The intention being to trial the method on the four piles at the landward end of the wharf.

Reinforcement

The use of FRP eliminated the risk of future corrosion and further deterioration and, importantly, was locally available. It offered higher tensile strength than steel, comparable bond strength, thermal properties and good fatigue and creep resistance. In addition, its lighter weight, approximately one quarter of the weight of equivalent steel made on-site handling much easier. This was important considering the need to locate reinforcement cages in the confined space under the wharf. The material is flexible enough to be 'sprung' into place, but unlike steel it cannot be bent to shape on site; any 'bends', including links, have to be applied at the manufacturing stage.

Replacement Concrete

The proposal included provision for the use of proprietary repair materials or site cast concrete. The use of proprietary materials, although potentially offering advantages over the site cast concrete for placement, was discounted because of cost.

The site cast concrete specification was based on the durability requirements for concrete in reinforced concrete structures in a marine environment (Exposure classification "C2" splash zone) (Standards Australia 2005). This called for a Class S40 grade with a minimum cement content of 400 kg/m^3 and a maximum water cement ratio of 0.4. These requirements, as with the New Zealand Standard for reinforced concrete (Standards New Zealand 2006), are primarily intended to provide additional protection to conventional steel reinforcement in the marine environment.

The small volumes (less than 1 m^3 per pile), uncertainty over the pouring schedule and a two hours' drive meant ready mix concrete was impractical. Accordingly, site batched concrete was chosen and to facilitate this a 700 litre tractor mounted concrete mixer was purchased. The tractor attachment made it possible to locate it wherever it was required on site so concrete could be mixed and poured without additional handling.

The choice of site mixed concrete also presented challenges for both placing and compaction in the restricted space beneath the wharf. Conventional placing techniques required clear access with the forms open at the top. To ensure adequate compaction, the concrete would need to be placed in lifts which could only be achieved if the mould was installed in sections as the pour proceeded. Access and time constraints between tides meant this would be impractical. Pumping would overcome some of the access issues allowing the concrete to be placed to the full height of the mould but still did not address the compaction requirement. It was also recognised this would add complexity and cost.

A solution which offered to address both issues was SCC. This could be poured from the top of the wharf into the forms without pumping and did not require additional compaction after placing. In addition, typical SCC mix designs would comply with the specified concrete mix design parameters. Fortuitously, the University of Waikato, which was running student research projects on the historic structures in the area, had teaching staff with experience of SCC mix design. Using this experience a preliminary mix was developed based on a published mix design (Hudd & Edwards 2001).

The mix design had a cement content of 350 kg/m^3 with 150 kg/m^3 of limestone flour as a filler for stability and flow. To meet the concrete specification for the trial repairs, the limestone flour was replaced with fly ash. This combination not only met the given specification but also the New Zealand standard requirement for concrete in a marine environment - a minimum binder content of 450 kg/m^3 with 30 percent fly ash (Standards New Zealand 2006).

Laboratory Tests

Local aggregates were obtained, and laboratory tests were carried out at the University of Waikato using the following mix design:

General Purpose Cement	350 kg
Fly Ash	150 kg
Nuhaka black Sand	900 kg
Nuhaka 13mm Aggregate	800 kg
Water	175 litres

Sika® Viscocrete® -5-555 (NZ) superplasticiser to give the required flow characteristics

The tests were used to confirm that acceptable flow spread using an inverted slump cone, could be obtained with the mix (Figure 3). Stable flow spreads between 650 and 750 mm were achieved with water: binder ratios between 0.35 and 0.4 and superplasticiser dosed at 0.3 to 0.5 litres per 100kg of binder (Figure 3). At higher flow spreads bleeding and aggregate segregation were observed.

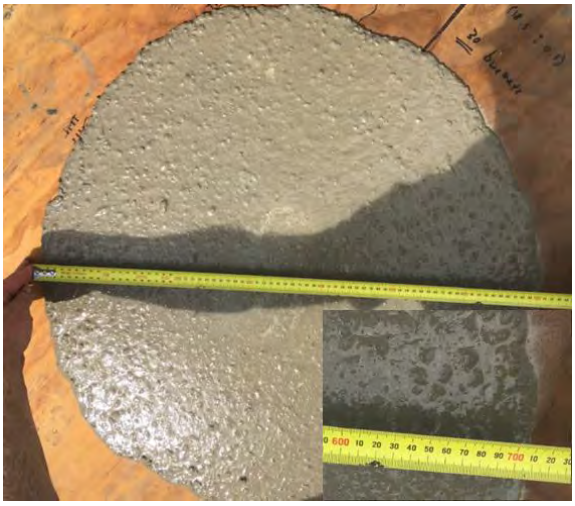

Figure 3. On-Site Flow Test of Trial Self-Compacting Concrete Mix

Cylinders were cast for compressive strengths testing at 7 and 28 days. Strength tests showed the mix would meet the Class 40 minimum strength requirements with 7 day strengths typically 30 - 40 MPa and 28 day strengths in excess of 50 MPa. Cylinders were water cured for three days after demoulding, then wrapped in polythene. It was felt this would be more representative of site curing although it is likely the strength performance was reduced, especially with the fly ash in the mix.

SITE TRIALS

Having obtained satisfactory performance of the mix in the laboratory, a series of site tests were carried out prior to the trial repairs to identify any issues with the proposed mix or method in practice.

These tests showed that the same mix properties were achievable on site. For simplicity, the batch size was based on whole bags of cement and fly ash, with aggregates being weighed into buckets. Without an accurate means of determining aggregate moisture content on site, the admixture dose rate was fixed and water added to give the desired flow properties.

A trial pour was carried out using a mock-up of a section of a pile. A section of the mould with reinforcement, delivery pipe and hopper was set up on the beach with the mixer at the wharf

deck level. An initial attempt was unsuccessful due to poor flow through the pipe. This was attributed to the length of the delivery pipe which hadn't been pre primed. For subsequent pours, this was addressed by shortening the delivery pipe and priming it with a cement slurry. Having resolved these issues the mock pour was carried out successfully. The SCC easily filled the mould, encapsulated the reinforcement and gave an acceptable off-form finish. The satisfactory outcome of these tests gave confidence that the material and methodology could be used for the trial repairs.

Concrete Surface Preparation

Successful repairs require all damaged concrete and reinforcement to be removed from the repair area. For repairs to load bearing elements, as in this case, the load must be relieved during the repair process so the repaired section will carry load once finished. For this project steel frames were fabricated and positioned either side of the bent being repaired with legs bearing on the seafloor and hydraulic jacks positioned under the wharf beams to take the load.

Once this loads were transferred to the frame, preparation of the piles stared with removal of the damaged concrete and rebar. An additional 300 mm of sound concrete was removed below the repair area to ensure the repair had a sound surface to bond to. It was noted that all of the steel exposed during this operation, both longitudinal and spiral, was in excellent condition with little or no corrosion visible and original wire ties still present.

Reinforcement Fixing

The FRP reinforcement cages were assembled in two halves each consisting of eight 22 mm bars arranged in pairs with each bar centred 35 mm from the corner of the links (Figure 4). Links were spaced at 150 mm centres secured with plastic zip ties at each intersection. Gloves were recommended when handling the longitudinal bars as they were machined during manufacture to give a ribbed profile resulting in exposed glass fibres.

The reinforcement cage sections were positioned either side of the piles with the top ends tied to stainless steel starter bars bolted to a purpose made bracket (Figure 5). The bottom of each cage was positioned over the undamaged pile section using spacers. The sections were secured at points around the pile with short lengths of GFRP bar fixed into the substrate concrete. The two halves of the cage were tied together with additional links to give continuity around the pile.

Figure 4. FRP Reinforcement Cage Half

Figure 5. Starter Bar Connection

Once the reinforcement was installed, the sections of the mould were lowered into place and assembled around the pile. The bottom of the mould had a reduced section to match the pile profile. The position relative to the pile and the reinforcement was fixed using bolts threaded

through the sides of the mould. There was a concern raised that, as the mould would be immersed in sea water prior to the concrete pour, normal oil based form release agents might become ineffective. To avoid potential issues this could create, a 'homemade' beeswax based form release was prepared.

Trial Concrete Pours

One of the many challenges with this project was weather and sea conditions. Clear settled conditions were required over several days to allow time to fix the reinforcement, install the mould and pour the concrete. On several occasions planned pours had to be postponed due to poor conditions. Once a suitable forecast was obtained, the reinforcement and mould were installed and preparations made for the concrete pour.

Prior to pouring, the mould was flushed with fresh water which was drained from the inlet port at the bottom of the mould. The delivery pipe was primed with a cement slurry then connected to the inlet pipe. The concrete was mixed and flow checked then discharged into the feed hopper at the upper end of the delivery pipe. Once the mould was full the inlet port was closed off and the delivery pipe removed. Using this method, two trial repairs were carried out in February 2021.

The forms remained in place for seven days, their removal, as with the concrete pours, being subject to the weather and sea conditions. After stripping the repairs were wrapped with wet hessian and plastic.

FUTURE WORK

During the course of this project a number of areas for future research were identified:

- Although the repair methodology was successful, the oversize repairs detract from the original form of the structure. Options to repair the piles to the original profile are being investigated;
- No site testing has been conducted to confirm the cause or determine the extent of the deterioration beyond what is visible, future projects are planned to address this;
- It is anticipated that some deterioration of the repairs may take place. Long-term monitoring of the repairs is required to assess and address any issues identified;
- A method needs to be devised to address the deterioration in the headstocks and longitudinal beams;
- Spalling and reinforcement corrosion is apparent on the underside of the concrete deck. Research is being undertaken to identify practical, non-intrusive, methods to address this.

CONCLUSIONS

At over 80 years old, the concrete wharf at Tokomaru Bay exhibits deterioration typical of chloride induced reinforcement corrosion in marine environments. The closure of the wharf in 2017 prompted efforts by the local community to save the structure and see it reopened. This culminated in a proposal to trial a repair methodology incorporating advanced concrete materials as the practical first stage of a restoration process. Research conducted by the University of Waikato and site trials carried out in the summer of 2020-2021 successfully demonstrated the viability of the proposed materials and method.

REFERENCES

Gisborne District Council (2017) “Historic wharves closed amid safety concerns”, see https://www.gdc.govt.nz/historic-wharves-closed-amid-safety-concerns/ (accessed 11/03/2021)

Gundry S (2014) “European History”, *The Tokomaru Bay Heritage Site Project Nga Tapuwae o Te Aotawarirangi In the footsteps of Te Aotawarirangi, feasibility study an application for funding presented by the Tokomaru Bay Heritage Trust*, June 2014, pp 20- 27

Hudd R and Edwards M (2001), “Self Compacting Concrete - A New Zealand Perspective”, *Proceedings of The Concrete Conference 2001*, Rotorua, New Zealand, pp. 25-31

Hudd R, Dyer M, and Brott J (2021), “Historic wharf restoration using modern materials”, *Paper accepted for the Australian Engineering Heritage Conference*, 17 - 18 November 2021, Dunedin, New Zealand

International Council on Monuments and Sites (2003), “ICOMOS Charter - Principles for the analysis, conservation and structural restoration of architectural heritage”, *Ratified by the ICOMOS 14th General Assembly in Victoria Falls*, Zimbabwe, in 2003

New Zealand Historic Places Trust (2007), “Sustainable Management of Historic Heritage Guidance Series, Discussion Paper No.2, Assessment of Effects on the Historic Environment”, *New Zealand Historic Places Trust*, 3 August 2007

Pattison L (2013) “Tokomaru Bay Wharf”, *Heritage New Zealand, Pouhere Taonga*, https://www.heritage.org.nz/the-list/details/3565 (accessed 11/03/2021)

Reed P, Schoonees K and Salmond J (2008) “Historic concrete structures in New Zealand Overview, maintenance and management”, *Science & Technical Publishing,* Department of Conservation, Wellington, New Zealand

Tokomaru Bay Heritage Trust (2014), “The Tokomaru Bay Heritage Site Project Nga Tapuwae o Te Aotawarirangi In the footsteps of Te Aotawarirangi, feasibility study an application for funding, June 2014”, https://docplayer.net/62860932-The-tokomaru-bay-heritage-site-project.html

Standards Australia (2005) Australian Standard AS 4997:2005 “Guidelines for the design of maritime structures”, *Standards Australia*, Sydney, Australia

Standards New Zealand (2006) NZS3101.1:2006 Concrete structures standard Part 1: The design of concrete structures, *Standards New Zealand*, Wellington, New Zealand

Williams L (2009) “Tologa Bay Wharf*”, Heritage New Zealand, Pouhere Taonga,* https://www.heritage.org.nz/the-list/details/3516 (accessed 30/05/2021)

concretenz BUILDING RESILIENCE
CONFERENCE 2022
13-15 October 2022
Energy Events Centre | Rotorua

HALF MOON BAY MARINA PRECAST CONCRETE BREAKWATER: PRODUCTION LESSONS LEARNT

JAMAL ALMULLA[1]

[1] *Wilco Precast Ltd, Auckland, New Zealand*

SUMMARY

This paper discuss making the precast concrete panels of the "Breakwater Structure" for Half Moon Bay Marina – Auckland. There are 150 panels in total which need special requirements due to the shape of the panels and the site environment, so I will discuss some of the obstacles that the precast team could face in order to finish such type of panels.

This project posed significant challenges such as:

- Choosing the right mix design for a special site environment.
- Ordering a special steel mould to ensure a high quality, reduce labour and speed up production.
- Method of pouring the concrete and vibration.
- Lifting and handling of the panels.
- Trapped Air bubbles and finishing.
- Curing of the panels.
- Storage of the panels on flat surface which needs a lot of space to store 150 panels.

INTRODUCTION

Breakwater structure is built near the shoreline to protect the shore area, harbour and anchorage of basin from the wave disturbance, they are built within a distance of tens meters from the shore, there are many types of breakwaters structure and could be detached or attached, emerged or submerged. This paper will cover the Half Moon Bay breakwater which is a vertical precast concrete breakwater wall (see Figure 1). The project consists of 150 panels which are all the same but with two types of rebate one reflecting Rangitoto Island (i.e. 75 panels) and another 75 panels reflecting the sea waves, to make both rebates we used rubber formlinear. Each panel consist flat slab of 212 mm thick and four Hooks for hanging the panel on two circular steel waler (i.e. Steel Beam), the total weight of each panel is 14.5 ton.

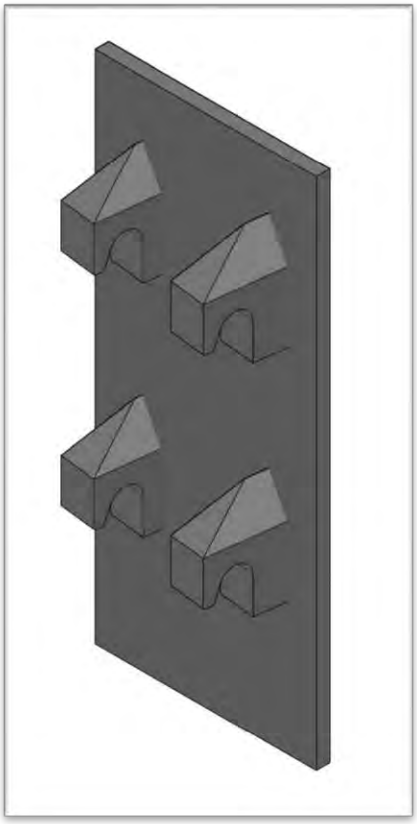

Fig 1. Half Moon Bay Precast Concrete Breakwater Wall.

Exact location of the project shown in Figure 2. Steel structure is installed on site to hold these panels (see Figure 3).

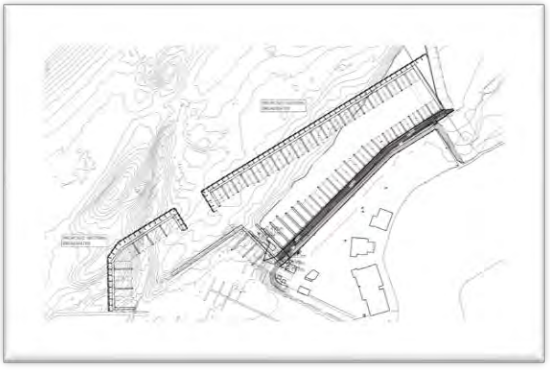

Figure 2. Shown the Project Location.

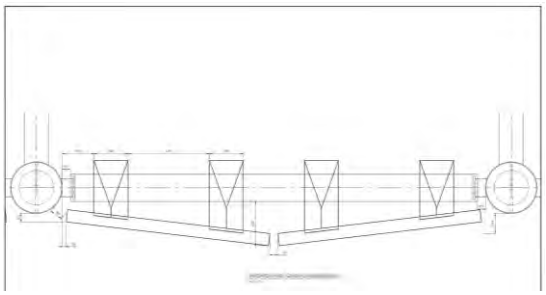

Figure 3. Left and Right Hand Side Panels.

Steel Mould and Finishing

Due to the high number of panels 150 it's more practical for precaster to make steel mould that consist of shutters and four hooks (see Figure 4) this will save time, labour and improve quality with accurate dimensions, which is very critical in these types of projects. Discussing the steel mould with architect we found that the steel waler beams on site will be wrapped with protection wrapping for durability reasons and will cause the inside diameter of the hook to change by a few millimetres, and therefore the steel hook mould will also change accordingly.

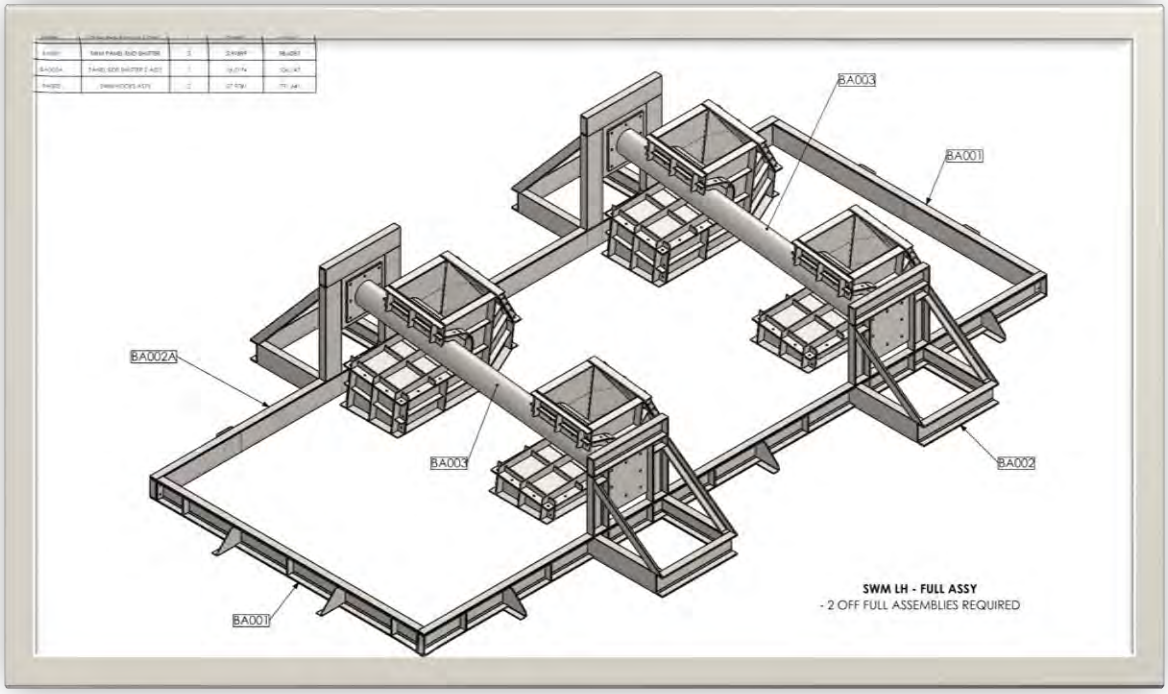

Figure 4. Steel Mould

The geometry of the panel make it very hard to store in vertical position on our toast rack, so we decide to strip, store and ship these panels flat, but in this situation with 150 panels we need an area of about 5000 meter square for storage. Our factory was going through an expansion so we had extra space in the yard to use as a storage area (see Figure 5).

Figure 5. Storage Area

To break the solid concrete looks the architect chose two rubber Formlinear reflecting the site environment, first one in the shape of Sea Waves and the second option gives the Rangitoto Island look (see Figures 6 and 7), but using the rubber lead to:

- Finalise thickness changes: because the minimum thickness of the panel is 180 mm and the maximum rubber thickness is 30 mm so they decided to make the panel thickness as 212 mm.
- In the area where we use the rubber Formlinear we omit the plastic chair to avoid seeing them on the mould face (Plastic chairs are used to hold the steel mesh and give the right concrete cover), for that we hang the double mesh of the reinforcement on the two sides of the mould shutters by using a steel pipe, but what we found is by using a tie wire to hold the heavy mesh and keep the right concrete cover we notice that before pouring the concrete if someone step on the reo mesh for some reason they will cause the mesh to go down and reduce the concrete cover (which is critical for durability reasons) and to avoid this we put few timber planks for labour to step on across the mould setup.
- From the first trial we notice that using the same “Mould Release Agent” for both steel and rubber will cause a colour stains, so we used a special release agent for the rubber and different agent for rest of the steel mould to solve this problem.
- Ordering the rubber formlinear in February 2020 (summer time), then working throughout the year with the rubber we found that at mid-winter the rubber will shrinks by 20 to 30 mm, so we asked the supplier to give us few strips of rubber in different width and we used them to fix the size of the rubber.

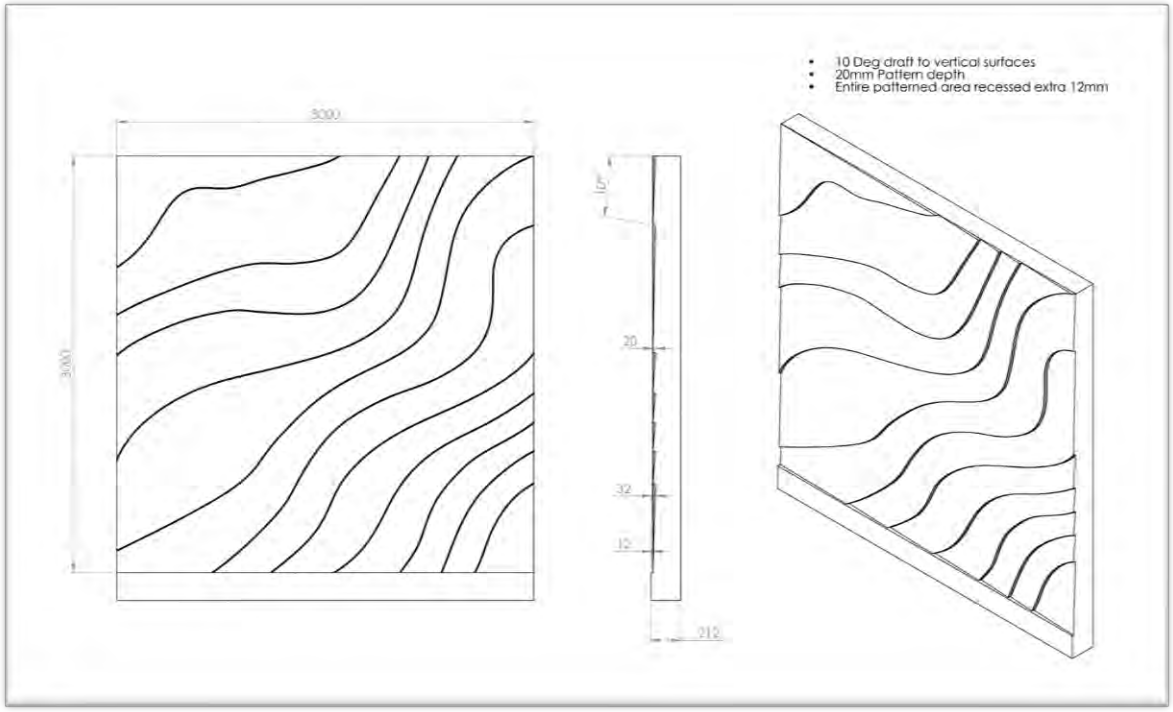

Figure 6. Rubber Formlinear in Shape of Sea Waves

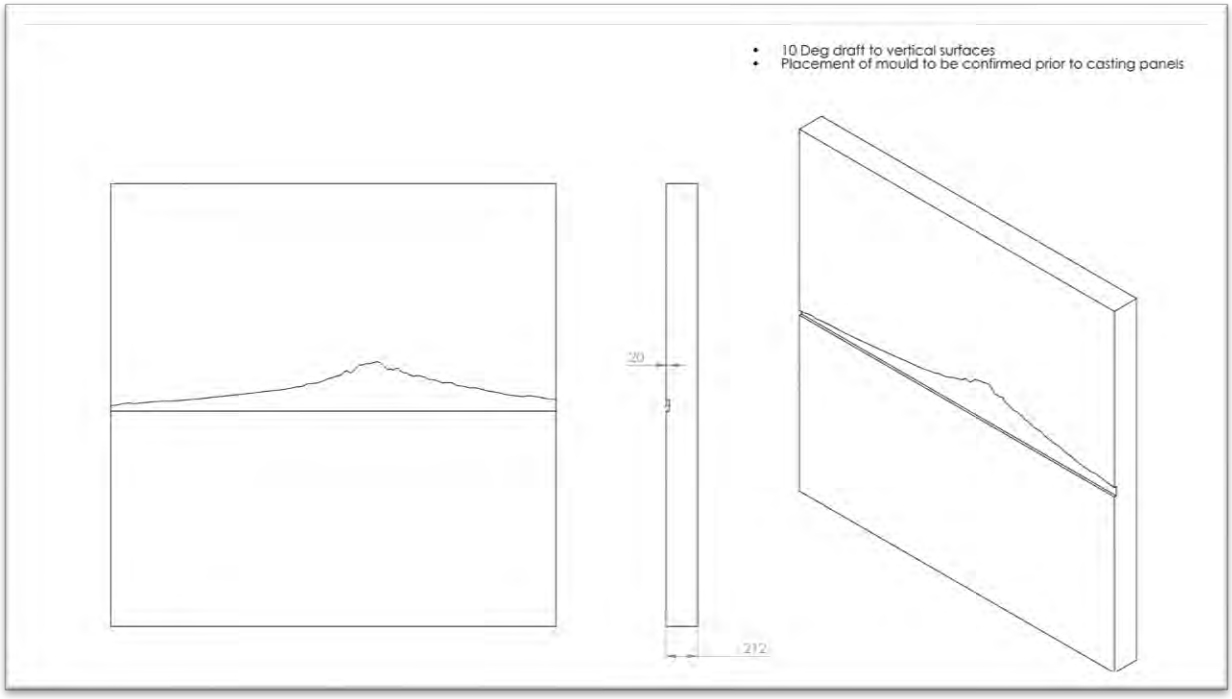

Figure 7. Rubber Formlinear in Shape of Rangitoto Island

For the four hooks we started to assemble the reinforcement of each hook relying on the detailer's sheet and the drawings, but when we try to assemble it inside the steel mould of the hook we found the reo is either small or big which meant we have to spend more time to fix them. So we made a wooden template for each hook then started to assemble the reo in them and move them to the final position in the steel mould, by doing this we saved a lot of time and got accurate results, (see Figure 8).

Figure 8. Wooden Template for Hooks Reinforcement

Mix Design and SCC

The final position of these panels will be half-submerged in sea water and according to the requirement of the NZ building code NZS 3101 and for durability reasons the exposure class will be “class C” in which we have to:

- Use 30% Fly Ash.
- Specified strength of 50 MPa, with minimum concrete cover of 50 mm.
- Minimum binder content > 350 kg/m^3 with Water-binder ratio < 0.45.
- Minimum curing period is 7 days.

The engineer suggested to use 15 kg/m^3 galvanised steel fibre, we started the job by doing a trial using conventional concrete and we reached the following conclusions:

- The mix is too sticky and hard to work with, this is due to the heavy reinforcement used (using HD12 at 150 both way each face).
- Pouring the flat part takes only 15 minutes but vibration process takes about 45 minutes, due to the Fibre.
- Casting has to be in two stages: First casting the flat slab then leave it for about two hours, nearly set up then do the second stage of filling the four hooks, this stage have to start before the setup of the concrete slab to prevent any cold joint, but if we pour it while the slab is still fresh then due to the vibration of the hooks a leakage could happen (see Figure 9), so the timing is really important and critical.
-

Figure 9. Leaking Due Pouring the Hooks While the Slab Still Fresh

To solve these difficulties of working with conventional mix and to pour the hooks without vibration, we decided to use SCC (Self Compacting Concrete) and get the following benefits:

- Reduce the casting time.
- No need to use vibration.
- Better finishing quality.
- All the other benefits the SCC offers.

We have to test the spread flow of SCC before pouring the concrete to make sure that we are using the right concrete consistency, and to reduce the time for standard testing we got a solid steel cone which is graduated in a way that you drop it in truck and that gives you the spread flow of the SCC, but due to the presence of the steel fibre we couldn't get accurate results (see Figure 10).

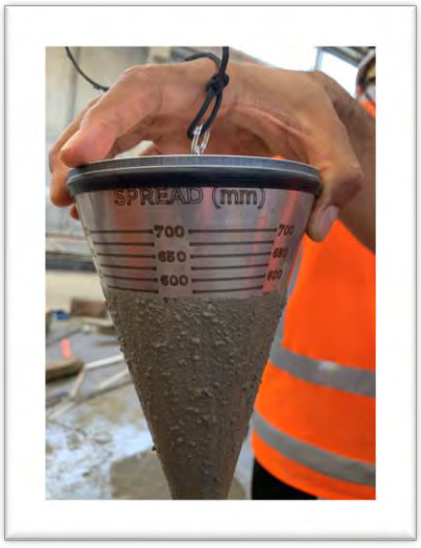

Figure 10. Quick Spread Tet for SCC

Lifting Anchors

The first design of the lifting anchors is to use 8 face lifters for handling and two top edge lifters for installation on site, the geometry of the panel showed that the centre of gravity is with trowel surface of the panel, which means if we use the two top lifters for the final installation on site then the panel will not be a pure vertical and it is very hard to put it on the waler beam, so the designer recommended to only use the face lifters. Considering we needed to fill the recess former of the lifters after installation, they recommended to use only four lifters for handling and shipping, then on site use only two top face lifters for the final installation and this will reduce the amount of remedial work later. To make sure everything will run smoothly and without problems we did a trial in our yard for lifting a panel to see if using the top face lifters is the right choice, the trial went very well in the presence of the contractor (see Figure11).

Figure 11. Trial for Lifting a Panel with Two Face Lifters Only

Casting Trials

The first trial was really helpful to understand what is the critical points that we have to consider to get high finishing quality. From the start we know that the four hooks are a big challenge. The trail shows lots of voids in the hook area even when we change the mix from conventional concrete to SCC (see Figure 12), we then used very little vibration in the hook and pouring the hooks in two levels but there are still a few voids due to the trapped air, so we drilled few inspection holes in the top of the first level in the hook (see Figure 13), this reduced the number of the voids but did not eliminate them, so we decided to cut the top cover of the first level completely and fix it by bolts so the finishing team can remove this cover and finish this area before the concrete setup.

Figure 12. Voids in the Hook

Figure 13. Inspection Holes to Reduce the Voids

Curing

As mentioned earlier the requirements of these panels need to have 7 days curing due to the exposure to sea water, this operation for this number of panels with this size in this condition of the storage area which is away from the main yard it will make the area a big mess with a lot of labour involvement, so we suggested to the engineer to use a curing compound that we can spray directly after the end of the finishing process for the near face and apply it for the side and mould face in the next day after stripping the panel this will save lots of labour and provides good quality.

Shipping and Site work

Programme was set for factory production to cast two panels a day and for that reason we ordered two steel moulds, the target strength was 50 MPa at 28 days and the actual strength was over 60 for that reason there were no issues in handling the panel flat and strip it the next day at strength of 25 MPa. Minimum age to leave the panel on our yard for one month before delivery, the sequence of the work is to strip the panel the next day do the remedial work then spray it with curing compound and store it in the new yard. Panels were delivered to site on flat deck truck for the site team to install where they lifted them flat (using four lifters) and put a group of panels on the barge (see Figure 14) directly after that they started filling the recess former of the bottom lifting anchors because they will be under the water level after installing the panel in its final position (see Figure 15).

Figure 14. Groups of Panels on the Barge Figure 15. Final Panel's Positon

CONCLUSION

With repeatable precast panels of that number (150 panels), we can conclude the following:

- Using steel mould makes the job easier and saving a lot of labour with high quality results.
- High quality by moving from the conventional concrete to SCC with all the benefits of using the SCC.
- Visually appealing to use the rubber formlinear with the two pattern which matching the area of the project giving the solid concrete different look.
- This project would not have been easy to finish without the cooperation between all the parties: Owner, Architect, contractor and the precaster.
- In conclusion now 150 panels of SCC Breakwater have been installed at Half Moon Bay Marina (see Figure 16).

Figure 16. Panels on Site

ACKNOWLEDGEMENT

Thanks for Wilco Precast Ltd team for all the help in finishing this work

SESSION 4B

Chair:
Kerry Newton

concretenz
BUILDING RESILIENCE
CONFERENCE 2022
13-15 October 2022
Energy Events Centre | Rotorua

RUBBERISED CONCRETE: MATERIAL CHARACTERISATION AND MECHANICAL BEHAVIOUR

E. HERNÁNDEZ, R. LIU, A. PALERMO, G. CHIARO, A. SCOTT

Department of Civil and Natural Resources Engineering, University of Canterbury, New Zealand

SUMMARY

Worldwide, it is estimated that one billion scrap tyres are produced per annum. This underlines the importance of finding an environmentally and economically sustainable way to manage the sheer number of waste tyres being produced. Traditionally, waste tyres have been used for low-value applications such as cheap fillers or fuel. What has been overlooked is that waste tyres offer a source of sustainable, high-quality and cost-competitive materials that, after processing, can be employed in a broad spectrum of civil engineering applications. This paper investigates the opportunities for structural engineering use of shredded waste tyre rubber particles in concrete by characterising its mechanical properties, flexural behaviour, and dynamic characteristics. To this end, a 50 MPa control mix (28 days) was designed and optimised. Besides the control mix, two rubberised mixes were designed, where 10% and 20% of the aggregate in the control mix were replaced, by volume, with fine and coarse rubber particles. All mixes were manufactured by a ready-mix concrete plant, allowing, the feasibility of mixing, transportation, and casting at a large scale to be evaluated. The experimental work was conducted in three phases: material property tests, four-point bending tests of reinforced beams, and vibration tests of unreinforced beams. Results show that, despite rubberised concrete exhibiting a lower compressive strength than conventional concrete (reduction of up to 60% at 20% replacement), its effect on the flexural resistance of reinforced concrete beams was found to be minor (less than 13% reduction). Based on considering multiple performance metrics simultaneously (material strength, stiffness, and equivalent viscous damping), it was concluded that the rubberised concrete mix with 10% aggregate replacement exhibited the best potential for structural use.

INTRODUCTION

The management and disposal of waste tyres has been recognised as a global environmental issue because of their lack of biodegradability, flammability, chemical composition, and the large volumes required to be managed. Globally, more than one billion waste tyres are generated every year, with more than five million being produced annually in New Zealand (MfE, 2015). Stockpiling and dumping have been common disposal methods to date but have led to serious environmental and public health hazards in recent years. The unfeasible nature of recycling automobile tyres for their original purpose makes their disposal more challenging. Furthermore, regardless of existing applications such as playground surfaces, sports fields, asphalt, or energy recovery, over 30% of the global generation of waste tyres remain unrecycled (WBCSD, 2018).

Due to its large worldwide consumption and variety of uses, concrete has the potential to integrate recycled rubber (from waste tyres) for specific applications, non-structural and structural, developing a new eco-friendly type of concrete with a lower carbon footprint. This new composite material called rubberised concrete (RuC) is a cementitious composite in which recycled rubber aggregates are included in the concrete matrix as a partial replacement of natural aggregates (fine and coarse). Thus, the sustainability of RuC lies in both the use of waste tyres and the reduction in the use of natural mineral aggregates, in particular, sand which is in short stock worldwide.

However, to successfully implement RuC, a thorough understanding is necessary at a material level (engineering properties) and member level (mechanical behaviour of reinforced RuC). RuC, as a composite material, depends significantly on the properties of its constituents. It is evident that the mechanical properties of mineral aggregates and rubber aggregates are fundamentally different. Rubber aggregates have a much lower modulus of elasticity and large strain capacity, whereas mineral aggregates are stiffer and more brittle. As a result, the properties of RuC depend significantly on the amount of rubber in the mix. Several authors have studied the effect of rubber aggregates on the mechanical properties of concrete (Eldin and Senouci, 1992 ; Bompa et al, 2017). Furthermore, published experimental investigations have reported that rubber aggregates enhance energy absorption capacity, crack control and damping ratio, but at the cost of lower strength and stiffness relative to conventional concrete (CC).

Nonetheless, it has also been proven that strength reductions of reinforced RuC members, particularly in flexure-dominant members, are far lower than would be indicated based off the strength of the plain RuC alone (Ismail and Hassan, 2016). Youssf et al. (2016) compared the response of conventional concrete and rubberised concrete columns under cyclic loads. The RuC specimen incorporated recycled rubber at 20% by volume of sand. Results indicated that despite the compressive strength of RuC being 28% lower than CC, the RuC column sustained a lateral load of approximately 98% of the conventional column (at the same axial load), all whilst dissipating 2.5 times more energy up until a drift ratio of 4%. Moustafa et al. (2017) investigated the dynamic response of CC and RuC columns (20% rubber content, by volume of sand) through shaking table tests. The authors reported that the RuC column displayed a higher drift capacity than the CC column: 5.4% drift compared to the 4.8% drift. In addition, an increase in the cumulative dissipated energy of 16.5% was measured. The performance improvements were attributed to the higher equivalent viscous damping of RuC compared to CC.

This paper presents preliminary results of an experimental programme focused on developing and characterising the material properties of RuC mixes (10% and 20% by aggregate volume), in addition to investigating the flexural and dynamic response of RuC beams. First, modifications to mix design procedures for RuC are explained. Then, results of the material characterisation (compressive, splitting tensile, modulus of rupture, stress-strain curves and modulus of elasticity values) are presented. Lastly, the flexural behaviour and dynamic properties investigated through four-point bending tests of reinforced beams and impact resonance tests on unreinforced beams are examined.

EXPERIMENTAL PROGRAMME AND METHODOLOGY

As part of the MBIE funded project titled “Eco-rubber seismic-isolation foundation systems” being undertaken at the University of Canterbury (Chiaro et al., 2019; Hernández et al., 2020), the authors are investigating the opportunities for structural use of rubberised concrete mixes. To this end, a control mix (50 MPa) and two rubberised mixes with 10% and 20% recycled tyre rubber by volume of aggregates were investigated (Figure 1).

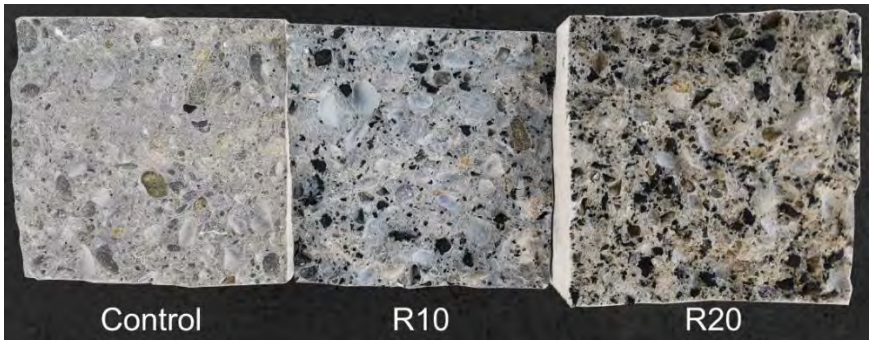

Figure 1. Comparison of the cross-section of control concrete, 10% rubber replacement (R10) and 20% rubber replacement (R20).

Material characterisation

***Materials*.** The design of the mixes prioritised the use of locally available materials in New Zealand. Natural river sand (<4.75 mm) and round coarse aggregates (maximum size of 13 mm) were use in all mixes. Two grades of recycled rubber aggregates (free of steel wires and textile reinforcement), 0.8-to-2.5mm (RA-1) and 4-to-8 mm (RA-2), replacing sand and coarse aggregate respectively, were obtained from a local supplier. The physical properties and grading of aggregates used are given in Table 1 and Figure 2, respectively. Potable water was used in all mixes. A two-phase binder consisting of a general purpose (GP) cement and Fly ash (FA) class F was utilised in all mixes. The workability of the mix was improved by using polycarboxylic-ether-polymer-based superplasticiser (SP).

Table 1. Physical properties of aggregates

Properties	Sand (FA)	Gravel (CA)	RA-1	RA-2
Grain size [mm]	< 4.75	< 13	0.8-2.5	4-8 mm
Specific gravity [–]	2.63	2.66	1.15*	1.15*
Bulk density [kg/m^3]	1550	1640	602*	650*
Water absorption [%]	0.8	0.8	-	-
* From Tasalloti et al. (2020; 2021)				

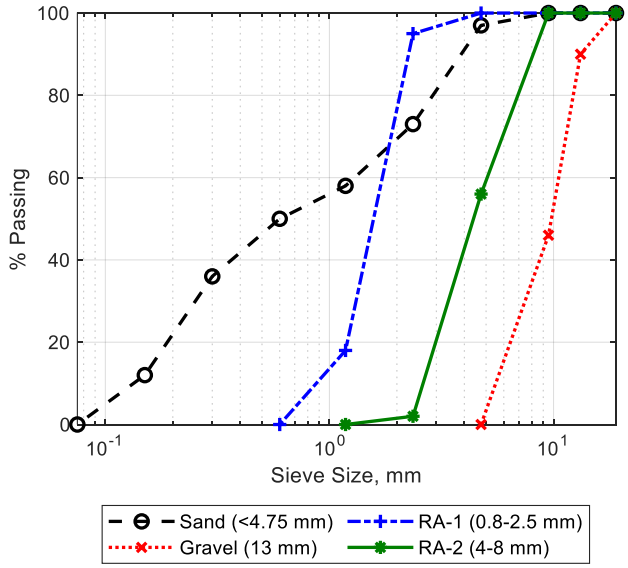

Figure 2. Particle size distribution of natural and rubber aggregates

Mix Design. The rubberised concrete mix was designed using the absolute volume method as presented in Steven and Kosmatka (2011). In order to consider the effect of rubber aggregates in the compressive strength, a reduction factor (Equation 1) was calculated using the strength-to-rubber content relationship proposed by Aslani (2015).

$$RF = 0.986e^{-0.051 \cdot R} \tag{1}$$

Where:

RF: Reduction factor
R: Rubber replacement by the total volume of aggregates, %

Then, using equation (1) and the modified Abram's law proposed by Mackechnie (2015), the target compressive strength was determined using Equation (2):

$$f'_c = \frac{150}{5^{1.5 \cdot w/b}} \times RF \quad \text{(MPa)} \tag{2}$$

Where:

f'_c: Target compressive strength at 28 days, MPa
w/b: water-to-binder content

Finally, the proportions of aggregates were adjusted to integrate the chosen rubber content as follows:

$$W_{agg} = W'_{agg} \times (1 - R) \quad \text{(kg)} \tag{3}$$

$$W_R = \frac{G_R}{G_{agg}} \times R \times W_{agg} \quad \text{(kg)} \tag{4}$$

Where:

W'_{agg}: Aggregate weight, kg
W_{agg}: Final adjusted aggregate weight, kg
W_R: Final adjusted rubber weight, kg
G_R: Specific gravity of rubber aggregate
G_{agg}: Specific gravity of mineral aggregate

A brief description of the proposed mix design methodology for rubberised concrete is presented in Figure 3.

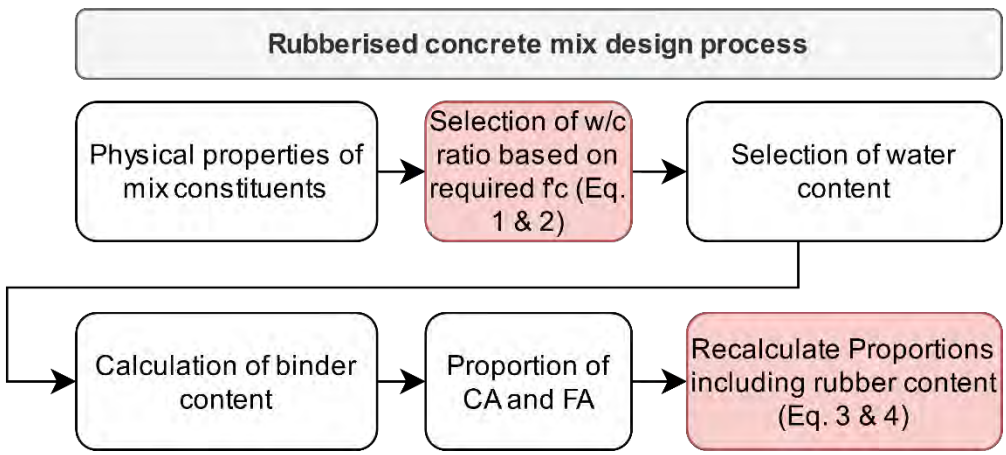

Figure 3 Proposed mix design process

The final proportions of the mixes used in this work are shown in Table 2.

Table 2. Mix proportions investigated in this work.

Material		Control	R10	R20
Cement	[kg]	305	305	305
Fly Ash, Class F	[kg]	75	75	75
Sand, McLeans Island	[kg]	900	810	720
13mm aggregates, McLeans Island Rounds	[kg]	940	846	752
Rubber 0.8-2.5mm	[kg]	0	40	80
Rubber 4-8mm	[kg]	0	40	80
Water	[L]	160	160	160*
Superplasticizer	[L]	0.6	1	1
Retarder	[L]	0.8	0.8	0.8
Water-to-binder ratio (w/b)	[-]	0.42	0.42	0.5
Note: *Additional water of 30 L was used to keep similar slump value (~140 mm) in all mixes.				

Concrete manufacturing. A ready-mix concrete plant manufactured all the mixes assessed in this work. In order to ensure suitable characteristics, crucial aspects such as the mixing process and mixing time were adjusted in conjunction with concrete plant engineers. Figure 4 shows the delivery and pouring of the RuC mix with 20% rubber content at the Wing Structural Laboratory. At least 1.5 m3 were poured for each mix.

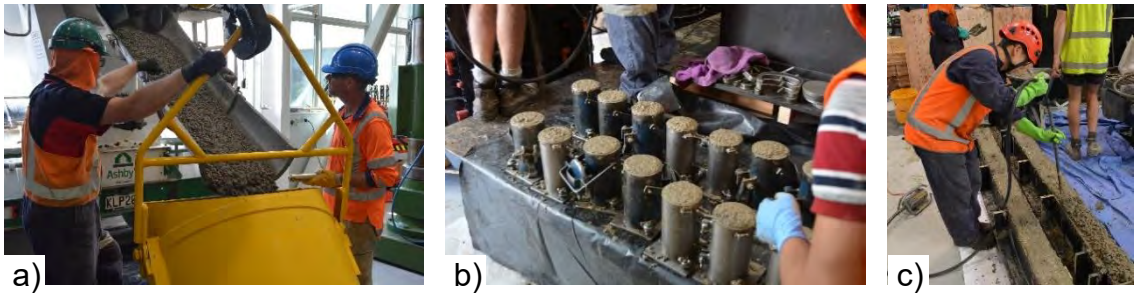

Figure 4. Concrete pouring of R20 mix: a) Delivery of R20 mix (slump test 180 mm), b) concrete cylinder for compression and splitting-tensile tests, c) Pouring of reinforced concrete beams

Experimental testing. Material tests were performed according to NZS 3112:2 (Standards New Zealand, 1986). Figure 5 shows the typical setups use to determine the material properties. The compressive strength and modulus of elasticity of the mixes were assessed using concrete cylinders of 100x200 mm, tested at 28 days of age after curing in water at 20° C (Figure 5a). For each mix, at least three replicate specimens were tested at a load rate of 0.25 MPa/s. Two cylinders of 100x200 mm were used to evaluate the splitting tensile strength (Figure 5b). Prisms of 100x100x400 mm under a four-point bending test setup were used to determine the flexural strength/modulus of rupture (Figure 5c).

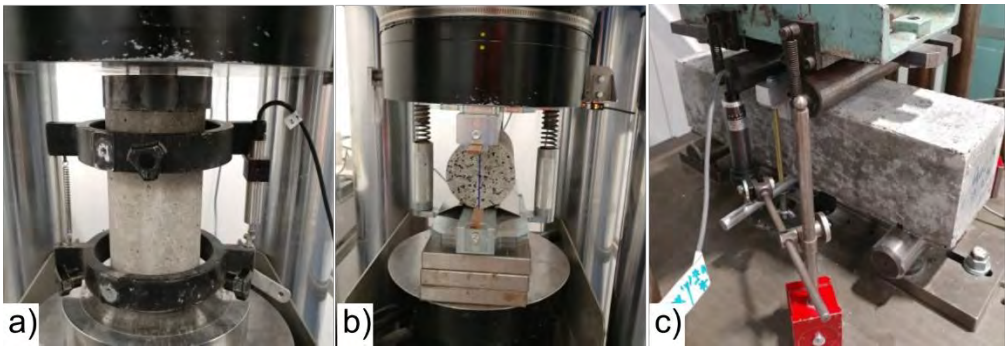

Figure 5. Test setup: a) Compression and modulus of elasticity, b) Splitting-tensile test, c) Flexural strength

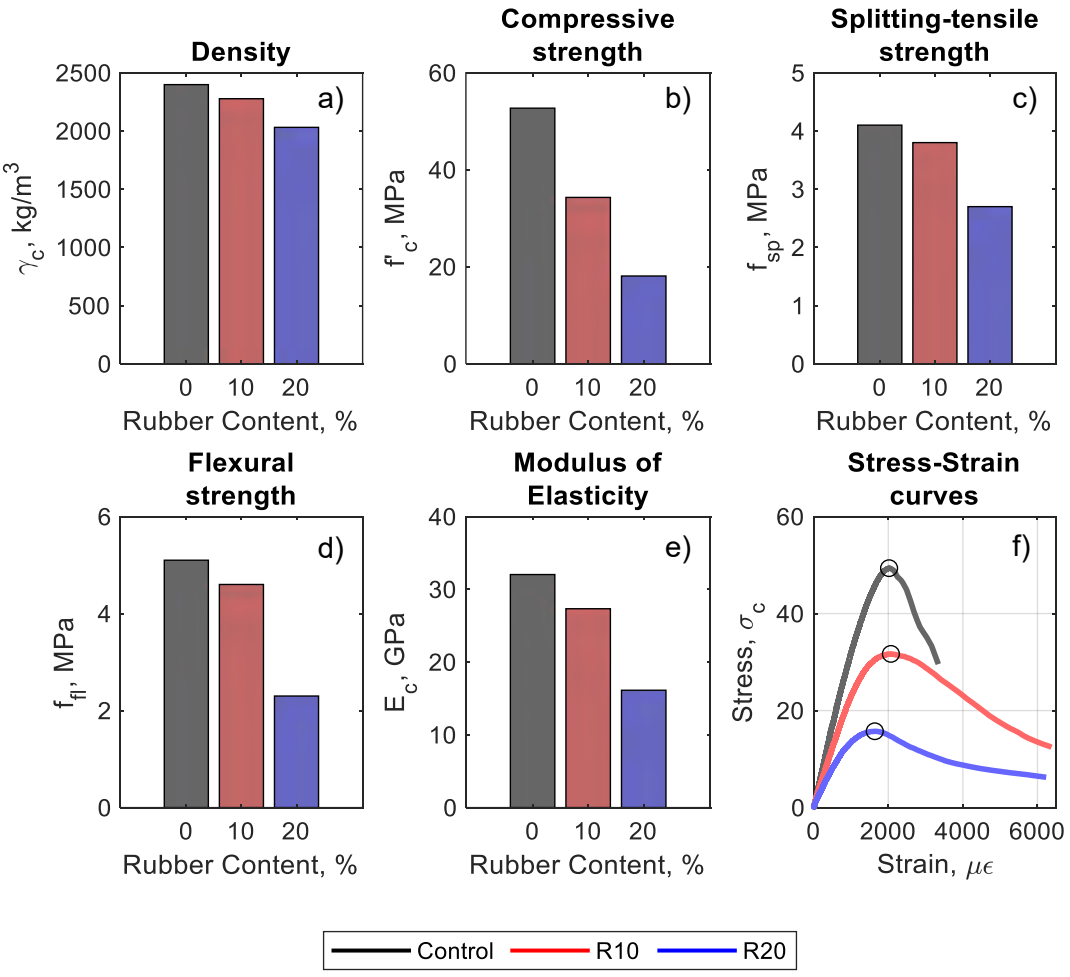

Figure 6. Comparison of the mechanical properties of rubberised mixes against the control mix.

Results. Figure 6 presents the mean values of the measured concrete material mechanical properties. The typical stress-strain curves for each mix, obtained from testing in a load-controlled machine, are presented in Figure 6f. Table 3 summarises the changes in properties with respect to the control mix. It can be observed form Table 3 that the substitution of aggregate with rubber significantly reduced the compressive strength of the concrete mixes. The higher w/b ratio, 0.5 compared to 0.42 of control mix, also affected the mechanical properties of the R20 mix. Using equations 1 and 2, a reduction of 3 MPa (21 to 18 MPa) can be estimated due to the increase in w/b ratio. That is a minor effect compared to the drop in strength caused by the addition of rubber. In general, lesser strength reductions were observed

for other mechanical properties, e.g., spitting tensile strength etc. However, a considerable drop in the modulus of elasticity and flexural strength occurred from the rubber content increasing from 10% to 20%. This effect is particularly important for choosing a suitable rubber content to use if rubberised concrete is to be used in applications such as raft foundations, where adequate flexural strength is a key design parameter.

Table 3: Effect of rubber content in mechanical properties

Property	Percent change (%)	
	R10	R20
Density [kg/m^3]	-5	-15
Compressive strength [MPa]	-35	-65
Splitting-tensile [MPa]	-7	-34
Flexural strength [MPa]	-10	-55
Modulus of Elasticity [GPa]	-15	-50
Strain at peak stress [με]	+2	-19

Static properties of reinforced beam members

A set of 9 doubly reinforced beams (three control concrete, three R10 concrete and three R20 concrete) were tested under four-point bending (Figure 7). The beams were rectangular in section with a depth of 200mm and a width of 100mm. Within each set of three beams, the amount of tension reinforcing provided was varied: 3 x D10, 2 x D12, and 2 x D16 (Figure 7). All beams had 2 x D12 compression reinforcing and R6 stirrups spaced at 100mm spacing. In terms of test setup, the span between support centres was 2.7m, and the span between applied point loads was 600mm. At the time of writing, only the control concrete beams, R20 beams and one reinforced R10 beam had been tested. The beams were loaded using a manually powered hydraulic ram following an asymmetric cyclic loading protocol.

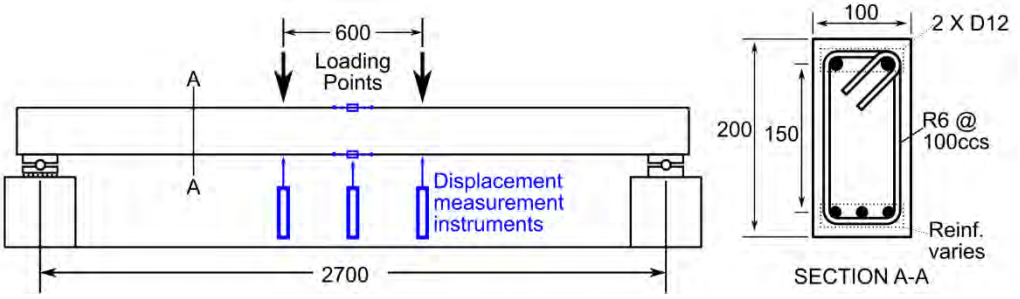

Figure 7. Test setup elevation and beam reinforcing details

Results. In terms of force-displacement response (Figure 8), the rubberised concrete beams displayed: lower stiffness (initial and cracked) than the control concrete beams, a near perfectly plastic post-yield response, and lack of spalling. The reduction in stiffness was expected because its effect had been reported previously and the fact that rubber has a lower elastic modulus than concrete. The largest changes in stiffness were seen for the initial stiffness. For the R10 and R20 beams, respectively, a 16% and 48% reduction in initial stiffness relative to the control concrete beams was observed. Table 4 compares the effect of rubber content on the flexural properties of the D10 reinforced beams. A possibly useful consequence of stiffness reduction is the reduced post-yield stiffness that rubberised concrete offers (Table 4 and Figure 8). If used in plastic hinge regions for seismically designed structures, it has the potential to greatly reduce construction costs related to plastic hinge overstrength demands. In terms of the effect of rubberised concrete on strength, despite rubberised concrete having a lower compressive strength than the control mix, only a minor reduction in strength was observed (Table 4). All beams were pushed to approximately 100mm displacement (displacement

ductility of approximately 10), and no reduction in strength was observed for the rubberised concrete beams, and no further strength reduction was observed for the control concrete beams after spalling.

In terms of the effect of rubber on concrete damage (Figure 9), two observations were made: firstly, the rubber had a beneficial effect on distributing tensile strains such that flexural cracks were of more similar width over the length of the constant moment region. Secondly, even with only 10% rubber replacement, a crushing rather than spalling type failure was observed in the compression zone: That is, the formation of many longitudinal cracks, but, where the fractured concrete is still joined requiring forceful effort to break apart. In the case of the control concrete beams, at the point of spalling, a crack initiated at the top of the beam and suddenly propagated along the longitudinal axis, just above the compression reinforcing (Figure 9a. and 9b.), resulting in a complete loss in the top cover concrete and a drop in strength (Figure 8). For the rubberised concrete beams, the rubber aggregates acted as a sort of fibre, preventing uncontrolled crack propagation and thus preventing spalling of the top cover concrete.

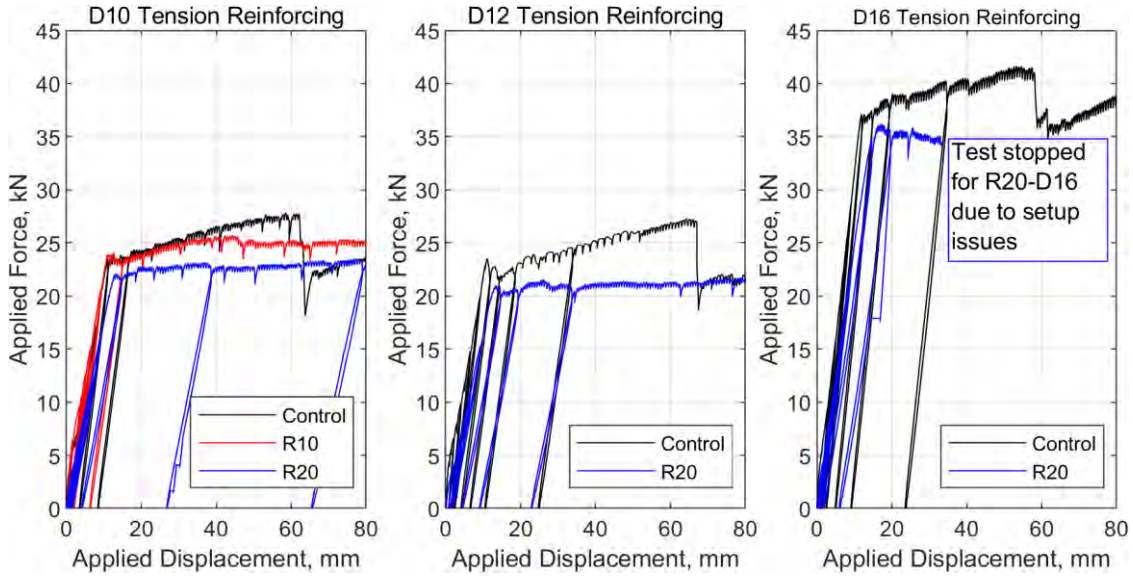

Figure 8. Comparison of force-displacement plots for control and rubberised concrete beams using different tension reinforcing.

Table 4. Comparison of static flexural properties of the D10 reinforced control and rubberised concrete beams.

Reinforcing: 2 x D12 compression, 3 x D10 tension			
	Control	R10	R20
Initial Stiffness [kN/mm]	3.09	2.59	1.6
Cracked stiffness [kN/mm]	0.98	0.95	0.84
Elastic unloading stiffness [kN/mm]	1.71	1.37	1.05
Post-yield stiffness [kN/mm]	0.05	0.04	0.03
Yield Curvature [1/mm]	3.015e-3	2.975e-3	2.722e-3
Yield Moment [kNm]	12.39	12.3	11.54
Max Moment [kNm]	14.6	13.5	12.69
Strain at spalling (s)/crushing (c) [με]	3660 (s)	2839 (c)	2290 (c)

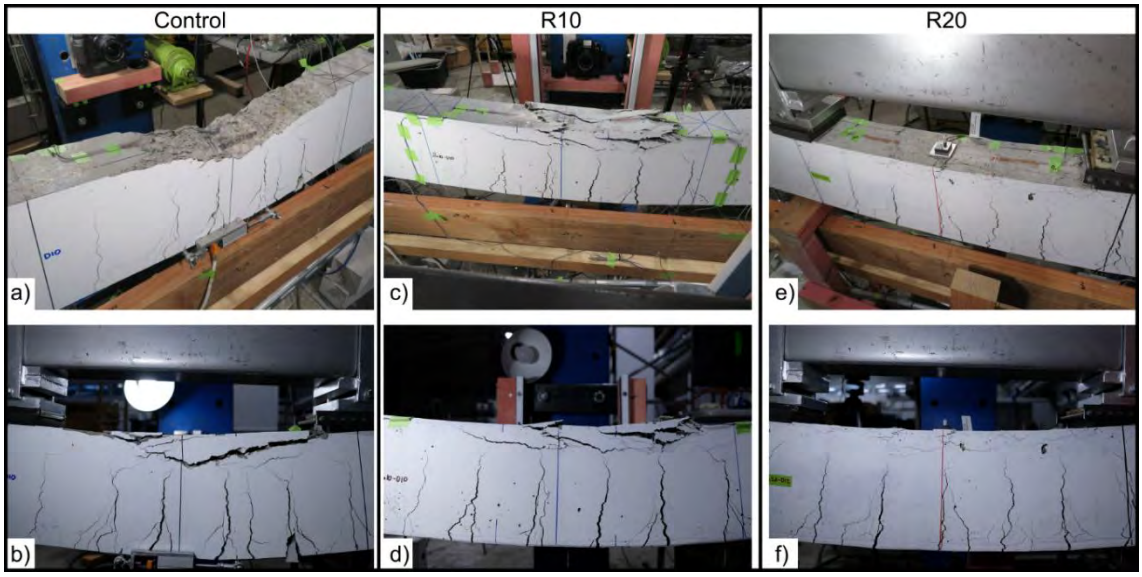

Figure 9. Comparison of the effect of rubber content on concrete damage.

Dynamic properties of beam members

A set of three unreinforced beams (CC, R10, and R20 beams) were subject to free vibration testing to compare the dynamic stiffness and vibration damping response. These unreinforced beams had the same overall dimensions and span as the reinforced beams. For the vibration testing, specialised knife-edge supports were used to support the beams. The beams were set into free vibration using two modal impact hammers: 250g and 5.5kg. These two hammer sizes were used to elicit low and high levels of vibration excitation and are shown in Figure 10. The modal impact hammers had an inbuilt loadcell which was monitored to measure the impact force applied. The beam response was measured using an array of 5g accelerometers (Figure 10a) and a high-speed data logging system. Damping and frequency were estimated using two methods: Modal Analysis and the logarithmic decrement method (Figure 10c).

Figure 10. Vibration testing. a) small modal hammer and accelerometers, b) large modal hammer, c) typical hammer pulse and acceleration decay curve

Results. The measured and inferred dynamic properties of the unreinforced beams tested are presented in Table 5 below. Rubberised concrete was found to have a higher value of equivalent viscous damping (EVD). The R20 concrete displayed a 16-27% increase in EVD depending on the level of vibration excitation applied, whilst the R10 concrete displayed a 9-18% increase in EVD also depending on the level of vibration excitation applied. The frequencies of vibration of the rubberised concrete beams were lower than that of the control concrete beam due to the reduction in elastic modulus being greater than the reduction in mass (owing to the rubber replacing mineral aggregate). Respectively, the dynamic elastic modulus of the R10 and R20 beams were found to be 78% and 53% of the dynamic elastic modulus of

the control concrete beam. The dynamic elastic moduli were found to be in agreement with the static elastic moduli shown in Figure 6.

Table 5: Effect of rubber content in dynamic characteristics of unreinforced concrete beams

	Concrete Type			
	Control	R10	R20	Vibration mode shape
Fundamental Frequency [Hz]	46.8	41.8	37.2	
2nd mode [Hz]	187.3	136.8	122.3	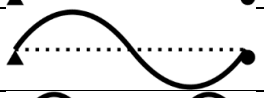
3rd mode [Hz]	418.5	361.7	352.5	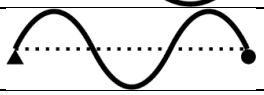
Modal EVD [%] (low level excitation)	0.66	0.78	0.84	
Logarithmic Decrement EVD [%] (high level excitation)	0.74	0.81	0.86	
Measured beam mass [kg]	142.95	132.70	118.7	
Dynamic Elastic Modulus [GPa]	32	25	17	

CONCLUSIONS

Rubberised concrete is a potential solution to the issue of waste tyre management. In this study, the effect of two levels of rubber replacement content in concrete was investigated (10% and 20% replacement of aggregates by volume) relative to a 50MPa control mix. A mix design methodology was proposed and shown to be able to predict the compressive strength for the control, R10, and R20 mixes successfully with an error between 3-12% (1.6 MPa -2.2MPa).
It was shown that rubberised concrete could be successfully produced by ready-mix concrete plant and no issues regarding the production and transportation of rubberised concrete mixes were found. Moreover, no significant differences in workability or sensitivity to handling were observed during the casting and curing of the rubberised concrete compared to conventional concrete. It was found that rubber content had a strong effect on reducing compressive strength. The modulus of elasticity, flexural and splitting tensile strength presented minor reductions for the R10 mix (up to 15%); however, they dropped significantly in the R20 mix (up to 55%) compared to the control mix. The four-point bending of reinforced rubberised concrete beams showed that compared to conventional concrete they exhibit similar flexural strength, lower stiffness (initial, cracked and post-yield), near perfectly plastic post-yield response, and lack of spalling. From free vibration testing of unreinforced beams, it was found that rubberised concrete displays a higher level of equivalent viscous damping than conventional concrete ranging from 9-27% depending on rubber content and level of vibration excitation. Overall, the R10 mix demonstrates the greater potential for structural use in flexure-dominant members such as raft foundations, beams, or slabs due to it having a practical balance of performance metrics: material properties, flexural response, and dynamic characteristics. Nonetheless, additional investigations into properties such as durability or fire resistance, still need to be completed.

ACKNOWLEDGEMENTS

Research funders: Ministry of Business, Innovation and Employment (MBIE) and QuakeCoRE; Sponsorship and material supply: Complete Reinforcing and Allied Concrete, in particular, Dave Barker, Gary Hanser, and Nasser Almesfer for their contribution and insightful feedback in the production of the mixes at a large-scale; Contributions to experimental work: UC technical staff Tim O'Connell, Mosese Fifita, Tim Perigo, and John Maley.

REFERENCES

Aslani, F. (2015). Mechanical properties of waste tire rubber concrete. Journal of Materials in Civil Engineering, 28(3), 4015152.

Bompa, D. V., Elghazouli, A. Y., Xu, B., Stafford, P. J., & Ruiz-Teran, A. M. (2017). Experimental assessment and constitutive modelling of rubberised concrete materials. Construction and Building Materials, 137, 246-260. https://doi.org/10.1016/j.conbuildmat.2017.01.086

Chiaro G., Palermo A., Granello G., Tasalloti A., Stratford C. & Banasiak L.J. (2019). Eco-rubber seismic-isolation foundation systems: a cost-effective way to build resilience. In: Proc. of the 2019 Pacific Conference on Earthquake Engineering, 4-6 April, Auckland, New Zealand, pp. 8.

Eldin, N. N., & Senouci, A. B. (1992). Engineering properties of rubberised concrete. Canadian journal of civil engineering, 19(5), 912-923.

Hernández, E., Palermo, A., Granello, G., Chiaro, G., & Banasiak, L. J. (2020). Eco-rubber Seismic-Isolation Foundation Systems: A Sustainable Solution for the New Zealand Context. https://doi.org/10.1080/10168664.2019.1702487

Ismail, M. K., & Hassan, A. A. A. (2016). Ductility and Cracking Behavior of Reinforced Self-Consolidating Rubberized Concrete Beams. Journal of Materials in Civil Engineering, 29(1), 04016174-04016174. https://doi.org/10.1061/(asce)mt.1943-5533.0001699

Mackechnie, J. R. (2015). Moving towards model specification guidelines for the supply of ready-mixed concrete in New Zealand. Concrete Industry Conference, Rotorua.

MFE. (2015). Waste tyres economic research. Ministry for the Environment.

Moustafa, A., Gheni, A., & ElGawady, M. A. (2017). Shaking-Table Testing of High Energy–Dissipating Rubberized Concrete Columns. Journal of Bridge Engineering, 22(8), 04017042. https://doi.org/10.1061/(asce)be.1943-5592.0001077

Standards New Zealand, 1986. Methods of Test for Concrete, NZS 3112.2:1986, Wellington, New Zealand.

Steven H. Kosmatka, M. L. W. (2011). Design and Control of Concrete Mixtures (15th ed.). PCA.

Tasalloti A., Chiaro G., Palermo A. & Banasiak L.J. (2020). Effect of rubber crumbs volumetric content on the shear strength of gravelly soil in direct shear apparatus. Proc. of Geo-Congress 2020, 25-28 Feb., Minneapolis, Minnesota, USA; ASCE Geotechnical Special Publication, 319: 259-266.

Tasalloti A., Chiaro G., Banasaik L. & Palermo A. (2021). Experimental investigation of the mechanical behaviour of gravel-granulated tyre rubber mixtures. Construction and Building Materials, 273: 121749, https://doi.org/10.1016/j.conbuildmat.2020.121749.

WBCSD. (2018). Global ELT management - A global state of knowledge on collection rates, recovery routes, and management methods. World Business Council for Sustainable Development.

Youssf, O., ElGawady, M. A., & Mills, J. E. (2016). Static cyclic behaviour of FRP-confined crumb rubber concrete columns. Engineering Structures, 113, 371-387.

concretenz BUILDING RESILIENCE
CONFERENCE 2022
13-15 October 2022
Energy Events Centre | Rotorua

CHEMICAL AND MINERAL ADMIXTURE CONCRETE MIX DESIGN FOR SUSTAINABILITY USING SIMPLEX CENTROID MODEL

EZRA JONES, JAROD WILSON

Sika NZ Ltd, Auckland, New Zealand

SUMMARY

Replacing cement with industrial waste material streams is a highly effective way to reduce the carbon footprint of concrete. Mineral admixtures (pozzolans) such as fly ash (FA) and ground granulated blast-furnace slag (GGBS) however typically show delayed set and decreased strength particularly at early ages compared to type GP cement. Chemical admixtures (set accelerators and strength enhancers) are necessary to overcome these negative aspects and facilitate high mineral admixture replacement levels in order to maximise sustainability while still maintaining acceptable fresh and hardened concrete properties. The concept of simplex centroid mix design method and cement efficiency factor (*k*-value) as it applies ternary blended cements will be introduced. The chemical composition of the supplementary cementitious materials (SCMs), water/binder ratio and replacement level are shown to play a major role in determining their cement efficiency.

INTRODUCTION

SCMs may be divided into natural and artificial materials. To the former belong true pozzolanas and volcanic tuffs while the latter belong siliceous waste by-products, such as fly ashes, condensed silica fume and slags (blast-furnace slag, steel slag, non-ferrous slags). The SCMs can be used in concrete production either as blended cement constituents or as separate concrete mineral admixture. The use of SCMs at high replacement levels has a significant impact on the sustainability of concrete since cement has far and away the highest embodied carbon contribution [NZGBC].

Table 1. Concrete Component Embodied Carbon [TCC/05/24]

Material	**Embodied CO_2 (kg/tonne)**
Type GP Cement	860
Fly Ash	0.1
Ground Granulated Blast-furnace Slag (GGBS)	79.6

However, due to significant variation in physical, chemical, and mineralogical composition the SCMs exhibit different activity, therefore an efficient procedure has to be developed for their optimum use in concrete.

The efficiency factor (or *k*-value) is defined as the part of the SCM in a pozzolanic concrete which can be considered as equivalent to Portland cement, having the same properties as the concrete without the SCM (*k*-value = 1). The quantity of the SCM in the mixture can be multiplied by the *k*-value to estimate the equivalent cement content, which can be added to the

cement content for the determination of the water cement ratio, minimum required cement content, etc. Knowing *k*-values, the mix design can be easier and more accurate.

The concept of *k*-value for SCM has found its way into British and European standards [BS EN 206, PD CEN/TR 16639].

$$w_o = \frac{w_a}{c_a + k.a}$$

When normalized to the cement content c_a:

$$k = \frac{\frac{w_a}{w_o - 1}}{\frac{a}{c_a}}$$

Where:

w_o is the water/cement ratio of reference concrete without addition.
w_a is the water content of the concrete with addition.
c_a is the cement content of the concrete with addition.
k is the efficiency factor.
a is the addition content.

Accepted *k*-values for fly ash and GGBS are 0.4 and 0.6 respectively [BS EN 206] with some limitations around replacement levels.

EXPERIMENTAL

Concrete Equivalent Mortar (CEM) Mini-Cone Test Methods

The concrete equivalent mortar (CEM) is based on a standard concrete mix design [Assaad *et al*, Schwartzentruber & Catherine]. The coarse aggregates are replaced with an equivalent surface area of fine aggregates (e.g. Normensand) where workability is measured as spread rather than slump using a scaled down Abrams cone as shown in the figure below.

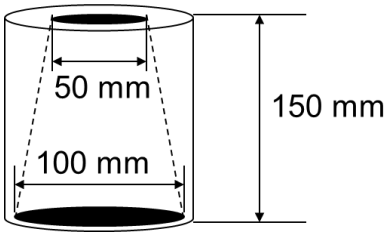

Figure 1. Concrete Equivalent Mortar (CEM) cone dimensions.

Set time is measured using Calmetrix F-Cal 8000 semi-adiabatic calorimeter and specimens moulded into prisms 40 x 40 x 160 mm for compressive strength.

Selected properties of the cementitious materials are listed in the table and particle size distribution (PSD) figure below. The fly ash belongs to the type class F and is slightly finer than the cement and GGBS.

Table 2. Selected cementitious properties.

Properties	Type GP	GGBS	Fly Ash
SiO_2	19.7	33.1	48.1
Al_2O_3	5.9	13.2	22.0
Fe_2O_3	2.9	0.6	13.4
CaO	64.2	42.5	6.7
MgO	1.4	5.9	5.0
$SiO_2 + Al_2O_3 + Fe_2O_3$			77.9
$CaO + MgO + Al_2O_3 / SiO_2$		1.86	
Relative Density	3.1	2.84	2.64

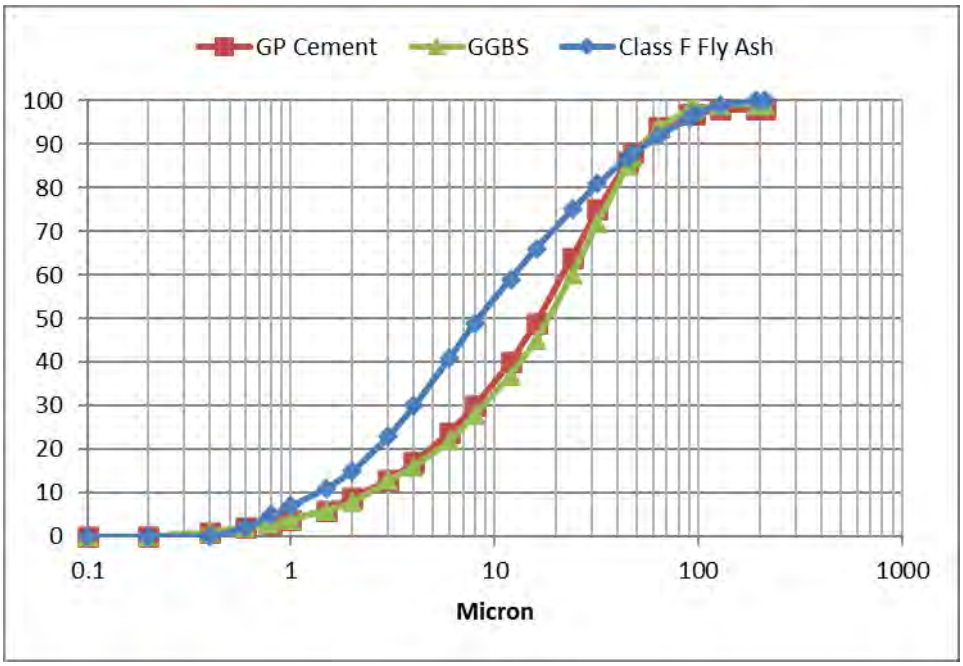

Figure 2. Particle size distribution of Type GP (general purpose) cement, GGBS and fly ash.

Simplex Centroid Design of Experiment (DoE)

The simplex-lattice design was introduced by Scheffé in 1958 [Scheffé]. Based on the simplex-lattice design, some modified designs have since been developed, including the simplex-centroid design [Jiao *et al*].

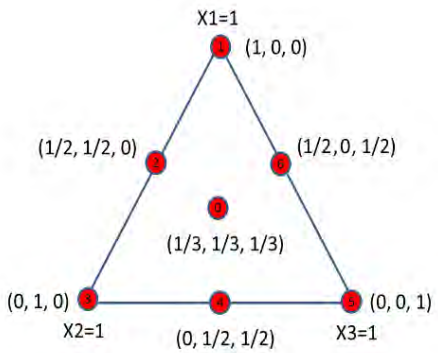

Figure 3. Simplex centroid mix design for a ternary blended system.

In the ternary blends of CEM mortars, the proportion bounds of cement, GGBS and fly ash are:

$0.5 \leq x_1 \leq 1.0$, $0.0 \leq x_2 \leq 0.5$, and $0.0 \leq x_3 \leq 0.3$, respectively.

According the DoE discussed above, the seven design points were obtained (given in Table 3). Based on the results of the seven design points, the equations of mortars made with Portland cement, GGBS and fly ash blends could be regressed by special cubic polynomial models [Dehuai & Zhaoyuan, Douglas & Pouskouleli]:

$$Y = \beta_1 x_1 + \beta_2 x_2 + \beta_3 x_3 + \beta_{12} x_1 x_2 + \beta_{13} x_1 x_3 + \beta_{23} x_2 x_3 + \beta_{123} x_1 x_2 x_3$$

The table below shows the mix proportions for the ternary systems under investigation, with the water binder ratio fixed at 0.5.

Table 3. Simplex Centroid Mix Proportions

Cement (x_1)	GGBS (x_2)	Fly Ash (x_3)	Designation
1.00	0.00	0.00	100OPC 0GGBS 0FA
0.75	0.25	0.00	75OPC 25GGBS 0FA
0.50	0.50	0.00	50OPC 50GGBS 0FA
0.75	0.00	0.25	75OPC 0GGBS 25FA
0.60	0.10	0.30	60OPC 10GGBS 30FA
0.50	0.25	0.25	50OPC 25GGBS 25FA
0.66	0.17	0.17	66OPC 17GGBS 17FA

To examine he effect of the water binder ratio on compressive strength and *k*-value, a chemical admixture (water reducer) was used to obtain mix designs of 0.3, 0.4, 0.5 and 0.7 water binder ratio of a ternary blend 50OPC 30GGBS 20FA. The addition of a chemical activator to enhance strength and set is also investigated.

RESULTS AND DISCUSSION

CEM Workability

SCMs, particularly fly ash can enhance the paste and concrete workability which can be used to reduce the water content for the same workability if desired:

- Increase in paste volume owing to lower density of the SCM compared to that of cement.
- Fly ash reduces the flocculation of the cement particles due to dilution effect.
- Reduced growth of hydration products at early age due to the slower reaction of the fly ash.
- The spherical shape of fly ash particles facilitates the movement of neighbouring particles at high replacement levels by ball bearing effect.

GGBS has a smooth surface texture but is irregular in shape, with sharp edges and higher early reactivity leading to slightly lower workability.

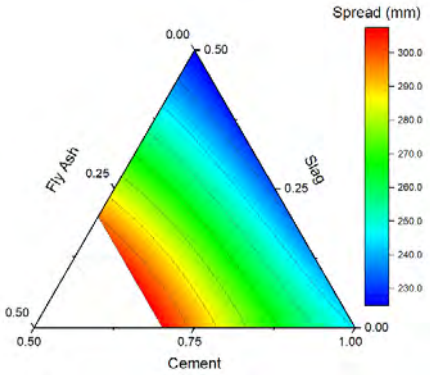

Figure 4. CEM workability as measured by spread.

CEM Compressive Strength and K-Value

Increasing the proportion of SCM decreases compressive strength at a fixed water cement ratio (0.5) at all ages. GGBS has higher strength compared to fly ash at ages 7 – 28 days. Fly ash contribution to strength occurs at later ages 28 – 56 days.

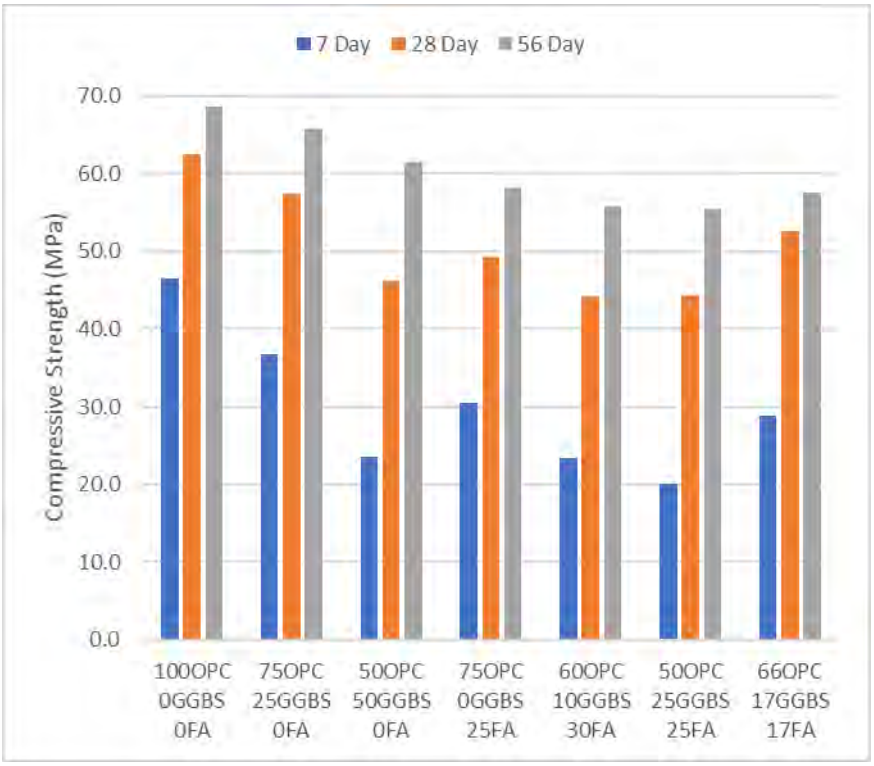

Figure 5. CEM compressive strength.

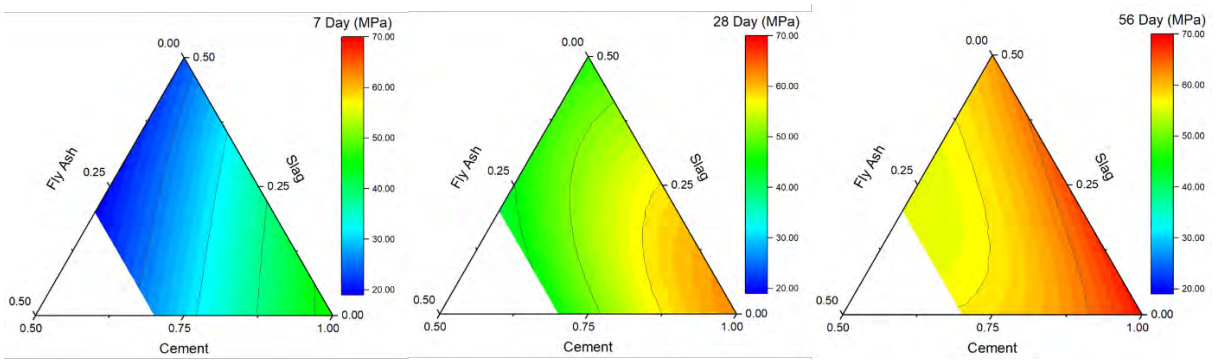

Figure 6. CEM compressive strength simplex centroid.

During the hydration of cement with water, tricalcium silicate (alite) and dicalcium silicate (belite) react chemically with water to produce a calcium silicate hydrate (C-S-H) phase, which is the major contributor to strength in concrete, as well as lime (calcium hydroxide) and heat:

$$2Ca_3SiO_5 + 6H_2O \rightarrow 3CaO.2SiO_2.3H_2O + 3Ca(OH)_2 + heat$$

$$2Ca_2SiO_4 + 4H_2O \rightarrow 3CaO.2SiO_2.3H_2O + Ca(OH)_2 + heat$$

Calcium hydroxide, $Ca(OH)_2$, is more soluble and migrates into the pore solution where pozzolans such as GGBS and fly ash which contain significant amounts of silica (SiO_2) reacts with the $Ca(OH)_2$ to form more C-S-H.

$$3Ca(OH)_2 + 2SiO_2 \rightarrow 3CaO.2SiO_2.3H_2O$$

As a result, pozzolans have been characterised with a delayed strength development, as they only act as fillers before $Ca(OH)_2$ becomes available.

The *k*-value calculated from the compressive strength data shows that it increases with age and is higher for GGBS than fly ash at the same replacement level. At 28 days the *k*-value is similar to values as described in BS EN 206 of 0.6 and 0.4 for GGBS and fly ash respectively.

GGBS is latently hydraulic, meaning it will react with water, all be it slowly [Menendez *et al*]. The basicity of GGBS is used as a hydraulic index and in many countries it is used as a standard measure of quality of GGBS and specify a minimum basicity/hydraulic index. In general as the hydraulic index increases the early age strength increases.

Class F fly ash as used here is purely pozzolanic and therefore only reacts at later ages with the by-product of the hydration of cement as shown above. The chemical composition determines the structure of glass materials and plays an important role in determining the pozzolanic reactivity of fly ash, calcium to alumina and calcium to silica ratios [Hemalatha & Ramaswamy].

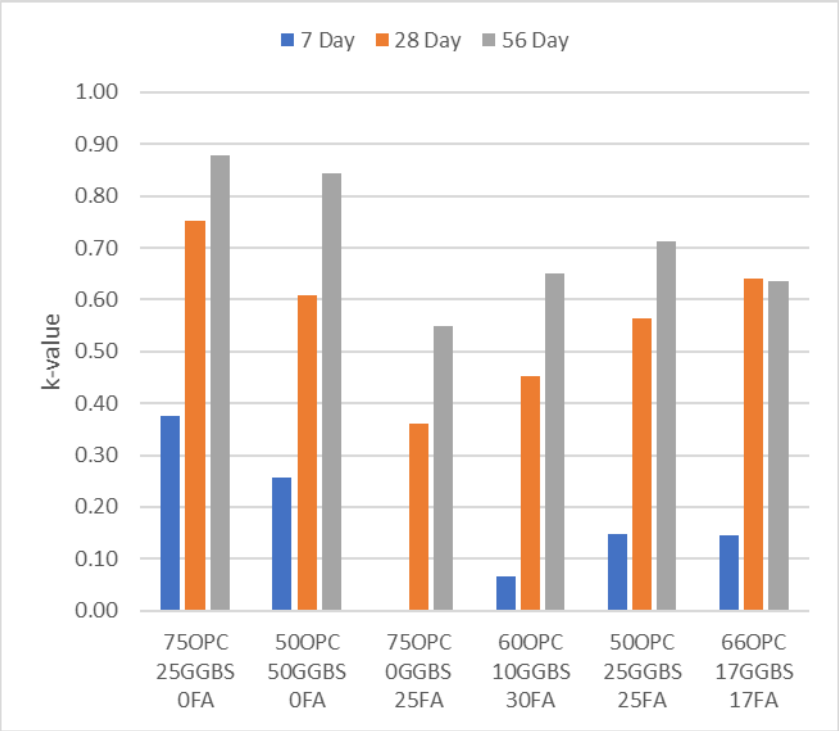

Figure 7. CEM *k*-value ternary blended system.

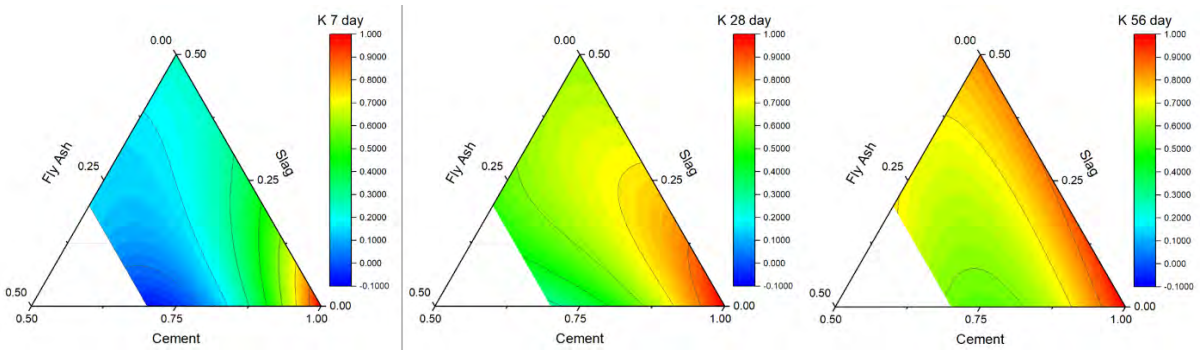

Figure 8. CEM *k*-value.

Heat of Hydration

Setting time of the CEM ternary blends shows that increasing the proportion of SCMs shifts the peak to the right (extends the set time), broadens and lowers its temperature, more so for fly ash than GGBS. The main peak is the heat is associated with the hydration of alite (C3S) while the secondary peak attributed to renewed hydration of tricalcium aluminate (C3A). Lower heat generation is desirable as it can minimise the risk of thermal cracking. Calorimetry is also a very useful tool to identify incompatibility in the binder system e.g. a deficiency of soluble sulphate with high addition rates of SCMs (in particular some class C fly ashes).

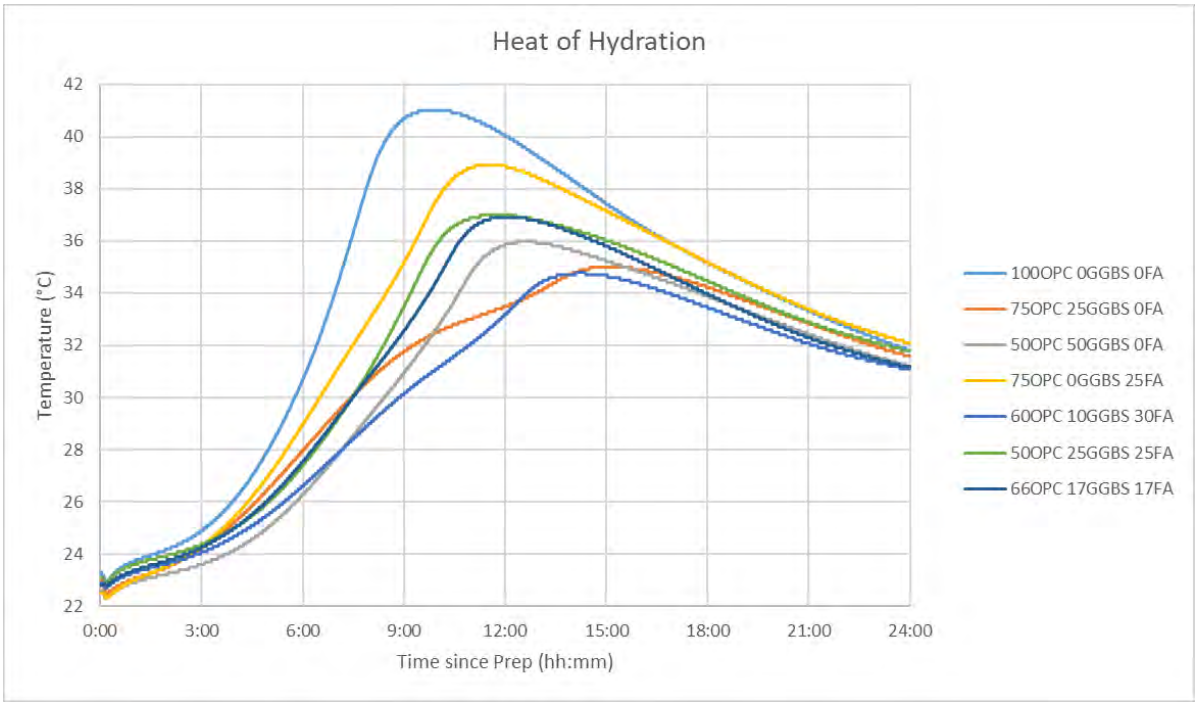

Figure 9. CEM semi-adiabatic calorimeter.

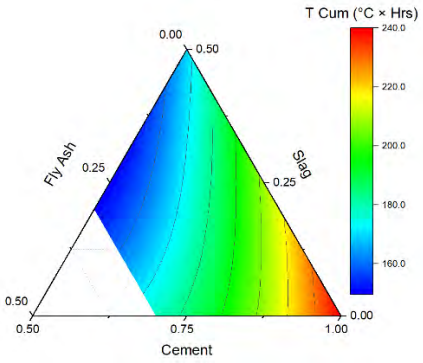

Figure 10. CEM semi-adiabatic calorimeter cumulative heat.

As shown in the figure below the cumulative heat, the area under the peak of “heat of hydration”, from the semi-adiabatic calorimeter shows a very good correlation (R^2 ~ 0.99) to compressive strength, particularly at early age which can enable it to be used as a predictor for strength.

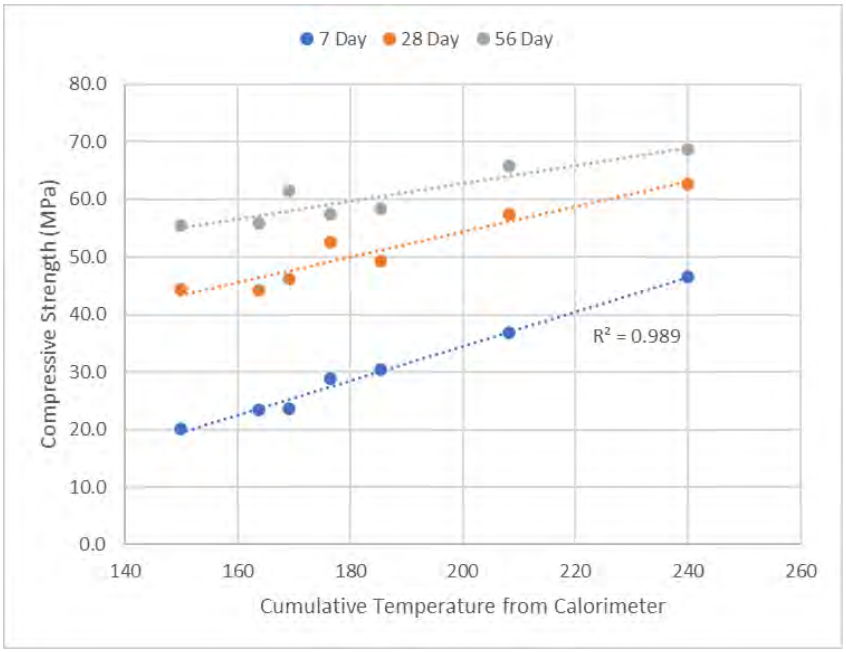

Figure 11. CEM cumulative temperature from semi-adiabatic calorimeter vs compressive strength.

CEM Water Cement Ratio and Chemical Activation of Ternary Blend

The effect of the water cement ratio on strength of a ternary blend containing 50 % OPC, 30 % GGBS and 20 % FA is investigated and shown in Figure 12. It shows that decreasing the water binder ratio has a marked impact on the strength and consequently the *k*-value of the ternary blend below a water binder ratio of ~ 0.5. At a water binder ratio of < 0.4 the 50 % OPC replaced ternary blend CEM exceeds a *k*-value of 1 at 56 days.

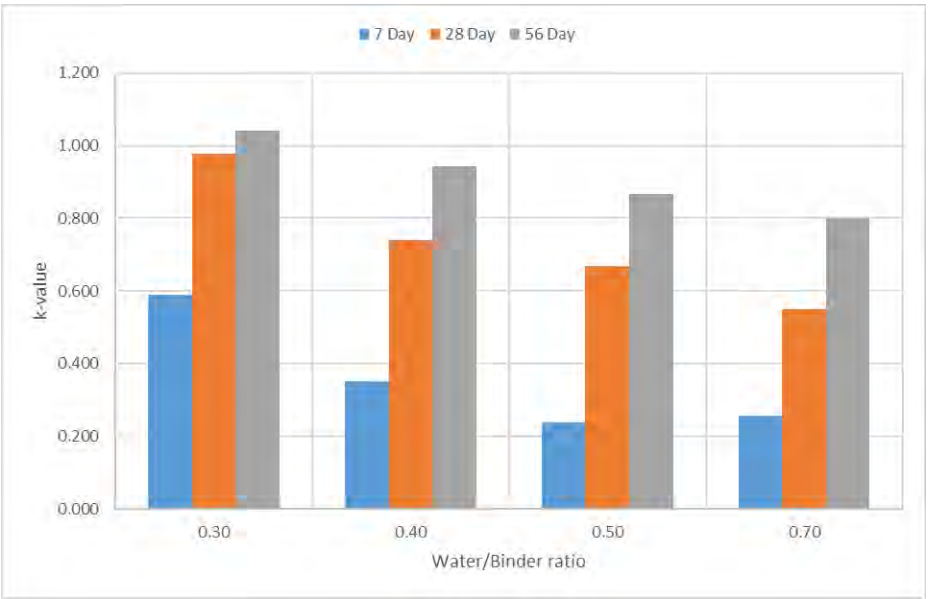

Figure 12. Ternary blend *k*-value (50OPC 30GGBS 20FA)

Figure 13 below shows the *k*-value of the ternary blend at a water/binder ratio of 0.5 with the addition of a chemical activator is more effective than reducing the water/binder ratio from 0.5 to 0.4.

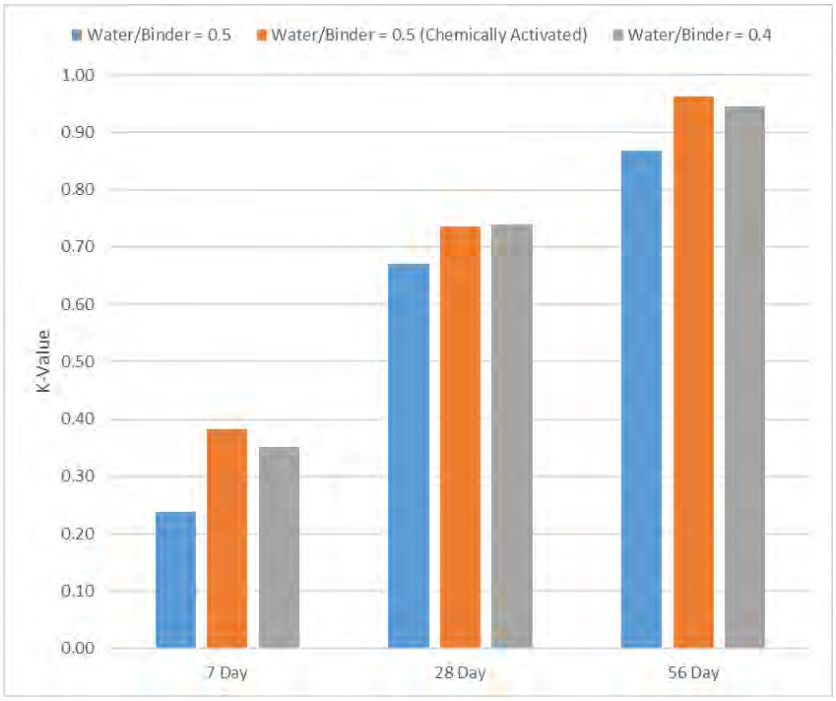

Figure 13. CEM *k*-value with chemical activation.

Chemical activators can act on the cement or SCM (or both) to accelerate its strength and/or set development. Common chemical activators used in concrete are salts of [SINTEF]:

- Chloride
- Nitrate
- Sulphate
- Silicate
- Thiocyanate

CONCLUSION

- Concrete equivalent mortar (CEM) test is an effective means for rapidly screening cement binder systems.
- The addition of SCMs significantly improves the sustainability of concrete.
- Fly ash increases workability whereas GGBS marginally decreases workability.
- Fly ash and GGBS extend set time and lower the heat of hydration.
- Semi-adiabatic calorimetry can be used as a predictor for compressive strength.
- Fly ash has a lower *k*-value than GGBS.
- *K*-value increases with age and lower water/binder ratio.
- *K*-value increases with the use of chemical activators.

REFERENCES

Assaad, J. Harb, J & Chakar, E. Relationship between key ASTM test methods determined on concrete and concrete equivalent mortar. Journal of ASTM International. 2009, 6 pp 1-13.

BS EN 206:2013+A1:2016. Concrete. Specification, performance, production and conformity. British Standards Institute.

Dehuai, W. Zhaoyuan, C. On predicting compressive strengths of mortars with ternary blends of cement, GGBFS and fly ash. Cement and Concrete Research. 1997, 27 pp. 487-493.

Douglas, E. Pouskouleli, G. Prediction of compressive strength of mortars made with Portland cement – blast furnace slag – fly ash blends. Cement and concrete research. 1991, 21 pp. 523-534.

GreenStar Technical Manual V3.2 2017 New Zealand Green Building Council (NZGBC).

Hemalatha, T. Ramaswamy, A. A review on fly ash characteristics Towards promoting high volume utilization in developing sustainable concrete. Journal of Cleaner Production. 2017, 147 pp. 546–559.

Jiao, D. Shi, C. Yuan, Q. An, X. Liu, Y. Mixture design of concrete using simplex centroid design method. Cement and Concrete Composites. 2018, 89 pp. 76-88.

Menendez, G. Bonavetti, V. Irassar, E.F. Strength development of ternary blended cement with limestone filler and blast-furnace slag. Cement and Concrete Composites. 2003, 25 pp. 61-67.

PD CEN/TR 16639:2014 Use of *k*-value concept, equivalent concrete performance concept and equivalent performance of combinations concept. British Standards Institute.

Scheffé, H. Experiments with Mixtures. Journal of the Royal Statistical Society: Series B (Methodological). 1958, 20, pp. 344-360.

Schwartzentruber, A. Catherine, C. Method of the concrete equivalent mortar (CEM) - A new tool to design concrete containing admixture. Materials and Structures. 2000, 33, pp 475-482.

SINTEF COIN P1. Accelerating admixtures for concrete. 2007. Concrete Innovation Centre.

TCC/05/24 Specifying Sustainable Concrete. 2020. The Concrete Centre.

EFFECT OF CURING CONDITION AND WEATHER ON CONCRETE CYLINDER COMPRESSIVE STRENGTH

O SAGGI[1]; N ALMESFER[2]; C BEZETT[3]

[1] National Technical Manager, Allied Concrete Ltd
[2] South Island Plant Engineer, Allied Concrete Ltd
[3] National Systems Manager, Allied Concrete Ltd

SUMMARY

To ensure concrete strength is reliably assessed, accurate sampling and testing are required. Concrete strength depends substantially on the curing conditions. There has been an increased number of specifications where design engineers or specifiers have requested concrete test specimens to be sampled and cured on site. They would like it to attain the specified strength required in the structural design based on the actual “site cured” conditions that the structure experiences. However, the strength result for the site cured specimens does not represent the actual strength of the structure due to the difference in heat of hydration between site cured specimens and the actual structure.

Concrete test specimens cured on site are typically lower in strength and more variable compared to specimens cured to the standard lab curing conditions specified in NZS 3112.2. This lower and more variable strength is due to various factors such as improper curing, disturbance during initial set, specimens exposed to sunlight or cold weather, and no protection for specimens from loss or gain of moisture. Also, the primary cause for this discrepancy relates to the permitted temperature range that samples are initially stored at. NZS 3112.2 (1986) Clause 3.5 stipulates laboratory curing shall be in the temperature range of 21 ± 2 degrees, whereas site cured specimens need to be maintained in a much wider band, 10 to 26 degrees, for up to 80 hours. This introduces significant variance in strength development, which is corroborated by inconsistencies and variances in test results which means a significantly increased coefficient of variation for site cured specimens.

An experimental programme was initiated to investigate the effect of weather and curing condition on concrete strength along with the effect of aggregate temperature on concrete properties. This paper utilizes several trial and production mix data to explore the effect on strength of 30MPa & 40MPa grade concrete at 3, 7 & 28 days and effect of aggregate temperature on fresh properties of concrete at different ambient temperatures. The data concludes with some certainty that tests taken on site are consistently underperforming with respect to samples taken at the plant and cured under lab conditions as stated in NZS 3112.2.

INTRODUCTION

Concrete is obviously a popular construction material, being the most widely used building material on earth, partially due to its excellent mechanical and durability properties, relative affordability, and availability. It is fundamental that out of the thousands of concrete mixes produced around New Zealand, properties are measured and controlled, and importantly are understood by all stakeholders including the producer, contractor, and engineer/designer/specifier. It is also important for all stakeholders to have the best possible understanding of how concrete behaves and gains strength, what factors affect strength, how strength is measured, and how to interpret the data from different methods of testing concrete strength, or basically, what the results from strength testing are telling us or not telling us. This is because on most job sites, the strength of the concrete poured is a critical piece of information. There are various methods of determining concrete strength, and some methods may be more cost effective and arguably better in some way, but the concrete cylinder remains the standard for acceptance and has been a pillar for compression strength testing in the construction industry. Strength testing using cylinders is only an indicator of structural performance, as there are several factors which affect in situ concrete strength, but at least the number that comes out of the cylinder test is a measure of quality, potential strength, a way of ascertaining compliance with the specification, and can sort out contractual obligations. Also, many properties of concrete are related to compressive strength (Neville and Brooks 2010).

Ready-mixed concrete companies typically undertake two main types of testing, one related to quality control and the other related to quality assurance. Quality control is mostly done randomly across production at the concrete plant to provide evidence of production control and performance of individual concrete mixes as per NZS 3104:2021 Clause 2.15.8.1. Quality assurance testing can be done where tests are requested for specific concrete mixes going to projects, with testing being done at the plant or on-site, commonly referred to as testing requested by the customer. There is a lot dependent on the correct acceptance of concrete and interpretation of compressive strength results, with potentially significant costs in time and cash if there are discrepancies, especially with regards to testing requested by the customer to be undertaken on site. For example, one of the complications faced by producers is when the engineer or purchaser argues that the concrete must be accepted based on site-cured test cylinders, without realising that strength depends on curing conditions and that the producer has no control over the curing conditions of concrete on site. Another complication faced is when there is considerable difference in results between cylinders made at the plant compared to cylinders made on site. Hence, the intention of the information reported herein is to provide basic information on some factors (irrespective of the concrete mix design) which affect concrete compressive strength and show what the effect of different curing conditions have on concrete cylinder compressive strength. Curing conditions refers to conditions used to promote hydration of cement and relate to control of temperature and moisture.

The content of this paper is nothing new, and hence it serves as a reminder to the industry. As you read this paper, it is recommended to keep in mind that the underlying parameter which concrete strength depends on is the number and size of pores in the hardened cement paste.

SOME FACTORS WHICH AFFECT CONCRETE COMPRESSIVE STRENGTH

Temperature

The effect of concrete curing temperature on concrete compressive strength is shown in Figure 1. A higher casting and curing temperature than normal results in more rapid hydration of cement, higher early age strength, but lower long term strength of hardened concrete, and vice-versa for a lower casting and curing temperature than normal. At higher concrete temperatures there is a less uniform distribution of cement gel established with a poorer

physical structure which is also more porous than the structure formed at normal temperatures. At higher temperatures there is insufficient time available for the cement hydration products to diffuse away from the cement particles to allow a uniform precipitation in the interstitial space, and as a result, a concentration of cement hydration products is built up within immediate proximity of the hydrating cement particles, limiting subsequent cement hydration and strength development (CCANZ 2010; Neville & Brooks 2010). With low initial temperatures, there is a more uniform distribution of cement gel and microstructure to account for the higher long term strength.

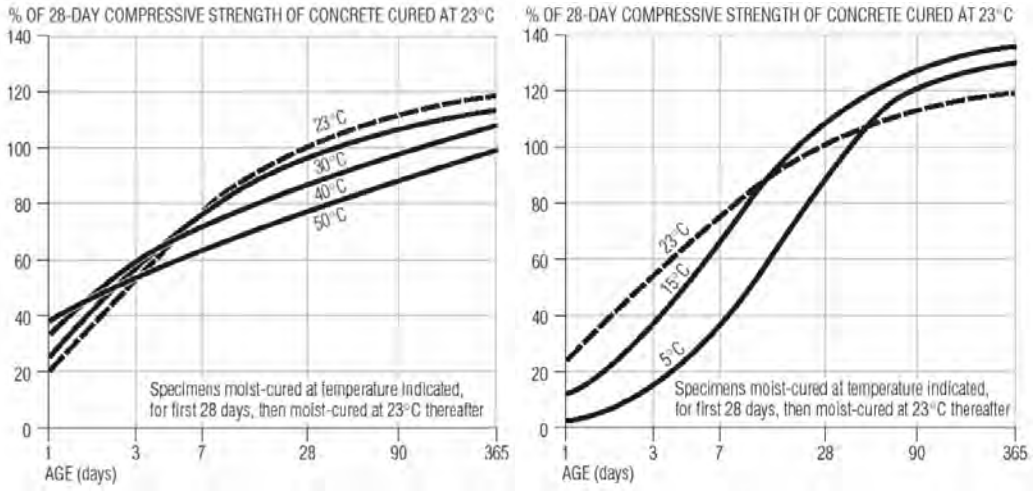

Figure 1. Effect of curing temperature during the first 28 days on concrete compressive strength (CCANZ, 2010)

Keep in mind that the curing temperature is far more important to achieve long term strength than the initial casting/placement temperature, as supported by Figure 2. Adequate temperature levels are needed for sufficient time for cement hydration to proceed unhindered, especially for thin concrete elements.

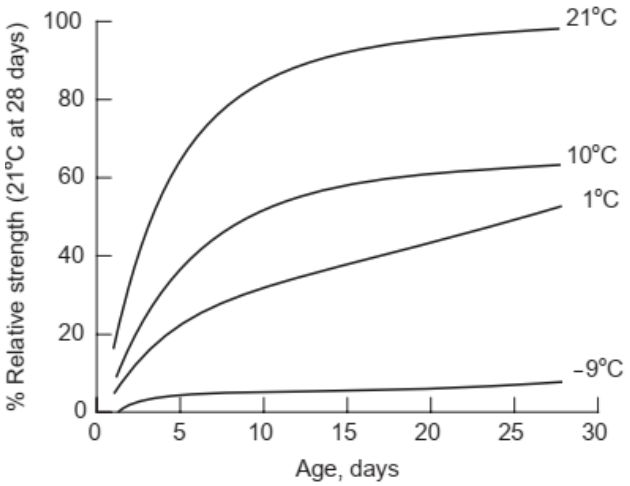

Figure 2. Influence of curing temperature on concrete strength - specimens were cast and maintained at 21ºC for 6 hours, then cured at indicated temperature (Mehta & Monteiro, 2006)

Moisture

The hydration of cement can only occur in the presence of moisture, hence why it is important to prevent loss of water by evaporation from the capillaries of the paste. The reaction between cement and water is time dependent, and hence moisture needs to be present for sufficient time to allow full strength to develop. The compounds which contribute most to the strength of the hardened cement paste and hence strength of the concrete react relatively slowly, and hence they require the paste to be kept moist until the concrete gains its strength. If the paste were allowed to dry out, the effects of rewetting the paste on subsequent strength may be permanently impaired or reduced (CCANZ, 2010). Obviously in practice it is important for curing to commence as early as possible due to effects on shrinkage and cracking. Generally, the longer the moist curing period, the higher the strength, as shown in Figure 3.

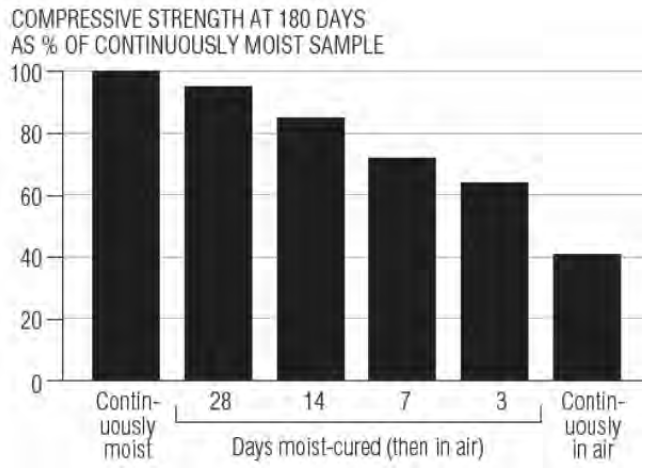

Figure 3. Effect of moist curing on compressive strength (CCANZ, 2010)

EXPERIMENTAL PROGRAM

The purpose of tests reported herein is to get a better understanding of the effect of curing condition on compressive strength development of standard 30MPa and 40MPa concrete mixes. Concrete was representatively sampled from trucks at the Allied Concrete Ltd production plant at Penrose, Auckland, as per NZS 3112:1 Section 3. Immediately after sampling, the fresh concrete was tested for slump, air content, temperature, after which the required number of standard 100 mm diameter by 200 mm height cylinders were cast as per NZS 3112.2 Section 3. The curing methods used in the study are summarised as follows:

Method 1: As per NZS 3112.2 Clause 3.5.1, concrete cylinders were cast and stored undisturbed overnight in the laboratory at 19-23^{o}C. After approximately 16 to 24 hours, cylinders demoulded and cured in a saturated condition at a temperature of 19-23^{o}C until testing for compressive strength in a saturated surface dry condition. This method is referred to as PP (plant made and plant cured) later in this paper.

Method 2: Concrete cylinders were cast and stored overnight outside the laboratory at ambient temperature ranging from 11-25^{o}C. After approximately 16 to 24 hours, cylinders demoulded and cured in a saturated condition at a temperature of 19-23^{o}C until testing for compressive strength in a saturated surface dry condition. This method is referred to as SP (site made and plant cured) later in this paper.

Method 3: Concrete cylinders were cast and stored overnight outside the laboratory at ambient temperature 11-25°C. After approximately 16 to 24 hours, cylinders demoulded and cured outside the laboratory in air at ambient temperature until testing for compressive strength in the air-dry condition. This method is referred to as SS (site made and site cured) later in this paper.

Method 4: Concrete cylinders were cast and stored overnight outside the laboratory at ambient temperature 11-25°C. After approximately 16 to 24 hours, cylinders demoulded and cured outside the laboratory while wrapped in a sealed plastic bag at ambient temperature until testing for compressive strength in the air-dry condition. This method is referred to as SS(W) (site made and site cured (wrapped)) later in this paper.

Note that as per NZS 3112.2 Section 3, if cylinders are to be stored on site, they need to be suitably protected such that the specimens remain at a temperature between 10-26°C, however based on the authors experience this is rarely done on site. Therefore, curing Methods 2 (SP), 3 (SS), and 4 (SS(W)) stated earlier are more resemblant of what essentially happens on site regarding curing. For each curing method, five trucks were sampled for testing. Cylinders were tested at 3, 7, and 28 days.

In the lower South Island, with freezing temperatures, the effect of aggregate temperature on concrete compressive strength is generally forgotten or not emphasised enough. Hence, supplementary modelling has been conducted to get a better understanding on what the effect of aggregate temperature would be on early age concrete compressive strength.

RESULTS

The average test results for compressive strength of concrete cured according to the different conditions mentioned earlier for various ages are shown in Figure 4 for the 30 MPa concrete mixes, and Figure 5 for the 40 MPa concrete mixes. The results are the average of the five trucks sampled and tested for each curing method. For all the curing methods, the compressive strength of concrete increased with age. There was no clear difference in compressive strength of PP cylinders and SP cylinders, although the lowest compressive strength was clearly attributed to the SS cylinders. For the 30 MPa concrete, PP and SP cylinders were approximately 37%, 30%, and 36% greater than SS cylinders at 3, 7, and 28 days respectively. For the 40 MPa concrete, PP and SP cylinders were approximately 25%, 21%, and 26% greater than SS cylinders at 3, 7, and 28 days respectively. This is due to the reduced porosity and improved pore structure in the PP and SP cylinders resulting from a greater degree of cement hydration. The effects of curing the cylinders outside the laboratory until testing are considerable at all ages of testing. These results should make the reader appreciate the effects of leaving concrete cylinders outside air curing until testing (SS), even with the moderate ambient temperatures experienced with the SS cylinders in this study. For 30 MPa concrete, cylinders wrapped and sealed (SS(W)) have similar 3 day and 7 day strengths to the PP and SP cylinders, but unfortunately at 28 days the strengths are considerably lower. For 40 MPa concrete, the SS(W) cylinders have considerably lower strengths from 7 days onwards when compared to the PP and SP cylinders. Although cylinders on site are better being sealed to help retain moisture, the effects of a much wider band of temperature experienced on site reduced the strengths after 3 days.

An important point to note is that the results of compressive strength are significantly affected by parameters involving the test specimen. Site made cylinders are not only negatively affected by not having sufficient temperature and moisture for cement hydration, but based on the authors experience, site made cylinders by contractors have various discrepancies, such as wrong procedures of casting cylinders due to inadequate training and experience, incomplete compaction, inadequate squareness, flatness, effect of disturbance/vibration on site, and other

defects due to cylinders not being stored properly during transportation from site to lab. These factors need to be considered when assessing the viability of site made cylinders. NZS 3104:2021 Clause C2.15.8.1 addresses the aforementioned point.

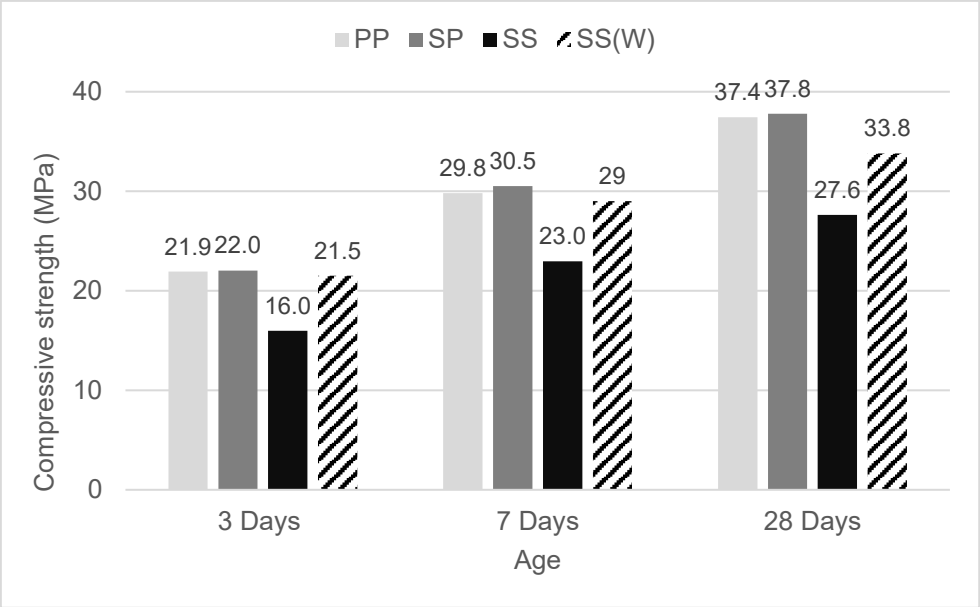

Figure 4. Effect of curing conditions on compressive strength of 30 MPa concrete

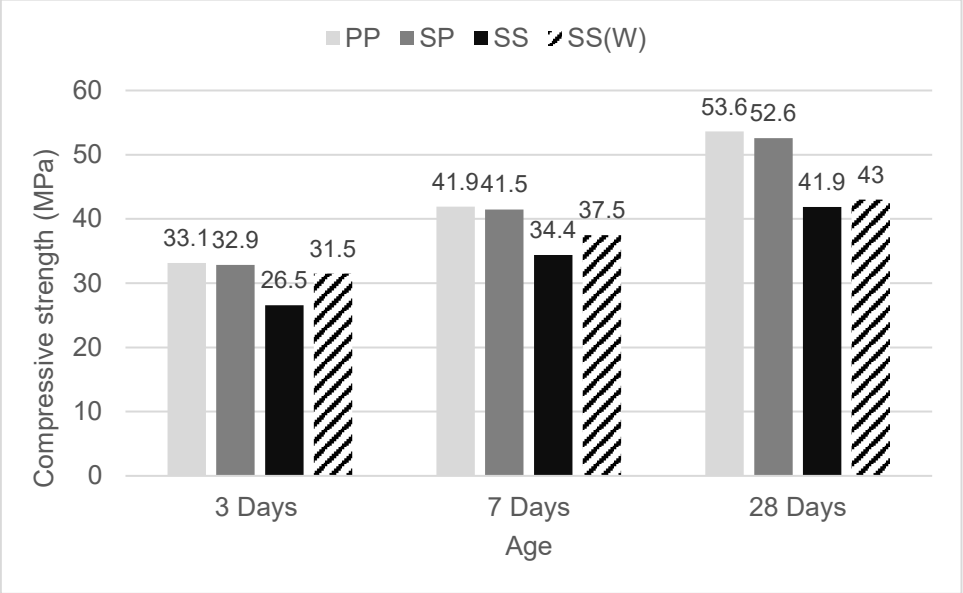

Figure 5. Effect of curing conditions on compressive strength of 40 MPa concrete

Figure 6 is related to a project in the South Island which Allied Concrete supplied concrete to, and cast concrete cylinders at the plant for testing, the same as Method 1 (PP), whilst the contractor cast cylinders on site and transported to the plant after demoulding, like Method 2 (SP). Although in Figure 4 and Figure 5 the PP and SP cylinder strengths were similar, Figure 6 shows that SP cylinders were up to 10% lower in compressive strength compared to PP cylinders, and gradually getting lower during the duration of the project. A couple of important observations here which were not present during the lab trials conducted. As mentioned earlier, it is not surprising for site made cylinders by contractors to have defects, usually due to inadequate training and experience, and during the project, unfortunately it seems as though there was less care about the quality of the specimens during casting and transportation,

leading to a greater difference in strength between the PP and SP cylinders. Another factor to consider on construction sites is the effect of disturbance and vibration on cylinders stored with fresh/green concrete.

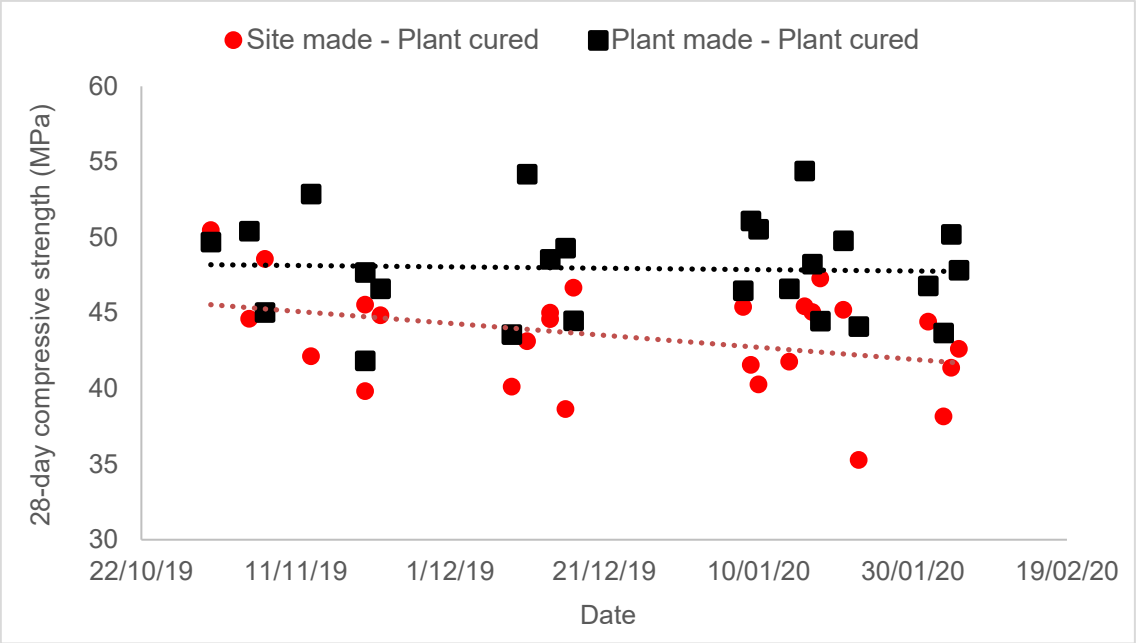

Figure 6. 28-day compressive strength comparison on same truck between site made plant cured (SP) and plant made plant cured (PP) cylinders

The SP and PP cylinder results of another project in the North Island which Allied Concrete Ltd supplied concrete to, and cast concrete cylinders at the plant for testing, the same as Method 1 (PP), and cast cylinders on site, like Method 2 (SP). As shown in Figure 7, the SP cylinders on average were lower in compressive strength compared to PP cylinders, in this project also by 10%. It was believed that the differences relate to the temperature range that samples were initially stored at.

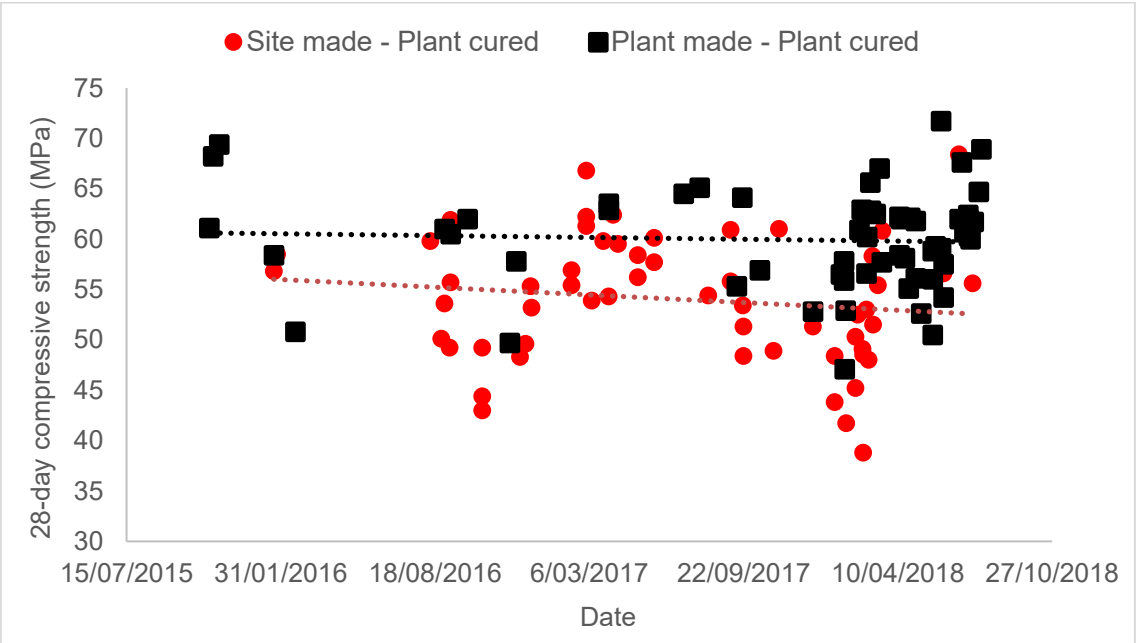

Figure 7. 28-day compressive strength comparison between site made plant cured (SP) and plant made plant cured (PP) cylinders

Given that it is the concrete temperature which cement hydration and hence strength development depends on, one needs to appreciate what the effect of the temperature of different concrete components has on the concrete temperature. The three main concrete components are water, cement, and aggregate. Each mass of water has roughly five times as many available heat units in it compared to each mass of aggregate, however due to the significantly larger proportion of aggregate in a mix compared to water, the effect of aggregate temperature on concrete temperature is greater than that of water temperature. For a standard 30 MPa concrete mix with 160 L/m3 water, 300 kg/m3 cement, and 1900 kg/m3 aggregate, to achieve a 1°C change in concrete temperature, water temperature would have to change by 4.1°C, or cement temperature would have to change by 9.7°C, or aggregate temperature would only have to change by 1.5°C. To appreciate the effect of weather and hence aggregate temperature on overnight concrete compressive strength, once can correlate the aggregate temperature to concrete temperature and then overnight compressive strength. An example of this is shown in Figure 8, which indicates the significant effect aggregate temperature will have on early age concrete strength.

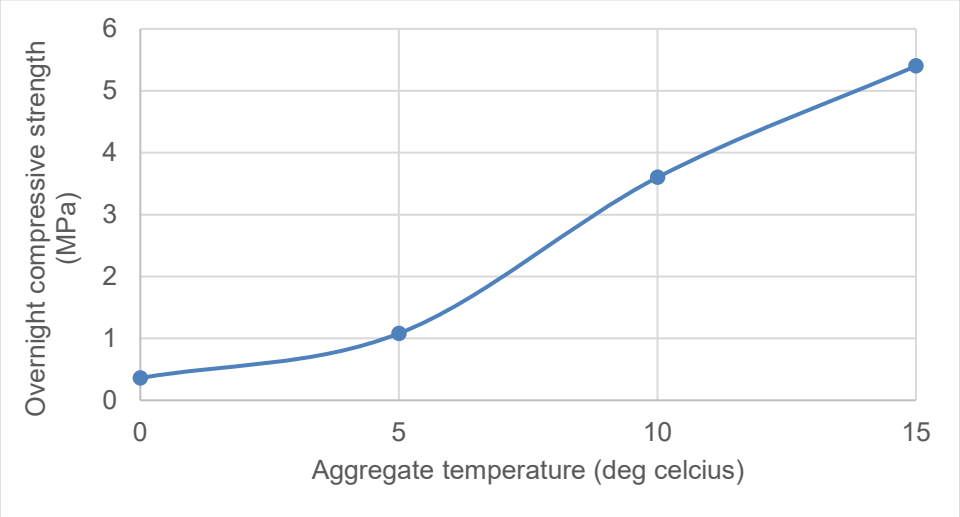

Figure 8. Overnight compressive strength for 30 Mpa concrete depending on aggregate temperature – if water remains at 5°C and cement remains at 10°C

CONCLUSIONS

This paper sought to provide basic but important information on some factors which affect concrete compressive strength and show what the effect of different curing conditions is on concrete cylinder compressive strength, by utilizing several trial and production mix data. It is important that this information is understood by all stakeholders including the producer, contractor, and engineer/designer/specifier, so that results are understood and interpreted correctly.

It was shown that excessive early loss of moisture with cylinders left on site air curing leads to significantly reduced strength, hence why tests taken on site and left on site until testing consistently underperform when compared to cylinders taken at the plant and cured in saturated condition until testing. Cylinder left on site until testing show improved strength if they are wrapped in a sealed plastic bag, however strengths are still below that of cylinders cured at the plant in saturated condition and controlled temperatures, especially at 28 days.

Projects were given as examples to show effects of curing condition on cylinder compressive strength. Two projects which Allied Concrete supplied concrete to showed that cylinders made

on site and left overnight before being returned to the lab the next day after demoulding for curing are approximately 10% lower in strength than concrete cylinders cast and stored undisturbed overnight and cured in the laboratory as per NZS 3112.2 Clause 3.5.1.

It is hoped that the supplementary data on aggregate temperature and early age compressive strength, along with all the aforementioned literature on curing temperature effects on compressive strength are taken into account to further appreciate how weather affects concrete compressive strength.

More data on different mixes including lower strength and higher strength concrete at the different curing conditions would be useful. Also, exposing the SP and SS cylinders to different temperatures would further increase understanding of temperature on cylinder compressive strength. If SS (site made and site cured) cylinders are being requested to estimate the strength of the in situ concrete, it is recommended that the maturity of the concrete is taken into account, which is a summation of the product of temperature and time during which it prevails, with wireless sensors available for measuring concrete temperature and maturity.

REFERENCES

CCANZ. (2010). *The New Zealand Guide to Concrete Construction.* Cement and ConcreteAssociation of New Zealand.

Mehta, P. K., & Monteiro, P. J. (2006). *Concrete - Microstructure, Properties, and Materials.* McGraw-Hill.

Neville, A. M., & Brooks, J. J. (2010). *Concrete Technology.* Essex, England: Pearson.

THE REVISED NZS 3104 SPECIFICATION FOR CONCRETE PRODUCTION AND THE CONCRETE NZ PLANT AUDIT SCHEME

JAMES MACKECHNIE, ROB GAIMSTER, ADAM LEACH, DAVE MCGUIGAN

Concrete NZ

SUMMARY

This paper looks at two the recent revision of NZS 3104 – Specification for concrete production and the New Zealand Plant Audit Scheme (NZPAS). The revised concrete production standard was published in April 2021 and includes several changes to improve sustainability, encourage excellent quality control and mandated several important practices that were previously only voluntary. Key changes that are reviewed in this paper include daily moisture content of fine aggregates, increased frequency of yield testing, 7-day testing, encouragements for plants showing excellent production control, longer-term strength testing at 56 days when using SCM concrete and several simplifications of analysis and reporting. The Plant Audit Scheme has been a pillar of the New Zealand concrete industry since the 1960s providing the building industry with confidence that concrete is reliably produced in accordance with relevant Standards by participating batching plants. In recent years, the former New Zealand Ready Mixed Concrete Association (NZRMCA) Plant Audit Scheme has transitioned to become the Concrete NZ Plant Audit Scheme. With this transition there has been a need to ensure that industry is aware of the Plant Audit Scheme and the benefits it brings. This paper also explains how NZS 3104 and NZPAS are connected and the mechanisms of audit certificate of concrete batching plants.

REVISION OF NZS 3104 – SPECIFICATION FOR CONCRETE PRODUCTION

NZS 3104 was revised in April 2021 and superseded the previous 2003 version. Concrete NZ funded the review and performed the project management required for the revision process, to complement Standards NZ roles of facilitating the consultation and publication process. A key driver to revise this Standard was to address sustainability and provide increased incentives for concrete batching plants that demonstrate rigorous production control.

NZS 3104 prescribes the minimum requirements for the production of fresh concrete. Compliance with NZS 3104 ensures compliance with the requirements for the supply of fresh concrete given in NZS 3109, which in turn meets the materials requirements of the Concrete structures standard NZS 3101 and therefore provides a means of demonstrating compliance with the New Zealand Building Code.

The committee consisted of representatives from the following organisations:

- Building Research Association of New Zealand (BRANZ)
- Concrete NZ
- Concrete NZ – Learned Society
- Concrete NZ – Precast Sector group

- Concrete NZ – Readymix Sector Group
- Engineering NZ
- Structural Engineering Society of New Zealand (SESOC)

Overview of NZS 3104:2021 Specification for concrete production

The fundamental structure of the document remains unchanged from the previous version. The key sections of the Standard are as follows:

1. General – covering scope, interpretation, definitions, abbreviations.
2. Provisions for ready mixed concrete – sets out the requirements for the production of ready mixed concrete at batching plants. The requirements of this section cover:
    a. Personnel – the requirements and responsibilities of the Plant Engineer and Plant Supervisor.
    b. Material requirements.
    c. Batching plant requirements including storage, measuring and weighing
    d. Concrete mixing and transportation.
    e. Responsibility for mix design for normal concrete and special concrete (any concrete defined with performance criteria other than strength, such as shrinkage, tensile strength; or strength greater than 50MPa, is considered 'special concrete').
    f. Variability control.
    g. Control tests of concrete such as – slump, yield, air content, and cylinder strength tests.
    h. Quality audits – setting out requirements that a batching plant can demonstrate compliance with NZS 3104 by holding a current Certificate of Audit.
3. Provisions for prescribed mix concrete – provides material proportions for concrete mixes for concrete strength ranging from 10MPa to 25MPa.
4. Concrete Mixers – sets out the requirements for the performance of concrete mixers covering stationary, truck mixers and continuous mixers.

PRINCIPAL CHANGES IN NZS 3104:2021

Several important changes were made to NZS 3104 to improve sustainability, quality control and testing efficiencies. The relevance and impact of these changes is discussed in this paper.

Daily moisture content measurement of fine aggregates

Control of moisture content of fine aggregate is key to improving quality control since fluctuations cause variations in strength and directly affects the yield of concrete. While moisture contents of fine aggregate can be inferred from the amount of water used when batching concrete mixes, this approach can be misleading since water demand is also affected by environmental effects, cement fluctuations, sand grading variations and contaminants such as silt and clays.

Improved moisture control and measurement of fine aggregate is critical for being able to predict the strength of each batch of concrete produced. This is important since testing is not done on every batch of concrete but typically occurs on every 10-50 loads depending on annual production levels.

Increased frequency of yield testing

Yield testing of fresh concrete is routinely undertaken to ensure that batching produces the correct volume during production. Previously the required yield testing frequency was set at one test per week regardless of the production level at the concrete plant. The latest revision to NZS 3104 has increased the frequency of yield testing since not only can this be used to check the volume supplied but significant changes can infer cement under- or over-weighs. This is illustrated in Figure 1 where changes in yield may be related to expected 28-day compressive strength of concrete.

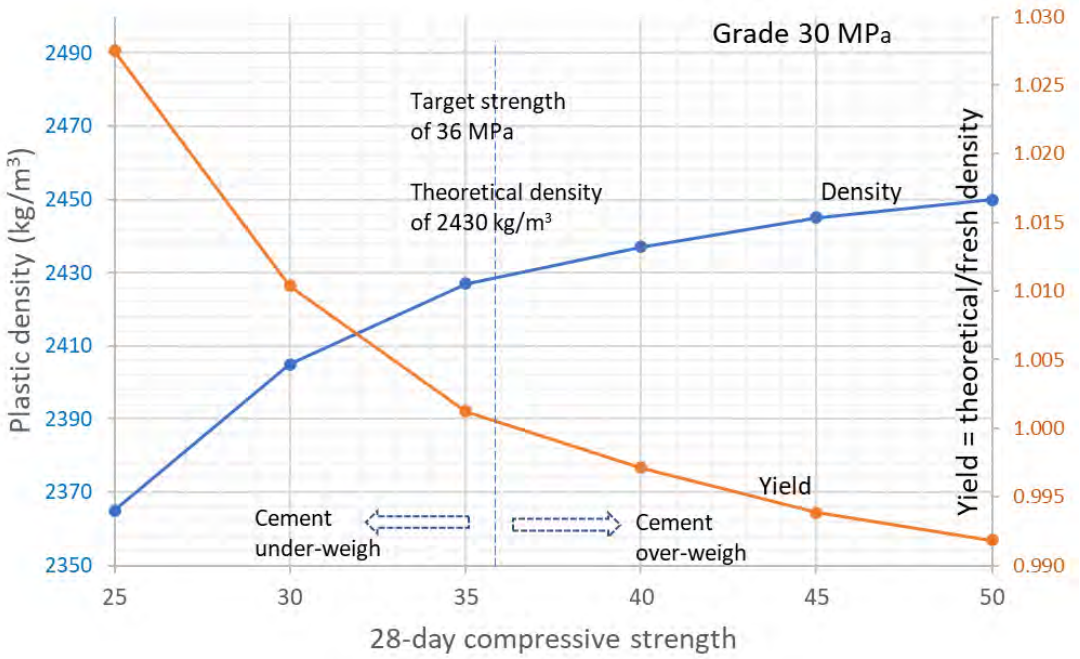

Figure 1: Effect of cement weigh up tolerances on strength and yield

Mandatory 7-day strength testing

NZS 3104:2003 did not mention 7-day strength testing of concrete, which was left to the discretion of the supplier or specifier. More recently in 2016 it became mandatory to report 7-day strengths for concrete plants under the NZ Plant Audit Scheme. When NZS 3104 was revised in 2021, 7-day strength testing became mandatory for all plants who require audit certification. Figure 2 shows how 7-day strength are used to predict 28-day strength and how lack of performance can trigger further action. Using this early warning system has been able to pick up structural issues in a timely manner.

Figure 2: Using 7-day strength to predict 28-day strength of concrete

Excellent production control incentives

Concrete plants that invest in more rigorous production control are able to use lower target mean strengths (TMS) that ultimately reduce cementitious content of selected concrete mixes. These savings are not just economic but may result in lower embodied carbon dioxide and improve the sustainability of concrete. This only applies to major series of more than 30 tests per annum and with demonstrated low variability in strength results. A detailed statistical analysis of test results from different sized plants showed that strengths tended to be well above TMS and adopting the new table would allow plant engineers to trim cement in larger concrete mixes showing excellent control. The standards committee also investigate the approach used internationally in setting target strengths and findings showed the methodology produced in NZ is sufficiently conservative (e.g. failures below 5%).

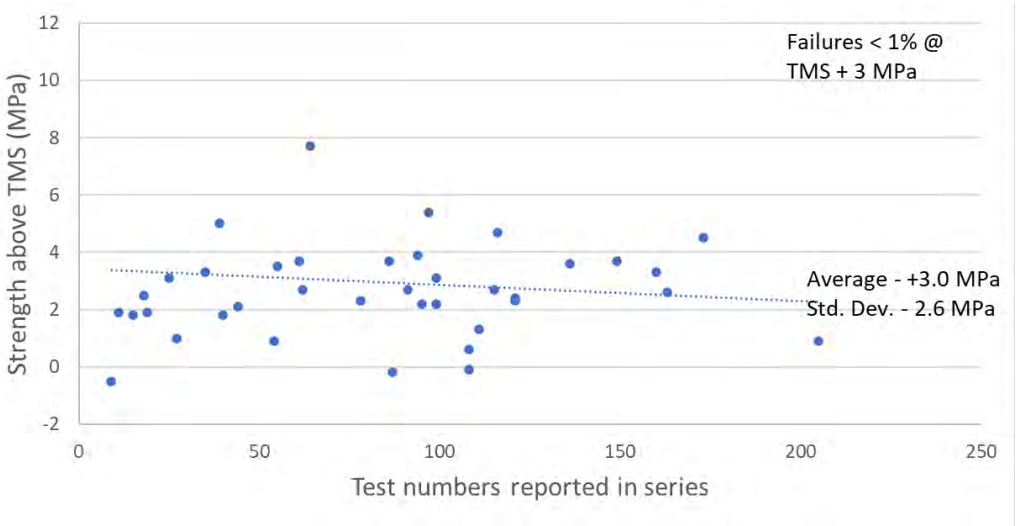

Figure 3: Strength above target for different plants across New Zealand (2019 survey)

Longer-term strength testing of SCM concrete

With the increased use of SCM in concrete, provisions need to be made for the longer strength development of these materials. Recommendation are made to use 56-day testing rather than 28-day of strength for SCM concrete. The slower and longer strength development of these concrete mixes is shown in Figure 4, which compares strength development of concrete with different binder systems.

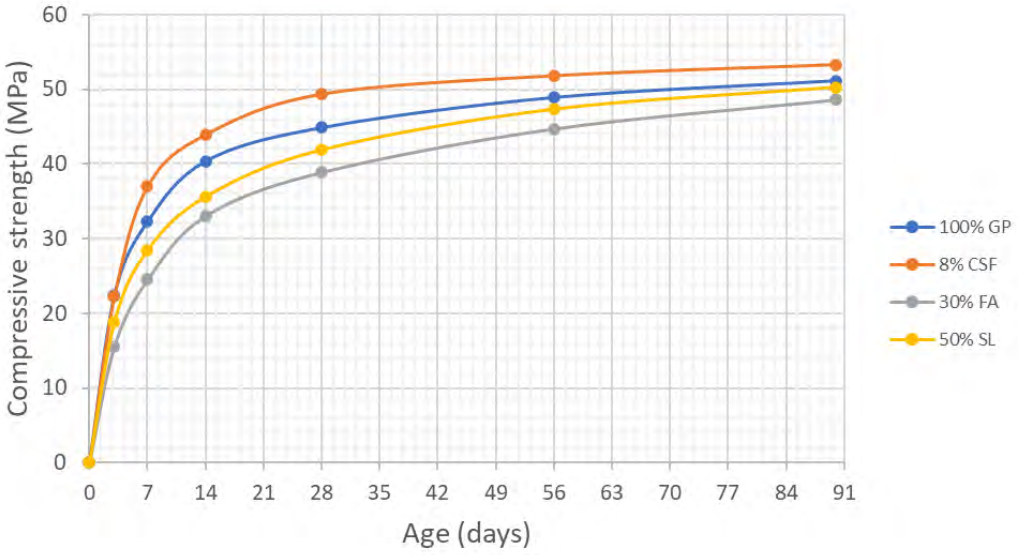

Figure 4: Strength development of GP versus SCM concrete (wet cured at 21 ^{0}C)

THE CONCRETE NZ PLANT AUDIT SCHEME

The Concrete NZ Plant Audit Scheme, formerly the New Zealand Ready Mixed Concrete Association (NZRMCA) Plant Audit Scheme, has existed for nearly 60 years – the protocols for a concrete quality control scheme, which included a monitoring requirement to see if plants were adhering to the Scheme, were developed in May 1963 (Barnard, 2013). With the consolidation of the New Zealand concrete industry associations in 2017 the former NZRMCA Plant Audit Scheme transitioned to become the Concrete NZ Plant Audit Scheme.

The Plant Audit Scheme provides an independent and rigorous audit of the quality systems in place at a ready mixed concrete plant which in turn provide suppliers, designers and clients confidence that participating audited plants, that hold a Certificate of Audit, are reliably supplying concrete in accordance with the requirements of NZS 3104.

There are currently almost 200 audited batching plants across New Zealand. The location of the current audited plants can be found at https://rmcplantaudit.org.nz/audited-plants/

Plant Audit Scheme requirements and operations

Further to complying with NZS 3104 Specification for concrete production each batching plant must have:

- a Plant Engineer who is either a Chartered Professional Engineer (CPEng), a Chartered Member of Engineering New Zealand (CMEngNZ) or a Registered Engineering Associate (REA),
- an appropriately qualified employee who carries out concrete testing; and
- properly maintained records of concrete productions and testing.

Experienced and qualified auditing engineers, appointed by the Plant Audit Committee, perform the audits of the participating plants (refer to Figure 5 below).

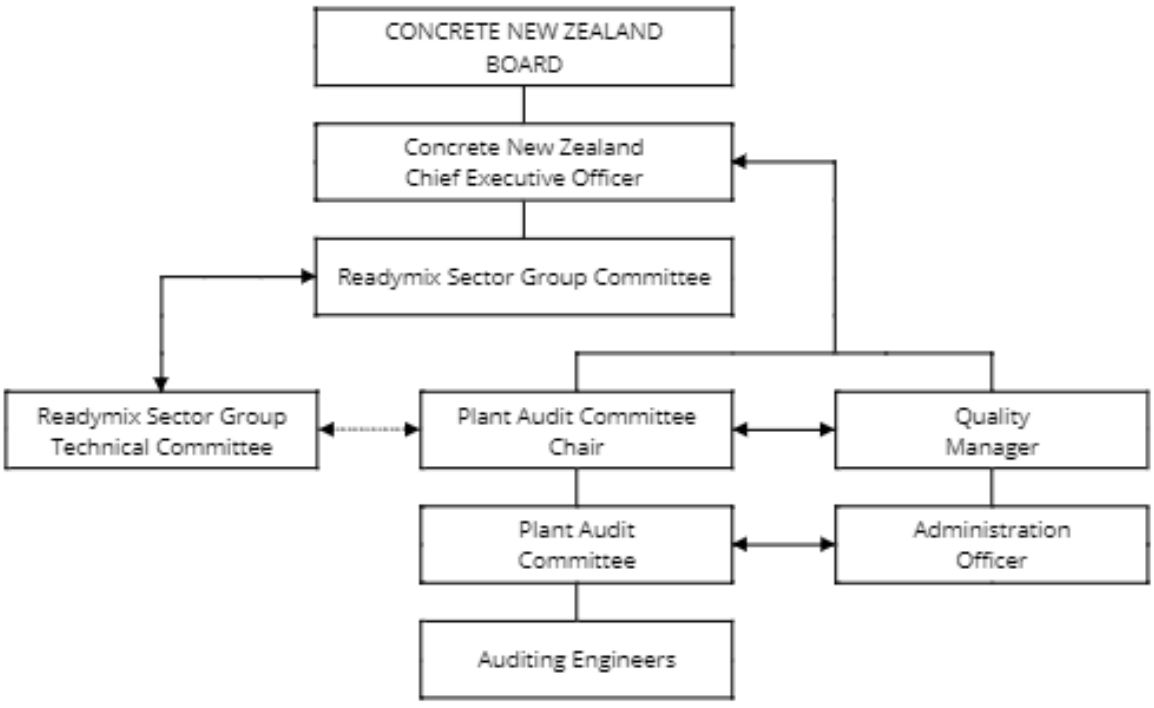

Figure 5: Organisational structure of the Plant Audit Scheme

The Plant Audit Committee is comprised of Professional Engineers and Registered Engineering Associates who have extensive experience in the concrete production industry. The Committee has two externally appointed members. One member is appointed by Engineering NZ and the other by the Concrete NZ Learned Society. The current chair of the Plant Audit Committee is James Mackechnie.

The auditing engineers review the submitted test records and undertake site visits of the batching plants on a two-year cycle (refer to Figure 6. Operation of the Plant Audit Scheme). For the purposes of operating the Plant Audit Scheme New Zealand is divided into four zones.

All batching plants participating in the scheme report their performance and testing data to the Committee annually. Among the performance criteria audited and reported on are:

- Mean concrete strengths and coefficients of variation
- Aggregate quality by testing and monitoring
- Weigh scale calibration and accuracy
- Mixer efficiency tests
- Laboratory equipment calibration
- Production and testing record keeping
- Technician training
- Plant operator performance
- Effectiveness of plant engineer's monitoring of quality controls

In addition to the above criteria, the frequency of testing within each quarter year must be submitted to the Plant Audit Committee. Failure to maintain testing requirements can result in the withdrawal of an Audit Certificate.

All participating batching plants will also have an on-site audit every second year to verify that the information reported regularly by the Plant Engineer accurately represents the performance of the plant. It provides an opportunity to check that personnel, equipment and systems at a batching plant are meeting the requirements of NZS 3104. Random site audits may also be carried out without warning at any time.

The Plant Audit Committee meet quarterly to assess the audit reports for a specific zone. They will then determine if the plants are acceptable for issuing a Certificate of Audits or if they need to respond to identified non-conformances prior to the issue of a Certificate of Audit (refer to Figure 7. Example Concrete NZ Certificate of Audit Compliance). The Certificate includes the maximum MPa (up to 50 MPa) that a batching plant can supply. A Certificate of Audit is typically issued for a 12-month duration in which time it must be revalidated. An interim certificate of audit, valid for 3 months may also be issued to allow a plant to rectify minor deficiencies.

Any new batching plants assessed for the first time, after receipt of a plant report, will be subject to a site inspection of the plant. If the plant meets the requirements of the Plant Audit Scheme, an interim Certificate of Audit will be issued with a three-month duration. In this three-month period the batching plant will be reassessed and if it continues to meet the requirements it will be issued a Certificate of Audit with a maximum twelve-month duration.

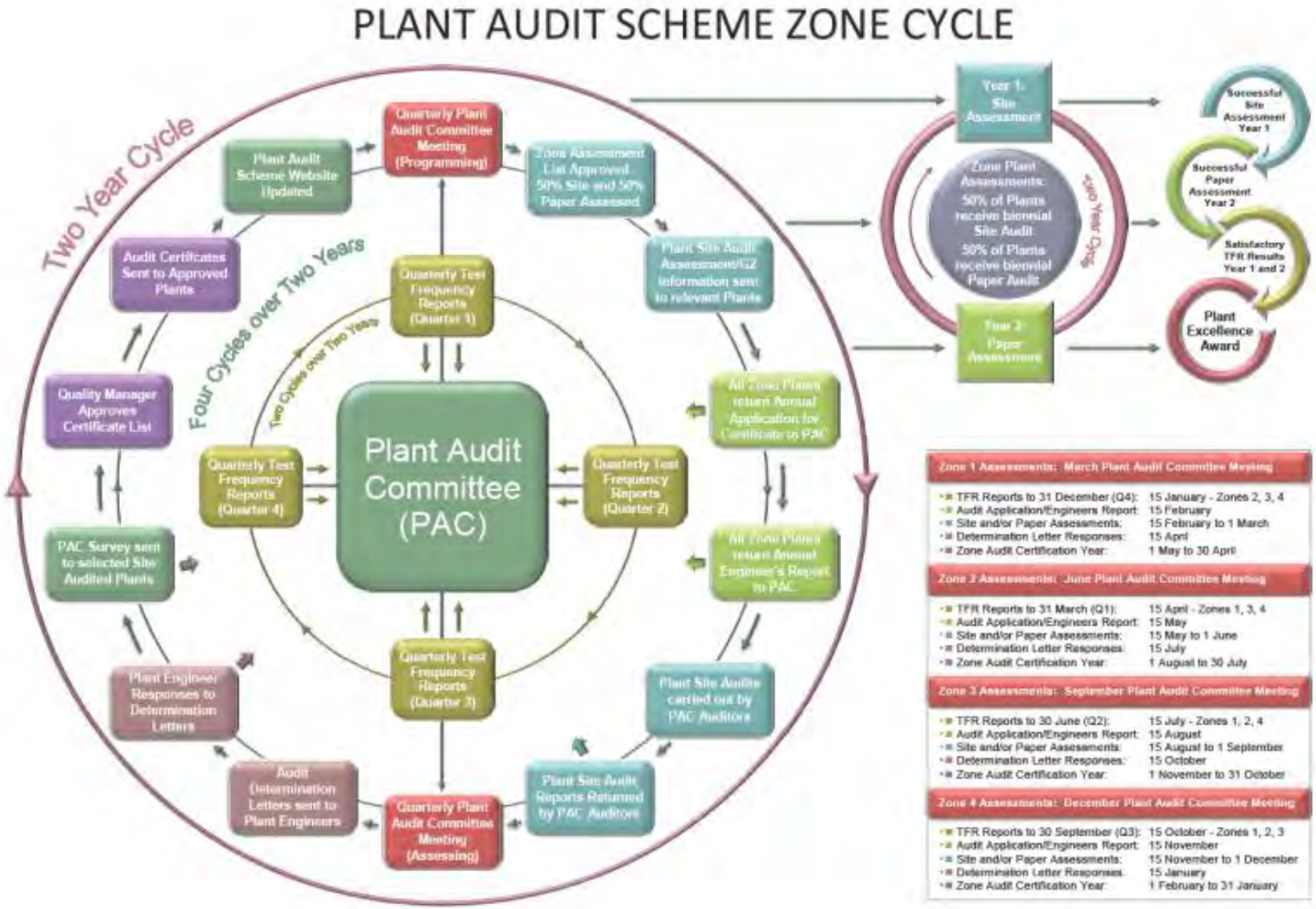

Figure 6: Operation of the Plant Audit Scheme

concretenz
BUILDING RESILIENCE
AUDITED PLANT
Quality Assured NZS 3104

CERTIFICATE OF COMPLIANCE

COMPANY McGregor Concrete Limited

PLANT LOCATION Te Anau

This is to certify that the above ready mixed concrete plant has been audited as having a production quality control system which complies with the quality assurance requirements of NZS 3104:2003

CERTIFIED UP TO 50 MPa CONCRETE PRODUCTION

CERTIFICATION START DATE 1 May 2021

CERTIFICATION EXPIRY DATE 30 April 2022

PLANT AUDIT COMMITTEE CHAIR

PLANT AUDIT SCHEME ISO 9001 CERTIFIED 16023

Figure 7: Example Concrete NZ Plant Audit Scheme Certificate of Audit

It should be noted that it is not mandatory for a concrete batching plant to hold a Certificate of Audit. It is therefore important to be aware that when concrete, specified to meet the requirements of NZS 3104, is supplied from an un-audited plant, the purchaser and/or the designer is responsible for the implementation of the audit process and/or project testing to ensure the concrete complies with New Zealand Building Code.

The management of the Concrete NZ Plant Audit Scheme is certified to ISO 9001 and undergoes an external audit by BVQI (Bureau Veritas Quality International) on an annual basis to maintain its ISO 9001 certification (refer to Figure 4. Certificate confirming management of the Concrete NZ Plant Audit Scheme is certified to ISO 9001).

BUREAU VERITAS
Certification

Certification

Awarded to

CONCRETE NZ

LEVEL 4, 70 THE TERRACE, WELLINGTON, 6011
NEW ZEALAND

Bureau Veritas certify that the Management System of the above organisation has been audited and found to be in accordance with the requirements of the management system standards indicated below

STANDARD

ISO 9001:2015

SCOPE OF SUPPLY

THE MANAGEMENT OF THE CONCRETE NEW ZEALAND PLANT AUDIT SCHEME

Original Approval Date: **29 June 1994**

Subject to the continued satisfactory operation of the organization's Management System, this certificate is valid until: **16 August 2022**

To check the validity of this certificate please call tel. **0800 473 613**

Further clarification regarding the scope of this certificate and the applicability of the Management System requirements may be obtained by consulting the organisation.

Certificate Number: NZ9001748-1 Date: 3 September 2019

Andrew Mortimore
Vice President – I&F Pacific Region

Managing office: Bureau Veritas Pty Ltd, 3435 Wilkinstown Road, Port Melbourne, Victoria, 3207

Issuing office: Bureau Veritas Pty Ltd, 3435 Wilkinstown Road, Port Melbourne, Victoria, 3207

JAS-ANZ

Figure 8. Certificate confirming the management of the Concrete NZ Plant Audit Scheme is certified to ISO 9001

Acknowledging that a new version of NZS 3104 has been published some aspects of the Plant Audit Scheme Handbook, that sets out the requirements for performing plant audits, are being updated.

More general information on the Concrete NZ Plant Audit Scheme, such as the current status of a batching plant, is available at https://rmcplantaudit.org.nz/.

CONCLUSIONS

NZS 3104 has been revised and published in April 2021 and has several significant changes that are intended to improve technical control, cement efficiency and sustainability of concrete. Many of these changes, such as daily moisture content measurement, increased yield testing frequency and 7-day strength testing, were voluntarily being undertaken at most readymix concrete plants before the revision of the standard. Other changes such as lower target mean strengths for test series that demonstrate excellent technical control and longer-term strength testing of SCM concrete will help reduce carbon emission associated with concrete production.

The Concrete NZ Plant Audit Scheme continues to provide independent and rigorous audits of the systems in place at a concrete batching plant, providing concrete purchasers and designers confidence that concrete produced by an audited plant meets the requirements of the NZS 3104, the New Zealand Standard for concrete production. Given the recent changes it is important that designers review and check that their specifications correctly reference the new revisions of NZS 3104:2021 and the Concrete NZ Plant Audit Scheme to ensure the concrete for a project meets the requirements of the New Zealand Building Code.

REFERENCES

Australian Standards, AS 1379:2007, Specification and supply of concrete, Australia, 2007.

American Concrete Institute, ACI 318-08, Building code requirement for structural concrete, Michigan, 2008.

Barnard, D. P. (2013), *Plant Audit Scheme, Where is it and where is it going?*, NZ Concrete Industry Conference 2013, Queenstown

British Standards Institute, BS 5328-1, Guide to specifying concrete, London, 1997.

European Standard, EN 206-1:2013 Concrete, specification, performance, production, conformity, European Standard, 2013.

Standards NZ (2016), *NZS 3101:2006 Concrete Structures including Amendments 1,2,3*, Wellington, New Zealand.

Standards NZ (2003), *NZS 3104:2003 Specification for concrete production*, Wellington, New Zealand.

Standards NZ (2021), *NZS 3104:2021 Specification for concrete production*, Wellington, New Zealand.

Standards NZ (2004), *NZS 3109:1997 Concrete Construction including Amendments 1.2*, Wellington, New Zealand.

concretenz BUILDING RESILIENCE
CONFERENCE 2022
13-15 October 2022
Energy Events Centre | Rotorua

WASTE END-OF-LIFE TYRES AS A SUBTITUTE FOR COAL IN CEMENT MANUFACTURING AT GOLDEN BAY

G RAFFAINER

Golden Bay, a division of Fletcher Concrete & Infrastructure Ltd.

SUMMARY

Golden Bay began using waste end-of-life tyres (WELT) as an alternative fuel at its Portland cement manufacturing plant in March 2021. For the period 1st July 2021 to 30th June 2022, over 25,000 tonnes of WELT were used to displace over 25% of coal in the clinker manufacturing process. Achieving these substitution rates resulted in reduction in CO_{2e} emissions of over 22,000 tonnes CO_{2e} and a reduction in iron sand usage by 6,000 tonnes. This initiative has diverted over 3 million waste tyres from landfill in the first 15 months since commissioning.

INTRODUCTION

Golden Bay operates the Portland cement manufacturing plant, which is New Zealand's only fully integrated cement manufacturing plant, approximately 15 km south of Whangarei. It is strategically located near two quarries that supply the necessary raw materials for cement manufacturing, and the Whangarei Harbour to allow for costal shipping of cement product to the service centres located around New Zealand.

The plant is a modern, cement plant with the capacity of close to 1 million tonnes of cement per annum and supplies approximately 60% of the country's cement to New Zealand's unique and stringent building and seismic standards.

Over its more than 100-year history, the plant has developed a reputation for supplying high quality products to the New Zealand building industry, while striving to maintain world best available technology for energy efficiency and environmental controls. Golden Bay, part of the Fletcher Building Group, is committed to a Science-Based Target to reduce our 2018 baseline carbon emissions 30% by 2030. Alternate fuels have been used at Golden Bay since 2004 when biomass wood waste was first introduced to the process as a substitute for coal. Alternate fuels usage was increased in 2021 when the plant completed a successful upgrade of its precalciner to accommodate new feed and combustion equipment suitable for handling waste end-of-life tyres (WELT).

WELT usage in the cement manufacturing industry is common practice globally. Several characteristics make WELT an excellent fuel for the cement kiln. The very high temperatures controlled oxidising combustion conditions and long fuel residence times in the kiln precalciner ensures complete combustion of the WELT. There is no smoke, odour or visible emissions from the process and because leftover tyre steel and ash from the WELT is incorporated into the final product, there is no waste or by-product.

WELT also helps offset iron sand usage with the steel belting and reinforcing in the WELT acting as a direct replacement for this necessary raw material. This has resulted a 6,000t reduction in iron sand usage for the July 2021 to June 2022 period.

WELT emits approximately 26% less CO_{2e} in combustion compared to coal (see Table 1). In New Zealand WELT is currently a waste product that has predominately been sent to landfills as alternative solutions are limited.

Table 1: Coal vs. Waste Tyres Emissions Factors.

Thermal Fuel	Emissions factor (t CO_{2e} /TJ)
Coal	88.28
Waste Tyres	60.00

The target for the first full financial year of operation (July 2021 to June 2022) to use WELT to replace 15% of coal as a fuel in the manufacturing process. At 15% substitution rate (17,000 tonnes of WELT), the natural rubber content of the tyres results in a minimum reduction of 13,000 tonnes CO_{2e} per annum.

In addition to the WELT, Golden Bay also substitutes an additional 20% of coal with biofuel (wood waste). An overall alternative fuels substitution of approximately 50% was achieved in the 2022 financial year, avoiding a total of over 90,000 tonnes of CO_{2e} emissions. This has lowered the embodied carbon of our products, and Golden Bay GP cement now has a Global Warming Potential (GWP) 25% lower than the ISCA 2020 baseline.

BACKGROUND

Cement manufacturing is an inherently carbon emissions intensive process, largely due to the production of the intermediary product, clinker. Two main factors contribute to the carbon emissions profile of cement manufacturing, both relating to the production of cement clinker. Firstly, the chemical reaction, which is required in the formation of clinker, drives off CO_2, as shown in equation (1) below

$$CaCO_3 \xrightarrow[T=890\,^{\circ}C]{} CaO + CO_2 \quad (1)$$

Secondly, the high temperatures required in the process of clinker formation are normally achieved using coal as the primary fuel. As a mass balance, 1 tonne of clinker produces 0.9 tonnes of CO_{2e} for a fully coal fired manufacturing plant. Between 55-60% are process emissions, and 40-45% are from the process combustion fuels.

Golden Bay is committed to a Science-Based Target to reduce its carbon emissions by 30% by 2030 compared with 2018 baseline levels. Science-based targets provide companies with a clearly defined path to reduce emissions in line with the United Nations Paris Agreement goals (United Nations 2015). The focus is on achieving a carbon reduction that would keep global warming to less than 1.5°C.

Solutions for the capture and sequestration of direct process emissions are not currently proven as commercially viable. This is something that Golden Bay anticipate as a future solution for further carbon reduction initiatives.

An important part of Golden Bay's carbon reduction has been and continues to be the substitution of coal with alternative fuels. Golden Bay's long history of use of alternative fuels resulted in Golden Bay's GP cement having 20% lower embodied carbon than ISCA 2020 baseline, before the introduction of WELT. This was demonstrated by the 2019 Golden Bay Environmental Product Declaration (EPD) (thinkstep 2019) with GWP of 732kgCO_{2e} per tonne of GP cement.

WASTE END-OF-LIFE TYRES PROJECT

WELT is recognised as a major waste stream and are recycled at rates of up to 95% internationally (see Figure 1).

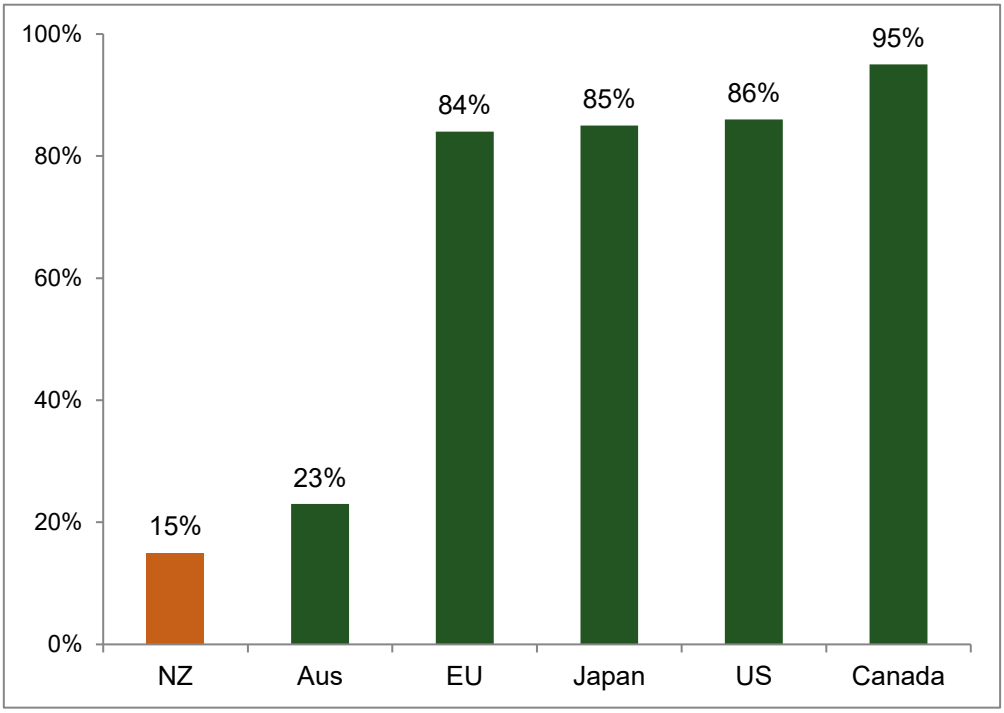

Figure 1. Percentage of Tyres Recycled Internationally in 2017.

Over 5 million tyres are imported into New Zealand per annum. This equates to approximately 50,000 tonnes of WELT, much of which would end up in landfills or abandoned in hazardous stockpiles around the country. These stockpiles were frequently the target of arson attacks and had other environmental and biosecurity concerns.

Technology Selection

Golden Bay began investigating the use of WELT as a process fuel in 2015. A review of all engineering solutions for the feed system was undertaken and the equipment selected was from Engineering Danish Company – FL Smidth. The solution chosen called a Hotdisc is a combustion reactor allowing for WELT to be combusted in the precalciner to provide thermal heat for the clinker manufacturing process.

The Hotdisc consists of a rotating disc in the kiln riser where alternative fuels are burnt. The fuel is fed onto the slowly rotating disc where it meets tertiary air and burns in oxidizing conditions. Fuels can be resident on the hot disc for up to 45 minutes meaning large particle sizes such as whole tyres can be successfully burnt. The fuel is transported 270º on the disc where it meets a scraper that scrapes any ash and remnants into the kiln. At least 80% of calciner fuel can be substituted through the Hotdisc. Figure 2 provides a cutaway view of the Hotdisc.

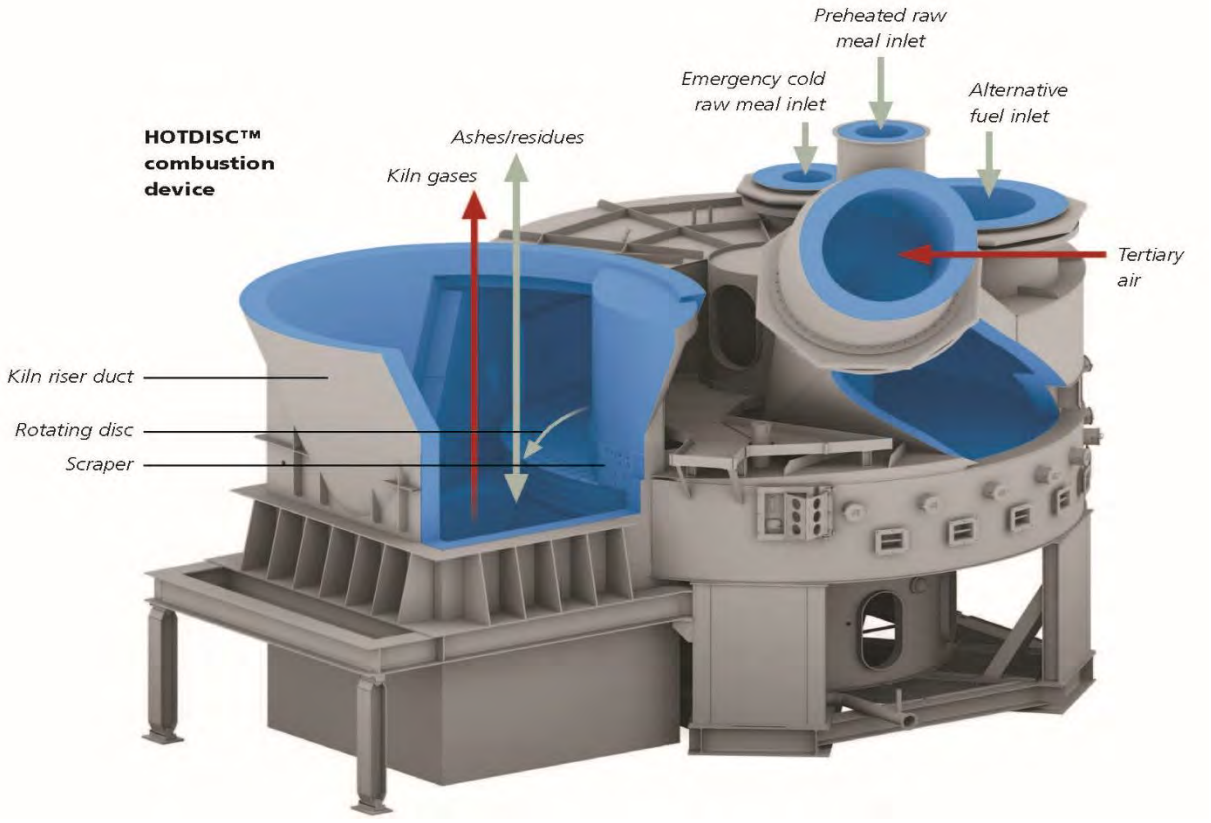

Figure 2. The FLSmidth HotDisc

Project Development and Execution

The Ministry for the Environment (MfE) had declared WELT as a priority product for Waste Minimisation funding, and in 2017 Golden Bay, MfE and Waste Management collaborated to offer an end-to-end solution to sustainably dispose of New Zealand's waste tyres. Waste

Management New Zealand became a strategic partner for collection and shredding of the waste tyres. Winstone Aggregates became transport partners, backloading the shredded tyres from the processing plant in Auckland to Whangarei to maximise transportation efficiency. During project scoping, it was determined that WELT could replace up to 30% of coal as a fuel in the manufacturing process without affecting the manufacturing process, product quality and without more than minor environmental impacts.

The project gained significant funding from the MfE Waste Minimisation Fund, allowing it to be financially viable. Collectively this is one of NZ's largest ever waste minimisation initiatives – diverting 3 million waste tyres per year away from landfill, to be chipped by Waste Management and used by Golden Bay as an alternate fuel to substitute coal. As well as offering a solution to the imported tyres coming into the country, it also offers a solution to hazardous nuisance stockpiles.

A comprehensive resource consenting process was undertaken, to change the conditions of consent for the operations of the cement plant at Portland to enable the addition of WELT into the list of allowable fuels for process heat. This included consultation with the local community, local Iwi groups, and members of the wider Whangarei community.

A full assessment of environmental effects (AEE) was completed, including assessing potential impacts on air, land, and freshwater and marine environments. This also included the potential human and animal toxicology assessments, with potential for contact with possible contaminants via air, drinking water and soils. The AEE concluded that there would be no change in the potential environmental or toxicological impacts with the addition of WELT at the 30% substitution rate assessed. Table 2 shows the change in stack emissions when using WELT vs base case. Resource consent change was granted by the Northland Regional Council in 2019.

Table 2. Predicted Changes in Stack Emissions When Using WELT vs Base Case.

Main Kiln Stack Gas Composition and Flow			
Gas	**Base Case**	**30% WELT**	**Units**
CO_2	17.8	17.7	% by volume
H_2O	18.6	18.8	% by volume
N_2	56.4	56.3	% by volume
O_2	7.2	7.2	% by volume
Flow volume at stack	60.0	60.3	Sm^3/sec (STP, dry)
Flow volume at stack	102.1	102.8	AM^3/sec
Temperature at stack	105	105	°C
Pressure at stack discharge	101.325	101.325	kPa
Stack diameter	2.48	2.48	m
Discharge velocity	21.14	21.14	m/sec
Elevation of stack	73.53	73.53	Meters above datum (sea level)

Plant modifications

Integration and installation of the Hotdisc into the process required significant structural modifications to the existing plant. A collaborative approach was taken to design and construction – leveraging off the knowledge of local contractors and consulting engineers to improve constructability. Due to the complex nature of the project, Golden Bay established a project management team made up of inhouse engineers as well as national and international industry and construction specialists. The team worked alongside day-to-day operations to facilitate safe and efficient work execution while maintaining the ability to act quickly with key decisions as needed as there was no intermediary major contractor.

While the majority of the structural work was done while the plant continued to operate, the installation of the Hotdisc itself required a full 35 days of round the clock work to complete the project and make all the required process modifications. Figure 3 shows the as built 3D Model (derived from laser scan) used to sequence installation and highlight any potential clashes ahead of time. GBC completed its upgrade project in February 2021.

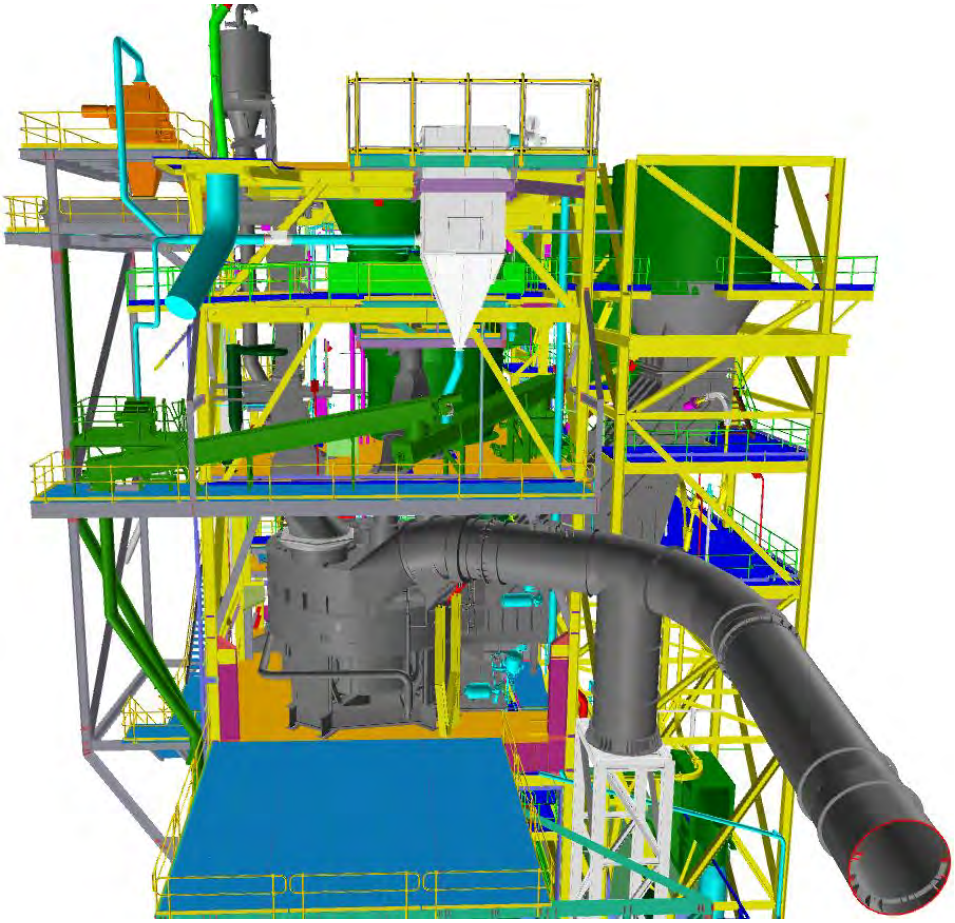

Figure 3. 3D Laser Scan and As Built Model of Precalciner and HotDisc.

OUTCOMES

The WELT project has taken 5 years in planning and a 35-day plant shutdown for the installation of the equipment. This nationally significant initiative uses WELT as a kiln fuel, displacing up to 30% of coal. These tyres would otherwise present a significant environmental hazard, most being destined for landfill in New Zealand.

This $30 million project was installed in partnership with the Waste Minimisation Fund, which contributed $16 million. One of the most significant Waste Minimisation Fund projects to date. Use of WELT at Golden Bay solves multiple problems at a national level. As well as carbon reduction, there is a significant decrease of waste to landfill, international transportation emissions are reduced (to export waste tyres), and there is a reduced risk of uncontrolled tyre stockpile fires.

Use of WELT has been tracking ahead of plan, with an overall substitution rate of more than 25% achieved in the 2022 financial year. This has resulted in the use of over 25,000 tonnes of WELT and a reduction in CO_{2e} emissions by over 22,000 tonnes over that period. This has far exceeded the original target of 15% substitution. This initiative has diverted over 3 million waste tyres from landfill in the first 15 months since commissioning. The use of WELT is one part of Golden Bay's wider decarbonisation roadmap.

In addition to the WELT, the use of biomass wood waste has meant that Golden Bay has been able to reach a total substitution rate (TSR), at its peak, of 53% of alternative fuel use. For the 2022 financial year total WELT substitution surpassed 25% and biomass wood waste surpassed 20% achieving a TSR of just short of 50% for the period (see Figure 4). This resulted in a total reduction of over 75,000 tonnes of CO_{2e} emissions when compared against using 100% coal for thermal fuel.

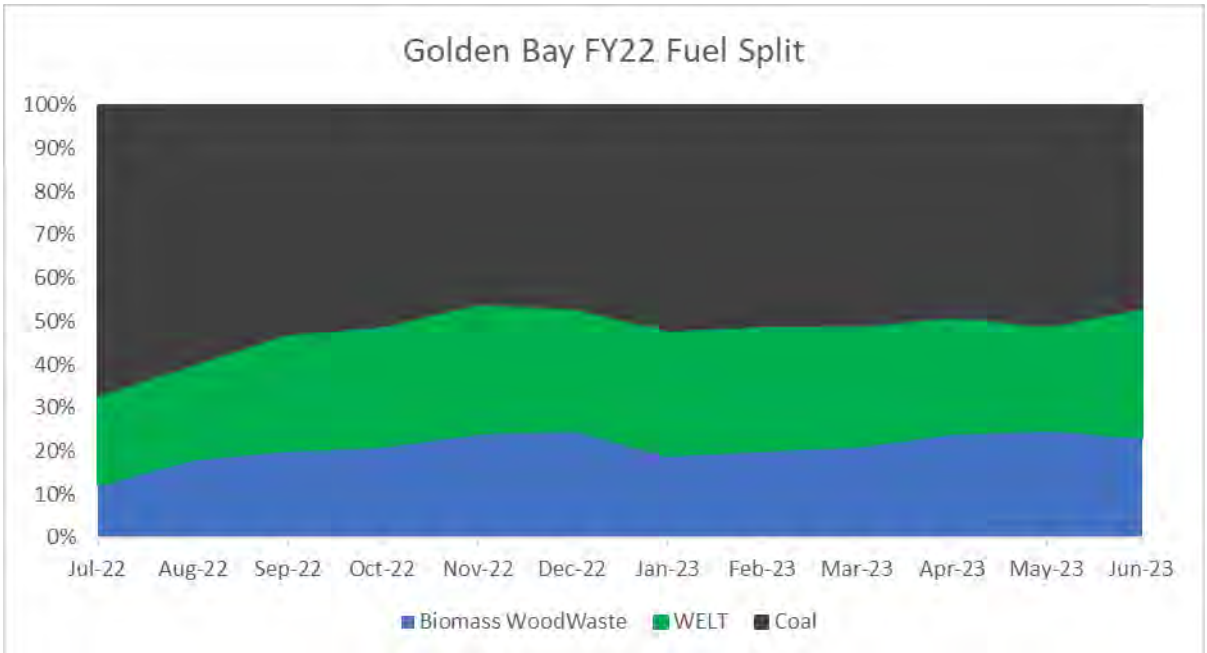

Figure 4. Golden Bay Financial Year 2022 Alternative Fuels Usage.

As verified by the updated Golden Bay EPD data, the GWP of Golden Bay GP cement has now reduced to 699kgs of CO_{2e} per tonne of cement, making this product 25% lower than the ISCA 2020 baseline GWP.

REFERENCES

Thinkstep Limited, (2019), “Golden Bay Cement Environmental Product Declaration”, (https://www.goldenbay.co.nz/assets/Uploads/d310c4f72a/GoldenBayCement_EPD_2019_HighRes.pdf).

United Nations, (2015), “Paris Agreement”, Paris: United Nations.

SESSION 5A

Chair:
Ralf Kessel

concretenz BUILDING RESILIENCE
CONFERENCE 2022
13-15 October 2022
Energy Events Centre | Rotorua

CASE STUDY OF SOLAR PANEL INSTALLATION AT CONCRETEC NEW ZEALAND LTD

JUSTIN BRAGG

Director, Concretec New Zealand Ltd

SUMMARY

This paper discusses the benefits and assessment process for the installation of a solar panel array at an industrial manufacturing site – firstly from an economic perspective for return on investment, and secondly from an environmental perspective, been CO2e emissions reduction, both locally and globally. The solar installation was motivated by the increasing demand for more sustainable business practices. The site is Concretec New Zealand Ltd precast concrete manufacturing facilities located in the Bombay hills south of Auckland. It operates on a purpose built site which has allowed the development to be environmentally friendly from conception. The site is self sufficient with water with 200,000 litres of storage for rainwater, sewerage is treated on site, and incorporates a green belt border of several hectares which has been planted with hundreds of native plants and trees. Hence to move to generate clean electricity on site to further the sustainability of the operation was a natural next step. The resulting solar installation which went live in December 2020 has proven to be both economically viable, and has a positive impact on the environment by reducing demand on the national electricity grid, which results in lower CO2e emissions for New Zealand.

Photo 1:The Solar array on a north facing Concretec NZ factory roof.

ASSESSING THE FINANCIAL RETURN OF A SOLAR INSTALLATION

The Financial return ($/kWhr installed) of a solar installation is dependant on a number of factors including:

- Size of array versus power consumption (in kWhrs)
- Time of power demand relative to daylight hours.
- Number of days per week the demand occurs.
- Cost of power at location
- Wholesale rate available for exported solar kWhrs.
- Location, orientation and angle of inclination of array.

Size of array versus power consumption

The key criteria impacting financial return of a solar installation are the size relative to power demand, and when the demand occurs relative to daylight hours. Simple examples to demonstrate the above follow:

The highest financial returns ($ return per total kWhr generated) occurs when a maximum proportion of solar power generated is consumed directly by the business, and the amount exported is minimal. Graph 1 below reflects this ratio with a typical seasonal profile of solar generation by month, versus a steady consumption across the year decreased for public holidays in December & January. It also assumes power consumption occurs between 8am and 5pm.

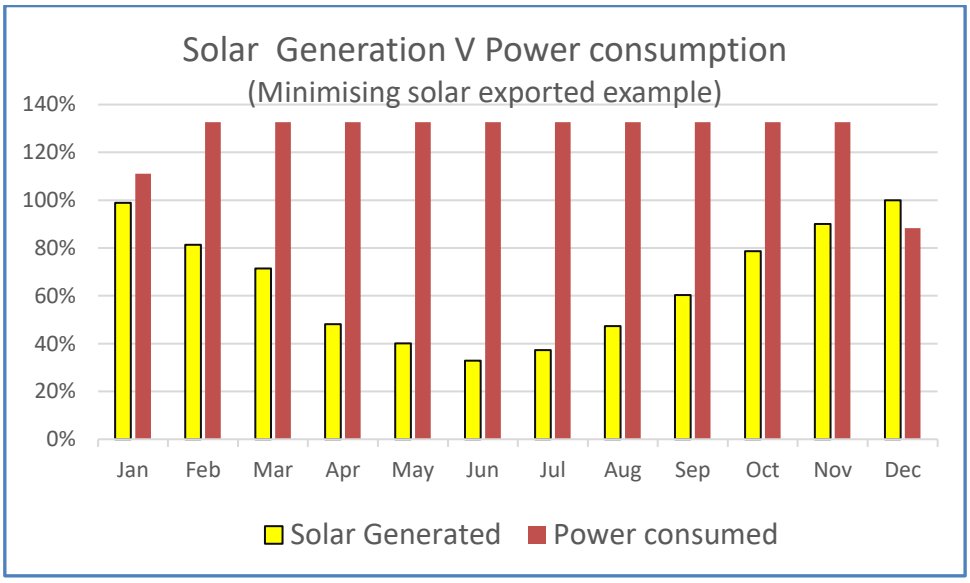

Graph 1: Optimising financial return model

For the minimising solar exported example, the array is purposely sized small relative to demand so little solar is exported on a work day. This results in generation of approximately half of the power consumed. Then the ratio exported will be relative to working days, and assuming the business does not work statutory holidays will be:

5 working days – 32% solar exported
6 working days – 18% solar exported
7 working days - 3% solar exported

By factoring in power cost and export power price, the financial benefit per kWhr of solar generated can be calculated. For typical power costs of 24c per kWhr, and example export price of 7c per kWhrs, table 1 shows benefits based on days worked per week.

Days worked per week	% solar consumed directly	% solar exported	Savings for direct consumption cents/ kWhrs generated	Export revenue cents/kWhrs generated	Total savings cents/kWhr of solar generated
5	68%	32%	68% x 24c	32% x 7c	18.56
6	82%	18%	82% x 24c	15% x 7c	20.94
7	97%	3%	97% x 24c	3 % x 7c	23.49

Table 1: Savings from solar generation for minimum power export

The second example below also compares returns as per to table 1, but from an array that is sized to offset the total power consumed, and hence have a minimal carbon footprint with respect to load on the national grid. Graph 2 below shows the system has excess generation in summer months to offset lower output during winter months.

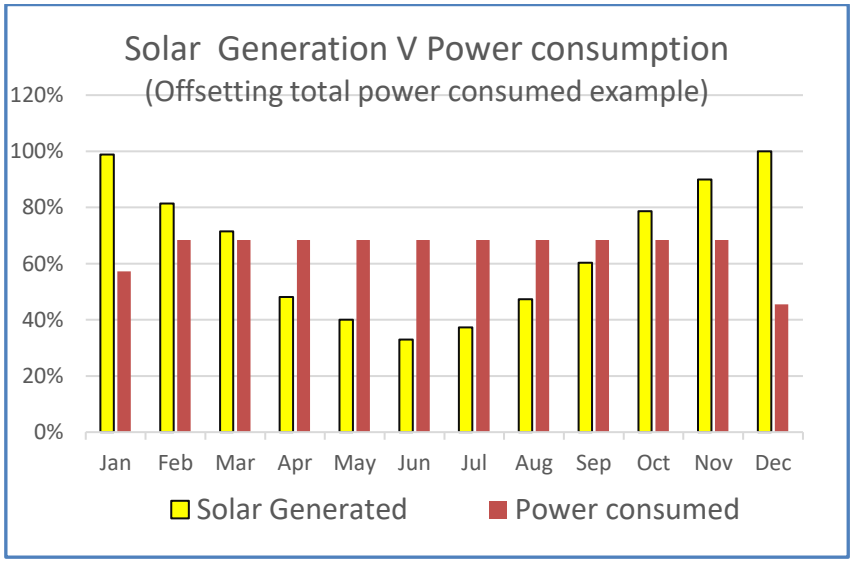

Graph 2: Covering all consumption model

Table 2 again shows total saving per solar kWhr generated, but increases the ratio exported by approximately 20% of total generated to account for the excess generation 6 months of the year.

Days worked per week	% solar consumed directly	% solar exported	Savings for direct consumption cents/ kWhrs generated	Export revenue cents/kWhrs generated	Total savings per kWhr of solar generated
5	48%	52%	48% x 24c	52% x 7c	15.16
6	62%	38%	62% x 24c	38% x 7c	17.54
7	77%	23%	18.48	1.61	20.09

Table 2: Savings from solar generation for solar generation covering all consumption

Table 2 can be modified again for the impact of running a 15hr shift, for operations from 6am to 9pm, while still generating sufficient solar to offset all the demand. Then approximately 30%

of power demand occurs outside of the hours the solar is generating, with a higher ratio of solar exported. This is approximated in table 3.

Days worked per week	% solar consumed directly	% solar exported	Savings for direct consumption cents/ kWhrs generated	Export revenue cents/kWhrs generated	Total savings per kWhr of solar generated
5	33%	67%	16% x 24c	84% x 7c	9.72
6	44%	56%	30% x 24c	70% x 7c	12.1
7	54%	46%	45% x 24c	55% x 7c	14.65

Table 3: Savings from solar generation for with a 15 hour work day

Hence from the table 1 to 3 the financial return can vary widely depending on the array size and hours of work. To calculate the annual return from a given installation is then simply obtained by multiplying the estimated total savings per kWhr of solar generated by the total kWhrs of solar generation per annum.

How much will a solar array generate at your site location.

Solar array output is a function of sun light intensity falling on the solar panel surface, which will vary with clear and cloudy weather, atmospheric conditions, plus the seasons as the sun intensity alters due to angle of impact on the earths surface. This can be modelled as sunlight radiation data is available from NIWA[(1)], for any location in New Zealand, which can be downloaded via csv files. The data is averaged based on at least 10 years of history from the closest of one of 100 weather stations across the country, allows for the input of the orientation and inclination of the panels, takes into account temperature and wind speed which impact panel output, providing watts of energy per m2 falling on the panels. The data is split into hourly units for every hour of the year. The solar panel supplier will take this data and apply an efficiency factor (approx. 21%) to convert the suns watts/m2 into solar panel watts of electrical generation. However a quick estimate can be calculated by multiplying the installed kW capacity x 1350 to provide annual kWhrs of generation.

Sizing Concretec New Zealand's array.

With Concretec's power demand commencing at 5am and continuing until 8pm or later, clearly the solar generation would not cover all of the usage. However by sizing the array sufficiently large, power in excess of demand could be generated during the sunshine hours, to offset some or all of the early morning and late evening demand not covered. Concretec selected a 102kW solar array, which applying the NIWA data and solar conversion factor gave a forecast annual generation of 138,000 kWhrs compared to a total usage of approximately 191,000kWhrs. The size chosen was both a compromise in financial return and amount of power offset, coupled with a practical constraint of the size of the north facing roof of the factory building chosen for the installation.

Assessing the ratio of solar consumed to solar exported.

Concretec typically runs a 12 to 15 hour day, and works 5 ½ to 6 days per week. Hence to assess the financial return, we needed to obtain the consumed / exported ratio as discussed above. Using the tables above, for solar generation at 72% (138/191MWhrs) of power consumed, one could interpolate approx. a 60/40 ratio of consumed to exported. However to obtain a more accurate estimate we matched historic power usage data from our electricity provider in kWhrs for every hour period across 24 hours per day for a full year from April 19 to Mar 20 with the NIWA based hourly data, pairing estimated solar output with consumption for

a sample year in hourly intervals. This was aggregated to provide solar generated and power consumed as shown in graph 3, and the data allowed a further split of solar into solar consumed and solar exported shown in graph 4.

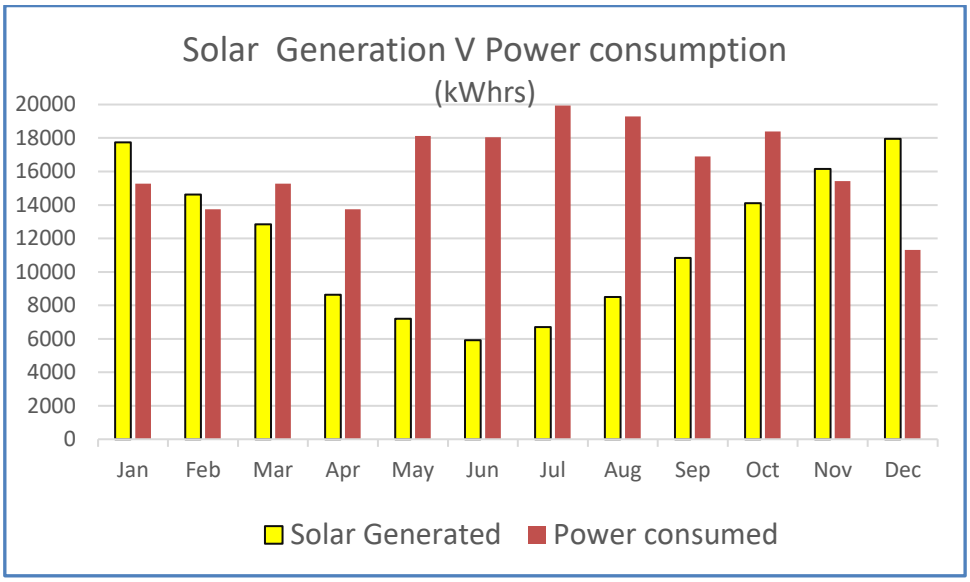

Graph 3: Concretec generation V consumption model

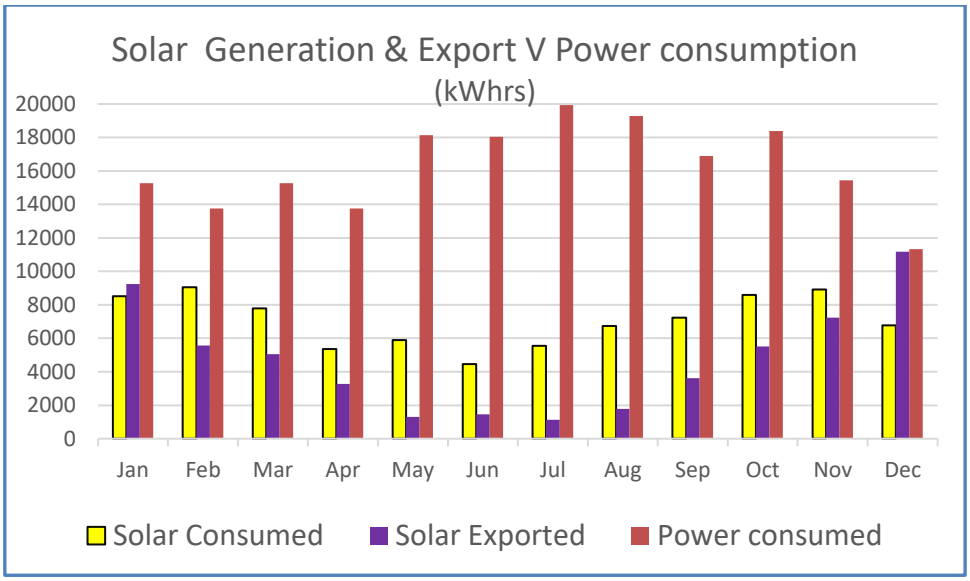

Graph 4: Concretec generation V consumption model

The total figures for the analysis were:
Total estimated power consumption = 191,000 kWhrs p.a.
Total estimated solar generation = 138,000 kWhrs p.a.
Estimated solar direct consumption = 84,000 kWhrs p.a.
Estimated solar exported = 54,000 kWhrs p.a.

The financial benefit can be calculated as:
Savings from direct reduction in consumption = 84,000 kWhrs x 24c / kWhr = $20,160 p.a.
Additional savings from export earnings = 54,000 kWhrs x 7c /kWhr = $ 3,780 p.a.
Hence a total savings of approximately $24,000 p.a. compared to a total cost prior to solar of $46,000 p.a., or 52%.

The resulting economics of this are quite favourable. Concretec financed 100% of the system using a 10 year term loan from a major bank. This provides a near neutral cash flow from year 1, climbing to a slightly positive cashflow at year 10 assuming a small inflation in electricity cost. After 10 years the savings are all banked, with the life of the system estimated at 35 years, and 92% of initial output guaranteed after 25 years. These savings can be summarised in a simple model:

Initial cost of total system:	$210,000
Interest cost @ 4% for 10yr payback	$ 42,000
Savings over 35 yrs assuming no inflation	$800,000
Net present value of investment	$548,000

Electricity costs across New Zealand.

A number of precast concrete manufactures provided their current 2021 electricity costs to compare with the Concretec example as follows. These costs exclude line and daily charges.

Location	Electricity cost cents per kWhr
Whangarei	26.5
Ruakaka	28.5
Ngaruawahia	23
Mt Maunganui	21.4
Palmerston North	21.3
Christchurch	23.5
Ashburton	22
Cromwell	28
Invercargill	19.5

Table 4

Comparing investment returns for this industry sized solar to other renewable generation methods.

Two common methods of assessing the cost of a power generation investment are total cost per kW generation capacity, and total cost per kWhrs generated over the life of the system, referred to as Levelized Cost of Energy (LCOE).

On the first measure Concretec's installation has a total installed cost of approx. $2100/kW.
For the LCOE measure, using a 35 year life, this provides a LCOE of 5.6c per kWhr using a 4% cost of capital and zero maintenance.

This can be compared with new wind farm installations, which MBIE forecasts[(2)] will be an important and significant source of NZ's future renewable energy generation.
Two examples are the Genesis Waipipi and Mercury Energy's Turitea, totalling 354MW total output, and will cost $740m[(2)] or $2090/kW.
The LOCE is estimated in the range of 5.5 to 7c per kWhr for the more favourable wind sites in NZ.[(2)]

Hence the cost of the Concretec solar installation is currently similar to much larger national scale wind farms per kWhr. An obvious advantage for the smaller solar installation is no additional real estate is required as this is typically existing in the form of a building roof, and no need for transmission lines back to the grid. This implies that smaller businesses installing a solar array can provide a similar investment benefit for NZ compared to large wind farm installations.

Use of batteries with a solar array.

Batteries are added to solar systems to provide one or more of the following benefits:

- Capture excess power generation during sunlight hours to be used when most demand does not align with generating sunlight hours. This is common with many residential installations.
- Provide security of power supply when mains power is not available, or is unpredictable in supply. (note this is not provided by a solar array alone without batteries)
- Remove the peaks off demand, reducing overall grid power costs. This is less common, and would apply to special industrial situations.

For a Concretec type installation, while the first two of these benefits would have some application, it was not seen as a financial viable option. The current cost of batteries to store solar generation are in the order of $1000 per kWhr, and the current life of such batteries is half the life of the system at best. A full assessment of battery use is outside the scope of this paper, but would include a cost comparison of increasing the solar array size, which while it has diminishing financial returns, it probably will provide better returns than installing batteries, but increases environmental benefits.

THE ENVIRONMENTAL BENEFITS FROM SOLAR POWER.

The primary reason for installing a solar array at Concretec was to have a positive impact on the environment. The question then was what would this impact be. By installing solar power generation, demand is reduced on the NZ's national grid system, firstly by directly reducing demand when the solar power generated is used onsite, and secondly when excess solar power is sold back to the grid. This is in line with the government's current desire to increase green renewable electricity generation capacity, and therefore allow the retirement of fossil fuel fired (thermal) generation, especially eliminating coal consumption.

The Concretec array is estimated to produce approx. 138,000 kWhrs p.a. and this will reduce demand of the same amount on the mains grid as discussed above. Over the expected 35 year life of the system over 4 GWhrs of demand will be reduced from the NZ national grid.

Current NZ emissions from electricity generation

While close to 80% of New Zealand's electricity is generated from renewable sources, New Zealand currently emits over 4 million tonnes[3] of CO2e per year into the atmosphere to produce around 43,000 GWhrs p.a. Most of these emissions are produced from the use of coal and gas fired power plants, which are used to generate the constant shortfall New Zealand has from clean sources such as hydroelectric, wind, solar, and geothermal, although the later can emit some CO2e.

The initial investigation to understand the impact of the solar installation took reference from the NZ Governments publication "Measuring Emissions: A guide for Organisations-2020 detailed guide", where table 9 provides historic data up to 2018 for the average emissions for purchased electricity from the NZ grid at about 110gms of CO2e per kWhr. For 2021 this figure will be slightly higher due to increase in coal burn. While this figure may be appropriate for current users to estimate there carbon footprint from electricity use, it is not appropriate to calculate the change of CO2e emissions due to changes of demand or type of generation.
A better understanding of this can be gained from a historic view of demand and generation type. Graph 5 below, sourced from MBIE data[5] electricity usage stats for NZ, shows from the early 1980's when NZ had it's "cleanest" generation peaking at 89% (mostly hydro), declining to the "least clean" in 2001 with only 64% renewable generation. Since 2001 an increase in renewable generation – geothermal and wind, have offset the fossil fuel burn of coal and gas. Hence graph 5 shows the relationship between total demand, renewable generation, and

thermal generation, with thermal balancing the first two. This relationship was also checked across a 12 month period, to check seasonal influences did not create periods of zero thermal generation. Graph 6 for the most recent 12 months shows the logic holds.

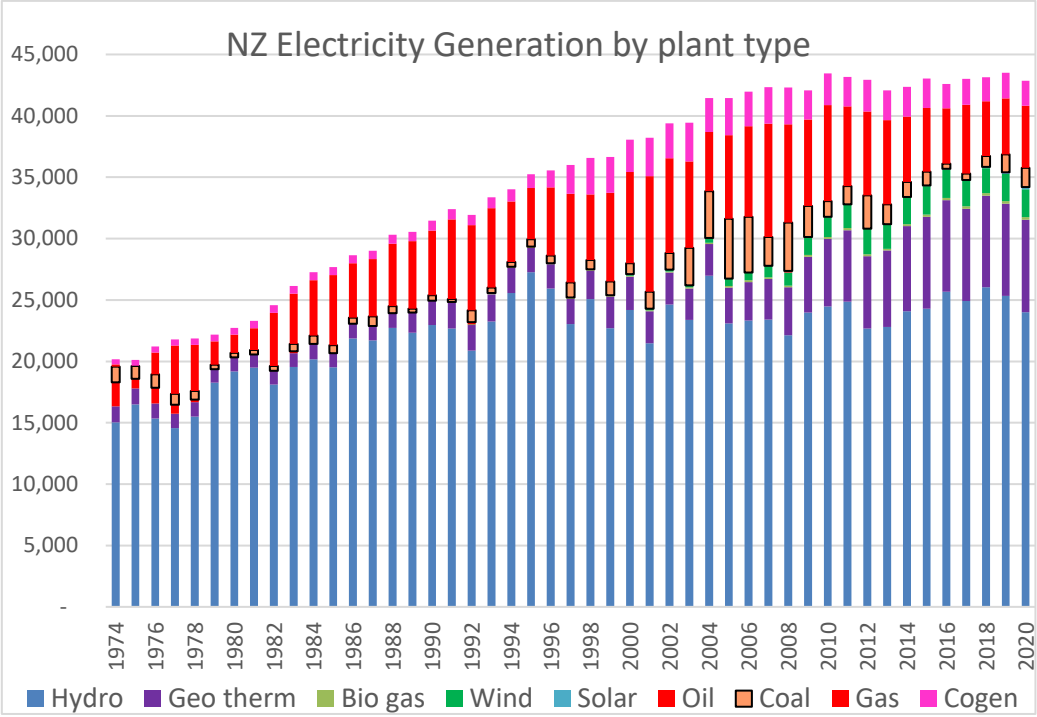

Graph 5: Renewable V thermal generation annual history

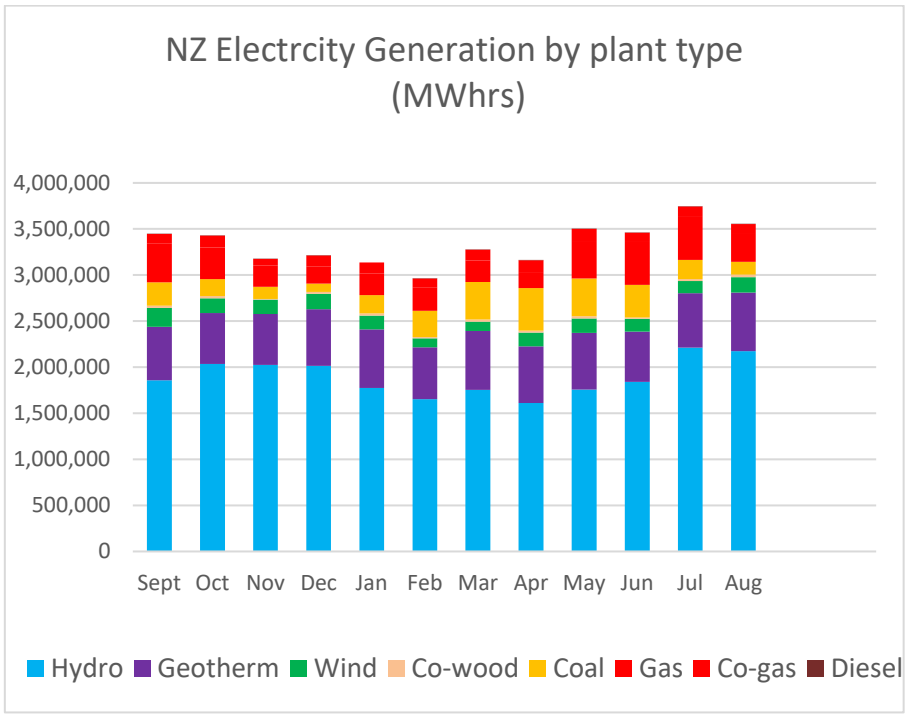

Graph 6: Renewable V thermal generation by month

<u>CO2e emissions reduction from a solar installation</u>

Using this relationship between total demand, renewable & thermal generation, the solar array generation will offset thermal generation, and CO2e savings from the Concretec solar generated kWhrs is probably somewhere between coal and gas generation emissions x the solar generation.

Emissions from gas and coal fuelled generation are approx. 400 and 1000g/kWhr respectively[3], so the savings will fall somewhere between these two figures. From graph 5 we can see historically coal fired generation has been considerable less than gas, and over the past 3 years has been less than 25% of total. 2021 will be an exception due to gas shortages in the first half of the calendar year with coal generation been similar to gas for that period. Taking the lower figure of 400gms per kWhr, the Concretec's solar installation could reduce emissions by 400gms x 138,000 kWhrs p.a. = 55 tonnes of CO2e p.a. However in the short term it is probably higher.

As a comparison Genesis[4] is forecasting saving of 250,00 tonnes of CO2e emissions p.a. from their recently commissioned wind farm at Waipipi Taranaki which is forecast to generate 455GWh per year. This equates to 0.55 tonnes per MWh, or 550 gms per kWhr. Using this figure the Concretec solar array will reduce emissions by 76 tonnes of CO2e per year. By observation these are not exact figures, and will trend down with time as coal is eventually retired from NZ's generation mix.

It is expected gas will be consumed in NZ power generation beyond 2035[7], hence emissions savings will continue for many years yet. Ultimately when NZ reaches its targets of 100% (or close to) of renewable energy, the environmental benefits for additional solar systems will mostly disappear.

<u>How do the CO2e savings compare with the carbon footprint due to the concrete in Concretec's head office building?</u>

Photo 2: Concretec NZ Head Office building

Photo 2 above shows the Concretec head office building, a 2 level 600m2 concrete structure comprising concrete foundations, floors, 260mm thick insulated precast concrete panels, precast concrete beams, columns, stairs and balcony. In total around 225 m3 of concrete was used in the construction. Using a C02e figure of 0.3 tonnes per m3 of concrete, the embodied CO2e in the 225m3 of concrete used in the office building = 67.5 tonnes. Hence in the current power generation regime of NZ, it could be argued the solar array will offset the carbon emissions from the concrete component of our office building in close to 12 months.

Checking for carbon leakage - the environmental impact of manufacturing solar panels.

The REC (Renewable Energy Corporation) panels used in the Concretec system had industry leading low embodied C02e in the manufacture of the panels, and the low energy amortisation time, or energy used in the manufacturing process payback time. Due to REC's use of industry leading low energy methods to produce the silicon wafers required (the energy usage for the purification of silicon is 80% of the total energy usage aspects of the full production process) and manufacturing these in Norway where approx. 96% of their electricity comes from hydroelectric sources. This allows these panels to have a leading energy payback time of approx. 1 year, and a C02e payback time of less than a year.

CONCLUSIONS

Installing solar power generation can be a viable financial investment for industry, especially when the bulk of the demand coincides with the solar generation during sunlight hours. The investments cost per kWhr has been shown to be similar to large commercial renewable electricity scheme such as wind farm, therefore providing efficient use of NZ investment funds.

The reduction of demand on the national grid provided by a solar installation currently has a direct benefit on reducing demand on the national thermal power generation, and hence the associated CO2e emissions from such. This will continue until NZ reaches a zero or minimal requirement for thermal generation, which is not expected until 2035.

REFERENCES

1. Solarview.niwa.co.nz
2. MBIE Wind Generation Stack Update – Version 2.0: Final 30 June 2020 – Roaring40s Wind Power Ltd
3. Ecotricity – New Zealand Electricity emissions https://ecotricity.co.nz/electricity-emissions
4. https://www.genesisenergy.co.nz/about/media/news/taranaki-windfarm-energised,-tilting-new-zealand-t (ex Energy Link NZ 12 months emissions 2020)
5. EMI – Electricity Authority – wholesale data sets https://www.emi.ea.govt.nz/Wholesale/Datasets/Generation/Generation_MD
6. https://www.genesisenergy.co.nz/about/media - August 2021
7. Climate Change Commission - 2021 Draft Advice for Consultation.

Appendix: Solar panel specifications

230 No REC Alpha HJT Mono 445W panels totalling 102.35k
4 x 25kW Fronius ECO 3 Phase inverters
REC offer a 25 year product warranty, guarantees of 92% power output after 25 years, a real life of 35 to 40 years, with a high degree of recyclability.
Fronius provide connectivity to the internet to allow real time monitoring of panel performance as well as historic power generation.

GETTING AHEAD OF THE CURVE ON DECARBONISATION AND SUSTAINABILITY

BERNIE NAPP[1]

[1]Concrete NZ

SUMMARY

Worldwide the cement and concrete industry is responding to the call to lower the carbon and environmental footprint of this energy and emissions-intensive industry. Aotearoa New Zealand is making strides in this space, and Concrete NZ has taken an ESG approach to meeting the challenge. “Environmental, Social and Corporate governance” is a response to growing environmental regulation and societal expectations of our industry; at the same time concrete also makes an essential contribution to the four wellbeings. We are working to identify pathways for industry decarbonisation (roadmap), and on a pan-industry sustainability report. Both programmes will benefit operators who seek to prosper in rapidly changing times.

INTRODUCTION

The contribution of the cement and concrete industry worldwide to global greenhouse gas emissions has been estimated at 8 percent. This makes it among the most emissions intensive in the world[1], and a call to climate change action. The Global Cement and Concrete Association (GCCA) aligned with the 2015 Paris Agreement goal of stabilising world climate at between +1.5 and +2°C, and produced in 2021 a decarbonisation roadmap titled *Our Concrete Future*[2].

The GCCA document sets out seven levers for moving the global cement and concrete sector to net zero carbon by 2050. In publishing it, the GCCA laid out a challenge to the industry worldwide, including in New Zealand, to reduce carbon dioxide emissions. (Concrete NZ is an affiliated member of the GCCA.)

In parallel, the United Nations Organisation (UN) published 17 Sustainable Development Goals[3] (SDGs) for the world in 2015. The SDGs include health and wellbeing, clean water, renewable and affordable energy, jobs and economic growth, industry and infrastructure, sustainable cities, waste and circular economy, climate action, and partnerships.

Concrete is relevant to all the above SDGs[4], and the SDGs in turn feed into the New Zealand Treasury’s “living standards framework”[5], (which defines wellbeing in terms of human, social, natural, and financial and physical capitals). As a building and construction material, concrete therefore occupies centre stage in the pursuit of sustainability and climate change action.

Even so, concrete has an image among some quarters in New Zealand of being energy and emissions intensive, compared with some alternative materials.

In evidence, government initially expressed a preference for timber over concrete in building and construction, which Concrete NZ contested in a submission on the Building for Climate

Change Programme[6]. The draft National Adaptation Plan[7] (NAP) for climate change contained no reference to concrete, and emphasised nature-based solutions to sea level rise (e.g., creating wetlands), and "managed retreat". Following Concrete NZ's advocacy[8], the final NAP does mention "sea walls" as a climate change adaptation option[9].

At the 2022 NZ Bridge Summit in Wellington in August, Waka Kotahi NZ Transport Agency presented on its new mission of building highway bridges out of timber, and asked if concrete would "lead to an over-reliance and bias in bridge construction"[10].

To meet these challenges, and to influence the sustainability and climate change debate, Concrete NZ has adopted an approach known as ESG, which stands for "environmental, social and corporate governance". This is defined below.

ESG - ENVIRONMENTAL, SOCIAL AND CORPORATE GOVERNANCE

In a nutshell, ESG concerns the material impacts, positive and negative, of a business or sector on people and the environment, and how the external world impacts on the business or sector[11]. To quantify or describe these impacts, organisations use sustainability reporting to improve their environmental (including carbon) and social footprint over time.

The ESG concept was coined in 2005[12], and since then its use has grown exponentially, particularly from 2018[13].

ESG differs from earlier, voluntary approaches to sustainability, e.g., "triple bottom line" and "corporate social responsibility"[14]. ESG is a response to the threats, risks and opportunities to businesses posed by their stakeholders. They include government policymakers and regulators, financial markets[15], customers, local communities and indigenous people, environmental NGOs, and people seeking rewarding and ethical careers.

A related concept is "stakeholder capitalism", which the World Economic Forum (WEF) discussed in a 2020 report[16] that coalesces several international reporting standards for sustainability.

ESG allows entities to position themselves in a sustainability-conscious world, in which trade-offs and dilemmas are inevitable, and which can be solved, methodically and transparently[17]. Note that the ESG approach accepts the profit motive remains paramount for businesses. By adopting "enlightened self-interest", the social and environmental aspects are also important.

In the case of concrete, the industry has a positive and verifiable story to tell, of rapidly decarbonising and otherwise reducing its environmental footprint.

Bringing this together allows businesses/sectors to challenge the polarised, adversarial debate on many issues in New Zealand, and invite a collaborative, informed approach - which the Government itself promotes – to create a positive vision for concrete.

CONCRETE NZ'S ESG RESPONSE

In 2022 Concrete NZ started developing a decarbonisation Roadmap, and a Sustainability Report for the sector. Australasian consultancy thinkstep is carrying out both projects with Concrete NZ as project manager and co-ordinator. Outputs are due later in 2022.

Both workstreams feed into Concrete NZ's government relations, including on New Zealand's first Emissions Reduction Plan[18], and on the case for concrete in building and construction, and in concrete roads and bridges.

Communications is an essential part of Concrete NZ's advocacy in this space. A portion of BRANZ, and Ministry of Business, Innovation and Employment (MBIE) funding for the decarbonisation Roadmap is allocated to its promotion.

Decarbonisation Roadmap

Underpinning the decarbonisation Roadmap is Concrete NZ's support for the Government's goals for climate change action, i.e., net zero carbon Aotearoa New Zealand by 2050. Thus, we are aligning with the GCCA, which produced in 2021 a decarbonisation roadmap that applies to the sector worldwide[19].

Further inspiration comes from the progress the New Zealand sector has made to date. Between 2005 and 2018 the New Zealand cement and concrete sector reduced CO_2 emissions by 15 percent, against a 13 percent volumetric increase in ready-mixed concrete production over that time[20]. Thinkstep verified the data in early 2020, and is updating this report.

This success has led Concrete NZ, in consultation with members, to set emissions reduction targets of 30 percent by 2030, and net zero carbon by 2050.

The GCCA report identified several levers or pathways for CO_2 emissions reductions. The thinkstep work will evaluate these for applicability and impact in the New Zealand context. Levers include lower-emissions kiln fuels and other savings in clinker production; supplementary cementitious materials; concrete design; transport emissions; and electricity.

Sustainability Report

In April 2021 Concrete NZ's Sustainability Committee met online to approve management's proposal to develop a pan-industry Sustainability Report, and to conduct a materiality assessment on the sector's impacts on people and the environment. The overall approach was consistent with an international standard, the Global Reporting Initiative. The material topics the sustainability committee chose are: energy and emissions; freshwater; built environment; health and safety; socio-economic benefits; and waste and circular economy. On the last, the significant advances the industry is making also contribute to CO_2 emissions reductions.

Subsequently Concrete NZ developed metrics for quantifying the above, and consulted on the list with the ready-mixed concrete sector. We will be collecting data from New Zealand's 10 largest cement and concrete companies to begin with.

In August 2022 Concrete NZ finalised a contract with thinkstep to produce a New Zealand cement and concrete industry Sustainability Report. Thinkstep will be linking reporting on the six identified material topics with the relevant UN SDGs and related targets, to place our sustainability journey into an international context.

The first Sustainability Report constitutes an industry baseline. In successive reports, Concrete NZ will develop a time series of data and descriptive information, and over time this will allow the identification of any trends, areas where the sector can improve, and importantly, document our sustainability journey.

CONCLUSIONS: BENEFITS FOR THE CEMENT AND CONCRETE SECTOR

ESG is increasingly a must-do approach to business in a world of tightening regulation, and rising societal expectations of the private sector, including the energy and emissions-intensive cement and concrete sector.

Ultimately, ESG is about company or industry performance and transparency, and requires monitoring, measurement and reporting. Many companies in our sector are already pursuing decarbonisation, obtaining Environmental Product Declarations, and/or are preparing their own sustainability reports, e.g., in no particular order: Allied Concrete[21], Fletcher Building[22], and LafargeHolcim[23].

The New Zealand concrete industry is expressing our sense of purpose in an ESG-driven world, not before time. Larry Fink, founder and CEO of Black Rock, a US$10 trillion investment fund, wrote in 2022 in his annual letter to company CEOs: “Putting your company’s purpose at the foundation of your relationships with your stakeholders is critical to long-term success”[24].

In May 2022 Prime Minister Rt Hon Jacinda Ardern met Black Rock in New York, while leading a New Zealand trade delegation to the US. Although there was no mainstream media coverage of the event, it seems likely that Black Rock’s requirements for climate change and sustainability disclosures of the companies it works with formed part of the agenda.

Concrete NZ and the sector we represent will benefit from this juncture in world affairs, and in domestic politics and policy. Via the pan-industry decarbonisation Roadmap and the Sustainability Report, we will be able to insert cement and concrete firmly into the sustainability conversation underway in New Zealand. Examples include implementation of the Emissions Reduction Plan, the Building for Climate Change Programme, and a programme of work at Waka Kotahi to write concrete specifications for its Highway Structure Construction Guide.

At the forefront of Concrete NZ’s work are good information, and constructive engagement with government and other stakeholders as we pursue “green concrete”, and gain increasing recognition for the industry’s work to reduce our environmental and CO_2 footprint. Improved policy settings; and better knowledge of concrete among specifiers of materials, designers and builders of infrastructure and other construction are measures of success.

REFERENCES

1. Chatham House (2018). *Climate change: the massive CO_2 emitter you may not know about*. BBC News, 17 December 2018
2. Global Cement and Concrete Association (2021). *Our concrete future*. GCCA
3. United Nations Organisation (2015). *Sustainable Development Goals*. United Nations Environment Programme
4. Concrete NZ (2022). *Concrete and the UN SDGs*. Unpublished
5. New Zealand Treasury (2021). *Living Standards Framework*. The Treasury
6. Concrete NZ (2020). *Building for Climate Change: Transforming Operational Efficiency and Reducing Whole-of-Life Embodied Carbon*. Submission, Concrete NZ
7. Ministry for the Environment (2022). *Draft National Adaptation Plan*. MfE
8. Concrete NZ (2022). *Adapt and Thrive: Building a Climate-Resilient Aotearoa New Zealand & Draft National Adaptation Plan*. Submission, Concrete NZ
9. Ministry for the Environment (2022). *Adapt and thrive: Building a climate-resilient New Zealand – New Zealand's first national adaptation plan*. MfE
10. Netley, J. (2022). *Engineered timber highway bridges*. Presentation to the 2022 NZ Bridge Summit, Waka Kotahi NZ Transport Agency
11. Aggregate and Quarry Association (2022). *Road Map for the Aotearoa New Zealand Quarry Sector*. AQA
12. Kell, G. (2018). *The remarkable rise of ESG*. Forbes
13. Neufeld, D. (2021). *Visualising the sustainable ETF universe*. Visual Capitalist
14. Shergold, S. (2021). *Webinar: Risk or opportunity? What is ESG and why should you care?* Dentons
15. Pomeroy, R. (2022). *ESG - how can we measure how ‘good’ companies are?* World Economic Forum

16. World Economic Forum (2020). *Measuring Stakeholder Capitalism Towards Common Metrics and Consistent Reporting of Sustainable Value Creation*. WEC
17. Australasian Institute of Mining and Metallurgy (2022). *Professional certificate course: ESG and social performance*. AusIMM
18. Ministry for the Environment (2022). *Emissions Reduction Plan*. MfE
19. Global Cement and Concrete Association (2021). *Our Concrete Future*. GCCA
20. Concrete NZ (2020). *Concrete industry on track to meet emissions reduction target*. Media statement, Scoop
21. Allied Concrete Ltd (2019). *Sustainability report 2019*. Allied Concrete
22. Fletcher Building Ltd (2021). *Building Momentum: Annual Report 2021*. Fletcher Building
23. LafargeHolcim (2021). *Integrated Annual Report 2020*. LafargeHolcim
24. Fink, L. (2022). *Letter to CEOs: the power of capitalism*. Black Rock

concretenz BUILDING RESILIENCE
CONFERENCE 2022
13-15 October 2022
Energy Events Centre | Rotorua

HAWKES BAY AIRPORT TERMINAL REDEVELOPMENT

J. BEHAN; J. JACKS; B. CORNELL

WSP, Wellington, NZ

SUMMARY

With the bold aspiration of being New Zealand's most vibrant and successful regional airport, for the last few years Hawkes Bay Airport has been growing physically and strategically to meet that goal. A crucial part of that growth is the redevelopment of the terminal, which will greatly enhance and bolster this key infrastructure asset for the Hawkes Bay region. The terminal utilises a combination of precast concrete wall panels and structural steel frames that provided the benefits of off-site fabrication, speed of on-site erection, strength, stiffness and robust connection detailing to future-proof the resilience needs of the airport.

This paper discusses the technical structural design process, project challenges, NZBC compliance changes to cast-in elements during the construction phase and the team's solutions for completing an operational airport terminal.

INTRODUCTION

In late 2015, WSP New Zealand Ltd (WSP) was engaged by Hawkes Bay Airport Ltd (HBAL) to undertake structural, mechanical, electrical and civil engineering services for HBAL's Terminal Expansion project. The design phase was completed in mid-2017 and in late 2017 the construction contract was awarded to Arrow International Ltd (Arrow). The terminal construction works began in January 2018 and are due for completion mid-November 2021. HBAL's Entry Forecourt project, which links the WSP-designed carpark to the Terminal, is due for completion in early 2022. Figures 1 and 2 show perspective views of the WSP Revit model.

Figure 1. Terminal perspective views WSP's Revit model viewed from the Southeast

Figure 2. Terminal perspective views WSP's Revit model viewed from the Northeast

Project Brief

HBAL's initial brief for the design team was that upon completion, the project would provide an extended terminal, designed to Importance Level 3 (IL3), with architectural wow-factor that high-lights the local culture, along with the creation of new drop-off/pick-up areas. The project would provide a new terminal experience with Hawkes Bay hospitality/retail in the central area of the terminal. The central area would be buffered at the North end by the new arrivals, baggage claim, anchor retail space and car rental area and at the South end by the departures area, check-in, BOH / baggage hall and airline offices, all while still allowing for future growth. It was essential for the airport to remain operational throughout the refurbishment, which required careful planning and phasing to ensure operations could run as normal. Factored into the planning and phasing was the requirement for the airline check-in areas to be relocated to the southern end of the terminal, with a new automated baggage collection system installed at the northern end.

Project Team

Over the 6 years of the project, the design team and the Main Contractor changed for various reasons. Table 1 below includes the main team members, with those members that completed the project shown in bold text.

Table 1. Project Team

PROJECT TEAM	
Principal:	**Hawkes Bay Airport (HBAL)**
Project Manager:	Impact Project Management; Integrating Architecture
Main Contractor:	Arrow International; **Hawkes Bay Airport Construction Ltd (HBACL)**
Main Subcontractor/PM:	**Tararua Construction Management (TCM)**
Quantity Surveyor:	MCC Cost Management; **Millard Construction Cost Consultants & PB Consult Ltd**
Architect:	**Designgroup Stapleton Elliott - formerly Paris Magdalinos Architecture (PMA)**
Landscape Architect:	**Mauvan Scott**
Structural Engineer:	**WSP New Zealand Ltd (WSP) – formerly Opus International Consultants**
Structural Peer Reviewer:	**Geoff Kell Consulting**
M&E Engineer:	**WSP**
Civil Engineer:	WSP**; Infir**
Fire Engineer:	**Holmes Fire**
Geotechnical Engineer:	**Tonkin & Taylor (T&T)**

The most significant change to the project's team was that of the Main Contractor, Arrow International, when they went into voluntary administration in early 2019. However, due to some early warning signs and quick action by HBAL and their advisors to address the risk, HBACL was set up and became the new main Contractor. The existing Arrow International

project manager formed TCM, and their quantity surveyor formed PB Consult. Both TCM and PB Consult and all of the other sub-contractors were secured for the remainder of the terminal's construction works. In all, only approximately 5 weeks of down-time resulted on site and there were many benefits that resulted from this significant change to the construction phase of the project.

Site Location

Located just North of the Napier suburb of Ahuriri, Hawkes Bay Airport is sited on the former Ahuriri Lagoon, part of an area that was raised above sea level up to 1.5m by the 1931 Hawkes Bay Earthquake.

BUILDING DESCRIPTION

The completed terminal is approximately 135m x 34m footprint and has increased in size by approximately 70%. The North end is single storey, as is the South end, while the majority of the central hospitality precinct is a two storey structure. For building footprint comparison of before and after works, Figure 3 below shows a ground floor plan image from a 2002 extension design by Opus, along with a 3D image of the final 2021 structure taken from the steel detailing model in 2021, courtesy of the Napier-based steel fabricator, Red Steel.

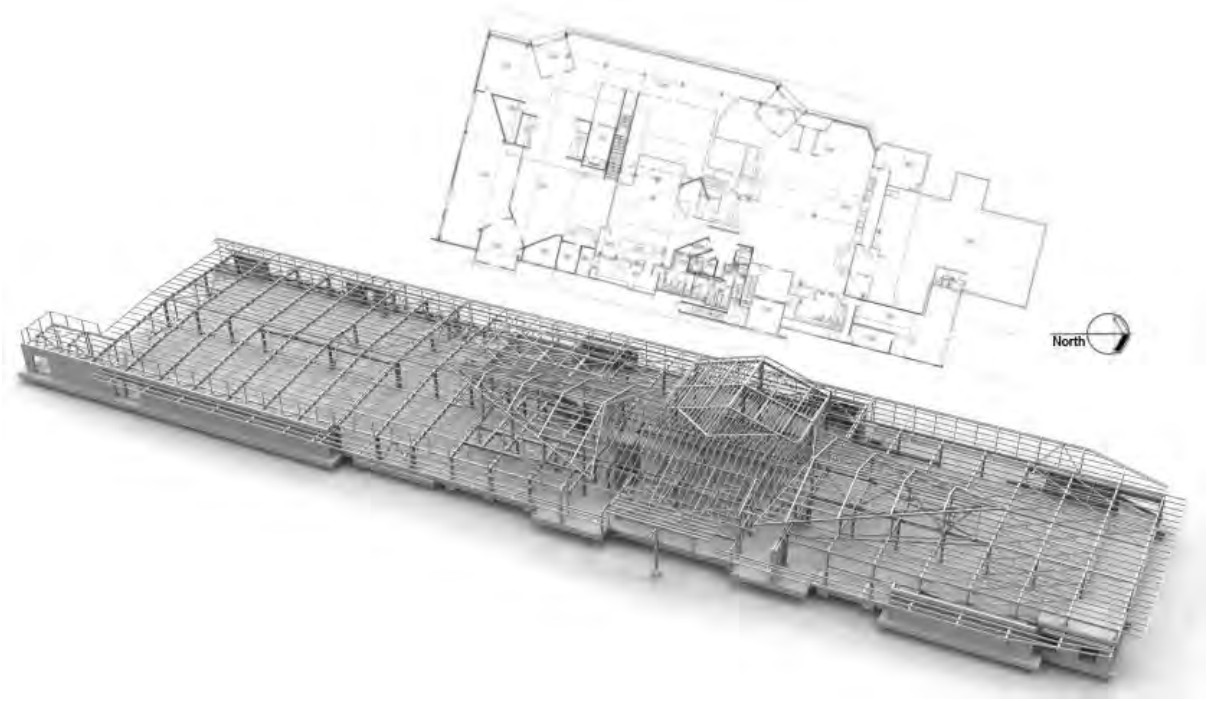

Figure 3. Above - terminal plan pre-construction. Below - steel model 3D perspective view

During the design phase and for the majority of the construction phase, the intention was to maintain and use a large proportion of the existing steel structure. However, as the construction phase progressed, it was determined that there were sufficient benefits to the project in demolition of existing structure, fabricating off site and installing new structure. In the end, of the existing terminal building prior to the construction works beginning, it was only 6 columns and associated floor beams that support the Regional Lounge and the 2014 lift structure that remained. The rest of the building's superstructure is new.

Geotechnical Parameters & Foundations

The geotechnical conditions and design parameters were described in detail in the T&T geotechnical report, which recommended shallow foundations, suitable for the soils encountered at this site. The risk of liquefaction and lateral spreading at this site was assessed

as low and the site was generally categorised as subsoil “Class D – Deep Soil” in accordance with NZS 1170.5.

A shallow foundation solution was adopted following these recommendations. For the higher foundation design loading, the foundation preference was for wide ground beams to meet hold-down and soil bearing requirements. This avoided the likely high costs of multiple establishments and disestablishments for a piling contractor on a potentially staged construction project to suit the decanting of an operational airport. The risk of high tidal water table was another reason to adopt shallow foundations. New slab-on-grade forms the floor structure of the majority of the terminal ground floor, having removed all of the existing timber framed ground floor structure and leaving only a relatively small portion of existing slab-on-grade in the central area below the new mezzanine. Reinforced concrete pad foundations are provided below portal frame columns and gravity posts, which are typically tied together by tie beams. Large grounds beams support steel concentrically braced frames (CBFs) and precast concrete shear walls, as shown in Figure 4, a photograph taken at the Southwest elevation.

Figure 4. Photograph of PC Wall panels on large ground beams. Control tower beyond.

Gravity Superstructure

The gravity support structure is primarily of structural steel using portal frames, gravity beams and transfer structure where columns would clash with baggage handling systems and the like. The Plant and MSB Rooms located at the Northeast corner are formed by concrete blockwork masonry with ceilings formed by precast concrete flat slab and insitu concrete topping for acoustic insulation and fire resistance purposes.

The three separate upper floor areas in the central precinct that house the mezzanine waiting area, Air New Zealand Regional Lounge and HBAL’s office are steel moment frame, braced frames and gravity frames with timber floor joists.

The various roof areas are framed by a mix of cold-formed steel DHS purlins, timber and LVL rafters/purlins, and timber trusses over some of the Regional Lounge, all supported by structural steel frames.

Lateral Load Resisting Systems

The terminal’s structure has been designed as an elastically responding structure for IL3-associated design loading. Steel connections for the two storey areas of the building have been designed for MCE loading due to the complication of combining existing and new structure and for life safety in the event that the design level earthquake, relating to a 1000 year return period for this IL3 building, is exceeded. Robust connection detailing was used to support the resilience requirements of the designed Importance Level.

Typically, steel moment-resisting frames are provided in the transverse (East-West) direction for the single storey and two storey areas and in some areas of the South end steel CBFs are provided where stiffer structure was required.

For much of the single storey areas, precast wall panels are located on perimeter wall lines where they perform as stiff shear walls for the longitudinal (North-South) direction and also to celebrate local Maori themes by way of carefully planned and set-out patterns, as shown in Figure 4 above.

An example of the profiled steel formwork used by Lattey Group to produce these special wall panels is shown in Figure 5.

Figure 5. Photograph of steel formwork for the feature PC Wall panels

A strong influence in the use of precast wall panels for the structure was the airport's precast concrete predecessor – the control tower, built circa 2002 using 175mm thick and 17m tall PC panels. The control tower's structural design was provided by Carl Ashby, now WSP's Structures Director – Wellington, and architectural design by PMA Architecture. It was quite fitting that both Carl and PMA would later play their part in the architectural wall panels for the terminal's redevelopment.

Elsewhere, stiff structural elements were provided by steel braced frames.

Roof structural steel cross bracing is provided in the lower roof area, plywood diaphragm is provided to the skillion roof over the West end of the Regional Lounge and strap-type bracing is provided to the roof trusses over the East end of the Regional Lounge. Roof bracing is utilised to transfer loads to the vertical lateral load resisting structures and also to even out some of the transverse displacements where different stiffnesses of adjacent moment-resisting frames occurred.

The North Arrowhead roof structure is formed by upper transverse steel moment-resisting frames over the arrival lounge's main moment-resisting frames. LVL feature roof structure is incorporated along the spine of the North Arrowhead, as shown in Figure 6. Longitudinal steel bracing is provided in the perimeter walls.

Figure 6. Photograph of structure within the North Arrowhead, looking South.

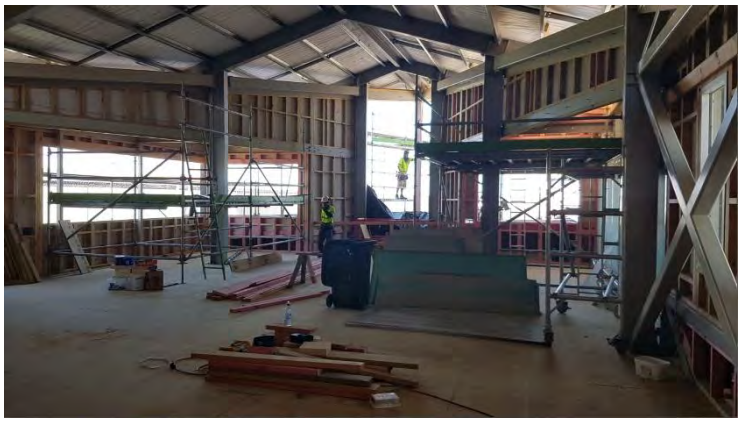

The two storey South Arrowhead structure is formed by transverse steel moment-resisting frames and is braced in the longitudinal direction by steel CBFs. A view taken within the upper level of the South Arrowhead, where the HBAL office will be, is shown in Figure 7.

Figure 7. Photograph of structure within the South Arrowhead, looking South.

CULTURAL INFLUENCE ON STRUCTURAL SOLUTIONS

Hawkes Bay Airport is a key threshold and gateway for much of what happens in the region, be it social, environmental, financial or cultural. For the terminal's visual form, it was important that upon arrival and throughout their visit, passengers and welcoming whānau should experience strong representations of the region, to the point that the terminal's visual form was made to reflect the Hawke's Bay wider context and stories. Designgroup Stapleton Elliott collaborated with local artist Jacob Scott of Mauvan Scott and representing Mana Ahuriri. Inspiration was drawn from the Kuaka (godwit) bird, which nests at the tidal flats of the nearby Ahuriri estuary. The long slender terminal with steel framed arrowhead-like roof projections facing North and South has been designed to emanate the wings of the Kuaka in flight. In earlier times the annual return of the Kuaka to Aotearoa from the North was considered by Maori as a great event, with the bird featuring prominently in mythology as a bird of mystery.
Early in the concept design phase it was considered whether the North and South arrowhead roof projections might be formed by use of timber framing or engineered timber, but the resulting overall thickness for the long cantilevering spans were excessive and did not meet the aesthetic requirements of slenderness.

Structural steel was the choice of material that provided the slender and stiffness needs of the "wings" and it also allowed large, fabricated sections of the arrowheads to be erected in one go. The North Arrowhead's fabricated tip by Red Steel is shown in Figure 8. The large, fabricated sections had the knock-on benefit of minimising the erection time and thereby reducing the hazards of working at height.

Figure 8. Photograph, courtesy of TCM, of the North Arrowhead's tip looking south.

The almost complete terminal's East elevation is shown in Figure 9 below.

Figure 9. Photograph of the terminal's East elevation at the central region. North and South Arrowhead structures prominent.

The cultural architectural features of the precast wall panels created another early design challenge for the structural team due to their varied projection beyond the main structural section of the wall panels. Their overall thickness added a considerable amount of additional mass to be resisted by the steel moment-resisting frames, which exacerbated lateral displacements when subjected to earthquake actions. Part of the solution was to provide partial fixity of the wall panels at their base by sandwiching them between two halves of large ground beams and also to provide sufficiently stiff steel moment-resisting frames.

The two halves of the wall panel's ground beams were tied together with Reid bars with flange nuts for anchorages at the bar ends. Refer to Figure 10. The inside half of the ground beam was tied into the concrete slab.

During the construction phase, Amendment 3 of the Concrete Structures Standard NZS 3101:2006 was issued. It relates to the use of cast iron mechanical anchorages. In essence, it resulted in a change during the construction phase to the material of the Reid bar flange nuts and half nuts used and how they were to be installed. Close collaboration with Lattey Group for the precast wall panel reinforcing and with TCM for the insitu concrete works aided in lead times and the smooth transition from cast iron anchorages to steel anchorages with associated epoxy fill.

Figure 10. Photograph of Eastern half of reinforcing cage of wall panel ground beams.

Careful attention was given to concrete covers to reinforcing and concrete mix designs to address the relatively high tidal water table and the harsh coastal environment. Following return of the construction team to the site once HBACL became the Main Contractor, much of the lower reinforcing in foundation excavations was washed down due to the build-up of salts from the tidal water.

The pattern for the features on the precast wall panels was closely coordinated between Designgroup Stapleton Elliott and WSP and sufficient set-out provided to Lattey Group to make it a reality. Figure 11 shows an Eastern part-elevation of the feature wall panels at the South end.

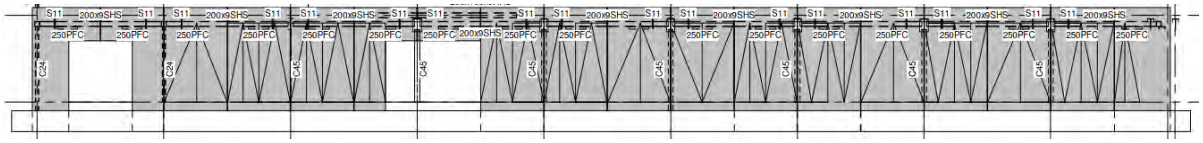

Figure 11. Feature PC wall panels on East elevation, from WSP's structural drawings.

The challenge for forming the feature thickenings on the structural sections of the wall panels was solved by use of “Z bars” of varying thickness tied into the structural reinforcing cage and an outer layer of mesh of closely spaced wires. These are shown in the Figures 12,13 and 14.

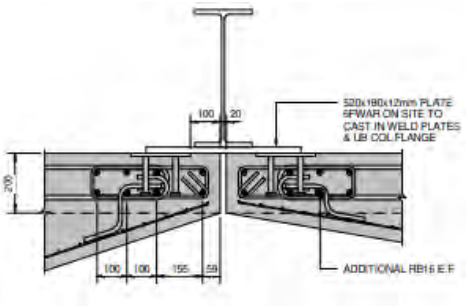

Fig 12. Horizontal cross section through a feature PC wall panel.

Fig 13. Photograph of reinforcing “Z bars” being tied for a PC wall panel.

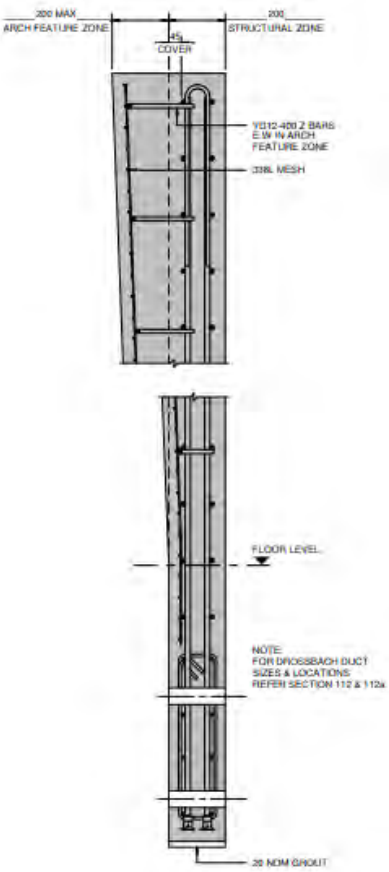

PROJECT CHALLENGES

The Hawkes Bay Airport terminal redevelopment had many challenges, not least of which was the liquidation of the original Main Contractor and other changes to the project team, along with the effects of Covid 19. These all had an effect on the longer than anticipated construction period. There were various other challenges and many lessons learnt, but the following relate to design changes and implementation of the solutions.

It was essential that the airport remain operational throughout the refurbishment, which created significant challenges for sequencing the design and in particular for the construction phase. Additionally, the overall scale of development was changed several times during the design phases. More significant changes occurred partway through construction, via the airport’s instruction in mid-2018 to increase the Southern extension by a further three bays and the Air New Zealand Regional Lounge by a combined 540 m^2. The increase was driven by forecast growth in passenger movements through the terminal, the strong likelihood of future security screening requirements, and additional flight announcements by two incumbent airlines with the potential for new revenue opportunities.

Fig 14. Vertical cross section through a Feature PC wall panel.

The challenges the delivery team faced from the decision to provide additional space resulted in fast-tracking an updated design, while at the same time maintaining construction monitoring services.

The solution involved splitting the design packages and phases of construction works into three main stages:

- Stage 1, opened in January 2019, delivered the new Northern terminal, providing a dedicated arrivals gate, baggage claim area and a rental car concierge.
- Stage 2, opened in November 2019, delivered a new Southern terminal with new airline check in, baggage handling system, airline offices, cargo area and dedicated departures gate.
- Stage 3, opened in early August 2021, delivered an upgraded central hospitality and retail area. The final portions of the terminal's ancillary works, cladding install and fitout construction for Stage 3 is due for completion in mid-November 2021.

Adopting a staged design approach, the design team, the airport and contractors collaborated closely, which ensured that construction continued while a redesign of the terminal occurred in the background.

WSP's structural team became, temporarily in mid-2018, the lead consultant by firstly undertaking a concept design for the increased Southern extension and central hospitality and retail area, with an additional seismic gap between both areas.

Combined with the already seismically separated North end, this resulted in three separate structures, making it easier for staging the design, consenting, construction and decanting.

COLLABORATION WITH THE CONTRACTOR

During early 2020, during Stage 3, there were further significant design changes with the decision to demolish the existing HBAL office over which the South Arrowhead was to be constructed and construct a new structure due to the benefits of off-site construction. A new design for the front entry canopy was also undertaken in 2020. Thankfully, the design team's models and drawing documentation was fully coordinated during the initial consented design and a period of value engineering was utilised once the original Contractor, Arrow International, was brought on board. As large changes were made during the construction phase, the design team's documentation continued to be coordinated.

However, for the revised South Arrowhead structure and the new front entry canopy it became more efficient for Red Steel's steel detailer to document the revised structure based on WSP's sketches, supplemented with close coordination via regular remote detailing workshops using the Tekla model. The reason for this approach was that the steel detailer's model was more up to date than WSP's Revit model, which was effectively frozen in early 2019 following the delivery of WSP's Stage 3 drawings. The result of utilising Red Steel's detailing capability was a package of documentation that was as realistic as possible with respect to set-out, members fitting and buildability.

OFF-SITE FABRICATION

The opportunity to fabricate off-site all of the precast concrete for wall panels and the ceiling panels over the plant and MSB rooms, along with the structural steel of the new North end of the terminal was well understood early in the design and Stage 1 construction phase. It was expected, initially, that the South end phase of work would include a mix of new and existing steelwork. However, when the three-bay extension to the South end was announced in mid-2018 and the three stage solution was adopted, Red Steel highlighted the opportunity to speed up construction by removal of the last of the existing steel portal frames in the current South end and fabricating new replacement steel frames off-site.

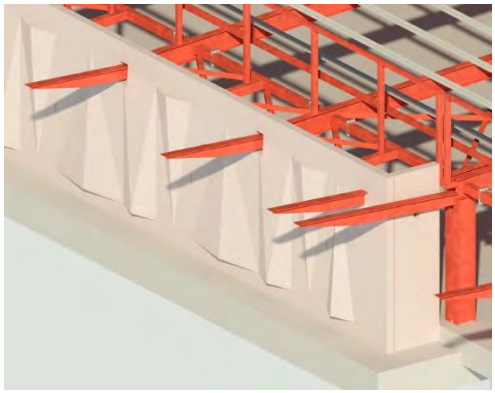

Off-site fabrication would also result in far less site welding and hence overall improved quality of fabrication under controlled environmental conditions. This solution for speedier construction was adopted again when the decision was made in early 2020 to replace the existing HBAL office structure below the proposed South arrowhead with a new steel structure.

That decision to demolish and fabricate off-site had another advantage – removal of unknown existing members and their potentially poor conditions.

Fig 15. Render from WSP Revit model showing PC wall panels and structural steel, all fabricated off site

The precast concrete wall panels were also fabricated off site to aid construction speed and sequencing, as well as to ensure high quality and to not take up valuable lay-down area at an operational airport site.

CONCLUSIONS

The Hawkes Bay Airport terminal redevelopment is an exciting landmark project for the Hawkes Bay region providing a new terminal experience that showcases Hawkes Bay hospitality and retail with a strong local and cultural theme. The terminal design is a careful blend of structure, architecture and culture, while also ensuring structural robustness, resilience and future proofing is provided, along with durable materials that are easily maintained in a harsh coastal environment.

Instead of hiding the elements of strength, HBAL and Designgroup Stapleton Elliott made the bold move to expose and thereby celebrate much of the structure, while at the same time ensuring that key local cultural narratives of Mana Ahuriri are communicated at this important gateway to the Hawkes Bay region. The feature precast wall panels is just one example of this. From an airport operational perspective, the expanded terminal with automated baggage collection system, along with re-modelled departure and arrivals gates, will increase capacity significantly and improve the feel and flow of the airport for passengers. Crucially, it meets the airport's current and future operational needs. The result is a beautifully crafted structure that strongly aids HBAL's aspirations of being New Zealand's most vibrant and successful regional airport.

ACKNOWLEDGEMENTS

This project was a success largely due to the close collaboration between HBAL and the design and construction team who continued to work through and resolve challenges with determination and great skill and at all times with a "best for project" approach.

The authors would like to thank and congratulate the following teams for their significant contributions to the project: The WSP wider group (Keegan Hampshire, Matthew Gonzalez, Ryan Baker, Carl Ashby, Mariusz and Mariusz Tarnowski), HBAL (Stuart Ainslie, Gareth Mentzer et al.), Andrew Millard from MCCCL, Designgroup Stapleton Elliott (Chris Ainsworth, Alison Miranda et al.), TCM (Callum Sutherland, Kevin Hinton), PB Consult (Paul Banister), GSB (Graham Scarf et al.), Integrating Architecture (Steve Birkhead et al.), Lattey Group (Richard Flanagan et al.), Red Steel (Bob Hawley, Bill Halpin et al.) and Kadmon Ltd (Dave Smith, steel detailer).

concretenz
BUILDING RESILIENCE
CONFERENCE 2022
13-15 October 2022
Energy Events Centre | Rotorua

PROPOSED TEST PROGRAMME FOR CONCRETE-FILLED METAL DECK APPLICATIONS: BRIDGING THE GAP FOR ETA APPROVED MECHANICAL ANCHORS

EMANUELE NACCINI[1]; ENRIQUE DEL REY CASTILLO[2]

[1] Reid Construction Systems
[2] University of Auckland

SUMMARY

Post-installed anchors used for the restraint of engineering systems as per NZS/4219, must be qualified for seismic loading in accordance with ACI 355.2, but approved and designed according to ETAG 001 Annex E and TR 045 respectively, if using NZS 3101. The majority of anchors available in New Zealand have an ETA seismic approval, which doesn't cover applications on the soffit of composite steel deck floor units, a very common application. We propose an approach and methodology to determine the relevant design parameters, including seismic tension and shear, of ETA approved anchors by following the provisions of AC193 for concrete-filled metal deck applications testing and results interpretation.

INTRODUCTION

Post-installed mechanical fasteners, typically made of steel, are installed into hardened concrete to transfer loads from either structural or non-structural elements into the concrete structure. Multiple types of mechanical fasteners are available on the market, but the most commonly used for the applications discussed in this paper are concrete screws and torque-controlled expansion anchors, both of which require a hole predrilled into the concrete substrate (figure 1, left). Concrete screws are screwed inside the hole and the thread of the fastener cuts its way into the concrete substrate thus forming the required mechanical interlock (Figure 1, centre). Expansion anchors are set by pulling a conical bottom nut inside one or more sleeves through the application of torque, which expands the sleeve(s) against the sides of the hole, thus causing the expansion and the mechanical interlock (Figure 1, right).

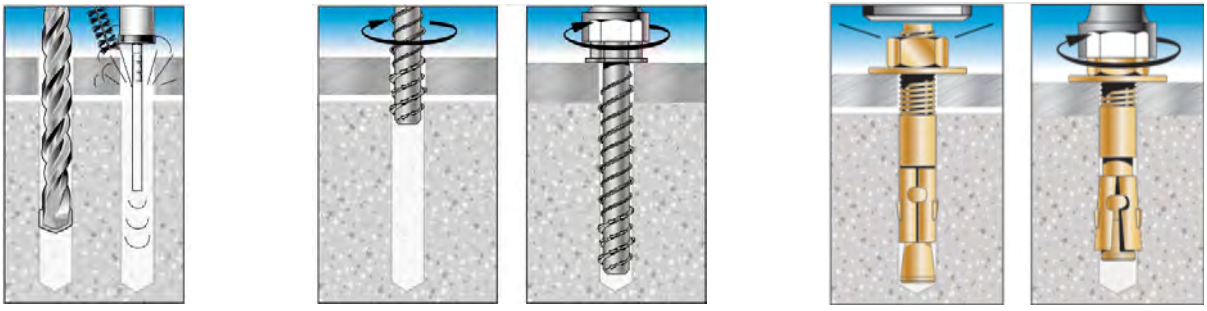

Figure 1. Typical post-installed fasteners installation: predrilled hole (left), concrete screw installation (centre), torque-controlled expansion anchor (right)

The application discussed in this paper is when these fasteners are installed in the soffit of concrete-filled metal deck floor units to support and brace non-structural engineering services such as cable trays and sprinkler systems. Figure 2 shows an example of concrete screws installed in the upper flute and lower flute positions.

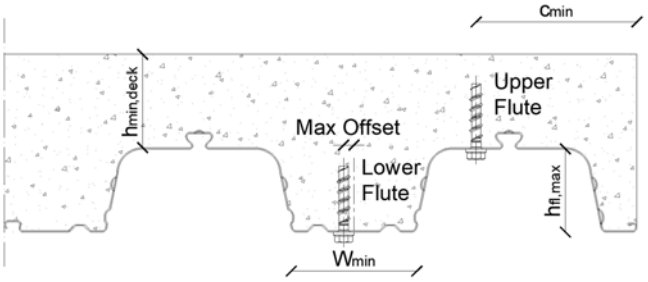

Figure 2. Example of anchors installed in the soffit of concrete filled metal deck floor

REQUIREMENTS FROM THE NEW ZEALAND REFERENCE STANDARDS

For the above-mentioned applications of post installed mechanical anchors, the main reference standards in New Zealand are NZS 3101, NZS 4219 and NZS 4541.

NZS 3101:2006 A3 “Concrete structures standard”

Prior to the release of its third amendment in 2017, NZS 3101 included post installed mechanical anchors in the scope of Chapter 17 with similar provisions to cast in anchors. Amendment 3 modified the requirements for post installed anchors, departing from those of cast in anchors. Clause 17.5.5 requires post-installed anchors to “pass the prequalification testing stipulated in ETAG 001, Annex E and be designed in accordance with EOTA TR045”. ETAG 001 is a guideline for European technical approval of metal anchors for use in concrete, and Annex E specifically addresses seismic action. This standard was superseded by EOTA TR049, which in turn is now included in EOTA EAD 330232-01-0601 “Mechanical fasteners for use in concrete”. EOTA TR045 is a technical report providing guidance for design of metal anchors for use in concrete under seismic actions, which is now superseded by EN 1992-4 “Design of fastenings for use in concrete” that also includes verification for seismic loading. The use of post installed anchors with a European Technical Approval (ETA) for seismic loading has become prevalent in New Zealand since 2018, when NZS 3101 A3 was cited by the Building Code.

NZS 4219:2009 “Seismic performance of engineering systems in buildings”

Clause 3.10.5 requires for all post-installed and proprietary anchors used for restraint of engineering systems components to have passed the seismic qualification test stipulated in ACI 355.2 “Qualification of post-installed mechanical anchors in concrete and commentary”. ACI 355.2 prescribes the testing and evaluation requirements for post-installed mechanical anchors intended for use in concrete design under the provisions of ACI 318. For the design of qualified anchors in concrete, NZS 4219:2009 refers to NZS 3101, which cites European Standards as described above.

NZS 4541:2020 “Automatic fire sprinkler systems”

Clause 4.3.13.3.6 requires for post-installed and proprietary anchors to be assessed against seismic loads using either ACI 355.2 or ETAG 001, or otherwise listed by the Sprinkler System Certifier.

THE KNOWLEDGE GAP

The use of concrete-filled metal deck floor units in New Zealand has significantly increased in the last few years, resulting in an increase of post-installed mechanical anchors on these floor units. NZS 4219 requires anchors to pass the seismic qualification tests stipulated in ACI 355.2, but this document does not have provisions for testing and validation of anchors on concrete-filled metal deck floor units. AC 193 is a document produced by ICC Evaluation Service (ICC-ES), which is an industry leader in performing technical evaluations of building products, materials and systems for code compliance in the United States of America. AC 193 sets the acceptance criteria for anchors validated by ICC-ES according to ACI 355.2, and includes some provisions for this type of applications. The issue is that this document is not referenced in the relevant New Zealand Standards discussed above. Additionally, NZS 3101 A3 requires the use of ETA documents, but the European Standards do not include provisions for testing and evaluation of post-installed anchors on concrete-filled metal deck floor units either.

AC 193 "ACCEPTANCE CRITERIA FOR MECHANICAL ANCHORS IN CONCRETE ELEMENTS"

As described above, AC 193 is the only relevant document that has provisions for testing post-installed anchors in steel deck composite floor units. The purpose of AC 193 was to establish requirements for recognition of mechanical anchors in concrete elements in ICC-ES evaluation reports under the International Building Code (IBC section 104.11), and International Residential Code (IRC section R104.11). The criteria include static and seismic loading applications in uncracked and cracked concrete, for both normal weight and light weight structural concrete, and also concrete-filled metal deck floor and roof assemblies, which, as mentioned, is not included in ACI 355.2 nor in any of the EOTA published documents.
The authors would like to point out a couple of observations. First, this document is not published by ACI like other standards (e.g. ACI 318 and ACI 355.2), it is a document published by ICC-ES, which is a certification body and not a recognized industry association like ACI. And second, despite being part of the test programs for evaluation of anchors in cracked and non-cracked concrete, the specific tests for concrete-filled metal deck soffit applications only include static loading conducted on non-cracked concrete condition.
Among the 51 test cases included in this document, only the following two will be relevant for the scope of this paper, which for simplicity is limited to non-redundant soffit applications:

- Test N. 21 from Table 4.2 – Service-condition tension test in concrete fill on deck-soffit installation, single anchor in tension away from edges, non-cracked concrete
- Test N. 22 from Table 4.2 – Service-condition shear test in concrete fill on deck-soffit installation, single anchor in lower flute, shear towards nearest edge of flute, non-cracked concrete.

It is to be noticed that other four test cases are specific for composite steel deck floors but two of those are limited to redundant applications (test N. 13 and 14 from Table 4.3), and the other two are for anchors installed on the top surface of the floor (test N. 15 and 16 from Table 4.2).

AC 193 results interpretation for tension load

AC 193 provides some guidance to calculate the cracked concrete and seismic loading capacity based on the results of the non-cracked concrete static load tests (N.21 and N.22). Clause 10.3 stipulates that the uncracked concrete pull-out capacity from test N. 21 ($N_{p,deck,uncr}$) shall be used to extrapolate the cracked concrete pull-out capacity using the ratio of the pull-out capacities in cracked and non-cracked concrete (from testing with normal concrete slabs):

$$N_{p,deck,cr} = \Psi_{3,pullout} \times N_{p,deck,uncr} = (N_{p,cr} / N_{p,uncr}) \times N_{p,deck,uncr} \quad (1)$$

AC 193 results interpretation for shear load

From clause 10.4, the characteristic shear capacity from test N. 22, $V_{sa,deck}$, will be taken as the steel strength of anchor in shear, V_s, in uncracked and cracked concrete. AC 193 does not mention seismic loading on steel deck applications, but further guidance is included in the ESRs, the evaluation reports published by ICC-ES.

OUR INTERPRETATION OF ICC-ES EVALUATION REPORTS' DATA (ESR)

The authors have reviewed the Evaluation Reports (ESR) produced by ICC-ES for several manufacturers' anchors, validated for composite steel deck seismic applications, and have observed that the following content is consistent across the board.
There is always a clause "4.1.8.2 Seismic Tension", that states that the nominal steel strength and concrete breakout strength for anchors in tension must be calculated according to clause 17.6.1 and 17.6.2 of ACI 318-19 respectively, and the value for nominal pull-out strength in tension for seismic load, $N_{p,eq}$ or $N_{p,deck,cr}$, must be used in lieu of N_p. In other words, for seismic load steel deck applications, the reference pull-out strength is $N_{p,deck,cr}$, which, as per AC 193, is actually the uncracked concrete pull-out strength on steel decks, adjusted for cracked concrete with the factor $\Psi_{3,pullout}$.
There is always a clause "4.1.8.3 Seismic Shear", that states that the nominal concrete breakout and pry-out strength for anchors in shear must be calculated according to clause 17.7.2 and 17.7.3 of ACI 318-19 respectively and the value for nominal steel strength in shear for seismic load, $V_{sa,eq}$ or $V_{sa,deck,eq}$, must be used in lieu of V_{sa}.
Although not explicitly stated, from the published values of the ESR certificates, it can be deducted that the steel deck seismic load capacity is extrapolated from the steel deck static load capacity that is multiplied times the ratio between the seismic load and the static load capacities on concrete slab applications:

$$V_{sa,deck,eq} = V_{sa,deck} \times (V_{sa,eq} / V_{sa}) \quad (2)$$

OUR PROPOSED METHODOLOGY

Enough similarities and overlap exist between the two models, ACI and Eurocodes, that we might be able to bring those two "worlds" closer to each other. Acknowledging that the majority of mechanical anchors available in NZ now come with an ETA certificate, our proposed approach is to conduct the monotonic tests on the uncracked concrete steel deck units, as per AC 193, and to utilize the test results to determine the seismic loading design resistance to be used with the ETA and the Eurocode model. The resulting capacity will be different, depending on the governing failure modes, in tension and shear.

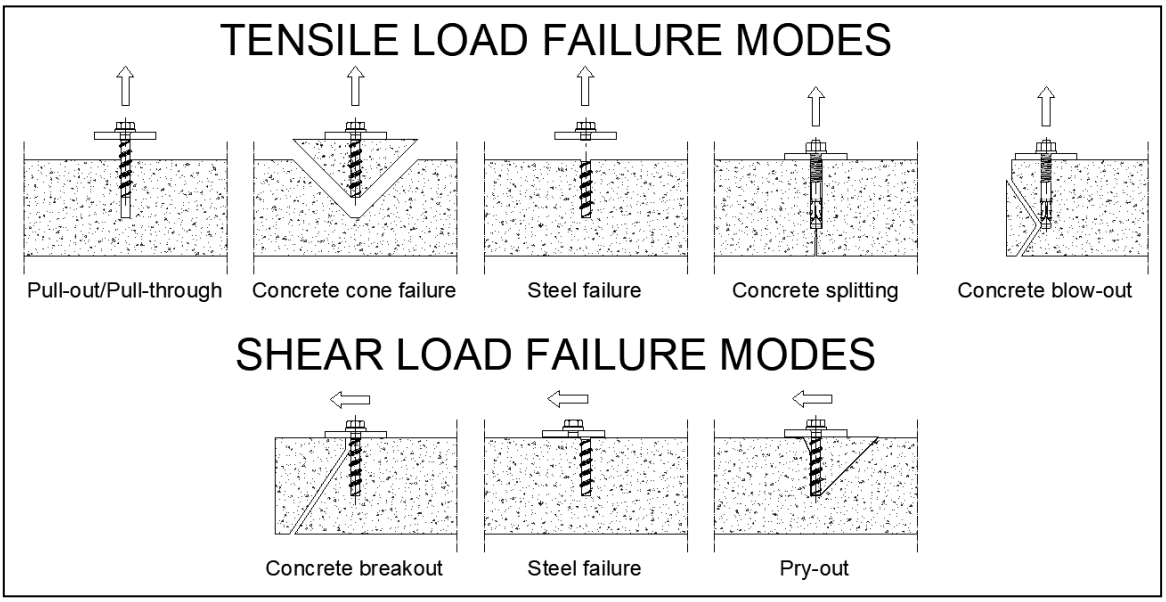

Figure 2. Main failure modes to be considered in tension and in shear

The compressive strength of the concrete might determine which failure modes are governing, so we recommend the test metal deck slabs to be prepared with the lowest concrete class generally specified in practice.
A compressive strength adjustment might be required for concrete failure modes, depending on the difference between the compressive strength of the floor units used for the tests and the ones used for the design or reference. If steel failure governs, and the resulting characteristic capacity is higher than the corresponding value for uncracked concrete in the ETA, the outcome of the test will be considered redundant and the data from the ETA will be used instead.
For seismic load conditions, the ACI model has only one category, which is called simulated seismic load, whilst the Eurocode model has two categories, C1 and C2. The simulated seismic load condition of the ACI model is remarkably similar to that of the seismic category C1 of the Eurocode model, in terms of test conditions and load cycles. On the other hand, category C2 of the Eurocode model, with a larger and pulsating crack width and a tighter displacement tolerance, is much more demanding. As such, the authors have decided to limit the proposed metal deck seismic load capacity to category C1. Both models have specific provisions for fasteners that are used for redundant non-structural applications. However, for simplicity, those have not been included in our proposed method.

TENSION LOAD

The first step is to determine the failure mode and the lower characteristic value (5%-fractile, 90% confidence level) for the ultimate tension load measured on a number of tests conducted on steel deck concrete filled units ($N_{Rk,deck}$), as per test N. 21 of AC 193 above.
For concrete governed failure modes, $N_{Rk,deck}$ is adjusted for the seismic cracked concrete condition and for the concrete strength. And finally, the design resistance is determined applying the appropriate partial and reduction factors, as per EN 1992-4 which superseded TR 045 cited by NZS 3101 A3.

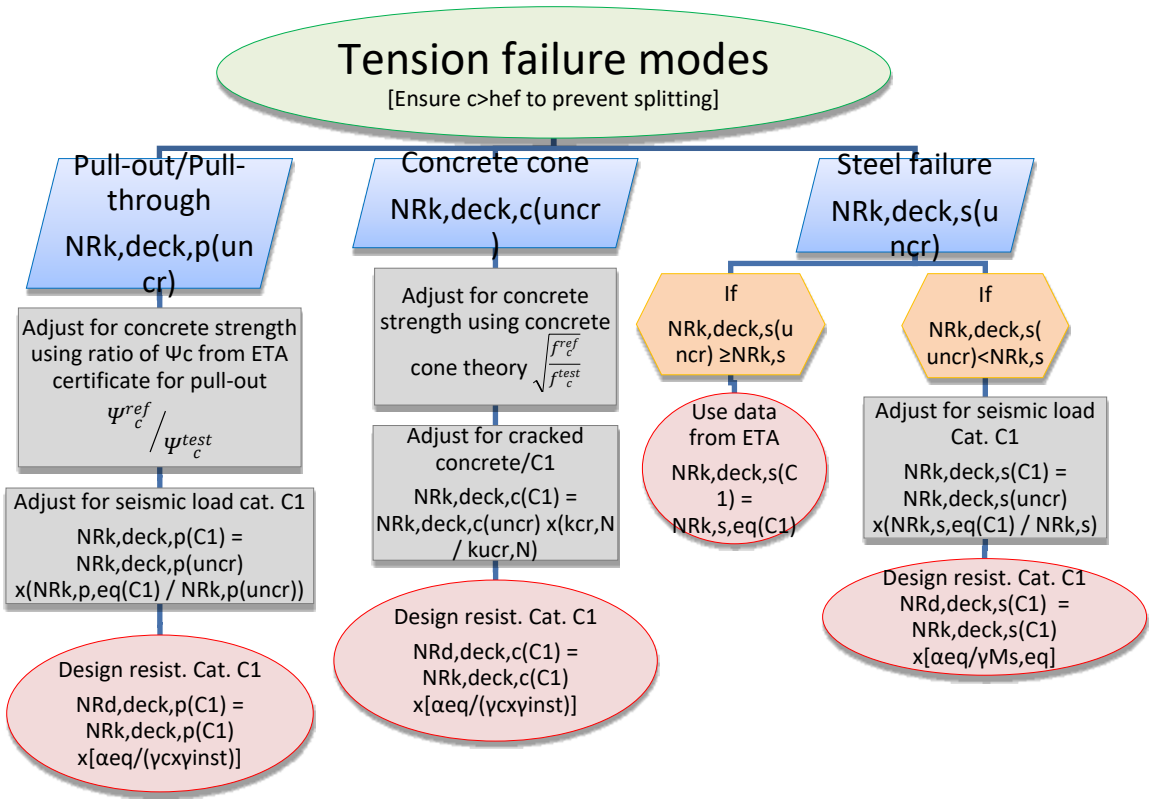

Figure 3. Summary of the proposed methodology for tension loads

Pull-out / pull-through (concrete failure)

The pull-out strength values for non-cracked and for cracked concrete are represented by $N_{Rk,p}^{(uncr.)}$ and $N_{Rk,p}^{(cr.)}$ respectively published in the ETA certificates (Eurocode model). These correspond to $N_{p,uncr}$ and $N_{p,cr}$ respectively on ESR certificates (ACI model). The adjustment for the compressive strength of the concrete is made by the multiplication factor Ψ_c also included in the ETA.
Our proposed approach is to create a new value for pull-out / pull-through capacity in tension for steel deck applications suitable for the Eurocode system: $N_{Rk,deck,p}^{(uncr)}$. When pull-out is the governing failure mode, this corresponds to $N_{p,deck,uncr}$, the lower characteristic value from test N. 21 of AC 193 (non-cracked concrete pull-out failure). Consistently with the Eurocode model, $N_{Rk,deck,p}^{(uncr)}$ shall be adjusted for different values of the concrete compressive strength in accordance with the Ψ_c factors published on the ETA for normal slabs: ($\Psi_c^{(ref)}$ / $\Psi_c^{(test)}$). For cracked concrete, instead of multiplying times $\Psi_{3,pullout}$, which is $N_{p,cr}$ / $N_{p,uncr}$ for the ACI model, we propose to multiply it times $N_{Rk,p}^{(cr)}$ / $N_{Rk,p}^{(uncr)}$:

$$N_{Rk,deck,p}^{(cr)} = N_{Rk,deck,p}^{(uncr)} \times (N_{Rk,p}^{(cr)} / N_{Rk,p}^{(uncr)}) \quad (3)$$

According to the ACI model, $N_{p,deck,cr}$, that in our proposal corresponds to $N_{Rk,deck,p}^{(cr)}$, should be used not just for cracked concrete but also for seismic load applications. To be more conservative, we propose to determine the characteristic pull-out capacity for seismic loading using the category C1 seismic load pull-out capacity, $N_{Rk,p,eq}^{(C1)}$, instead of $N_{Rk,p}^{(cr)}$:

$$N_{Rk,deck,p}^{(C1)} = N_{Rk,deck,p}^{(uncr)} \times (N_{Rk,p,eq}^{(C1)} / N_{Rk,p}^{(uncr)}) \quad (4)$$

For the design resistance:

$$N_{Rd,deck,p}^{(C1)} = N_{Rk,deck,p}^{(C1)} \times [\alpha_{eq} / (\gamma_c \times \gamma_{inst})] \quad (5)$$

α_{eq} = 1 [single fastener] or 0.85 [fastener group] ; γ_c = 1.5 ; γ_{inst} [from ETA cert.]

Concrete breakout (concrete failure)

Concrete breakout failure mode is related to the concrete cone capacity, which is more likely to occur on lower flute positions because the cone may not fully develop depending on the geometry of the flute. This failure mode might be triggered by the proximity to the sides of the flute, particularly if the edge distance is closer than $1.5h_{ef}$. For the ACI model, $N_{b,cr}$ and $N_{b,uncr}$ are the concrete breakout capacity for cracked and uncracked concrete respectively. From ACI 318, for post-installed anchors in normal weight concrete:

$$N_b = (f'_c)^{0.5} \times h_{ef}^{1.5} \times \Psi_{c,N} \quad (6)$$

$\Psi_{c,N}$ = 1.4 [for non-cracked concrete] ; 1 [for cracked concrete]

For the Eurocode model, $N^{\circ}_{Rk,c}$ is the basic concrete cone capacity. From EN 1992-4:

$$N^{\circ}_{Rk,c} = k_1 \times (f'_c)^{0.5} \times h_{ef}^{1.5} \quad (7)$$

$k_1 = k_{cr,N}$ = 7.7 [cracked concrete]; $k_1 = k_{ucr,N}$ = 11 [uncracked concrete]

It's worth mentioning that old ETAs, instead of referring to EN 1992-4, might still refer to ETAG 001 Annex C, which had slightly different values for k_1: 7.2 for cracked concrete, 10.1 for uncracked concrete. Considering all the above, we propose to create a new parameter called $N_{Rk,deck,c}^{(uncr)}$, which represents the lower characteristic value from test N. 21 of AC 193 (non-cracked concrete breakout failure) when concrete breakout is the governing failure mode in tension. Consistently with the Eurocode model, $N_{Rk,deck,c}^{(uncr)}$ is adjusted for different values of the concrete compressive strength with the square root proportion of f_c: $(f_c^{(ref)}/ f_c^{(test)})^{0.5}$.
We propose using the ratio ($k_{cr,N}$ / $k_{ucr,N}$) adopting the values from EN 1992-4 to adjust $N_{Rk,deck,c}^{(uncr)}$ from uncracked to cracked concrete. These values are up-to-date, and the outcome is also slightly more conservative.

$$N_{Rk,deck,c}^{(cr)} = N_{Rk,deck,c}^{(uncr)} \times (k_{cr,N} / k_{ucr,N}) \quad (8)$$

As per C.5 of EN 1992-4, no further adjustment is required between cracked concrete condition and seismic loading category C1 ($N_{Rk,deck,c}^{(C1)} = N_{Rk,deck,c}^{(cr)}$). For the design resistance:

$$N_{Rd,deck,c}^{(C1)} = N_{Rk,deck,c}^{(C1)} \times [\alpha_{eq} / (\gamma_c \times \gamma_{inst})] \quad (9)$$

α_{eq} = 0.85 [single fastener] or 0.75 [fastener group]; γ_c = 1.5 ; γ_{inst} [from ETA cert.]

Steel failure

For the ACI model, N_{sa} represents the steel strength in tension, without any another specific parameter to account for seismic load conditions. For the Eurocode model, the steel strength in tension is represented by $N_{Rk,s}$, and for seismic load conditions, by $N_{Rk,s,eq}$.
The lower characteristic value of the steel failure mode capacity ($N_{Rk,deck,s}^{(uncr)}$) is determined, using test N.21 of AC 193, and compared with $N_{Rk,s}$ from the ETA certificate.
If $N_{Rk,deck,s}^{(uncr)} < N_{Rk,s}$, the new data is used to determine the tensile load steel capacity for category C1, as follows:

$$N_{Rk,deck,s}^{(C1)} = N_{Rk,deck,s}^{(uncr)} \times (N_{Rk,s,eq}^{(C1)} / N_{Rk,s}) \quad (10)$$

If $N_{Rk,deck,s}^{(uncr)} \geq N_{Rk,s}$, the new data is conservatively made redundant and the characteristic tensile load steel capacity for category C1 is adopted ($N_{Rk,deck,s}^{(C1)} = N_{Rk,s,eq}^{(C1)}$).
For the design resistance:

$$N_{Rd,deck,s}^{(C1)} = N_{Rk,deck,s}^{(C1)} \times [\alpha_{eq} / \gamma_{Ms,eq}] \quad (11)$$

α_{eq} = 1 [for single fastener & fasteners group]; $\gamma_{Ms,eq}$ [value published in ETA cert.]

Considerations for other failure modes

Other possible failure modes in tension are concrete splitting and concrete blow-out. Clause 7.2.1.7 (1) of EN 1992-4 specifies that concrete splitting during installation is avoided by compliance with the minimum edge distances, spacing and concrete thickness, with these values being stated in the ETA. No verification is required for concrete splitting under tension load if the characteristic resistance for concrete cone failure and pull-out failure are calculated for cracked concrete, and reinforcement resists the splitting forces and limits the crack width to $w_k \leq 0.3$mm (EN 1992-4 clause 7.2.1.7 (2) b) 2)). As such, considering the confinement effect of the steel deck and the adjustment for cracked concrete and seismic loading applied on the concrete breakout capacity, we propose to disregard splitting failure mode. Clause 7.2.1.8 (1) of EN 1992-4 states that verification of concrete blow-out is required only if the edge distance $c \leq 0.5h_{ef}$, which would never be the case for the short anchors typically used for these applications. However, for particularly long anchors on lower flute installations, it might be necessary to apply restrictions for the effective depth and the maximum offset from the centre of the flute.

SHEAR LOAD

As for tension, the first step is to determine the failure mode and the lower characteristic value (5%-fractile, 90% confidence level) for the ultimate shear load measured on a number of tests conducted on steel deck concrete filled units ($V_{Rk,deck}$) as per Test N. 22 of AC 193 above.
For concrete governed failure modes, $V_{Rk,deck}$ is adjusted for the seismic cracked concrete condition and for the concrete strength. And finally, the design resistance is determined applying the appropriate partial and reduction factors, as per EN 1992-4 which superseded TR 045 cited by NZS 3101 A3.

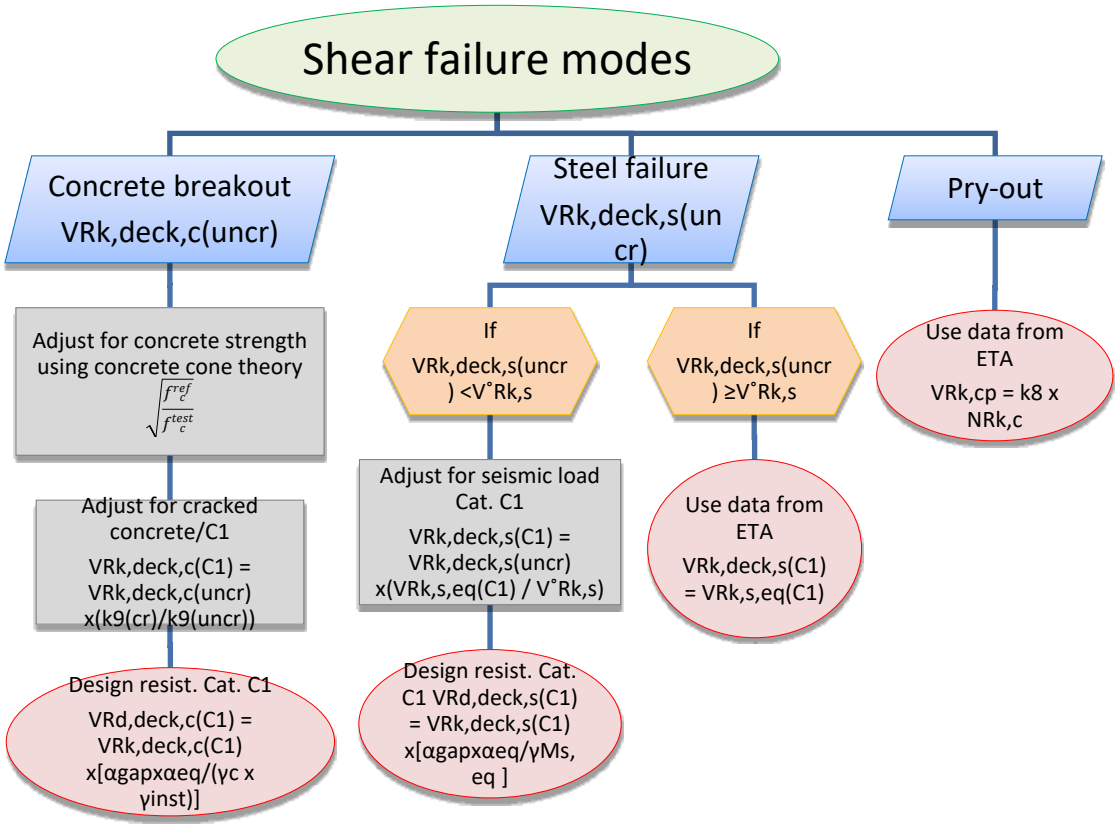

Figure 4. Summary of the proposed methodology for shear loads

Concrete breakout (concrete failure)

This failure mode is more likely to occur for lower flute positions when the load direction is perpendicular to the orientation of the flute.
For the ACI model, the basic concrete breakout shear capacity (V_b) is proportional to the square root of f'_c and, for uncracked concrete condition, there is a multiplication factor $\Psi_{c,V}$ = 1.4 that is applied in the more generic formula of the breakout strength in shear V_{cb}.
For the Eurocode model, $V^{\circ}_{Rk,c}$ is the initial value of the characteristic resistance of an anchor loaded towards the edge. From 7.2.2.5 of EN 1992-4:

$$V^{\circ}_{Rk,c} = k_9 \times d_{nom}^{\alpha} \times l_f^{\beta} \times (f'_c)^{0.5} \times c_1^{1.5} \quad (14)$$

$k_9 = k_9^{(cr)} = 1.7$ [cracked concrete]; $k_9 = k_9^{(uncr)} = 2.4$ [uncracked concrete]

Therefore, the concrete compressive strength is accounted for by its square root and the cracked/uncracked concrete condition is accounted for by different values of k_9.
Considering all the above, we propose to create a new parameter called $V_{Rk,deck,c}^{(uncr)}$, which represents the lower characteristic value from test N. 22 of AC 193 (non-cracked concrete) when concrete breakout is the governing failure mode in shear.
Consistently with the Eurocode model, $V_{Rk,deck,c}^{(uncr)}$ is adjusted for different values of the concrete compressive strength with the square root proportion of f_c: $(f_c^{(ref)}/ f_c^{(test)})^{0.5}$.
We propose using the ratio $(k_9^{(cr)} / k_9^{(uncr)})$ to adjust $V_{Rk,deck,c}^{(uncr)}$, from uncracked to cracked concrete.

$$V_{Rk,deck,c}^{(cr)} = V_{Rk,deck,c}^{(uncr)} \times (k_9^{(cr)} / k_9^{(uncr)}) \quad (15)$$

As per C.5 of EN 1992-4, no further adjustment is required between cracked concrete condition and seismic loading category C1 ($V_{Rk,deck,c}^{(C1)} = V_{Rk,deck,c}^{(cr)}$).
For the design resistance:

$$V_{Rd,deck,c}^{(C1)} = V_{Rk,deck,c}^{(C1)} \times [(\alpha_{gap} \times \alpha_{eq}) / (\gamma_c \times \gamma_{inst})] \quad (16)$$

α_{gap} = 0.5 [hole clearance between fastener and fixture] or 1 [no hole clearance]

α_{eq} = 1 [single fastener] or 0.85 [fastener group] ; γ_c = 1.5 ; γ_{inst} [from ETA cert.]

Steel failure

For the ACI model, V_{sa} represents the steel strength in shear for static loading in concrete applications. For seismic loading, in concrete and in steel deck applications, the nominal steel strength in shear, $V_{sa,eq}$ and $V_{sa,deck,eq}$ respectively, must be used in lieu of V_{sa}.

$$V_{sa,deck,eq} = V_{sa,deck} \times (V_{sa,eq} / V_{sa}) \quad (17)$$

For the Eurocode model, the steel strength in shear is represented by $V_{Rk,s}$, and for seismic load conditions, by $V_{Rk,s,eq}$, which can be different for category C1 and C2.
The lower characteristic value of the steel failure mode capacity ($V_{Rk,deck,s}^{(uncr)}$) is determined using test N.22 of AC 193 and compared with $V^{\circ}_{Rk,s}$ from the ETA certificate.
If $V_{Rk,deck,s}^{(uncr)} < V^{\circ}_{Rk,s}$, the new data is used to determine the shear load steel capacity for category C1, as follows:

$$V_{Rk,deck,s}^{(C1)} = V_{Rk,deck,s}^{(uncr)} \times (V_{Rk,s,eq}^{(C1)} / V^{\circ}_{Rk,s}) \quad (18)$$

If $V_{Rk,deck,s}^{(uncr)} \geq V^{\circ}_{Rk,s}$, the new data is conservatively made redundant and the characteristic shear load steel capacity for category C1 is adopted ($V_{Rk,deck,s}^{(C1)} = V_{Rk,s,eq}^{(C1)}$).
For the design resistance:

$$V_{Rd,deck,s}^{(C1)} = V_{Rk,deck,s}^{(C1)} \times [(\alpha_{gap} \times \alpha_{eq}) / \gamma_{Ms,eq}] \quad (19)$$

α_{gap} = 0.5 [hole clearance between fastener and fixture] or 1 [no hole clearance]

α_{eq} = 1 [single fastener] or 0.85 [fastener group] ; $\gamma_{Ms,eq}$ [from ETA cert.]

Considerations for other failure modes

Other possible failure modes in shear are concrete pry-out and steel failure with lever arm.
Generally speaking, pry-out tends to occur on short and stiff anchors away from concrete edges, and the authors have not encountered this failure mode during the tests that have been conducted on a series of concrete screws and wedge anchors of various sizes. It's also likely that the steel deck has a beneficial confinement effect, preventing this kind of failure.
However, should this failure mode occur, the characteristic capacity from the steel deck tests should be superior to the capacity from the Eurocode model, which is just for concrete, without the confinement effect of the steel deck. As such, using the Eurocode model for concrete pry-out failure, disregarding the results from the steel deck shear load tests, would be our recommended solution, because it's more conservative.
We have not investigated the behaviour of anchors loaded in shear with lever arm, because this option is not available for seismic loading applications from the Eurocode model.

CONCLUSION

The methodology proposed in this paper is an attempt to provide a practical solution for the determination of the design parameters, including seismic tension and shear, of ETA approved mechanical fasteners when installed in the soffit of composite steel deck floors. It's based on the review of the most relevant national and international standards from Europe and the US, and on the experience and results of several test programs that were conducted by the authors, following the principles of AC 193, on multiple sizes of concrete screws and expansion anchors installed in composite steel deck units. The intent is to instigate comments and contributions from industry experts and academics to further develop and refine a methodology that might eventually be adopted across the market by fasteners suppliers in New Zealand. This would

bring more consistency to how the technical data, for composite steel deck applications, is presented by each supplier, and of course more confidence on the data for the specifiers.

REFERENCES

American Concrete Institute, (2019), “Building Code Requirements for structural concrete and Commentary” (ACI 318-19)

American Concrete Institute, “Qualification of post-installed mechanical anchors in concrete and Commentary” (ACI355.2-19)

European Organization for Technical Assessment (EOTA), (2016), “Post-installed fasteners in concrete under seismic action” (EOTA TR 049)

European Organization for Technical Assessment (EOTA), (2019), “Mechanical fasteners for use in concrete” (EAD 330232-01-0601)

European Standards, (2019), “Eurocode 2 – Design of concrete structures – Part 4: Design of fastenings for use in concrete” (EN 1992-4)

ICC Evaluation Service, (2017), “Mechanical anchors in concrete elements” (AC193)

ICC Evaluation Service, (2022), ESR-3699, Report holder: ITW Red Head

ICC Evaluation Service, (2021), ESR-3027, Report holder: Hilti, Inc.

ICC Evaluation Service, (2021), ESR-2713, Report holder: Simpson Strong-Tie Company Inc.

ICC Evaluation Service, (2022), ESR-2502, Report holder: DeWalt

Ramset, (2019), “Specifiers Anchoring Resource Book ANZ Edition 2”

Standards New Zealand, (2017), “Concrete Structures Standard” (NZS 3101:2006, incl. Amendment 3)

Standards New Zealand, (2009), “Seismic performance of engineering systems in buildings” (NZS 4219:2009)

Standards New Zealand, (2020), “Automatic fire sprinkler systems” (NZS 4541:2020)

concretenz BUILDING RESILIENCE
CONFERENCE 2022
13-15 October 2022
Energy Events Centre | Rotorua

CARBON MITIGATION OPTIONS IN THE CEMENT INDUSTRY

ALLAN SCOTT[1], CHRISTOPHER OZE[2], VINEET SHAH[3]

[1] University of Canterbury, [2] Occidental College, [3] Callaghan Innovation

SUMMARY

The production of Portland cement is responsible for a significant percentage of industrial CO_2 emissions. There are many options that make use of existing technologies that can help reduce these CO_2 emissions. In addition to the traditional use of SCMs, new pozzolanic materials and alternative binder systems can aid in reducing the amount of clinker require in concrete construction. Here we review some of the major options for reducing carbon emissions associated with concrete usage. Further, we present a possible new solution for carbon capture which could help dramatically reduce the carbon footprint or Portland cement.

INTRODUCTION

Concrete is one of the most versatile and widely materials used construction material on Earth. While concrete's benefits to the construction of infrastructure are undeniable, the production of Portland cement is also responsible for approximately 8% of the global CO_2 emissions (Andrew 2018, Wallis and Provis 2016). Given the growing concern regarding climate change, there is an urgent need for the cement industry to reduce its carbon emissions to help create a more sustainable future for society.

Many options are available to both cement producers and the construction sector in general. Supplementary cementitious materials (SCMs) have been known for years, if not millennia when counting the Romans, to be effective partial replacements for the major carbon producing component of cement. In addition to SCMs, alternative binder systems include alkali-activated binders, reactive calcium silicates, precipitated calcium carbonates, reactive belite-rich Portland cement (RBPC) clinkers, Belite-Ye'elimite-Ferrite (BYF) clinkers, carbonatable calcium silicate clinkers (CCSC) and magnesium oxide based binder systems (Gartner and Sui 2018).

Another potential option which would allow for the continued use of Portland cement is the ability to economically capture the carbon (i.e., CO_2) while the cement is being produced. Currently, a number of promising new materials and methods for rapid carbon capture are being explored.

Here we review selected major options for reducing carbon emissions associated with concrete usage. Additionally, we present a potential new solution for carbon capture which could help dramatically reduce the carbon footprint or Portland cement.

LOW CLINKER CONCRETE

Supplementary cementitious materials (SCMs) have been used extensively to reduce the carbon footprint of Portland cement concrete construction. Slag, fly ash and limestone are the most commonly used SCMs. Slag can typically replace approximately 50% of Portland cement, though higher replacement levels are possible, and fly ash is usually used at a replacement level of around 30%. In addition to the benefits of a reduced clinker factor and lower CO_2 emissions there are also many other reasons to use SCM's including better chloride resistance, reduced permeability and increased concrete resistivity, lower temperatures for mass pores, better Alkali-Silica Reaction (ASR) resistance and improved workability to name a few.

While SCM's provide many benefits, one of the greatest limitation to their more wide spread adoption is the limited availability of these materials, particularly in New Zealand. Total global slag production is only 5 to 10% of the amount of clinker produced and most of it is already in use (Scrivener et al. 2018). Fly ash is more generally available than slag; however, there can be considerable more variability in the material which limits its application. Effectively ~10% of Portland cement could be replaced with fly ash at current production levels. With the increased pressure to reduce carbon emissions, closure of existing coal fire power plans as they are replaced with gas plants and other forms of power generation will further reduce the long term availability of fly ash.

Limestone calcined clay cement (LC3) is being proposed as a promising alternative to reduce the carbon emissions and improve the sustainability of concrete construction. Through a coupled substitution of clinker with calcined (700 – 850^{o}C) kaolinite clay and limestone, LC3 cement has been reported to obtain better or similar mechanical and durability properties in concrete compared to Portland cement based concrete. The pozzolanic reaction between calcium hydroxide produced on hydration of clinker with calcined clay and the reaction of the aluminate phase of calcined clay with limestone results in the formation of carboaluminate phases which imparts excellent performance in the LC3 binder system (Shah et al 2020, Dhandapani and Santhanam 2020). Using LC3 technology, the clinker factor of cement can be reduced to the levels of ~ 0.50 and reduce the CO_2 emissions compared to Portland cement by ~30% (Scrivener et al. 2018). Clays with a kaolinite content of ~40% are fairly widespread across the world providing an almost limitless resource, relative to the amount of cement produced.

Reactive belite-rich Portland cement (RBPC) clinkers and Belite-Ye'elimite-Ferrite (BYF) clinkers present another potential method to reduce clinker carbon emissions. RBPC typically contain more than 40% belite and less than 35% alite. The firing temperature for RBPC is around 1,350^{o}C which results in lower energy consumption and CO_2 emissions, ~10% less than conventional clinker. RBPC typically show lower water demand, similar setting times and lower heat evolution and lower early strength but improved long term strength (Gartner and Sui 2018).

As the name indicates BYF clinker contains belite, Ye'elimite which is the main phase from calcium sulfoaluminate (CSA) and ferrite. BYF clinker contains ~20-30% less limestone, requires kiln temperatures between 1,250 – 1,350^{o}C, and needs 15% less energy. BYF binders are considered to have similar characteristics to conventional Portland cement (Gartner and Sui 2018).

ALTERNATIVE BINDERS

Many different binder systems do not rely on $CaCO_3$ as the main feedstock for production. Alkali activated materials (AAM), also known as geopolymers, have been in use since the 1970's (Scrivener et al. 2017). The main materials used in the production of AAM include a source of alumina and silica which has traditionally been fly ash or slag plus the addition of an

activator such as sodium silicate (water glass). The challenge with traditional sources of alumina and silica (slag and fly ash) is that most of the limited quantities that are produced are already in use as SCMs. Calcined clays may provide a viable future option, but at present they require considerable quantities of expensive and energy intensive sodium silicates. As a result there may not be significant environmental benefit to the use of these materials. However, alternative activators such as silicate activators from olivine and near neutral salts, (Shi et al. 2019) may improve the viability of AAM for practical use in the future.

Magnesium oxide (MgO) based binder have been in use for 150 years (Walling and Provis 2016). Among the different types of MgO-based cements, magnesium oxy-chloride cement (Li and Chau 2008, Deng 2003) and magnesium phosphate cement (Yang et al. 2014, Soudée and Péra 2000, Yang and Wu 1999) have received the most attention and practical application. Widespread adoption, however, has been limited in part due to long term instability issues when permanently exposed to water.

Magnesium silicate hydrate (MSH) based binders were first proposed by Wei et al (2006) and have gain considerable attention due to their good overall performance characteristics and similarities with traditional calcium silicate hydrate (CSH) based binder systems (Jin and Al-Tabbaa 2015, Shah and Scott 2021). Compressive strengths of almost 90 MPa have been reported for the MSH system (Tran and Scott 2017). While the MSH system has shown considerable promise, the majority of research has been conducted using MgO calcined from $MgCO_3$ which generates as much if not more CO_2 than calcination involving limestone ($CaCO_3$) despite the lower calcination temperature. Figure 1 shows a comparison of compressive strengths for MSH concrete produced from traditional $MgCO_3$ derived MgO and also olivine derived MgO. It should also be noted that most of the silica used in research to date has been silica fume which is not sustainable or economically viable. Scott et al. (2021) have demonstrated a novel technique to extract both MgO and amorphous silica from olivine for use in the creation of truly carbon zero binder system.

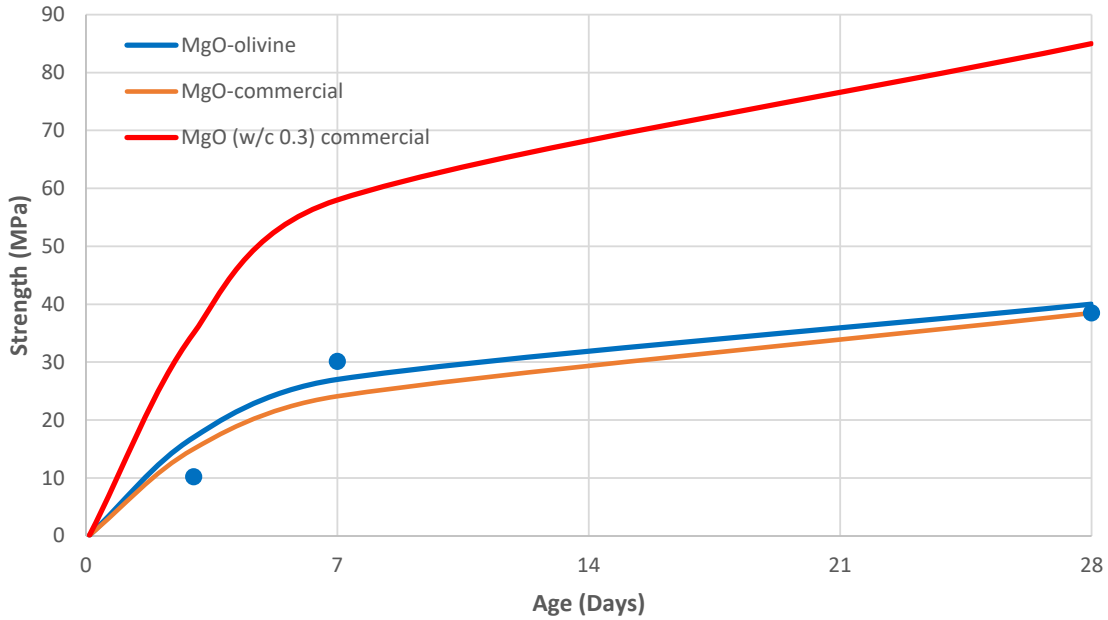

Figure 1: Comparison for MSH concrete produced using commercial MgO ($MgCO_3$) and MgO derived from olivine (W/C 0.4).

CARBON CAPTURE AND SEQUESTRATION

Carbon capture and storage has gained considerable attention to reduce industrial CO_2 emissions. Of the approximately 37 billions tonnes of CO_2 was released into the atmosphere in 2018 (Tollefson 2018), ~60% of global emissions can be attributed to point sources such as power generation and industrial production, including cement plants (IPCC 2005). The two major approaches to long-term storage are either geological burial/sequestration or carbon mineralization. The use of deep geological sequestration techniques requires there is suitable geologic formations close to each industrial point source or that the captured and compressed CO_2 can be effectively transported the required distance for injection. In some cases this may be thousands of kilometres. Carbon mineralization can occur in a number of different ways but one of the most practical is the ability to transport the required solid material to the point source for sequestration of the CO_2.

One of the most reactive materials for carbon mineralization is Mg-hydroxide (Kelemen et al. 2019). While there are other materials which are known to sequester CO_2, Mg-hydroxide is exceptionally efficient. The challenge with Mg-hydroxide for sequestration is similar to that of MgO for cementitious binder production in that most traditional manufacturing processes require lime additions or the calcination of $MgCO_3$ both of which generate considerable amounts of CO_2 in their production.

PROPOSED METHOD

The use of olivine for the production of $Mg(OH)_2$ for point source carbon sequestration and reactive silica as a partial replacement for traditional Portland cement provides a viable method to substantially reduce the carbon emissions associated with concrete construction. The overall approach to the mineral recovery from olivine can be seen in Figure 2.

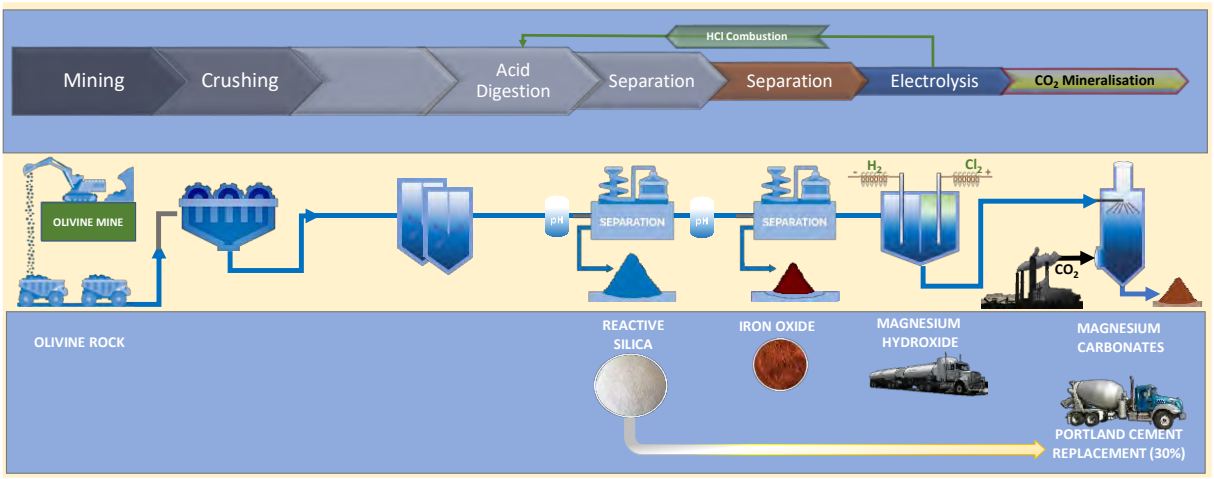

Figure 2: Process for carbon sequestration and SCM utilization

In the proposed method, olivine is used as a feedstock to supply the required silica and magnesium. Iron,also produced, can be utilized in iron production; however, this a relatively minor component compared to the other materials. Olivine is widely available around the world and significant deposits exist within New Zealand. After crushing, the olivine is initially digested in acid which produces a solution containing magnesium, silica and iron. The pH of the solution is increased to precipitate the silica which is removed through a filtration. The iron is removed through another pH swing and filtration step which leaves a relatively pure solution of magnesium ions. If HCl is used as the acid for digestion then $MgCl_2$ is the remaining soluble solution. The $MgCl_2$ is sent to an electrolyzer which results in the formation of $Mg(OH)_2$ and H_2 gas at the cathode and Cl_2 gas at the anode. The H_2 and Cl_2 gases can be recombined to form HCl for the next olivine digestion. The recombination of H_2 and Cl_2 also produces heat energy

which can be used for drying or other process activities. For every tonne of $Mg(OH)_2$ ~880 kg highly reactive silica and 235 kg of iron oxide are also recovered. The overall energy input per tonne of recovered materials is approximately 3.2 GJ.

One of the key parameters in assessing the environmental benefit of any new or alternative production method is the amount of CO_2 emissions it generates. While it is easy to claim zero carbon emission in New Zealand, due the vast of majority of electricity coming from hydroelectric power, a more realistic assessment would be somewhere with a mix energy supply such as California. Using California with approximately half of the electricity generated from fossil fuels, the CO_2 emissions per tonne of material produced is approximately 220 kg, which is much lower than the 800+ kg/tonne emitted in the production of Portland cement.

The recovered silica has been shown to replace up to 30% of Portland cement when used as an SCM. Figure 3 compares the strength development, up to 28 days, for a 15% replacement of Portland cement by the recovered silica. The recovered silica provides enhances early age strength which could be beneficial for precast concrete applications and fast track construction.

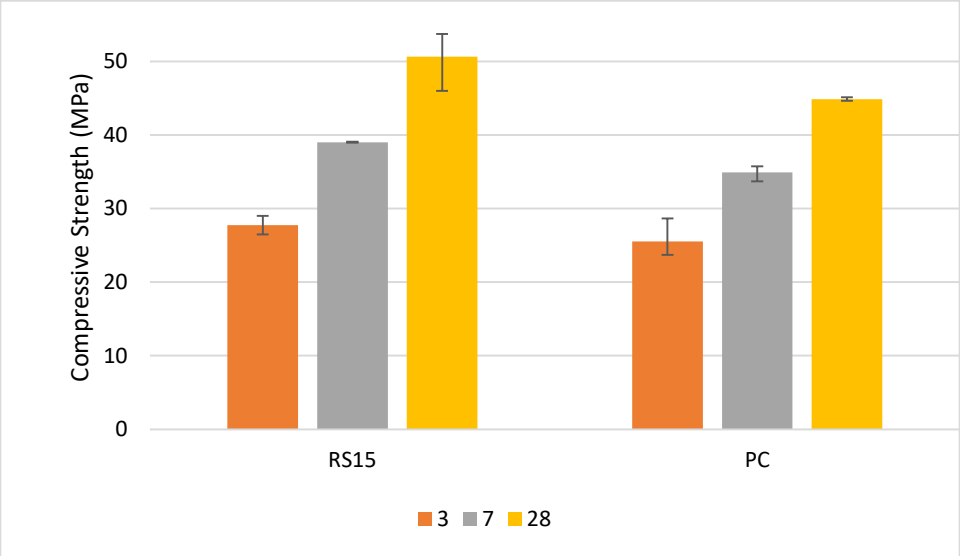

Figure 3: Comparison of 15% recovered silica with Portland cement control for cube strength up to 28 days.

The recovered $Mg(OH)_2$ can be transported to any industrial site, including cement plants, and used as sorbent for CO_2 producing a stable Mg-carbonate containing material. Every tonne of $Mg(OH)_2$ can potentially sequester approximately 770 kg of CO_2. The overall combination of the recovered silica for use as an SCM and the capture of CO_2 from a cement plant through the use of $Mg(OH)_2$ can dramatically reduce the overall carbon footprint of Portland cement.

CONCLUSION

Many options are available that can help reduce the carbon footprint associated with the use of concrete in construction. The success and familiarity of traditional SCMs such as fly ash and slag has helped prepare the way for the use of more widely abundant materials such as calcined clays, natural pozzolans, and silica recovered from ultramafic minerals such as olivine. Additionally, the ability to produce a low-carbon $Mg(OH)_2$ that can sequester CO_2 from a point source industrial process, such as cement production, will further dramatically reduce concrete construction related emissions.

ACKNOWLEDGEMENTS

The authors would like to acknowledge of the contributions of Matt Watson and Mark Chadderton.

REFERENCES

Andrew, R.M., 2018, “Global CO_2 emissions from cement production”, Earth system science data, 10, pp. 195-217

Deng, D. 2003, The mechanism for soluble phosphates to improve the water resistance of magnesium oxychloride cement. Cement and Concrete Research, 33(9): p. 1311-1317.

Dhandapani, Y. Santhanam, M. 2020, Investigation on the microstructure-related characteristics to elucidate performance of composite cement with limestone-calcined clay combination, Cem. Concr. Res. 129.

Gartner, E. Sui, T. 2018, Alternative cement clinkers, Cement and Concrete Research, 114, 27-39.

IPCC, 2005, IPCC Special Report on Carbon Dioxide Capture and Storage. Prepared by Working Group III of the Intergovernmental Panel on Climate Change (eds Metz, B., O. Davidson, H. C. de Coninck, M. Loos, and L. A. Meyer). pp. 442 (Cambridge University Press, Cambridge, United Kingdom and New York, NY, USA, 2005).

Jin, F., and A. Al-Tabbaa. 2014. “Strength and hydration products of reactive MgO-silica pastes.” Cem. Concr. Compos. 52 (Sep): 27–33.

Justnes, H. 2009, Pozzolana from minerals–State of the art. COIN P1 Advanced cementing materials and admixtures. SP 1.4 F Alternative pozzolans. Concrete Innovation Centre Project report.

Kelemen, P., Benson, S. M., Pilorge, H., Psarras, P. & Wilcox, J. 2019, An overview of the status and challenges of CO_2 storage in minerals and geological formations, Front. Clim. 1, 9

Li, Z. and C.K. Chau, 2008 Reactivity and Function of Magnesium Oxide in Sorel Cement. Journal of Materials in Civil Engineering, 20(3): p. 239-244.

Scott, A. Shah, V. Oze, C. Shanks, B. Cheeseman, C. 2021 Use Of Olivine For The Production Of MgO-SiO_2 Binders, Frontiers in Built Environment, May, pg. 8.

Scott, A. Oze, C. Shah, V. Yang, N. Shanks, B. Cheeseman, C. Marshall, A. Watson, M. 2021 Transformation of abundant magnesium silicate minerals for enhanced CO_2 sequestration, Communications Earth and Environment, 2 (25), p 6.

Scrivener, K.L. Martirena, F. Bishnoi, S. Maity, S. 2018, Calcine clay limestone cements (LC3), Cement and Concrete Research, 114, pp. 49-56.

Scrivener, K.L et al. 2017, UN Eco-efficient cements: Potential economically viable solutions for a low-CO_2 cement-based materials industry, United Nations Environment Programme, Paris. 64.

Shah, V. Parashar, A. Mishra, G. Medepalli, S. Krishnan, S. Bishnoi, S. 2020, Influence of Cement Replacement by Limestone Calcined Clay Pozzolan on the Engineering Properties of Mortar and Concrete, Adv. Cem. Res. 32, pp. 101–111

Shah, V. Scott, A. 2021, Use of kaolinite clays in development of a low carbon MgO-clay binder system, Cement and concrete research, 144, pg. 13.

Shi, C. Qu, B. Provis, J.L. 2019, Recent progress in low-carbon binders, Cement and Concrete Research, 112, pp. 227-250.

Soudée, E., J.J.C. Péra, and C. 2000, Research, Mechanism of setting reaction in magnesia-phosphate cements. Cement and Concrete Research, 30(2): p. 315-321.

Tollefson, J. 2018 Global industrial carbon emissions to reach all-time high in 2018. Nature, 3, 4.

Tran, H. M., and Scott, A. 2017. Strength and Workability of Magnesium Silicate Hydrate Binder Systems. Construction Building Mater. 131, 526–535

Yang, Q., X.J.C. Wu, C 1999, Factors influencing properties of phosphate cement-based binder for rapid repair of concrete. Cement and Concrete Research, 29(3): p. 389-396.

Walling S.A., Provis J.L., 2016, “Magnesia-Based cements: A journey of 150 years, and cement for the future?”, Chemical Reviews, 116, pp. 4170-4204

Wei, J., Y. Chen, and Y. Li. 2006. “The reaction mechanism between MgO and microsilica at room temperature.” J. Wuhan Univ. Technol. 21 (2): 88–91.

Yang, N., et al., 2014, Research Progresses in Magnesium Phosphate Cement – Based Materials. Journal of Materials in Civil Engineering, 26(10): p. 040140711-8.

SESSION 5B

Chair:
Paul Dillon

THE SOUND OF MUSIC: UNIVERSITY OF OTAGO – MUSIC AND THEATRE REDEVELOPMENT PROJECT

ALEX KELLY[1], JOHN HEENAN[2], NEILL LEWIS[3]

[1] Structural Engineer, Beca, Christchurch
[2] Technical Director, Structural Engineering, Beca, Christchurch
[3] Structural Engineer, Beca, Dunedin

SUMMARY

Te Korokoro o te Tūi is the new recording studio building constructed as part of the Music and Theatre Redevelopment Project at The University of Otago. This studio was designed to feature world-leading performing arts spaces and includes a live studio with space for a full orchestra, three control rooms, two percussion rooms, four practice booths and social spaces.

Acoustic performance is of utmost importance in a recording studio and hence the structural design was governed by acoustic requirements. To achieve the high level of acoustic separation and isolation required, a minimum 150mm structural concrete thickness was used for floors and 200mm for walls.

The recording studio and practice rooms feature acoustically isolated 150mm thick floor slabs and standalone timber framed walls surrounded by the main structural floor slabs and precast concrete walls, creating a “box within a box” to acoustically isolate the spaces from each other and the surrounding building. The overall net thickness of concrete floor is typically 300mm in these areas, driving the use of shorter beam spans and secondary columns to mitigate deflection and vibration issues.

The external precast panels are profiled and feature exposed aggregate, adding additional concrete thickness of up to 75mm on top of the 200mm structural thickness of the panels. Precast panels internally and to the perimeter form the lateral load resisting system, whilst the internal gravity frame is comprised of structural steel with suspended Comflor concrete slabs at both first floor and roof level, again to achieve the acoustic integrity of the building. The additional seismic mass from the acoustic slabs, the concrete roof and architectural build-up of the panels led the design of the precast panels and led to use of large panel tie plates, to allow the individual precast panels to act together to resist the lateral loads.

The two-storey recording studio facility is supported by deep concrete piles with reinforced concrete foundation beams to mitigate the poor ground conditions on site and resolve the high lateral forces from the building.

The structure was modelled in ETABS due to the complex geometry of the building. The building has three principal axis to consider due to the triangular shape, and therefore six directions of loading. The distribution of walls is also somewhat irregular leading to large diaphragm transfer forces between elements.

The precast fabricator used steel forms to produce the profiled finish of the external panels. A number of test pours and refinement of the formwork was required to achieve the finish and appearance required by the architects. Beca devised a construction methodology that would minimise propping and speed up construction, reducing programme and construction risk. The panels were designed such that, once erected, they were propped below the first-floor slab level, to allow for the slab to be poured without temporary penetrations or additional staging.

The collaborate and collegial approach of all involved resulted in this valuable University asset opening on-time for the 2020 academic year following an 18-month construction programme.

Figure 1: Architects Render of Completed Building

INTRODUCTION

In May 2016, the University of Otago embarked on a project to relocate and consolidate the University's Music and Theatre Department as part of the campus capital works programme.

The Music and Theatre Department was spread through several areas within the existing campus with part of the department located at "The Music Building" at 180 Albany Street, Dunedin. The Music Building was the old New Zealand Broadcasting building constructed in 1967 and used by the University of Otago as a rehearsal and recording facility since 2008. Unfortunately, the building contained asbestos containing materials and was deemed not fit for purpose and scheduled for demolition in 2018.

The Music and Theatre department was relocated to accommodate performance and recording facilities along with office, teaching, research and public circulation spaces. The most suitable location for the relocated department was on the existing College of Education campus located on Union Street, Dunedin. The project required new buildings for specific uses, along with the refurbishment and reuse of existing buildings such as the Mary Hopewell theatre and Auditorium.

After initial project briefing and consultation the project comprised of five separate elements;

- Construction of a new purpose-built Music and Theatre building incorporating recording studios, practice studios, and rehearsal studios
- Redevelopment of the existing two storey music building associated with the College of Education

- Construction of a new link building between the existing music building and the adjacent three storey Teaching Block
- Redevelopment of the Teaching Block
- Redevelopment of the College of Education Tower Block for academic offices

The redevelopment of the existing College of Education buildings required the detailed seismic assessment of the buildings probable seismic capacity and the subsequent seismic strengthening in accordance with the University of Otago's earthquake prone buildings policy.

The link building consists of a two and three storey building which provides an accessible path between the old College of Education music building and the adjacent teaching block. The building essentially consists of a stair core and lift well providing covered access between the two buildings and linking with the new Music and Theatre recording studio building.

The new Music and Theatre building is a two-storey high stud building housing a new recording studio, various practice, rehearsal and teaching spaces, student areas and public circulation areas.

The location of the relocated Music and Performing Art faculty is at the College of Education campus on Union Street, Dunedin. The new Music and Theatre building is situated on an old car park area between the original College of Education music building and the adjacent Bill Robertson library to the west. The site was very constricted by the proximity of the adjacent building at the Water of Leith stream on the southern side of the site.

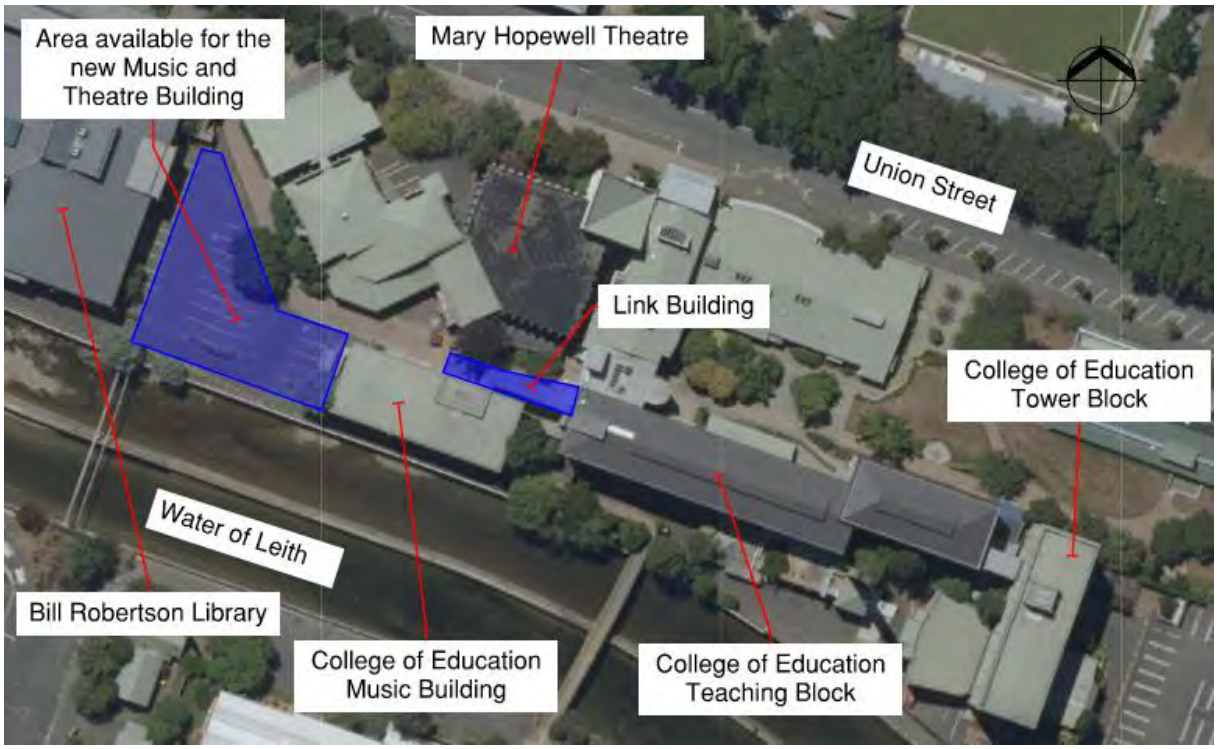

Figure 2. Location Aerial Photo

The key project drivers for the University of Otago was to,

- Provide a cohesive and unified Music and Theatre campus,
- Provide facilities which are fit for purpose, and support modern pedagogies for teaching music including collaborative educational environments and student focused student commons,
- The programme and desire to vacate the existing University recording studios at 180 Albany Street and the subsequent demolition of same,

- New recording and practice studios
- While the preference is for the redevelopment of the University's existing College of Education campus, this was to be tested against other potential options.

In conjunction with Baker Garden Architects (Dunedin) and CCM Architects (Wellington), Beca were engaged to undertake the design and construction monitoring of the new Music and Theatre building along with the adaptive reuse of the noted adjacent buildings.

This paper will describe the novel elements of the design and construction of the new Music and Theatre building.

DESIGN PHILOSOPHY

The structural design philosophy adopted for the new Music and Theatre building was based around several governing factors.

- The site has difficult access for construction materials and plant, being bounded on three sides by existing buildings and on the south by the Water of Leith
- The retaining wall which confines the Water of Leith on the south side of the site was of unknown and variable construction with the capacity of this retaining structure to support construction equipment required to be determined for the design of prefabricated elements and their access to the site
- Geotechnical investigations revealed that the site contained soft materials to a depth of approximately 7.5m – 10.0m where a rock cobble horizon was determined to be suitable for bearing. The intermediate ground was not considered to be potentially liquifiable at either the SLS or ULS condition in general but some areas of the site investigation did suggest that liquefaction induced settlement may occur with up to 60mm of settlement predicted.
- A Dunedin City Council foul sewer main traversing the site along the western edge parallel to the Bill Robertson Library.

Notwithstanding the site constraints above, the primary design requirement was to develop a world class teaching, performing and recording facility with suitable characteristics to enable full acoustic isolation for specific recording and practice areas within the building.

The acoustic drivers for the design dictated the construction type and material selected for the design of the building. The materials and construction type had to provide sufficient mass to dampen out any external noise and any internally generated noise which may affect or influence the functionality of the recording spaces.

Marshall Day Acoustics provided a comprehensive specification for the acoustic performance of all building construction and materials for the design and detailing of the building spaces including the recording studio (live studio, isolation booths, control room and isolation lobbies), rehearsal, practice and teaching studios, teaching, staff, student and common areas within the building. The specification included for the generation of internal noise including building services plant, reverberation and transmission of sound and external noise.

The resulting design philosophy was to construct a "building within a building" for the specific areas where sound control was dominant, with the construction of a fully acoustically separated structure within the portions of the building envelope.

The implications of the acoustic demands on the structural design of the building required that reinforced concrete construction was adopted for primary walls, floors and roof, with a minimum average thickness of 150mm required to mitigate the sound management within the building.

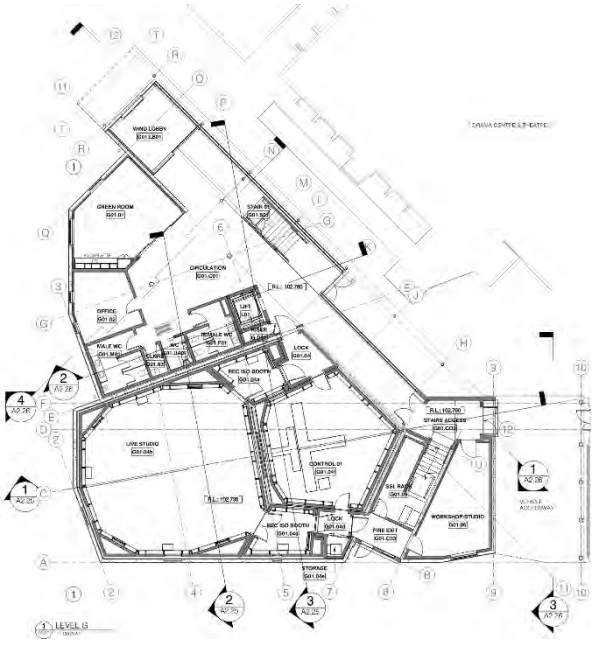

Figure 3. Ground Floor Plan

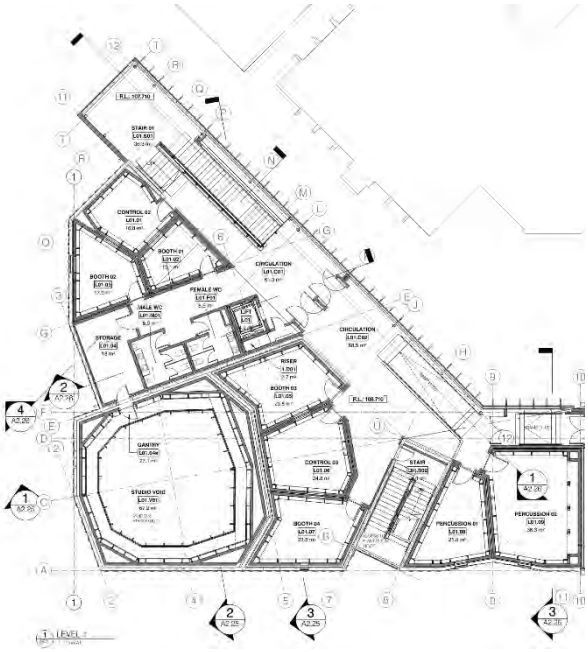

Figure 4. First Floor Plan

(Baker Garden Architects)

The acoustically isolated spaces within the building were achieved by constructing a fully suspended floor over the structural slab supported on acoustic isolators with a completely separated self-supporting acoustic shell within the structural walls.

DESIGN CRITERIA

The structural design criteria that were adopted for the building design is as follows,

- Importance Level 2 as required by AS/NZS 1170.0 for the building type and occupancy. There was no specific client/owner driver to adopt a higher importance level for the building nor any further requirement for low damage design or serviceability limit state 2 requirements.
- Design Life of 50 years was adopted as per AS/NZS 1170.0 with a period to first maintenance of 15 plus years for durability requirements
- The site subsoil category adopted was for class D soils (Deep soils) based on the geotechnical assessment of the site and ground conditions with a cobble bearing horizon at between 7.5 and 10.0 metre depth.

<u>Foundations</u>

The geotechnical report indicated that there was a potential for some liquefaction induced settlement in parts of the site and that a deep piled solution would be an appropriate foundation solution for the relatively heavy Music and Theatre building.

Driven piles were discounted based on the likely disruption to adjacent buildings and occupants and as such large diameter bored piles were adopted for the foundations design.

Although load demands suggested that smaller piles would be suitable, we adopted a 900mm diameter pile for all foundation locations. This was due to the cobble layer to be encountered for our founding horizon. At this location, based on previous experience, the cobble layer was expected to consist of rounded rock cobbles bound with silty material ranging from fines up to 600 mm large dimension stones. In order to allow for embedment of the piles into this cobble

layer some excavation and extraction of the cobbles would be required. Therefore the larger diameter piles were selected to allow for the extraction of these cobbles.

The ground floor slab was designed as a fully suspended floor between large foundations beams tying the pile caps together. The shape of the building resulted in complicated reinforcement arrangements at non-rectangular beam-beam connections. To indicate the required arrangement of reinforcement a typical beam-beam connection reinforcement detail was modelled in 3D and provided as an example for the reinforcement detailers and suppliers.

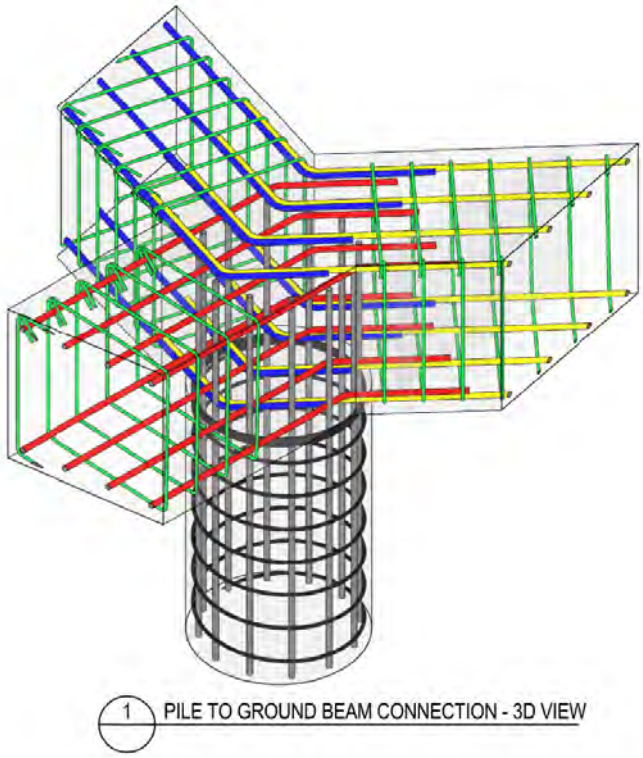

Figure 5. Foundation Reinforcement Arrangement example

Early engagement with the reinforcement sub-contractor was also undertaken to work through any issues and difficulties with detailing the reinforcement.

Gravity Load System

The primary gravity load system adopted for the building consisted of the precast concrete walls with a composite metal and concrete floor system. The atrium and circulation spaces to the north of the building are supported on structural steel beams and columns. This was adopted for the ease and speed on construction along with allowing to the restricted site access requirements.

The Comflor 60 system was used with an over all thickness of 180mm to create an average thickness of 150mm required for acoustic purposes. This also allowed for the punching shear loads from the floating floor isolators to the first floor. The same system was adopted for the roof system over the building foot print. The concrete roof structure was required primarily for acoustic purposes.

Lateral Load System

The lateral load resisting system of the new building for the Music and Theatre redevelopment is required to resist loads from either seismic (earthquake) or wind. Seismic loads are the critical governing lateral load condition.

The triangular nature of the building and the acoustic requirements of the building envelop dictate the structural form of the external walls and roof level structure. A minimum of 150mm thick reinforced concrete is required to achieve the required acoustic demands. The number of precast concrete walls therefore dictate that these should also function as the lateral load resisting system. The new recording studio building uses precast concrete shear walls full height of the building to resist lateral loads.

Although not part of the original brief, the stiffness of the precast concrete walls will protect the building from damage or minimise the need to vacate or repair the structure under moderate to large level earthquake events. It is expected that minor to low level damage may occur at the ULS event. The panels are to be connected at first floor and roof level with cast in weld plates to provide continuity of the wall panels over the length of the wall.

The panels are to be connected at first floor and roof level with cast in weld plates to provide continuity of the wall panels over the length of the wall.

This has the effect of:

- significantly reducing the reinforcement content of the wall panels.
- increasing the stiffness of the building.
- avoidance of localised damage at the first floor and roof concrete diaphragms at panel connections.
- aiding in the constructability of the wall panels on site.

The structure was modelled in ETABS due to the complex geometry of the building. The building has three principal axis to consider due to the triangular shape, and therefore six directions of loading. The distribution of walls is also somewhat irregular leading to large diaphragm transfer forces between elements.

The lateral load from the structural steel gravity frames is transferred back to the precast shear walls via diaphragm action of the floors at first floor and roof. While this means the diaphragms cantilever beyond the extent of the shear walls, these frames are relatively narrow and do not place excessive stress on the concrete diaphragm.

Structural Walls

The structural walls were designed as the lateral load system shear walls; as such the slenderness of the wall panels had to be considered for the in-plane loading particularly where the panels span between the ground floor level and the level 2 roof slab (10.850m clear height).

The structural thickness of the walls was designed as 200mm thick with the Architectural faceted finish to the external face as additional non-structural finish.

The panels were specifically designed to be propped below first floor level during construction with the upper portion of the panels cantilevering above the propping (8.0m) during construction. During the design phase it was assumed that the panel erection would precede the structural steel and Comflor erection requiring the panels be propped. In order to avoid large props penetrating through the floor diaphragms during construction the panels were checked for construction period loads (25 year return period loading for wind and seismic) with the crack moment of the panels not to be exceeded for these load events.

This did result in significant portions of the panels projecting above the propping line and the panels did noticeably deflect under face loading however we are not aware of any cracking due to construction loads of the erected panels.

As can be seen in figure 6 below the external Architectural finish to the wall panels was quite complex and intricate. The finish involved angled faceted shapes to the panels with both off the form finish and exposed aggregate finish with each panel matching the pattern in the adjacent panel. This required that each external wall panel was bespoke in terms of Architectural finish.

The internal walls required for both structure and for acoustic purposes used the same panel arrangement where appropriate. The width of the panels was restricted to less than 4.0m and typically around 3.0 m in width. This was to allow for transportation to site and attempting to keep the panel size and weight to a manageable level for cranage on the site. Given the height of some of the panels this did prove to be a challenge for cranage on a constricted site. The bespoke Architectural finish was adapted to work with the proposed panel width as an early point of design coordination which also determined the optimum width of panels.

Horizontal jointing of the panels was discounted at an early stage as continuity of the panels would be difficult to achieve and did not fit with the Architectural bespoke finishes.

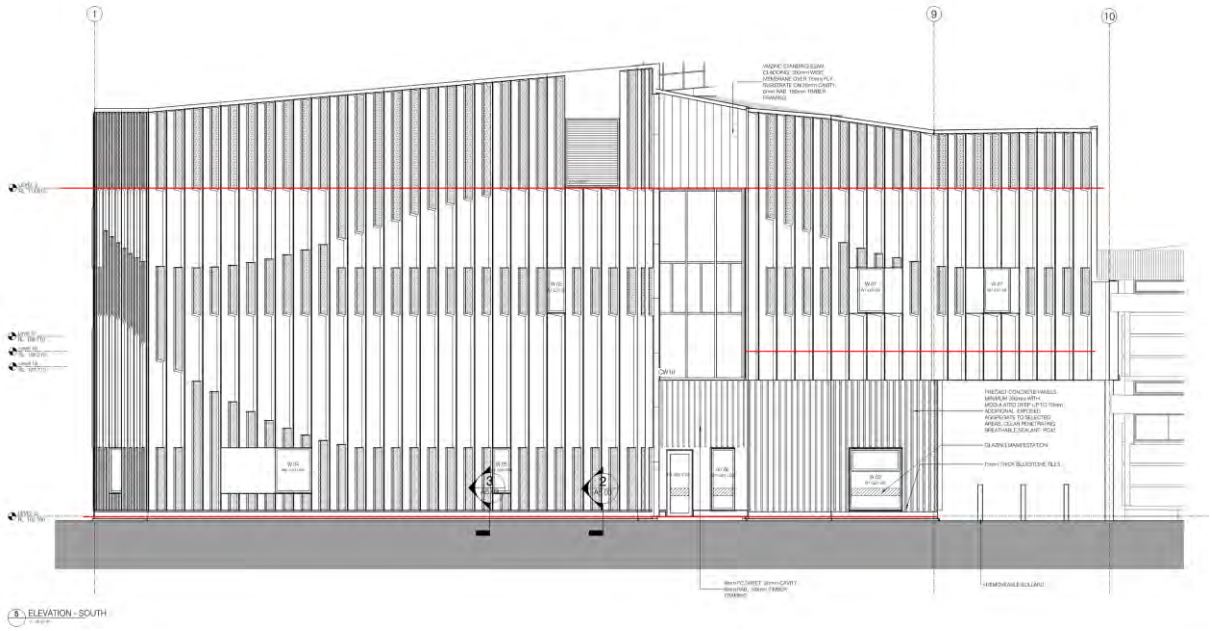

Figure 6. South Wall Elevation (Baker Garden Architects)

<u>Displacements and Serviceability Limit State</u>

The building drifts calculated from the analysis model are significantly less than required by design codes as would be expected from a very stiff concrete wall structure. Floor drifts were calculated as less than 0.2% in most instances at ULS loading. The building stiffness was generally dictated by the acoustic requirements for the building rather than a specific limitation on building drift for structural performance.

In order to provide a building which meets the daily functionality required for a music and teaching building, floor vibrations were modelled to restrict potential vibrations to acceptable levels. Although there was not identified any specific installation in the building that would require special consideration, floor vibrations were assessed again the criteria of the BRANZ Study Report No.57, “Serviceability Limit State Criteria for New Zealand Buildings” and with “Floor Vibrations due to Human Activity” by Murray et al (1997).

Typically a limit of response factor of 2-4 was targeted for recording and rehearsal areas as an acceptable compliance for the type of building use with a more relaxed approach taken for the general teaching and circulation areas. Refer Figure 7 below.

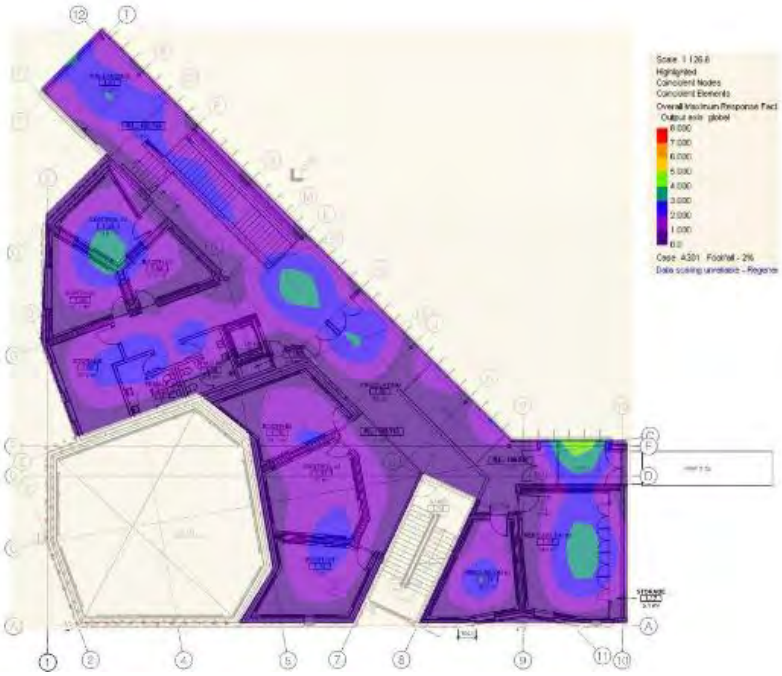

Figure 7. Response Factor Output of Level 1 Floor with 2% Damping Applied

Acoustic Isolation

The acoustic isolation of the Live Recording studio, control room, recording booths, percussion rooms and associated sound lobbies required that a fully isolated structure was required within the structural building elements.

The floors for the isolation areas were designed as suspended reinforced concrete floors (150mm thick) supported on specialised acoustic isolators. The design of the isolators remained as a contractor design elements as these are a specialist product subject to supplier design details and load criteria. The load demands on the suspended floors was specified to include high concentrated loads from shifting heaving equipment on the floors such as moving a grand piano around the recording studio. The contractor had to allow for the uneven distribution of loads and account for any uplift loads in the concrete floor due to a moving concentrated load.

The isolated floors are cast on the structural slab with a suitable bond breaker, then after strength is achieved, the floors are screwed up to the required height with the adjustable floor isolators. The floating slabs were also restrained from lateral displacement with discrete packing around the floor panels to the structural walls or slab recesses.

The building layout dictated that several acoustically isolated rooms were located on the first floor which required the isolated floors to be cast in a floor recess created in the Comflor floor and structural steel frames. The Comflor was specifically designed for acoustic separation and for the localised punching shear from the individual floor isolators.

Floating concrete floors typically have a natural frequency around 20 Hz, so we just need to avoid a matching acoustic resonance with the structural floor below. Typically this means

separating the natural frequencies by a factor of 3. For example, <5Hz natural frequency for structural floor will allow for floating floor natural frequencies down to 15Hz.

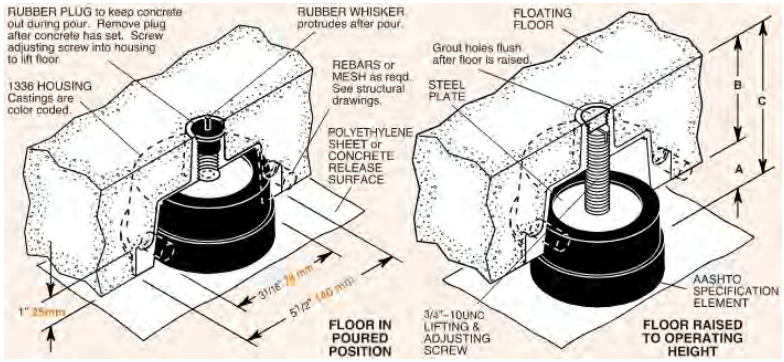

Figure 8. Mason Industries Floor Isolators

The super structure of the isolated rooms was typically constructed with a structural steel frame and timber infill with multiple layers of GIB board to achieve the acoustic ratings. Additional acoustic panels and baffles were fixed to the internal faces of the acoustic walls.

CONSTRUCTION

The construction period was estimated to be 18 months, from an initial start on site in August 2018 through to opening in February 2020 for the start of the academic year.

Piling took the first four months. Typical pile lengths were 7m and 10.5m long. Cobbles were encountered throughout the drill depth. A dense cobble layer at 12-13m depth prevented drilling the steel pile casings beyond this point and the two pairs of 20m long piles, located under two short but highly stressed concrete shear walls, were substituted for three piles ranging from 9m to 12.9m long, depending on the local material encountered and assessed pile capacity by the structural and geotechnical engineer reviewing the drilling work.

As shown in Figure 2 the site is heavily constrained in terms of access and space on site. Initially the contractor was to be restricted to a single site entry point, accessed from the east alongside the Water of Leith. Due to the relocation of a major sewer pipe, a second access point onto Union Street was able to be created, greatly improving the access to site and changing and simplifying the contractor's construction methodology.

The contractor decided to construct the primary structure in two halves. Foundations were poured with Reid couplers in the main longitudinal bars at the junctions of ground beams and buried again to allow the site to be infilled, and precast panels erected and floors poured completely in the southern half of the building before continuing and finishing the northern half. As the precast panels were erected in a cellular structure and floor diaphragms poured before removing propping and moving to the next stage, the half structure erected was self supporting and did not require temporary bracing or propping.

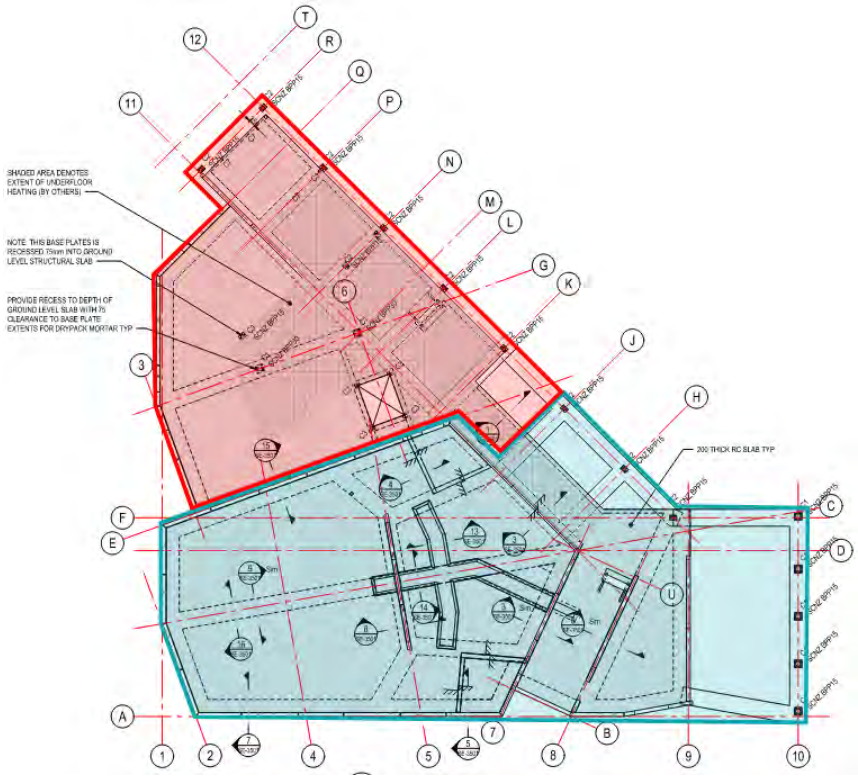

Figure 9. Construction Sequence (First Stage in Blue, Second in Red)

Site concrete was poured under all ground beams to create a clean surface to form off and provide support to the reinforcing cages during placement and pouring. We engaged early with the reinforcing subcontractor to agree on sections of these cages which could be premade and craned into position on site, and actively engaged with their detailers to co-ordinate the junction reinforcing, which in some cases included up to four beams intersecting, none at right angles, on a pile head. Apart from some minor comments made on site with the contractor, no issues were noted during pre-pour inspections.

Figure 10. Reid Couplers Cast at Beam Junction

Figure 11. Reinforcing Cages in Place

The shop drawing process required a large amount of co-ordination between the design engineer and the precast and steel fabricators. The complicated shape, faceting of the panels, and the interaction between precast shear walls and steel beams fixed to cast-in weld plates required the two fabricators to co-ordinate their models closely. The overall shop drawing process took 10 months, undertaken in stages to allow elements to be fabricated and brought to site as required by the programme. While the steel shop drawing model was completed in 3D, the precast panels were completed in 2D. While there could have been benefits if both these elements were modelled and co-ordinated in 3D, all panels arrived to site without issue,

none were rejected and there were no site alterations required to either steel or precast to make the structure work, a testament to the co-ordination undertaken.

Panels were fabricated in Christchurch. The local round greywacke aggregate was used in the manufacture, which differed from the architectural design intent to use local Dunedin basalt aggregate, although this was not specified on the drawings or documentation explicitly. The initial test panels showed the exposed aggregate finish was not as dark as the architect would have liked, to enhance the contrast between exposed aggregate and form finished sections. Concrete additives or surface coatings were rejected due to the likelihood they would need to be re-applied over the life of the panels. An alternate source of crushed greywacke aggregate was sourced which was found to give a suitably dark finish to the exposed aggregate sections and was used for the faceted panels on the project.

Erection on site was typically done with two cranes, lifting the panels off trucks and into place. To allow erection of such large panels, the cranes were located as close to the panel final locations as possible. The contractor planned ahead and requested during the foundation construction that some of the panel starter bars be removeable to allow the cranes to drive into the building footprint. Sections of the starter bars were cast in with Reid couplers on the top face of the ground beams, and the starter bars threaded in after the other panels were lifted into place.

Panels were typically propped below first floor level as described above. While it was noted by the contractor on site that the panels visibly wavered in strong winds during construction, no cracking occurred to the panels during the propped period on site prior to the floor slabs being poured.

Figure 12. Internal Panels in Recording Studio Space

The contractor identified the acoustic slab jacking as a construction risk. The supplier of the isolators provided a detailed methodology along with the shop drawings indicating the layout of the floating floor isolators. The methodology typically consisted of raising each jack incrementally one at a time in a concentric pattern across the extent of the floating floor, slowly raising the whole floor to flush with the surrounding slab. The contractors followed the

supplier’s methodology and found the process very simple and risk free, with no damage to the acoustic slabs occurring during the lift process.

Figure 13. South Elevation of Building with Panels In Place

Figure 14. Completed Building (Naylor Love)

LESSONS LEARNED

In this age of 3D modelling of buildings and structures the Level of Detail (LOD) is typically limited at LOD 300 for practically and economics from a design perspective. This LOD still relies heavily on a coordinated approach from the design team and the production of shop drawings for precast concrete and structural steel elements.

For specific elements where there is a complex reinforcement arrangement or structural steel detail, the modelling of these connections during the design phase adds a considerable amount of value both for the structural engineer and the detailer/fabricator.

The 3D modelling of a representative pile/beam/beam connection does not resolve all of the potential clashes with reinforcement but it does highlight the important criteria from the structural engineer and allows the reinforcing detailer to see the preferred arrangement of bars in a practical application rather than interpreting a 2D drawing.

The early engagement between the reinforcing detailer/supplier is also invaluable for describing the important issues to the structural engineer and setting basic ground rules for detailing. This leads to a much more collaborative approach to an early trade where this has been traditionally over looked in the past.

The precast concrete wall panels detailed by the structural engineer typically only show the structural content of the panels and reliance by the contractor is again required for coordination between the Architectural and structural drawings for specific or bespoke finishes. In the instance of the Music and Theatre building the set out of Architectural finishes was provided solely on the Architectural drawings with no modelling of this in the structural drawings. The precast shop drawings were undertaken in 2D format and as such was a long drawn out process. Notwithstanding and with full respect to McKendry Construction the panel production was relatively smooth and the finished product looks very impressive. Modelling of the precast wall panels in 3D for shop drawings including the reinforcement is now becoming common place and does provide both the structural engineer and the fabricator some degree of confidence the design intent will be achieved and that buildability issues can be identified early and resolved before cost implications become insurmountable.

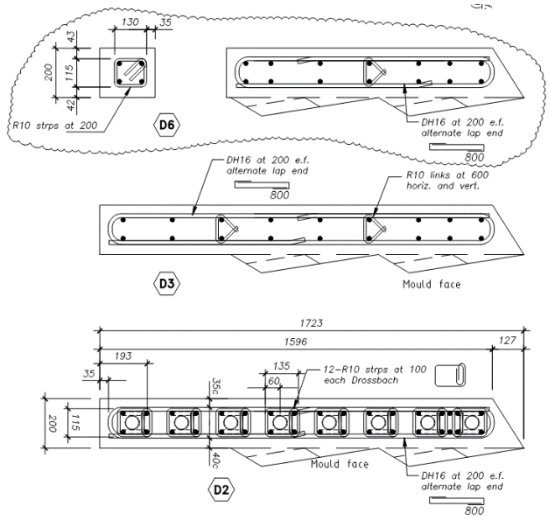

Figure 15. Music and Theatre 2D Shop Drawing Example

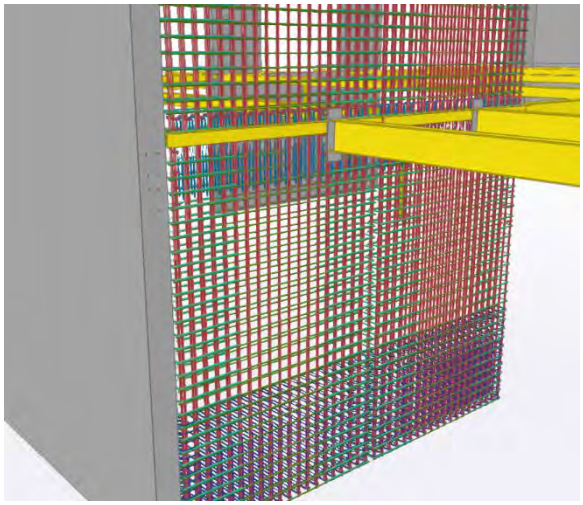

Figure 16. Recent Example 3D Precast Modelling

We also encourage the precast shop detailer to model the structural steel or coordinate models with the structural steel detailer. This does tend to resolve any issues with clashes and alignment of weld plates and cast in items.

Typically it is the contractor's responsibility to design and construct any temporary works for the support of structural elements in a building. We firmly believe that this is where this responsibility should lie. It is not appropriate for the designer to dictate how, when and in what order the contractor should build the works. However we consider it is important for the designer to understand construction practice and prepare designs that are buildable and affordable. Although we did not specify on the drawings the propping points for the precast panels for Music and Theatre, we did discuss what the panels had been designed for with the contractor and the assumptions that we had made in design. This allowed the contractor more options for temporary works and resulted in a simpler build.

In simple terms we discussed what was important to us in the construction as designers and the contractor similarly discussed what was important to them for the construction sequence. This led to an excellent working relationship with the head contractor and allowed any problems and issues to be identified and headed off early.

Sustainability

This project was completed prior to the current considerations we provide for sustainability in the built environment and as such no carbon counting was undertaken and no comparison was made to other forms of construction. Notwithstanding, reinforced concrete was the most appropriate material to be used to achieve economically the required acoustic performance of the building.

It is unlikely that all reinforced concrete will be able to be substituted with alternative lower embedded carbon materials and it will not be appropriate to make this substitution in many instances. However consideration needs to be provided for lowering the embedded carbon on concrete by using cement replacements and have responsible and sustainable practices in the industry.

ACKNOWLEDGMENTS

Client
University of Otago

Design Team
Baker Garden Architects
CCM Architects
Marshall Day Acoustics
Pedersen Reid : Electrical Engineering
Beca : Structural, Building Services, Fire, Civil Engineering

Construction Team
Naylor Love Construction
Smith Crane and Construction: Piling Sub-Contractor
McKendry Construction Ltd : Precast Concrete
Steel and Tube: Reinforcement
Complete Reinforcing: Reinforcing
Allied Concrete: Ready Mix Concrete

concretenz
BUILDING RESILIENCE
CONFERENCE 2022
13-15 October 2022
Energy Events Centre | Rotorua

EFFECT OF MULTIFACETED TECHNOLOGIES ON CONCRETE IN THE 2020S

MARY ANN HALLIDAY, SUE FREITAG

WSP New Zealand Limited

SUMMARY

Concrete has now evolved from a simple blend of aggregates, Portland cement, and water. Admixtures, additives, supplementary cementitious materials, and alternative binder materials have enabled improvements in construction process, structural performance, and durability. These more complex mixtures may have unexpected side effects on the fresh or hardened concrete, including greater sensitivity to small changes in mix design or use.

Based on the authors' experiences, this paper demonstrates how considering concrete materials, structural design, and construction processes as a system will identify potential shortcomings of the proposed combination before construction begins. Lower-risk options can then be selected to prevent significant defects.

INTRODUCTION

Concrete has evolved from a simple blend of aggregates, Portland cement, and water. Admixtures have allowed construction practices to improve, and in turn the demands for more efficient and safer construction have increased the range of admixtures available. For example, most concrete is now pumped, which increases placement speed, facilitates consolidation, and removes hazards related to manual handling. Retarders help to accommodate warm weather and extended delivery times, and enable large placements to be made in a continuous process, obviating the need for construction joints. Additives (such as fibres and densifying fillers) and supplementary cementitious materials (SCMs) provide further benefits to specific fresh and hardened concrete properties. Admixtures, additives, and SCMs are also used specifically to reduce the amount of Portland cement needed to achieve the specified concrete strength (and other properties) with readily available aggregates. Issues around the supply of ideal aggregates in some locations and the drive to reduce the carbon footprint of construction will lead to a greater variety of admixtures, additives, and cementitious binders being used in future.

Admixtures, additives, SCMs (and alternative binder materials) may have side effects that affect the fresh or hardened concrete. Disregarding or overlooking their potential shortcomings may result in substandard or unacceptable construction quality. Materials technology raises expectations of concrete performance but sometimes delivers concrete that does not always handle within expected design and construction parameters, leaving the contractor vulnerable to culpability when the final product is deficient.

If anticipated early in the project, potential disadvantages of a particular combination of materials can be avoided by appropriate specification, design, and construction practice. Unfortunately, designers don't always have detailed knowledge of local concrete materials at the project location, and in many projects, particularly when 'normal concrete' as defined by

NZS 3104 is used, the procurement process creates no natural opportunity for all parties in the supply chain to discuss materials-related issues that may affect construction process, structural performance, or durability. Consequently, the designer, contractor, and placer may remain unaware of potential risks that their individual actions may impose on overall concrete performance, and thus unable to address them. Such 'silo' working is increasingly unlikely to produce acceptable results as concrete materials become more complex to meet demands for fast, structurally- and cost- efficient, low carbon construction.

Concrete is one of many components of a construction system. Improving the constructability of the concrete component will benefit its structural performance, serviceability and durability, adding to the overall success of the project. Using examples based on projects, this paper describes how considering concrete materials, structural design, and construction processes as inter-related parts of a construction system will help designers and contractors identify and address potential 'concrete problems' before they arise. Applying this approach at the design and tendering stages will enable early identification of aspects requiring more investigation. It will also help to ensure new technologies are adopted successfully.

MATERIALS (CONFORMANCE WITH THE STANDARD DOES NOT MEAN EQUAL PERFORMANCE)

Concrete's properties are determined by the properties of the raw materials from which it is made. Aggregates, cements, and SCMs from different sources – natural or manufactured - all have different characteristics even if they conform to the same relevant product specifications. The nuances between the different products affect fresh and hardened concrete properties. Designers and contractors are usually familiar with their local materials but may not be aware of the specific characteristics of materials in projects elsewhere. With inter-regional and international project teams now common, input from the local industry from the project's inception is needed to manage expectations about the local resources, and thus minimise unforeseen costs, delays, and defects.

Admixtures (and additives) add a further level of complexity. While suppliers can advise on the inherent compatibility of the proposed combination of materials, it is much harder to predict accurately the performance limits of a specific combination of admixtures, additive and cementitious materials with the particular delivery conditions, placement methods, and site conditions during placement, curing, and hardening.

Examples of local variation in aggregates and cementitious binders are described below. Examples of other aspects are described later in the paper.

Aggregates

Different rock types, sources, and processing produce aggregates with different properties. NZS 3121:2015 purposely specifies performance properties for concrete aggregates to enable concrete producers to make the most of local aggregate supplies and thereby reduce the need to 'import' aggregates from further afield to meet minimum requirements. This approach reduces the cost and carbon footprint of concrete aggregate supply.

The variability of concretes made from different aggregate sources throughout New Zealand was demonstrated by Mackechnie (2003), whereby hardened properties of concretes made from each of 26 aggregates were compared at three water to cement ratios using the same GP cement, stone content, slump, and air content. The results showed that within a strength grade, other hardened concrete properties can vary between aggregate types and sources and were subsequently used to update NZS 3101 design criteria for static elastic modulus, drying shrinkage, creep, and thermal movement.

Natural sands sourced from the same river catchment may vary in grading, fines content, and minor components depending on the specific source and method used to process the raw

material. Similarly, the particle shape and grading of manufactured sand may demand a different mortar volume to produce suitable workability. And some aggregates may not have the crushing resistance or surface characteristics to produce high strength concrete.

An often-cited example of how aggregate properties affect concrete properties is the shrinkage characteristics of Wellington concretes. Greywacke in the lower North Island has a higher moisture movement than upper North Island greywackes, and much of the concrete sand in Wellington is manufactured. Higher sand contents (and mortar volumes) needed to achieve satisfactory workability, combined with high aggregate moisture movement result in some Wellington concretes having inherently higher drying shrinkage than concretes of the same grade made in other regions using natural sands.

The wide range of aggregates available throughout New Zealand, the performance-based approach of NZS 3121:2015, and the effect of individual aggregate properties on the properties of fresh and hardened concrete mean that the concrete producer must optimise concrete mix designs for the particular blend of aggregates being used in each individual plant. Within a region, producers have supply agreements with specific aggregate suppliers, and a particular aggregate supplier may not supply every local concrete producer. Between regions, the nature of the aggregates and therefore the concrete may vary significantly. And concrete colour can only be replicated with the same aggregates, cementitious binder, and mix design. Therefore mix designs cannot be transferred between individual concrete plants or producers within or between regions, design criteria may vary between regions depending on the aggregate used, and construction practices may also vary to accommodate local concrete materials.

Cementitious binder systems

Changes in Portland cement introduced from the 1960s to the 1980s to improve the rate of strength development up to 28 days and thereby increase construction rates had unanticipated side effects. In particular, the combination of lower cement contents and earlier removal of formwork (which had provided a degree of curing) resulted in more permeable and therefore less durable concrete. Today, Portland cement varies between manufacturers, cement type, and the specifications with which each product is manufactured to conform. In many countries, even general purpose Portland cements (such as New Zealand's type GP cement) may contain other materials known as 'mineral additions', often added simply to reduce the cement's embodied carbon content. The different types and quantities of such additions may also affect the properties of the fresh and hardened concretes.

Natural pozzolans were used in concretes in major New Zealand power development projects as far back as the 1950s. In the 1990s, other SCMs such as fly ash, natural amorphous silica, silica fume, ground granulated blastfurnace slag (GGBFS) and metakaolin were introduced to the New Zealand market. In countries where fly ash, silica fume, and GGBFS are produced they are added to concrete as a means of disposing of a waste industrial byproduct. In New Zealand, their main collective use to date has been to increase the potential durability of concrete that would be exposed to aggressive conditions in service. Current pressure to significantly reduce the carbon footprint of all concrete construction encourages the use of SCMs in concretes that do not need their additional benefits, including in 'normal concrete'.

Like Portland cement, different types of SCM have different characteristics, as do individual materials of the same type. For example, fly ashes produced by the combustion of different coals will have different properties even if produced at the same plant. In New Zealand, this is exemplified by slight variations in fly ashes from Huntly's geothermal power station as it burns coals from different sources. Natural pozzolans, too, are highly variable. Each pozzolan deposit must be processed and optimised for its proposed use, e.g. for use in a cement blend or for addition at plant, and compatibility with specific cements and admixtures.

New Zealand general purpose Portland cements have traditionally all been very similar. In contrast, each SCM imparts its own behaviour on concrete such as workability, bleed and

setting, strength gain, dimensional stability, and resistance to ingress of water and chemical attack. In future, designers and contractors will need to become familiar with the behaviours associated with the various SCMs used in cementitious binders, including those used in 'normal concrete'. Close liaison between suppliers, contractors, and designers will enable design and construction practices and the binder combinations themselves to be modified where necessary, as happened when mineral addition contents were increased in New Zealand general purpose cements about 10 years ago.

WORKABILITY AND RETEMPERING (SLUMP IS NOT THE END OF THE STORY)

The quality of hardened concrete is determined not only by the quality of the materials and mix design (which determine the volume and continuity of voids within the hardened cement paste) but also whether the fresh concrete can be readily placed and fully consolidated without bleeding or segregating significantly and without entrapping significant amounts of air within the body of the concrete, around reinforcement and other embedded items, or against the formwork. If the concrete is too stiff when placed, then it will be difficult to consolidate. Consequently, when hardened it will probably contain excess entrapped air in the form of relatively large voids that may be locally interconnected. The location, size, and connectivity of these voids will determine the hardened concrete's load capacity, watertightness, and durability irrespective of the mix design and materials used. For example, large, interconnected voids in the cover concrete will reduce bond to the reinforcement and cause it to corrode prematurely.

When a batch is stiffer than specified when it arrives at site, its workability can sometimes be adjusted successfully by adding water (and/or admixture) to the concrete before it is discharged from the mixer. 'Retempering' in this way can be used to address small between-batch variations in slump caused by variations in aggregate moisture content or residues of concrete or washwater from the previous load, or to overcome slump loss caused by evaporation of free water in transit. It is not intended to remedy significant shortfalls in slump compared to the specified value. Slump loss related primarily to concrete setting cannot be addressed by retempering because the additional water will remain as free water and the bonds within the early-formed cement hydrates will be disturbed.

Retempering must be controlled by the concrete supplier so that appropriate amounts of water (or admixture) are added and fully mixed into the concrete. In 2003, NZS 3109 introduced an allowance for up to 10 L/m^3 of water to be added to 'normal concrete' at site to achieve the required workability if the concrete is delivered at less than the specified slump and less than an hour old, and then re-mixed at least 30 revolutions before re-measuring the slump. The basis for the 10 L limit is uncertain, but may have originated from a former rule of thumb that strength decreases 1-2 MPa per 25 mm of slump. Adding up to 10 L/m^3 of water assumes the benefit to consolidation overcomes the slight increase in free water to cement ratio and related reductions in concrete performance, including strength reduction of up to 10%.

Retempering with water to produce a slump higher than the specified slump will, however, reduce the overall quality of the hardened concrete. For example, ConcreteNZ (2018) reports that "no compaction" reduces strength by 20-30%, and that "more water" reduces strength 20%, increases the risk of shrinkage cracking, and increases dusting and wear of floor surfaces. It also reports that an addition of 10 L/m^3 in trials increased slump by 50 mm, decreased strength by 20%, and increased drying shrinkage by 20%.

More than 10 L/m^3 of water may be needed to restore workability to concrete with low water cement ratio, low slump, concrete that has stiffened due to unforeseen interactions between the constituents, or concrete that is starting to set due to (e.g.) delayed delivery or higher than anticipated temperatures. Adding water to restore workability to such concretes will reduce strength by a greater amount and may have undesirable effects on highly optimised blends of aggregate, cementitious binder, and admixture. For example, retempering a pump mix inappropriately may result in segregation or blockage within the delivery line, depending on the nature and grading of the aggregate, the overall mix design, and the line geometry. Even a

slight increase in water to cement ratio will increase the permeability of high-performance concrete, therefore concrete designed for watertightness or with specific durability requirements such as chemical or abrasion resistance, or for marine or coastal conditions, should not be retempered without pre-determined acceptable limits for water addition.

With most concretes now relying on combinations of admixtures to deliver the required workability, and the volume of added water or admixture not always easy to control (particularly if part of the load has been discharged), concrete should be retempered only as a last resort and within pre-agreed limits based on the maximum acceptable water to cement ratio determined in consultation with the concrete producer, designer, and contractor. For 'special concrete', or if a new mix design is being used, or excessive slump loss is likely because of haul time or anticipated warm weather, trial mixes or a trial placement may help to determine the required workability, limits of conditions such as delivery time, slump loss, temperature, and mix volume within which retempering is acceptable, and the maximum acceptable water or admixture additions. Nevertheless, any retempering of such concrete still needs to be approved by the designer and producer and implemented by a concrete technician.

Technology now exists for maintaining workability by automated control of water and admixture additions within acceptable ranges, during transit and upon arrival at site. The improved quality control and assurance offered by such systems could reduce the number of rejectable concretes and concretes being accepted inappropriately. However, a system's reliability and the acceptable limits of water/admixture additions would still need to be pre-determined for the anticipated range of concretes and conditions for which it would be used.

Even if the amount of additional water (or admixture) can be accurately controlled and reported, rejecting the load may be a more pragmatic solution. Creating a construction joint to enable the replacement batch to be placed at a later time may be quicker, more reliable, and cheaper for a project than determining the acceptable range of water to cement ratios or the effects of a stiff or retempered mix after it has hardened and potentially having to remediate or re-cast the placement. For example, a small top-up batch for the top of a pile in a recent wharf development was delivered stiffer than specified but was placed nonetheless, relying solely on a drop height of 1-1.5 m for consolidation. Compressive strength test results from three cores taken to assess the quality of the in-situ concrete varied from 24 to 50 MPa. The effect of the potentially low strength on structural performance was considered insignificant, but the effect on the risk of reinforcement corrosion was a concern and the designer required an acceptable durability assessment as a condition of signing the producer statement. A durability specialist's opinion was requested three months after construction, by which time remediation was not practical. Rejecting the final load or manually compacting it would have addressed concerns more effectively.

AIR ENTRAINMENT (YOU DON'T KNOW WHAT YOU DON'T KNOW – AND OTHERS DO)

Between about 2015 and 2019, anecdotal evidence indicated an increase in reported cases of floor slab delamination in New Zealand. Some cases were attributed to issues with specific admixtures. Around the same time, WSP received a set of cores from a medium-sized industrial floor in the North Island that had delaminated, with a request to measure the concrete compressive strength to ascertain whether the concrete supplied was consistent with the 30 MPa 'normal concrete' specified. The core sides exhibited many round air voids up to 2 mm across, suggesting the concrete was air entrained. A similar case was reported from a different location, but no samples from that site were received for testing.

The opportunity to investigate the cause of delamination finally arose some months later, when cores from a large commercial site were submitted for investigation. The measured core compressive strengths were within expectations for the grade of 'normal concrete' that had been specified. Air bubbles were visible on the core sides, and indeed the concrete supplier's mix design indicated a target air content of 4.5% in the fresh concrete. Petrographic analysis

of four core samples indicated the hardened concrete had a total air content of 5-7 %, including entrapped and entrained air. The petrographer saw no evidence of consolidation issues, excess fines, bleeding or bleed channels, but in all samples he observed more entrained air at depth than in the 4-10 mm surface zone consolidated by power-floating. In this surface zone he observed entrained air voids that had coalesced to form larger elongate surface-parallel voids, some of which were connected by fine [micro]cracks. He also reported a partial delamination in one core. He concluded that the total and entrained air contents had contributed significantly to the development of the surface cracking and delamination, the eventual widespread delamination probably being caused by differential stresses at the concrete surface, possibly due to subsequent drying shrinkage or loading of the slab surface. These stresses would have initiated further [micro]cracking from tips of existing [micro]cracks and related elongate air voids, eventually leading to complete separation of the cracked surface layer from the underlying sound concrete.

The possibility that air entrainment can contribute to delamination is well-known. For example, Suprenant and Malisch (1998) reported air entrainment as the consistent factor resulting in delamination in a site trial comparing the effects of entrained air and finishing techniques. CCANZ (2002), ACI (2015, 2020), and RILEM (2018) report that air entrainment increases the likelihood of delamination in addition to more familiar causes such as the combination of temperature, bleeding and setting rates, and finishing operations. On the basis that air entrainment increases the likelihood of delamination, ACI (2015, 2020 and earlier versions) prohibit the use of air entraining admixtures or fresh concrete air contents exceeding 3% at point of placement for floor slabs that will be hard-trowelled. Similarly RILEM (2018) recommends fresh concrete [total] air contents not exceeding 3% when a floor is to be machine-trowelled, based on US and European experience.

‘Normal concrete’ produced in accordance with NZS 3104:2003 and 2021 may be air entrained at the producer’s discretion to improve workability. Consequently, simply specifying ‘normal concrete’ for a slab that’s to be machine-trowelled will increase the possibility of delamination if the concrete supplied is air entrained or its air content elevated due to the combination of admixtures, additives, and mixing and delivery processes.

An informal poll of 10 experienced designers in New Zealand revealed none were aware that air entrainment is used for purposes other than freeze-thaw durability and that ‘normal concrete’ supplied to their projects may be air entrained at the producer’s discretion. Contractors may like the improved workability and finishability of air entrained concrete but not appreciate that it increases the risk of delamination. Similarly, most designers, contractors, and producers assume delamination is related to the nature and timing of finishing operations. The contribution of entrained air thus seems to be widely overlooked in New Zealand. In the above case, however, the end user was an international brand with many similar sites. Such companies may well have in-house designs specifying concrete with less than 3% air content.

For concrete floor slabs that are to be machine-trowelled, specifying concrete with a maximum fresh air content of 3% at the point of placement will reduce the risk of delamination, irrespective of whether air entrainment is intentional or arises from the combination of materials and mixing / delivery processes. For some concrete supplies, a higher grade may be needed to improve workability in lieu of air entrainment. This may in turn affect detailing for crack control.

Early discussions between all parties, including the owner/end-user and subcontractors, will help to ensure they understand the likely risk factors and can make informed decisions about the measures needed to ensure the concrete supplied can be placed and finished satisfactorily without increasing the risk of significant defects such as delamination.

SHRINKAGE (ALL CONCRETE SHRINKS. THE DEVIL IS IN THE DETAIL.)

Concrete contracts as it hardens and dries, and subsequently expands and contracts with changes in temperature and moisture conditions. It will crack if such movements are restrained.

Early age shrinkage may facilitate the removal of formwork, but generally shrinkage is a potential problem that needs close attention to detail and careful management to prevent uncontrolled cracking, especially in floor slabs.

Floor slabs are usually cast on polythene damp proof membrane to reduce friction between the slab and the substrate. A double layer is very effective. To address restraint from other sources, joints are usually needed. Prestressing is another, less common, option.

Sometimes features that will restrain contraction in the completed structure are overlooked. This may happen when attention is focused on deadlines, demanding service requirements or construction conditions, or changes are made late in the design process or during construction, resulting in movement joints being absent, incorrectly located, or cut too late. Examples of restraint that have caused significant shrinkage cracking in industrial floor slabs are:

- An element cast into the slab. This can be as simple as a guide rail for a door.
- A rebate cast into the slab for an architectural element.
- A load bearing element added to the slab.
- A slab cast on a slight slope to achieve a required fall and thus subject to a gravity component in addition to shrinkage strain.
- A slab tied into a footing.
- Services and other penetrations.
- Cold joints.
- Re-entrant corners.

Unless it compromises structural or seismic performance, shrinkage cracking may be acceptable in a floor slab that will remain dry in service and where aesthetics are not important, for example where a decorative floor covering will be applied. But it may not be acceptable where the floor surface is required to meet hygiene requirements, or withstand moisture ingress, cleaning regimes, aggressive chemicals, or impact and abrasion from mechanical equipment, such as in food processing, chemical manufacturing and storage facilities, or in high-performance warehouse floors. To minimize the risk of unacceptable shrinkage cracking, all parties involved in the project, including the owner/end-user, need to recognize the contributing factors and associated risks, and collaborate to manage them to an acceptable level. This may involve changing how the floor is used.

PUSHING THE ENVELOPE
(CONCRETE IS A ROBUST MATERIAL, BUT HAS ITS LIMITS)

As the list of design and construction parameters and the complexity of materials to address those needs grow, so does the likelihood (and consequence) of something going wrong. Identifying and managing risks in multi-faceted technologies is also more challenging.

Many failures are related to projects that extend the bounds of materials, construction process, and design. For floor slabs, aspects that flag potential difficulties are listed in Table 1. If a specific slab design has more than, say, a third of these features it may be starting to push the limits of concrete materials and construction technologies.

Table 1. High risk aspects in floor construction

Construction conditions	Service conditions
Remote site	Heavy design loads
Congested site	Sloping floor
Site access limited, e.g. by topography, or timing of other activities	Watertightness
Variable, weak, or aggressive soils	Chemical resistance
High groundwater level, pressure or aggressivity	Saline environment
Difficult weather conditions (freezing, elevated, or highly variable temperatures, wind, precipitation)	Abrasion resistance
Placing under water	Impact resistance
Concrete to be pumped over large distance	Freezing, elevated, or highly variable temperatures
Continuous pour	Saline environment
Minimum construction joints	Hygiene requirements
Traffic delays	Resistance to cleaning regimes
Contractors not familiar with the proposed concrete	Limited access for inspection, maintenance and repair
	Slip / skid resistance
	Aesthetics
	Low carbon footprint
	Concrete recyclable at end of service life
	Structure can be repurposed at end of service life

Some of these aspects can be addressed by the concrete materials and mix design, and some by the physical design of control joints and other detailing. Some combinations of construction methods and materials are tried and true. But concretes containing more than one cementitious component, or multiple admixtures or additives, are unlikely to have been tested or previously used in combination with the other risk factors in a specific placement to predict accurately how they will perform during construction and in service. For example, the risk of plastic cracking and delamination is high if a fibre-reinforced SCM concrete is placed outdoors in mid-summer in a continuous pour over several hours by a contractor who's never placed such concrete before, to construct a jointless, free-draining floor that will be directly exposed to aggressive materials handled by front end loader.

The habit of individual parties thinking that a potential issue is nothing to do with them, or assuming they know what the other parties need or want, or that what they did in a previous project will work in the current one is unlikely to achieve a good outcome in a complex project or with new materials. Similarly, congratulating themselves on 'getting away with it' this time, and on that basis repeating the same practices on future projects, will leave those future projects susceptible to the same risks – where the good luck may not continue. The new technology itself may then be blamed, and thus the opportunity to use it more effectively next time is lost.

Each party in the project team (including individual designers and contractors) will understand some of the individual risk factors and their significance, but may not appreciate how one factor may impact on others. Utilising their collective knowledge will ensure the combination of risks in the construction system remains acceptable. Involving the owner and, where possible, the end users, in dialogues and critical decisions about risk right from the start of the project ensures their needs and interests are fully understood and addressed as well as possible, and their expectations managed. This is particularly important when planning to use highly specialized materials designed for demanding construction and operating conditions, structural performance, and cradle-to-grave considerations. The early stages involve the designer

ensuring that the owner understands the options available, their effects on constructability, structural performance, durability, in-service operations and maintenance, carbon emissions, and cost (capital and maintenance), and the inherent risks associated with each option. Such consultation is not a new idea: industry already implements embodied carbon reduction and safety-in-design, and the process of durability planning as part of the concept design phase has been documented (CIA, 2014). Design detailing, construction process, and concrete materials should then be determined by discussions between designer, contractor and subcontractors (as required by NZS 3104 for 'special concrete') to ensure the designer's intentions can be achieved with the proposed materials and placement methods within the planned construction period, and the owner's expectations thus met. For example, installing and commissioning a new process or plant item in a food production facility between seasons may mean a specialist industrial floor topping designed to meet the client's specific operational and maintenance regimes is a more reliable solution than a crack-free, joint-free, chemical resistant structural floor slab. Or a sacrificial concrete surface may be more suitable in a waste transfer or coal handling facility.

THE VALUE OF TRIAL MIXES, TRIAL PLACEMENTS, AND PRE-POUR MEETINGS (TRY BEFORE YOU BUY)

Failures in large or complex projects are rarely attributable to a single factor or party, and reparation/liability is usually divided between parties. A specifically designed large floor slab is likely to be very expensive ($100,000s) to replace/remediate, plus the costs of determining liability. The owner often bears much of this cost, as well as costs associated with delayed occupancy or reduced value for onselling. The end users may incur ongoing maintenance and repair costs, or reduced functionality. Arguably the only clear winners are the lawyers of the various parties involved, and the repair contractors.

Harnessing the collective knowledge and experience of the project team to reduce the risk of failures, as discussed above, will also reduce the commercial risk to all parties involved. It requires good communication and co-operation between all parties, and one party to take responsibility for the total package. This may involve a change in contract relationships and project management. In complex projects or with new materials and technologies, consultation and collaboration may not be enough to anticipate and address potential problems: trial mixes and placements may be needed.

When developing a new mix design, a trial mix enables key properties such as workability [and its retention], air content, and rate of strength development to be measured in controlled (and therefore repeatable) conditions so that if necessary the mix design can be amended to achieve the required properties. Trial mixing might be prompted by a new raw material, logistics associated with a project, or properties requested for a project (e.g. drying shrinkage, maturity, heat evolution, resistance to carbonation or chloride ion ingress, water absorption or permeability, or benchmark testing of in-situ properties). Trial mixing and testing also enables the producer to provide data for future projects that may use the same concrete.

A trial placement, whereby the contractor places a batch of the proposed concrete in a mock-up of critical or typical formwork and reinforcement configuration, and finishes the exposed surface using the proposed finishing techniques will show whether the proposed mix design is suitable for the likely delivery times and conditions and the contractor's planned methodology. This can reveal potential incompatibilities of materials, formwork, reinforcement details, and placing and finishing processes, and can enable architectural finishes to be evaluated so that materials and processes can be modified before the first placement. Trial placements are particularly useful in critical or challenging (e.g. congested) pours to ensure that the concrete will get to the right place in the right condition within the structure. Protocols for trial placements of sprayed concrete are already well-established and widely used in New Zealand. The same mindset could readily be adopted for other materials and applications.

To make an informed decision based on the test results, trial mixes and placements must be carried out in time for relevant results to be obtained and assessed before construction starts. Producers and test labs can advise on suitable testing regimes, and the logistics involved. For example, early age strength development may be important for planning subsequent or adjacent activities. Durability testing of concretes designed for aggressive environments may only start when the concrete is 56 days old and then take a further two months to complete. In practice, mix design is often one of the last steps before the first pour, therefore trials require forethought and planning. Submitting a new mix design for 'special concrete' the day before the first pour is too late for it to be evaluated other than by measuring fresh concrete properties of the first truckload before discharge.

A recent example involved a concrete based on an existing product, but with higher slump to accommodate longer and more variable anticipated haul times and slightly different use. The supplier submitted the mix design for approval the day before the first pour. The design team and contractor noted the high slump and commented that formwork was not designed for self-compacting concrete. The casting sequence resulted in significant localised honeycombing. The designer, contractors, and producer discussed the events of the first pour and the resulting defects in the hardened concrete and identified changes that were then implemented in subsequent similar placements. The large scale of this project and the contract type enabled the first placement to be treated as a trial and the opportunity to learn from it to be utilised.

On smaller projects and one-off placements, the potential cost and inconvenience of remedials may be better avoided by carrying out a small 'mock-up' trial placement. One example of this involved piles cast with a tremie mix. Several piles were cast successfully. When the next pile was completed, on another part of the structure, an extra truckload of concrete was left over after the casing was filled. Investigation revealed that the piles in this location had a tighter reinforcement spacing, through which the concrete was unable to penetrate to fill the cover zone. Unfortunately, no-one recognised the inherent incompatibility until it was too late. In a subsequent project, the same contractor initiated a trial placement for a series of stitch joints between precast panels. This enabled them to refine their methodology and manage risk, giving the designer confidence in their process, and satisfying quality assurance requirements.

Whether or not any trials have been carried out, a pre-pour meeting before the first placement is essential to ensure all parties understand and agree on the goals to be achieved and to identify potential problems (and solutions) in time for them to be rectified. Follow-up meetings should be held if problems are encountered and when changes in materials, key personnel, processes, or delivery or placing conditions are anticipated. In longer projects, regular pre-pour meetings will help to maintain focus, familiarize new personnel, and provide an opportunity to suggest improvements to materials or processes. These discussions should involve representatives of the owner/end-user, design team, supplier, and contractors. They should have an agenda involving all parties, be minuted, and actions assigned and followed up. Even if no problems arise, the process and meeting records will improve understanding and instill habits of co-operative and collaborative communication that will benefit all participants in future projects.

SUMMARY AND RECOMMENDATIONS (HOW TO GET THE BEST FROM CONCRETE MATERIALS IN THE 2020s)

Today's concrete is no longer the simple blend of aggregates, Portland cement, and water on which much of the industry's practices are based, but a complex blend of aggregates, binders, admixtures and additives designed to optimise resources and satisfy many different demands during and after construction. It is more sensitive to small changes in materials and mix design, and the specific conditions in which the fresh concrete is handled. Coupled with a rapidly increasing range of raw materials with different characteristics, plus project teams often comprising multiple (and possibly independent) designers and contractors, this means

potential shortcomings of a proposed mix design and construction process are becoming harder to identify, increasing the likelihood of significant defects.

To ensure that concrete materials of the 2020s meet expectations means considering concrete design and construction as a system where every component affects the performance of every other component. This will involve some changes in approach from the wider concrete industry, irrespective of individual pour and project complexity, including:

- Understanding the characteristics of concrete constituents and their effects on fresh and hardened concrete and how to accommodate them (including differences between individual products, regional variations, and limitations associated with particular types of raw materials and concretes);
- Setting and adhering to limits for maintaining and restoring workability in mixes or project logistics, without compromising other concrete properties, particularly where the 10 L/m^3 rule does not apply;
- Paying close attention to design details that may compromise construction process or the performance of the fresh or hardened concrete;
- Harnessing the knowledge and experience of all parties in the project team, including the owner/end-user, designers, suppliers, and contractors, via contracts and consultation processes that encourage and facilitate collaboration and co-operation throughout the project;
- Utilising trial mixes and trial placements (with appropriate associated testing), and pre-pour meetings to identify and address potential problems before construction and whenever significant changes in materials or construction processes are anticipated.

By reducing the risk of significant defects, these practices will improve the standard and performance of concrete construction and maintain its reputation as a reliable, adaptable, and economic system, and thus a preferred option for future projects.

REFERENCES

ACI 301-20 *"Specifications for structural concrete"* ACI Manual 2021

ACI 302.1R-15 *"Guide to concrete floor and slab construction"* ACI Manual 2021

CCANZ (2002) *"Surface delamination in slab on ground construction"* TR09. Cement and Concrete Association of New Zealand.

Concrete Institute of Australia (2014) *"Recommended practice for Durability Planning"* Z7/01

ConcreteNZ (2018) *"Uncontrolled water addition"* ConcreteNZ Readymix Technical Note 6, June 2018.

Mackechnie J. R. (2003) *"Hardened properties of concrete containing New Zealand aggregates"* SESOC Journal Vol. 16, No. 20-29

RILEM Technical committee TC 268-SIF *"Surface delamination of concrete industrial floors and other durability related aspects guide"* RILEM 2017.

Standards New Zealand (2003 and 2021) *"Standard specification for concrete production"* NZS 3104

Suprenant B.A. and Malisch W.R. (1998) *"Diagnosing slab delaminations. Is improper finishing the only cause?"* The Aberdeen Group publication C980029.

A REVIEW OF CONCRETE SPECIFICATIONS IN THE NEW ZEALAND INDUSTRY AND THE COMPLICATIONS ASSOCIATED WITH THEM IN PRACTICE

P. DONOGHUE[1], T. SAWYER[2]

[1] Firth Concrete Materials Manager, Hamilton, New Zealand
[2] Firth Concrete Materials Manager, Christchurch, New Zealand

SUMMARY

Over the years there have been many discussions over what is a good specification and what is a poorly written specification. This work is a light hearted summary of specification clauses that are currently being used within the industry and a practical approach to the interpretation of the specification, how it gets priced with some of the more common tags that would be included, and discusses the chances of the specification being followed or implemented on site. The biggest risk with the best written specification is the management of the details and ensuring all parties are clear on what is expected. With loosely written specifications there is scope for interpretation or the opportunity for the less educated to take simplest route and ignore all the detail buried in the jargon in random paragraphs within a document that has become part of the clutter in a shelf.

The primary topics addressed in this paper are the specification of mix constituents or an individual mix constituent specified where achieving the limits is not possible with local materials, specification of mix characteristics without consideration of the suitability of the mix for the application and the specification of mix properties that applicable and relevant but are unlikely to be followed as the placer and pump operator dictate the type of concrete based on their skill level and competency.

Our challenge as an industry is to produce a set of instructions that everyone can read and understand without increasing risk of failure but being environmentally conscious at the same time.

We hope to point out some of the confusions, some of the short falls and make some recommendations, all with the intention to open a dialog to develop clear and concise specifications.

INTRODUCTION

Over recent times there has been a lot of debate and discussions amongst the practicing concrete technologists in New Zealand that review the specifications for pricing and mix design compliance and there has been a concern raised that the specifications are often vague or excessively onerous, in some cases simply impossible to achieve.

There is an understanding that the quality of concrete that is going into the structures is a major concern, and the specifying engineers are attempting to produce a specification that meets the structural requirements and limits the risk.

THE ROLE OF THE CONCRETE TECHNOLOGIST

In the scope of the NZS3104 the Plant Engineer is a responsible for the concrete mix designs and the quality of production at the plants they are responsible for. All of the CNZ audited plants have well experienced plant engineers that are responsible for the concrete and ensuring it meets required standards and generally have many years of experience on any different types of concrete projects. In line with global trends this role is more commonly filled by a concrete technologist. This is often a miss quoted term as this is a formal post graduate qualification and not a nominated status, but the qualified concrete technologist when reading a concrete specification will be taking into consideration the design engineers specification, but will include the intended application, the element to be cast and any risk during the plastic or hardened state, the transport and delivery requirements including transit time, placing, compacting and finishing requirements, and design a concrete that will satisfy all of these. It is no simple task at tender stage as there are often a series of assumptions that need to be made that are typical of the New Zealand industry and local environment. These would often raise conflicts or concerns around the specification, and these will be tagged on the quotation to highlight these to the customer.

A closer collaboration between the design engineers, the plant engineers and CNZ technical team at the time of compiling a specification will result in a specification that will meet the structural requirements, technical needs in terms of hardened and plastic performance, environmental sustainability and practical requirements for any project ensuring the best possible outcome for the client.

THE QUALITY OF THE SPECIFICATION

The specifications that are received are often made up of several different parties and it is common to have the same concrete specified in two or three different ways. It is common for the concrete specification to have a different set of requirements to the drawings. In this case the pricing team would typically quote on both concrete types and let the contractor resolve the concrete selection with the project managers or design engineers. Although the concrete producer may well have read the specification, at the time of delivery there is no possible way the concrete producer can manage the concrete selection based on the specification. The concrete producer will deliver what ever the customer orders and they will be delivering the concrete to the specifications supplied by the customer at the time of ordering. The challenge here is that our industry has become so familiar with ordering concrete on strength alone and leaving the pump operator and placer to define the slump the control has gone out of the window and the chance of the concrete meeting the specification has reduced significantly.

Probably the biggest challenge with specifications is having limits or tolerances that cannot be tested or verified. When a 30MPa concrete is specified with a w:b ratio of 0.45 there is very little that can be done to test the w:b ratio other than checking the batch records, but this is a rather time-consuming task and unlikely to be undertaken by a consulting engineer so strength of the concrete is then relied upon as the guiding factor.

ON SITE WORKMANSHIP AND SUPERVISION

Concrete is specified by a qualified professional. The production of the concrete is covered by NZS3104 and all concrete for commercial and structural work should be supplied from a plant that holds a Certificate of Audit from CNZ which requires a suitably qualified Plant Engineer to design the concrete and manage the quality of the concrete. Once the concrete has been delivered it is then left to the concrete placing fraternity. In most specifications there is little or no mention made of this process which is equally important in achieving the serviceability and design life of the concrete element or structure. It is all good and well specifying properties of the concrete that will lead to less shrinkage but proper compaction, protection and curing renders these specified requirements meaningless.

The great majority of cracking issues are not caused by poorly designed or batched concrete but rather by the need of the pump operator to 'wet her up' or the poor placing and compacting techniques, protection and curing. Lack of correct compaction/vibration techniques, lack of protection of the plastic concrete and lack of suitable curing will result in a lower quality final product and poor-quality cover-crete which is the critical part of the element. Specification of the placing and compaction methodology, protection of the fresh concrete, curing and location of and timing of saw cuts all needs to be included in a prescriptive specified but a specification without a measurement is meaningless so site supervision is critical if the engineers are accepting responsibility and specifying the materials in a prescriptive manner.

PRESCRIPTIVE VS PERFORMANCE BASED SPECIFICATIONS

Prescriptive specifications give the client and design engineer a (false) sense of security about the end product when they make their final investment decision. The assumption here is that the specifications are understood by all and the intention is adhered to by all. The trouble here is that there are so many variables, new technologies and a drive to produce an environmentally sustainable product that these prescriptive based specifications become counterproductive to the industry at large.

Performance based specification is a result, output or quality-based approach gives the contractor and suppliers more scope to innovate, adopt cost effective methods of work, and deliver a material that is fit for the design life, environmentally sustainable and potentially offering better value for money. It generally ties in a portion of the contactor's payment into a service period to deal with the high risk of issues and failure in the early stages of the life of an asset – commonly referred to as the 'Bathtub Effect' but asset managers.

To draft an appropriate performance specification, the design engineer needs know exactly what is needed as an end product. The simplicity of this statement is deceiving as this type of specification needs an intimate understanding of the end performance and they need to have a method of compliance testing. Performance based specifications will rely heavily on a team of people coming together to work towards a single goal. This requires a well-defined outcome and collaboration with the broader team of experts who can define the performance based specifications and detail testing methods to verify the outcome.

ConcreteNZ published Technical Report TR10 Specifying Concrete for Performance which was updated in 2013. This is a great guide and this can be used to draft a reliable performance based specification, the challenge is to overcome the need to write a performance based specification and add in some 'key' prescriptive specifications just for good measure. These can often be counterproductive and will lead to concrete be over designed, expensive and generally not environmentally sustainable.

REVIEW OF SPECIFICATIONS

The specification samples below are some extracts from specification documents where we highlight the challenges and propose an alternative method of specifying the performance.

Specification 1

Concrete shall not be pumped without the Contract Administrator's approval Where such approval is given, only standard structural concrete mix designs may be used. The use of a pump mix design will not be accepted.

In a market where probably 80%+ of the concrete is pumped this is a clause that is unlikely to be adhered to. The assumption here is that pump mixes are going to be significantly different in engineering properties to the desired material. It is unclear why the design engineer does not want a pump mix to be used and is would be valuable to include a set of characteristics that must be met and let the concrete technologist do what they are qualified to do and design a composite material that will meet the hardened concrete requirements and the placing techniques. These could be a limit on drying shrinkage or durability specification.

Specification 2

The plant engineer shall specifically design the concrete mixes for this project to eliminate the occurrence of plastic shrinkage cracking and early age thermal cracking.

This is becoming more common and is impossible to achieve. The term 'eliminate' is sometimes replaced with 'reduce the risk' but this gives no reference to the baseline. The plant engineer can design concrete to reduce the risk of plastic shrinkage cracking, but this will increase the risk of plastic settlement cracking and at what point does this become a problem? Plastic shrinkage cracking and early age thermal cracking are both due to environmental aspects and are dealt with through proper protection and curing. A performance-based specification that limited cracking to occur only within saw cuts and any random or unplanned cracks would be repaired at the contractors cost to reinstate the concrete element to its intended serviceable state would be a reasonable specification and this would require some level of discussion between the concrete supplier and the concrete placer.

Specification 3

Minimum binder (cement and fly ash) content is recommended to be 10kg/m3 of binder per MPa of strength +/- 5%. For example:
- *40MPa Concrete = 400kg/m3 of binder*
- *30MPa concrete = 300kg/m3 of binder*

This recommendation has no place in a specification document where the concrete plant holds a valid NZS 3104 certificate of Audit. The strength of the concrete would need to meet the requirements of the NZS3104 and there are no prescriptive binder-based specifications. Binder content has absolutely no bearing on compressive strength without the water being specified.

Self-Compacting Concrete
Allowable range of water:cement ratio 0.35
Total binder (GP cement, and SCM) content 520 kg/m3
Maximum water content 170 L/m3
SCM, as percentage by weight replacement of cement, either:
- *30% Fly Ash, or*
- *65% Slag, or*
- *8% Amorphous Silica (micro silica)*

Maximum 56 Day Shrinkage 350 Microstrain (TBC)
Shrinkage control admixture (Sika Control 40) to be added at nominal 2% by volume

Allowable range of water:cement ratio 0.35 – 0.45
Total binder (GP cement, and SCM) content 330 kg/m3 to 430 kg/m3
Maximum water content 170 L/m3
SCM, as percentage by weight replacement of cement, either:
- *30% Fly Ash, or*
- *65% Slag, or*
- *8% Amorphous Silica (micro silica)*

Maximum 56 Day Shrinkage 350 Microstrain (TBC)
Target including 70% or greater of coarse aggregate in the total mix volume (including sand > 7mm, 12/13 mm and 19 mm aggregate sizes)
Shrinkage control admixture (Sika Control 40) to be added at nominal 2% by volume

The two specifications above are unlikely to be achieved and are confusing prescriptive and performance specification. The water content of 170 litres per m^3 is unrealistic for an SCC, the binder content is counterproductive for the shrinkage requirement, and a shrinkage requirement of 350 microstrain for an SCC with this binder content is unrealistic, even with the use of a shrinkage reducing admixture. The second of the two mixes above specifies 70% or greater of coarse aggregate. It is unclear 70% of what – it is assumed that this is 70% of the total volume of the aggregate must be coarse aggregate above 7mm. This concrete is going to be a nightmare to place, compact and finish. In a large unreinforced base this could work, but if this concrete is to be placed around reinforcing there is likely to be honeycombing and a myriad of other problems as this concrete will not be workable.

If there was a clear intention of what the desired outcome needs to be the concrete technologist could provide the design engineer and the contractor a few solutions that could meet the hardened concrete requirements as well as the placing techniques, but with this specification there is no opportunity for collaboration.

Specification 4

The Contractor shall perform a bleed test on each trial mix in accordance with NZS 3112.1 Section 8 by pouring a proportion of the mix into a 200 litre drum. The mix shall be vibrated until only a trace of small air bubbles is observed percolating through the mix. The top surface of the concrete shall be screeded flat and measurements shall be taken of the depth and extent of bleed water.

The extent of bleeding that will be deemed as acceptable depends on the water-to-cement ratio used for Contractor's mix design and the early age performance of the concrete. Sufficient bleeding is desirable to prevent premature drying of the concrete surfaces and consequent plastic shrinkage cracking of the concrete.

Excessive bleeding which delays the Contractor from properly finishing the concrete or significantly reduces the concrete water-to-cement ratio is undesirable. The Contractor shall monitor the early age performance of the concrete to determine the acceptable extent of mix bleeding during the trial mixes. The Principal may request concrete mixes with excessive bleeding to be modified to reduce the quantity of bleed water.

This is unlikely to be accepted as a test method and it is unlikely that repeatability and reproducibility would be reliable. The bleed test should be specified to a National Standard. There is a New Zealand standard for bleed although the more common specification for bleed is the Australian Standard. It would be appropriate to specify this as a test method with a set of bleed limits.

Specification 5

Based on experience from previous contractor supplied mix designs where cracking has occurred, the failure is typically contributed to the Engineer not reviewing the mix design, incorrect material proportions and inadequate curing controls put into place. Other issues we have come across in mix design are higher than normal sand contents and the typically specified small aggregate size (<13mm max). This causes weaker bond between aggregates, which may cause potential cracking risk to slabs. The higher sand content specified also absorbs water from the mix, slowing the hydration reaction with the cement, and causing inadequate curing of the concrete. To avoid this it is important that the sand is saturated prior to being added to the mix.

If the contractor increases the water content to maintain workability, the risk of cracking increases due to plastic shrinkage within the concrete.

The assumed intention is to produce a concrete with a low risk of cracking and the use of smaller aggregate increases the risk of cracking. It would be beneficial to remove this clause completely and write a clause that makes the contractor liable for any cracking outside of induced cracks.
The concerns about sand and hydration of cement are technically incorrect.

Specification 6

Use air entraining admixture in accordance with ASTM C 260 to provide a total air content of 4% ± 1.5% provided that when the mean daily ambient air temperature in the vicinity of the work falls below 5 degrees Celsius for more than one day the total air content provided shall be of 6% ± 1.5%

The addition of entrained air is common in concrete exposed to freeze thaw cycles where freeze thaw is a form of mechanical weathering. The risk here is entrained air particularly above 5% will reduce the abrasion resistance of the concrete significantly. If the freeze thaw cycles are not daily then the benefits of entraining 6% air will be outweighed by the loss in abrasion resistance. An understanding of the environment and service life of the concrete would enable the concrete technologist to add value to this specification if it was performance based.

Specification 7

Recycled water shall not be use. The water shall be potable, with a pH greater than 6.5 and total dissolved solids not exceeding 200 mg/kg.

The maximum concentration of chlorides shall not exceed 200 mg/litre. The maximum concentration of sulphates shall not exceed 4% by weight.

In the current market it is unlikely that concrete is made without recycled water. Ready Mix Concrete plants generate a huge amount of waste water and generally recycle water by passing it through settlement tanks and then using the water in the concrete. There are a set of limits that the water must comply with but using recycled water to produce concrete is done by the majority of concrete plants in New Zealand. This is becoming more common with the use of recycled aggregates becoming more common too.

Specification 8

Fine aggregate shall be well graded sand, shall be selected to minimise the content of material finer than 75 microns, and shall not exceed the content limits set out in NZS 3121. The percentage of fines passing a 150 micron sieve shall be limited to 3.5 percent of the total volume of coarse and fine aggregate.

The intent of this clause is unclear and very generic. In high strength concrete this may be a valid comment, particularly where a variety of binders are being used to achieve a specific performance, but this would yield disastrous effects in a 25MPa concrete for columns. A sand of this nature would need an air entrainer to keep the concrete stable and prevent excessive bleed and segregation.

Specification 9

All concrete shall have a maximum nominated (pre-additive) slump of 100mm.
Concrete workability shall be assessed using;
a slump cone test in accordance with NZS 3112.1 before the addition of additives,
a slump cone test in accordance with NZS 3112.1 after the addition of additives, and
by placing and finishing a test section.

Strictly No Super Plasticizers are to be used in any mix. Plasticisers and water reducers may be used provided the dosage is at the lower end of the recommendation and is being provided to reduce shrinkage and not to reduce cement in the mix. A preference is placed on the use of organic admixtures over synthetic.

The challenge with these specifications is they are not conducive to the batching process and are unlikely to be followed. Admixtures are a constituent material, and they are added with the mixing water. By dosing the admixtures with the mixing water better dispersion is achieved and more effective use of the admixture. Adding admixtures to the back of the truck after batching the concrete is risky and will lead to a higher variability and will in effect double the required mixing time. Admixtures, whether super plasticisers, PC, PCE's old generation admixtures, mid-range water reducers or the basic plasticisers or water reducers are all constituents of the concrete mix design, and they are added to the concrete to achieve a given outcome – generally a cost-effective concrete that meets the specified slump and strength. If the concern is managing the water for a specified slump, most modern concretes with a 160mm slump will have less than a 60mm slump without the admixtures.

It must also be mentioned that a concrete designed for a 100 slump cannot be increased to a 160mm slump simply by adding a super. The concrete will segregate and will give poor results.

A better result would be achieved if the final outcome was specified and it is unclear as to the intention of the testing of the slump prior to adding the admixture.

concretenz
BUILDING RESILIENCE
CONFERENCE 2022
13-15 October 2022
Energy Events Centre | Rotorua

HIGH AND ULTRA-HIGH PERFORMANCE CONCRETE FOR NEW ZEALAND BRIDGES: A NATURAL PATHWAY TO SUSTAINABLE DESIGN

ROSIE PAGEL[1], HANNAH WEISE[2], ALESSANDRO PALERMO[3], ERNESTO HERNANDEZ[4]

[1] University of Canterbury, Christchurch, New Zealand
[2] WSP, Tauranga, New Zealand
[3] University of Canterbury, Christchurch, New Zealand
[4] University of Canterbury, Christchurch, New Zealand

SUMMARY

High performance concrete (HPC) and ultra-high performance concrete (UHPC) show significant potential to decrease the environmental impact of concrete. This research explores the feasibility of these materials for New Zealand bridges in three phases: (i) testing the mechanical properties of the concrete mixes which primarily use locally sourced materials, (ii) parametric analysis of the structural performance in a prototype bridge and (iii) assessment of the economic and environmental impacts. It concludes that HPC is the cheapest, most sustainable and constructable option over its lifespan, while UHPC could become more sustainable as low cement alternatives are investigated.

INTRODUCTION

Integrating sustainability into infrastructure is increasingly becoming a crucial aspect of the engineering industry. The environmental damages caused by the production of cement, the major component of concrete, have been widely documented (Habert and Roussel 2009, Dong 2018). Despite its large carbon footprint, concrete remains widely used as its mechanical properties allow it to be implemented for a variety of applications and construction methods.

Two strategies to improve the sustainability of concrete are gaining momentum: improving the concrete properties to reduce material required ant the replacement of cement with supplementary cementitious materials (Habert and Roussel 2009). Both strategies aim to reduce the total carbon dioxide emissions. High performance concrete (HPC) and ultra-high performance concrete (UHPC) can fulfil these goals, as proven by research (e.g. Aïtcin 1998, Fehling et al. 2015). However, there is limited research into HPC and UHPC within a New Zealand context, thus this research aims to investigate the potential of these materials (Figure 1). This study has three phases: (i) testing the mechanical properties of the concrete mixes which use locally sourced materials, (ii) parametric analysis of the structural performance in a prototype bridge and (iii) assessment of the economic and environmental impacts.

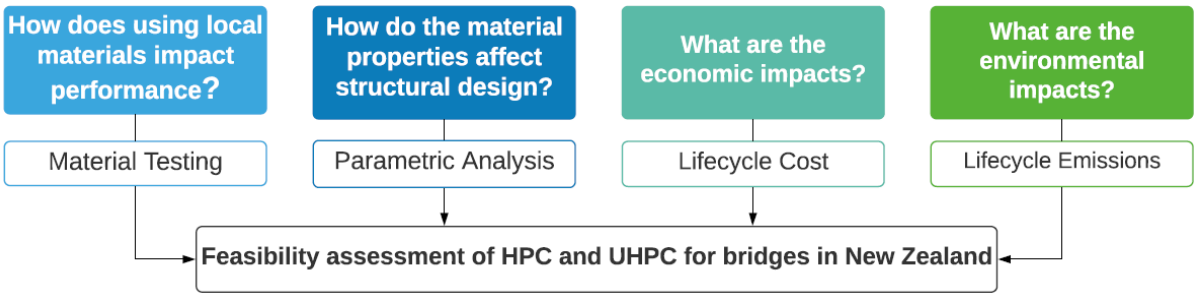

Figure 1. Flow chart outlining research objectives and activities

LITERATURE REVIEW

History of Modern Concrete Technologies

HPC technology was first developed in the 1970s and gained popularity as a group of designers saw its potential for use in high rise buildings. The superior mechanical properties of HPC, including high compressive and flexural strength, allowed taller structures to be built (Aïtcin 1998). In the 1980s research proved that decreasing the water/binder ratio from approximately 0.7 for conventional concrete to 0.3 – 0.4 could improve the compressive strength (Aïtcin 1998).

In 1981 Bache developed a concrete which achieved a compressive strength of 280 MPa, while his peers struggled to consistently achieve strengths of 30 MPa (Azmee and Shafiq 2018, Bache 1981). Despite the increased compressive strengths, these concretes became more brittle (Azmee and Shafiq 2018).

To overcome this brittleness, Richard and Cheyrezy investigated using steel fibres, which provide tensile strength by transferring forces across cracks, in their concrete mixture (Azmee and Shafiq 2018). The increased ductility of this steel fibre reinforced concrete resulted in more favourable distribution of stresses and cracking before failure (Fehling et al. 2015). This concrete formed the basis of modern UHPC. Widespread research into both HPC and UHPC demonstrated that improved mechanical properties could be consistently attained (e.g. Larrard and Sedran 1994, Richard and Cheyrezy 1995, Shah 1997). Following this, several proprietary mixes were developed including Ductal ® (LaFargeHolcim), BCV (Vicat) and BSI Ceracem © (Sika-Eiffage).

Table 1. Typical properties of concrete types

Concrete Type	Compressive Strength (MPa)	Tensile Strength (MPa)	Other Properties
CC	15 – 50	2 – 5	-
HPC	50 – 150	5 – 8	Durable
UHPC	> 150	> 8	Highly durable

HPC and UHPC Use in Bridges

As concrete suppliers investigated the commercial potential of this material, researchers and engineers began to investigate its structural applications. In 1997, the world's first UHPC bridge was constructed in Sherbrooke, Canada. The superstructure consisted of a precast space truss entirely constructed out of UHPC (Aïtcin 1998). With design compressive strengths of 200 – 350 MPa, this bridge signalled a new era in the international concrete bridge industry.

Since then, HPC and UHPC have been used extensively in bridges internationally. In 2013, the Federal Highway Associated (FHWA) identified 55 bridges that used UHPC and HPC in North America alone (FHWA 2013). Similar advancements can be seen in France, Germany, Italy, China, Japan, Malaysia and South Korea (Azmee and Shafiq 2018). However, these materials remain underutilised for bridges in New Zealand with few bridges using the materials.

The Papatoetoe Pedestrian Bridge was the first, and currently one of few, bridge in New Zealand to include UHPC as the primary structural material (Rebentrost 2005). Section sizes were reduced due to increase material strength, resulting in a more economic structure (Rebentrost 2005). Reduced loading, therefore, minimised the seismic design requirements and the use of steel fibre UHPC removed the need for steel reinforcing bars (Figure 2).

(a) (b)

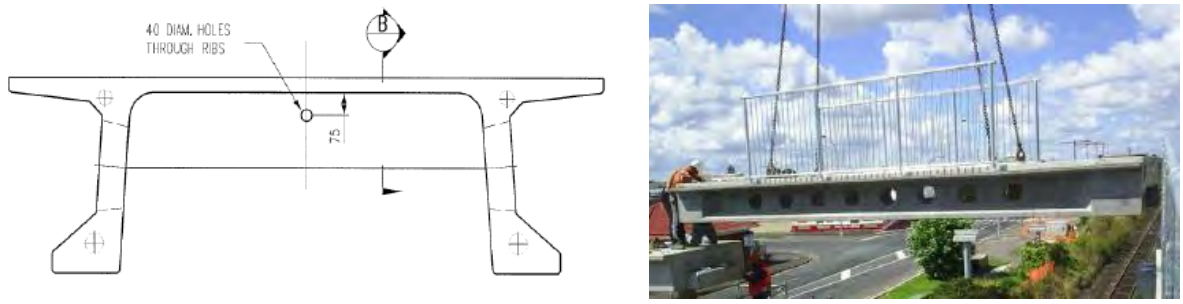

Figure 2. (a) Beam element (b) Precast segments being lifted into place (Source: Rebentrost 2005)

For an altogether different purpose, HPC was utilised the bridge girders of the Tauranga Harbour Bridge in 2009. This bridge links two communities, and thus a short construction time was required to minimise disruption to the communities. To achieve this, an incremental launch construction methodology was used, and the high early-age strength of HPC enabled sections of the bridges to be installed every day (McSaveney et al. 2011).

High initial costs and apparent lack of construction expertise appear to be limiting factors to the uptake of these materials. However, use in recent bridges have shown that the high strengths allow for reduction in section sizes (Rebentrost 2005). To fully understand their potential, economic and environmental analyses should be undertaken that consider the reduced section sizes and therefore material use.

MATERIAL TESTING OF HPC AND UHPC

In this second phase of this research, HPC and UHPC mix designs were sourced from literature and adapted to incorporate primarily locally sourced materials (Table 2). A total of five HPC mixes and three UHPC mixes were experimentally tested under compression, tension and flexure.

Table 2. Concrete mix designs in kg/m^3

Concrete Ingredients		GP Cement	Silica Fume	Class C Fly Ash	Visco Crete 5-555	Steel Fibres	Sand < 5 mm	Fine Silica Sand	Gravel 7 – 13 mm
Mix Design	HPC	384	48	59	4.76	Refer Table 3	925	-	822
	UHPC	1114	169	-	40		-	1072	-

Mix Design Sources: HPC (Hernández 2020), UHPC (Azmee and Shafiq 2018)

Three main parameters were investigated for HPC and UHPC (Table 3, Table 4).

1. Water/binder ratio to validate the theory that reduced water/binder increases compressive strength.
2. Steel fibre content to assess whether this improved tensile strength as suggested in literature (Schmidt et al. 2012, Dong 2018, Song and Hwang 2004).
3. Steel fibre length to optimise the particle packing within each matrix (e.g. Aïtcin 1998, El-Tawil et al. 2020, Larrard and Sedran 1994).

The strengths achieved in testing was assessed against the target strengths and behaviour for each test was compared with typical behaviour observed in literature. These results will provide an indication about whether using locally sourced materials affects the mechanical performance.

Table 3. Key mix parameters

	HPC (Hernández 2020)					UHPC (Azmee and Shafiq 2018)		
Mix Type	A	B	C	D	E	F	G	H
w/b ratio	0.31	0.31	0.31	0.31	0.31	0.24	0.17	0.17
v_f (%)	0	1	1	0.5	0.5	1	1	2
Steel Fibre	-	5D 60mm	4D 35mm	4D 35mm	5D 60mm	OL 13/.20	OL 13/.20	OL 13/.20

Table 4. Target strengths for steel fibre mixes (MPa)

	Compression	Tension
HPC	100-120	5 – 8
UHPC	160-180	> 8

RESULTS

The target compressive strength for HPC mixes was achieved in the testing (Figure 4). However, the highest average compressive strength (UHPC mix G) was nearly 20 MPa below the target strength of that mix design (Figure 3). HPC displayed moderately brittle behaviour, with minor cracking before failure, unlike UHPC, which had several microcracks prior to failure (Figure 5).

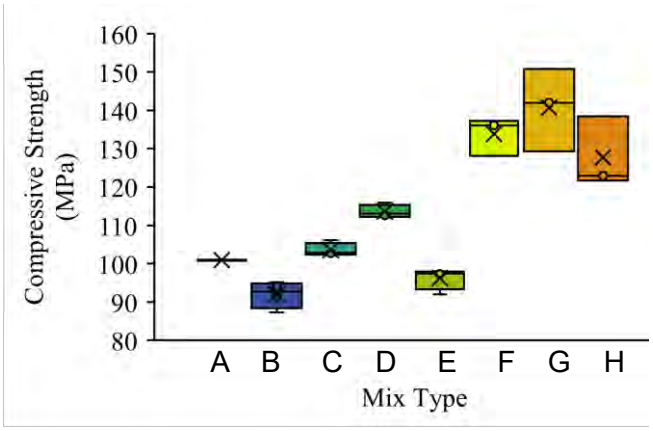

Figure 3. HPC and UHPC compressive strengths

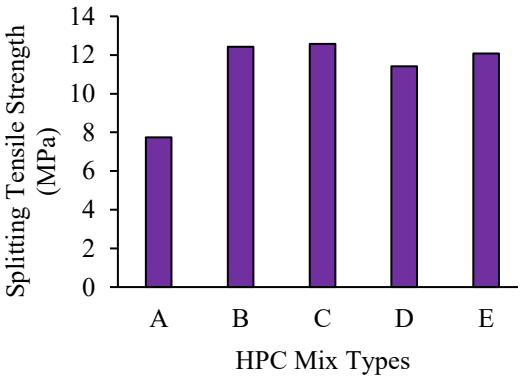

Figure 4. HPC splitting tensile strength

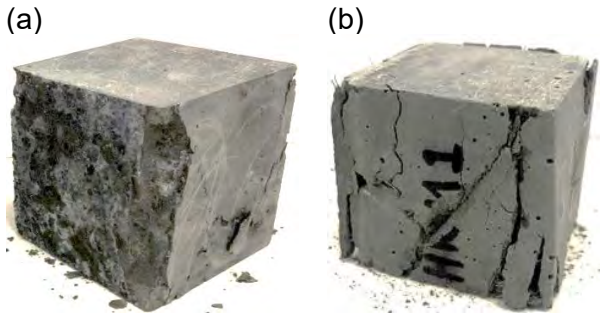

Figure 5. Specimens after compression testing (a) HPC (b) UHPC

None of the UHPC mixes achieved the target strength unlike the HPC mixes, which all achieved tensile strengths greater than the target. The UHPC mixes exhibited strain-softening behaviour in tension (Figure 6).

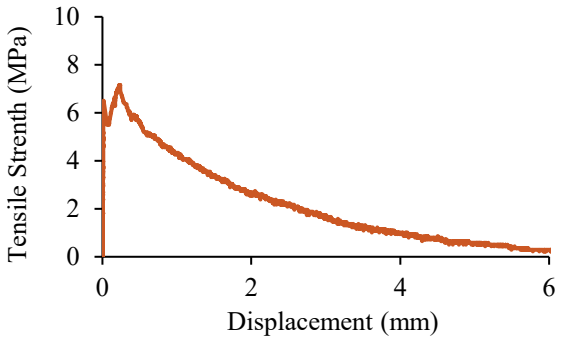

Figure 6. Typical tensile behaviour of UHPC

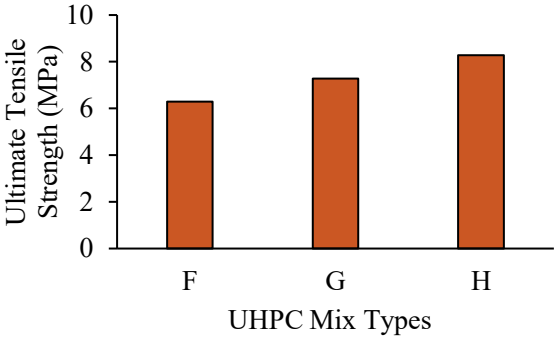

Figure 7. Ultimate tensile strengths of UHPC

HPC and UHPC mixes exhibited different post-peak behaviour when tested in flexure. HPC specimens showed strain softening after first cracking (Figure 8), while UHPC specimens displayed strain-hardening (Figure 9). Ductile behaviour, which was more pronounced for UHPC than HPC, was observed for both materials in the flexural testing.

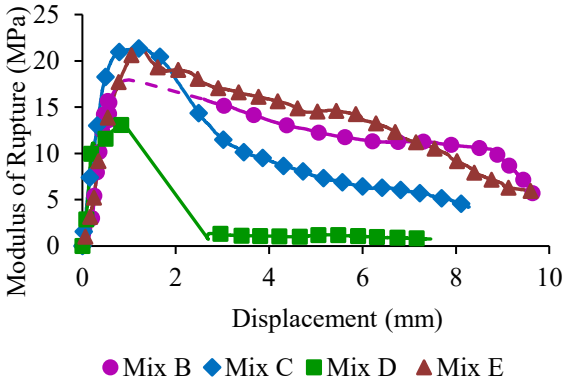

Figure 8. Flexural behaviour of HPC

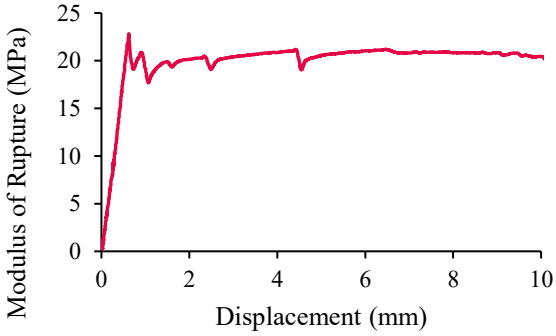

Figure 9. Typical flexural behaviour of UHPC

For a water/ binder ratio of 0.31, HPC achieved compressive strengths of 90 – 115 MPa, and for a ratio of 0.17 the UHPC achieved strengths of 125 - 140 MPa. This generally indicates that reductions in the ratios can increase the compressive strength.

An increase in splitting tensile strength of 47% and 62% was achieved for the 0.5% and 1% fibre reinforced HPC mixes, respectively, compared to the baseline. Similar trends were observed in the UHPC mixes from the 1% to 2% fibre content. Thus, it can be concluded that the inclusion of fibres generally increases the tensile strength of the concrete. Both 35mm and 60mm long fibres were added into the HPC mixes. Testing results indicate that the specimens with 35 mm fibres produced higher compressive strengths than the specimens with 60 mm fibres. These trends were not replicated in the tensile testing, thus further testing is required to validate which fibre is most appropriate for the HPC mix design.

All HPC specimens achieved the target strengths, while none of the UHPC specimens met the targets. HPC specimens exhibited minor cracking occurred prior to compressive failure and strain-softening under flexure. This semi-ductile behaviour has been extensively reported in literature (e.g. Aïtcin 1998, Azmee and Shafiq 2018). UHPC specimens exhibited microcracking under compression, strain softening under tension and some strain hardening under flexure. Microcracking and flexure induced strain hardening were both observed by researchers (e.g. Fehling et al. 2015) although the specimens were expected to show strain hardening under tension, due to the inclusion of steel fibres.

Several researchers agree on the importance of the ingredients when developing UHPC. Larrard and Sedran (1994) first proposed how particle packing affects overall concrete quality. Similarly, Azmee and Shafiq (2018) outline how ingredients with similar physical and chemical properties to the original mix design should be used, to accurately replicate the matrix. However, the materials used in this testing likely were different to the original mix design, due to being locally sourced (the original mix design used American-sourced materials). This adversely affected the particle packing, resulting in weaker strengths and poorer behaviour. To the author's knowledge, there are no open source UHPC mixes based on ingredients commonly used in New Zealand.

This testing indicated that when well designed, HPC and UHPC has excellent mechanical properties, and if exploited, have the potential to improve bridge design in New Zealand. A parametric analysis was therefore undertaken to quantify the effect of these materials on structural design. A variety of concrete grades were used in this analysis, with testing results from Mix D being used as the first HPC concrete grade. Other concrete grades had hypothetical strengths, based on strengths achieved in literature (Table 5).

PARAMETRIC ANALYSIS

A parametric analysis was used to explore how the material properties of HPC and UHPC affect structural design of a bridge superstructure. The prototype structure comprised of three 25 m spans (Figure 10), where each span consisted of nine standard prestressed hollowcore units (New Zealand Transport Agency 2008). It was designed as simply supported with unrestricted and restricted movement in longitudinal and transverse directions, respectively.

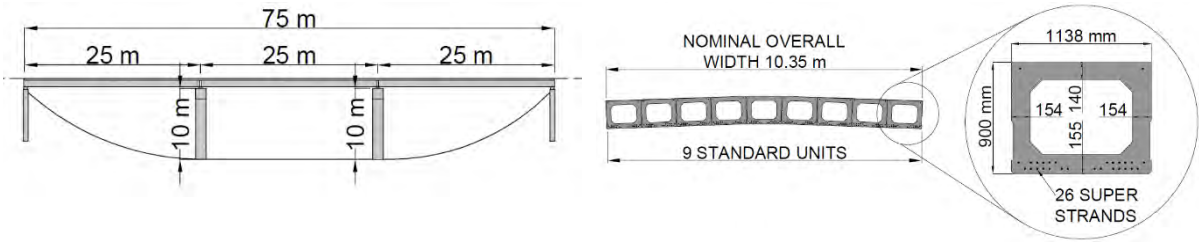

Figure 10. General arrangement and cross section of the prototype bridge including section details

Cross sections of the hollowcore unit were optimised by reducing web and flange thickness, and number of prestressed strands, while maintaining original outer dimensions. The simplified analysis assumed that the top and bottom flanges carried flexure, while the web carried shear.

Materials, Loading and Losses

Four concrete grades were assessed and compared to the baseline CC case (Table 5). The increased compressive and tensile strengths could sustain additional applied stress, allowing for reduction in the cross section. One optimised cross section was produced for each material.

Table 5. Material strengths for redesign of beam (MPa)

	CC	HPC1*	HPC2	UHPC1	UHPC2
Compressive Strength	50	105	120	150	250
Tensile Strength	-	8	10	12	16

* HPC1 is based on Mix D testing results

Dead load, superimposed dead load and live loads were assessed according to the Bridge Manual (NZTA 2018). The dead load varied between cases depending on the cross-sectional area of the beam. Live load was determined using the standard HN-HO loading with uniformly distributed load and point loads placed on the superstructure for worst case loading. Elastic shortening, friction and relaxation losses were assumed to be the same as the baseline case. Creep and shrinkage losses were assumed to be smaller for HPC and UHPC than CC due to the material composition (Fehling et al. 2015).

Flexure and Shear Analysis (Ultimate Limit State)

The compressive and tensile stresses at the extreme fibres were computed and checked against the permissible stress limits stipulated in NZS 3101 Section 19.3 (Standards New Zealand 2006). These stresses were located at the maximum moment, assumed to be at midspan of the beam. Stress was analysed using four cases; at prestressing, at transfer of load, after superimposed load was applied and at service load. Worst case stresses and factors of safety are shown in Table 6, where “+” refers to maximum compression and “–” to tension.

Table 6. Compressive and tensile stress demands and limits

	HPC 1		HPC2		UHPC1		UHPC2	
	+	-	+	-	+	-	+	-
Max. stress (MPa)	25.2	-2.96	26.97	-3.62	30.48	-4.16	29.72	-5.79
Stress limits (MPa)	45	-4	54	-5	67.5	-6	113	-8
Factor of safety	1.8	1.4	2.0	1.4	2.2	1.4	3.9	1.4

The shear demand was analysed at the critical section, located at half the section depth from the support. This was checked against the shear resistance of the beam (Table 7). Shear strength comprised of concrete shear strength (the lesser of web shear and flexure shear strength) and shear strength provided by steel reinforcement (including steel fibres). Standard equations from NZS 3103 (Standards New Zealand 2006) were used in this analysis.

Table 7. Shear stress demands and capacities

	HPC 1	HPC2	UHPC1	UHPC2
Max. shear stress (MPa)	405	372.4	354.2	345.7
Shear strength (MPa)	738.8	590.4	720.9	591.1
Factor of safety	1.8	1.6	2.0	1.7

Deflection Analysis (Serviceability Limit State)

Deflections were checked according to NZS1170.0, where the deflection limit was determined to be span/500 (Standards New Zealand 2002). The maximum computed deflections consisted of deflections due to point load, dead and superimposed dead load moments, live load moments and thermal stresses under worst case loading (Table 8).

Table 8. Deflection demands and limits

	HPC 1	HPC2	UHPC1	UHPC2
Max. deflection (mm)	36.6	40.3	41.7	38.9
Deflection limit (mm)	50	50	50	50
Factor of safety	1.4	1.2	1.2	1.3

Results

The optimised cross-sections of the hollowcore units are shown in Figure 11.

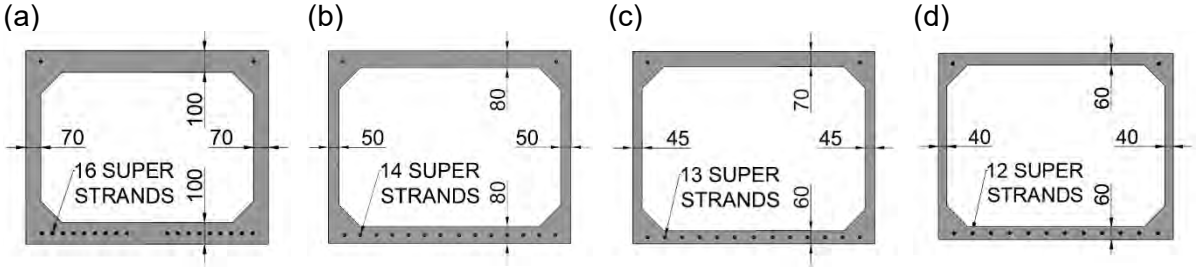

Figure 11. Cross sections (a) HPC1 (b) HPC2 (c) UHPC1 (d) UHPC2 (dimension in mm)

This parametric analysis highlighted the benefits of designing a lightweight superstructure (Table 9). Several cascade effects can be seen, such as reduced steel reinforcement and tendon requirements. These improvements can only be made when the structure is optimised for the high strength concrete. Tensile strength, not compressive strength, governed the design of the bridge beam, indicating that concrete with a high tensile capacity could improve bridge beam design most significantly. The design is governed by serviceability limit state deflections, so for future design, any reductions in cross section need to adhere to the deflection limits.

Table 9. Summary of structural improvements compared to the baseline case

Parameter	HPC1	HPC2	UHPC1	UHPC2
Weight (%)	36	49	56	60
Maximum Moment (%)	42	54	60	64
Steel Reinforcement (%)	50	50	50	50
Steel Tendons (%)	36	43	46	50

LIFE CYCLE ANALYSIS

A life cycle analysis was undertaken to investigate the environmental and economic impacts of the increased lifespan of HPC and UHPC. Bridge life cycle analyses have previously concluded that the production of raw materials phase was the largest contributor to the environmental impact, followed by the maintenance phase (Penadés-Plà 2017, Habert et al. 2012). Similarly, life cycle economic analyses generally include the initial cost and the maintenance costs (El-Tawil et al. 2020, Lounis and Daigle 2006). Thus, only the construction and maintenances phases were assessed.

These analyses investigated the environmental and economic impacts of the prototype bridge superstructure across a 100-year timeframe. The carbon dioxide equivalent (CO_2-e) emitted by construction and maintenance over the bridge lifespan were used to evaluate the environmental impact of each superstructure. Raw material carbon dioxide emissions were obtained from environmental product declarations and literature (Table 10) while construction and maintenance emissions were estimated (Dong 2018, Flower and Sanjayan 2007).

Table 10. Emissions factors for raw concrete ingredients (kg CO_2-e/kg)

Cement (GP)[1]	Silica Fume[2]	Fly Ash[2]	SP[2]*	Sand[2]	Silica Sand[3]	Gravel[2]	Steel Fibre[3]	Steel Rebar[4]	Steel Tendon[3]
0.73	0.03	0.03	0.0052	0.014	0.010	0.046	1.50	3.97	5.64

[1] Golden Bay Cement 2019; [2] Flower & Sanjayan 2007; [3] Shi et al. 2019; [4] Pacific Steel 2018
*Superplasticizer

The lifetime cost of each prototype superstructure was calculated using a net present value analysis. This analysis included construction and maintenance costs expected over a 100-year timeframe (Table 11). Maintenance requirements were estimated used the New Zealand Transport Agency Bridge and Inspection Manual (New Zealand Transport Agency 2001) and information from Lee et al. (2019).

Table 11. Cost of raw concrete ingredients ($/kg)

Cement[5]	Silica Fume[6]	Fly Ash[5]	Super-plasticizer[6]	Sand[8]	Gravel[8]	Steel Fibre[7]
0.45	1.93	1.93	20.43	0.04	0.03	3.85

[5] Golden Bay; [6] Sika; [7] Bosfa; [8] Parkhouse Garden Supplies; [9] Urban Pavers

Results

The emissions of the optimised superstructures varied significantly (Figure 12). Using a combination of steel fibres and steel reinforcement produced fewer emissions than using steel reinforcement alone, as is used in CC bridges. The high cement content of UHPC appeared to counter this decrease in emissions, unlike HPC superstructures which had both decreased cement and steel emissions (Figure 12).

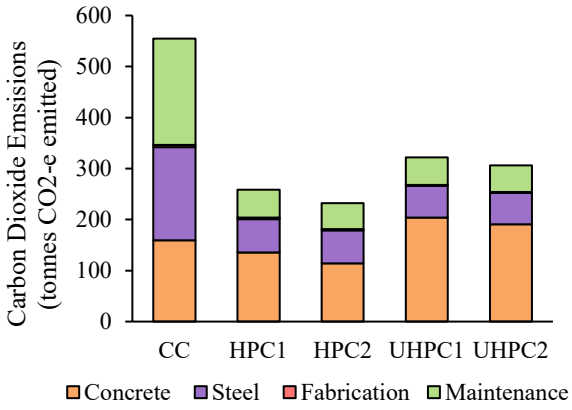

Figure 12. Emissions of the entire bridge superstructure

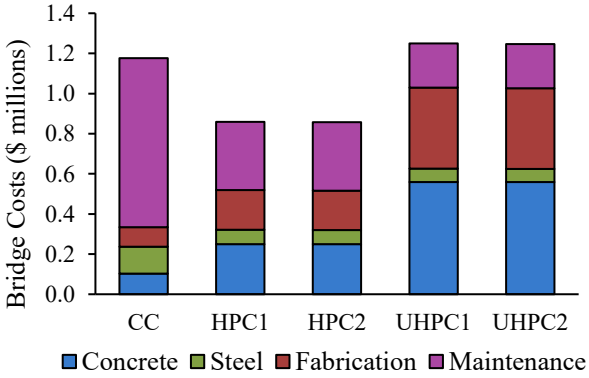

Figure 13. Cost of the entire bridge superstructure

The cost of CC and UHPC bridges was relatively similar (Figure 13). However, the HPC bridges had a decreased lifetime cost compared to CC bridges, which is primarily attributed to the reduced maintenance costs. Both HPC1 and HPC2 produced fewer emissions and were

cheaper than the CC bridge. However, UHPC1 and UHPC2 resulted in reductions in emissions but minor increases in cost (Table 12).

Table 12. Summary of economic and cost improvements relative to the baseline

	HPC1	HPC2	UHPC1	UHPC2
Emissions (%)	-49	-53	-39	-42
Cost (%)	-27	-27	+6	+6

CONCLUSION

The feasibility of high performance concrete (HPC) and ultra-high performance concrete (UHPC) was assessed by characterisation of the mechanical properties, a parametric analysis of the structural performance and an assessment of the economic and environmental impacts.

Characterisation of the materials indicated that using locally sourced materials could produce high quality and well performing HPC but not UHPC. It was suggested that UHPC is highly dependent on the ingredients and many UHPC mix designs utilise materials not commonly used in New Zealand. HPC is likely to be more feasible to develop and implement commercially than UHPC in New Zealand.

These high strength materials can enable bridge beam section sizes to be reduced, having cascade effects such as reduced steel reinforcement and tendon requirements. The simplified analysis indicated that tensile strength, not compressive strength, governed the design. Therefore, concrete with a high tensile capacity can benefit structural design of bridges most significantly.

Steel and cement were primary contributors to emissions, and both HPC and UHPC prototype structures produced less emissions than the baseline CC bridge, due to reduced material requirements. The HPC mixture produced fewer emissions than the UHPC mix due to its lower cement content, and thus to reduce emissions of the UHPC bridges, lower cement UHPC mixtures could be explored. The lifetime cost of the CC and UHPC prototype bridges were relatively similar, while the HPC prototype structure was cheaper than the baseline structure.

When the material properties can be exploited, HPC is the best option for New Zealand bridges as it is currently the cheapest and most sustainable option over its lifespan. UHPC has the potential to become more sustainable as low cement alternatives are investigated and may be more viable for longer spans or when high durability is essential. Using these materials, bridges in New Zealand could become cheaper and more sustainable than ever.

ACKNOWLEDGEMENTS

This project would not have been possible without support from Prof. Alessandro Palermo. Thank you for your constant enthusiasm and guidance. To Ernesto Hernández and Dr. Royce Liu, thank you for providing us with technical resources and your time.

We would also like to acknowledge the support and technical guidance provided by Timothy Perigo (University of Canterbury); Nicholas Brazzale (Stahlton); Michael Cowan (WSP); and Assoc. Prof. Allan Scott (University of Canterbury).

REFERENCES

Aïtcin, P.-C. (1998). *High performance concrete*, CRC press.

Azmee, N., and Shafiq, N. (2018). "Ultra-high performance concrete: From fundamental to applications". *Case Studies in Construction Materials*, 9, e00197.

New Zealand Transport Agency. 2008. *Standard precast concrete bridge beams,* New Zealand Transport Agency Research Report 364.

Dong, Y. (2018). "Performance assessment and design of ultra-high-performance concrete (UHPC) structures incorporating life-cycle cost and environmental impacts." *Construction and Building Materials*, 167, 414-425.

El-Tawil, S., Tai, Y.-S., Belcher II, J. A., and Rogers, D. (2020). "Open-Recipe Ultra-High-Performance Concrete." *Concrete International,* 42(6), 33-38.

Federal Highway Administration. (2013). *Ultra-High Performance Concrete: A State-Of-The-Art Report for The Bridge Community,* Federal Highway Administration.

Fehling, E., Schmidt, M., Walraven, J., Leutbecher, T., and Fröhlich, S. (2015). *Ultra-high performance concrete UHPC: Fundamentals, design, examples*, John Wiley & Sons.

Flower, D. J. M., and Sanjayan, J. G. (2007). “Green house gas emissions due to concrete manufacture.” *International Journal of Life Cycle Assessment,* Springer Verlag, 12(5), 282–288.

Golden Bay Cement. (2019). *GP Cement Environmental Product Declaration.*

Habert, G., Arribe, D., Dehove, T., Espinasse, L., and Le Roy, R. (2012). "Reducing environmental impact by increasing the strength of concrete: quantification of the improvement to concrete bridges." *Journal of Cleaner Production,* 35, 250-262.

Habert, G., and Roussel, N. (2009). "Study of two concrete mix-design strategies to reach carbon mitigation objectives." *Cement and Concrete Composites*, 31(6), 397-402.

Hernández, E. (2020). “Seismic performance of rubberised concrete members”. Unpublished PhD thesis.

Larrard, F. de, and Sedran, T. (1994). “Optimization of ultra-high-performance concrete by the use of a packing model.” Cement and concrete research, 24(6), 997–1009.

Lee, J. H., Choi, Y., Ann, H., Jin, S. Y., Lee, S. J., and Kong, J. S. (2019). “Maintenance cost estimation in PSCI girder bridges using updating probabilistic deterioration model.” *Sustainability (Switzerland)*, MDPI AG, 11(23).

Lounis, Z., and Daigle, L. (2006), “Life cycle cost analysis of high-performance concrete bridges considering environmental impacts.” *Institute for Research in Construction*, 1-17.

McSaveney, L., Papworth, F., and Khrapko, M. (2011). "Self compacting concrete for superior marine durability and sustainability." *Concrete in Australia*, 37 (2), 69-64.

New Zealand Transport Agency. (2018). *NZTA Bridge manual SP/M/022.*

New Zealand Transport Agency. (2001). *Bridge inspection and maintenance manual*.

Pacific Steel. (2018). *Environmental Product Declaration*.

Penadés-Plà, V., Martí, J. V., García-Segura, T., and Yepes, V. (2017). "Life-cycle assessment: A comparison between two optimal post-tensioned concrete box-girder road bridges." *Sustainability,* 9(10), 1864.

Rebentrost, M. (2005). "Design and Construction of the First Ductal® Bridge in New Zealand." *Proc., 22nd Biennial Conference of the Concrete Institute of Australia.*

Richard, P., and Cheyrezy, M. (1995). “Composition of reactive powder concretes.” Cement and concrete research, 25(7), 1501–1511.

Schmidt, M., Fehling, E., Glotzbach, C., Fröhlich, S., Piotrowski, S. (2012). “Ultra-High Performance Concrete and Nanotechnology in Construction.” *Structural Materials and Engineering Series*, 19, 425.

Shah, H. (1997). “Material aspects of high performance concrete.” High Strength Concrete - First International Conference, 504–516.

Shi, Y., Long, G., Ma, C., Xie, Y., and He, J. (2019). “Design and preparation of ultra-high performance concrete with low environmental impact.” *Journal of Cleaner Production*, Elsevier Ltd, 214, 633–643.

Song, P. S., and Hwang, S. (2004). “Mechanical properties of high-strength steel fibre-reinforced concrete.” *Construction and Building Materials*, 18(9), 669-673.

Standards New Zealand. (2002). AS/NZS 1170.0 *Structural design actions Part 0: general principles standard,* Standards New Zealand, Wellington.

Standards New Zealand. (2006). NZS 3101.1&2:2006 *Concrete structures standard,* Standards New Zealand, Wellington.

concretenz BUILDING RESILIENCE
CONFERENCE 2022
13-15 October 2022
Energy Events Centre | Rotorua

PROJECTS AND PEOPLE – WHAT DOES THE RIGHT WORKFORCE LOOK LIKE

MARK WILLIAMS

Building and Construction Industry Training Organisation

SUMMARY

The concrete industry needs to have the right people in the right numbers with the right skills in the right place at the right time - but how do we know what 'right' is?

For the past eight years, BCITO has supported the construction industry through economic forecasting and modelling to project future workforce needs. This model worked in a business as usual environment but cracks showed in 2020 following the March COVID-19 lockdown, when economists were collectively forecasting a drop in construction activity and wide scale redundancies. Fortunately, the drop did not happen, but what do workforce forecasts look like now and how do we know what 'right' is?

The future pipeline of work is the best indicator of future construction activity. While it did not falter following the March 2020 COVID-19 lockdown, it needs to be unpacked to understand the relationship between project and workforce demands. Waihanga Ara Rau the Workforce Development Council for Construction and Infrastructure came into existence in October 2021 as part of the Review of Vocational Education (RoVE) It has picked up the mantel of providing insightful commentary about workforce demands through the Construction and Infrastructure Workforce Information Platform in balance with listening to and promoting the voice of industry to answer the question - '*what does right look like*?'

The answer to this question starts with the pipeline of work that drives workforce demand. The pipeline is growing but it is also being delayed. Graph 1 on the following page compares the pipeline of construction and infrastructure work in the Construction and Infrastructure Workforce Information Platform[1] June 2020 to the same pipeline of work in July 2021. The July 2021 data shows a noticeable increase in the value of the project pipeline. However, both the June 2020 and July 2021 forecasted peak in activity occur nine months after the reporting date. This data points to the continual delay of project work, due in part to workforce shortages, but also materials supply and demand.

The next component in identifying how close we are to having the right workforce is understanding the supply side of the equation. This includes the existing workforce, numbers of people entering the 'concreting-services' sector, and an estimate of workers likely to leave. Graph 2 on the following page shows the sector employment over time and the forecasted number of replacement staff. Graph 3 shows the activity of people before entering the concreting-services sector. Graph 4 brings the sector workforce supply and demand forecasts together to highlight the gap between incremental growth in the workforce and the project-based demand.

[1] Construction and Infrastructure Workforce Information Platform https://wip.org.nz/project-pipeline/

The paper concludes with an insight into the current labour market and what appropriate actions look like now. It draws on research across New Zealand to identify what issues and opportunities are impacting and exist for the construction and infrastructure industry.

DISCUSSION

In June 2020 the pipeline of construction and infrastructure work peaked at $14.85B in March 2021. By June 2021 the pipeline had increased to $20B in March 2022.

Graph 1. Pipeline of construction and infrastructure work June 2020 August 2022

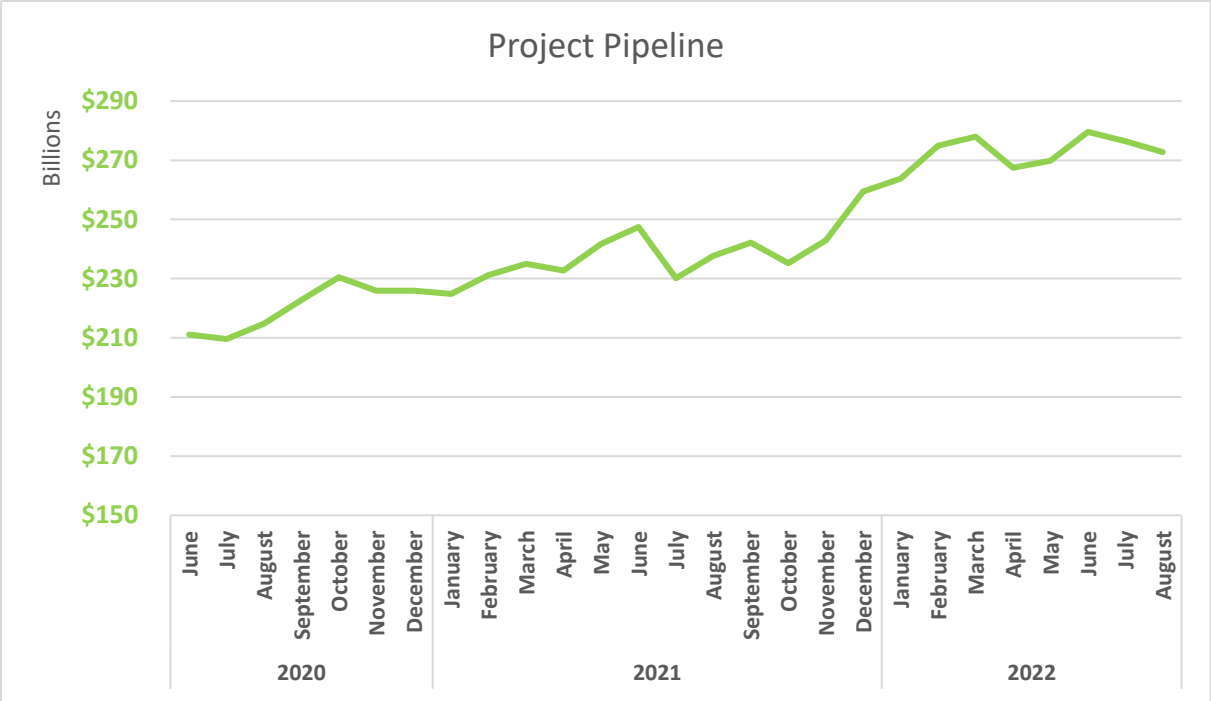

Sector data shows a steady increase since 2011. However, replacement numbers needed just to maintain the existing workforce, have also grown to over 600 per year.

Graph 2 Concreting Services, Ready-Mix and Concrete Construction Sector employment over time

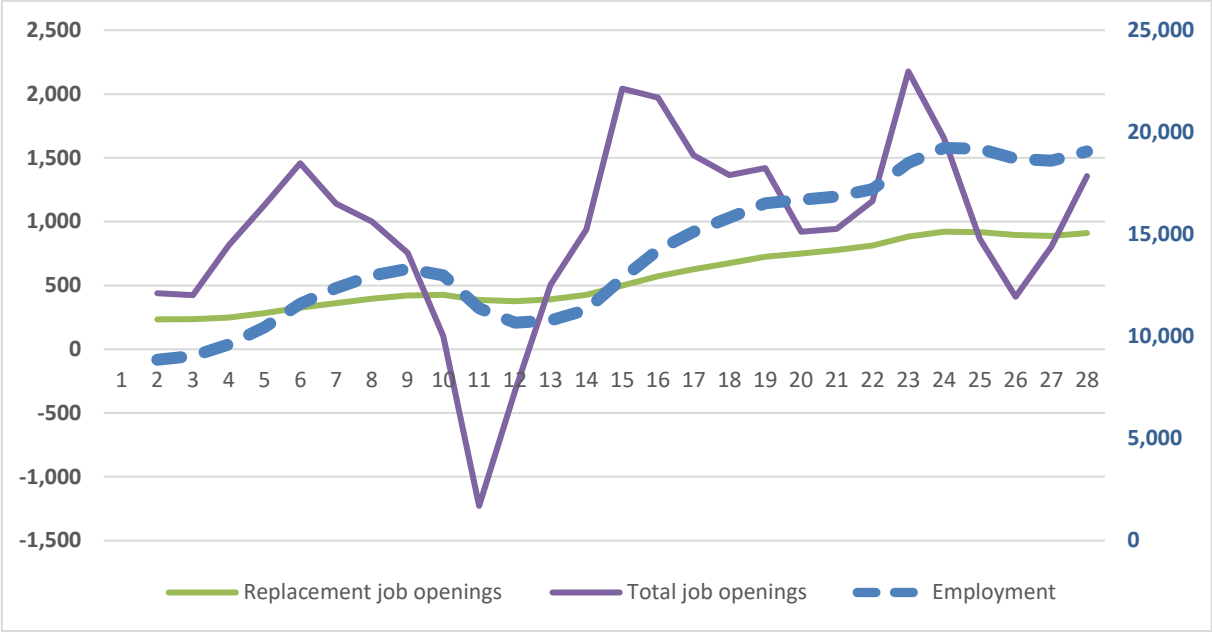

While the construction industry in general has a focus on school leavers as a source of new workers, the percentage of people who were at school directly before entering the concreting - services sector is relatively low. Numbers straight from school entering the sector varied between 3% and 5% of new people in the workforce between 2016 and 2021, while the number of career changers entering the sector in the same period ranged between 51% and 59%.

Graph 3 Workforce supply channels into the Concreting Services Sector

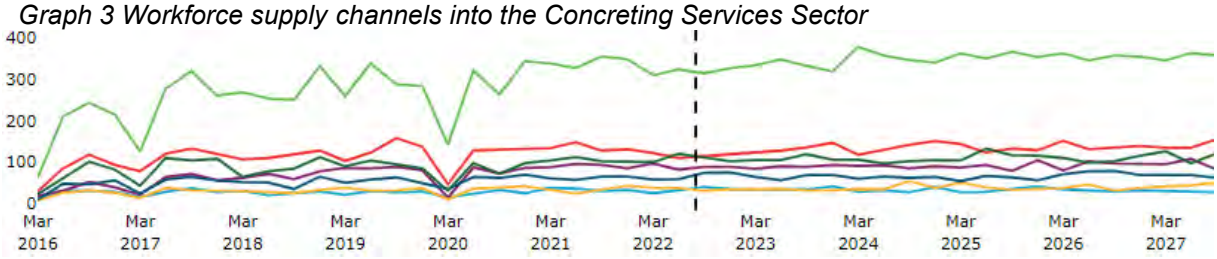

The graph below shows the workforce needed to put past and future building consent predictions and project pipeline in place for the Concreting Services Sector. Everything above the labour supply line is an activity- based workforce gap.

Graph 4 Concreting Services Sector workforce supply and demand comparison

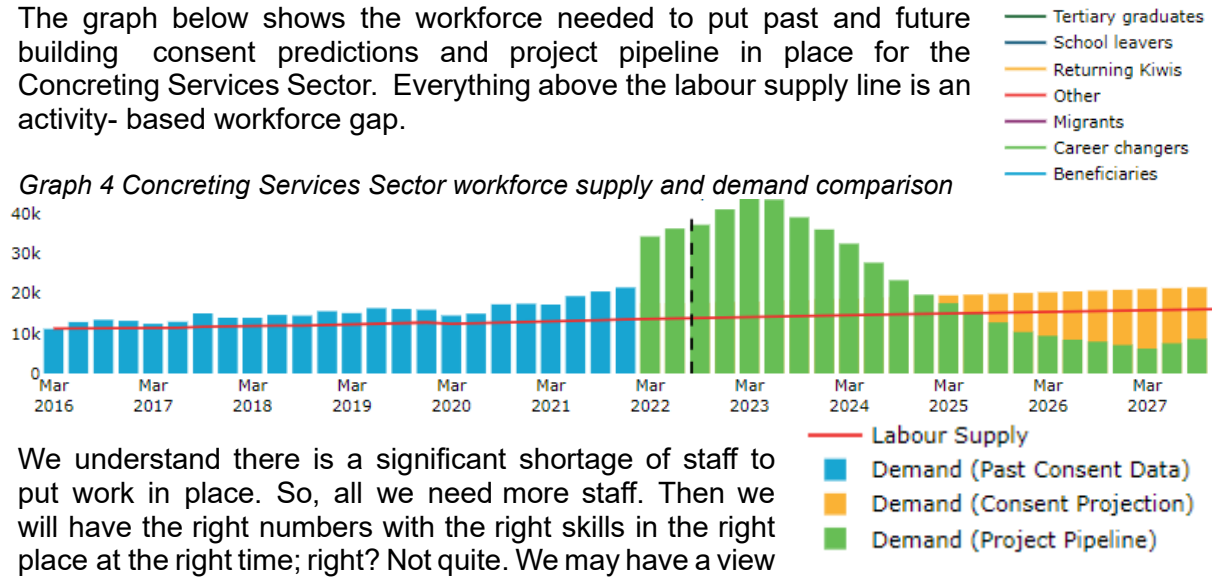

We understand there is a significant shortage of staff to put work in place. So, all we need more staff. Then we will have the right numbers with the right skills in the right place at the right time; right? Not quite. We may have a view of how many people are needed to deliver the forecast pipeline of work, but there are only three ways to get great staff. You can grow them, you can pinch them and you can import

them. At the time of writing, importing staff was off the table so the only two options left are growing or pilfering them from other firms.

Pinching staff does not grow the workforce so it is not a sector solution to demand. Accordingly, the second part of the paper looks at the issues and opportunities affecting the supply of labour and the growth of organisations across the country to meet the project pipeline demand.

This paper is not suggesting that the right number of people in the concreting-services sector is the 44,000 suggested at the peak of the supply and demand gap in graph 4. The mountain of work will continue to be levelled off and pushed out as shown in graph 1. However, the current gap of over 20,000 people needed to put project work in place, along with the need to replace over 800 people leaving the sector annually, means we need to employ more people than the 2,500 who are currently recruited in 2021 into the Concreting Sector. What are the issues and opportunities relating to recruitment?

As noted in relation to graph 3, the largest supply channel into the concrete-services sector are career changers. These people account for between 51% and 59% of those entering the sector. This is an opportunity in itself, as it opens up the potential market for recruitment. However, there are a range of enablers (as identified through construction and infrastructure industry consultation), which the sector needs to have in place, including:

1. Support for employers
2. Support for workers
3. Training/upskilling availability and support
4. Attracting people to the sector
5. Retaining workers
6. Immigration changes

Opportunities to address these needs are many and varied. Details will be available in the BCITO's Regional Construction and Infrastructure Workforce reports. You can access these or sign up to get sent copies sent to you at: https://wip.org.nz/.

Finally, the workforce solutions below came from the Regional Construction and Infrastructure Workforce initiative. These have been sorted in order of highest priority and themed according to trends. Many of these themes had solutions that impacted more than one area.

1. Education/Training
2. Improve Culture/wellbeing/flexibility
3. Workforce mobility
4. Immigration
5. Better promotion of the sector
6. Improve perception of the sector
7. Government regulations and programmes
8. Diversity & inclusion
9. Collaboration across the industry
10. Youth outreach
11. Procurement/supply chain (what? I'm not sure what this means)
12. Ageing workforce support and work opportunities

The challenge facing employers in the industry is to look at culture and practices of employment environments and adapt these to be the workplace of choice. Yes, you do have to compete with other employers to attract quality candidates – that is a feature of the current

landscape that will endure for some time. Integration of the themes above into the culture of your workplace can promote firms: great workplaces have great cultures derived from great leadership.

Four things to consider:

Workforce dynamics - the construction workforce has grown exponentially, from 33.3 workers per 1,000 in the whole workforce in 2000 to 53.5 in 1,000 in 2020. Given the employment market is currently, and predicted to continue to be,

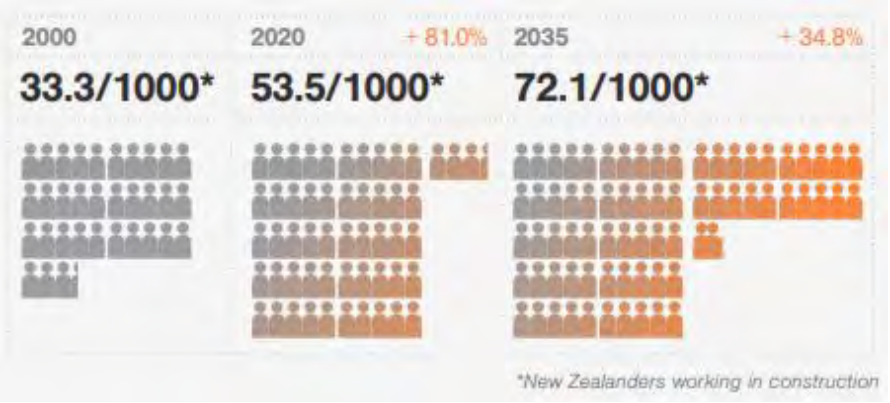

highly competitive with widespread shortages, the question must be asked: Is it realistic to continue industry practices that require so many people?

Improve productivity - Historically, the focus of the construction workforce has been on increasing the number of people on the tools. Our future efforts must include working smarter and looking at ways to achieve more with a sustainable workforce.

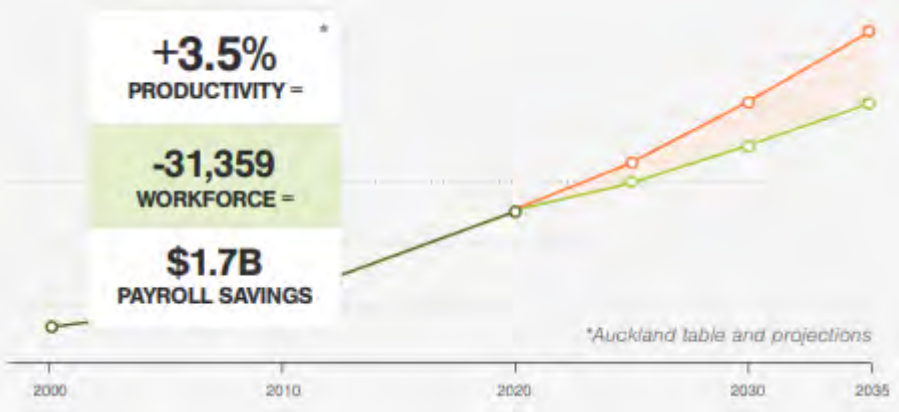

Reactive decimation – culling the workforce in response to market conditions – is counter-productive to managing demand and improving productivity. Continuing to manage our workforce in line with a boom–bust economic cycle perpetuates a backlog of work which is more expensive to deliver and prone to reduced quality due to a heightened sense of urgency. An example of this is the current housing shortage, compounded by the Global Financial Crisis, which saw us fall behind by an estimated 40,000 houses. For better long-term outcomes we can build the workforce to the trendline

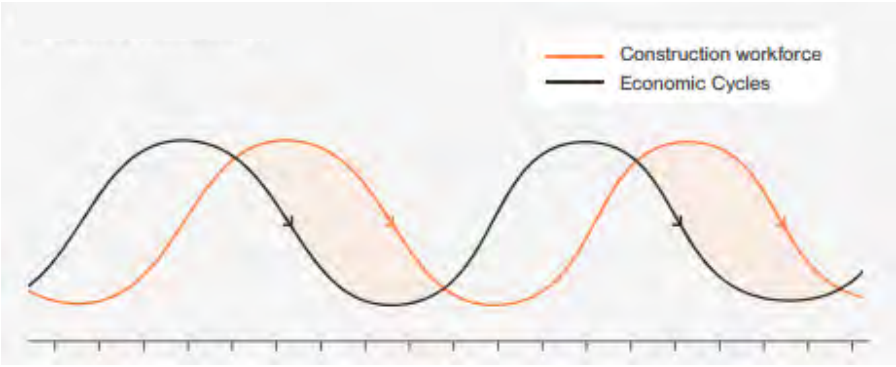

Making better choices – prioritising construction work to align with regional needs. We must create an alternative way of prioritising construction work to align with regional needs and based on a project's impact on society. That's why we formulated WEW, an Impact Criteria Model; a holistic approach to construction activity and activity outcomes – Wellbeing, Enabler and Wealth. Any society needs a balanced investment in all three categories to be sustainable. When faced with excessive demand we can use these criteria as part of the investment decision-making process, for example prioritising projects that correct an imbalance and avoiding projects that create one.

SESSION 6

Chair:
Rick Henry

A SUSTAINABILITY CHECK OF A RECENTLY CONSTRUCTED CONCRETE BRIDGES PROJECT – M2PP EXPRESSWAY - A CASE STUDY

JAMIL KHAN

Technical Director - Structural Engineering, Beca Ltd, Wellington, New Zealand

SUMMARY

The concept of sustainability is getting popular among Kiwis; do our bridge engineers understand what sustainable development is? According to United Nations World Commission on Environment and Development (UNWCED), it is a development that meets the needs of the present without compromising the ability of future generations to meet their own needs.

A bridge development is a large investment of resources associated with significant social, economic, and environmental impacts. Kiwi bridge engineers can deliver their environmental and social obligations by applying the sustainable practices to bridge design, construction, and maintenance.

To assist our Kiwi bridge engineers in developing an understanding of a sustainable bridge development, a case study is conducted on a recently constructed project using a framework, developed for assessing sustainability in bridge design, construction, and maintenance. The framework consists of a green rating system, which is divided into three categories: design, construction, and maintenance.

This paper will present the outcomes of the case study. The authors believe that the outcomes of the study will tell us how sustainable our recent bridges are and steer the Kiwi bridge engineers for future improvements in their practices to achieve more sustainable bridge developments.

SUSTAINABLE DEVELOPMENT

“Sustainable development is a development that meets the needs of the present without compromising the ability of future generations to meet their own needs" as defined in Brundtland Commission Report of United Nations presented in United Nations General Assembly 1987.

Daniel Whittemore in his article “Sustainable Structures for Bridge Engineers” published in 2010 in Structure Magazine wrote “A sustainable bridge can be defined as the one that is conceived, designed, constructed, maintained and eventually put out of service in such a

fashion that these activities demand as little as possible from the natural, material and energy resources from the surrounding community."

To bridge engineers, it is planning, designing, constructing, and managing bridges that maintain a balance between social, economic, and environmental considerations, which are three pillars of sustainability. Adams, in 2006, presented a Venn diagram to express the relationship of these three pillars. Sustainability is achieved where the tree circles overlap, which means that all three elements have been satisfied. All three pillars must be addressed before we can have a balanced world that can satisfy the needs of both present and future generations.

Figure 1: Venn diagram expressing relationship of 3 pillars of sustainability.

KEY COMPONENTS OF SUSTAINABLE BRIDGE DEVELOPMENT

Bridge engineers have a role to play here by building resilience into our bridges so that the bridges we design today can resist the loads that could be applied as the climate changes. Making developers and bridge owners aware of how a changing climate may affect their bridge, with intensity of rainfall, associated flooding levels, hail, and windstorms. These key items are to be considered and discussed with developers, owners, and operators. Sustainability can be explained under:

1. Structural Sustainability
2. Environmental Sustainability in the context of bridges.

Structural Sustainability

Structural design can have a significant impact on the overall sustainability of a bridge. The sustainability of a structure can be considered with respect to embodied energy of structural materials, durability, design flexibility, optimality, and deconstruction, to name a few. Current structural practice has just begun to address these issues. The bridges have unique sustainable principles that warrant a special focus.

With regards to structural sustainability, in the American Concrete Institution (ACI) Fall 2010 Convention, it is stated as:

- A structural sustainable concrete bridge should provide an overall life of 100 to 150 years.
- They should have a minimum of shrinkage (plastic, drying, chemical shrinkage) and cracking.

- Long service life of bridge decks over 100 years can be achieved with low shrinkage, low permeability high performance concrete (HPC), compared to only 20 years for normal strength concrete decks.

Environmental Sustainability

United States Environmental Protection Agency (EPA) in 2006 defined that “Environmental sustainability deals with the environmental impacts of the product or the process in all life cycle stages of the bridge, i.e. to measure the environmental impacts and performance of the product or process over the design, construction, use, maintenance, and disposal stages”.

SUSTAINABILITY OBJECTIVES

The following are some of key Objectives of a sustainable development:

- Reduce virgin material use
- Reduce the waste
- Reduce energy use
- Reduce emission to air
- Maintain or improve hydrologic regime characteristics
- Engage community values and sense of place
- Have a resilient structure
- Improve safety
- Improve local economy
- Increase life cycle efficiency
- Promote innovation.

CURRENT SUSTAINABILITY PRACTICES

Several articles, theses, journals, books, and magazines were consulted to review current sustainable approaches in bridge design, construction, and maintenance. The current sustainable practices are grouped in three categories, which are Sustainable Bridge Design, Sustainable Bridge Construction and Sustainable Bridge Maintenance.

Sustainable Bridge Design

The design of a bridge is an important phase where most decisions can impact later stages. Incorporating sustainability approaches and methods in the design stage is important for achieving sustainability. For example, site selection, material selection for design, service life design, span arrangement, substructure type, geometry, and foundation types are some of the factors that should be taken into consideration during the design stage.

Lounis and Daigle, in 2007, performed a simplified life cycle environmental analysis of two bridges with high performance concrete (HPC) decks and normal performance concrete (NPC) decks, by focusing on two impacts: a) emissions of CO_2 and b) waste production (or landfill use). They concluded that:

- HPC deck results in a reduction in the number of maintenance and repair actions.
- HPC deck yields a reduction of 65% in CO2 emissions compared to NPC.
- It was also found that based on the onset of corrosion as the end of service life criterion, the HPC deck alternative incorporating supplementary cementitious materials (SCMs)

has a service life that can vary from 3 to 10 times the service life of a normal concrete deck having the same water-to-cementitious materials ratio.

Sustainable Bridge Construction

The key elements during a bridge construction are operation and transportation, which are responsible for energy consumption and emissions. The operation involves the construction procedures and transportation involves the transport of construction materials, plants, and precast/prefabricated components of bridges.

Accelerated Bridge Construction (ABC) is bridge construction that uses innovative planning, design, materials, and construction methods to provide a safe and cost-effective approach to reduce the onsite construction time that occurs when building new bridges or replacing and rehabilitating existing bridges. ABC techniques have demonstrated significant time savings and improved construction quality.

- ABC techniques improve site constructability, quality, durability, safety, and total project delivery.
- ABC techniques reduce the onsite construction time, weather-related time delays and traffic impacts.
- ABC techniques also minimise environmental impacts, impacts to existing roadway alignment and utility relocations and land requirement for the construction works.

Different road equipment such as trucks and other vehicles are used during construction operations to transport materials to and from site, which consumes fuel and releases wastes to the atmosphere. Similarly, various non-road construction equipment such as excavators, bulldozers, compactors, pressure washers, cement and mortar mixers, pumps, trenchers, rollers, and other construction equipment used during operation consumes fuel and releases energy. Non-efficient fuel vehicles can increase fuel consumption and release GHG emissions. The EPA recommends non-road construction equipment to have engines that meet the current EPA Tier emission standards.

Table 1: CO_2 Emission per gallon Fuel

Fuel	Diesel	Gasoline	Natural gas	Natural gas
CO_2/gallon	22.37 lbs	19,54 lbs	12.66 lbs	11.7 lbs/1000ft^3

If ways are implemented to reduce fuel use by 3%, 2.02 MMT of CO_2 emission will be reduced (EPA 2009). Using biofuels for trucks and non-road equipment can reduce significant GHG emission (EPA 2009).

Sustainable Bridge Maintenance

Bridge maintenance is a major part of the bridge life cycle. There are several activities involved in bridge maintenance that may significantly impact on the environment. An attempt should be made to reduce the number of maintenance activities, which in turn reduce environmental impacts. The use of durable material extends the service life of the bridge components, thus decreasing the need for maintenance activities. Development and evaluation of improved visual inspection procedures, innovative non-destructive testing methods and an automated method to gather and manage data should be encouraged.

SUSTAINABILITY FRAMEWORK FOR BRIDGE DEVELOPMENT

In this section an attempt is made to develop a framework to assess the sustainability of bridge developments in New Zealand. It is based on the framework “Implementation of Sustainability in Bridges Design, Construction and Maintenance” developed by Michigan State University for Michigan Department of Transportation (MDOT) in 2012. The framework consists of a green rating system, which is divided into three categories, which are design, construction, and maintenance.

The design section involves selection of site, materials, and other design considerations. The construction section is based on construction techniques, water use, use of renewable energy, and minimising the construction waste and fuel efficiency of equipment and plants. The maintenance section highlights sustainability issues in bridge painting, cleaning, drainage and impact on aquatic and wildlife.

SUSTAINABLE BRIDGE DESIGN ASPECTS

At the design stages, key focuses shall be on measures that can be taken during the design of bridges. The aim is to create a plan and employing methods in the design that result in achieving sustainability that are the intent of this stage. The section is split into sites’ selection, materials’ selection, and other design considerations. Guidance is provided under each criterion for assigning points to each design aspect.

Site Selection

In the planning of a bridge project, the focus shall be given on the facts that the new development does not impact on the environment and the historic sites. It shall reduce the pollution and rehabilitate the contaminated sites. The design intent and scoring criteria for site selection, historic site preservation, brownfield redevelopment and stormwater management are described in the following sections.

Site Selection (6 Points)

The intent is to select the sites that do not have impacts on the environment due to the location. Three points shall be awarded for meeting any of the following two requirements and six points for meeting all the following four requirements.

- Avoid sites of habitats of any species.
- Avoid placing footings and piers in water bodies.
- In case of river/stream bridges, avoid placing footing in water ways.
- Reconstruct the bridge at the same location.

Historic Site Preservation (3 Points)

The intent is to avoid development on historic sites and reduce the social-cultural environmental impact from the location of a bridge on the site. Three points shall be awarded for meeting the following requirements.

- No historical bridge is demolished
- Local history and culture are preserved.

Soil Erosion and Sedimentation (5 Points)

The intent is to reduce pollution from soil erosion, which may be due to winds or water, sedimentation, and dust and particularly during the constructions. Two points shall be awarded if one or more of the following requirements are met, and five points for meeting all the following requirements.

- Develop a comprehensive erosion and sedimentation control plan.
- Develop a schedule and implement a maintenance program.
- Follow the Resource Consent Conditions.

Brownfield Redevelopment (2 Points)

The intent is to rehabilitate contaminated sites and reduce pressure on undeveloped lands. Three points shall be awarded for meeting the following requirements.

- Identify and analysis environmentally contaminated information and take appropriate action accordingly.
- Conduct preliminary site investigation accordingly.
- Follow the Resource Consent Conditions.

Stormwater Management (4 Points)

The intent is to reduce the amount of stormwater run-off and pollution that is discharged into surface waterways or storm-sewers. Two points shall be awarded for meeting the minimum requirements and four points shall be awarded if all requirements are met.

- Implement a Stormwater Management Plan (SWMP) include plans to accomplish illicit discharge elimination, public education, and stormwater pollution to meet the nation standards.
- Follow the approved best Management practices
- Comply with the Resource Consent conditions.

MATERIALS

The two main concerning issues are the environmental impact of materials brought to the bridge project and disposal of materials that leave the bridge project. Using recycled materials, regional materials, reducing the quantity of materials, and reusing materials will help in minimising environmental impacts associated with material use. Therefore, the following measures are suggested to minimise environmental impacts associated with materials selection, waste disposal and waste generation:

a. Selecting sustainable materials
b. Practicing waste reduction
c. Reusing and Recycling.

Use of Recycled Materials (4 Points)

The intent is to increase the demand for materials that incorporate recycled content, thereby reducing impacts resulting from the extraction and processing of virgin materials. The points shall be awarded based on the percentage of recycled materials used on the project. One point shall be awarded for 10% recycled material, two points for 20% recycled material used and four points 30% recycled material used.

Supplement Cementitious Materials (3 Points)

The intent is to reduce the embodied energy associated with cement by replacing a portion of it with supplement cementitious materials. The points shall be awarded based on the percentage of Supplemental Cementous Materials (SCM) used on the project. One point

shall be awarded for 10% SCM, two points for 20% SCM, and three points for 30% SCM used on the Project.

Reduction in Quantity of Materials (3 Points)

The intent is to reduce the amount of material used in the construction of bridges by using innovative civil engineering techniques. The points shall be awarded based on the percentage of material reduced on the project. One point shall be awarded for 10% reduction in quantities of the material, two points for 18% reduction and three points if at least 25% of the total materials are reduced.

Materials Reuse (2 Points)

The intent is to reuse the demolished bridge materials in road construction to reduce demand for virgin materials and reduced waste; thereby lessening impacts associated with the extraction and processing of virgin resources. Two points shall be awarded for 10% reused material and one point for 5% reused material.

Regional Materials (3 Points)

The intent is to increase demands for materials and products that are extracted and manufactured within the region, thereby supporting the use of indigenous resources, and reducing the environmental impact resulting from the transportation. One point shall be awarded if 15% of all the material and products are from the region, two points for 18% and three points for 25% are from the region.

OTHER DESIGN CONSIDERATIONS

Here several miscellaneous design aspects are considered, which have environmental impacts on bridges due to their design. These design aspects are renewable energy use, use of bikes/pedestrian lanes, design for future expansion, reduction in Greenhouse Gas (GHG) emission, and energy consumption.

Renewable Energy Use (1 Point)

The intent is to reduce the electricity consumption and promote the use of renewable energy technologies. One point shall be awarded for using renewable energy systems.

Bicycle/Pedestrians Pathways (2 Points)

The intent is to promote the use of alternative transportation through bicycling and walking, thus minimising pollution, and energy demand. One point shall be awarded if bike lanes are provided. One point shall be awarded if pedestrian pathways are provided.

Lane Adaptability (1 Point)

The intent is to provide a framework that allows for additional lanes should there be any unforeseen conditions. One point shall be awarded if provisions for adding one or more travel lanes in the future are maintained in the design plan.

Resilience Seismic Design (6 Points)

The intent is to provide a resilience bridge structure stand up to the design and major earthquake events. The bridges are required to be designed to ensure that collapse does not occur under a Major Earthquake (ME). Six points shall be awarded for low damaged seismic design of bridges, four points for bridges where plastic hinges are restricted in elements

above the ground, and two points for bridges where plastic hinges will be developed in elements below the ground.

Life Cycle Cost Analysis (5 Points)

The intent is to estimate the overall costs of project alternatives and to select the design that ensures the facility will provide the lowest overall cost of ownership consistent with its quality and function. Five points shall be awarded for conducting Life Cycle Cost Analysis (LCCA) of a complete bridge project.

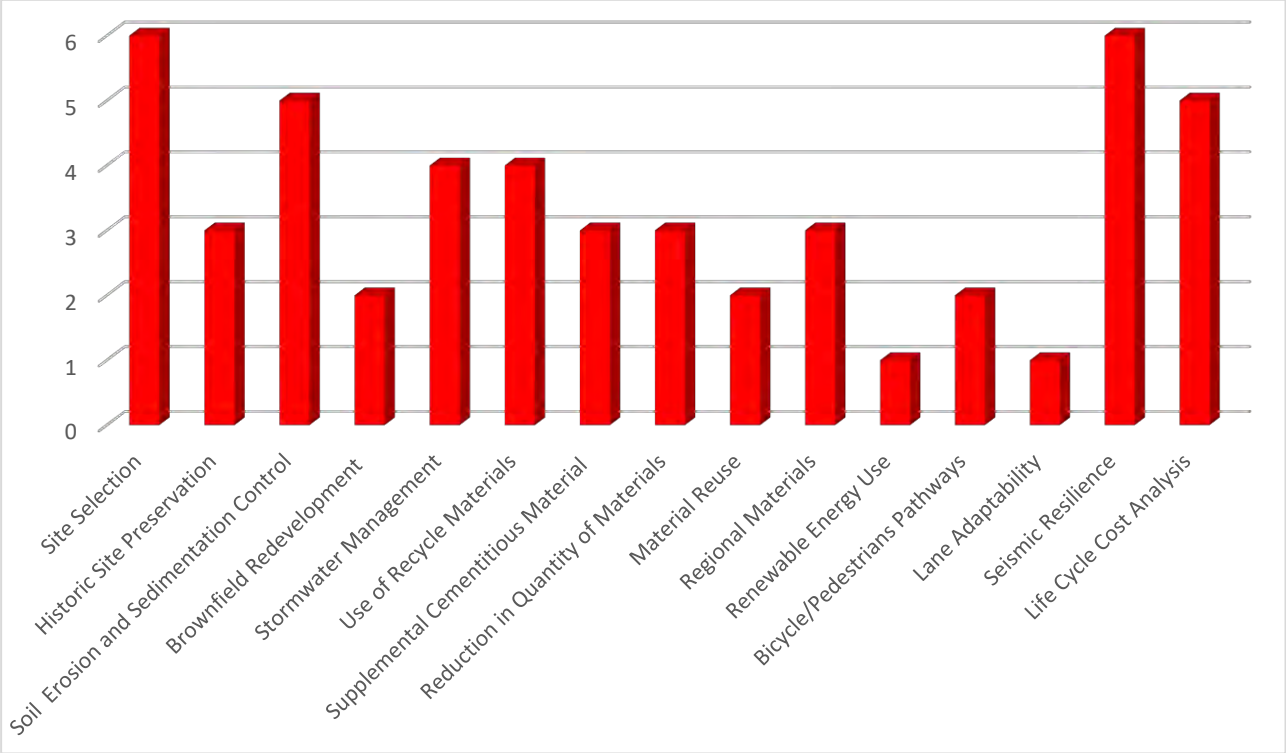

Figure 2: Points Distribution for Design Stage (50 Points)

SUSTAINABLE BRIDGE CONSTRUCTION ASPECT

Construction of bridges is another important phase of the project that incorporates the rehabilitation, replacement, or addition of an entire structure. A successful completion of a bridge project includes timely completion, cost-effectiveness, high quality, and safety. The following sections define the criteria and standards recommended to incorporate in bridge projects during the construction phase. These credits help in promoting a sustainable environment and lessen the impacts on nature by integrating recycled or reused materials, efficient water use, managing waste material on-site, utilising sustainable energy resources, and employing fuel efficient vehicles in the construction process.

Accelerated Bridge Construction Techniques (ABCT) (14 Points)

The intent is to reduce the construction time of the project, thereby reducing the environmental and traffic mobility impact. It also improves the safety in construction and the quality of the final product. The points shall be awarded based on the number of initiatives adopted to improve the construction relative to the conventional practices.

Table 2: Point for Different ABC Initiatives

S No	ABC Initiatives	Points shall be awarded
1	Pad footing without piles	1
2	Single column on single pile	1
3	Bank seat for abatement	1
4	Coolum cages plunge into pile top	1
5	Pre-cast beam	1
6	Pre-cast beams without deck formwork	1
7	Pre-cast beams without deck slab	1
8	Pre-cast crosshead	1
9	Precast Pier columns	1
10	prefabricated abutment r/f cage	1
11	Pre-cast Barriers	1
12	precast facing /facia panels	1
13	Use of RE walls to build embankment	1
14	Not more than 3 different sizes of elements	1

Corrosion Resistant Steel Reinforcements (7 Points)

The intent is to prevent bridge reinforcement from corrosion by penetration of chloride, thus preventing the bridge from early deterioration and extending the service life of the bridge. Three points shall be awarded if the concrete cover is provided to higher exposure conditions. Two points shall be awarded if epoxy coated reinforcement is used on the project and four points will be awarded for both stainless steel reinforcement and epoxy coated reinforcement.

Effective Water Use (2 Points)

The intent is to efficiently use water during bridge construction and incorporated water efficiently and conservation in equipment washing. Two points shall be awarded if 30% water is reduced using water efficiency techniques and one point for 20% water reduction.

Non-Road Equipment Emission Reduction (2 Points)

The intent is to reduce air emissions from non-road equipment. Two points shall be awarded if 75% of the equipment meets the following requirements and one point if 50% of equipment meets.

- Use non-road equipment that meets at least one of the following criteria.
  - Have engines that meet the current NZ Environmental Protection Agency (EPA) Tier emission standards.
  - Have diesel retrofit device for after-treatment pollution control verified by EPA for use with non-road engineers.

Construction Waste Management (4 Points)

The intent is to divert construction and demolition debris from disposal in landfills and incineration facilities. Redirect recyclable recovered restoration back to the manufacturing process and reusable material to appropriate sites. The points shall be awarded based on percentage of total construction waste diverted from landfills. Four points for 80% Construction waste diverted, three points for 60%, two points for 40% and one point for 20%.

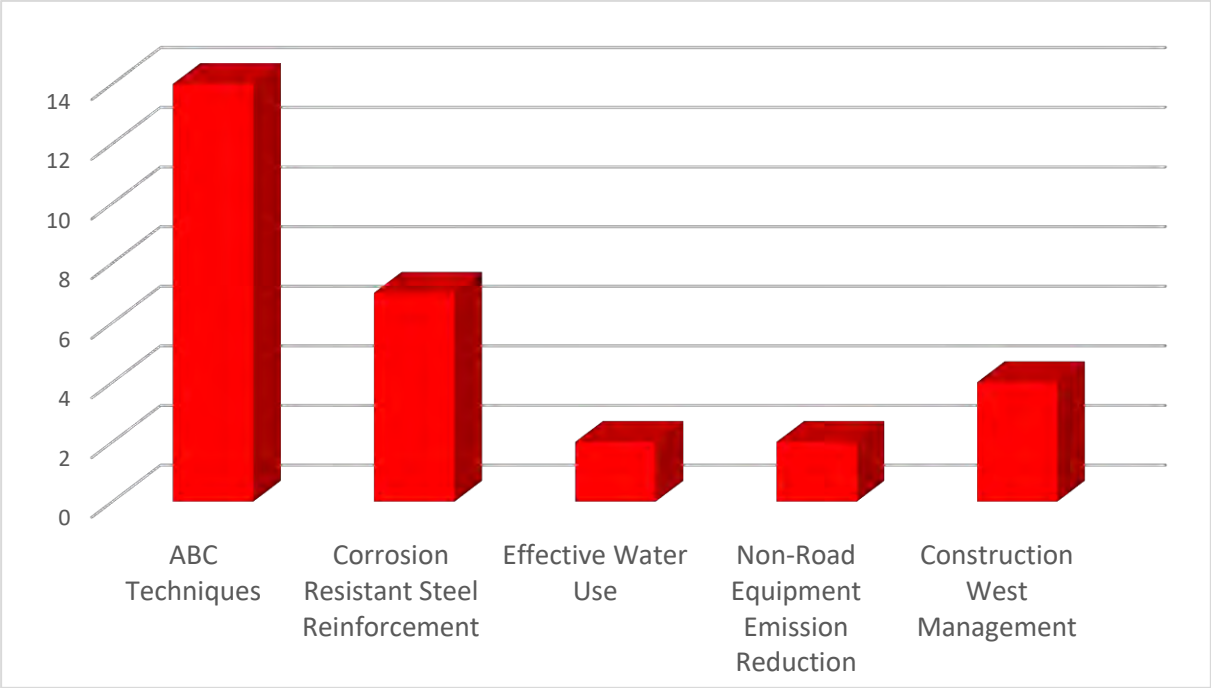

Figure 3: Points Distribution for Construction Stage (29 Points)

Sustainable Bridge Maintenance

A majority of the bridges built around the 1960's and 1970's need significant repair and maintenance actions (Helms, 2011). Lead and chromate-based paints and coatings removal may have significant impacts on the environment, workers, and public. This section outlines the requirements of inspection technologies, bridge painting, cleaning, deck drainage, and impacts to fish and wildlife that should be met in order to reduce associated environmental impacts.

Efficient Inspection Technology (3 Points)

The intent is to use efficient inspection technologies and process for proper maintenance action decision, thus enhancing the service life and reducing associated environmental and reducing associated environmental impacts. Two points shall be awarded for meeting the first requirements and three points will be awarded on meeting both requirements.

- Follow recommended framework for a Bridge Inspection Program of NZTA Bridge Manual.
- Use of specialised bridge equipment such as under bridge inspection vehicles, mobile inspection platforms, non-destructive evaluation equipment and data collection and analysis equipment.

Bridge Painting/Coating (6 Points)

The intent is to prevent bridge components from deterioration due to corrosion, thus increasing the life expectancy of bridges and protect workers and the environment from paint-related by products. Three points shall be awarded if zinc rich coatings are used for all steel components and six points will be awarded for meeting NZTA Painting Coating Guidance.

Bridge Cleaning (2 Points)

The intent is to clean components of bridges vulnerable to dirt, bird drops, accumulation, etc, thus increasing the longevity of the bridge components and lessening future maintenance requirements. One point shall be awarded for developing the schedule of cleaning operations. Two points shall be awarded if bird proofing around the services, bearings and other inspectable bridge components is provided.

Bridge Deck Drainage (2 Points)

The intent is to avoid impacts on the deck structure and reinforcing bars due to inefficient drainage. One point shall be awarded for meeting any of the following two requirements and two points for meeting all the following requirements.

- Gutter flow from roadways should be interrupted before the bridge.
- Avoid zero gradients and sag vertical curves on bridges.
- Larger gates and inlet structures are used onto the subsequent roadway sections to collect runoff from bridge decks immediately.

Avoiding and Minimising Impacts to Fish and Wildlife (1 Points)

The intent is to avoid impacts on fish and wildlife due to maintenance activities. One point will be awarded for meeting the following requirements.

- Seek ways to build durable structures, and in an environmentally sound fashion. Identify opportunities to avoid and minimise impacts.
- Schedule maintenance and improvements so that minimal time is spent in sensitive environments. Schedule maintenance outside egg spawning seasons.

Corrosion Control Materials (3 Points)

The intent is to prevent or minimise the corrosion of bridge elements due to penetration of chloride base dicers. This minimises early deterioration of the structures. Each recommended method would either result in an increased amount of time between maintenance cycles or extend the bridge's service life. Two points shall be awarded if any one of the following requirements is met. Three points will be awarded for meeting both requirements.

- Consider using galvanic anodes in all concrete patches that extend below the top layer of reinforcement.
- Consider using Carbon Fibre Reinforced Polymer wrap. This increases the strength, is lightweight, and provides additional resistance.

Bridge Deck Joints and Deck Joint Seals (4 Points)

The intent is to minimise or eliminate poorly maintained bridge deck joints and seals, thus maintaining the service life of the bridge. Two points shall be awarded for eliminating bridge deck joints (when possible). One additional point shall be awarded if the use of compression seals in new bridges is discontinue. One additional point shall be awarded if a routine maintenance procedure is established to inspect the joints.

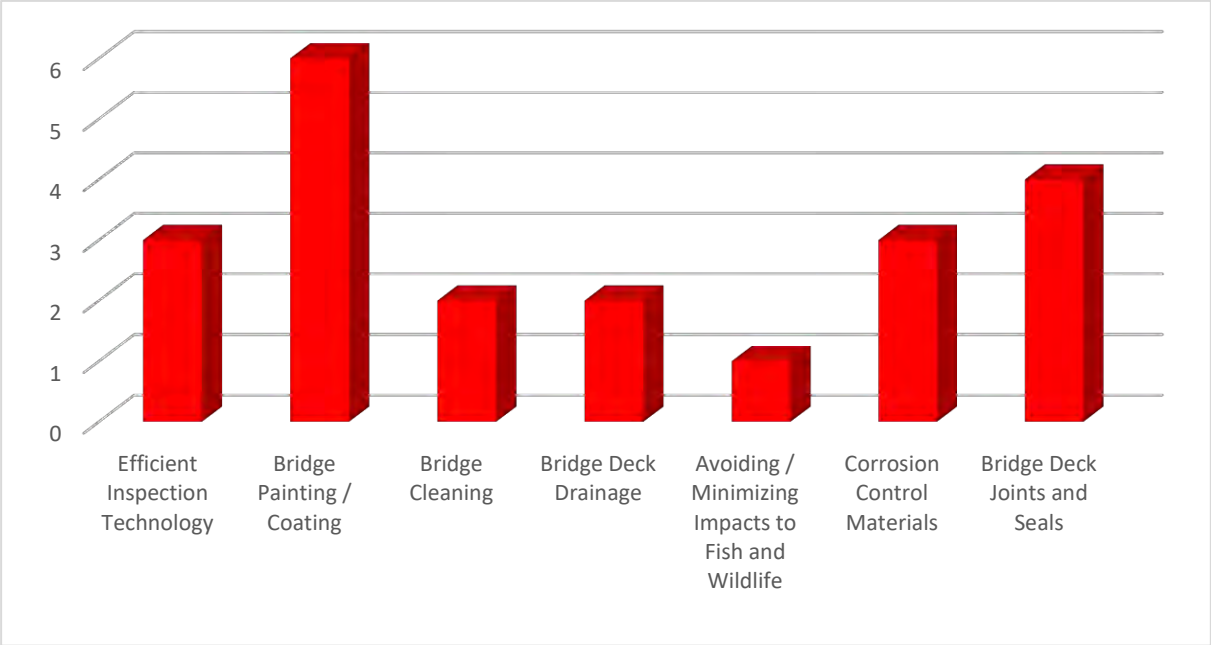

Figure 4: Point Distribution for Maintenance Stage (21 Points)

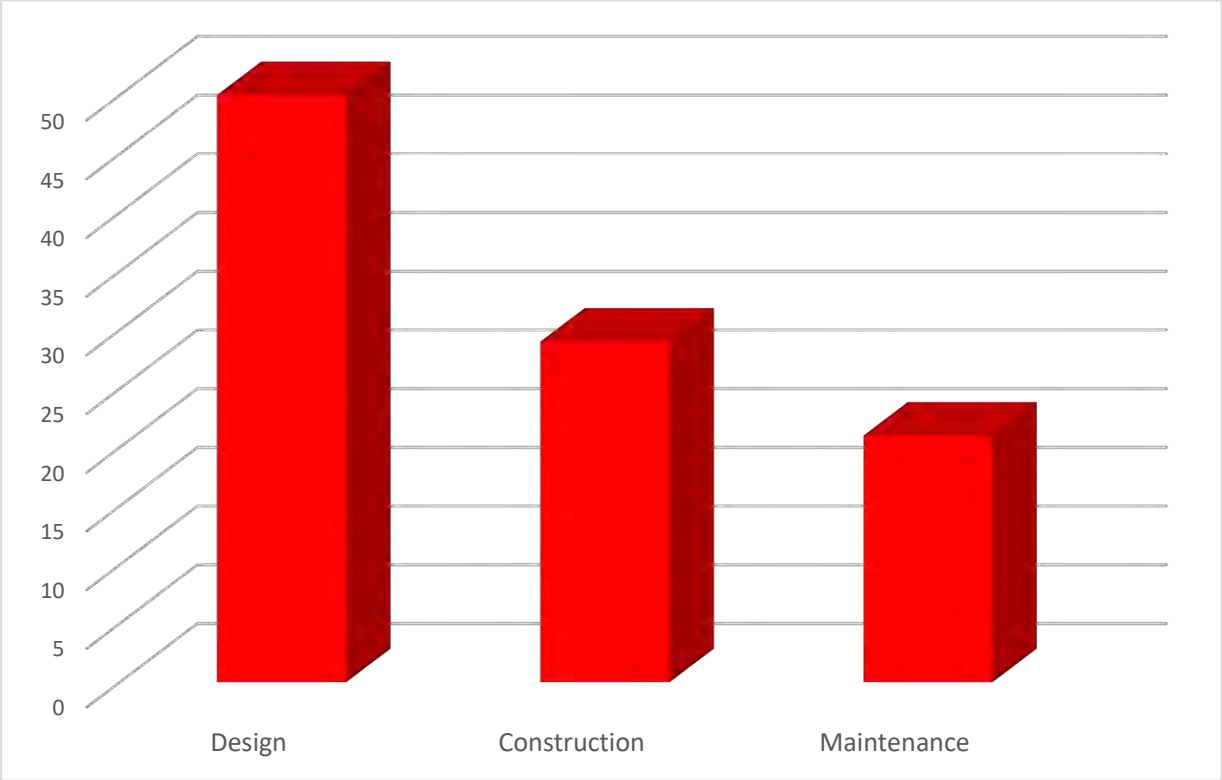

Figure 5: Point Distribution for Complete Life Cycle of the Bridge Development

CERTIFICATION LEVELS

After assigning points to each bridge design, construction and maintenance aspect, the next step is to decide certification levels to categorise sustainable bridges. It is recommended to adopt the same rating system as adopted by MDOT.

The score range is divided into three major levels: 0-33 representing the lower range, 34-64 representing the middle range, and 65-100 representing the higher range. The lower range and the higher range are further divided into two halves. This is because some of the criteria are easy to achieve and are very basic components of every bridge design and construction project. Those seeking certification are likely to achieve the Green certified level in any project, as they can easily obtain at least 1 or 2 points. The lower range consists of the Non-Green level, followed by Less Green. Similarly, the higher range consists of the Total Green level, followed by Evergreen; this raises the bar for an elevated objective for sustainability. The certification levels are shown in the Table 3 below.

Table 3: Certification Levels for Bridge Green Rating System

Certification level	Score Range
Non-Green	0-16
Less Green	17-34
Green	35-64
Total Green	65-82
Evergreen	83-100

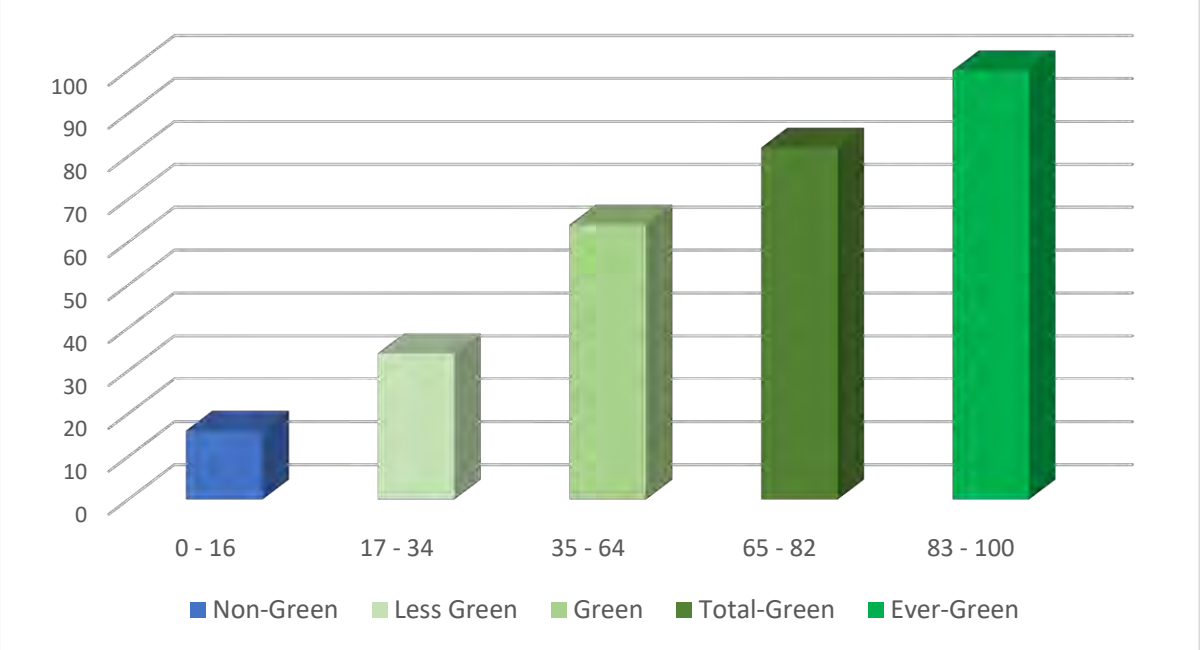

Figure 6: Certification Levels

A CASE STUDY – M2PP EXPRESSWAY PROJECT

The Mackays to Peka Peka (M2PP) Expressway is an 18km, four lane highway that takes State Highway 1 along the Kāpiti Coast. It was built by an alliance made up of the Waka Kotahi NZ Transport Agency (NZTA), Beca Ltd, Fletcher Construction and Higgins Group, supported by Goodmans Contractors and Boffa Miskell. The project included 17 multi-span and single-span bridges, including a new 182m long crossing over the Waikanae River. The use of high-quality concrete has delivered structures that fit seamlessly into the local urban

and rural landscape, while maintaining construction efficiency and allowing the project to be delivered to a very high standard.

Figure 7: Location plan of M2PP Expressway Project

Sustainable Design Aspects of M2PP Expressway Project

In the planning stage, several alignment options were considered to avoid sites with habitats of any species, avoid placing footing in water bodies/waterway of river and avoid demolishing any historical structure. The local history and culture were preserved by protecting the local sacred land by installing the Te Kakakura retaining wall with motifs demonstrating the cultural values of the region using the concept of a kaitaka (cloak). The motifs are embossed into the precast wall panels and the river stone aggregate is exposed for contrast.

Peat deposits were present along the alignment. These peat deposits can cause significant post construction settlements due to high compressibility which, without treatment would have resulted in poor rideability, settlement of services and adjacent properties, altered surface drainage patterns and increased maintenance. Several ground improvement techniques were adopted to improve the ground without excavation and replacement of peat deposits. This was to minimise the environmental impacts of construction by not excavating and replacing the peat deposits and use of the brownfield to reduce pressure on undeveloped land. A comprehensive Stormwater Management plan was implemented at the site to reduce the pollution that is discharged into surface waterways or storm-sewers.

The excavated materials were used initially to overload the peat deposit area along the alignment to improve the ground for highway construction, and later this material was used in the formation embankment of the road. The recycled polystyrene had been used in eight bridges along the expressway. The compacted blocks of recycled polystyrene had been placed in areas where concrete formwork was too complex to construct and remove. This includes filling the gap in between concrete barriers to prevent the collection of debris in between the barriers resulting in a reduction in the maintenance cost, and below the land span slab to eliminate the formwork. The project used about 180 cubic meters of recycled polystyrene material.

Up to 30% Supplementary Cementitious Material (SCM) was used in large diameter piles and large abutment foundation pilecaps to control the heat of hydration and to reduce the embodied energy associated with cement. To support the local business and community,

one of the Alliance's objectives was to get most of the construction material from the region. This also reduced the impact on the environment resulting from the transportation.

A separate 3m wide pedestrian and cycleway is provided along the full length of the expressway and a 2.5m wide shoulder is provided alongside the expressway for occasional bicycle users. The bridge structures are designed to behave in ductile manners by allowing the plastic hinges to form in the piles below the ground. During the concept stage, several options were developed, and a full life cycle cost analysis was carried out of all options to select the option with the lowest overall cost consistent with its quality and function.

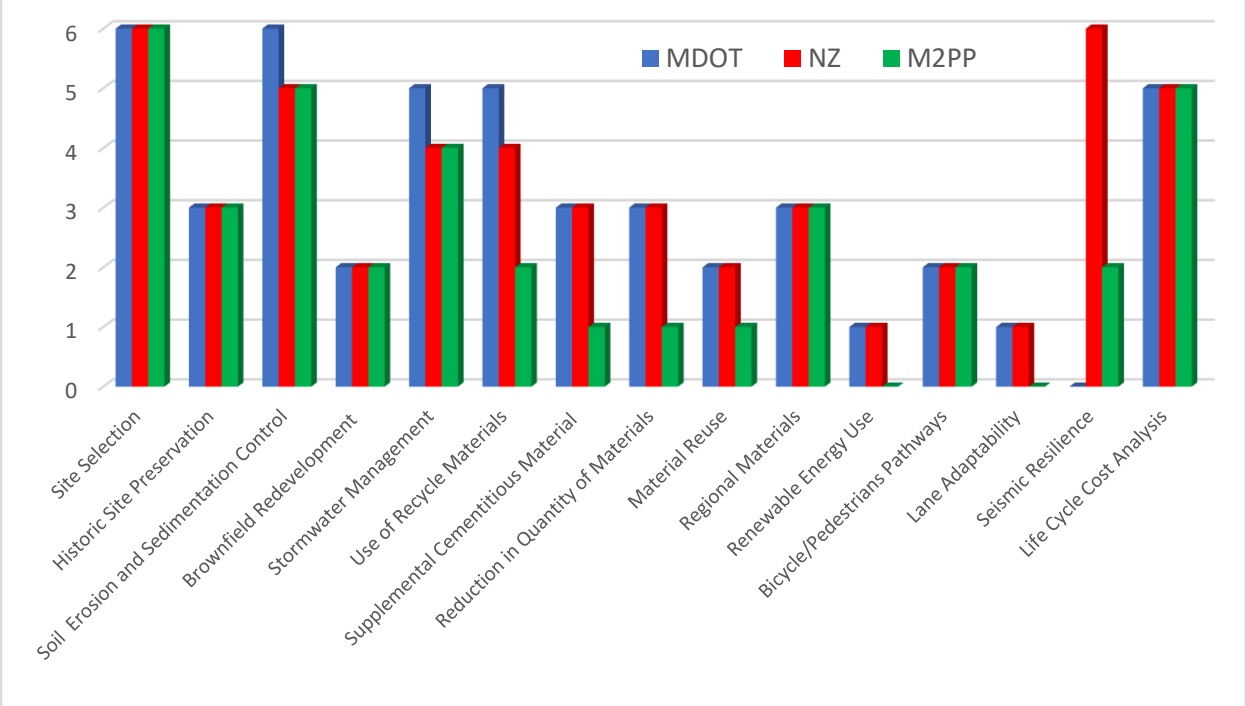

Figure 8: Points for a Sustainable Bridge Design

Sustainable Construction Aspects of M2PP Expressway Project

A number of efficiencies were achieved through the use of Accelerated Bridge Construction (ABC) techniques. The ABC approach utilised innovative planning, design, material, and construction methods in a safe and cost-effective manner to reduce the onsite construction time for the new bridges.

The exposure environment for the project site was “B1 – Costal perimeter” in accordance with Table 3.1 of NZS 3101. The concrete covers to reinforcement/prestressed strands were provided for exposure classification “B2 – Coastal frontage”. The concrete cover for exposure environment B2 is 10mm thicker than for exposure environment B1. The flow-able concrete mix with high cement and fine particles content produced a dense concrete with low permeability/porosity. A dense concrete with thicker concrete cover than required for the exposure environment enhances the durability of the structures and will minimise potential weathering effects. The concrete members should achieve a 100-year design life and should require minimal maintenance during the in-service life of the bridges.

A precasting yard was established as a part of the project, where hundreds of precast beams and other elements were produced. All storm water from the precasting yard had to be treated and was drained to a pH treatment facility that could fully neutralise up to 36,000L of

highly caustic water per hour. A CO_2 dosing system was installed to manage the high alkaline water from the precasting yard without the need for harsh chemicals, to protect the environment.

The project team made all possible efforts to reduce the construction waste. Material used for overloading the soft soil zones was used in the construction of road embankment, construction waste of reinforcements was donated to local community projects for retaining wall construction.

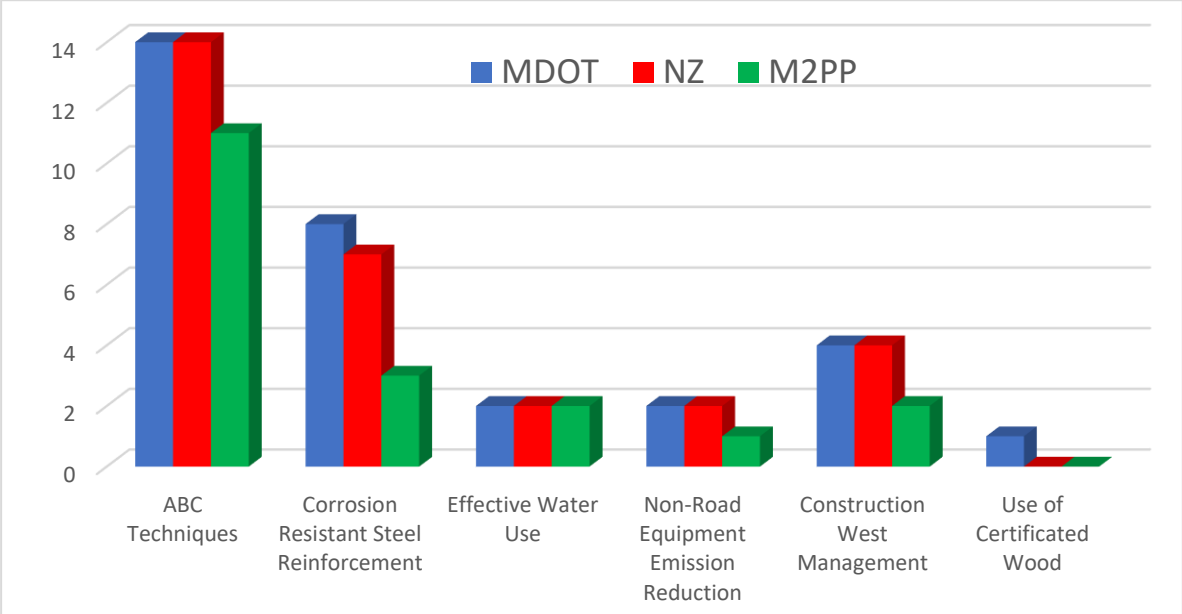

Figure 9: Points for a Sustainable Bridge Construction

Sustainable Maintenance Aspects of M2PP Expressway Project

For the inspection of bridges during the operation of the expressway, the framework for the Bridge Inspection Programmes as recommended in the Bridge Manual is adopted. To prevent steel bridge components from deterioration due to corrosion, painting and coating to bridge steel components is specified in accordance with the NZTA Painting Coating Guidance. Stainless steel bird proofing nets are provided around the services, bearing shelves and other bridge components which require regular inspections, to keep these areas clean. Only six bridges have movement joints out of 12 road bridges. Four bridges have single seal joints, and two bridges have multi-seal joints. A routine maintenance procedure is established as recommended in the Bridge Manual for inspecting the movement joints.

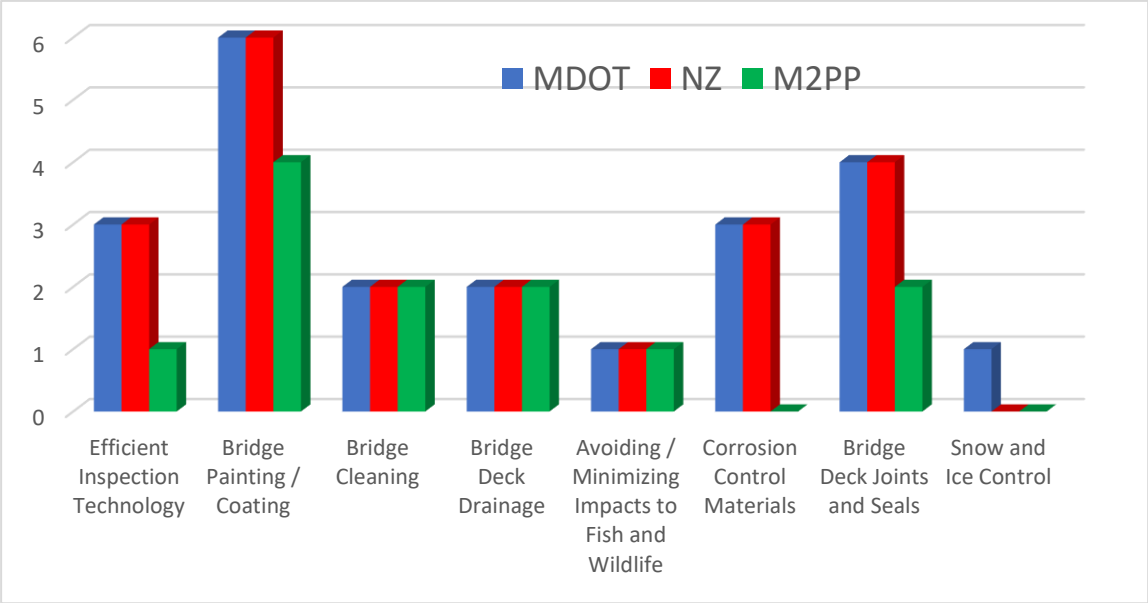

Figure 10: Points for a Sustainable Bridge Maintenance

Sustainable Rating of M2PP Expressway Project

In the light of above, it is found that the Mackays to Peka Peka Expressway Project can scores 37 sustainability points for its design, 19 sustainability points for its construction aspects and 12 sustainability points for the maintenance aspects. Overall the M2PP expressway project can scores 68 points out of 100 sustainability points and can achieve a "Total Green (65-82)" certification level.

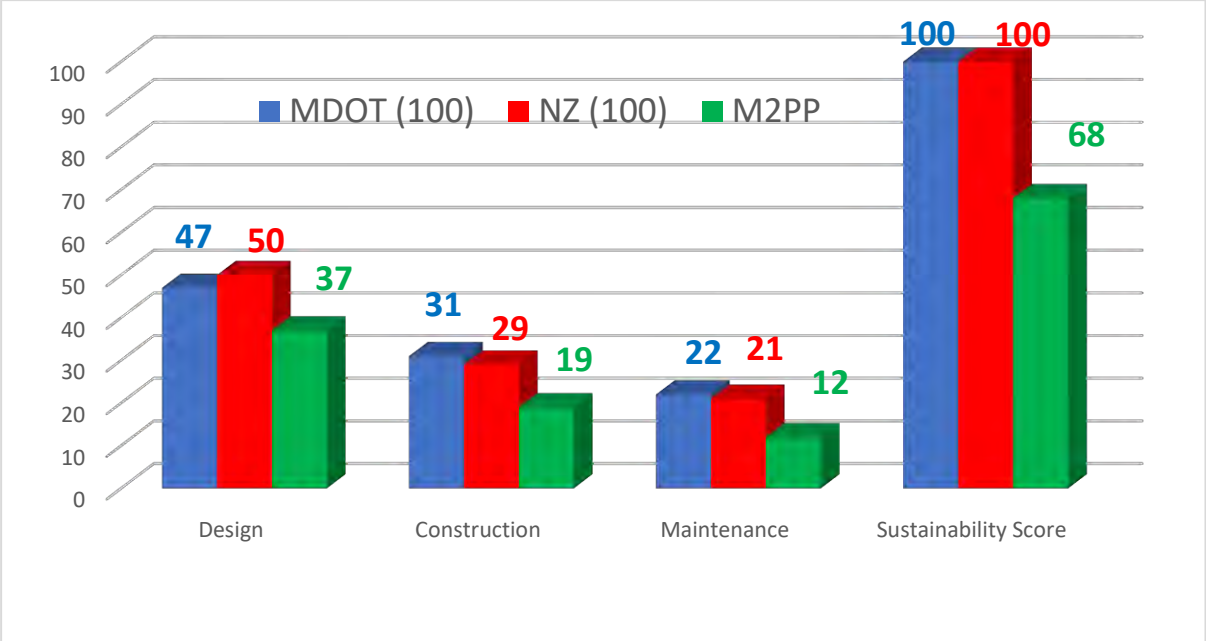

Figure 11: Sustainable Score

CONCLUSION

A framework was developed to implement sustainable strategies in bridge projects for New Zealand. The framework includes a green rating system, which is divided into three major categories, Design, Construction, and Maintenance. Design, construction, and

maintenance sections are further divided into various criteria. For each criterion, the description, intent, and requirements have been established.

A scorecard for the rating system is developed based on the common practices in the New Zealand bridge industry. Certification levels are developed to categorise sustainable bridges. The certification levels are Non-Green (0-16), Less Green (17-34), Green (35-64), Total Green (65-82), and Evergreen (83-100).

The framework can be used as a tool to find out how sustainable our current bridges are and will steer us for future improvements in our current practices.

A case study was conducted for the Mackays to Peka Peka Expressway Project using this framework and found that M2PP projects scored:

- 37 points out of 50 points for the design stage
- 19 points out of 29 points for the construction stage
- 12 points out of 21 points for the maintenance stage.

It is also found that that M2PP Project scored 68 points out of 100 sustainability score and can achieve a “Total Green (65-82)” certification level.

REFERENCES

Report No. RC-1586, “Implementation of Sustainable and Green Design and Construction Practices for Bridges”, by Kasim A K, Matt Syal, Ronald S, Sinem K, School of Planning, Design and Construction of Michigan State University, Sponsored by Michigan Department of Transportation

Sustainability Assessment: The state of the art, by Alan B, Angus M and Jenny P, Impact Assessment and Project Appraisal Vol 30, No 1, March 2012.

Sustainable Bridge Construction Through Innovative Advances, by A E Long, P A M Basheer, S E Taylor, B G I Rankin and J Kirkpatrick, Proceedings of the Institute of Civil Engineer, Bridge Engineering 161, June 2011.

Sustainability for the Concrete Bridge Engineering Community by Dr Tess Ahlborn, ASPIRE, Winter 2008.

A design approach for sustainable bridges – Part 1: Methodology, by Helena M D S G and Luis A P S, Proceedings of the Institution of Civil Engineers, Engineering Sustainability 166 August 2013 Issue ES4.

Sustainability – A Bridge Engineer’s Viewpoint, by Man-Chung Tang, T.Y Lin International, San Francisco, California, 94104 USA.

The Sustainability Considerations for Bridges, Transportation Association of Canada, October 2015.

The components of sustainable development - a possible approach, by Dan C D, Luminita M G, Alin A and Vasile D, 4th World Conference on Business, Economics and Management, WCBEM, 2015.

Our Common Future, Report of the World Commission on Environment and Development, General Assembly of the United Nations, by Gro Harlem Brundtland, Oslo, 20 March 1987

“Sustainable Structures for the Bridge Engineer” By Daniel Whittemore, the article published in Structure Magazine Oct 2010.

“The Future of Sustainability: Re-thinking Environment and Development in the Twenty-first Century”, Report of the IUCN Renowned Thinkers Meeting, by Adams, W.M. 29-31 January 2006.

concretenz BUILDING RESILIENCE
CONFERENCE 2022
13-15 October 2022
Energy Events Centre | Rotorua

CONSTRUCTION OF TEKAPO A NEW INTAKE GATE AND SHAFT

MARK HEDLEY[1], ALEX PARFITT[2]

[1] Downer NZ, Christchurch, NZ, [2] Parfitt Construction Limited, Christchurch, NZ

SUMMARY

In October 2018, Downer was awarded a $15.3M contract by Genesis Energy for the supply, construct, and commissioning of the new Intake Gate for Tekapo A Power Station. The new gated water intake will allow Genesis Energy to stop the flow of water to Tekapo A Power Station in an emergency. Water from Lake Tekapo flows through the existing 1.6km long tunnel to the Tekapo-Pukaki canal and to the power stations on the rest of the Waitaki scheme.

The work involved building a shaft extending down to the tunnel, exposing and cutting into the tunnel, fitting a steel "stent" section into the tunnel and installing the gate with its guide slots and hydraulic ram. Genesis required works to be carried out between specific time periods so that there would be minimal disruption to the generation of power.

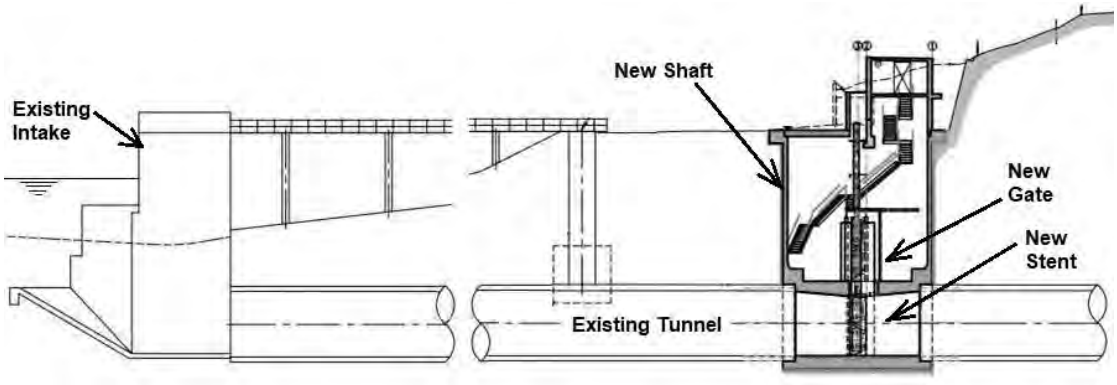

Downer and Parfitt Construction Ltd worked collaboratively with the client, Genesis Energy, and the design consultants, AECOM to overcome challenging conditions and develop innovations which reduced risks and saved time, ensuring that the Client's expectations were met.

Some of the challenges and construction smarts included:

- Innovative construction methods for the concrete shaft and roof
- changes to the concept of the "stent"
- specialist concrete mix designs
- unique risks including the remote nature of the site, cold temperatures, confined space tunnel work, and working through the COVID-19 lockdowns of 2020
- fabrication and handling of very large, precision engineered components.

All works were completed on time and to the revised budget of $17.6M, with no impact on power generation activities outside of the agreed shutdown periods.

Key words: concrete shaft, shotcrete, concrete pour, power station, outage, tunnel, excavation

1. INTRODUCTION

Five years from planning to completion, the project had to overcome a number of unique engineering challenges, including how to integrate modern gate technology into infrastructure and tunnels originally designed and built in the 1940s. This included developing an innovative permanent stent option for the existing tunnel to allow flows during construction and a methodology to construct the shaft in layers, expediting this critical piece of work.

Construction of the permanent stent and concrete shaft was completed within the constraints of two non-negotiable shutdowns or “outages” of 17 weeks and 8 weeks respectively, plus a third outage for final install and commissioning. The shaft required excavation to a depth of 21m, just 50m from the shore of the lake, to a depth of almost 15m below lake level, with over 4,000 tonnes of concrete poured in this sensitive environment.

Figure 1: A project of national significance, Tekapo A Intake Gate project was completed on time and under budget, ensuring continued powering of over 125,000 Kiwi homes

Given the depth of the existing tunnel and shaft, this work needed to be delivered under the Health and Safety at Work (Mining Operations and Quarrying Operations) Regulations 2016, to manage these critical risks.

Genesis wisely engaged Cromwell local Les Topping as Engineer’s Representative and Joe Edwards as Engineer to the Contract.

1.1 Shaft innovations

To closely align the works with Genesis’ programme expectations, Downer and key subcontract partner, Parfitt, collaboratively developed and proposed an alternative approach for the construction of the shaft.

The original solution detailed at tender time for the shaft was to construct the permanent shaft walls “top-down” in 1.5m sections, using formwork and in-situ poured concrete. This had the advantage of minimising temporary retaining works but had programme, cost and potential quality implications. The joins between concrete pours for this method of construction pose a risk of leakage and each section would be slow and difficult to build effectively.

The alternative approach was to dig and temporarily support the shaft using shotcrete and soil nails all the way to the base followed by “bottom-up” permanent construction. This method reduced the timeframe for each 1.5m section from two weeks to just one week, allowing the Client’s deadlines to be met. The choice of shotcrete for time critical activities also reduced delivery and temperature risks.

1.2 Stent innovations

For the original sequence, all permanent works were to be constructed prior to the opening of the tunnel for generation at the end of the planned first (17 week) outage. Completing this quantum of work in a relatively short time period created programme risk and so an intermediate stage was developed which utilised a “stent” installed at the base of the shaft to allow full generation to occur while the permanent works were completed.

Subsequently, all works were completed on time and to budget with no additional impact on power generation activities.

1.3 Construction Risks Managed

Access to Tekapo via State Highway 8 posed some risk, as any incidents on either the Tekapo to Fairlie or Tekapo to Twizel portions of the road could effectively cut off access, with no other routes available on either side of the township. The COVID-19 lockdowns of 2020 created additional challenges on top of the remoteness of the site, with transportation and supply chains significantly affected. Careful planning was required to manage these risks, along with advance ordering and stockpiling of materials on site.

Figure 2: Extreme temperatures were a risk to concrete quality

Isolation was an issue to consider for the time critical shaft construction and, accordingly, the decision for Parfitt to self-perform most activities was made. This allowed accommodation to be booked out and a great project culture to be developed amongst the close-knit project team led by Project Manager, Alex Mowe and Site Supervisor, Don Hayward.

Local general and precision engineers Gibson Brothers in Fairlie were called upon frequently to make urgent repairs to keep the job going.

All reinforcing was supplied and placed by Complete Reinforcing, Christchurch. All concrete was supplied by Kiwi Concrete, Twizel. In-situ concrete was placed using a skip and shotcrete was fed from a trailer pump.

To mitigate the potential risk of voids and water erosion, a 60MPa self-compacting mix was developed for the gate slot secondary concrete. Kuniseal hydrophilic sealants and a waterproofing admixture were used in all in-situ concrete pours.

Some winter concreting was required but fortunately, during this time, the temperature in the tunnel and shaft was slightly higher inside than the ambient outside temperature. This helped to mitigate the risks posed by cold temperatures.

A full scale heat of hydration analysis was completed for the base slab staging pours.

All quality requirements were met despite the cold weather and remote site.

2. CONSTRUCTION

2.1 Soil Nailed Retaining Wall

To facilitate a clear, level construction area, a 6m high retaining wall was constructed, containing 100 x 5.5m long soil nails and shotcrete. These works were completed 22 days ahead of programme. This work also provided an opportunity for the design and construction team to refine procedures for installing the soil nails and shotcrete for the shaft leading down to the tunnel.

Figure 3: Completion of 6m high retaining wall

2.2 Excavating the Shaft

A 14m diameter circular shaft with reinforced concrete walls was required to access the tunnel and to house the new gate.

An early innovation of Downer and Parfitt was to temporarily support the sides using shotcrete and soil nails so that the excavation could proceed at pace. Construction of the 400mm thick

reinforced concrete walls could then follow on in parallel with other work since it would no longer be on the critical path.

Temporary access to the bottom of the shaft was via a “hanging” Layher scaffold, with new modules added underneath the tower at each lift.

Excavation was carried out by a 13t zero tail swing excavator, and removed by filling a kibble skip, which was lifted in and out of the shaft with a 120t crane. Fill was carted 3km off site and stored for use later in the project as backfill between the control building and temporary retaining wall.

Excavation of the shaft and the removal of material was a challenge, particularly as the depth increased. Key communication protocols were developed for removal of each kibble. Up to 20 lifts of 15t each were made in a single day, and daily briefings were held with the team to ensure each days lifting was properly planned and reviewed.

Protocols included:

- Top and bottom dogmen for controlling all lifts
- Top dogmen stationed in a crow’s nest on the edge of the shaft to gain full view
- Bottom dogmen controlling lifts leaving the shaft base and rigorously handing over to the top dogmen at the top of the shaft for clearing the shaft and landing the kibble topside
- The controlling dogman always having direct line-of-sight visibility
- All personnel down in the shaft stationed in a refuge area or ‘safe-zone’ during all lifts, including the excavator operator
- Careful filling of the kibble to avoid overloading or spills.

Figure 4: Excavation of the shaft

The glacial till material could be excavated to a vertical face but was prone to fretting and spalling. To prevent dropouts during drilling, mesh was placed and shotcrete was sprayed on the newly exposed face prior to drilling the soil nails. Shotcrete was delivered using a Putzmiester BSA1002 piston pump and a 4” hard line reduced down to a 2” soft line at the base of the shaft. A knife gate valve was always positioned at the base of the shaft. Shotcrete was originally specified as 30MPa and this was successful for the retaining wall and upper shaft, however as depth progressed, blockages were more common. The mix design was increased to 40MPa which provided more fines and assisted pumping. With the batching plant up to an hour away and the shotcrete process taking 30 minutes per truck, all parties needed to work together. It was important that the drivers continuously spun their bowls and that slump tests were taken before and during truck discharge. Superplasticiser was on hand to increase the slump when required.

At each excavation stage, 21 hollow bar soil nails were installed using a neat cement grout flush with a Hutte HBR504 drill rig and Krupp drifter. The rig was well sized for the job, having just enough space to fit in the 14m diameter excavation while still having ample power to maintain productivity. Generally, all 21 nails could be installed in a single shift. All grout was mixed topside and pumped down in a 1” line to the drill rig. A valve was available at the rig to help control flow. All pull-out tests exceeded requirements with sacrificial tests not being able to move the bar before yield was approached, indicating good bond. Soil nail lengths were reduced following sacrificial testing. Generally, grout volumes per nail were as expected except for nails on the lake side of the shaft which occasionally hit voids and often required up to 20-30 bags to maintain flush during and after drilling. Historical photos indicated that this was an area disturbed by excavation and backfill activities during the 1950’s tunnel portal

works. Shaft temporary works design was completed by Soil and Rock and A O'Sullivan and Associates, and included modelling of each permanent and temporary construction phase.

Communication between topside and shaft teams was via ear-muff mounted radio. Noise from the ventilation fan, drill rig engine, shotcrete operation and drifter operation in the shaft was deafening at times threatening to turn simple tasks or requests into safety hazards.

Excavation, shotcrete, and soil nail works were constructed down to a level 4m above the tunnel crown while the tunnel was operational and pressurised. No further work was carried out until the tunnel was emptied of water. This ensured that the worst-case internal water pressure did not overcome the overburden weight leading to potential tunnel failure. This analysis was completed by AECOM tunnel engineers in Sydney.

Progress to this level above the tunnel was faster than forecast, providing a window to commence the permanent walls before the first outage period. This was a valuable programming advantage which allowed a portion of the shaft walls, 3.6m high, to be constructed early. However, this also meant that this 180t ring of concrete would be undermined when excavation was recommenced. To ensure that there was no possibility of this ring sliding down the shaft, temporary support was required. The desirable solution was to "hang" the wall from the ring beam above, using the reinforcing steel, but that meant that all of the laps in the reinforcing would have to be positively tied together (and welding was not allowed.) Appropriately sized "bulldog" grips were sourced, but no load data was available for bulldog grips holding reinforcing steel bars, so testing was carried out by Holmes Solutions. A simple and effective temporary support design was developed using these test results.

Figure 5: View inside the existing tunnel

2.3 Opening up the Tunnel

The tunnel was dewatered (drained) at the commencement of the first planned maintenance outage. This relieved the internal pressures in the tunnel and allowed shaft excavation to continue.

The tunnel was never designed to be exposed from above so a cautious approach was taken. AECOM carried out a review of tunnel stability and certain loading restrictions were imposed. There was great conjecture on whether the tunnel segment bolts had been left in place during original tunnel construction in the 1940's. Such bolts may have been rare, and if they had been removed, this would have made a difference to the restrictions. The segments were conservatively assumed to be unbolted.

To access the tunnel, a 'letterbox' opening was cut into the crown of tunnel. This opening was restricted to 4.2m in width. This size determined maximum size of liner plates (and the amount of welding). A wire saw was used to cut a neat hole in the tunnel crown. (Bolts were present!) The existing tunnel, now 70 years old was found to be in excellent condition, and very close to dimensional expectations.

The next stage was to install the steel liners. These liners were critical to continued progress – they effectively extended the length of the stent, upstream and downstream, and were doweled, grouted and sealed to the tunnel walls to provide additional strength to the existing tunnel in these critical areas. All this work had to be done through the relatively small 'letterbox' opening so that the stability of the tunnel was not compromised.

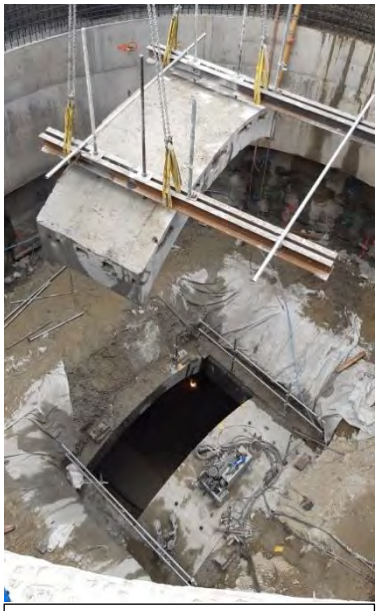

Figure 6: Removal of tunnel crown for access

The tunnel liners were manufactured in halves, totalling four curved sections upstream and four curved sections downstream. The restriction in 'letterbox' size provided a challenge to install the liners in a short time. The bottom half was lowered in to the tunnel on its side (3m wide), rotated to horizontal within the tunnel and slid on skids using a snatch block and the crane winch up into the tunnel, away from the opening. The top section was then lowered in and rotated to horizontal inside the tunnel, before the bottom half was then pulled back beneath the top half (using a tirfor) and secured. The liner set was then winched along the tunnel and into position. Comprehensive lifting and rigging plans were prepared well in advance to ensure this lifting could all be done safely without damaging the liner sections. A trial tunnel was set up at the Parfitt fabrication workshop to check the method. All eight liner rings were installed over a one-day period using this very efficient method. The liners were levelled, doweled, welded, grouted and painted in place.

The tunnel circumference was cut using a 3m diameter wall saw blade by Concut Christchurch from inside the tunnel. This provided an accurate cut face in the tunnel, upstream and downstream at the location of the future stent.

Figure 7: Tunnel liners arriving on site

A simple and safe working platform was created in the tunnel by filling the tunnel with gravel. Two bulkheads were constructed, one upstream and one downstream to confine the gravel platform and this allowed construction of the lower part of the shaft to continue using the same proven method used for the upper part of the shaft. The gravel platform was progressively lowered as the remaining stages of the shaft were constructed. During each stage, part of the tunnel was demolished using a breaker on the excavator until finally the invert was reached, some 21m below ground level.

2.4 Installing the Stent

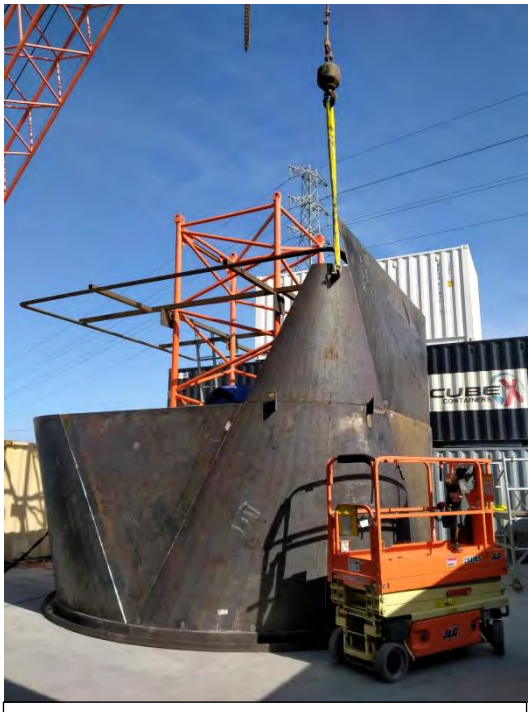

Figure 8: Fabrication of stent underway in vertical position

To achieve programme and complete works within the required shutdown periods, the team were required to install a steel “stent” to carry water beneath the shaft construction area. Initially designed as a temporary measure, the original stent was smaller in diameter than the tunnel itself, which would have reduced the flow of water and limited power generation. Working with the client and designer, Downer offered an alternative:

- support the tunnel either side of the shaft construction area with permanent tunnel liners
- install a permanent steel stent that met the diameter of the original tunnel and provided a slot for the new gate.

The stent was made of 8mm skin plates and a series of fabricated T sections of web and flange at 300mm centres. It transitioned from an upstream egg-shaped tunnel to the rectangular gate and back to the downstream egg-shaped tunnel, making for quite a complex, fully welded geometrical structure more akin to an ocean going ship than a civil structure. The 40t stent was fabricated and painted at the Parfitt workshop in a vertical orientation to minimise jig costs (a set of 120t crane booms in the vertical position were used). Vulcan supplied, cut and tip folded all plate. Each stent was rotated to horizontal and transport was via an ultra-low bed trailer designed for tank transport and operated by Jackson Heavy Haulage.

Figure 9: Installing the Stent in two halves

With the liners in place, and the existing tunnel removed within the shaft footprint, the two stent halves could be lowered into place. The two sections were lifted in one at a time. The cylindrical ends were butted against the sawcut faces of the tunnel with the square ends meeting in the centre of the shaft. Placing the second section was a challenge, with extremely tight tolerances at either end. There was only 100mm of space between the stent piece and the stair tower, and a similar distance between each section once these were actually in place. Although challenging, each section was successfully slotted into place and connected using a combination of temporary and permanent sealing plates. To ensure stability of the stent during full tunnel operation (6m diameter of water), 1.5m of concrete was poured at the base of the shaft to encase the invert of the stent. Pour heights were limited due to the concrete pressures acting on the stent.

With the tunnel liners and stent fitted and tightly sealed against the slightly oval tunnel circumference, water could again flow through the tunnel. Works continued above in the shaft and generation of power resumed. The permanent stent option also meant that further works were not required on completion of the project to re-enter the tunnel and remove temporary measures.

Robert Bird Associates completed heat of hydration analyses which modelled the internal tunnel water temperature, the ground temperature, the height of each pour stage and the time between pours to ensure critical temperature differentials did not occur in the 1000m3 concrete raft at the base of the shaft. AECOM confirmed a slight reduction on concrete strength to 25MPa could be employed in the raft concrete to assist with temperature control.

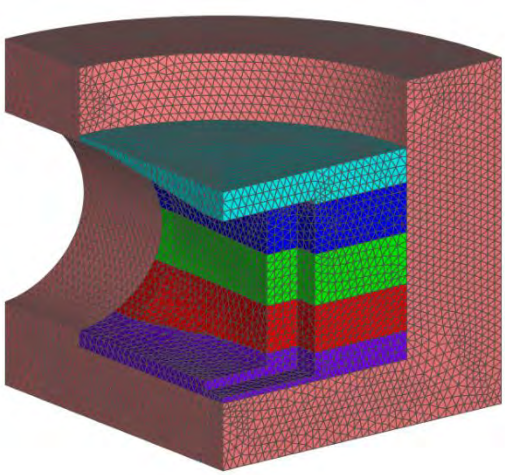

Figure 10: Heat of hydration analysis staging

Above the shaft base slab, a Doka circular formwork system was used to form the permanent shaft walls. Generally, 1.2m lifts were chosen for the pour height. A modular access platform was fixed to the formwork for each pour and boom lifts and the crane were used to jump the forms up to the next lift or to complete any remedials. A one-week turnaround was achieved.

2.5 Shaft Roof and Control Room.

The roof slab over the shaft was originally designed and detailed as fully in-situ. While possibly being simpler to detail, an in-situ slab is slow and requires substantial falsework, so the project team developed a precast + topping alternative. This method offered programming advantages but there were still challenges to overcome such as large spans, loads relating to mobile crane outriggers, access provisions and the not insignificant weight of the control room structure.

Figure 11: Precast roof layout

To meet these requirements a post tensioned beam, hollow core slab and in-situ topping slab option was chosen with the result that all falsework and temporary propping for the roof was eliminated.

The largest lift was the 45t “T beam” which was the main spanning member and was 2.4m high (also being the lower part of the control building walls). Beams and roof elements were made at the Parfitt precast yard in Christchurch and transported to site by Smith Crane and Construction.

Figure 12: Control room structure

The control room was a “Ministry of Works” style, fully in-situ concrete bunker. Doka Frami formwork was used to form wall, floor and roof elements. A horizontal rough sawn timber finish was provided in keeping with the surrounding concrete work.

2.6 Installing the Gate

The gate was manufactured in two halves – a 32t lower half and a 17t upper half, and fabrication was an exacting task. Installation tolerances were extremely tight and placing the gate was challenging.

Each section was lifted into place in the pre-formed metal slot with just 5mm of free space each side. Care was needed to avoid damaging the all-important gate seals and seal faces. Installation was successfully achieved in just nine hours, a testament to the good planning, precision engineering and the quality assurance carried out in the manufacture of all of the static and moving parts.

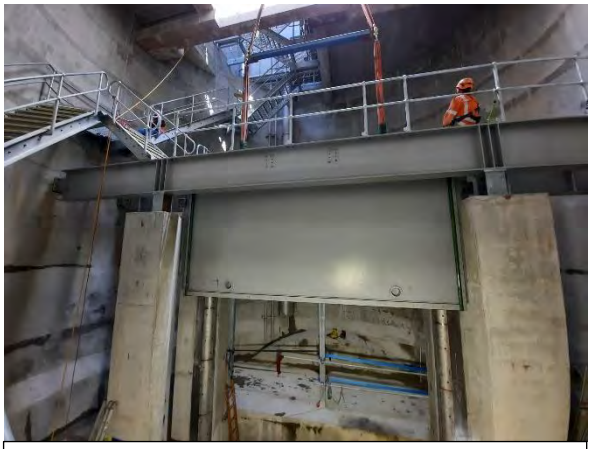

Figure 13: Gate installation

2.7 Next-level' quality control

With key elements of work needing to align to very tight tolerances (e.g. the prefabricated sections of the gate), quality was regularly and thoroughly monitored.

A key quality consideration was the temperature during concrete pours, especially in winter. Weather forecasts were reviewed against concrete/shotcrete pour schedules to align pours and volumes with the warmer parts of the day.

The concrete used to encase the plates for the gate runners was specified as 60MPa and the space for placing it was either very tight, or inaccessible. In some places it was so tight that the use of normal compaction equipment was not possible. The high strength concrete with its high cement content and short workability period further exacerbated the problem.

To address these challenges, a high strength, self-compacting mix was developed with Kiwi Concrete that would give sufficient time to place, whilst also taking into account the one-hour delivery time to site from Twizel. Trial pours were conducted by setting up a typical pour lift on site and placing the mix to check if it would fill all of the voids. The trials were successful.

Farra Engineering Ltd (Dunedin) were chosen to manufacture the gate and the associated components since they had the ability to machine these large and complex fabrications. The stainless steel plates on which the gate wheels would run, and to which the seals would come into contact, had to be machined to exacting tolerances. For example, the bottom seal plate was checked against a reference straight edge for a flatness deviation of no more than 0.5mm, and the gate had to seal such that there was no more than five litres of water per second leaking when it was closed. On completion, the leakage rate was measured and found to be a minimal one litre per minute.

All concrete and grout testing was carried out by Downer's own ISO accredited Road Science laboratory.

Three external audits were undertaken by Rileys (working for Environment Canterbury) as part of the Building Consent requirements.

2.8 Protecting Lake Tekapo

There were a number of environmental challenges on the project, given its location on the shores of the pristine Lake Tekapo. Storm water and surface runoff were carefully managed by a combination of silt fences, drainage channels, soak pits and the natural permeable nature

of the glacial till ground. Lined skips were used for collecting wash-down water from concrete trucks.

Dewatering was flagged as a big risk item given that all discharge into the lake had to meet critical sediment requirements. Four wells were drilled around the perimeter of the shaft using the Hutte rig used for soil nailing. Each had a submersible pump with high and low alarms and cut-out and ran 24hrs a day for the project. Care was taken to position wells away from soil nails to avoid grout ingress into the dewatering system.

Figure 14: Working on the shores of Lake Tekapo

Water pumped from de-watering wells was contained in sediment tanks before being discharged into soak pits or other prescribed outlets and regular monitoring of water quality confirmed that PH limits were never exceeded.

Figure 15: Successful completion was second only to the view.

CONCLUSIONS

In February 2021, after 18 months of construction, the Tekapo Intake Gate Project was completed on time and on budget, protecting one of the South Island's key hydro power schemes from the risk of uncontrolled water discharge due to significant earthquakes.

Downer NZ and Parfitt Construction Ltd worked collaboratively with Genesis and designers AECOM, to overcome significant engineering challenges and develop engineering smarts that led to a successful outcome:

- Innovative construction methods were developed for the concrete shaft and roof which saved time
- Changes to the concept of the "stent" added value and reduced risk
- Specialist concrete mix designs contributed to a quality outcome
- Unique risks were managed including site remoteness, cold temperatures, confined space tunnel work, and working through the COVID lockdowns of 2020
- Very large, precision engineered components were successfully produced, installed and commissioned.

The project won the CCNZ "Category 3" award at the national conference in Wellington on 30th July, 2021.

ACKNOWLEDGEMENTS

- Genesis Energy – Client
- Les Topping and Associates (Engineer's Representative)
- Joe Edwards (Engineer to Contract)
- AECOM – consultant
- Kiwi Concrete – concrete supplier
- Farra Engineering Ltd – gate
- Queensland Hydraulics – hydraulic ram
- JLE - Electrical
- ABB - Automation

concretenz BUILDING RESILIENCE CONFERENCE 2022
13-15 October 2022
Energy Events Centre | Rotorua

TESTING OF FLANGE HUNG DOUBLE TEE UNITS WITH LOOP BARS

MATTHEW JENKINS, RICK HENRY, KEN ELWOOD

University of Auckland

SUMMARY

Double tees are a common form of precast floor unit that have been implemented in a range of buildings in New Zealand, many of which used the flange hung loop bar support detail. Concerns were previously raised about the seismic performance of double tees with loop bar supports and as a result the detail is no longer used in new construction. The seismic performance of existing buildings with double tees remains of concern, with damage observed to such support details in both the Canterbury and Kaikoura earthquakes. A test programme was initiated on double tee floor units as part of the wider ReCast floor project that is investigating retrofit solutions for existing precast concrete floors. A total of 6 tee units with loop bar support details were tested to investigate their seismic capacity and proposed retrofit solutions. Three tests focused on the vertical load capacity of the loop bar support with varying degrees of delamination simulated at the unit-topping interface. A further three tests focused on the capacity of the support connection when subjected to combined rotation and elongation demands.

INTRODUCTION

Double tee precast floor units have been implemented in a range of New Zealand buildings since the late 1960s. Many of these double tees used the flange hung loop bar support detail, as shown in Figure 1a. The loop bar detail (also referred to as a pig tail) consist of reinforcing bars that project up diagonally from the bottom of the web, looping around in the flange support region and then tying back into the unit. Concerns about the compliance of the loop bar detail and the capacity under both vertical and seismic actions were raised during the early 2000s and are summarised in the paper by Hare et al. (2009). As shown in Figure 1b, a strut and tie model of the loop bar support detail showed a tension tie required across the interface between the insitu topping and the precast unit when subjected to gravity loading. In addition to relying on the concrete tensile strength, the tension capacity across a cold joint is particularly unreliable and may be influenced by potential delamination of the topping concrete when subjected to different load combinations. Despite having a roughened surface to the double tee units, delamination of the topping from the units was observed in the double tees that collapsed in Statistics House building during the Kaikōura earthquake (2017).

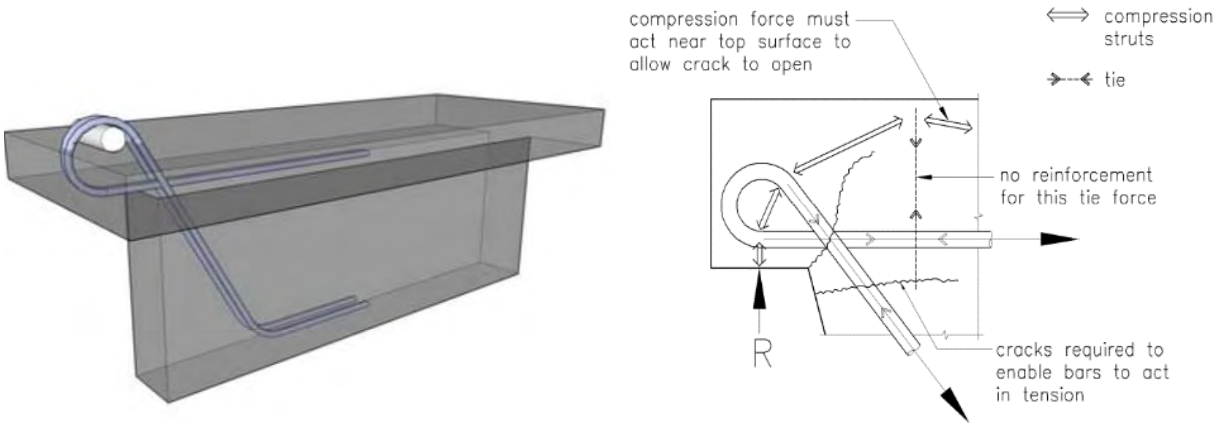

a) 3D drawing showing the loop bar b) Strut and tie model

Figure 1. Typical loop bar support connection (Hare et al. 2009)

Despite concerns being raised and significant research into the seismic performance of hollowcore precast floor units, the performance of double tees has received significantly less attention. Observations from buildings damaged during both the Canterbury and Kaikōura earthquakes confirmed some of the prior issues raised for flange hung double tees with loop bar support details as well as identifying new failure modes that should be considered (Corney et al. 2014, Henry et al. 2017). In particular, the partial collapse of double tees in the Statistics House building during the Kaikōura earthquake highlighted the potential for loss of support due to cumulative frame dilatation from beam elongation and the spalling of the double tee nib and support beam ledge that reduces the available bearing support length (MBIE 2017, Hare et al. 2019). In recognition of the identified issues, preliminary guidance was included for the assessment of flange hung double tees in the revised version of the C5 seismic assessment guidelines, commonly referred to as the 'yellow chapter' (MBIE 2018).

A test program was initiated on double tee floor units as part of the wider ReCast floor project aimed at developing retrofit solutions for existing precast concrete floors (Brooke et al. 2019). The double tee tests focused on the assessment and retrofit of flange hung units with loop bar support details and included investigations into both the vertical load and seismic capacity. The tests are described along with preliminary results from the initial tests completed.

LOOP BAR DETAILING

Prior to testing, an investigation into the typical details of existing buildings with double tee loop bar units was undertaken. The review included of over 20 New Zealand buildings and double tee fabrication drawings, ranging from 1979 to 2008. Table 1 shows the range of key design parameters from existing construction as well as the most common or typical details used to inform the testing. In general, the detailing of the loop bar reinforcing has remained similar from the 1970s to 2000s, with between 2 to 4 R12 bars used depending on the support loads. However, the position of the loop bar within the double tee was varied and a potential critical change in the standard detail occurred between the 1970s and 2000s. Standard support details from 1979, as shown in Figure 2a, indicate the loop bars would be placed with a cover of ~30 mm from the end of the unit flange/nib. Fabrication drawings from 2000 onwards show the detail was changed to reduce the loop bar cover close to zero, as shown in Figure 2b. The influence of loop bar placement is expected to have a significance impact on the seismic capacity as the effective seating or overlap of the loop bar is critical to the loss of support calculations with nib spalling occurring when subjected to beam rotations (Hare et al. 2019).

Table 1. Details representing typical double tees in New Zealand buildings

Design parameter	Approximate range	Most common / typical
Unit depth	200-600 mm	350 mm
Span	6-15 m	10 m
Parallel beams	Varied	Two bays of frames
Seating length	50-100 mm	75 mm
Topping thickness	65-125 mm	65-75 mm
Starter bars	Varied	D12 @ 400 mm

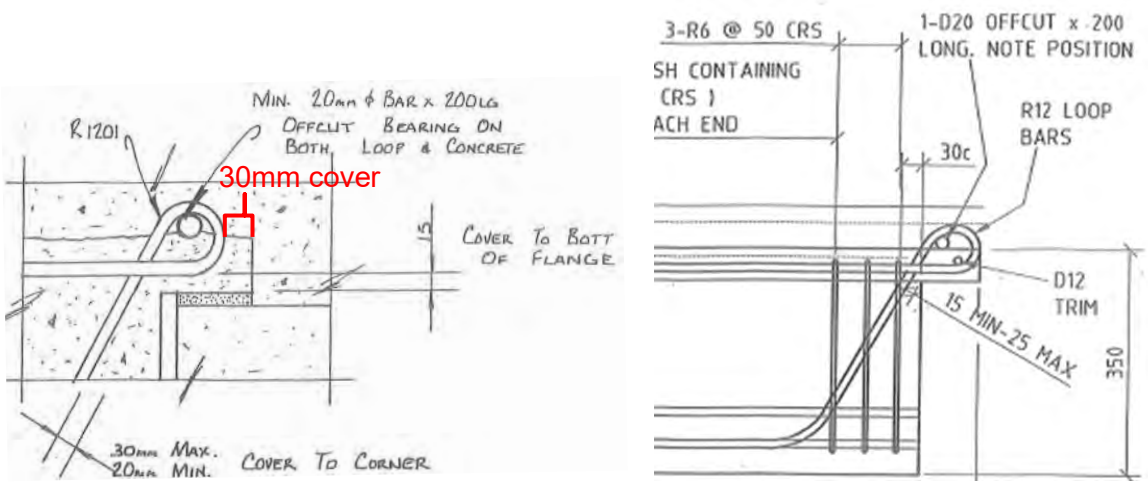

a) 1979 drawings b) 2000 drawings

Figure 2. Standard loop bar support detail

TEST PLAN

Sub-assembly tests were conducted that consisted of precast single tee units and a portion of the support beam. Single tee units were chosen for testing due to their accessible handling and the ability to isolate the test to a single loop bar support. The single tee units were 350 deep, 3.2m long, and 1.2m wide. A drawing of the loop bar support end is shown in Figure 3. One end of each unit was fabricated to represent a typical flange hung loop bar support detail, which included three R12 loop bars in the web region. The flange support end was seated 75 mm on a precast beam, both the beam and single tee unit were topped with 75 mm in-situ concrete with D12-400 starter bars and topping mesh were installed.

A total of 6 tests were conducted in two phases, with key details summarised in Table 2. The first series of tests focused on the vertical load capacity and failure mode of the loop bar detail. Based on the strut and tie model in Figure 1b, the unit-to-toping interface was identified as a key variable that effected the load path in the support. The three test units varied the condition of the topping-to-unit interface to simulate varying degrees of joint strength and potential delamination. The first precast unit had a U6 “wire broom” roughened surface (NZS 3114), representing a the typical as-designed unit. The second unit was finished with a smooth surface during fabrication. The third unit had a smooth surface finish and a piece of polyethylene plastic placed on its surface at the support end prior to the topping being poured to simulate delamination.

The second series of tests investigated the seismic capacity and failure mode of the loop bar detail. The three tests investigated the influence of loading protocol (drift vs. drift + elongation) as well as cover to the loop bar based on changes to standard detailing between older and newer double tees, as described earlier.

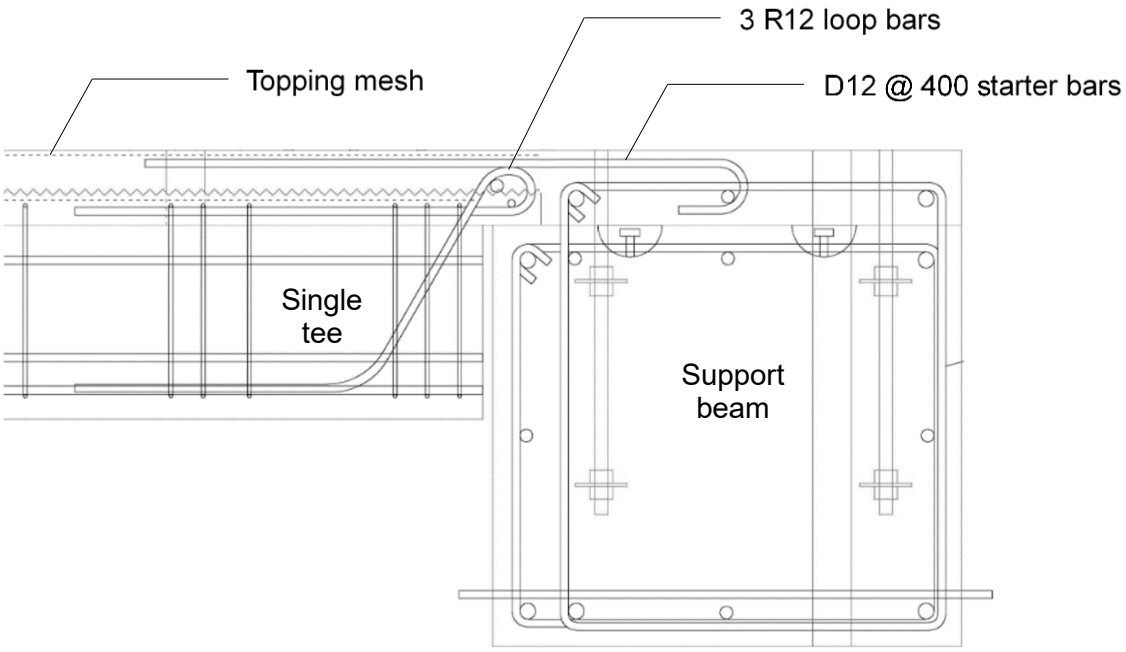

Figure 3. Drawing of test connection detailing

Table 2. Test matrix

Series	Unit name	Cover to loop bar (mm)	Topping interface	Loading protocol
Vertical loading	1. ST.PL.Non	0-10	Roughened	Point load
	2. ST.PL.Smooth	0-10	Smooth finish	Point load
	3. ST.PL.Plastic	0-10	Plastic sheet	Point load
Seismic loading	4. ST.Drift.30	30	Roughened	Drift only
	5. ST.DE.0	0-10	Roughened	Drift and elongation
	6. ST.DE.30	30	Roughened	Drift and elongation

The vertical load test setup is shown in Figure 4a. The support beam was fixed to the floor while the opposite end of the unit rested on a pin-roller support 2800 mm from the support beam. Vertical load was applied using hydraulic jacks located 550 mm from the flange support end of the unit. This loading point ensured the vertical stresses were transferred through the single tee web to engage the loop bars while reducing the flexural demands on the support connection. Vertical loads were applied monotonically until failure, pausing at key stages to observe and document damage to the support.

The seismic load test setup is shown in Figure 4b. Similar to previous sub-assembly testing of hollowcore, the end of the unit was attached to two hydraulic actuators to apply a combination of rotation and elongation to the support connection. An additional mass consisting of steel billets was applied to the single tee unit to simulate the support reaction consistent with the seismic load combination.

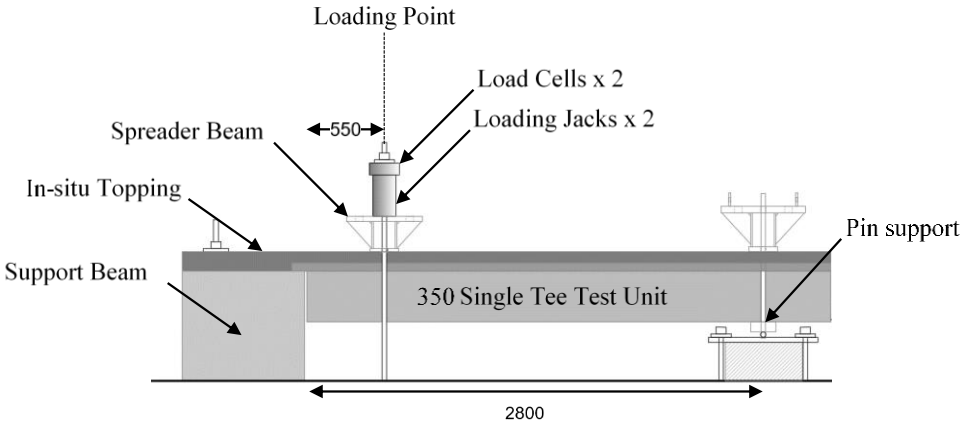

a) Vertical load tests

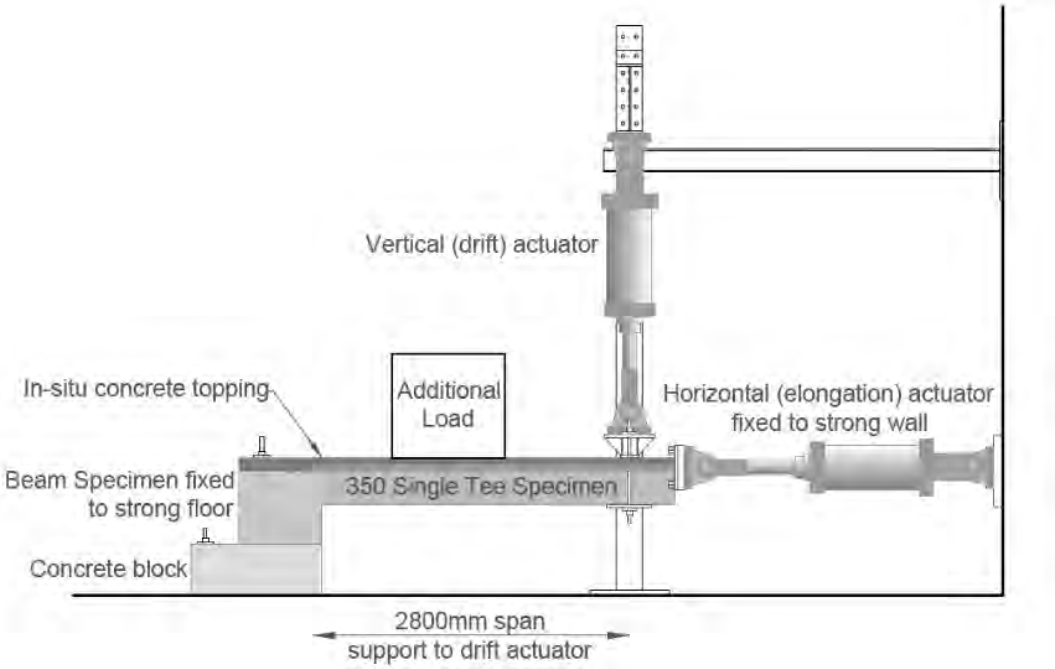

b) Seismic load tests

Figure 4. Test setups

VERTICAL LOAD TESTS

Photos of the typical damage progression for the vertical load test units are shown in Figure 5. A crack opened early at the interface between the topping and the support beam as the tee unit was loaded. At 100% ULS support load cracking was visible at the web-to-flange corner on the underside of the unit (Figure 5a). Such cracks are commonly observed in existing buildings and propagate at approximately 45 degrees across the flange. Upon further loading a second crack occurred along the top of the web, with the web deflection increasing as the crack width increased (Figure 5a). The unit failed with separation occurring between the web and flange regions and significant deflections occurring as the load capacity degraded (Figure 5b). Following an examination of the support after testing, it was observed the loop bar had deformed significantly rotating backwards from the ledge and being dragged down as the web separated (Figure 5c).

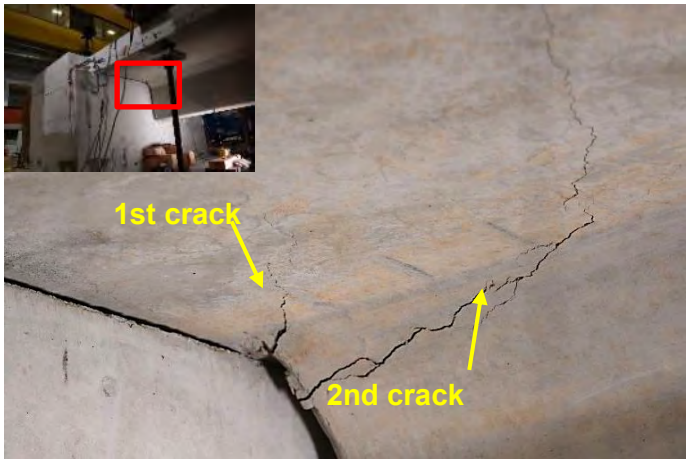

a) Web-flange corner cracking

b) Failure – web separation

c) End of test – deformed loop bar

Figure 5. Vertical load test observations

After removing concrete at the end of each test to examine the failure mode, the web separation was attributed to a crack that started at the web-flange corner and propagated up to the topping-to-unit interface in an arc profile. Additional cracking was observed across the entire width of the topping-to-unit interface. Figure 6 provides an illustration of the presumed crack pattern based on visible observations. Further analysis is required to confirm the degree of cracking and separation at key loading stages.

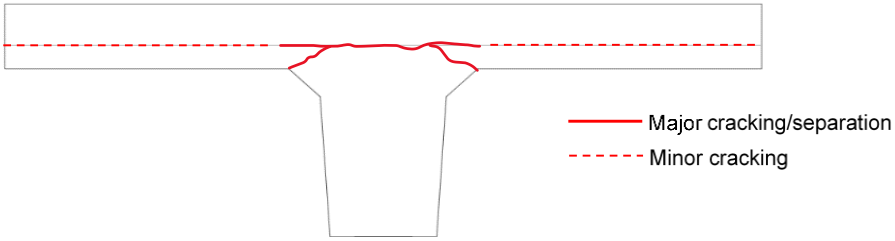

Figure 6. Illustrated cross-section cracking at support

Despite the variations to the topping-unit interface to simulate delamination, the reduction in vertical load capacity was only ~10% for test units 2 and 3. However, the observed damage patterns did indicate that the simulated delamination was effective. For Unit 3 that used a polythene sheet to debond the interface, slip was observed at the toping-unit interface during loading and significant movement occurred along the interface at failure, as shown by the photos in Figure 7.

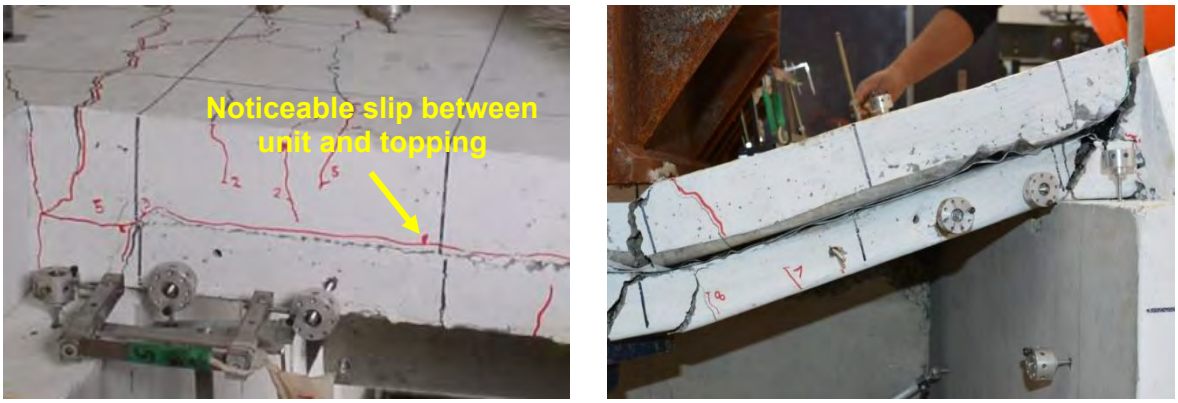

a) Slip at the toping-unit interface during loading

b) Movement along toping-unit interface at failure

Figure 7. Unit 3 toping interface cracking

SEISMIC LOAD TESTS

For the seismic tests, both of the test units subjected to combined rotation and elongation resulted in a loss of support failure, as shown in Figure 8. Significant spalling occurred to the support beam ledge, initially concentrated at the loop bar location but later propagating along most of the beam length. The units dropped as the loop bars slid down the support beam and the web of the units was eventually caught by retrofits that had been installed. Upon inspection at the end of testing, significant spalling was also observed to the nib of the tee unit which combined with the ledge spalling and elongation led to a loss of bearing length causing the support to fail. This observation is consistent with the failure mode observed in Statistics House. Additional analysis of the test results is required to compare the observed spalling and drift capacity with the procedures in the C5 seismic assessment ‘yellow chapter’.

a) Unit 5 b) Unit 6

Figure 8. Seismic load test loss of support

SUMMARY

A series of subassembly tests were conducted to investigate double tee precast concrete floor units that used flange hung support connections with loop bar reinforcing details. The first phase consisted of vertical load tests to assess the support load path and influence of delamination between the unit and topping. The second phase consisted of simulated seismic loading with a combination of rotation and elongation imposed on the support connections. The test results have helped to understand the failure modes of flange hung double tee with loop bar details and preliminary observations were presented. Additional analysis of the test results is required in order to provide recommendation to the seismic assessment and retrofit of precast double tee floor units.

REFERENCES

Brooke, N. J., Elwood, K. J., Bull, D. K., Liu, A., Henry, R. S., Sullivan, T., Hogan, L. S., Del Rey Castillo, E. (2019). 'ReCast Floors - Seismic assessment and improvement of existing precast concrete floors', *SESOC Journal*, 32(1), 50-59.

Corney, S. R., Henry, R. S., Ingham, J. M. (2014) 'Performance of precast concrete floor systems during the 2010/2011 Canterbury earthquakes', *Magazine of Concrete Research*, 66(11), 563-575

Hare, J., Fenwick, R., Bull, D. & Built, R. (2009). 'Precast double tee support systems', *SESOC Journal*, 22(1), 10-44.

Hare, J., Bull, D. K., Elwood, K. J., Henry, R. S., Brooke, N. J. (2019). 'Precast Double Tee Support Systems -10 Years On', *SESOC Journal*, 32(1), 32-40.

Henry, R. S., Dizhur, D., Elwood, K. J., Hare, J., Brunsdon, D. (2017) 'Damage to concrete buildings with precast floors during the 2016 Kaikoura Earthquake', *Bulletin of the New Zealand Society for Earthquake Engineering*, 50(2), 174-186.

MBIE. (2017). Investigation into the Performance of Statistics House in the 14 November 2016 Kaikoura Earthquake. Ministry of Business, Innovation, and Employment, Wellington, New Zealand, 36p.

MBIE. (2018). The seismic assessment of existing buildings. Technical Proposal to Revise the Engineering Assessment Guidelines. Part C5. Concrete Structures. 189.

concretenz BUILDING RESILIENCE
CONFERENCE 2022
13-15 October 2022
Energy Events Centre | Rotorua

UNDERPINNING OF AUCKLAND'S CHIEF POST OFFICE BUILDING

NIRAJ RANJIT[1], NICK CRAIG[2] ,MICHAEL CHUNG[3]

[1] Freyssinet New Zealand
[2] Downer Soletanche Bachy JV
[3] Aurecon

SUMMARY

The Chief Post Office (CPO) building was built in 1912 and occupied by the NZ Post Office until the early 1990s. It was later converted into Auckland's Britomart Transport Centre in 2001 where the city's commuter train services currently terminate. Two decades later, it has undergone another transformation as part of the city-changing City Rail Link (CRL) project.

Construction of twin rail tunnels beneath the Category 1 heritage CPO building in one of New Zealand's largest railway stations presented major challenges for CRL delivery. These challenges led to several NZ first innovations, including the underpinning of the CPO building.

The primary objective of the underpinning works was to take approximately half of the gravity load of the building from existing foundations and transfer it onto new concrete diaphragm walls (D-walls). This operation was necessary to allow the existing foundations to be removed for the construction of the rail tunnels themselves.

Once the tunnel was constructed, the building load was transferred off the temporary works and onto new foundations on the tunnel roof and back into the D-walls. Approximately 6,000 tonnes of building load (close to half the weight of the entire building) was incrementally transferred without impacting the building's structural or architectural integrity - a feat of delicate engineering not seen in this country before.

PROJECT DESCRIPTION

Auckland's top transport priority, the CRL project includes the design and construction of a 3.4km double-track underground rail line from Britomart Station through the CBD to connect with the existing western line at Mt Eden station.

In 2016, the Downer NZ and Soletanche Bachy JV (DSBJV) was awarded CRL Contract 1 (C1), an enabling works contract at Britomart. The design was managed by a team comprising CRLL, Aurecon, Grimshaw, Mott Macdonald, Jasmax, and Arup, working very closely with DSBJV.

CRL C1 includes construction of tunnels from Britomart Station, westwards underneath the CPO building and lower Queen Street, connecting to cut and cover tunnels in Albert Street

delivered under Contract 2 (C2). However, the new tunnel clashed with the building's existing foundations.

This article outlines the main steps that enabled the construction of these tunnels including:

- Construction of the diaphragm walls and jet grouting that served as new foundations for the building
- Construction of the permanent and temporary underpinning structures
- The load transfer from the existing to the new foundations
- The construction of the tunnels
- The release of the temporary underpinning structures

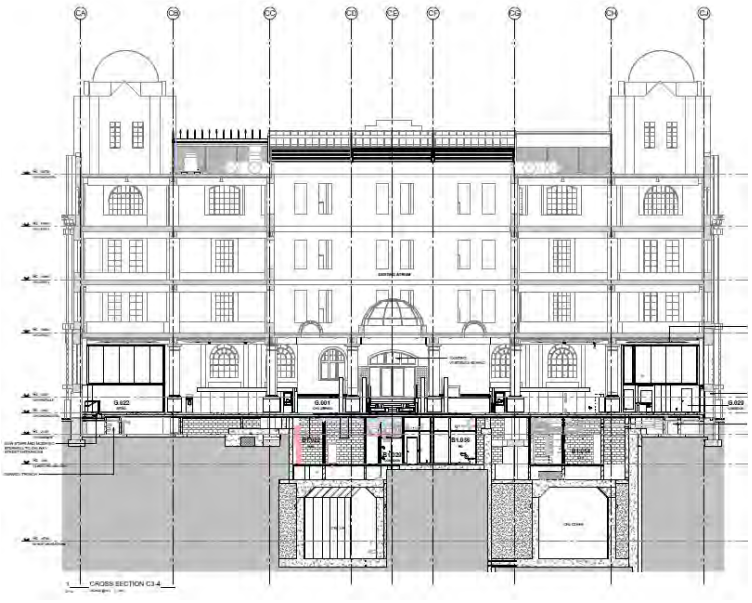

Figure 1: CPO Building with twin rail tunnels constructed underneath

During the works, the behaviour of the building was monitored very closely to ensure that the load transfer activity was conducted with precision, without impacting the building's structural or architectural integrity. Monitoring prisms were installed throughout the building and continuously monitored over the duration of the project. Real time movement of the building during the load transfer was also monitored using traditional survey techniques to ensure that the building was not 'lifted' during the load transfer by more than 3 millimetres.

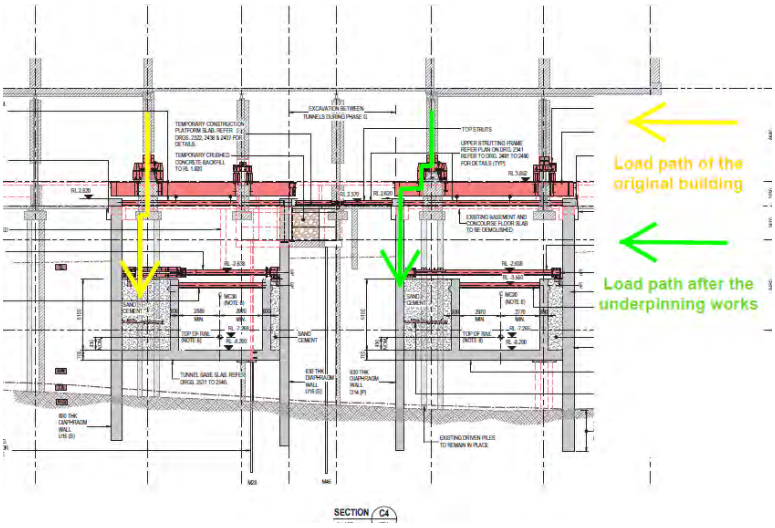

Figure 2: Original vs Underpinned Load Paths of CPO Building

DESIGN CONCEPT

Extending the railway from Britomart Station required the construction of two shallow tunnels below the CPO building. The tunnel alignment clashed with the driven piles supporting twenty building columns and the façade walls on the eastern and western sides. However, in recognition of the CPO building's heritage value, the visible sections of the façades, upper floor levels and tiled vestibule had to remain undisturbed throughout construction. In addition, the high water-table and soft ground conditions on reclaimed land heightened the risk of ground movements affecting the CPO and surrounding properties during excavation.

To address these constraints, the tunnel design utilised a cut and cover sequence, whereby the building was first underpinned before excavating within a water-tight cofferdam. This required significant temporary works to be undertaken within the confines of the CPO building.

The construction sequence began with the demolition of the ground floor slab, followed by D-Wall installation from basement level. Subsequently, underpinning frames were installed to support the existing columns and walls and transfer loads onto the D-wall.
During excavation, the existing foundations were demolished leaving the CPO structure suspended over the cofferdam. Two levels of steel strutting were installed to reduce wall deflections and internal forces. The top strutting level ran between the tunnels to prevent racking towards the central column of remaining ground.

Following excavation, the tunnel boxes were constructed bottom-up. The tunnel boxes re-supported the building columns and spanned the D-walls each side. This approach allowed the temporary underpinning frames to be removed, enabling re-construction of the ground floor and new basement space.

CONSTRUCTION OF PERMANENT STRUCTURES

The following sections of this paper describe the major phases of work required to tunnel under the CPO building, including D-wall construction, underpinning of the building foundations, and tunnel box construction.

Diaphragm walls (D-walls)

The overall D-wall is made of 64 panels, varying in width from 2.8m to 5.2m, approximately 17m in depth (3m socket into rock). These were drilled with two different thickness; 630mm and 800mm (approximately 50-50 difference in thickness).

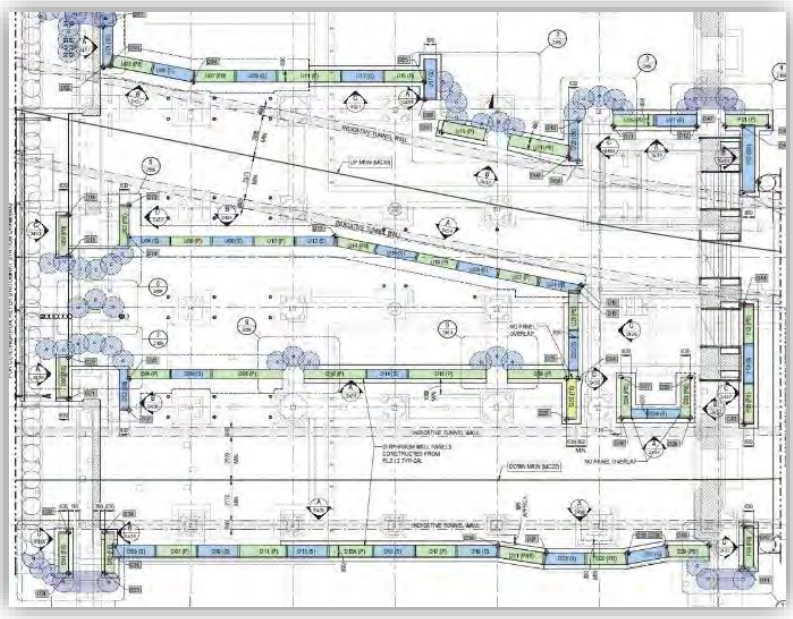

Figure 1: CPO D-wall panels

Excavation and drilling of the D-walls was carried out using a Hydrofraise Compact HC05 last generation machine. The machine was equipped with a detachable power-pack which was positioned on a crawler and connected by an umbilical to the drill. This was due to the column orientation highly constraining the machines movement around the CPO ground floor.

Figure 4: Hydrofraise D-wall machine (left). D-wall Power Pack detached (right). The Hydrofraise compact was the only machine capable of constructing the D-walls inside the building and was the first time this equipment was used in New Zealand

The 64 concrete panels were poured using a tremmie mix with design strength of 40 MPa at 28 days. The average concrete volume for each panel was 45 m3. Pours were completed in approximately 2- 3 hours. Given that most of the pours were constructed inside the CPO building, it was not possible to use the traditional D-Wall method of pouring straight out of the truck. Due to the limited 7 m headroom, DSBJV worked with Allied Concrete on a pumped tremmie concrete mix design with 3-4 hours workability.

The initial D-wall design included a double row of 40mm diameter longitudinal reinforcing steel. A construction review identified a bar congestion and constructability risk associated with the number of manual interventions inside suspended cages. This led to the design of a single row of high strength 50mm primary reinforcing bar, a first for New Zealand. New procedures for manufacture and testing were developed while keeping to programme and maintaining a minimal carbon footprint.

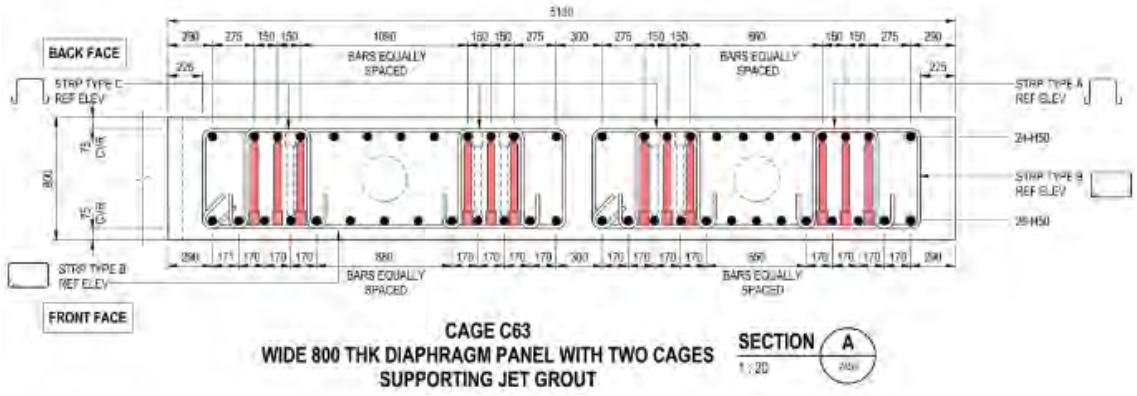

Figure 5: Section of D-wall showing single row H50 bars, each face.

Jet Grout Arches

To create the arches between the D-wall panels and complete the temporary retaining structures, DSBJV used a jet grouting method as the Hydofraise was not able to access certain areas due to space restrictions. The overall jet grouting is made of 81 columns with a minimum diameter of 1.4m, approximately 17m deep.

A jet grout mix design was developed that achieves a minimum in-situ characteristic unconfined compressive strength of 5MPa. The jet grout mix used Holcim Ultracem type GP mixed with water and was pumped under high pressure using a jet grout piling machine.

The plant to undertake both the D-wall and jet grouting operations was built on site and maintained by the self-performing team throughout the works.

Figure 6: Bentonite D-wall and jet grout plant (left) Jet Grout Piling Machine (right)

Capping Beams

The D-wall capping beams had several objectives as part of the main works:

- Tie the D-wall panels together and distribute forces throughout the beam through the top level struts
- Provide temporary seating for the steel underpinning beams
- Provide a jacking surface for load transfer works (refer load transfer sequence)
- Provide permanent seating for the concrete underpinning beams
- Provide temporary seismic support for the front façade concrete underpinning beam
- Some capping beams included starters bars with couplers to enable permanent walls to be built above as part of the CPO rebuild works, following tunnel construction.

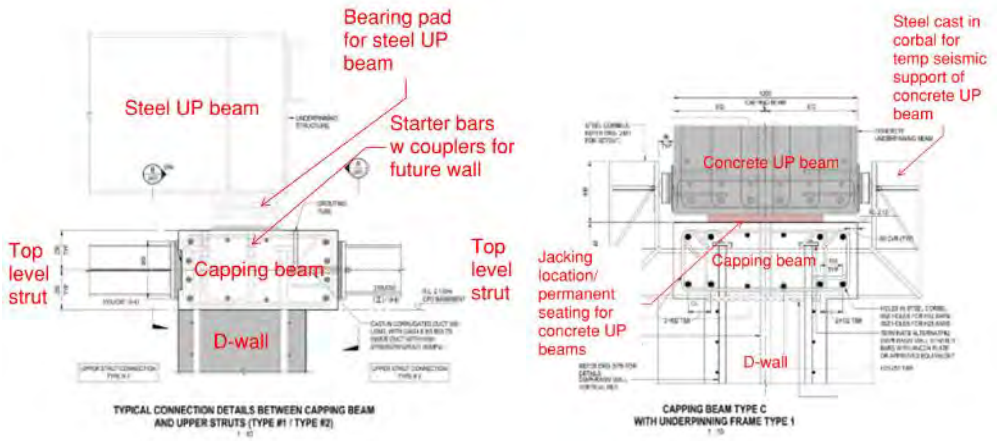

Figure 7: : Capping beams for steel and concrete underpinning works

Reinforced Concrete Underpinning Beams

Concrete underpinning beams consisted of approximately 830t of concrete structures comprising 38 reinforced concrete beams. 32 of these were post-tensioned using a series of stress bars and post-tensioning multi-strand tendons. The areas depicted below in plan and 3D were identified around the façade and vestibule area of the CPO where additional strengthening was required to stiffen the structure.

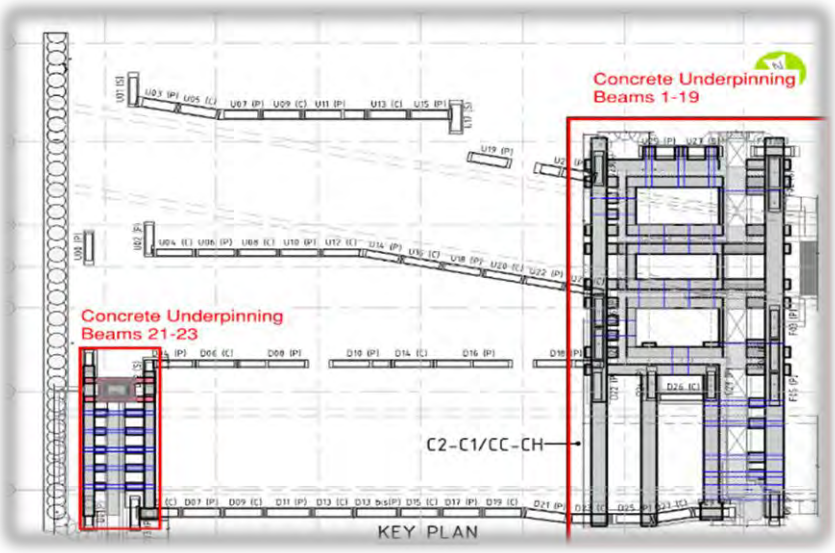

Figure 8 : Concrete underpining beams layout

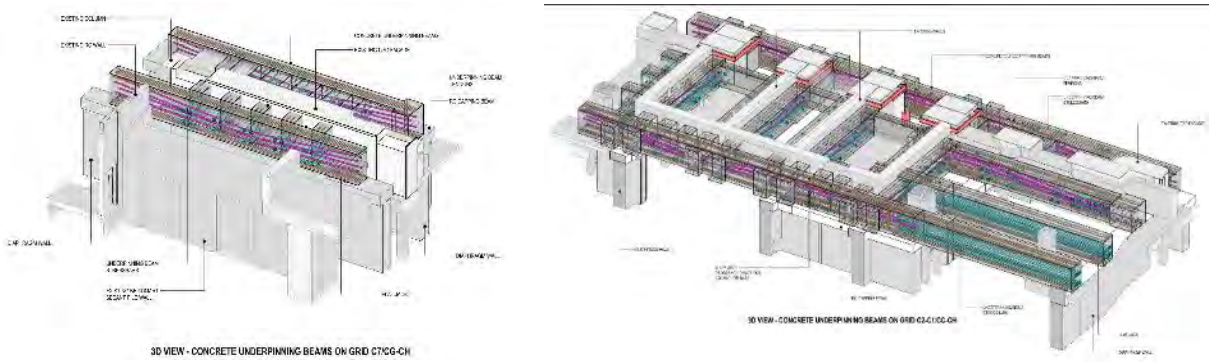

Figure 9 : Concrete underpining beams layout

Post tensioned, reinforced concrete beams were located at the front and rear façade areas of the CPO building where it was imperative that the heritage elements were not compromised (Beam 22 shown below). The beams were cast against the existing concrete wall structures, many of which were unreinforced during the early 1900 build. Figure 10 below illustrates the typical details of concrete underpinning beams interfacing with existing walls.

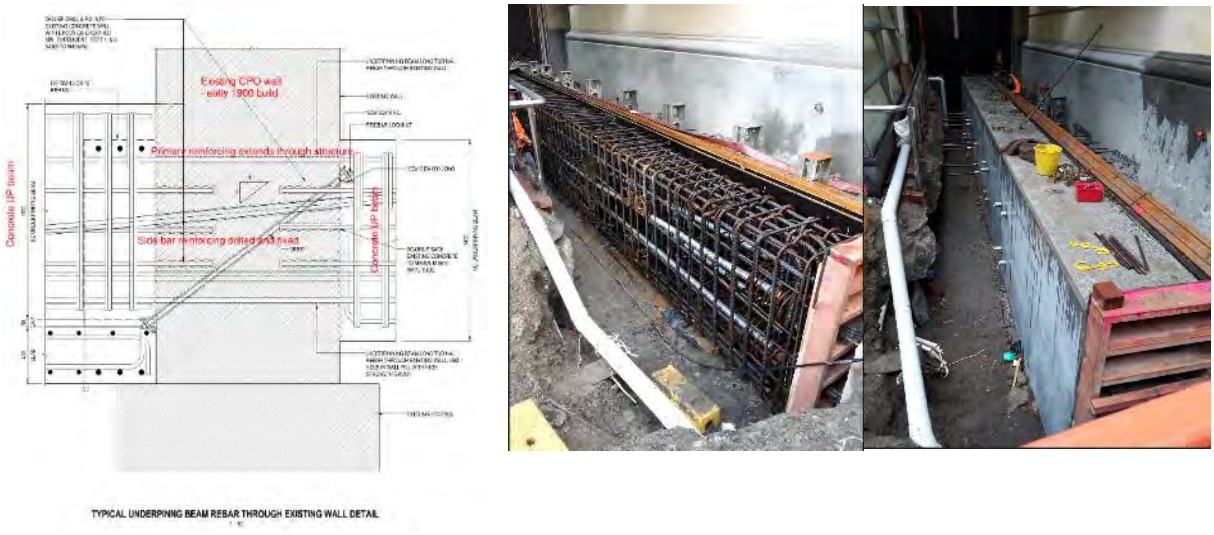

Figure 10: Typical Underpinning Beam through existing wall (left) Concrete Underpinning beam – North east façade (right)

The primary reinforcing and post tensioning in the beams extend through the existing walls and connect to adjacent beams in the particular group (using starter bars, couplers and corrugated ducts), effectively forming a grillage structure. The post tensioning enabled the loads to be transferred from the existing walls to the new concrete beams. Figure 11 below shows Beam 10 cast with PT ducts, side face bars and primary reinforcement couplers for transverse BM09. The left of the image shows holes cored for post tensioning elements between BM09 and BM10.

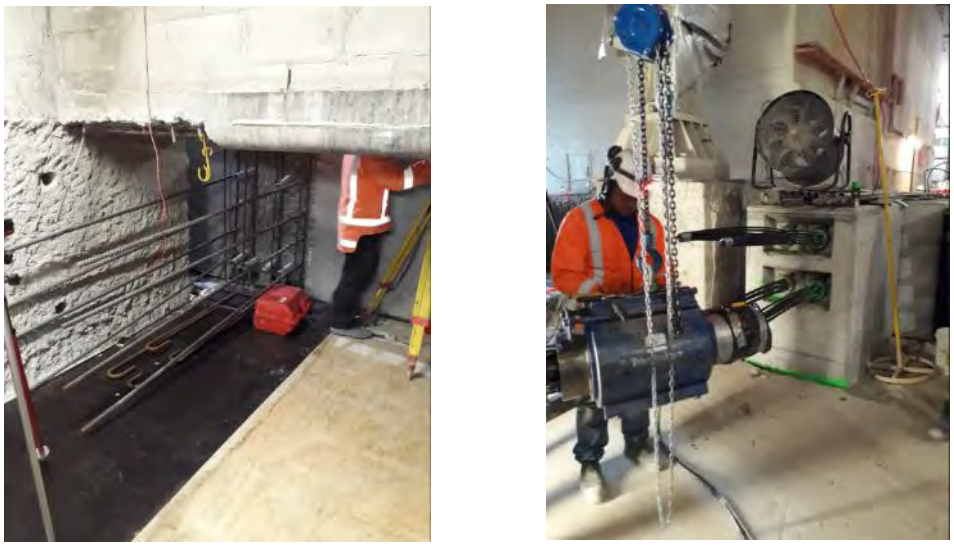

Figure 11: Concrete underpinning reinforcing and PT ducts through structures (left) Post tensioning works (right)

LOAD TRANSFER WORKS

Load transfer was conducted using Freyssinet's 'Flatjack' system. Flatjacks were used for their versatility and their load capacity. They require minimal clearance of 40-50mm and can be engaged using hydraulic fluid for temporary jacking or permanent grouts. They provide very high load capacity. Varying jack sizes with capacities from 62 ton to 585 ton per jack were utilized on this project efficiently and cost competitively.

Two distinct areas were identified for the load transfer works, which required specific methodologies to be developed:

1. Steel underpinning load transfer (internal columns)
2. Concrete underpinning load transfer (Eastern and Western facades)

The sequencing of the works involved the internal columns to be lifted before the western and eastern facades.

Steel Underpinning Load Transfer

The steel underpinning structures were constructed on top of the capping beams within the internal columns section of the building. This included fabrication and construction of nine steel frames and three standalone collar structures. These structures, totalling 350t, were all located within the CPO Building and positioned on the capping beams of the D-walls.

The primary function of the steel underpinning works was to support the internal columns of the CPO Building during excavation and tunnel construction and provide a suitable means of undertaking the load transfer works.

In the figure opposite, the steel structure can be seen in red and the concrete underpinning beams can be seen in grey.

Individual frames were constructed of welded beams, transverse steel beams, collar assemblies and shear boxes welded to the existing steel columns. Each collar assembly then had a specially designed low-shrink concrete poured inside the collar on a temporary falsework soffit. The collars were subsequently post tensioned.

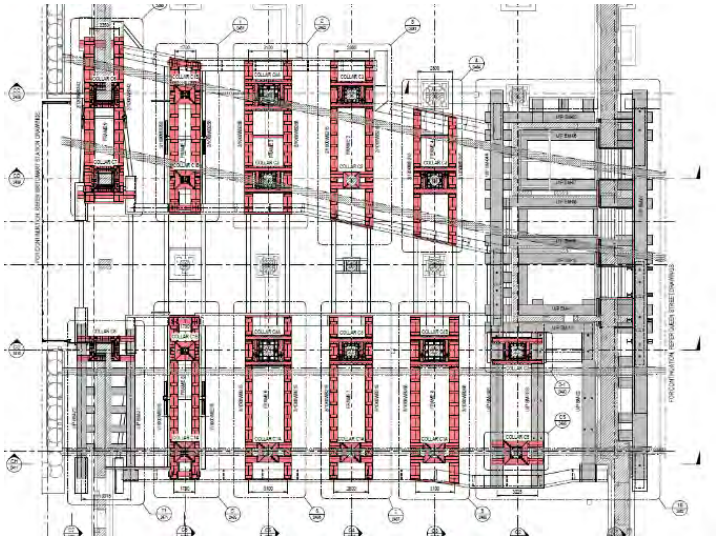

Figure 12: : Steel Underpinning Beams

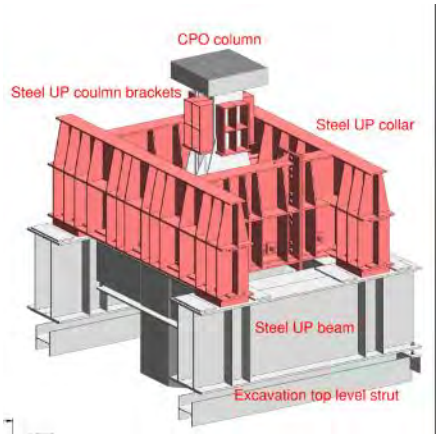

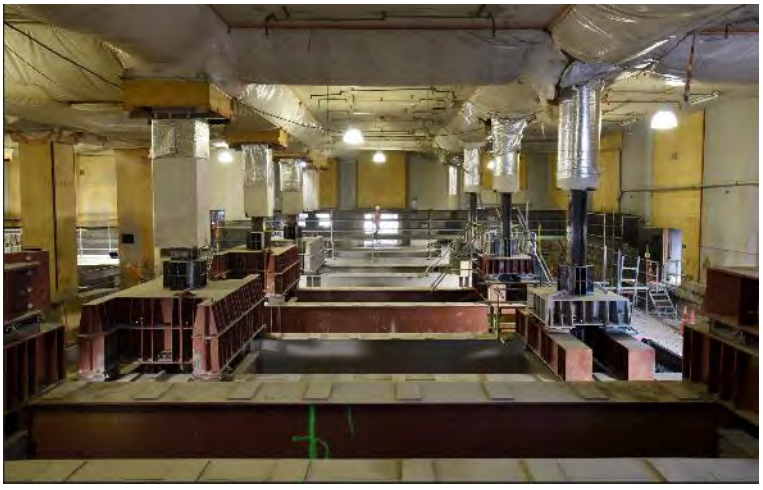

Figure 13: Steel Underpinning Collar (left) North Tunnel Trench from top of Underpinng Beams (right)

The internal column section was split into 9 zones. Each zone included a steel ‘Frame’ connected to the D-wall and two internal columns. Incremental load transfer in this section involved jacking up the columns one zone at a time.

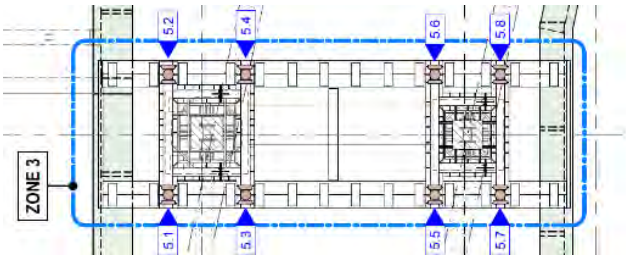

Figure 14: : Typical Flat Jack Zone

The critical features of these works:

- Flatjacks were positioned around each column to ensure the load applied was centred on the column to avoid imposing any bending moment on the column. This was achieved by surveying the position of each jack as well as designing a hydraulic circuit that enabled equal loading on all four corners.
- Maximum loads of up to 79 ton per flatjack. Total of 64 flatjacks between 270mm to 420mm were used.
- To minimise losses during the transfer of load between the flat jacks and adjacent shims, project specific design of a tapered shim was conducted to achieve the required accuracy
- Accounting for the unpredictable behaviour of the building and given its age, there was a degree uncertainty on the load carried by each column. Contingency was built into the load transfer methodology by applying a factor of safety on the capacity of the flat jacks. In addition to the load control, alert levels were set on displacements to avoid over-jacking of the building.
- In order to allow for accurate detection of column lift-off, a laser “dot” was shot on the column. This laser was also used to monitor any vertical movement of the column during jacking. The Surveyor was able to detect movement of the laser dot to 0.25mm. Allowing for normal background vibration, reliable detection of 1mm lift off was achieved.

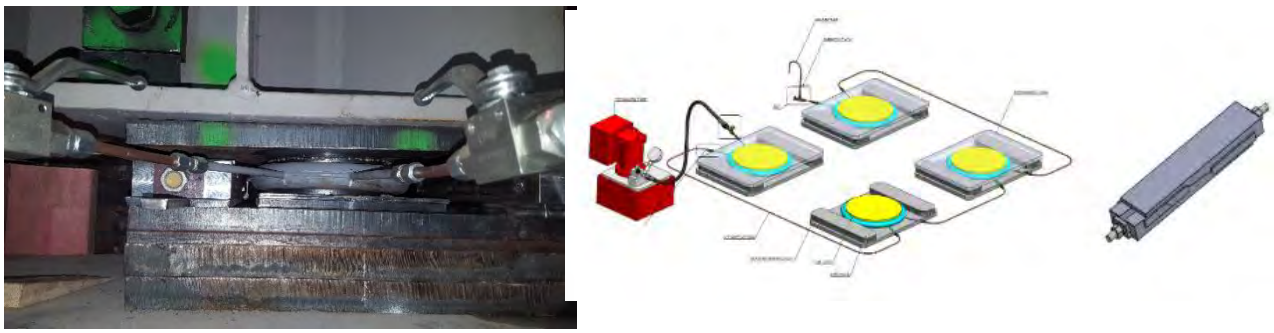

Figure 15: Hydraulically Linked Flatjacks (left), Flatjack circuit schematic (right)

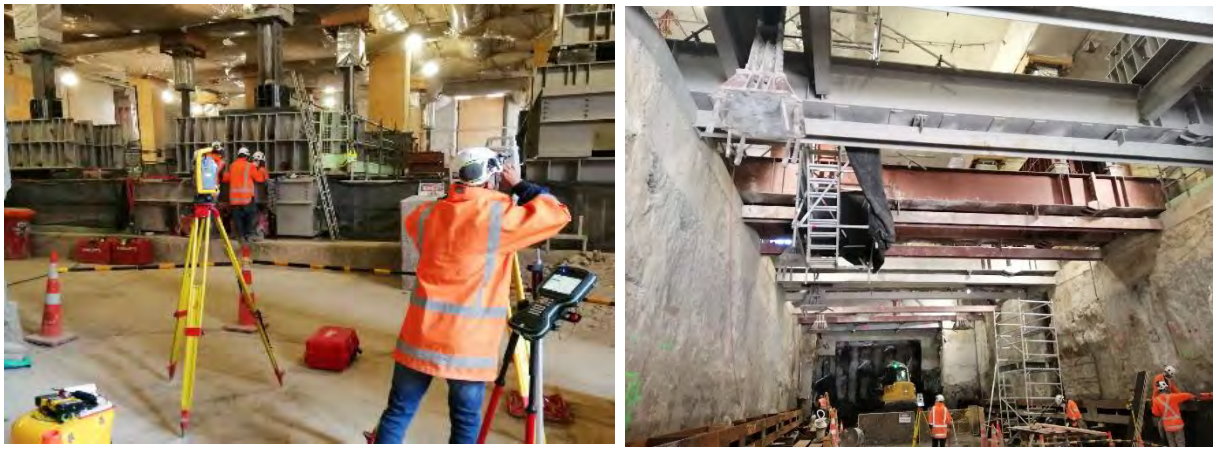

Figure 16: Multiple Survey Instruments to monitor the Load Transfer (left), Free hanging column footing after load transfer and partial excavation (right)

Concrete Underpinning Load Transfer

The eastern and western façade load transfer was also incrementally conducted in 4 zones.

The critical features of these works included:

- Much higher loads, with flat jack capacities up to 600 ton per jacking location. Total of 21 flatjacks between 350mm to 750mm were used.
- A much stiffer structure supporting a heritage structure including a mosaic floor, thus very sensitive to displacements. The façade load transfer was significantly more sensitive than internal columns as there was a significant risk of damage to the heritage façade and vestibule area. Additional monitoring locations were positioned during the load transfer of the façade.
- Flat jacks of varying sizes were used within a single zone, thus requiring a different setup to ensure proper sharing of the load between the different beams
- While all the jacks within a zone were required to be engaged simultaneously, they did not need to be linked in the same hydraulic circuit.

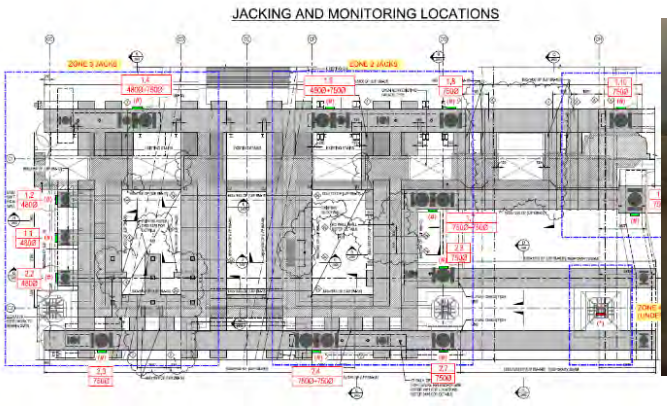

eam and Capping Beam

Construction of Tunnel, Roof Beams and Columns Between the D-walls

Following excavation of the tunnel trench, work commenced to construct the rail tunnels.

The tunnel base slab itself had a blinding layer with an underlying drainage system to dissipate buoyancy forces on the tunnels and building. The base slab was cast on a fully bonded waterproofing membrane and was tied into the D-walls using couplers that were positioned accordingly in the D-wall cages at an early stage of construction.

Once the base slab was cast, side-wall infills were constructed. These consisted of mass flowable fill. This structure provided a smooth, fair face for the wall waterproofing membrane. Similarly to the base slab, the roof was also tied into the D-walls using couplers positioned in the D-walls.

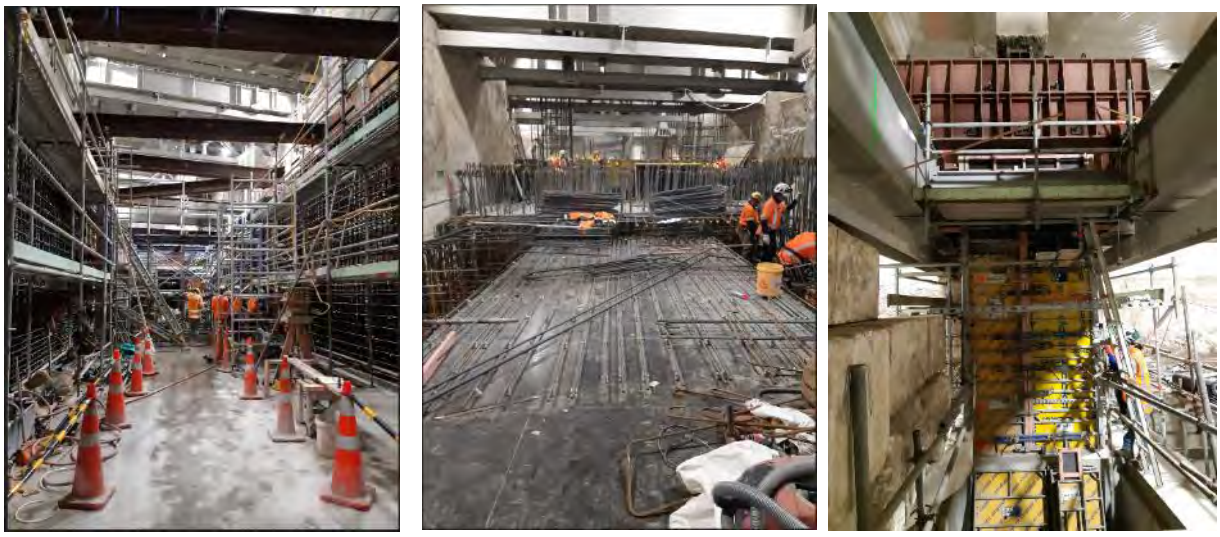

Figure 18: Tunnel Wall construction (left) tunnel roof construction (middle) CPO column construction while underpinned (right)

On top of the tunnel roof and in line with the overhead 'hanging' columns, DSBJV constructed the tunnel roof beams (typically 1.5m deep and 3.5m wide). These were constructed to support the new columns and spread the load across the tunnel roof and into the D-walls for the permanent state. Figure 19 below illustrates in detail the CPO tunnel construction works including roof beams and columns.
The tunnel box concrete design consisted of special grade concrete. In addition to meeting the requirements of normal concrete as specified in NZS 3104, the following was required:

- Blended cements were used (blended cement content: 35-50% fly ash / 50-65% Portland cement).
- The maximum drying shrinkage of concrete was 570 micro-strain at 3 weeks and 800 micro-strain at 8 weeks.
- Characteristic 28 day compressive strength, 40 MPa.
- Thermal expansion coefficient, 12 με/°C.
- Early-age concrete maximum temperature rise, 35 degrees.
- Permissible range of blended cement content: 370 kg/m3 – 445 kN/m3
- Maximum water / cementitious ratio, 0.45
- To mitigate spalling effects in the event of a fire, 2kg/m3 polypropylene monofilament fibres with a maximum of 32 micrometre diameter and 12mm length were added to the concrete mix.

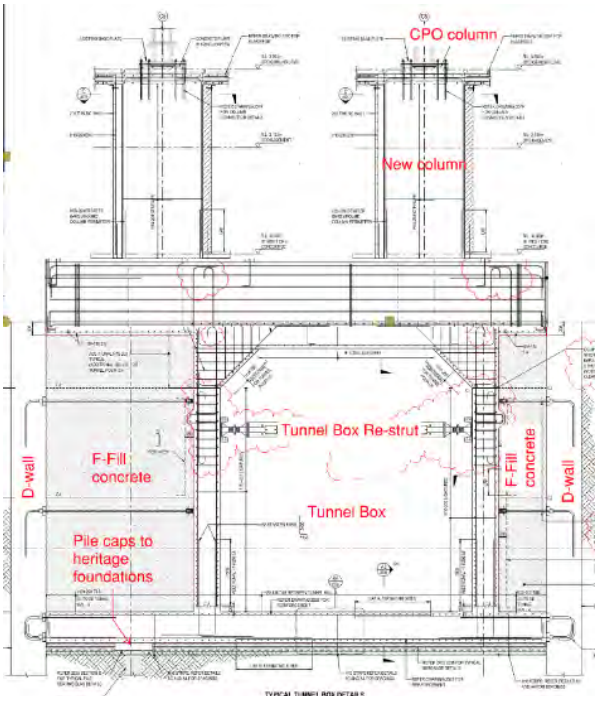

Figure 19: CPO Tunnel Construction details

During construction of the new columns, DSBJV worked closely with the architect to develop a concrete finish to the visible columns located on the B1 basement level as a departure to the specification and design. The columns were left exposed to assist in 'telling the story' of the recent construction works. Figure 20 shows the finished columns inside the public toilets, seen to the public on level B1.

Figure 20: CPO Columns exposed concrete appeal inside public toilets at B1 level

Load Transfer to Tunnel Roof

Once the tunnel roof was built, it was necessary for the building load path to be re-directed from the original column footings onto the tunnel roof. It was not desirable to leave the steel underpinning beams in place as they were occupying a large amount of space in what is now the Britomart Train Station foyer which thousands of people use for access daily. Controlled transfer was crucial as the steel underpinning beams had been storing large amounts of energy from the initial load transfer.

The works involved re-installing the flatjacks and hydraulic circuits and engaging the flatjacks to remove the tapered shims. The procedure was similar to the initial load transfer phase where specified loads were applied to each individual jacking zone. The columns and the facade were just sufficiently jacked up to loosen the tapered shims for removal.

CONCLUSION

The project required some 18 months of temporary works prior to any excavation, including the installation of underpinning structures to transfer approximately half the load of the 100-year-old CPO Building from its original piled concrete foundations - a feat of delicate engineering not seen in this country before.

Following the successful completion of the underpinning works, the tunnel construction and refurbishment activities were able to commence. Careful consideration of the CPO building's history and legacy resulted in successful reinstatement and refurbishment of the CPO basement level plant room, ground floor, rail ticketing facilities, station retail and all heritage features. Meticulous attention to detail was overseen by both client and contractor's appointed heritage architects to protect the heritage features.

DSBJV delivered this highly technical and challenging project, including specialist works and innovations new to New Zealand on time and on budget. DSBJV is proud to be part of a diverse and high-performing team. The power of collaboration between main contractor, specialist contractor, designer and client during early procurement phase through to contract execution phase has meant that what was once a challenging vision has now become a reality that will help to improve the quality of life for Auckland commuters.

ACKNOWLEDGEMENTS

- City Rail Link Limited
- Aurecon
- Grimshaw
- Mott Macdonald
- Jasmax
- Arup
- Allied Concrete

REFERENCES

Nil

concretenz BUILDING RESILIENCE
CONFERENCE 2022
13-15 October 2022
Energy Events Centre | Rotorua

BUILDING THE LARGEST FLOOR SLAB IN NEW ZEALAND AND THE FUTURE OF HIGH-PERFORMANCE FLOORS – A CASE STUDY ON FOODSTUFFS NORTH ISLAND DISTRIBUTION CENTRE (FSNIDC)

SAM DATLEN-CARTER[1]; TIM WALKER[2]

[1] Conslab Ltd
[2] Face Consultants Ltd/RDT Pacific

SUMMARY

The largest warehouse ever constructed in New Zealand, Foodstuff's North Island Distribution Centre, required careful design and planning to deliver the 75,000m^2 post-tensioned warehouse slab within a tight programme timeframe. Design of the slab needed to accommodate large expected joint openings and was optimised for construction to allow for a two-face methodology. The late addition of an extension to house a semi-automated shuttle racking system indicated the logistics industries shift towards automation, which is introducing new challenges to the design and construction of floors for logistics facilities.

INTRODUCTION

Foodstuffs North Island Distribution Centre (FSNIDC, referred to hereafter as DC) is the largest warehouse ever built in New Zealand. Constructed from 2019 to 2020, the DC consolidated operations from 8 Foodstuffs sites within the upper-North Island region into a single facility. The DC is located at Auckland International Airport's *The Landing* development, which was selected for its proximity to transport links and Foodstuffs chilled and frozen storage facilities ("Foodstuffs NI Makes A Move", 2021).

The original concept for the facility was a 64,300m^2 warehouse with selective pallet racking storage for 65,000 pallets. The concept included provision for a 10,700m^2 future expansion, however during the construction phase this was incorporated into the main build. The expansion was built to house a semi-automated shuttle racking system with capacity for 14,700 pallets, taking total storage capacity in the DC to 80,000 pallets.

Conslab was engaged by the Main Contractor, Macrennie Commercial Construction, to design and build the 75,000m^2 post-tensioned warehouse slab, and 25,000m^2 external pavement.

DESIGN

Floors are an important consideration in the construction, use and longevity of modern logistics facilities. A poorly designed or constructed floor can lead to a range of issues for tenants and asset owners, including excessive maintenance, limitations on logistics equipment, and inefficient operation of forklifts and materials handling equipment (MHE).

Equally, a high-quality, well-designed floor enables the efficient utilisation of logistics equipment (racking and MHEs) with minimal maintenance.

The key factors that characterise high-quality floors in logistics applications are:

1. Structurally sound – being able to carry appropriate racking and MHE loads while accommodating the site-specific ground conditions
2. Flat & Level – achieving the required surface regularity specification to enable efficient storage and minimise MHE maintenance and driver fatigue
3. Durable Surface – achieving required abrasion resistance classification to minimise maintenance cost and disruption

The developer's Structural Engineer (Day Consultants Ltd) provided a performance specification for design & construction of the floor which addressed these factors by specifying design loads (governed by a 75kN racking load), surface regularity (FM2 to TR34) and finish (steel trowelled/highly burnished).

This paper does not discuss floor performance specification or design in detail as this has been covered extensively by previous work (McGuigan & Walker 2008) (Marchant 2001) (Walker et al. 2007).

Selection of Floor Type

The primary solutions for large-scale industrial flooring in New Zealand are Post-tensioned (PT) or "Jointless" fibre reinforced slabs. Both solutions eliminate the need for saw-cut joints in the slab, which greatly improved the serviceability and durability of industrial floors. Saw-cuts are a common maintenance item in industrial buildings and require regular sealing to prevent deterioration by frequent MHE traffic.

Beyond the elimination of saw-cut however, there are significant differences between post-tensioned and jointless fibre slabs, which drive decisions by developers and tenants in favour of either solution. The most obvious difference is the frequency and design of movement joints. PT slabs can be designed with movement joint spacings of up to 150m. This distance is determined by practical limits on the ability to push PT strand through ducts over larger distances, and to reliably grout ducts after the strands have been tensioned. Jointless fibre slabs require movement joints at approximately 30-40m spacings. This is determined based on industry experience and is a "rule-of-thumb", with larger joint spacing correlating to an unacceptable risk of uncontrolled cracking.

Based on these maximum joint spacings, the potential slab layouts for FSNI using PT and jointless fibre slabs, shown in Figures 1 and 2 respectively, were developed.

The concept PT layout has a total movement joint length of 1,143m, with a maximum slab joint spacing of 120m and joint-free panels up to 11,390m^2. The concept Fibre slab layout has a total movement joint length of 4,296m, with maximum joint spacing of 35m and joint-free panels of up to 1,225m^2. As movement joints are the primary maintenance item within an industrial

floor, this difference in joint length correlates with a significant difference in maintenance burden which the developer and tenant would have to manage.

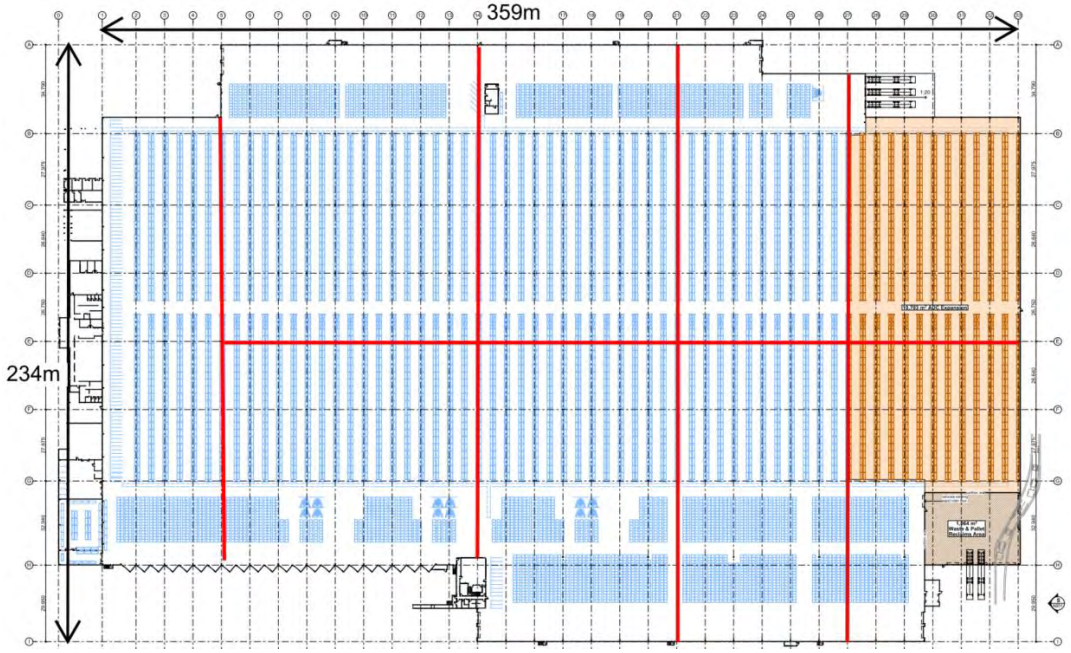

Figure 1. Concept PT Slab Layout (Movement Joints in red)

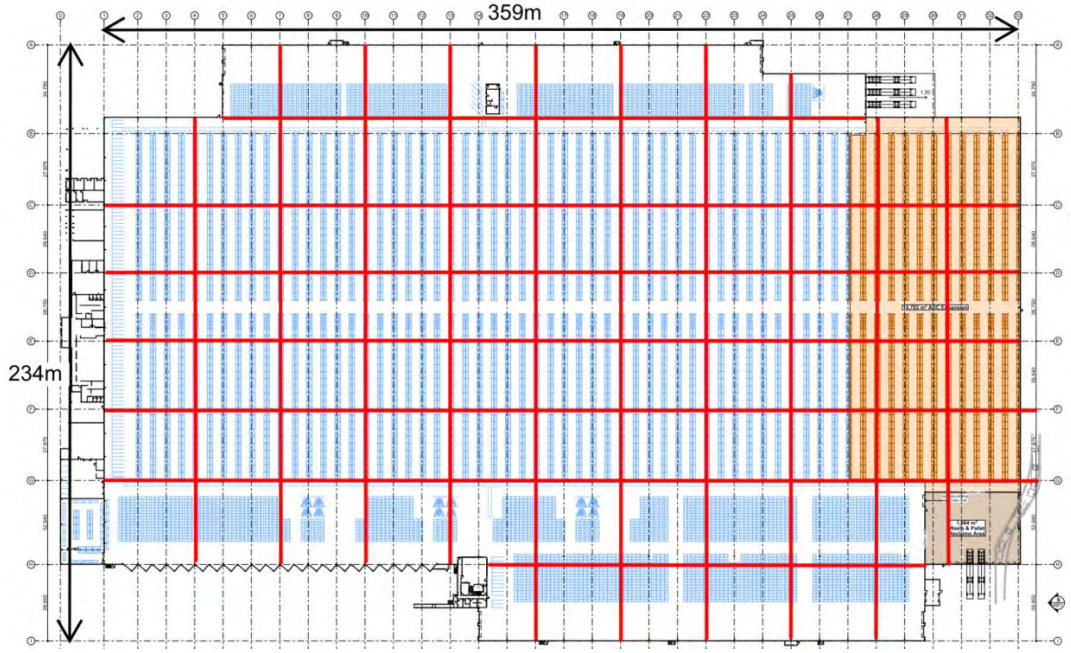

Figure 2. Concept Fibre slab layout (Movement Joints in red)

Based on these maximum joint spacings, the opening at movement joints is also significantly different. Industry generally estimates in-situ concrete shrinkage (very conservatively) as 1mm per 1m of slab length. This means movement joints between 120m long PT slabs could be up

to 120mm, whereas in a fibre slab with 35m joint spacing the opening would be 35mm. Commercially available movement joint systems can accommodate up to 85mm joint openings, which means joints between the PT slabs would require customised movement joints to accommodate large openings.

Another consideration in joint selection is the potential for slab curl. Curl is correlated with slab length, therefore is a significantly larger risk for large PT slabs compared to the fibre option. Curl is the result of moisture gradients within a concrete element. Slabs constructed on damp-proof membranes tend to curl upwards due to lower moisture resulting in higher drying shrinkage near the slab surface. Curling occurs at slab edges, both the perimeter and at movement joints (CCAA, 2006). Curl at joints could cause disruption to tenant activities by forcing MHEs to reduce their speed while crossing joints. Joints with significant curl are also prone to damage and deterioration, due to the loss of support as the slab curls away from the sub-grade, and increased impact from traffic crossing the joint, as shown in Figure 3.

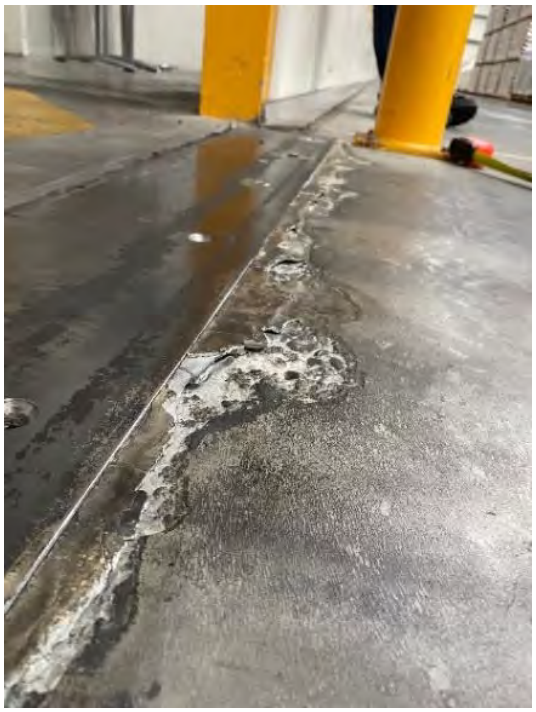

Figure 3. Joint arris damage due to MHE traffic on a slab with excessive curl

To mitigate the risk associated with large joint openings and slab curl, Conslab proposed a PT slab design which utilised Rhino Joint (Figure 4) to manage curl and accommodate large movements at opening joints. This proprietary joint system is anchored into a concrete ground beam to provide a resisting force that acts against upwards slab curl.

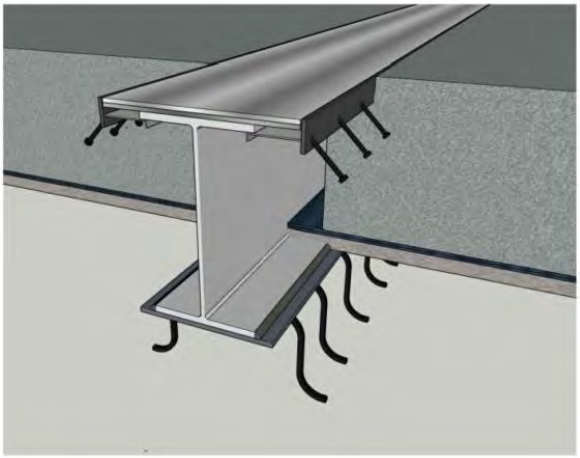

Figure 4. 3D view of Proprietary Joint designed to mitigate curl

The final design selected for FSNI was the Post-tensioned slab option. This was primarily driven by the developer and tenants desire to minimise future maintenance.

Build

At tender stage the warehouse comprised of 64,300m^2 warehouse space, with the option for a 10,700m^2 expansion in the future. The programme allowance for construction of the 64,300m^2 post-tensioned slab was 40 weeks, requiring production of approximately 1650m^2 per week.

During the early stages of construction, the tenant decided to incorporate the expansion option into the main build. The expansion area was built to accommodate an automated shuttle racking system, with higher post loads than the main build. This necessitated a re-design of the PT slab to add the expansion area, with an increased slab thickness to accommodate the higher racking loads.

The construction of the expansion area was to be undertaken within the original construction programme, a total area of 75,000m^2, with no extension to the time allowed for floor construction, requiring a floor production rate of 1875m^2 per week.

Many factors determine the productivity rate of PT slabs, including:

- Slab Size – Limited by:
  - Concrete supply rate determining maximum pour size
  - Concrete mix characteristics – initial/final setting time, bleed rate
  - Area that can be finished to a high standard within an appropriate timeframe
  - Availability of skilled labour
  - Width of pour face to avoid cold joints
- PT Slab layout
  - Location of joints – movement, coupled and day joints
  - Programming of adjacent slabs to allow access for stressing/grouting

- PT stressing and grouting timeframe
  - Initial Stress – typically 1-2 days after pour
  - Final stress – typically 7-10 days after pour
  - Grouting – following final stress

Typically PT slabs are constructed in a 3-week cycle, which includes preparation of the pour area, installation of the post-tensioning components, pouring, curing, tensioning PT strands and finally grouting the PT ducts (Figure 5). In the Auckland market with good availability of concrete and skilled labour, this 3-week cycle allows construction of approximately 5000m^2 of slab in two "back-to-back" pours.

Figure 5. PT Slab Construction Process (Strand install, pouring, stressing)

This typical cycle of PT slab construction would not allow for the target programme to be achieved. Conslab took the step of deploying two separate teams to set up PT slabs, allowing slab construction on two faces. This required careful consideration of the PT slab layout to ensure access for strand tensioning and grouting was not prevented by construction of adjacent slabs.

The first Post-tensioned slab was poured on September 5th 2019. In total 31 pours were required to complete the warehouse PT slab, with an average pour area of 2,395m^2, requiring an average concrete volume of 434m^3. A total of 13,459m^3 of concrete was required for the PT slabs.

On March 25th 2020, approximately two-thirds of the way through the PT slab construction, New Zealand was put into a month-long lockdown due to Covid-19. The FSNIDC site was entirely shut down during this period. Returning to site on May 11th, after New Zealand's Covid alert level was change to Level 2, PT slab production resumed with a pour on March 13th, and the final slab pour was completed on 10th June 2020.

Discounting the time spent in lockdown, the 75,000m^2 PT slab was completed within the 40 week programme.

The Future

The floor slabs at FSNIDC were designed to suit the logistics equipment that would be used at the facility. Primarily this consists of 7-8-high selective pallet racking, with operator-driven MHEs (forklifts, order pickers, pallet trolleys) used to transport pallets within the facility. This type of system has been widely used in the logistics industry for many decades.

Over recent years there has been significant advancement in the sophistication of available logistics systems, with a trend towards increasing automation of facilities, with a range of solutions including automatic guided vehicles (AGVs), autonomous guided robots (AMRs), automated storage and retrieval systems (ASRS) and others.

The expansion area at FSNIDC was built to accommodate a semi-automated shuttle racking system, which provides increased storage density and more efficient loading/unloading of pallets from the racking system.

The COVID-19 pandemic has accelerated the adoption of automated logistics systems, driven by increasing demand for e-commerce and labour shortages ("How Automation Will Change the Logistics Industry", 2022).

Most logistics facilities in New Zealand, including FSNIDC, are specified and constructed using a framework that was designed around non-automated logistics systems. The structural design is based on static and seismic post loading of selective pallet racking systems. Surface regularity of specified for the free movement of operator driven MHEs. Floor finish is specified to provide abrasion resistance to high-frequency traffic by MHEs with small solid-rubber tyres and high axle loads.

This specification framework may not be suited to the highly-automated logistics facilities of the future.

For example, the structural design of floors to carry ASRS systems is based on achieving very small deflection tolerances (L/3000 or larger). Traditional slab design methods have a linear inter-dependency between slab thickness and design loads (for a given sub-base stiffness), meaning if the slab design loads are specified then the slab thickness can be calculated. When designing for slab deflections, an iterative process is required. The racking designer provides the design loads to the slab designer, who then calculates the deflections. The slab designer provides those deflections back to the racking designer, who re-calculates the design loads taking the deflection into account. This process is repeated until the deflection limit is achieved.

Another example is AGVs and AMRs, that can require floor surface regularity properties which are not always achieved using existing established specifications, such as ConcreteNZ TS01:2021. Some AGV/AMRs require very small floor flatness tolerances that cannot be achieved through normal construction techniques and require significant post-construction correction of slab levels.

An example of this adoption of automated logistics equipment in New Zealand is a project currently under construction in South Auckland. This facility will house a 16,000m^2 ASRS system with capacity to store 65,000 pallets. Compared to FSNIDC, it will achieve approximately 3-4 times greater storage density in terms of pallets per m^2 of floor space and have a much lower labour requirement to operate.

Design of the slab to carry the ASRS system is governed by a slab rotation limit of L/1200. FEM modelling was used to calculate and plot slab deflections under the racking loads which are up to 267kN (Figure 6), which was repeated over several iterations to optimise design of both the slab and racking system. The slab design is a 400mm thick, reinforced with top and bottom mats of conventional reinforcing and a high dosage of steel fibre.

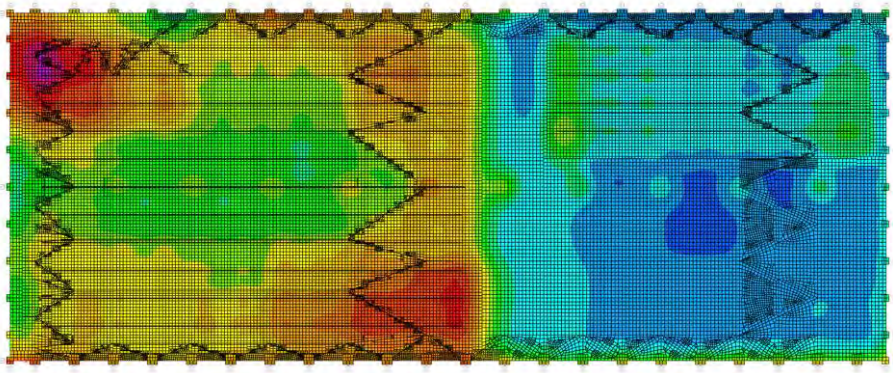

Figure 6. Deflection plot of ASRS slab

CONCLUSION

The FSNIDC floor slab is the largest ever constructed in New Zealand at 75,000m^2. It was designed to minimise the maintenance burden on tenants, allow for efficient operation of the tenant's logistics equipment, which consisted of selective pallet racking, semi-automated shuttle racking and operator-driven MHEs.

Construction within the programme was achieved through optimisation of the PT slab pour layout and required deployment of an additional PT installation team to allow slab construction on two-faces. Despite disruption due to the COVID-19 pandemic and the 2020 lockdown, the slabs were completed on schedule.

The late addition of a semi-automated racking system to the FSNIDC project is an example of the rapid adoption of automation in the logistics industry, which is introducing new challenges for the design and construction of industrial slabs-on-grade.

Methods of industrial floor slab procurement, design and construction developed over recent decades deliver excellent results for facilities operating conventional logistics systems such as FSNIDC. However, these methods may not be fit-for-purpose when higher levels of slab customisation are required for highly-automated facilities.

REFERENCES

Bogus, A., (1988), “Impulse Functions in Structural Mechanics”, *The Royal Society*, Vol. 77, December, pp. 2828–2832.

Cement Concrete & Aggregates Australia (CCAA), (2006) “Curling of Concrete Slabs”, Technical Data Sheet.

Foodstuffs NI Makes A Move (2021). Supermarket News, https://supermarketnews.co.nz/news/foodstuffs-ni-makes-a-move/

How Automation Will Change the Logistics Industry (2022). Industry Today, https://industrytoday.com/how-automation-will-change-the-logistics-industry/

Marchant, J. (2001), “Revival of Post-Tensioned Slabs on Grade”, NZ Concrete Industry Conference Proceedings 2001.

McGuigan, R., Walker, T. (2008), “Specifying Industrial Concrete Floors & Pavements”, NZ Concrete Industry Conference Proceedings 2008.

Walker, T., Mooney, B., Dallas, A., (2007), “Specification and Measurement of Floor Surface Regularity”, NZ Concrete Industry Conference Proceedings 2007.

THE CONCRETE NZ CONFERENCE 2022

To view or download the conference papers use this QR code or go to

https://concretenz.org.nz/page/conference_2022

(QR readers are easily installed at no cost from your mobile phone app store)

Please note: At the time of printing some papers were not available and so were not included in this version of the technical papers proceedings. Please visit the website above to view all papers.

CONCRETE NZ
CONFERENCE 2022